

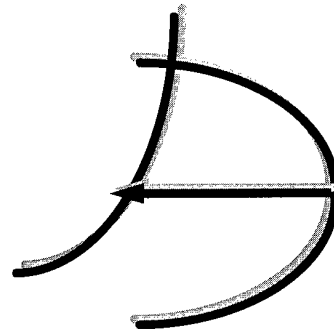


University of Leeds

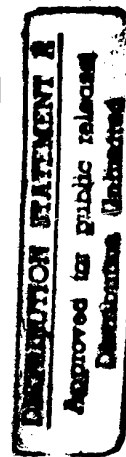
---

# 14th International Symposium on Gas Kinetics Book of Abstracts

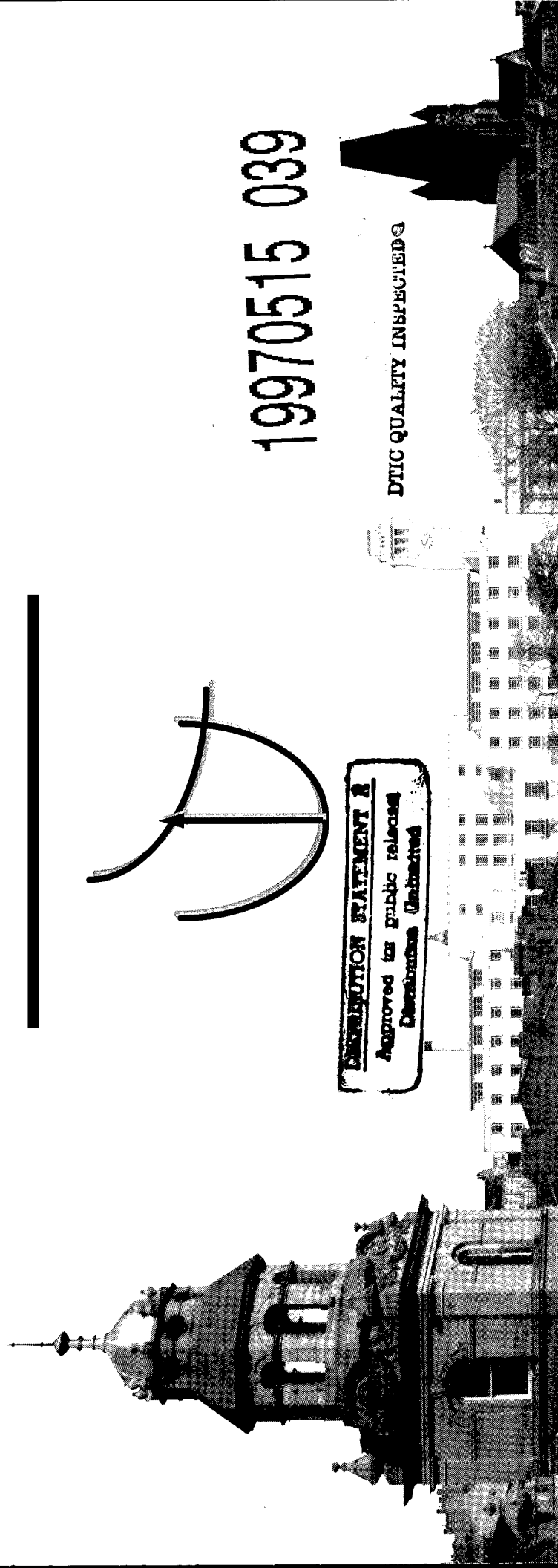
---



19970515 039



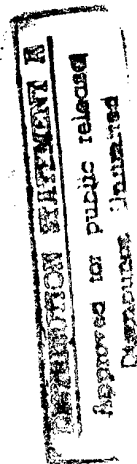
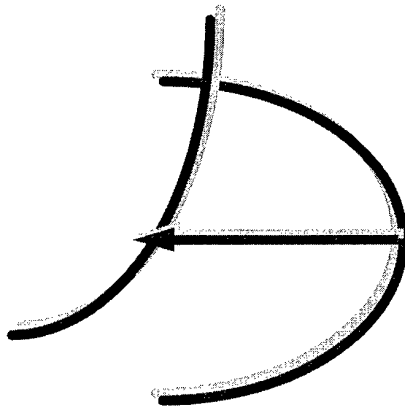
DTIC QUALITY INSPECTED



# 14<sup>th</sup> International Gas Kinetics Symposium

University of Leeds

1996



## Book of Abstracts

The Scientific Committee would like to thank the following Organisations for Sponsorship:

US Army European Research Office,  
Shell Research Ltd,  
Leybold Ltd,  
ICI Research & Development,  
Hiden Analytical,  
Coherent (UK),  
NERC (Laboratory Studies in Atmospheric Chemistry Thematic Programme).

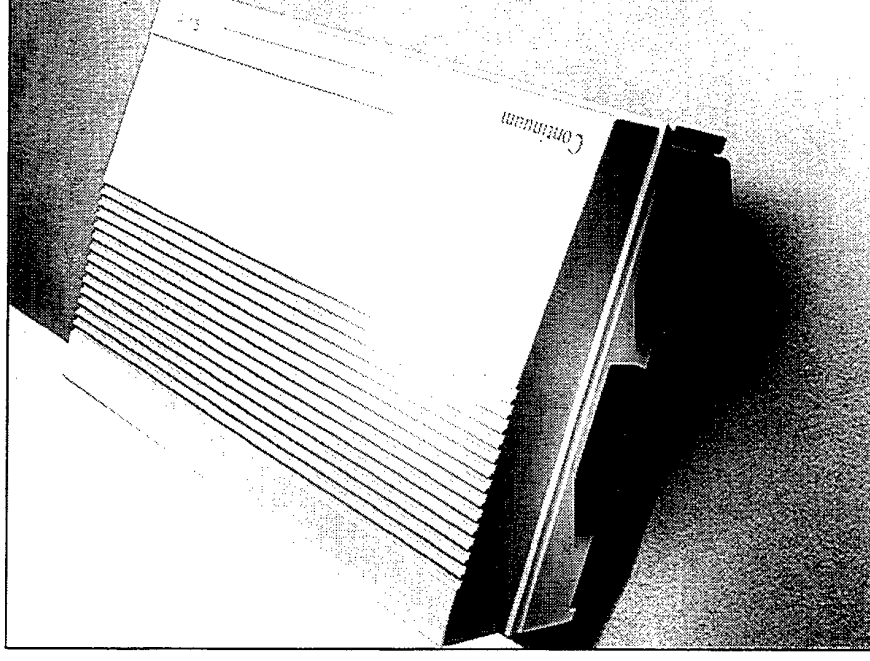
The Local Organising Committee would like to thank Ms Judith Davies for her help in the preparation of this book of abstracts.

## Introducing...

### The laser LITE guide from Continuum

- PowerLITE - pulsed Nd:YAG, up to 3.0J(Powerlite Plus)
- SureLITE - pulsed Nd:YAG, up to 800mJ (Surelite III-10)
- MiniLITE - mini pulsed Nd:YAG, 25mJ (now up to 20Hz)
- SunLITE OPO - 445nm – 1750nm,  $\Delta\nu < 0.1\text{cm}^{-1}$
- SureLITE OPO - 410nm – 2200nm
- HPO - diode pumped YAG, 3mJ 1000Hz (HPO-1000)
- EPO - diode pumped YAG, 250 $\mu\text{J}$ , 5kHz
- PY Series - picosecond YAG, up to 75mJ, down to 25ps

Custom solid state lasers, OPO's, ultrafast amplifiers, dye lasers.



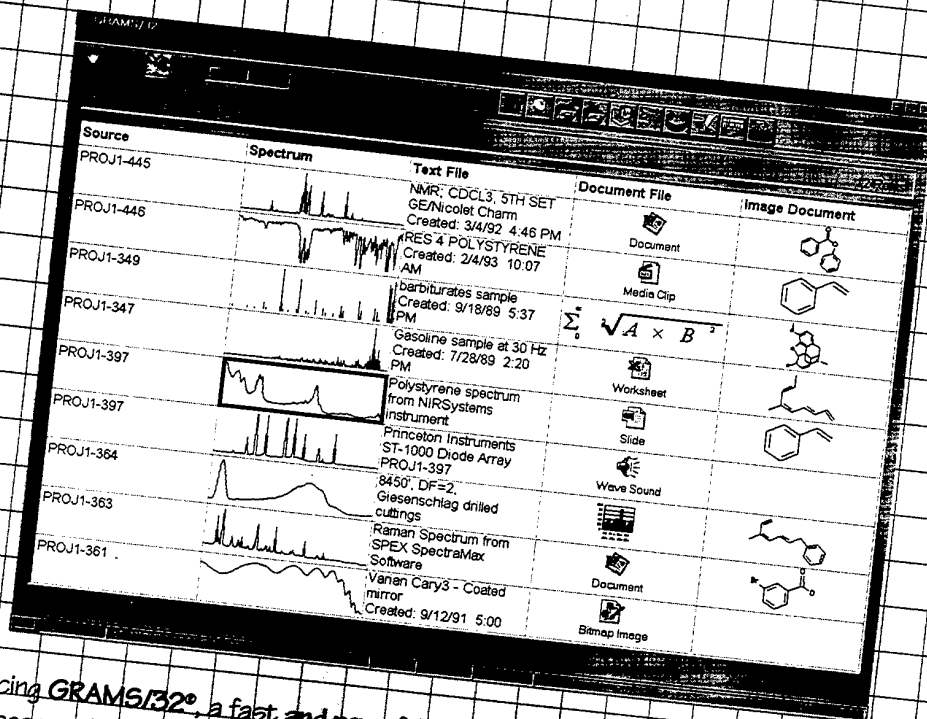
## Continuum

from Edinburgh Instruments Ltd, Riccarton, Currie, Edinburgh EH14 4AP

Tel: 0131-449 5844 Fax: 0131-449 5848

email:sales@edininst.com <http://www.edinst.com>

# Organise, Analyse, Search all your lab data with GRAMS/32



Introducing **GRAMS/32**, a fast and powerful software package that will change the way you process and organise your spectroscopic data and all of its associated information. **GRAMS/32** contains all the tools you need to run your lab smoothly and efficiently:

- ✓ **Automatic File Conversion:** Our library of hundreds of file converters supporting the most popular analytical instruments can transparently import your data files.
- ✓ **Easy-to-use Data Management:** Store and access all your spectra and its associated information - spreadsheets, documents, chemical information, graphics, video, voice - with the all-new Spectral Notebook™ feature.
- ✓ **Fast & Flexible Data Processing:** Our fully interactive data processing library includes peak fitting, baseline correction, data subtraction, smoothing, derivatives and much more!
- ✓ **Visual Programming Interface:** The Macro Wizard lets users build new applications from our existing data processing library - without coding!

GRAMS/32 runs on 386, 486 and Pentium processors under Windows 3.1 and Windows 95. GRAMS/32 supports UV, UV-Vis, IR, FT-IR, NIR, NMR, LC, GC, HPLC, DAS, CE, Mass Spec and Raman techniques.

**For a prompt response fax back to 01462 480213**

Please call, fill out and fax back or post this coupon to Adept Scientific for your **FREE GRAMS/32 Information Pack!**

DEPARTMENT \_\_\_\_\_

ADDRESS \_\_\_\_\_

NAME \_\_\_\_\_

TELEPHONE NO. \_\_\_\_\_

POSITION \_\_\_\_\_

COMPANY \_\_\_\_\_

TOWN \_\_\_\_\_

COUNTY \_\_\_\_\_

POST CODE \_\_\_\_\_



Adept Scientific plc  
6 Business Centre West, Avenue One,  
Letchworth, Herts, SG6 2HB  
Tel: (01462) 480055 Fax: (01462) 480213  
Email: [grams@adeptsience.co.uk](mailto:grams@adeptsience.co.uk)  
<http://www.adeptsience.co.uk/>

**GRAMS/32**

Your Spectroscopy Software Suite

## THE INS AND OUTS OF COLLISION COMPLEXES

J P Simons

*Physical and Theoretical Chemistry Laboratory, South Parks Road,  
Oxford OX1 3QZ*

The development of scientific innovation is often triggered by the advent of new experimental strategies which allow questions to be addressed by design rather than conjecture. At first, the new thinking is confined to a small group of laboratories but if the innovation is addressing important questions, the 'word soon gets around' and before too long, scientists in other laboratories or disciplines begin to get wind of the fact that something new and exciting is happening. This is the path that (may) lead, one day to Nobel prizes. When that day has come and gone, although a new sub-discipline has been created, the buzz may begin to subside and the new sub-discipline can become an esoteric speciality with its own high priests, language, priorities - and even biennial conferences.

A prime purpose of the Lecture will be to transmit some of the current buzz and passion that animates (the far from esoteric) world of molecular reaction dynamics, to show how some of the questions signalled by its Nobel Laureates can now be addressed, and to report some of the extraordinarily detailed insights into the nature of chemically reactive collisions that are being revealed through the application of Doppler resolved, polarised laser techniques - particularly those involving collision complexes. The central challenge is easy to state but far less easy to achieve: it is to present a three dimensional view of a reactive molecular collision, through the transition state from reagents to products.

## Acknowledgements.

Firstly, to Dr Mark Brouard and Professor Javier Aoiz, for their crucial contributions to the development and implementation of polarised, Doppler probe strategies. Secondly to the members of our research groups, and finally to our 'sponsors' for support granted through EPSRC and the Accion Integrada Anglo-Spanish collaboration programme.

## DYNAMICS OF INTRA-CLUSTER REACTIONS VIA ULTRAFAST TIME-RESOLVED SPECTROSCOPY

A. W. Castleman, Jr.

*Department of Chemistry  
The Pennsylvania State University  
University Park, PA 16802*

Studying the dynamics of reactive events in clusters provides a means of bridging an understanding of the mechanisms of energy transfer and reactivity of intermediate states of matter, with particular attention to the effects of solvation on the temporal evolution of the various phenomenon involved. Particularly interesting are reactions which ensue following the excitation of cluster moieties to various electronically excited states. The coupling of ultrafast laser techniques with pulsed molecular beams provides methods for probing the dynamical processes associated with reactions in clusters, as well as ionization phenomenon taking place in the excitation and/or detection schemes.

The study of van der Waals clusters and hydrogen-bonded systems are particularly valuable in gaining insight into the influence of solvation on intercluster hydrogen and proton transfer, as well as charge transfer reactions. In the context of elucidating the influence of solvation on the dynamics of molecular systems, two specific examples will be considered in detail, namely clusters of ammonia and acetone. Excitation of ammonia to various Rydberg states is found to result in predissociation events leading to the formation of  $\text{NH}_2$  and  $\text{H}$ , imparting little or considerable translational energy depending on the state of excitation. The formation of  $\text{NH}_2$  and its ionization, competing with its formation via direct ionization of ammonia and subsequent ion-molecule reaction is elucidated through ultrafast pump-probe spectroscopy.

Another example comes from studies of the femtosecond excitation dynamics of acetone. Work will be presented on the predissociation of acetone and acetone clusters after excitation to states corresponding to the upper  $\{\text{S}_1, \text{T}_1\}$  and 3s Rydberg states of the acetone monomer. Acetyl fragments are found to form at short times followed by subsequent dissociation to  $\text{CH}_3$  and  $\text{CO}$ , the temporal behavior of which is dramatically influenced by the initial excitation energy and clustering phenomenon.

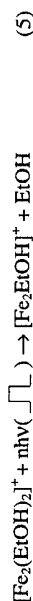
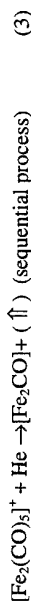
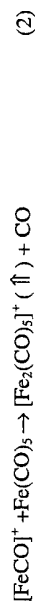
During the course of conducting these pump-probe experiments to reveal the ionization dynamics, a surprising observation was the sudden appearance of highly charged atoms in the individual cluster systems such as  $\text{N}^{+1.10.5}$  in the case of ammonia clusters, and  $\text{O}^{+1.10.5}$  and  $\text{C}^{+1.10.4}$  in the case of acetone. These phenomenon are shown to result in the Coulomb explosion of clusters with concomitant large kinetic energy release. Oscillations in the pump-probe spectra, along with investigations of the formation of high charge states in HI clusters resulting in  $\text{I}^{+1.10.4,17}$  and related high charge states in rare gas clusters, point to an ignition model as the underlying mechanism responsible for the initial ionization phenomena. Comparison with various theories will be made.

# PHOTOCHEMICAL STUDIES OF METAL CLUSTERS IN AN ION TRAP

D.A. Kirkwood and A.J. Stace.

*School of Molecular Sciences, University of Sussex, Falmer, Brighton, BN1 9QJ*

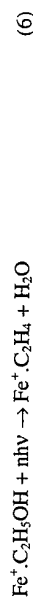
This series of experiments is concerned with the development of techniques for studying metal cluster photochemistry using a commercial ion trap in association with an infrared laser. The power of the trap is demonstrated by its capability for undertaking multiple mass-isolations to grow and react species, such as  $\text{Cr}^{3+}$  or  $\text{Fe}^{3+}$ , from volatile organometallic compounds. To generate for example  $[\text{Fe}_2(\text{EtOH})_2]^+$ , and monitor the photochemistry of the ion, the following sequence of events can be implemented within the trap:



In step (1) a range of different-sized carbonyl ions are generated by electron impact ionisation; the symbol ( $\uparrow$ ) is used to denote that the product ion from a particular reaction sequence is mass-isolated within the trap in preparation for the next step and that all other ions are discarded. In step (2) the isolated ion is allowed to react with background iron pentacarbonyl; a process that proceeds more efficiently with  $[\text{FeCO}]^+$  rather than bare  $\text{Fe}^+$ . In step (3) the kinetic energy of the ion is increased through the application of a small AC voltage ( $\sim 2\text{-}3\text{V}$ ) to the end caps of the trap, with the result that most of the CO ligands are stripped away. Following the isolation of  $[\text{Fe}_2\text{CO}]^+$ , a 200  $\mu\text{s}$  pulse ( $\square$ ) of ethanol is introduced into the trap from a Jordan nozzle which is triggered from the trap scan sequence via a delay generator [step (4)]. Finally, in step (5) the mass-isolated ion,  $[\text{Fe}_2(\text{EtOH})_2]^+$ , is irradiated with a 1000  $\mu\text{s}$  pulse ( $\square$ ) of infrared photons from a line tuneable  $\text{CO}_2$  laser (Edinburgh Instruments PL4) with a wavelength range of 910-1090  $\text{cm}^{-1}$ .

The laser enters and leaves the trap through two 1 mm diameter holes drilled on opposite sides of the central ring electrode. Since the ions are confined by an AC voltage of 1.1 MHz this, in conjunction with the presence of helium in the trap, ensures that ions take trajectories which pass through the centre giving maximum interaction time with the laser beam. For a 1000  $\mu\text{s}$  pulse, each ion should pass through the laser beam approximately 1000 times, which guarantees the absorption of large numbers (20-30) of infrared photons. Our experiments have shown IR excitation to be a very gentle approach, because the ions only absorb the photon numbers necessary to promote the lowest energy process. In addition, reactivity is most likely to proceed via the electronic ground-state.

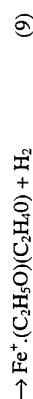
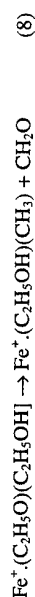
A series of experiments involving metal ion - alcohol clusters has provided some very interesting results. As an example, the IR excitation of  $\text{Fe}^+ \cdot \text{C}^2\text{H}_5\text{OH}$  at 950  $\text{cm}^{-1}$  gives:



In contrast, if we IR excite  $\text{Fe}^+ \cdot \text{C}_2\text{H}_5\text{O}$ , which absorbs approximately 50  $\text{cm}^{-1}$  to the blue of  $\text{Fe}^+ \cdot \text{C}_2\text{H}_5\text{OH}$ , then the observed reaction is



Both species appear to be ligated to iron via an oxygen atom; however, in the case of  $\text{Fe}^+ \cdot \text{C}_2\text{H}_5\text{O}$  the bond may be more covalent because of the loss of H. Finally, if we prepare  $\text{Fe}^+ \cdot (\text{C}_2\text{H}_5\text{O})(\text{C}_2\text{H}_5\text{OH})$  then the following reactions are observed:



The presence of  $\text{C}_2\text{H}_5\text{O}$  on the iron appears to influence the chemistry of the alcohol molecule; in contrast, if we place two alcohol molecules on  $\text{Fe}^+$  then reaction (6) is observed. Replacing  $\text{Fe}^+$  with  $\text{Mn}^+$  introduces yet further chemical reactions.

The phrase "molecular surface photochemistry" has been coined to describe these processes (*Chem. Phys. Lett.* **247**, 332 (1995)), and we believe that the future use of this approach in the study of chemical reactions on small metallic clusters offers some exciting prospects for new chemistry.

# UV CIRCULAR DICHROISM SPECTROSCOPY USING COHERENT LASER-INDUCED THERMAL GRATINGS

David W. Chandler, David W. Neyer, Larry A. Rahn

*Sandia National Laboratories*

and

Jon A. Nunes and William G. Tong

*Dept of Chemistry*

*San Diego State University*

A new pulsed four-wave mixing (FWM) technique for the detection and real-time measurement of circular dichroism (CD) in liquid samples is demonstrated. The technique is based on the formation and detection of transient thermal gratings formed by the interference of two laser beams whose polarizations are carefully modulated using a photoelastic modulator (PEM). Through an internal heterodyne process, coherent thermal gratings interfere to greatly enhance a weak circular dichroism signal. By measuring the ratio of the difference of scattered laser light from two different polarizations, DS, to the average amount of scattered light, S<sub>ave</sub>, one can determine the value of De/e for the compound under investigation. Samples of chiral camphorquinone are used to demonstrate the technique in the ultraviolet region of the spectrum. Camphorquinone, which has a value of De/e  $\times 10^{-3}$  at the 266-nm excitation wavelength employed in this study, produces values of DS/S<sub>ave</sub> which approach the limiting value of two when maximized. Possible extensions of the technique for measuring CD in very small sample volumes and monitoring time-dependence are discussed.

# STICKING AND REACTION OF HYDROGEN HALIDES ON MODEL STRATOSPHERIC ICE FILMS

H. Rieley<sup>a</sup>, H.D. Aslin<sup>a</sup> and S. Haq<sup>b</sup>

<sup>a</sup> *Department of Chemistry, University of Liverpool, Liverpool L69 3BX, UK*

<sup>b</sup> *IRC in Surface Science, University of Liverpool, Liverpool L69 3BX, UK*

A high vacuum methodology which employed a thermal molecular beam and grazing incidence FTIR was used to investigate the uptake dependent sticking coefficient for HF, HCl and HBr on bare ice films in the temperature range 85 -140 K. Sequential molecular beam titration of HCl and N<sub>2</sub>O<sub>3</sub> allowed an investigation of the kinetics and mechanism of the important stratospheric heterogeneous reaction: HCl + N<sub>2</sub>O<sub>3</sub> → ClNO<sub>2</sub> + HNO<sub>3</sub>. The initial sticking coefficients of the hydrogen halides on ice varied from zero, for HF, to approximately unity, for HCl and HBr and, in the latter two cases, the nature of the species retained at the surface was ionic.[1] A dissociative mechanism was confirmed in isotopic labelling experiments in which DCl was observed in temperature programmed desorption following the uptake of HCl on D<sub>2</sub>O.

In the study of the reaction of HCl with N<sub>2</sub>O<sub>3</sub>, FTIR revealed the existence of covalent ClNO<sub>2</sub> and HNO<sub>3</sub> at low temperature but, on warming only ionic species remained at the surface. Thermal beam "sticking" experiments conducted at a surface temperature above the thermal desorption threshold for ClNO<sub>2</sub> gave some insight into the reaction probability as a function of uptake. The results are interpreted in terms of a simple model for the uptake of hydrogen halides on ice and the potential relevance of these experiments to stratospheric ozone depletion will be discussed.

1) Rieley, H.D. Aslin and S. Haq, *J. Chem. Soc. Faraday Trans. 91* 2349 (1995).

# THE ADSORPTION OF ATMOSPHERIC GASES ONTO WATER CLUSTERS: A MIMIC FOR ATMOSPHERIC PROCESSES

C. J. Apps, N. E. Watt and J. C. Whitehead.

*Department of Chemistry, University of Manchester.*

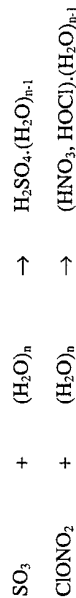
*Manchester, M13 9PL, UK*

The adsorption of various atmospherically-important species ( $\text{SO}_2$ ,  $\text{SO}_3$ ,  $\text{HCl}$  and  $\text{ClONO}_2$ ) onto the surface of large water clusters has been studied. Large water clusters ( $\langle n \rangle \sim 50 - 450$ ), produced by a supersonic molecular beam expansion of water vapour, can be considered as prototypes for Polar Stratospheric Cloud ice particles. The water clusters were produced by expanding pure water vapour ( $P_0 \leq 2$  bar) through a conical nozzle (0.3 mm diameter). The molecules were deposited onto the surface of the clusters using the "pick - up" technique, where the water clusters pass through an effusive spray of the molecule in the post-expansion region. The beam was modulated and passes through two stages of differential pumping before being detected by a quadrupole mass spectrometer. Electron diffraction studies and molecular dynamics simulations indicate that the clusters are crystalline having an amorphous structure with considerable surface irregularities and an abundance of non-bonding or "dangling" OH groups. The temperature of the clusters is  $\sim 180$  K.

By studying the intensity of the ion signal as a function of pick-up source pressure we can determine the relative sticking efficiencies for the various gases upon the water cluster. For the species  $\text{SO}_2$  and  $\text{HCl}$ , the relative sticking efficiencies are comparable to those found in a previous study for  $\text{NO}_x$  species ( $\text{N}_2\text{O}$ ,  $\text{NO}$  and  $\text{NO}_2$ ). On average, the pick-up process deposits no more than two molecules on the surface of each cluster. The mass spectral cracking patterns for the  $\text{HCl}$  and  $\text{SO}_2$  when adsorbed

onto the water cluster are identical to those for the isolated gas-phase molecules. This is taken to indicate that the picked-up molecule retains its identity whilst attached to the cluster and does not undergo any transformation or reaction as a result of being attached to the cluster. Theoretical calculations for the analogous processes for  $\text{N}_2\text{O}$ ,  $\text{NO}$  and  $\text{NO}_2$  on small water clusters,  $(\text{H}_2\text{O})_{10}$ , indicate that these molecules prefer to adopt a configuration where they are attached to the surface of the cluster rather than being incorporated into the bulk of the cluster. The interaction is then a weak physisorbed state.

In contrast, the mass spectral cracking patterns for  $\text{SO}_3$  and  $\text{ClONO}_2$  attached to the water clusters indicate that a transformation has taken place. In particular,  $\text{SO}_3$  has been converted to hydrated sulphuric acid,  $\text{H}_2\text{SO}_4$ , and  $\text{ClONO}_2$  has reacted with the water cluster to produce  $\text{HOCl}$  and nitric acid,  $\text{HNO}_3$



The latter heterogeneous processes mirrors that occurring for  $\text{ClONO}_2$  on ice films<sup>1</sup> and in polar stratospheric clouds creating active chlorine species and causing denitrification of the stratosphere both of which contribute to the reduction of ozone in the polar spring. The reaction of  $\text{SO}_3$  with the water cluster is a limiting case of the mechanism proposed by Morokuma and Muguruma<sup>2</sup> for the conversion of  $\text{SO}_3$  into sulphuric acid by reaction with water in which the reaction takes place *via* the participation of a water dimer



where the cluster or dimer offers an alternative transition state for the reaction which gives a small or zero barrier to reaction to  $\text{H}_2\text{SO}_4$ . These results parallel earlier studies by Hofmann-Sievert and Castleman<sup>3</sup>.

This work has been supported by NERC and EPSRC.

- (1) Hanson, D. R.; Ravishankara, A. R. *J. Geophys. Res.* **1991**, *96*, 5081.
- (2) Morokuma, K.; Muguruma, C. *J. Am. Chem. Soc.* **1994**, *116*, 10316.
- (3) Hofmann-Sievert, R.; Castleman, A. W. *J. Phys. Chem.* **1984**, *88*, 3329

## CHAOS CONTROLLED AND WAVES AMAZED RECENT ADVANCES IN COMPLEX KINETICS

S.K. Scott

*School of Chemistry, University of Leeds, Leeds LS2 9JT*

This lecture will review two particular aspects of recent advances in 'complex reaction systems', concentrating on the behaviour of systems exhibiting chemical feedback or 'nonlinear kinetics'. The areas of interest relate to exploiting the potential of *chaotic systems* and of *chemical waves*.

### *Chaos in Chemical Kinetics*

It is now well established that the quite simple requirements for oscillatory responses are met by a wide range of chemical reactions. In solution-phase, the Belousov-Zhabotinsky (BZ) reaction and its various cousins are frequently used as lecture demonstrations. In the gasphase, combustion processes such as the oxidation of  $H_2$  or CO support oscillatory ignition whilst many hydrocarbon oxidations lead to cool flames. For the  $H_2$  and CO systems, complex oscillatory wave forms have been observed and for some experimental conditions these may develop into *chaotic* behaviour. Initial, chaos was purely of academic interest, but more recent ideas have suggested ways in which this mode of operation can be exploited by elegant *control algorithms*. Examples of the control of chemical and other physical and biological systems will be discussed along with a brief introduction to the underlying strategy.

### *Chemical Waves*

Chemical waves correspond to typically narrow regions of reaction that propagate by diffusion into fresh reactants. The most familiar form is that of a flame, but solution-phase analogues are also of interest and relevance, e.g. to biological signalling processes. If the reaction has sufficient mechanistic feedback, successive waves can be initiated and propagate as a *wave train*. Such wave trains can give rise to organised spatial structures such as target 'patterns' or spiral waves. A variety of new experimental reactors have been constructed to study chemical waves in quantitative detail. Very recently, spirals and targets have been observed in gas-phase reactions (hydrocarbon oxidation). Various properties of chemical reaction-diffusion waves are now being exploited, with waves being trained through, capillary tubes, through labyrinthine mazes or used to construct logic gates for prototype chemical computers.

## THE INFLUENCE OF LOCALIZED BORON VIBRATIONS ON THE REACTION OF THE TRANSFER OF BORON ATOMS FROM THE SURFACE PHASE INTO THE SILICON CRYSTAL

I.P. Ipatova, O.P. Chikalova-Luzina, A.A. Maradudin\*

*A.F. Ioffe Physico-Technical Institute, Russian Academy of Sciences,  
Politekhnicheskaja 26, St. Petersburg 194021, RUSSIA,*

*\*Department of Physics, University of California, Irvine, CA 927127 U.S.A.*

In this study the reaction of the transfer of boron atoms from a two-dimensional gas on the surface of the silicon crystal into the crystal  $B(\text{surface}) \rightarrow B(\text{crystal})$  is considered and the temperature dependent contribution of the lattice vibrations to the coefficient of the boron distribution between the surface phase and the bulk of the silicon crystal is found.

As it is known [1], boron atoms can be obtained on the silicon surface from gaseous B-containing compounds, for instance  $HBO_2$ . At the temperature above  $700^\circ\text{C}$   $HBO_2$  dissolves and only B is deposited on the surface.

The boron atoms were found to form surface phases on silicon.[1] RHEED and AES experiments show [2], that the additional B atoms which are deposited on  $Si(111)$  surface after the completion of the  $\sqrt{3} \times \sqrt{3} R30^\circ$ -B superstructure on the surface, do not create chemical bonds with the silicon atoms and do not have any long-range order. Assuming that at low concentrations of the additional B atoms they can be regarded as an ideal two-dimensional gas on the crystal surface, we calculated the coefficient of the distribution of the boron atoms between the surface phase and the silicon crystal in which they penetrate. The distribution coefficient is defined as the ratio of the concentration of the boron atoms in the bulk of the silicon crystal to their concentration in the two-dimensional gas on the surface in thermodynamic equilibrium. That is the distribution coefficient is equal to the equilibrium constant of the reaction of the boron atom transfer [3]. The distribution coefficient is calculated with using the equilibrium condition of the equality of the chemical potential of boron atoms in the two-dimensional gas to the chemical potential of the boron atoms in the silicon crystal. In [4] the calculations based on the simple model of a crystal have shown that in the establishment of the equilibrium in the system crystal + gas a significant role is played by the distortion of the vibrational spectrum of the crystal due to presence of the impurities in the interior. In the present work the distribution coefficient is calculated by using a realistic model of the lattice vibrations of silicon [5]. The boron atoms in the silicon crystal are treated as mass defects, which leads to only a small error in the calculation of the frequency of the localized vibration modes they induced. It is shown that the boron localized vibrations impede the transfer of the boron atoms into the bulk of the silicon crystal and lead to the decrease of the distribution coefficient.

### References

- 1) Lifshits, A.A. Saranin, A.V. Zotov, Surface phases on silicon, Chichester: John Wiley and Sons (1994) 454p.

- 2) Hirayama, T. Tatsumi and N. Aisaki, *Surf.Sci.*, 193 (1988) L47
- 3) I.Prigogin and R.Defay, *Chemical Thermodynamics*. Longmans Green and CO, London- New York- Toronto (1954)
- 4) Bykhovskii, I.P. Ipatova, A.A. Maradudin, *Solid State Commun.* 82 (1992) 261
- 5) Herman, J. *Phys. Chem. Solids.* 8 (1959) 405

A8

# **OZONE DEPLETION ON THE SURFACE OF DRY SOOT AEROSOL PARTICLES**

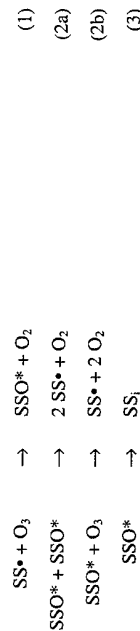
O. Möhler, K.-H. Naumann, H. Saathoff

*Forschungszentrum Karlsruhe, Institut für Meteorologie und Klimaforschung  
Postfach 3640, D-76021 Karlsruhe, Germany*

Over continental regions, soot particles may contribute up to 20% to the total lower tropospheric aerosol mass concentration [1]. Due to their aggregate structure, soot particles offer a large specific surface area for heterogeneous interactions with reactive trace gases like ozone. Depending on the reaction mechanisms and reaction probabilities, which are only poorly known, soot may significantly influence the tropospheric trace gas chemistry by its surface reactions. On the other hand, interactions with reactive trace gases can change the morphology, the chemical composition and the hydrophobic behaviour of soot particles. Thereby their optical properties, their efficiency to act as condensation nuclei and their lifetime with respect to deposition processes can be affected.

To obtain kinetic and mechanistic information about the catalytic ozone destruction on airborne soot we performed experiments in a stainless steel vessel of 3.7 m<sup>3</sup> volume and in a teflon bag of 2.7 m<sup>3</sup> volume at 297 K and 20% relative humidity [2,3]. A carbon sparc generator was used to produce dry soot particles having the typical fractal aggregate structure with monomer diameters around 5 nm. Ozone was formed by UV-photolysis of pure O<sub>2</sub>. The soot mass concentration was varied between 10 and 1000 µg/m<sup>3</sup> and the decrease of ozone was measured in the range 100 - 1 ppb with a commercial UV ozone monitor. Before and after each experiment, the ozone decay rate was measured in the reactors filled with dry synthetic air only. The soot aerosol was characterized with respect to number concentration (condensation nucleus counter), mass concentration (gravimetric and coulometric analysis of filter samples), and size distribution (mobility analyser, cascade impactor). The observed ozone depletion could be approximately described with a pseudo first order rate law. The obtained rate coefficients depend linearly on the soot mass concentration with a slope of 2·10<sup>-5</sup> m<sup>3</sup> µg<sup>-1</sup> min<sup>-1</sup>.

To facilitate a more detailed interpretation, the experimental data are compared with results from aerosol-dynamic model calculations. The simulation code COSIMA describes dynamic processes of irregularly shaped particles using fractal scaling laws [4]. The modelled processes include diffusion, coagulation, sedimentation, gas transport to the particle surface, surface adsorption, and surface reactions. The gas transport to the particle surface is modelled regarding the transition regime correction [5]. The modelled ozone surface reactions are:



# INFLUENCE OF O<sub>2</sub> AND O<sub>3</sub> ON THE KINETICS OF NUCLEATION UNDER PHOTOLYSIS OF HALOIDBENZENES OR TRIETHYLAMINE VAPOURS.

Skubnevskaya G.I., Dubtsov S.N. and Dul'tsev E.N

*Institute of Chemical Kinetics and Combustion of Siberian Branch of RAS  
Novosibirsk 630090, Russia.*

Among the pathways of degradation of organic compounds in the atmosphere the formation of ultra-fine aerosols under sunlight is of special interest due to ecological and toxic properties of organic portion of aerosols. Furthermore, the formation of the dispersed phase gives the chance to determine minor products and pathways of their origin.

The aerosol-forming potential of individual volatile organic compounds can be dependent on oxygen and ozone presence in the gas mixture. We have investigated the kinetics of photoaerosol formation for haloaromatics (PhX, X= Cl, Br, I) compounds similar to herbicides and pesticides, and triethylamine (TEA)- one of the precursors of toxic organic peroxynitrate. Aerosol formation in all of these systems studied was shown to take place only the UV irradiation [1-3, 6].

The experimental setup allows to study photonucleation of various gas mixtures in a quartz cylindrical flow reactor irradiated by unfocused high-pressure Hg lamp. Concentration (N<sub>a</sub>) and size distribution of particles was measured by automated aerosol spectrometer [5]. Composition of gas and aerosol products was analyzed by GC-, HPLC- chromatography, UV-, IR- and NMR-spectroscopy and electron microscopy [4]. The kinetics of the photonucleation of PhX and TEA was studied under a wide range of UV intensity ( $I_{UV} = 10^{-2} - 10^{-6}$ ) and irradiation time ( $t = 0.05-5s$ ).

The photonucleation kinetics in the air greatly differs from that in Ar for both PhX and TEA. It was found that O<sub>2</sub> has strong effect on aerosol concentration and size at the early stages of the process. Oxygen addition (1-7 %) to the flow of carrier-gas Ar increases N<sub>a</sub> values as great as 10-1000 folds for both PhX and TEA. Aerosol size distribution also changes in the presence of O<sub>2</sub>. Thus, the mean diameter of aerosols formed for TEA is 4 nm in Ar and increases up to 50 nm in the air. The similar increase of the particles size was observed for PhX also.

The existence of oxygen-containing products has been established by the analysis of physico-chemical properties and chemical composition of aerosols. Particles contain 23-33 % by mass of oxygen in the cases of PhX photolysis in the air. Bonds C=O and -OH are characteristic for these products. The available data indicate that O<sub>2</sub> effect on kinetics of photonucleation is connected with the involvement of oxygen in the chemical stages of the process [4].

Reaction 1 is the fast reaction of ozone with pristine surface sites SS<sup>\*</sup>. Reactions 2a (Langmuir-Hinshelwood mechanism) and 2b (Eley-Rideal mechanism) lead to slower ozone destruction. The possible conversion of SSO<sup>\*</sup> into inactivated sites SS<sub>i</sub>, which is considered by reaction 3, was found to be negligible on the time scale of our experiments. The theoretical analysis indicates that, after rapid formation of a monolayer of SSO<sup>\*</sup> (reaction 1), the Eley-Rideal mechanism (reaction 2b) dominates the long-term ozone depletion (Figure 1). The limiting reaction probability  $\gamma$  for this reaction was found to be  $(2.0 \pm 0.3) \times 10^{-5}$ . This value is of the same order of magnitude as for the reaction of ozone with oxygen atoms in the gas phase.

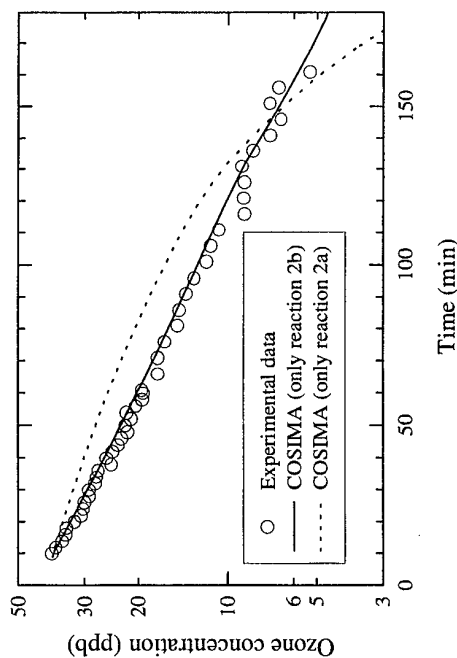


Figure 1. Comparison of measured and modeled ozone depletion.

Assuming an urban tropospheric soot concentration of  $20 \mu\text{g}/\text{m}^3$  with typical particles ( $100 \text{ nm}$  diameter and  $20 \text{ nm}$  monomers) we calculate a surface area concentration of  $1 \times 10^3 \text{ m}^2/\text{m}^3$  and a collision rate of  $6 \times 10^{-2} \text{ s}^{-1}$ . Using the obtained reaction probability this leads to a reaction rate of  $2 \times 10^{-6} \text{ s}^{-1}$ . Therefore we conclude that the ozone loss due to reaction on dry soot surface as an isolated process is probably too slow to be important in the atmosphere. However, if the surface loss rates of other reactive species (e.g. HO<sub>2</sub>, NO<sub>3</sub>) approach the collision rate with the soot particle surface, the impact of soot on the gas phase radical chemistry of the troposphere may be significant [6].

## References

1. A. D. A. Hansen, T. Novakov, *Aerosol Sci. Tech.* **12** (1990) 194.
2. O. Möhler, K.-H. Naumann, W. Schöck, *J. Aerosol Sci.* **25** (1994) S303.
3. O. Möhler, K.-H. Naumann H. Saathoff, and W. Schöck, *J. Aerosol Sci.* **26** (1996) S195.
4. K.-H. Naumann and H. Bunz, *J. Aerosol Sci.* **23** (1992) S361.
5. B. Dahneke, in *Theory of dispersed multiphase flow*, Academic Press, London.
6. U. Schurath, Aerosols in atmospheric chemistry, *Proceedings of the Eurotrac Symposium 1996*

The kinetics of the nucleation **PhX** - O<sub>3</sub> and **TEA** - O<sub>3</sub> system has been investigated as a function of a number of experimental variables. The ozone has large and an opposite influence on the photo-induced aerosol formation of **PhCl** and **PhI**. The most pronounced effect of O<sub>3</sub> is at relatively low particle concentrations. The variation of O<sub>3</sub> concentration from 6 10<sup>11</sup> cm<sup>-3</sup> to 1.5 10<sup>13</sup> cm<sup>-3</sup> leads to a 100-fold decrease in N<sub>a</sub> for **PhCl** and to a 300-fold increase for **PhI**. The monomer generation rate as a function of ozone concentration has been estimated [2]. It was concluded that reactions leading to the aerosol products are different in cases **PhCl** and **PhI**. It is quite probable that the aerosol formation in presence of O<sub>3</sub> is considerably promoted via the active particle **IO** in the **PhI**+O<sub>3</sub> photolysis. With **PhCl** the preferential formation of gas products are expected if ClO is an intermediate active particle. No influence of ozone on the photonucleation of TEA was detected.

On the base of available data the conclusion is that O<sub>2</sub> and O<sub>3</sub> active participate in the chemical stages of the photonucleation of **PhX** and TEA. Some free-radical mechanisms of **PhX** and TEA photolysis and aerosol forming reactions in presence of O<sub>2</sub> and O<sub>3</sub> are supposed.

## REFERENCES

- 1) Dubtsov S.N., Skubnevskaya G.I. and Koutzenogii, K.P. (1987), *Khim.Fiz.*, (in Russian), **6**:1061
- 2) Dubtsov S.N., Skubnevskaya G.I. and Koutzenogii, K.P. (1992), *J. Aerosol Sci.*, **23**:181
- 3) Dubtsov S.N., Koutzenogii, K.P., Levyikin A.N., and Skubnevskaya G.I. (1995), *J Aerosol Sci.*, **26**:705
- 4) Dubtsov S.N., Kondrat'eva L.N., Skubnevskaya G.I., and Polukhina A.I. (1989), *Izv. Sib. Otd.Akad. Nauk, ser. khim.*, (in Russian), **2**:51
- 5) Ankilov A.N. et al., (1991) *J. Aerosol Sci.*, **22**:223
- 6) Skubnevskaya G.I., Dul'tsev E.N., and Dubisov S.N. (1995), *Khim.Fiz.* (in Russian), **14**:93

## INFRARED DEPLETION SPECTROSCOPY OF ANILINE CLUSTERS

K. Sugawara, J. Miyawaki, T. Nakanaga and H. Takeo

*National Institute for Advanced Interdisciplinary Research and National Institute of Materials and Chemical Research, 1-1-4 Higashi, Tsukuba 305, Japan*

and

G. Lembach, S. Djafari, H.-D Barth and B. Brutschy

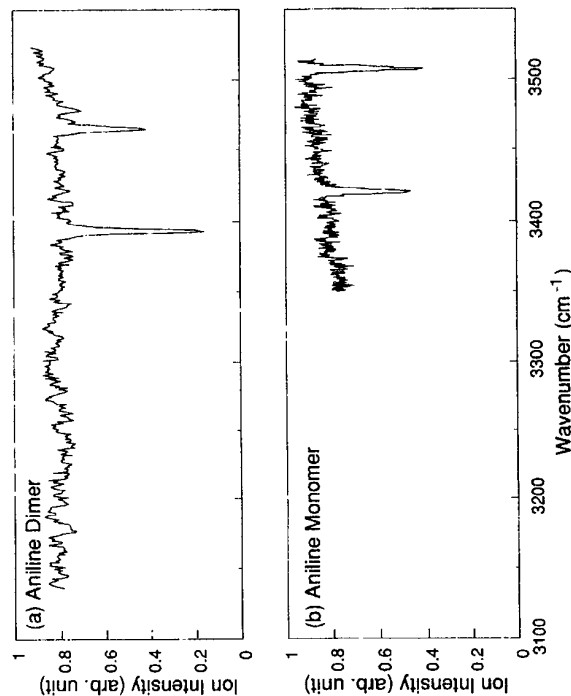
*J. W. Goethe Universität Frankfurt, Institut für Physikalische und Theoretische Chemie, Marie-Curie-Str. 11, 60439 Frankfurt am Main, Germany*

Hydrogen bonding interactions of molecules with the NH group are of great interest in view of their importance in biological systems. Recently we reported the infrared spectra of the aniline-Ar<sub>n</sub> (n=1,2) clusters and their cations using infrared depletion spectroscopy combined with REMPI/TOFMS [1]. This technique was applied to observe the N-H stretching modes of the aniline dimer to obtain direct information on its hydrogen bonding interaction. A configuration with mutual NH<sub>2</sub>... π bonds and phenyl groups stacked in parallel is suggested for the ground state aniline dimer.

Aniline clusters were formed in the supersonic expansion of a mixture of aniline vapor and helium, and detected by TOFMS after resonant two photon ionization with a UV laser at 299 nm. The infrared absorption bands of the aniline clusters were recorded as the attenuated ion signal induced by the depletion of the clusters in the ground state. The infrared light source was generated by difference frequency mixing of a dye laser with the fundamental of a Nd:YAG laser. The cluster beam was first irradiated with the IR laser and then probed with the UV laser pulse. The frequency of the UV laser was fixed on a resonance line of the aniline dimer, while the IR laser was scanned around the N-H stretching region.

The REMPI spectrum of the aniline dimer was in good agreement with that very recently reported [2]. In Fig. 1, the observed IR depletion spectra of the aniline dimer (a) and the monomer (b) are shown. Only two bands can be seen at 3394 and 3466 cm<sup>-1</sup> in the region 3130 - 3530 cm<sup>-1</sup>. These are red-shifted by 28 and 42 cm<sup>-1</sup> from the symmetric and asymmetric NH stretching vibrations of the aniline monomer, respectively. Yeh et al. calculated the structure of the aniline dimer in order to discuss their experimental results of REMPI spectroscopy [2]. They proposed a head-to-head structure, where the phenyl rings are stacked roughly parallel and the NH<sub>2</sub> groups of the two anilines form a normal hydrogen bond with each other. Another structure was a head-to-tail structure with the phenyl rings stacked in parallel, but displaced in such a manner that the amino hydrogens on each aniline point towards the phenyl ring of the other. Generally, in a hydrogen bond of type X-H...Y-H, the Y-H stretching vibration of the acceptor is only slightly affected while that of the donor is very sensitive to hydrogen bond formation. If the aniline dimer forms a hydrogen bond between the NH<sub>2</sub> groups (the head-to-head structure), one should observe largely shifted NH donor bands and slightly shifted NH acceptor ones. In the head-to-tail structure, both NH<sub>2</sub> groups are equivalent and therefore one may observe

only two bands, symmetric and asymmetric  $\text{NH}_2$  stretching ones. The latter reasonably explains the observed IR spectrum in which only two sharp peaks are observed. Thus, we suggest mutual H- $\pi$  bonds for the structure of the aniline dimer, and assign the peak at  $3394\text{ cm}^{-1}$  to the symmetric  $\text{NH}_2$  stretching and that at  $3466\text{ cm}^{-1}$  to the asymmetric stretching.



**Figure 1.** Infrared depletion spectra of (a) the aniline dimer and (b) the aniline monomer in the  $\text{NH}_2$  stretching region. The UV laser frequency was fixed to the respective 0-0 bands and the resulting ion intensity was measured as a function of the IR laser frequency.

- (1) T. Nakanaga, F. Ito, J. Miyawaki, K. Sugawara and H. Takeo, *Chem. Phys. Lett.*, in press.
- (2) J.-H. Yeh, T.-L. Shen, D.G. Nocera, G.E. Leroi, I. Suzuka, H. Ozawa and Y. Namuta, *J. Phys. Chem.* **100**, 4385 (1996).

## INTERACTION BETWEEN THE PEROXY RADICALS AND SOLID SUBSTANCES

R.H. BAKHCHADJYAN\*, I.A. VARDANYAN

*Institute of Chemical Physics of the Armenian National Academy of Sciences  
Paruyr Sevak st., 5/2, 375044 Yerevan, Republic of Armenia*

During the last years the interest to the heterogeneous reactions of radicals increased because of the development of heterophase model of ozone destruction in the atmosphere. The rise of the aerosols in the atmosphere, vulcanos activity and anthropogen factors lead to the realisation of heterogeneous processes with the participation of atmospheric organic compounds. The role of such reactions on the surface of aerosols for the destruction of the ozone stratum of Earth can become important.

The heterogeneous reactions of peroxy radicals play a role in the troposphere in the region far from the seashore and also at night when the concentration of  $\text{RO}_2$  increases. Particularly it is important to know the behaviour of the radicals on salts surfaces (NaCl, KCl and others). But the information about this type of heterogeneous reactions is rarely taken into account.

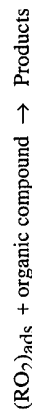
The aim of this work is to find the direct spectroscopic evidences on the possibility of radical reactions for example of  $\text{RO}_2$  radicals with aldehydes (intermediates of photochemical smog) on the solid surfaces  $\text{SiO}_2$ ,  $\text{KCl/SiO}_2$  and to study the kinetic peculiarities of the process dependent of the surface nature. As a simplest model of solid substances present in the atmospheric air the aerosol or KCl modified aerosol have been chosen.

The problem was solved by two ways. First, the aldehyde was adsorbed on the solid surface, the  $\text{RO}_2$  radicals attacked from the gas phase. The process was studied using IR spectroscopy. In the second way, the peroxy radicals were adsorbed on the solid surface

\*Present address of BAKHCHADJYAN : Ecole Nationale Supérieure de Syntheses de Procédés et d'Ingénierie Chimiques d'Aix-Marseille Avenue Escadrille Normandie Niemen-13397 Marseille, France

and the aldehyde attacked from the gas phase. The process was studied here using EPR spectroscopy and mass spectrometry.

In both cases the approach of Ready 1-Early mechanism of heterogeneous reaction has been assumed



In the first case the interaction of adsorbed propionaldehyde with the peroxy radicals has been carried out at 285-373°K. The obtained data show that the process proceeds by the breaking of CH bond in the aldehydic group and formation of the new adsorbed compound. On the surface of KCl/SiO<sub>2</sub> the process proceeds at the room temperature.

In the second case, the spectrum of adsorbed radicals on the surface were analyzed by EPR and the concentration of radicals was determined. The interaction of CH<sub>3</sub>CO<sub>3</sub> radicals and CH<sub>3</sub>CHO was studied in the range of temperature 423-503°K. In the presence of CH<sub>3</sub>CHO a significant decrease of the EPR signal intensity was observed.

The results of experiments clearly demonstrate the reactivity of the radicals, particularly of the peroxy radicals, on the surface of the solid substances. This conclusion has been drawn on the basis of direct spectroscopic observations. Although the lack of knowledge related to the heterogeneous reactions of free radicals does not allow us to make a quantitative estimation of this contribution in the atmospheric processes, the data shows the existence of an interaction between the radicals and pollutants on the surface of solid substances.

The obtained results represent an interest also for combustion processes.

# UPTAKE COEFFICIENTS OF OH AND HO<sub>2</sub> RADICALS ON MATERIAL SURFACES OF ATMOSPHERIC INTEREST

F. Grappanche, A. Ivanov\*, P. Devolder, Yu. Gershenzon\*, J.-P. Sawertysyn

*Laboratoire de Cinétique et Chimie de la Combustion URA-CNRS 876  
Université des Sciences et Technologies de Lille  
59655 Villeneuve d'Ascq - France*

*\*RAS Semenov Institute of Chemical Physics  
117977 Moscow -Russia*

HO<sub>x</sub> radicals (OH and HO<sub>2</sub>) play a central role in atmospheric chemistry. In the troposphere, the concentration of these radicals govern the vertical distribution of important minor gases such as O<sub>3</sub>, NO<sub>x</sub>, CO, SO<sub>x</sub> and other pollutants of type hydrocarbons. The possible influence of HO<sub>x</sub> heterogeneous sinks on the gas composition of the troposphere was firstly considered by Cadle et al.<sup>1</sup> and Isaksen and Cruzen<sup>2</sup>. Assuming that the uptake coefficients (γ<sub>OH</sub> and γ<sub>HO2</sub>) for OH and HO<sub>2</sub> radicals were both equal to 1 (due to a lack of experimental data), Isaksen and Cruzen<sup>2</sup> concluded that the photochemical model was very sensitive to HO<sub>x</sub> heterogeneous loss processes. Now, it is well stated that heterogeneous sinks of OH radicals on tropospheric aerosol materials play a minor part compared to their homogeneous sinks. In contrast of OH radicals, heterogeneous sinks of HO<sub>2</sub> radicals could be competitive with their homogeneous sinks in the tropospheric chemistry since their average concentration is largely higher than the one of OH radicals ([HO<sub>2</sub>]/[OH] ≈ 10<sup>3</sup>). The data available in the literature on HO<sub>x</sub>-uptake coefficients on aerosol materials are most limited. Measurements of γ<sub>OH</sub> were performed on sulfuric acid<sup>3,5</sup>, ice<sup>4</sup> and pure liquid water<sup>5</sup>, and solid salts<sup>6</sup>. Regarding γ<sub>HO2</sub>, only a few values determined on NH<sub>4</sub>HSO<sub>4</sub> and LiNO<sub>3</sub> solutions<sup>7</sup>, pure water and sulfuric acid solutions<sup>5</sup> and solid salts of atmospheric interest<sup>8,9</sup> were reported.

In this study, we report the results obtained for the measurements of HO<sub>x</sub>-uptake coefficients as on dry sea-salt surfaces (NaCl) over the temperature range 245-340 K.

All experiments were performed using a discharge flow tube technique coupled to an Electronic Paramagnetic Resonance (EPR) spectrometer as a detection method<sup>10</sup>. The experimental set-up created in Lille University is in its principle very similar to the one previously developed by Gershenzon et al.<sup>4,11</sup> at Moscow. A coaxial reactor with a passivated tube wall (covered with type 1500 halocarbon wax) and an active axial rod was used to determine the HO<sub>x</sub>-uptake coefficients on NaCl surfaces covering the rod. Heterogeneous losses of HO<sub>x</sub> radicals on the rod were measured as a function of time by moving the rod along the axis of the reactor by means of an external magnet. The temperature of the reactor was controlled by circulating ethanol through the inner jacket. The temperature of ethanol was regulated using a cryostat.

OH radicals were generated by the fast reaction  $\text{H} + \text{NO}_2 \rightarrow \text{OH} + \text{NO}$  with an excess of NO<sub>2</sub>. The OH concentration was (1-2) x 10<sup>11</sup> cm<sup>-3</sup>. H atoms were produced

# MASS ACCOMMODATION OF SUBSTITUTED AROMATIC COMPOUNDS ON AQUEOUS DROPLET SURFACES

M. J. Pilling, P. E. Titcombe, B. J. Whitaker,  
School of Chemistry, University of Leeds, Leeds, LS2 9JT

and M. R. Heal  
Department of Chemistry, University of Edinburgh, Edinburgh, EH9 3JJ

There is increasing recognition that many important heterogeneous processes occur in the atmosphere which can dramatically affect the sinks and chemical reactions of trace species on a global, regional or local scale. Model calculations have demonstrated that the inclusion of aqueous phase chemistry within tropospheric clouds exerts an influence (for example on ozone) significantly in excess of the volume fraction occupied (Lelieveld and Crutzen, 1991). A key parameter in the study of gas-liquid interactions is the mass accommodation coefficient,  $\alpha$ , which is defined in the absence of any other transport limitations, as the probability that a gas molecule will enter the condensed phase on collision with the liquid surface.

Volatile organic compounds (VOC) are an important class of trace species in the troposphere and aromatics form an important sub-class with a high ozone creation potential. Although these species are generally assumed to have such low Henry's Law constants and accommodation coefficients that the lifetime with respect to uptake by aerosol is long compared to gas phase reaction with OH or NO<sub>3</sub>, it is important to consider the variety of aromatic polar and oxygenated species generated as C<sub>y</sub> intermediates in the gas phase oxidation of these species (Becker, 1994; Madronich and Hess, 1990). These species are more soluble than their hydrocarbon precursors and fast rates of reaction have been measured for a variety of aromatic species with sulphate and nitrate radicals in the aqueous phase (Herrmann *et al.*, 1995). The relatively high concentrations of atmospheric aerosol found in urban and other areas provides considerable scope for reactions within the aqueous phase of aerosols and droplets to act as a net kinetic sink for organics in the atmosphere. Phenol and aniline have been chosen as models of these polar and oxygenated C<sub>y</sub> species. In order to determine the maximum rate of mass transfer and aqueous phase reaction of aromatics in tropospheric aerosol, it is necessary to measure the mass accommodation coefficients of the C<sub>y</sub> aromatics and also the co-reactants.

Mass accommodation coefficients of aniline and phenol have been measured here using a droplet train apparatus (Jayne *et al.*, 1991). A stream of mono-dispersed droplets (100-200 μm in diameter) is produced by the resonant break-up of a liquid jet forced

through a microwave discharge of He containing small (<1 %) addition of H<sub>2</sub>. OH radicals were directly detected by EPR in gas phase.

HO<sub>2</sub> radicals were formed by the reaction H + O<sub>2</sub> + M → HO<sub>2</sub> + M with an excess of O<sub>2</sub>. In order to have a pressure much higher in the source of H atoms than in the flow tube, these two parts were separated by a thin capillary. To be also detected in gas phase, HO<sub>2</sub> radicals were converted to OH radicals prior to the EPR cavity via the fast reaction HO<sub>2</sub> + NO → OH + NO<sub>2</sub>. Taking into account the set of possible secondary reactions, a linear correlation was checked by modelling between the concentration variations of HO<sub>2</sub> and OH.

The uptake coefficients of HO<sub>x</sub> radicals were calculated from the measured first-order loss rate coefficients using an analysis including the effects of gas phase diffusion as earlier described<sup>9</sup>. The results can be given in the Arrhenius form:

$$\gamma_{NaCl}^{OH} (245-340K) = (1.2 \pm 0.7) \times 10^{-5} \exp[(1750 \pm 200)/T]$$

$$\text{with } \gamma_{NaCl}^{OH} (295K) = 4.5 \times 10^{-3}$$

$$\gamma_{NaCl}^{HO_2} (243-293K) = 1.4 \left( \pm 1.5 \right)^{16.8} \times 10^{-8} \exp[(3780 \pm 700)/T]$$

$$\text{with } \gamma_{NaCl}^{HO_2} (295K) = 5.2 \times 10^{-3}$$

These results are compared with previous measurements and their potential atmospheric impacts discussed.

## References

- 1) Cadle R.D.; Crutzen P.J. and Elshalt D.H. *J. Geophys. Res.*, **1975**, *80*, 3381
- 2) Isaksen I.S.A. and Crutzen P.J. *Geophys. Norvegica*, **1977**, *31*, 1
- 3) Baldwin A.C. and Golden D.M. *J. Geophys. Res.*, **1980**, *85*, 2888
- 4) Gershenson Yu.M.; Ivanov A.V.; Kucheryavii S.I. and Rozenshtein V.B. *Kinetics and Catalysis*, **1986**, *27*, 923
- 5) Hanson D.R.; Burkholder J.B.; Howard C.J. and Ravishankara A.R. *J. Phys. Chem.*, **1992**, *96*, 4979
- 6) Jech D.D.; Easley P.G. and Krieger B.B. *Heterogeneous Atmospheric Chemistry*, Ed. D.R. Schryer. AGU Washington D.C. 107, **1982**
- 7) Mozurkewich M.; McMurry P.H.; Gupta A.; Calvert J.G. *J. Geophys. Res.*, **1987**, *92*, 923
- 8) Antuzupov E.V. *Khimicheskaya Fizika*, **1988**, *7*, 1082 (in Russian)
- 9) Gershenson Yu.M.; Griegorieva V.M.; Ivanov A.V. and Remorov R.G. *Disc. Far. Soc.*, **1996**, *100*, in press
- 10) Ivanov A.V.; Gershenson Yu.M.; Grapanche F.; Devolder P.; Sawerysyn J.-P. *Ann. Geophysicae*, **1996**, *14*, 659
- 11) Gershenson Yu.M.; Ivanov A.V.; Kucheryavii S.I.; Iyapunov A.Ya. and Rozenshtein V.B. *Kinetics and Catalysis*, **1986**, *27*, 928

# THE MEASUREMENT OF UPTAKE COEFFICIENTS FOR HETEROGENEOUS REACTIONS OF ATMOSPHERIC IMPORTANCE

J.A. Davies, J. Baker, R.L. Jones and R.A. Cox

*Centre for Atmospheric Science (CAS), Department of Chemistry,  
University of Cambridge, Lensfield Road, Cambridge, CB2 1EW, UK.*

Research into ozone depletion in the atmosphere has given much attention to the chemistry of chlorine compounds e.g. CFCs. More recently, research has focused on the compounds of other halogens, in particular bromine and iodine, since, molecule for molecule, their ozone destroying capabilities are far greater. Also research into heterogeneous rather than gas phase reactions is intensifying. Reactions on the surfaces of water ice particles and sulphuric acid aerosols are of particular importance due to their abundance in the lower stratosphere at mid and high latitudes.

A wetted-wall flow tube system has recently been built at Cambridge to measure uptake coefficients for the adsorption of gaseous halogen compounds on the surfaces of water ice and liquid sulphuric acid as a function of temperature (190K to 250K). The flow tube consists of a 900 mm long and 20 mm ID Pyrex tube which can be lined with a Teflon sleeve to allow external preparation of the solid or liquid layer on the inner surface of the sleeve. Alternatively the surfaces will be provided in the form of aerosols introduced into the reactor through a side arm. The aerosol preparation will enable the aerosol composition to be varied within a narrow size distribution, while the total aerosol surface area will be determined by optical methods. To attain temperatures similar to those in the stratosphere, the flow tube will be encased in two jackets, the inner one containing a coolant, while the outer jacket is evacuated. A sliding injector, 1000 mm long and 9 mm ID, is used to introduce the gaseous reactant into the flow tube and may be moved along its axis in order to change the reaction zone length (i.e. the overlap between the gas and the surface). A highly sensitive quadrupole mass spectrometer with a fast response time is used to detect neutrals and radicals at concentrations down to 10 ppb. Low electron energies of approximately 20 eV will be used to ionise the molecular gas sample thus minimising fragmentation. The "uptake" of the reactant gas on the liquid/solid surface will result in a decrease in the concentration of the reactant as measured by the mass spectrometer. Measurements will be made for a range of reaction zone lengths enabling the kinetics of the reaction to be ascertained. The products of any surface reactions with the substrate that subsequently desorb into the carrier gas will also be identified and quantified using the mass spectrometer.

At the conference, the design of the flow tube system will be described in greater detail and preliminary results shall be presented.

through a vibrating orifice. The droplets pass co-axially through a slower moving humid gas flow entrained with a trace species of interest. An experimental uptake coefficient,  $\gamma_{obs}$ , is obtained by measuring the relative change in trace gas concentration,  $(n_i/n_i)_t$ , for a given change in droplet surface area,  $\Delta A$ . A novel feature of this experiment is that trace gas concentrations are monitored using laser-induced fluorescence (LIF). Mass accommodation coefficients are determined from fits of  $\gamma_{obs}$  measured as a function of pressure and gas-liquid contact time (Davidovits *et al.*, 1995). The temperature of the droplets is regulated by the partial pressure of water vapour in the He carrier gas. Rapid evaporation of the droplet occurs at the point of generation until the liquid temperature has fallen to that at which the saturated vapour pressure of the water equals the surrounding partial pressure. The temperature dependence of the mass accommodation coefficients of aniline and phenol have been measured between 263K and 290K. The values of  $(1.8 \pm 0.5) \times 10^{-2}$  and  $(2.7 \pm 0.5) \times 10^{-2}$  obtained for aniline and phenol respectively at 283K (Heal *et al.*, 1995), indicate that a significant fraction of atmospheric  $C_7$  could be removed by heterogeneous processes and that the mass accommodation coefficients of intermediates in the VOC oxidation chain are important parameters for models of tropospheric chemistry.

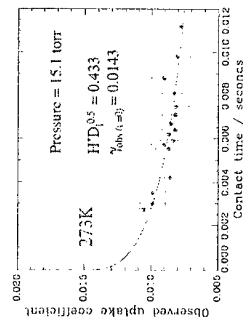


Figure 1. Variation of  $\gamma_{obs}$  with gas-liquid contact time for aniline onto 273K droplets.

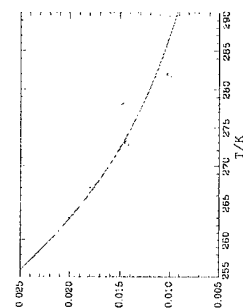


Figure 2. Variation of  $\alpha$  with temperature for aniline. Solid line is a fit to the function  $\alpha(1-\alpha) = \exp(-(\Delta H_{obs} - \Delta S_{obs} T)/T)$

## References

- Becker, K. H., EUROTRAC Symposium, Garmisch Partenkirchen, April 1994.
- Davidovits, P., J. H. Hu, D. R. Worsnop, M. S. Zahniser and C. E. Kolb, *Faraday Discuss.*, **100**, 65-81, 1995
- Heal, M. R., M. J. Pilling, P. E. Titcombe and B. J. Whitaker, *Geophys. Res. Letts.*, **22**, 3043-6, 1995.
- Herrmann, H., M. Exner, H. W. Jacobi, G. Raabe, A. Reese and R. Zellner, *Faraday Discuss.*, **100**, 129-53, 1995
- Jayne, J. T., S. X. Duan, P. Davidovits, D. R. Worsnop, M. S. Zahniser and C. E. Kolb, *J. Phys. Chem.*, **95**, 6329-36, 1991.
- Lelieveld, J. and P. J. Crutzen, *J. Atmos. Chem.*, **12**, 229-63, 1991.
- Madronich, S. and Hess, G. Angeletti and G. Restelli, (eds), *Physical-Chemical Behaviour of Atmospheric Pollutants*, Air Pollution Report EUR 15609/1, 1, 1-13, 1995

# COLLISION-INDUCED DISSOCIATION AND PHOTODISSOCIATION STUDIES OF THE $(\text{N}_2\text{O}\cdot\text{H}_2\text{O})^+$ CLUSTER ION

Michael J. Bastian, Rainer A. Dressler, Dale J. Levandier<sup>†</sup>, and Edmond Murad  
*Phillips Laboratory, PL/GPID, Hanscom AFB, MA 01731-3010 USA*

<sup>†</sup>*Orion International Technologies, Albuquerque, NM 01886 USA*

$(\text{N}_2\text{O}\cdot\text{H}_2\text{O})^+$  cluster ions are generated through low energy electron impact ionization of a pulsed supersonic expansion of  $\text{H}_2\text{O}$  seeded in  $\text{N}_2\text{O}$ . Following mass selection, the structure of cluster ions is probed in an octopole ion guide using collision-induced dissociation and photodissociation, and the decay products are examined mass spectrometrically. In both experiments, the three ionic products  $\text{H}_2\text{O}^+$ ,  $\text{N}_2\text{O}^+$ , and  $\text{N}_2\text{OH}^+$  are observed, for which collision-induced dissociation studies with Ar and Ne yield thresholds of  $0.65 \pm 0.15$  eV,  $0.85 \pm 0.20$  eV, and  $0.96 \pm 0.20$  eV, respectively. The difference in thresholds observed for  $\text{H}_2\text{O}^+$  and  $\text{N}_2\text{O}^+$  are consistent with the thermochemical asymptotes. The photodissociation spectra can be interpreted as deriving from a single cluster structure, in contrast to the suggestion by Graul and Bowers<sup>1</sup>, based on photodissociation measurements of thermal  $(\text{N}_2\text{O}\cdot\text{H}_2\text{O})^+$  clusters, that another isomer also exists ( $\text{N}_2\text{OH}^+\cdot\text{OH}$ ).

The photodissociation yields are obtained using the output of a Nd:YAG pumped OPO system that covers the entire visible range of the electromagnetic spectrum, thus providing additional insight with respect to the earlier studies.<sup>1</sup> The photodissociation yields shown in Figure 1 exhibit  $\text{H}_2\text{O}^+$  and  $\text{N}_2\text{O}^+$  production from an intense broad absorption band centered at  $21,000\text{ cm}^{-1}$  and  $\text{N}_2\text{OH}^+$  production from a weak band centered at  $17,000\text{ cm}^{-1}$ . The intense band is compared with the  $\text{H}_2\text{O}^+$   $\bar{A}$  state photoelectron intensities. The bending vibrational line positions have been shifted to higher energies by  $2420\text{ cm}^{-1}$  to match the photodissociation band maximum. The excellent agreement between the band shapes suggests that  $\text{H}_2\text{O}^+$  and  $\text{N}_2\text{O}^+$  are produced following the photo-induced charge transfer from a  $(\text{N}_2\text{O}\cdot\text{H}_2\text{O})^+$  cluster with the charge primarily situated on the  $\text{N}_2\text{O}$  moiety to a predissociating  $\text{N}_2\text{O}\cdot(\text{H}_2\text{O})^+$  complex. The energy shift of  $\sim 0.35$  eV with respect to the photoelectron band can be attributed to a smaller well depth of  $\sim 0.35$  eV of the predissociating excited state cluster.

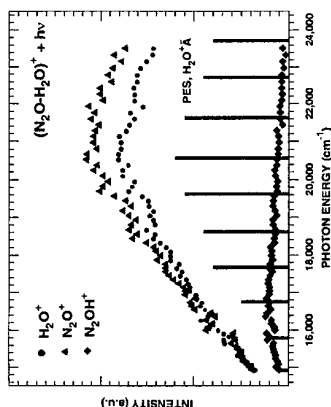


Figure 1.  $(\text{N}_2\text{O}\cdot\text{H}_2\text{O})^+$  photodissociation yields. The intense band is compared to  $\text{H}_2\text{O}^+$   $\bar{A}$  state photoelectron intensities on a corrected energy scale.

## References

- [1] S. T. Graul, H.-S. Kim and M. T. Bowers, *Int. J. Mass Spect. Ion Processes*, 117, 507 (1992).

## SPECTROSCOPY AND STRUCTURE OF AROMATIC - RARE GAS CLUSTER IONS

Ruth I. McKay, Evan J. Bieske and Alan E. W. Knight

*Molecular Dynamics Laboratory, Faculty of Science and Technology,  
Griffith University, Brisbane 4111, Australia.*

Ionic clusters consisting of a polyatomic ion surrounded by a few 'solvent' atoms or molecules, provide a connecting link between the isolated gas phase ion and the ion solvated in a condensed medium. Analysis of the vibrational structure associated with the motion of the cluster atoms can reveal details concerning the intermolecular potential. However, for large polyatomic ions, information concerning the cluster vibrational motion has been difficult to obtain using conventional spectroscopic methods.

We have developed a new combination of the previously available techniques of supersonic cooling, resonance-enhanced multiphoton ionization, time-of-flight mass spectroscopy, in concert with one-photon photodissociation spectroscopy. This technique takes advantage of the facile predissociation of an electronically excited cluster and affords us a method of studying the vibrational structure associated with the motion of a molecular cluster ion.

Using this technique we have obtained vibrationally resolved photodissociation spectra of a number of aromatic - rare gas cluster ions. Analysis of their vibrational structure permits structural details of the cluster cation to be deduced.

## TOWARDS A COMPLETE DESCRIPTION OF A MULTIPLE DISSOCIATION EVENT: A PHOTOION-PHOTONEUTRAL (pi-pn<sup>+</sup>) COINCIDENCE STUDY OF FRAGMENTATION IN RARE GAS CLUSTER IONS.

A.B. Jones, A.L.M. Buxey, P.R. Jukes, and A.J. Stace,

*School of Molecular Sciences, University of Sussex, Falmer, Brighton BN1 9QJ, U.K.*

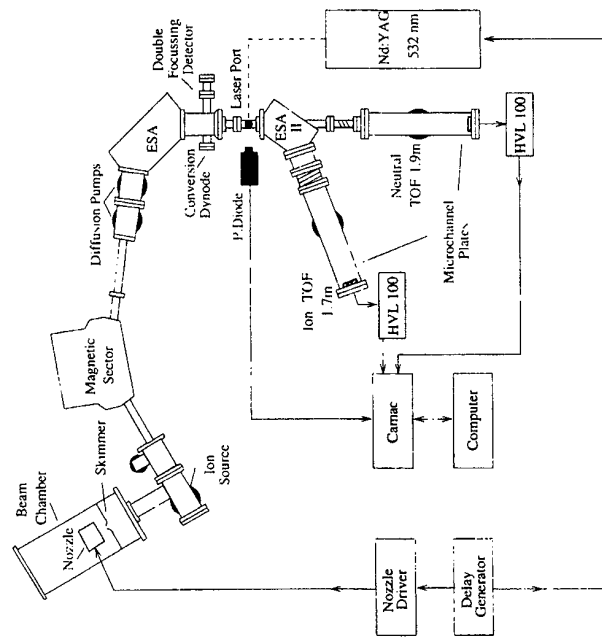
The photoexcitation of the rare gas cluster ions, e.g.  $\text{Ar}_n^+$ , at wavelengths in the region of 530 nm frequently results in complete dissociation:  $\text{Ar}_n^+ + h\nu \rightarrow \text{Ar}^+ + (n-1)\text{Ar}$ . We intend to present the first results from an experiment which we believe could ultimately provide a complete picture of multiple dissociation events of the type shown above for small cluster ions. The techniques of ion and neutral detection have been combined to give a method where we have sought to record, in coincidence, all the fragments from each photoexcitation step.

The core of the apparatus constructed to perform the coincidence experiments is a modified VG ZAB-E high resolution, double focusing mass spectrometer to which has been added a time-of-flight device for neutral collection. Ions with a laboratory frame kinetic energy of 8keV, are mass- and kinetic energy-selected using a magnet and an electrostatic analyser, and brought to focus at a laser port where they were photodissociated with a 10 ns pulse from a frequency doubled Nd:YAG laser operating at 532nm. The ionic photofragment,  $\text{Ar}^+$ , then passes through a second electrostatic analyser where the voltage (laboratory frame kinetic energy) is adjusted to transmit ions with a specific kinetic energy. Fragment ions are monitored using an MCP coupled to a discriminator, where the response to a single ion is a 2V spike with a FWHM (Full Width - Half Maximum) of 10 ns. A schematic diagram of the apparatus is shown below.

The neutral photofragments from each event, are allowed to continue in a straight line parallel to the original  $\text{Ar}_n^+$  flight direction and pass through a small hole in one of the analyser plates, where they enter a time of flight device 1.83m in length. At the end of the latter is a microchannel plate detector responds to the impact of neutrals

with high laboratory frame kinetic energies. The output from the MCP is fed to a second discriminator. For  $\text{Ar}_n^+$  ions with an initial laboratory frame kinetic energy of 8 keV, the neutral and ionic detection efficiencies are found to be approximately equal. Since the ionic fragments are detected first, their voltage pulse is used as a trigger to search for the coincident arrival of neutrals. On average, one in ten of all detected events proves to be coincident.

Results will be presented to show how the pi-pi<sup>+</sup> technique can be used to provide a complete description of photofragmentation patterns resulting from complex dissociation processes.



Schematic diagram of the apparatus used to perform pi-pi<sup>+</sup> experiments. The nozzle and mass spectrometer are used to deliver size and energy selected cluster ions to the laser port where they are photodissociated with a 10 ns light pulse at 532 nm.

# ON THE QUANTUM THEORY OF COLLISIONAL RECOMBINATION RATES

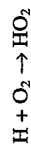
William H. Miller

*Department of Chemistry  
University of California  
Berkeley, California 94720-1460 USA*

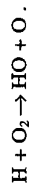
A rigorous quantum mechanical formulation has recently been given<sup>1</sup> for the venerable Lindemann mechanism of collisional recombination,



This theory and its application to the recombination of simple reactions, e.g.,



will be presented, with special emphasis on the effect of collisions on the reactive process



<sup>1</sup>J. Phys. Chem. **99**, 12387 (1995).

# A NEW METHOD FOR THE COMPUTATION OF QUANTUM VIBRATIONAL STATE DENSITIES IN ANHARMONICALLY COUPLED MOLECULAR SYSTEMS

Stephen J. Jeffrey and Sean C. Smith

*Department of Chemistry, University of Queensland, Brisbane, Qld 4072, Australia.*

The calculation of accurate rovibrational state densities  $\rho(E,J)$  in highly-excited unimolecular species is of fundamental importance in unimolecular rate theory, since this quantity appears in the denominator of the expression for the microcanonical dissociation rate coefficient  $k(E,J)$ ,

$$k(E,J) = \frac{N(E,J)}{h\rho(E,J)}$$

where  $N(E,J)$  is the cumulative reaction probability.

We present here an exact, non-perturbative algorithm for the calculation of quantum vibrational state densities  $\rho(E)$  in several-dimensional anharmonically coupled molecular systems.<sup>1</sup> The rationale for the method stems from the fact that there exist very fast algorithms for calculating an approximate density profile  $\rho_0(E)$  based on a reference Hamiltonian, viz. the Beyer-Swinehart algorithm for a harmonic Hamiltonian<sup>2</sup> and the Stein-Rabinovitch algorithm for an anharmonic (but separable) Hamiltonian.<sup>3</sup> In the *Density Correlation Method*, we calculate a density correlation function,  $D(E,E')$  which exactly corrects the reference vibrational state density profile,  $\rho_0(E)$ , to generate  $\rho(E)$ ,

$$\rho(E) = \int dE' D(E,E') \rho_0(E')$$

or, in discretized form,

$$\rho = D \rho_0$$

The elements of the density correlation matrix  $D$  may be readily computed by Lanczos reduction of randomly selected eigenfunctions of the reference Hamiltonian  $H_0$ . The Lanczos reduction process quickly generates a density distribution which shows how the (unit) density of an individual reference eigenfunction is spread over the spectrum of the full Hamiltonian. Statistical averaging of such distributions generates the columns of the matrix  $D$ .

We illustrate the application of the method to model two-dimensional Hamiltonians, including the Henon-Heiles potential.

# KINEMATIC AND POTENTIAL EFFECTS IN THE RECOMBINATION OF FREE RADICALS

Struan H. Robertson

*School of Chemistry, University of Leeds, Leeds LS2 9JT, UK*

Albert F. Wagner

*Chemistry Division, Argonne National Laboratory, Argonne, IL 60439, USA*

David M. Wardlaw

*Department of Chemistry, Queen's University, Kingston, ON K7L 3N6, CANADA*

Radical recombination typically involves large amplitude excursions from the reaction path in the form of hindered rotations. Variational Flexible Transition State Theory (FTST) incorporates such internal motion as well as external rotational motion. Recently, we have recast canonical FTST into a relatively simple expression containing an integral over only the internal coordinates of hindered rotational motion<sup>1</sup>. All the potential energy surface (PES) dependence resides in the argument of a Boltzmann-type term. In this formulation any kind of PES (harmonic, hindered, or free) can be treated. Kinematic factors in the integrand depend on the reaction path definition, i.e., what distance is held fixed between the reactions as the internal rotations are sampled (e.g., centre-of-mass separation, incipient bond distance)? The predicted rate coefficient is obtained by minimizing the rate coefficient expression with respect to the value and definition of the reaction path (as discussed by Klippenstein<sup>2</sup>). We report our most recent theoretical progress on this long-term project, namely systematic, closed-form expressions for the kinematic factors for arbitrary reaction path for all pairings of atomic, linear rigid top, and nonlinear rigid top fragments. Applications will be selected from ab initio surfaces for  $CX_3 + Y$  (where  $X$  and  $Y = H, D$ , and  $Cl$ ), for  $CH_2 + H$ , and for  $CH + H_2$ .

## References

- 1) S.H. Robertson, A.F. Wagner, and D.M. Wardlaw, *J. Chem. Phys.* **103**, 2917 (1995).
- 2) S.J. Klippenstein, *Chem. Phys. Lett.* **170**, 71 (1990); *J. Chem. Phys.* **94**, 6469 (1991).

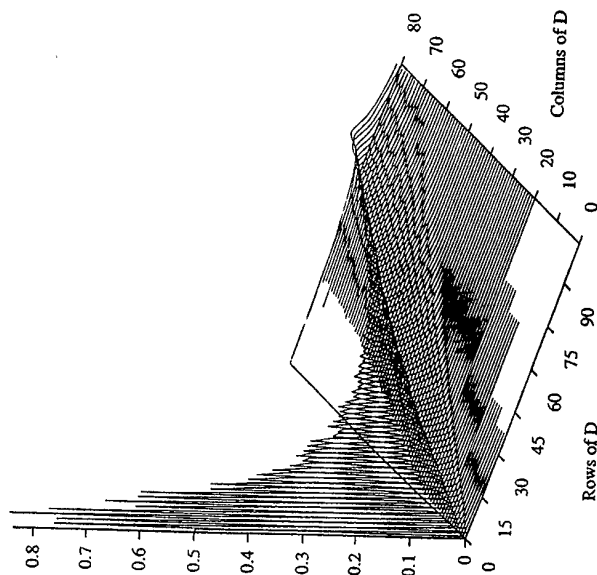


Figure: Elements of the Density Correlation Matrix computed for the two-dimensional Henon-Heiles Hamiltonian.

- (1) Smith and S.J. Jeffrey, *J. Chem. Phys.*, in press (1996).
- (2) Beyer and D.F. Swinehart, *Comm. Assoc. Comput. Machines* **16**, 379 (1973).
- (3) Stein and B.S. Rabinovitch, *J. Chem. Phys.* **58**, 2438 (1973).

## PHOTODISSOCIATION DYNAMICS OF FREE RADICALS

Daniel M. Neumark

*Department of Chemistry, University of California, Berkeley, CA  
94705, USA, and Chemical Sciences Division, Lawrence Berkeley National  
Laboratory,  
Berkeley, CA 94705 USA*

The photodissociation spectroscopy and dynamics of reactive free radicals are investigated using a novel fast beam technique. In this experiment, radicals are generated by laser photodetachment of a mass-selected beam of precursor negative ions. The resulting radicals are then photodissociated with a second laser, and the photofragments are detected.

Two types of measurements are performed. Photodissociation cross sections are measured by monitoring the total photofragment yield as a function of the dissociation laser frequency. At selected dissociation energies, photofragment energy and angular distributions are determined by detecting the fragments in coincidence on a position and time-sensing detector.

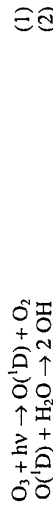
Results will be presented for the methoxy, vinoxy, and ketyenyl (HCCO) radicals. All three radicals have some structure in their photodissociation cross sections, indicating predissociation is occurring. However, the photofragment energy and angular distributions point to very different photodissociation dynamics for the three species. Preliminary results will also be presented for the photodissociation of mass-selected carbon clusters.

# ATMOSPHERIC PEROXY RADICALS: OBSERVATIONS AND MODELLING

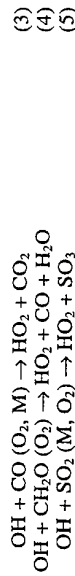
Chris A. Cantrell  
*National Center for Atmospheric Research*  
 Boulder, Colorado 80303 (cantrell@ncar.ucar.edu)

Peroxy radicals are important trace tropospheric constituents that are involved in the oxidation and production of many other atmospheric species. The peroxy radical family consists of  $\text{HO}_2$  and  $\text{RO}_2$ , where R is any organic group, but its members are also strongly coupled to the hydroxyl radical (OH). Peroxy radicals are responsible for ozone production in the troposphere, the formation of peroxides ( $\text{H}_2\text{O}_2$  and  $\text{ROOH}$ ), and act as intermediates in the oxidation of organic compounds.

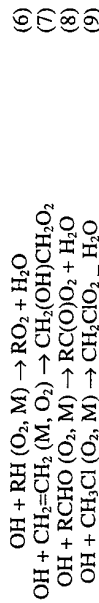
The sources of tropospheric peroxy radicals begin with processes that form OH. These include photolysis of ozone to  $\text{O}(^1\text{D})$  in the Huggins bands and the edge of the Hartley band (~2900 to 3200 Å), followed by the reaction of  $\text{O}(^1\text{D})$  with water vapor.



Hydroxyl radicals are also formed in the photolysis of nitrous acid ( $\text{HONO}$ ). Hydroxyl radicals are converted to hydroperoxy radicals by reaction with  $\text{CO}$ ,  $\text{CH}_2\text{O}$  and  $\text{SO}_2$ , for example.



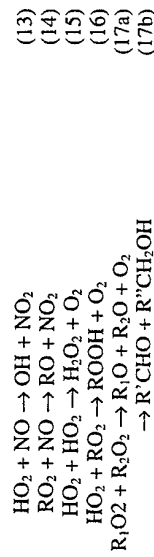
Organic peroxy radicals and  $\text{HO}_2$  are formed when OH reacts with organic compounds.



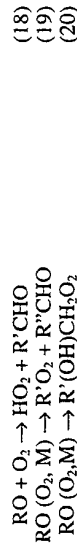
Peroxy radicals are also formed in the photolysis of carbonyl compounds.



During night-time hours, the nitrate radical,  $\text{NO}_3$ , reacts with some organic compounds (alkenes, aldehydes, dimethyl sulfide, etc.) to produce peroxy radicals much like OH during the day. Peroxy radicals are removed by reaction with NO and other peroxy radicals.



The alkoxy radical (RO) product of reactions (14), and (17a) can, depending on its structure and internal energy, react with  $\text{O}_2$  to produce  $\text{HO}_2$  and a carbonyl compound, decompose to lead to new  $\text{RO}_2$  radicals or in some case internally rearrange.



Ozone is produced in the troposphere from the photolysis of  $\text{NO}_2$  in the near ultraviolet spectral region (3000 to 4200 Å).



The efficiency of this process is limited because the NO formed in the photolysis reacts with the  $\text{O}_3$  formed in reaction (20).



Net ozone production can take place because peroxy radicals also oxidize NO to  $\text{NO}_2$ , leaving the  $\text{O}_3$  product of the  $\text{NO}_2$  photolysis intact (reactions (13) and (14)). It becomes a little more complex because  $\text{HO}_2$  also reacts with ozone.



Measurements of peroxy radicals in the troposphere have been accomplished through matrix isolation with electron spin resonance (MI-ESR), chemical conversion to OH followed by laser induced fluorescence (CCLIF), and chemical amplification (CA). We have also begun work on a new method based on chemical ionization mass spectroscopy for which some preliminary data will be shown. Results of recent measurement campaigns in remote and rural continental regions will be presented and the radical concentrations compared with various types of model estimates including a photochemical steady state model. This simply involves the assumption of balance between chemical production and loss for  $\text{HO}_2$ ,  $\text{RO}_2$  and OH, and neglect of the role of transport on the instantaneous radical concentrations. Measured quantities ( $\text{NO}_x$ , hydrocarbons, photolysis rates, temperatures, etc.) when available are input into the equations, and they are solved iteratively for the radical concentrations.

$$\begin{aligned}\frac{d[\text{HO}_2]}{dt} &= P_{\text{HO}_2} - L_{\text{HO}_2} \approx 0 \\ \frac{d[\text{RO}_2]}{dt} &= P_{\text{RO}_2} - L_{\text{RO}_2} \approx 0 \\ \frac{d[\text{OH}]}{dt} &= P_{\text{OH}} - L_{\text{OH}} \approx 0\end{aligned}$$

Reasons for agreement and discrepancy between the measurements and the models will be discussed in terms of measurement uncertainties and possible missing peroxy radical or OH reactions, including a probable loss of  $\text{HO}_2$  on aqueous aerosols and other gas phase processes.

# KINETICS, MECHANISMS AND PRODUCTS OF THE REACTIONS OF BR-ATOMS WITH HYDROCARBONS

I. Barnes, K.H. Becker, A. Bierbach, C. Sauer and T. Maurer  
*Bergische Universität - GH Wuppertal, Physikalische Chemie / FB 9*  
*Gaßstraße 20, 42097 Wuppertal, Germany*

Observations of the episodic destruction of boundary-layer ozone in the Arctic have shown that these events are accompanied by high levels of BrO radicals and also high concentrations of "filterable" bromine. Further, the degradation of acetylene during the events is more in keeping with Br-atom induced chemistry rather than OH-radical initiated oxidation. Although the source of the Br/BrO radicals and the exact nature of the filterable bromine is presently unclear the observations provide positive evidence for the involvement of bromine chemistry in this region of the troposphere.

In contrast to OH radical reactions the chemistry of the reactions of Br-atoms with hydrocarbons have not been the subject of intensive investigation. Results will be presented from a systematic investigation of the kinetics, mechanisms and products of Br-atoms with different classes of hydrocarbons including alkenes, dienes, aromatic hydrocarbons, unsaturated carbonyl compounds and the organic sulphur compounds dimethyl sulphide and dimethyl sulphoxide. The investigations have been performed in large volume reaction chambers using both in situ long path FTIR and GC-FID for the analyses and the photolysis of Br<sub>2</sub> as the Br-atom source. Most of the data has been obtained at room temperature (298±2 K) using the relative kinetic technique, however, for selected compounds both the kinetic and product studies have been performed in the temperature range 298 to 270 K. Table 1 lists the rate coefficients determined at room temperature K from this laboratory along with other values available in the literature. The investigations have considerably enhanced the kinetic and mechanistic data base for the reaction of Br-atoms with hydrocarbons. The data base has been used to look at possible correlations between the rate coefficients for reactions of Br-atoms with those for the reactions of OH, Cl, and NO<sub>3</sub> radicals with the same substrates, i.e. linear free energy relationships. General trends in chemical behaviour will be discussed. Finally, some possible implications from the investigations for the bromine chemistry occurring in the Arctic as well as possibly at mid-latitudes will be highlighted.

**Table 1:** List of rate coefficients determined for the reaction of Br-radicals with various VOC's at room temperature (°): Extrapolated values from listed Arrhenius parameters)

Compound	k [cm <sup>3</sup> molecule <sup>-1</sup> s <sup>-1</sup> ]	T[K]	Methods	Literature
<b>- A l k a n e s -</b>				
Ethane	(1.1 ± 0.5) 10 <sup>-19</sup>	298 <sup>1</sup>	FP-RF	Seakins et al. 1992
Propane	(4.3 ± 1.5) 10 <sup>-17</sup>	298 <sup>1</sup>	FP-RF	Seakins et al. 1992
n-Butane	(7.0 ± 2.2) 10 <sup>-17</sup>	298 <sup>1</sup>	FP-RF	Seakins et al. 1992
iso-Butane	(1.4 ± 0.3) 10 <sup>-15</sup>	298 <sup>1</sup>	FP-RF	Seakins et al. 1992

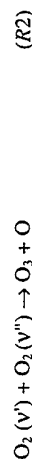
Cyclopentane	(1.2 ± 0.2) 10 <sup>-15</sup>	295	CP-GC	Wallington et al. 1989
2,3-Dimethylbutane	(6.4 ± 0.8) 10 <sup>-15</sup>	295	CP-GC	Wallington et al. 1989
2,2,4-Trimethylpentane	(6.8 ± 1.4) 10 <sup>-15</sup>	298	CP-GC	Barnes et al. 1989
<b>- A l k e n e s -</b>				
Ethene	(1.6 ± 0.3) 10 <sup>-13</sup>	298	CP-GC <sup>2</sup>	Barnes et al. 1989
	(< 2.3) 10 <sup>-13</sup>	295	CP-GC	Wallington et al. 1989
	(1.6 ± 0.2) 10 <sup>-13</sup>	296	CP-FTIR	Yarwood et al. 1992
Chloroethene	(7.4 ± 0.2) 10 <sup>-13</sup>	300	CP-GC	this work
1,1-Dichloroethene	(3.7 ± 0.1) 10 <sup>-13</sup>	300	CP-GC	this work
Trichloroethene	(9.0 ± 0.2) 10 <sup>-14</sup>	300	CP-GC	this work
Tetrachloroethene	(< 1) 10 <sup>-14</sup>	298	CP-GC	this work
Propene	(2.7 ± 0.5) 10 <sup>-12</sup>	298	CP-FTIR	Barnes et al. 1989
	(3.9 ± 0.4) 10 <sup>-12</sup>	295	CP-GC	Wallington et al. 1989
1-Butene	(3.4 ± 0.7) 10 <sup>-12</sup>	298	CP-GC	Barnes et al. 1989
trans-2-Butene	(7.5 ± 1.5) 10 <sup>-12</sup>	298	CP-GC	Barnes et al. 1989
	(9.5 ± 0.8) 10 <sup>-12</sup>	295	CP-GC	Wallington et al. 1989
2-Methyl-2-butene	(9.3 ± 0.7) 10 <sup>-12</sup>	300	CP-GC	this work
2-Methyl-1-butene	(1.9 ± 0.1) 10 <sup>-11</sup>	300	CP-GC	this work
2,3-Dimethyl-2-butene	(1.5 ± 0.1) 10 <sup>-11</sup>	298	CP-GC	this work
a-Pinene	(2.8 ± 0.2) 10 <sup>-11</sup>	300	CP-GC	this work
b-Pinene	(2.2 ± 0.1) 10 <sup>-11</sup>	296	CP-GC	this work
	(2.9 ± 0.1) 10 <sup>-11</sup>	296	CP-GC	this work
<b>- D i e n e s -</b>				
1,3-Butadiene	(5.8 ± 0.2) 10 <sup>-11</sup>	300	CP-GC	this work
Isoprene	(7.4 ± 0.1) 10 <sup>-11</sup>	298	CP-GC	this work
2,3-Dimethyl-1,3-butadiene	(8.2 ± 0.1) 10 <sup>-11</sup>	298	CP-GC	this work
<b>- A l k y n e s -</b>				
Ethyne	(3.6 ± 0.7) 10 <sup>-14</sup>	298	CP-GC	Barnes et al. 1989
Propyne	(5.2 ± 0.2) 10 <sup>-15</sup>	295	CP-GC	Wallington et al. 1989
	(1.5 ± 0.3) 10 <sup>-12</sup>	298	CP-GC	Barnes et al. 1989
<b>- A r o m a t i c s -</b>				
Furan	(< 1) 10 <sup>-14</sup>	298	CP-GC	this work
	(1.6 ± 0.1) 10 <sup>-15</sup>	300	CP-GC	this work

# THEORETICAL STUDIES OF COLLISIONAL DYNAMICS: THE ATMOSPHERIC REACTIONS $H + O_3$ AND $O_2(v') + O_2(v'')$

A.J.C. Varandas, H.G. Yu and W. Wang

*Departamento de Química, Universidade de Coimbra  
P-3049 Coimbra Codex, Portugal*

We report theoretical studies of the following four-atom atmospheric reactions:



For these studies we have employed realistic potential energy surfaces which have been determined by using the double many-body expansion [1] (DMBE) method to model empirical information and *ab initio* calculations. In all cases the dynamics has been studied using the quasiclassical trajectory method; in the case of the reverse of reaction (R2), a quantum dynamics approach has also been reported [2]. The results to be presented emphasize the comparison with the experimental thermal rate coefficients.

Figure 1 shows the calculated rate constant for the reaction (R1) using a novel DMBE potential energy surface [3] for ground state  $HO_3$ . This has been modelled at short range from properly scaled unrestricted single and double-electron excitation configuration interaction energies, while its long range part includes the electrostatic energy up to four-body terms and the dynamical correlation up to three-body ones. The agreement with experiment is seen to be good.

For the reaction (R2), we have studied [4] a wide range of combinations of initial vibrational states using the  $O_4$  DMBE potential energy surface reported elsewhere [6]. Besides the vibrationally resolved cross sections and rate constants for the reactive processes leading to  $O_3 + O$ ,  $O_2 + O + O$ , and O-atom exchange, an estimate of the corresponding vibrationally averaged rate constants is reported using the experimental distribution [7] of  $O_2(v)$  in the reaction of photodissociation of  $O_3$ . The implications of our results on a recently proposed hypothesis to explain the 'ozone deficit' problem are also tentatively assessed.

2-Methylfuran	(2.2 ± 0.1) 10 <sup>-13</sup>	300	CP-GC	this work
Furan-2-aldehyde	(2.2 ± 0.1) 10 <sup>-13</sup>	300	CP-GC	this work
2,5-Dimethylfuran	(1.9 ± 0.1) 10 <sup>-12</sup>	300	CP-GC	this work
5-Methylfurfural	(4.0 ± 0.1) 10 <sup>-13</sup>	300	CP-GC	this work
Benzene	(< 1) 10 <sup>-14</sup>	298	CP-GC	this work
Toluene	(< 1) 10 <sup>-14</sup>	298	CP-GC	this work
p-Xylene	(< 1) 10 <sup>-14</sup>	298	CP-GC	this work
<b>- Alcohols / Carbons -</b>				
3-Bromo-2-butanol	(2.2 ± 0.1) 10 <sup>-13</sup>	298	CP-FTIR	this work
Methylvinylketone	(1.9 ± 0.1) 10 <sup>-11</sup>	300	CP-GC	this work
Methacrolein	(2.3 ± 0.1) 10 <sup>-11</sup>	300	CP-GC	this work
Acrolein	(3.2 ± 0.1) 10 <sup>-12</sup>	300	CP-GC	this work
Formaldehyde	(1.6 ± 0.3) 10 <sup>-12</sup>	298	DF-ESR	Le Bras et al. 1980
	(1.1 ± 0.1) 10 <sup>-12</sup>	298	FP-RF	Nava et al. 1981
Acetaldehyde	(3.7 ± 0.1) 10 <sup>-12</sup>	298	CP-FTIR	Niki et al. 1985
Bromacetaldehyde	(1.8 ± 0.1) 10 <sup>-13</sup>	296	CP-FTIR	Yarwood et al. 1992

# ROLE OF EXCITED $\text{CF}_3\text{CFHO}$ RADICALS IN THE ATMOSPHERIC CHEMISTRY OF HFC-134a.

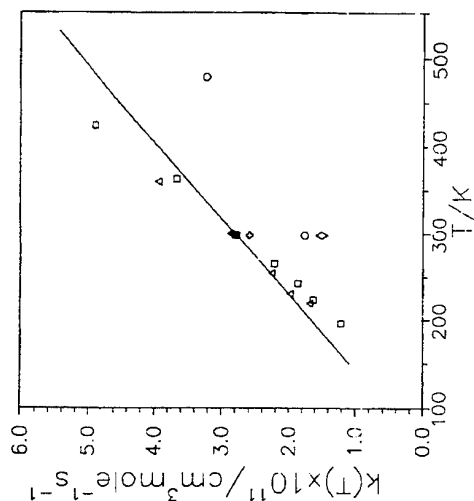
T. J. Wallington, M. D. Hurley  
Ford Motor Company  
Ford Research Laboratory, SRL-3083  
Dearborn, Michigan 48121-2053

J. M. Fracheboud, J. J. Orlando, G. S. Tyndall  
Atmospheric Chemistry Division  
National Center for Atmospheric Research  
P. O. Box 3000, Boulder, CO 80307

J. Sehested, T. E. Møgelberg  
Environmental Science and Technology Department  
Risø National Laboratory, DK-4000, Roskilde, Denmark

O. J. Nielsen  
Ford Motor Company  
Ford Forschungszentrum Aachen  
Dennewartstrasse 25, D-52068 Aachen, Germany

The atmospheric degradation of HFC-134a ( $\text{CF}_3\text{CFH}_2$ ) proceeds via the formation of  $\text{CF}_3\text{CFHO}$  radicals. Long pathlength FTIR environmental chamber techniques were used to study the atmospheric fate of  $\text{CF}_3\text{CFHO}$  radicals. Two competing reaction pathways were identified for  $\text{CF}_3\text{CFHO}$  radicals: reaction with  $\text{O}_2$ ,  $\text{CF}_3\text{CFHO} + \text{O}_2 \rightarrow \text{CF}_3\text{C(O)F} + \text{HO}_2$ , and decomposition via C-C bond scission,  $\text{CF}_3\text{CFHO} + \text{M} \rightarrow \text{CF}_3 + \text{HC(O)F} + \text{M}$ .  $\text{CF}_3\text{CFHO}$  radicals were produced by two different reactions: either via the self reaction of  $\text{CF}_3\text{CFHO}_2$  radicals, or via the  $\text{CF}_3\text{CFHO}_2 + \text{NO}$  reaction. It was found that decomposition was much more important when  $\text{CF}_3\text{CFHO}$  radicals were produced via the  $\text{CF}_3\text{CFHO}_2 + \text{NO}$  reaction than when they were produced via the self reaction of  $\text{CF}_3\text{CFHO}_2$  radicals. We ascribe this observation to the formation of vibrationally excited  $\text{CF}_3\text{CFHO}^*$  radicals in the  $\text{CF}_3\text{CFHO}_2 + \text{NO}$  reaction. Rapid decomposition of  $\text{CF}_3\text{CFHO}^*$  radicals limits the formation of  $\text{CF}_3\text{C(O)F}$  and hence  $\text{CF}_3\text{COOH}$  in the atmospheric degradation of HFC-134a. We estimate that the  $\text{CF}_3\text{COOH}$  yield from atmospheric oxidation of HFC-134a is 7-19%. Vibrationally excited alkoxy radicals may play an important role in the atmospheric chemistry of other organic compounds.



**Figure 1:** Calculated rate constant for the  $\text{H} + \text{O}_3 \rightarrow \text{HO} + \text{O}_2$  reaction. The symbols indicate the experimental results (Ref. 5, and references therein).

The support of Junta Nacional de Investigação Científica e Tecnológica, Portugal, under programmes PRAXIS XXI and FEDER (Contract 2/2/QUI/408/94), and EC (Contract #CHRX-CT 94-0436) is gratefully acknowledged.

## References

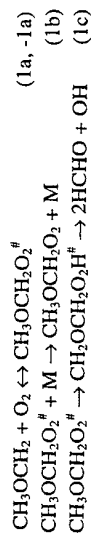
- 1) Varandas, Adv. Chem. Phys. **74**, 255 (1988); Chem. Phys. Lett. **194**, 333 (1992).
- 2) Szychman, A.J.C. Varandas, and M. Baer, J. Chem. Phys. **102**, 3474 (1995).
- 3) Varandas and H.G. Yu, (to be submitted for publication).
- 4) Varandas and W. Wang, (to be submitted for publication).
- 5) Steinfeld, S.M. Adler-Golden, and J.W. Gallagher, J. Phys. Chem. Ref. Data **16**, 911 (1987).
- 6) Varandas and A.A.C.C. Pais, in Theoretical and Computational Models for Organic Chemistry, edited by S.J. Formosinho, I.G. Czismadia, and L.G. Arnaut (Kluwer, Dordrecht, 1991), p.55.
- 7) Miller, A.G. Suits, P.L. Houston, R. Toumi, J.A. Mack, and A.M. Wodtke, Science **265**, 1831 (1994).

# DIMETHYL ETHER OXIDATION: KINETICS AND MECHANISM OF THE $\text{CH}_3\text{OCH}_2 + \text{O}_2$ REACTION AT 296 K AND 0.38-940 TORR TOTAL PRESSURE

J. Sehested, T. Møgelberg, J. Platz, H. Egsgaard, O. J. Nielsen  
*Section for Chemical Reactivity, EST Dept.*  
*Risø National Laboratory, DK-4000 Roskilde, Denmark*

T. J. Wallington, E. W. Kaiser  
*Ford Motor Company, Research Staff, SRL-3083*  
*P. O. Box 2053, Dearborn, Michigan 48121-2053, USA*

The title reaction was studied at 296 K and 0.38-940 Torr total pressure using a FTIR smog chamber technique. The overall rate constant for reaction of  $\text{CH}_3\text{OCH}_2$  radicals with  $\text{O}_2$ ,  $k_1 = k_{\text{RO}_2} + k_{\text{POD}}$ , was measured relative to that for the pressure independent reaction of  $\text{CH}_3\text{OCH}_2$  radicals with  $\text{Cl}_2$  ( $k_2$ ). There was no discernible effect of pressure on  $k_1$  in the range 200-940 Torr. Between 200 and 5 Torr total pressure  $k_1$  decreased by approximately a factor of 2. For pressures below 5 Torr  $k_1$  was again independent of pressure. The reaction proceeds via the formation of an activated complex,  $\text{CH}_3\text{OCH}_2\text{O}_2^*$ , that is either collisionally stabilized to form the peroxy radical,  $\text{CH}_3\text{OCH}_2\text{O}_2$ , or undergoes intramolecular H-atom abstraction followed by decomposition to give two formaldehyde molecules and an OH radical.



The products of reaction (1) were studied as a function of total pressure. The yield of formaldehyde increased from <2% at 700 Torr total pressure to ~100% at 0.38 Torr total pressure while the combined yield of methyl formate and methoxy methylhydroperoxide decreased from ~100% to 4% over the same pressure range. Fitting the product yields and relative rate data using a modified Lindemann expression gave the following rate constants:  $k_{\text{RO}_2}/k_1 = (1.97 \pm 0.28) \times 10^{-19} \text{ cm}^3 \text{ molecule}^{-1} \text{ s}^{-1}$ ,  $k_{\text{RO}_2}/k_2 = 0.108 \pm 0.004$ , and  $k_{\text{POD}}/k_1 = (6.0 \pm 0.5) \times 10^{-2}$  where  $k_{\text{RO}_2}$  and  $k_{\text{POD}}$  represent the overall bimolecular rate constants for formation of  $\text{CH}_3\text{OCH}_2\text{O}_2$  radicals and for the reaction of  $\text{CH}_3\text{OCH}_2$  radicals with  $\text{O}_2$  in the limit of low pressure, respectively. These data and absolute rate data from the literature were used to derive a rate constant for the reaction of  $\text{CH}_3\text{OCH}_2$  radicals with  $\text{Cl}_2$  of  $(1.13 \pm 0.30) \times 10^{-10} \text{ cm}^3 \text{ molecule}^{-1} \text{ s}^{-1}$ . The results are discussed in the context of the use of dimethyl ether as an alternative diesel fuel and the atmospheric chemistry of dimethyl ether.

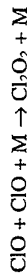
# DIMERS OF THE HALOGEN MONOXIDES: FORMATION KINETICS AND STABILITY

D.M. Rowley, M.H. Harwood, R.A. Cox and R.L. Jones

*Centre for Atmospheric Science, Department of Chemistry, University of Cambridge,*  
*Lensfield Road, Cambridge CB2 1EW, U.K.*

## Introduction

The halogen monoxide ( $\text{XO}$ ,  $\text{X} = \text{Cl}$ ,  $\text{Br}$ ,  $\text{I}$ ) radicals are important intermediates in the atmospheric breakdown of halogen containing compounds and are involved in several catalytic cycles leading to destruction of ozone<sup>1</sup>. The self-reactions of the  $\text{XO}$  radicals are rate determining in two important catalytic cycles. The formation of the  $\text{ClO}$  dimer in the reaction:

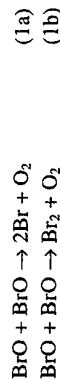


followed by its photolysis is the main cause of stratospheric ozone loss in the Antarctic ozone hole. The self-reaction of  $\text{BrO}$  to yield  $\text{Br}$  (1a, below), followed by the  $\text{Br} + \text{O}_3$  reaction is thought to be the cause of ozone loss in the arctic tropospheric marine boundary layer.

The  $\text{XO} + \text{XO}$  reactions all show complex kinetic behaviour arising from the existence of competing bimolecular and termolecular channels, leading to different products. As such they are of intrinsic interest to the understanding of elementary gas phase reactions. Early studies by Clyne and coworkers established the importance of the bimolecular self-reactions leading to halogen atoms as products but the formation of unstable halogen monoxide dimers has been established only recently. In view of its importance, much attention has been directed towards the  $\text{ClO}$  dimer, its formation kinetics, stability and photochemistry, which are now quite well-defined. Much less is known about dimers of  $\text{BrO}$  and  $\text{IO}$ , although there are some indications that they exist. The present study has provided the first characterisation of the  $\text{BrO}$  dimer and the competing channels in the  $\text{BrO} + \text{BrO}$  reaction.

## Experimental

The self-reaction of  $\text{BrO}$  radicals (1) has been studied as a function of temperature (222 - 298 K) and pressure (60 - 760 Torr) using flash photolysis/UV absorption.



The recently developed apparatus for the flash photolysis is unique and incorporates a charge coupled device (CCD) detector.<sup>2</sup> Use of a CCD enables rapid sequential UV absorption spectra of the photolysed gas mixture to be recorded in a single shot. Coupled with spectral decomposition algorithms, this enables unequivocal and accurate quantification of multiple species in the reaction mixture. Thus the advantages of spectral recording as with a diode array, along with the continuous temporal monitoring afforded by a photomultiplier tube are both realised.

Two distinct generation schemes were used for the BrO radicals in order to obtain channel specific kinetic information for reaction (1). In the first, flashlamp photolysis of Br<sub>2</sub> in excess ozone was used. In the second, excimer laser photolysis of oxygen in excess bromine was used. BrO radicals were monitored using the characteristic (A←X) structured absorption from 315–365 nm. Ozone, Br<sub>2</sub>, Br<sub>2</sub>O and OBrO were also monitored in some experiments.

In the bromine photolysis system, any bromine atoms produced in channel (1a) or other reactions are rapidly scavenged by the excess ozone. At 298 K BrO decays were second-order and therefore represented self-reaction of BrO along channel (1b) only. Results were in accordance with previous determinations. At lower temperature, the rate of BrO decay increased and, below 250 K, deviated from second-order. An additional absorption was also observed in the post flash spectra, after subtraction of the BrO. This was interpreted as a reversible termolecular channel of the BrO self-reaction at low temperatures, forming Br<sub>2</sub>O<sub>2</sub>. Inclusion of this channel allowed BrO decays to be successfully simulated. Experiments as a function of pressure confirmed the existence of a termolecular component and plots of  $k_{\text{initial}}$  vs pressure were used to separate the bimolecular and termolecular rate coefficients. Using  $k_{1b}$  and  $k_{1c}$  determined in this way enabled  $k_{1c}$  and the quantity of Br<sub>2</sub>O<sub>2</sub> to be determined, and a spectrum of Br<sub>2</sub>O<sub>2</sub> to be recorded. In separate experiments, the reactions Br + Br<sub>2</sub>O<sub>2</sub>; Br + BrO and Br + Br<sub>2</sub>O were also characterised.

In the oxygen photolysis system, all channels of the BrO self-reaction contribute to the observed decay. BrO decays were second-order under all conditions, presumably due to the scavenging of any Br<sub>2</sub>O<sub>2</sub> formed at low temperature by the excess of bromine atoms present. Rate coefficients for channel (1a) were determined at all temperatures studied and were independent of pressure.  $k_{1a}$  shows a very small temperature dependence above 250 K, but decreases rapidly at lower temperatures. The reaction O + Br<sub>2</sub> was also characterised.

Results for the bimolecular channels of the BrO self-reaction are shown in figure 1.

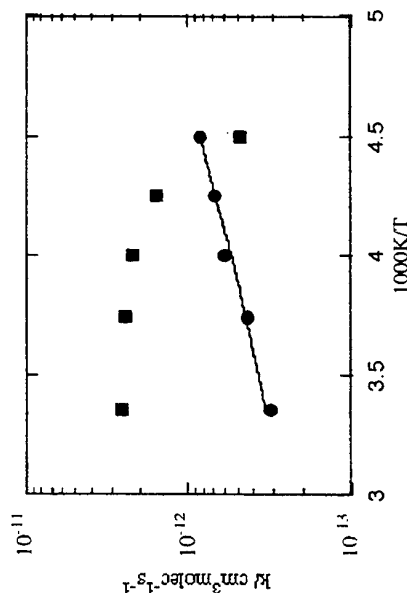


Figure 1: Arrhenius Plot for  $k_{1a}$  (filled squares) and  $k_{1b}$  (filled circles)

## Conclusions

There is now kinetic and spectroscopic evidence that dimers are formed in the self-reactions of ClO, BrO and IO. The formation rate coefficients and enthalpy (relative to 2 (XO)) are summarised in Table 2.

Table 2: Formation and Stability of Halogen Monoxide Dimers

Dimer	$k_f / \text{cm}^3 \text{molec}^{-1} \text{s}^{-1}$ ( $M = \text{N}_2$ )	$\Delta H_f / \text{kJ mol}^{-1}$	Structure
Cl <sub>2</sub> O <sub>2</sub>	$1.7 \times 10^{-32}$ (298K)	-72.3	ClOOCla
Br <sub>2</sub> O <sub>2</sub>	$8.2 \times 10^{-32}$ (222K)		BrOOBr
I <sub>2</sub> O <sub>2</sub>	$1 \times 10^{-30}$ (298K)	b	Unknown

Notes: a: Other structures, e.g. ClClO<sub>2</sub>, ClOClO are known but have lower stability; b: Stability unknown but appears stable at room temperature.

The formation rates for the dimers increase in the order Cl < Br < I, which is consistent with the pattern associated with other termolecular association reactions of the halogens. The BrO dimer is clearly less stable than Cl<sub>2</sub>O<sub>2</sub> and probably I<sub>2</sub>O<sub>2</sub> (which is not well-characterised), and is not a significant atmospheric species.

The temperature and pressure dependence of the bimolecular channels of the BrO + BrO reaction obtained in this work provides additional insight into the mechanism of these reactions. The reaction forming Br<sub>2</sub> + O<sub>2</sub> exhibits a small negative temperature dependence and is independent of pressure, indicating a mechanism involving a complex which is too short lived to be stabilised by collisions. Conversely, the channel (1a) producing bromine atoms appears to slow at temperatures where significant stabilisation of the BrO dimer can be detected, suggesting that this channel proceeds through an energised intermediate which can be collisionally stabilised.

## References

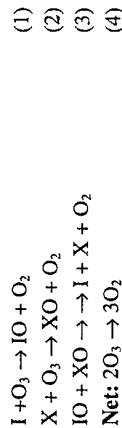
- 1) R.P.Wayne *et al.* "Halogen Oxides: radicals, Sources and Reservoirs in the Laboratory and in the Atmosphere" *Atm. Env.* **29**, 2675, (1995)
- 2) D.M. Rowley *et al.* *J. Phys. Chem.*, **100**, 3020, (1996)

# LABORATORY STUDIES OF THE KINETICS OF IO RADICALS

James B. Burkholder, Andrew Turnipseed, Mary Gilles, and A.R. Ravishankara

NOAA, 325 Broadway Boulder, CO 80303 and The Cooperative Institute for Research in Environmental Sciences, University of Colorado, Boulder, CO 80309

The impact of iodine chemistry on ozone catalytic destruction cycles in both the stratosphere and troposphere is currently under study. It is known that the oceans are a significant source of iodine to the atmosphere, primarily in the form of  $\text{CH}_3\text{I}$ . The possible role of iodine in the marine boundary layer and its possible role in the ozone loss observed in the Arctic spring after sunrise has received recent attention. Iodine may lead to catalytic ozone depletion via the reaction sequence:



where X represents Cl, Br, I, or OH. Reaction (3) is denoted with a double arrow to indicate that it may proceed by more than one elementary step. Because reaction (3) is the rate limiting step in this sequence, the rate coefficients for these reactions must be accurately known to ascertain the effectiveness of these cycles. Since the reservoir species for iodine in the atmosphere (i.e., HI, HOI, or  $\text{IONO}_2$ ) are photolytically unstable, most of the atmospheric iodine will be in the active forms of I or IO. Therefore, iodine is particularly effective at destroying ozone, and small amounts of iodine can make a significant contribution to ozone loss.

Previously, it was assumed that iodine could play a significant role only in tropospheric chemistry. However, it has been postulated that iodine-containing compounds can be rapidly transported to the stratosphere by strong convective transport in the tropics. Once in the stratosphere, these compounds would readily photolyze to release I atoms which then catalytically destroy ozone via reactions (1) - (3).

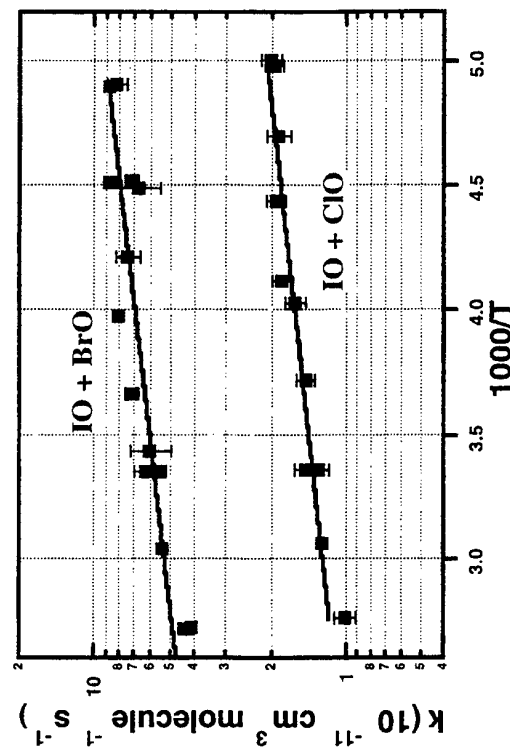
We have used the technique of pulsed laser photolysis/pulsed laser-induced fluorescence (LP-PLIF) to produce and monitor IO radicals. We have combined a discharge flow source for producing ClO and BrO radicals with UV absorption for determining their concentration and to measure the rate coefficients over the temperature range important in the atmosphere.

The reaction rate coefficient for  $\text{IO} + \text{ClO} \rightarrow \text{Products}$  was measured by coupling discharge flow and pulsed laser induced fluorescence techniques. Rate coefficients for  $\text{IO} + \text{ClO} \rightarrow \text{Products}$  were measured from 200 - 362 K by monitoring the temporal profile of IO in an excess of ClO. The rate coefficients are described by the expression:  $k(T) = (5.1 \pm 1.7) \times 10^{-12} \exp[(280 \pm 80)/T] \text{ cm}^3 \text{ molecule}^{-1} \text{ s}^{-1}$  where the quoted uncertainties include estimated systematic errors (data shown in Figure below).

Atomic iodine was identified as a major product of the reaction. A product yield,  $\Phi(\text{I})$ , for a channel(s) yielding an I atom was measured to be  $\Phi = 0.8 \pm 0.2$ .

The rate coefficient for  $\text{IO} + \text{BrO} \rightarrow \text{Products}$  (excluding channels that produce I atom) was measured in excess  $\text{O}_3$ . Under these experimental conditions we were insensitive to channels producing atomic iodine. This reaction was studied under pseudo-first order conditions in an excess of BrO at pressures between 6-15 Torr and 204-388 K. The Arrhenius expression obtained for non-iodine atom producing channels is  $k(T) = (2.32 \pm 0.40) \times 10^{-11} \exp[(269 \pm 85)/T] \text{ cm}^3 \text{ molecule}^{-1} \text{ s}^{-1}$  (data shown in Figure below).

These kinetic measurements will be described in this presentation. The implications of our findings to the ozone chemistry in the atmosphere will be discussed.



# TIME-RESOLVED FTIR ABSORPTION SPECTROSCOPY USING A STEP-SCAN INTERFEROMETER

Jürg Eberhard, Pey-Shiun Yeh, and Yuan-Pern Lee

Department of Chemistry, National Tsing Hua University, Hsinchu, Taiwan 30043  
Republic of China.

## Introduction

Whilst the kinetic data base for atmospheric chemistry is quite extensive today, comparably little mechanistic information is available.<sup>1</sup> Time-resolved vibrational spectroscopy can provide detailed information on dynamics and mechanisms of chemical reactions. Time-resolved IR absorption spectroscopy is an established method for chemical kinetic and dynamic investigations. Over the last few years time-resolved Fourier transform (FT) emission spectroscopy using step-scan interferometers has been applied to the study of photodissociation dynamics.<sup>2-4</sup> This technique has been applied in absorption mode for studies on biochemical systems.<sup>5</sup> The basic advantages of Fourier transform spectroscopy are retained in these applications. Time-resolved step-scan FT spectroscopy can be used for investigations of repeatable phenomena. The moving mirror of the spectrometer is moved in discrete steps. Once moved to a fixed position, the phenomenon is triggered and the temporal evolution of the signal is recorded. The triggering can be repeated for averaging. The mirror is then moved to the next position and the process is repeated. At the end of the experiment, the data are reshuffled to give the interferograms for different times after the trigger. Time-resolved spectra are obtained by Fourier transform these interferograms. The time-resolution is in principle only limited by the detector and acquisition electronics. Time-resolution for gas-kinetic studies in the micro- to millisecond range is easily achievable. Time-resolved FTIR absorption spectroscopy could be especially useful for determining branching ratios and identifying products of gas reactions because it is a multiplex technique working in the fingerprint region of the spectrum.

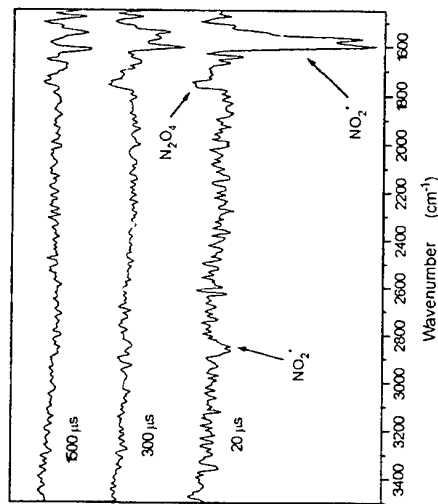
## Experimental Setup

The reaction cell (approximate volume 0.75 l) is mounted vertically into the sample compartment of a commercial step-scan spectrometer (Bruker IFS66v). The sample compartment is purged with N<sub>2</sub> and separated from the evacuable spectrometer optics with KBr windows. The reaction cell is equipped with a 20 cm base path White cell for multipassing the IR beam and multipass mirrors for the photolysis excimer laser beam. The cell is pumped with a 1400 l/min rotary pump. A fast photovoltaic MCT detector/preamplifier (50 ns response time) with simultaneous ac- and dc-coupled outputs is used. The signals are further amplified with low-noise preamplifiers and recorded using a 16-bit 200 kHz analog-to-digital converter (i.e. 5  $\mu$ s time resolution). The ac-coupled signal from the detector leads to the time-resolved spectral changes of the intensity  $\Delta S'(v)$ . The dc-coupled signal is used for obtaining the single beam

spectrum  $S_0(v)$  of the sample and for phase-correction of the ac-coupled signal. The spectral absorbance change at a specific time, a difference spectrum, is given as  $\log\{[S_0(v) + \Delta S'(v)]/S_0(v)]\}$ .

## Experimental results from the photolysis of NO<sub>2</sub> at 193 nm

NO<sub>2</sub> was photolysed at 193 nm in Ar bath gas. Typical difference spectra for specific times after the photolysis are given in the figure below. The conditions were 500 mtorr NO<sub>2</sub> in 1 torr Ar. The spectra were obtained without any filter at 8 cm<sup>-1</sup> resolution at a pathlength of 4 m averaging 50 laser shots. With a laser repetition rate of 50 Hz, the scan was completed in 25 minutes. The negative signals indicating product formation most probably arise from vibrationally excited NO<sub>2</sub>. The positive signal probably reflects the depletion of N<sub>2</sub>O<sub>4</sub>, which dissociates to reestablish the NO<sub>2</sub> / N<sub>2</sub>O<sub>4</sub> equilibrium.



Difference spectra at 20, 300 and 1500  $\mu$ s after the 193 nm photolysis of NO<sub>2</sub>.

## Conclusions

By observing transient signals arising from the photolysis of NO<sub>2</sub> at 193 nm, we demonstrate that time-resolved FTIR absorption spectroscopy for gas-kinetic investigations is feasible. The technique has to be improved with regard to resolution and signal-to-noise ratio.

## References

- (1) Atkinson, R. J. *Phys. Chem. Ref. Data* 1994, *Monograph 2*
- (2) Hartland, G. V.; Xie, W.; Dai, H.-L.; Simon, A.; Anderson, M. J. *Rev. Sci. Instrum.* 1992, **63**, 3261.
- (3) Heard, D. E.; Brownsworld, R. A.; Weston, D. G.; Hancock, G. *Appl. Spectrosc.* 1993, **47**, 1438.
- (4) Yeh, P.-S.; Leu, G.-H.; Lee, Y.-P.; Chen, I.-C. *J. Chem. Phys.* 1995, **103**, 4879.  
Uhmann, W.; Becker, A.; Taran, C.; Siebert, F. *Appl. Spectrosc.* 1991, **45**, 390.

# A NEW PUMP-AND-PROBE LIDAR TECHNIQUE TO STUDY TROPOSPHERIC OH RADICAL KINETICS

François Jeanneret, Robert Vajtai\*, Alain Clappier, Hubert van den Bergh and Bertrand Calpini

EPFL, DGR-LPAS LIDAR-Group,

Ecublens, CH-1015 Lausanne

Phone: ++41-21-693-6186 Fax: ++41-21-693-36-26

E-mail: francois.jeanneret@dgr.epfl.ch

\* Permanent: JATE, Department of Experimental Physics

**Abstract.** OH radical is the most important oxidising agent in the atmosphere. We are developing a new system to study the chemical kinetics of the tropospheric radical. A high concentration of OH is generated by flash photolysis and then its relaxation is followed by laser-induced fluorescence (LIF) method. By comparing the experiment with a numerical model, this experiment shall bring a new insight in the determination of thermodynamical constants for part of the reaction (the fastest one) involved in the atmospheric chemistry.

**Keywords:** atmospheric chemistry, OH radical, ozone, flash photolysis, laser induced fluorescence

## 1 Introduction

The hydroxyl radical dominates the daytime chemistry of the troposphere. It is responsible for the reactive removal of most trace gases such as hydrocarbons (in particular CH<sub>4</sub>) and is an active participant in the NO and NO<sub>2</sub> cycle.

We are developing a new LIDAR system, based on the well-known pump-and-probe principle allowing a new approach of the understanding of the atmospheric kinetic.

This method consist of an intense UV laser pulse (pump beam) to create a high concentration of OH by photodissociating O<sub>3</sub> in the presence of water molecules :



A second beam (probe laser) on axis with the pump beam excites the OH in the 282 nm absorption band and therefore the [OH] can be detected by LIF (~309 nm).

To check the well-referenced discrete absorption spectrum of OH, we measured first the OH laser-induced fluorescence in an OH-rich flame. In a second step, OH was generated by O<sub>3</sub> flash photolysis in a reaction cell : in the cell a flow of a controlled atmosphere (mixture of dry air, ozone, nitrogen, water vapour, methane and other gases) can be generated. Measurements of OH relaxation in the presence of different water vapour or methane concentrations in the cell show promising results and we succeed in measuring

the first "in situ" OH relaxation, that is by measuring the OH relaxation curve directly in the air of the lab, without cell.

A computer simulation based on both the chemical and physical properties of the atmosphere and including 53 species and 71 reactions allow a necessary comparison with the experimental measurements.

## 2. OH radical kinetic

The curves of the figure 1 show the decay time of OH in the presence of different concentrations of CH<sub>4</sub> in the reactor. In this figure, the pump step (the flash photolysis of O<sub>3</sub> to create OH) refers at a delay time = 0. The [OH] estimated from the LIF signal is of the order of 5\*10<sup>9</sup> molec./cm<sup>3</sup> which compared to the theoretical value (taking care of the initial O<sub>3</sub> / H<sub>2</sub>O concentrations, and the pump beam energy) is about 2 orders of magnitude lower than expected. By changing the delay between the Pump and the Probe beam, it is possible to "scan" the [OH] concentration versus the delay time, and to obtain a direct measurement of the OH life time. These curves reveal a clear decrease of OH relaxation time (46 ms → 6.5 ms) versus the increase of methane concentration (0 ppm → 500 ppm).

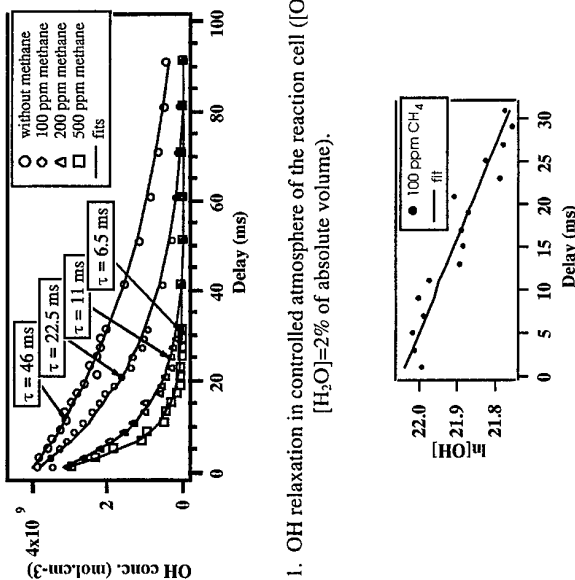


Figure 1. OH relaxation in controlled atmosphere of the reaction cell ([O<sub>3</sub>]=50 ppb, [H<sub>2</sub>O]=2% of absolute volume).

Figure 2. Slope of ln[OH] vs time in the 100 ppm CH<sub>4</sub> case.

The rate constant  $k_{\text{exp}}$  of this reaction was calculated from the slope of ln[OH] vs time (Figure 2) and the methane concentration :  $k_{\text{exp}} = 4 \cdot 10^{15} \text{ cm}^3/\text{molec.} \cdot \text{s}$ . This value is in a good agreement with  $k_{\text{ref}} = 7.7 \cdot 10^{15} \text{ cm}^3/\text{molec.} \cdot \text{s}$  [1] proving the validity of the method.

### 3. Conclusion

The technique is presented here as a local measurement but will be extended to a real range resolved method, with the possibility to measure different [OH] relaxation decay for different local air quality masses.

In the submillisecond time scale for the P-P delay, the Pump-and-Probe Lidar is a check of the "chemistry only" reactions, but for longer delay time, it will be also affected by the transport and diffusion induced by the wind, and therefore bring added information on the physical processes influencing the [OH] life time.

### 4. References

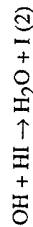
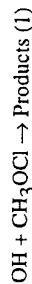
1. Warneck P.: Chemistry of the Natural Atmosphere, International Geophysics series, vol. 41 (1988).
2. G.H. Dieke and H.M. Crosswhite: The Ultraviolet Bands of OH. *J. Quant. Spectrosc. Radia. Transfer.* **2** (1962) 97-199
3. A. Clappier, B. Calpini, E. Durieux, L. Fiorani, L. Jaquet, H. van den Berg: Numerical Study of Pump and Probe Lidar Experiment For In Situ Tropospheric Measurement of The OH Radical. Submit. 17th International Laser Radar Conference, Sendai 1994, Japan.
4. T.J. McGee and T.J. McIlrath: Absolute OH Absorption Cross Sections (For LIDAR Measurement). *J. Quant. Spectrosc. Radia. Transfer.* **32** (1984) 179-184

### TEMPERATURE DEPENDENT KINETICS OF THE REACTIONS:



P. Campuzano-Jost, J.N. Crowley, G.K. Moortgat.  
*MPI für Chemie, Air Chemistry Division, 55020 Mainz, Germany*

The temperature dependence of the reaction of two expected stratospheric reservoir species, methylhypochlorite and hydrogen iodide with hydroxy radicals in the gas phase has been measured for the first time:

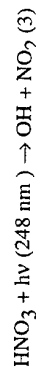


Methylhypochlorite has been shown to be a stable product of the reaction of methylperoxy with ClO at polar stratospheric conditions<sup>1</sup>. In order to evaluate the possible routes of chlorine release, the homogeneous reaction with OH and Cl radicals as well as the photodissociation rate has to be examined.

In recent times reactive cycles involving iodine chemistry has been proposed as an explanation of the arctic stratospheric ozone hole<sup>2</sup>. Formed by means of the reaction  $\text{HO}_2 + \text{I}$ , HI is believed to be one of the major reservoir species produced. As in the case of  $\text{CH}_3\text{OCl}$ , photodissociation and reaction with hydroxy radicals are the main expected sinks. Reaction 2 has been measured several times at room temperature<sup>3</sup>, but until now no temperature dependence has been examined.

The experiments were carried out in a newly build laser-photolysis/resonance fluorescence apparatus<sup>4</sup>. Rate constants were obtained directly at several temperatures by monitoring the decay of OH radicals in a large excess of  $\text{CH}_3\text{OCl}$  or HI. The sensitivity of the experimental setup towards OH is estimated as  $5 \cdot 10^{-7}$  counts  $\text{s}^{-1}$  [OH]-<sup>1</sup>. Reactants and radical precursors, diluted in argon bath gas, were flowed through a thermostated pyrex inlet before entering a teflon-coated stainless steel reaction vessel of ~150 ml volume.

OH formation was achieved by the flash photolysis of  $\text{HNO}_3$  at 248 nm:



<sup>1</sup>Crowley, J.N.; Helleis, F.; Müller, R. Moortgat, G.K.; Crutzen, P.J.; Orlando, J.J. *J. Geophys. Res.* 1994, 99, 20683.

<sup>2</sup>Solomon, S.; Garcia, R.R.; Ravishankara, A.R. *J. Geophys. Res.* 1994, 99, 20491.

<sup>3</sup>The current NASA-Panel evaluation is based on the data of Mac Leod, H.; Balestra, C.; Jourdain, J.L.; Laverdet, G.; Le Bras, G. *Int.J.Chem.Kinet.* 1990, 22, 1167.

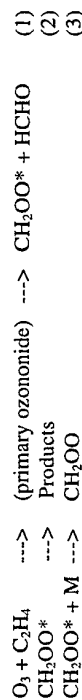
<sup>4</sup>Crowley, J.N.; Campuzano-Jost, P.; Moortgat, G.K. *J. Phys. Chem.* 1996, 100, 3601.

REACTIONS OF THE CRIGEE INTERMEDIATE  $\text{CH}_2\text{OO}$  WITH  $\text{HCHO}$ ,  
 $\text{HCOOH}$ ,  $\text{CH}_3\text{COOH}$ ,  $\text{CH}_3\text{OH}$  AND  
 $\text{H}_2\text{O}$  IN THE OZONOLYSIS OF SELECTED TERMINAL ALKENES

P. Neeb, O. Horie, F. Sauer, C. Schäfer, R. Winterhalter and G.K. Moortgat

Max-Planck-Institut für Chemie, Atmospheric Chemistry Department,  
 P.O. Box 3060, D-55020 Mainz, Germany  
 e-Mail: MOO@mpch-mainz.mpg.de

Despite numerous studies of the gas-phase ozonolysis of alkenes, reactions of stabilized Criegee radicals have received little attention. In the case of ethene, the initially formed excited Criegee intermediate  $\text{CH}_2\text{OO}$  partly decomposes to yield  $\text{CO}$ ,  $\text{CO}_2$ ,  $\text{H}_2$ ,  $\text{H}$ ,  $\text{H}_2\text{O}$ , etc, or is collisionally deactivated to form the stabilized intermediate  $\text{CH}_2\text{OO}^*$ :



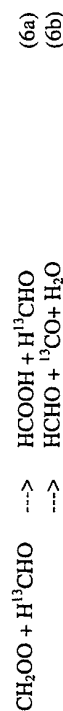
Ozonolysis of ethene and selected terminal alkenes  $\text{R}_1\text{R}_2\text{C}=\text{CH}_2$  (propene, isobutene, isoprene and  $\beta$ -pinene) was carried out in a 570 l spherical glass vessel at 296 K. Reactant concentrations were in the range 1-18 ppmv at a total pressure of 1 atm air. Relative changes in the product distribution due to the addition (in excess) of selected carbonyl compounds ( $\text{HCHO}$ ,  $\text{HCOOH}$  and  $\text{CH}_3\text{COOH}$ ) and hydroxy compounds ( $\text{H}_2\text{O}$  and  $\text{CH}_3\text{OH}$ ) were determined by means of FTIR-spectroscopy and/or HPLC. A detailed mechanism for gas-phase ozonolysis is deduced with the help of isotopic labelled carbon compounds.

Addition of  $\text{HCOOH}$  in the ozonolysis of ethene led to the formation of hydroperoxy methylformate  $\text{CHO-O-CH}_2\text{OOH}$  (HPMF), which was observed to slowly decompose to formic acid anhydride (FAN) [1].

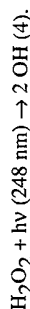


The FTIR spectrum of HPMF is identical to the spectrum assigned as hydroxy methylformate  $\text{CHO-O-CH}_2\text{OH}$  (HPMF, also known as "compound X") by Su *et al.* [1] and Niki *et al.* [2], and which is believed to be formed as a product of the reaction of  $\text{CH}_2\text{OO}$  with  $\text{HCHO}$ . In the absence of added  $\text{HCOOH}$ , the total yield of HPMF + FAN amounted to nearly 20 %, indicating that  $\text{HCOOH}$  is a main product formed in ozonolysis of ethene.

Upon the addition of  $\text{H}^{13}\text{CHO}$  to  $\text{C}_2\text{H}_4/\text{O}_3$  mixtures two reaction paths were identified:



The unfocused light of an excimer laser ( Lambda Physik Lextra 50 ) operated with a KrF<sub>6</sub> mixture was used. Laser energies were chosen so that secondary reactions due to  $\text{HNO}_3$  conversion and photolysis of  $\text{CH}_3\text{OCl}$  were reduced ( Laser fluence  $\sim 2\text{mJ cm}^{-2}$ ). For the HI experiments it was not possible to use  $\text{HNO}_3$  as the OH-radical source because of the fast reaction of HI with  $\text{HNO}_3$  under experimental conditions. Alternatively, hydrogen peroxide was used:



No energy dependence of the reaction system was observed within experimental error, so laser fluencies of about  $10 \text{ mJ cm}^{-2}$  were used.

$\text{CH}_3\text{OCl}$  was prepared by distilling methanol / KOH solutions saturated with gaseous chlorine at  $-10^\circ\text{C}$  and stored at  $-40^\circ\text{C}$  in the dark. Chlorine impurities were monitored by UV-Absorption.  $\text{HNO}_3$  was distilled from  $\text{KNO}_3/\text{H}_2\text{SO}_4$  mixtures and also kept in the dark at  $-40^\circ\text{C}$ .  $\text{H}_2\text{O}_2$  was used as a 75% aqueous solution (Solvay Interox). HI finally was made by drying hydroiodic acid (55%, Fluka) with  $\text{P}_4\text{O}_{10}$  at  $-30^\circ\text{C}$  and was stored at  $-50^\circ\text{C}$  in the dark after several distillations.

Typical experiments were carried out at 100 Torr and 0.5 sLm ( $\nu \sim 10\text{cm/s}$ , "slow-flow" - conditions), concentrations ranged from  $1\text{-}15 \times 10^{14} \text{ cm}^{-3}$   $\text{CH}_3\text{OCl}$  and  $7\text{-}50 \times 10^{12} \text{ cm}^{-3}$  HI. For the radical precursors,  $2.5 \times 10^{15} \text{ cm}^{-3}$   $\text{HNO}_3$  and  $3 \times 10^{14} \text{ cm}^{-3}$   $\text{H}_2\text{O}_2$  were chosen (corresponding OH concentrations of about  $2 \times 10^{11} \text{ cm}^{-3}$ ). Reaction temperatures were varied between 250 and 350 K ( $\text{CH}_3\text{OCl}$ ) and 280 and 360 K (HI).

Concentrations were calculated from flows. For HI, due to the very strong absorption on pyrex walls, concentrations were controlled a few times by ion chromatography of the aqueous solution.

The room temperature rate constants measured were:

$$k_1 = (7 \pm 1) \times 10^{-13} \text{ cm}^3 \text{s}^{-1} \quad \text{and} \quad k_2 = (6 \pm 2) \times 10^{-11} \text{ cm}^3 \text{s}^{-1}$$

No pressure dependence was observed for Reaction (1) in the range from 30 to 300 Torr. For Reaction (2), a control experiment at 160 Torr led to the same constant as at 75 Torr.

Arrhenius parameters measured for  $k_1$  were:

$$k_1(250\text{-}350\text{K}) = (2.4 \pm 0.8) \times 10^{-12} \exp(-(360 \pm 100)/T) \times 10^{-12} \text{ cm}^3 \text{s}^{-1}.$$

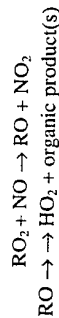
For  $k_2$  no temperature dependence in the range 280 - 360 K was observed within experimental error.

# THE CALCULATED FRACTIONAL RESPONSE OF THE CHEMICAL AMPLIFICATION TECHNIQUE TO TOTAL PEROXY RADICAL POPULATIONS ON BOUNDARY LAYER TRAJECTORIES OVER EUROPE

Michael E. Jenkin<sup>1</sup>, Richard G. Derwent<sup>2</sup> and Sandra M. Saunders<sup>3</sup>

<sup>1</sup>AEA Technology, Culham, UK; <sup>2</sup>Meteorological Office, Bracknell, UK; <sup>3</sup>University of Leeds, UK

The chemical amplification technique for the measurement of peroxy radicals is being increasingly employed in field studies of tropospheric chemistry. First developed by Cantrell and Siedman<sup>1</sup>, the technique is designed primarily for measuring the hydroperoxy radical, HO<sub>2</sub>, and relies on the HO<sub>2</sub> catalysed conversion of CO and NO into CO<sub>2</sub> and NO<sub>2</sub> by a rapid chain mechanism. Organic peroxy radicals, RO<sub>2</sub>, also contribute to the measured signal, if present in significant concentrations, since they are potentially converted to HO<sub>2</sub> in the presence of NO, via formation of the oxy radical, RO:

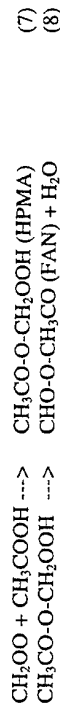


For simple RO radicals such as CH<sub>3</sub>O, the conversion to HO<sub>2</sub> occurs in a single step by reaction with O<sub>2</sub>. For more complex RO radicals, the mechanism may be multi-step, involving isomerisation and/or thermal decomposition reactions, but still usually yielding HO<sub>2</sub>. It is often assumed, therefore, that the amplification technique measures the total peroxy radical concentration, [HO<sub>2</sub>] + [RO<sub>2</sub>]. Owing to the existence of possible competing reactions for both RO<sub>2</sub> and RO, however, the fractional conversion of a given peroxy radical into HO<sub>2</sub> is influenced by the structure of the organic group "R". Depending on the precise peroxy radical population, therefore, the apparent total peroxy radical measurement made by the chemical amplification technique is potentially significantly lower than the true peroxy radical concentration under particular circumstances.

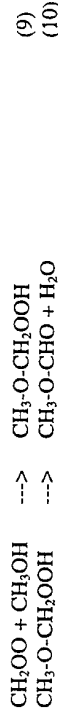
Available kinetic and mechanistic data on reactions of RO<sub>2</sub> and RO radicals have been used to estimate the fractional conversions of ca. 500 organic peroxy radicals into HO<sub>2</sub>, for typical reagent conditions in a chemical amplification instrument ([CO] = 5%; [NO] = 5 ppmv; P = 760 Torr; T = 298K). The peroxy radicals are those generated in a recent detailed chemical mechanism describing the degradation of 120 VOCs<sup>2</sup>. Examples of calculated fractional conversions are 73% for CH<sub>3</sub>O<sub>2</sub>, 87% for C<sub>2</sub>H<sub>5</sub>O<sub>2</sub>, 85% for *i*-C<sub>3</sub>H<sub>7</sub>O<sub>2</sub>, 16% for *t*-C<sub>4</sub>H<sub>9</sub>O<sub>2</sub>, 97% for HOCH<sub>2</sub>CH<sub>2</sub>O<sub>2</sub> and 73% for CH<sub>3</sub>C(O)O<sub>2</sub>. The chemical mechanism has been incorporated into a photochemical trajectory model<sup>3</sup>, and has been used to calculate peroxy radical populations on boundary layer trajectories over Europe. This has allowed the fractional response of the chemical amplification technique to total peroxy radical populations to be calculated for a range of realistic scenarios.

with a branching ratio (a):(b) of 4:1. This result indicates that CH<sub>2</sub>OO is in part converted via reaction path (3a) into HCOOOH, which then reacts with CH<sub>2</sub>OO to form HPMF.

The addition of excess CH<sub>3</sub>COOH suppressed the formation of HPMF and FAN, and an analogous compound hydroperoxy methylacetate (HPMA) was identified, decomposing to formic acetic anhydride [4]:



Also, CH<sub>3</sub>OH was found to react with CH<sub>2</sub>OO to yield methoxy methylhydroperoxide, which was observed to slowly decompose to CH<sub>3</sub>-O-CHO [5]:

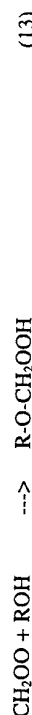


Hydroxymethyl hydroperoxide HOCH<sub>2</sub>OOH (HMHP) was found to be the sole product in the reaction of stabilized Criegee radical with water vapour. HMHP was converted to HCOOH in a heterogeneous reaction.

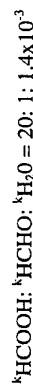


The yield of [HMHP + HCOOH] and thus of stabilized CH<sub>2</sub>OO Criegee radicals was measured relative to ozone consumption for a series of terminal alkenes: 42 % for ethene, 14 % for propene, 13 % for isobutene, 30 % for isoprene [5] and 18 % for β-pinene [Winterhalter, Diplom Thesis, 1995].

In conclusion, the stabilized Criegee biradical CH<sub>2</sub>OO was observed to yield in each case (except HCHO) a product which can be represented by the formula R-O-CH<sub>2</sub>OOH (R=CHO, CH<sub>3</sub>CO, CH<sub>3</sub> and H):



The reactivity was observed to increase in the following order: H<sub>2</sub>O << CH<sub>2</sub>OH << HCOOH = CH<sub>3</sub>COOH. Relative rates of reaction of CH<sub>2</sub>OO with HCOOH, HCHO and H<sub>2</sub>O were obtained with the help of computer simulation [Neeb, Ph. D. Thesis, 1996]:



The atmospheric relevance of the reactions involving Criegee biradicals will be discussed.

## References

- (1) P. Neeb, O. Horie and G. K. Moortgat, Chem. Phys. Lett., **246**, 150 (1995).
- (2) F. Su, J.G. Calvert and J.H. Shaw, J. Phys. Chem., **84**, 239 (1980); H. Niki, P.D. Maker, C.M. Savage and L.P. Breitenbach, J. Phys. Chem., **85**, 1024 (1980).
- (3) P. Neeb, O. Horie and G. K. Moortgat, Int. J. Chem. Kinet., in press (1996).
- (4) P. Neeb, O. Horie and G. K. Moortgat, submitted (1996).

# KINETICS OF THE THERMAL DECOMPOSITION OF THE CH<sub>3</sub>SO<sub>2</sub> RADICAL AND ITS REACTION WITH NO<sub>2</sub> AT 1 TORR AND 298K

A. Ray\*, I. Vassalli, G. Laverdet and G. Le Bras.

*Laboratoire de Combustion et Systemes Reactifs, CNRS, 45071 Orleans Cedex, France.*

CH<sub>3</sub>SO<sub>2</sub> radical is an important intermediate species in the atmospheric oxidation mechanism of dimethyl sulfide (DMS), initiated by OH radicals during daytime and NO<sub>3</sub> radical during night time. CH<sub>3</sub>SO<sub>2</sub> can decompose to produce SO<sub>2</sub> or be oxidized by species like NO<sub>2</sub> and O<sub>3</sub> to form CH<sub>3</sub>SO<sub>3</sub>, which is a precursor of methane sulphonic acid (MSA, CH<sub>3</sub>SO<sub>3</sub>H). Thus the fate of CH<sub>3</sub>SO<sub>2</sub> is a key process since it can influence the SO<sub>2</sub>/MSA yield which determines the possible regulatory influence of DMS on the Earth's climate through the formation of aerosols and cloud condensation nuclei (CCN)<sup>1</sup>. The kinetics and mechanism of the thermal decomposition of CH<sub>3</sub>SO<sub>2</sub> and its reaction with NO<sub>2</sub> have been investigated in a discharge-flow study of the Cl/CH<sub>3</sub>SH/NO<sub>2</sub> system. In this system, CH<sub>3</sub>S, produced by reaction of Cl atoms with CH<sub>3</sub>SH, initiated the following sequence of reactions:



CH<sub>3</sub> radical further reacted with NO<sub>2</sub> to produce CH<sub>3</sub>O radical, the time constant of CH<sub>3</sub> / CH<sub>3</sub>O conversion being less than 0.4 ms. The rate constants k<sub>1</sub> and k<sub>2</sub> are known. But no experimental determination of k<sub>3</sub> has been reported so far. The only one previous determination of k<sub>4</sub> had been obtained in our laboratory<sup>2</sup>, also from a discharge flow study of the Cl/CH<sub>3</sub>SH/NO<sub>2</sub> system, but in a more indirect way through determination of SO<sub>2</sub> by mass spectrometry, and omitting reaction (3) in the chemical mechanism used in model calculation. In the present study, the rate constants k<sub>3</sub> and k<sub>4</sub> have been determined by a fitting procedure of calculated kinetic profiles to experimental profiles of SO<sub>2</sub> and CH<sub>3</sub>O, obtained by laser induced fluorescence (LIF) analysis.

The discharge flow apparatus equipped with laser induced fluorescence and quadrupole mass spectrometric detection are described elsewhere<sup>3</sup>. The LIF excitation source was frequency doubled radiation of a Lambda Physik dye laser pumped by an excimer (XeCl) laser. The CH<sub>3</sub>O was detected by LIF via its electronic transition (A<sup>2</sup>A' - X<sup>2</sup>E) either at 292.8 nm or at 298.3 nm band. SO<sub>2</sub> was also detected by LIF via its electronic transition (A<sup>1</sup>B<sub>1</sub> - X<sup>1</sup>A<sub>1</sub>) around 300 nm. The clear observation of characteristic peaks of SO<sub>2</sub> and CH<sub>3</sub>O in the recorded (290-305 nm) excitation spectra of the products of the CH<sub>3</sub>S/NO<sub>2</sub> kinetic system, confirmed formation of CH<sub>3</sub>O and SO<sub>2</sub>. Fluorescence signal intensities of CH<sub>3</sub>O and SO<sub>2</sub> were measured as a function of reaction time in the reactor. Typical temporal profiles of CH<sub>3</sub>O and SO<sub>2</sub> LIF signals are shown in figure 1. Such temporal profiles were measured using the following ranges of initial concentrations of the reactants: [Cl]<sub>0</sub> = (1.4-2.4) × 10<sup>12</sup>, [Cl<sub>2</sub>]<sub>0</sub> = (1.9-9.4) × 10<sup>11</sup>, [CH<sub>3</sub>SH]<sub>0</sub> = (2.3-6.4) × 10<sup>12</sup>,

<sup>1</sup>Cantrell C.A. and Stedman D.H. (1982). A possible technique for the measurement of atmospheric peroxy radicals. *Geophys. Res. Lett.*, **9**, 846-849.

<sup>2</sup>Jenkin M.E., Saunders S.M. and Pilling M.J. (1996). Constructing a detailed chemical mechanism for use in tropospheric chemistry models. Report AEA/RAMP/18360008/003, AEA Technology, Culham, UK.

<sup>3</sup>Derwent R.G., Jenkin M.E., Pilling M.J. and Saunders S.M. Development and application of a master mechanism for regional scale photochemical ozone formation in Europe. Proceedings of the EUROTRAC Symposium, Garmisch-Partenkirchen, Germany, March 1996.

$[NO_2]_0 = (1.5 \times 10^{14})$  (units are in molecule  $cm^{-3}$ ). The high sensitivity of the temporal profiles of  $SO_2$  and  $CH_3O$  to  $NO_2$  concentration and the mass spectrometric identification of product MSA at  $m/e=96$ , suggested the reaction:

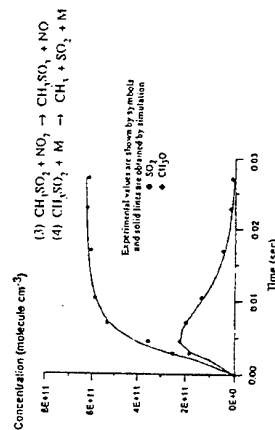
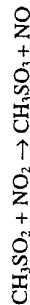


Fig. 1: Typical temporal concentration profile of  $SO_2$  and  $CH_3O$  in the  $CH_3S/NO_2$  system.

The observed concentration-time profiles of  $SO_2$  and  $CH_3O$  were compared to those obtained from simulation by the reaction mechanisms. A non-linear least square program, FACSIMILE, was used to simulate profiles of  $SO_2$  and  $CH_3O$ , using  $k_3$  and  $k_4$ , as variable parameters. The mean values of  $k_3$  and  $k_4$ , with one standard deviation were:

$$k_3 = (2.2 \pm 1.1) \times 10^{12} \text{ cm}^3 \text{ molecule}^{-1} \text{ s}^{-1}, k_4 = (510 \pm 150) \text{ s}^{-1}$$

The error on  $k_3$  is fairly high and mainly results from the complexity of the chemical mechanism used for modelling calculation. The present value of  $k_4$  at 298K, combined with an activation energy,  $E = 18 \text{ Kcal mol}^{-1}$ , reported by Benson<sup>4</sup> gives the following Arrhenius expression:

$$k_4 = 6.5 \times 10^{15} \exp(-1800/RT) \text{ s}^{-1}$$

The present study of the  $CH_3S/NO_2$  system has shown evidence for a competition between the thermal decomposition of  $CH_3SO_2$  to  $CH_3 + SO_2$  and the reaction with  $NO_2$  to form  $CH_3SO_3 + NO$ . It also provides some insight into the relative rates of reactions (3) and (4), which can influence the  $MSA/SO_4^{2-}$  ratio, the  $SO_4^{2-}$  species being produced from  $SO_2$  oxidation.

\*Present address: Bhabha Atomic Research Centre, Laser & Plasma Technology Division, Bombay 400 085, India.

## References

- (1) Charlson, J.E. Lovelock, M.O. Andreae, S.G. Warren, *Nature* **326**, 655, 1987.
- (2) Mellouki, J.L. Jourdain, G. Le Bras, *Chem. Phys. Lett.* **148**, 231, 1988.
- (3) Daele, A. Ray, I. Vassalli, G. Poulet, G. Le Bras, *Int. J. Chem. Kinet.* **27**, 1121, 1995.
- (4) Benson, *Chem. Rev.* **78**, 23, 1978.

## GAS-PHASE ULTRAVIOLET ABSORPTION CROSS-SECTIONS AND ATMOSPHERIC LIFETIMES OF SEVERAL $C_2 - C_5$ ALKYL NITRATES.

Kevin C. Clemitshaw<sup>1</sup>, Jonathan Williams<sup>2</sup>, Oliver V. Rattigan<sup>3</sup>, Dudley E. Shallcross<sup>4</sup>,  
Kathy S. Law<sup>4</sup> and R. Anthony Cox<sup>4</sup>

<sup>1</sup>Centre for Environmental Technology, Imperial College of Science, Technology and Medicine, Silwood Park, Ascot, SL5 7PY (UK)

<sup>2</sup>Aeronomy Laboratory, National Oceanic and Atmospheric Administration, R/E/AL6, 325, S. Broadway, Boulder, Colorado, CO 80303 (USA)

<sup>3</sup>Eugene F. Merkert Chemistry Center, Department of Chemistry, Boston College, Chestnut Hill, Massachusetts, MA 02167-3860 (USA)

<sup>4</sup>Centre for Atmospheric Science, Department of Chemistry, University of Cambridge, Lensfield Road, Cambridge CB2 1EW (UK)

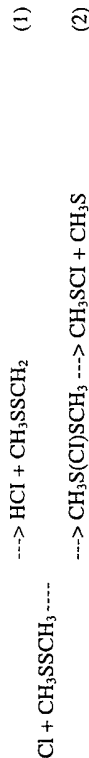
Gas-phase ultraviolet absorption cross-sections of ethyl nitrate, 1-propyl nitrate, 2-propyl nitrate, 2-methyl-1-propyl nitrate, 1-butyl nitrate and 1-pentyl nitrate have been measured over the wavelength range 220-340 nm using a dual-beam, diode array spectrometer. Each alkyl nitrate spectrum appears to be the sum of at least two Gaussian-shaped absorptions with an intense p-p\* band extending from 190-240 nm having a shoulder between 250-340 nm due to a n-p\* system. The absorption cross-sections recorded for ethyl nitrate, 1-propyl nitrate, 2-propyl nitrate and 1-butyl nitrate are within 10% of previous data: those of 2-methyl-1-propyl nitrate and 1-pentyl nitrate have been measured for the first time. For ethyl nitrate, absorption cross-sections between 280-340 nm in the tail of the near-ultraviolet band declined with decreasing temperature from 298-233 K. A two-dimensional numerical model of tropospheric chemistry was used to calculate atmospheric lifetimes with respect to photodissociation and OH radical reaction that are markedly dependent on season, latitude and altitude. Relatively long, surface level atmospheric lifetimes of several days to weeks confirm that the  $C_2-C_5$  alkyl nitrates may act as temporary reservoirs for NOx and suggest that they may also constitute a significant fraction of total reactive odd-nitrogen, NOy, particularly during winter at northern hemisphere high-latitudes.

## REACTION OF ATOMIC CHLORINE WITH DIMETHYLDISULFIDE

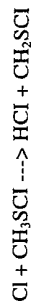
Kyriakos G. Kambanis, Yannis G. Lazarou and Panos Papagiannakopoulos

Department of Chemistry, University of Crete, Heraklion 71409, Crete, Greece.

The reaction of atomic chlorine with dimethyldisulfide  $\text{CH}_3\text{SSCH}_3$  was studied in the gas phase and over the temperature range 273 - 363 K with the very low pressure reactor (VLPR) technique. The reaction occurs via two competing pathways:



The hydrogen atom abstraction pathway proceeds with a temperature dependent rate that is given by the expression  $k_1 = (1.11 \pm 0.20) \times 10^{-10} \exp(-0.27 \pm 0.20/RT) \text{ cm}^3 \text{ molecule}^{-1} \text{ s}^{-1}$ , (R in kcal mol<sup>-1</sup> K<sup>-1</sup>). The S-S bond scission pathway proceeds via the formation of an intermediate  $\text{CH}_3\text{S}(\text{Cl})\text{SCH}_3$  adduct, which further decomposes to  $\text{CH}_3\text{SCI}$  and  $\text{CH}_3\text{S}$  fragments; its rate depends inversely on temperature and is given by the expression  $k_2 = (5.45 \pm 0.11) \times 10^{-11} \exp(0.78 \pm 0.02/RT) \text{ cm}^3 \text{ molecule}^{-1} \text{ s}^{-1}$ . The branching ratio  $k_1/k_2$  was 0.36 at room temperature, indicating that the second pathway is the dominant one. The secondary reaction of atomic Cl with  $\text{CH}_3\text{SCI}$  was also observed:



with a temperature independent rate ca.  $8.0 \pm 3.0 \times 10^{-11} \text{ cm}^3 \text{ molecule}^{-1} \text{ s}^{-1}$ .

KINETIC AND MECHANISTIC STUDIES OF THE FORMATION AND REACTION OF THE OHDS AND OHCS<sub>2</sub> ADDUCTS.

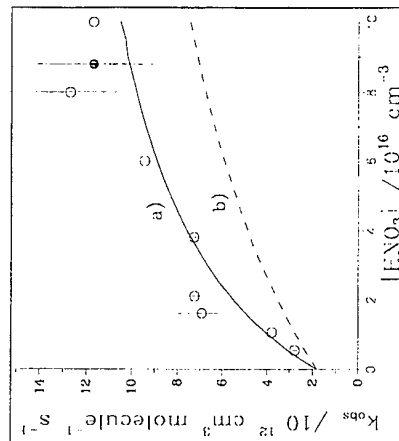
A. J. Hynes, C. J. Nien, R. C. Richter and E. Silvente

Division of Marine and Atmospheric Chemistry, Rosenstiel School of Marine and Atmospheric Science, University of Miami, 4600 Rickenbacker Causeway, Miami, FL 33149, USA

The important role which weakly bound complexes can play in atmospheric chemistry is well illustrated by the oxidation of two trace sulfur species carbon disulfide ( $\text{CS}_2$ ) and dimethylsulfide,  $\text{DMS}$ , ( $(\text{CH}_3)_2\text{S}$ ). In both cases, although there is some controversy about the detailed oxidation mechanisms, most experimental studies are consistent with mechanisms which involve the formation of a weakly bound adduct with OH followed by adduct reaction with  $\text{O}_2$ . Routes to determination of elementary rates include observation of biexponential decays or observation of rate enhancements in the presence of an adduct scavenger. These approaches have been used previously in studies of the reactions of  $\text{CS}_2$  and  $\text{DMS}$  with OH. Smith and co-workers have proposed that observations of the rate of vibrational deactivation of OH ( $\nu=1$ ) may offer a route to limiting high pressure association rates. If this approach is applicable to weakly bound species it offers a route to rate coefficients that would be extremely difficult, (particularly for OH +  $\text{DMS}$ ) to measure directly. In this work we report on a series of studies which are aimed at using these methods to determine elementary rates and detailed reaction mechanisms and also to examining adduct reactivity trends. Our studies utilize the Pulsed Laser Photolysis-Pulsed Laser Induced Fluorescence (PLP-PLIF) technique to monitor the decay of OH ( $\nu=3,2,1,0$ ) in the presence of reactants.

The equilibration of OH with  $\text{CS}_2$  has been directly observed at several pressures of  $\text{N}_2$  at 270K. Analysis of biexponential decays gives the elementary rates for adduct formation and decomposition. Fitting the forward addition rates to a fall-off curve gives a high pressure limiting rate of  $1 \times 10^{-12} \text{ cm}^3 \text{ molecule}^{-1} \text{ s}^{-1}$ , slightly higher than the current IUPAC recommendation. The adduct reaction with  $\text{O}_2$  has been measured at 270K and we obtain a rate coefficient of  $2.4 \times 10^{-14} \text{ cm}^3 \text{ molecule}^{-1} \text{ s}^{-1}$ .

We have examined the reaction of OH with  $\text{DMS}$  in the presence of high concentrations of nitric acid. We determined observed rate coefficients for the reactions of OH with both  $\text{DMS}$  and  $\text{DMS-d}_6$  over a range of pressures between 220 K and 350 K. The work reported here focuses on a systematic study of the  $\text{DMS-d}_6$  reaction between 280 K and 350 K at 700 Torr total pressure and nitric acid partial pressures of up to 3 Torr. Under atmospheric conditions the rate coefficient for the reaction of OH with  $\text{DMS}$  is dependent on oxygen partial pressure and appears to proceed by a two channel mechanism, involving either hydrogen abstraction or OH



# LABORATORY AND MODELLING STUDIES OF HO<sub>x</sub> FORMATION AND CYCLING.

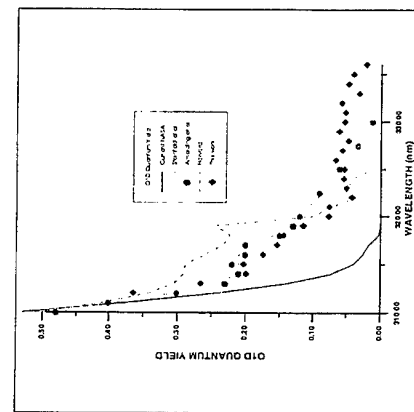
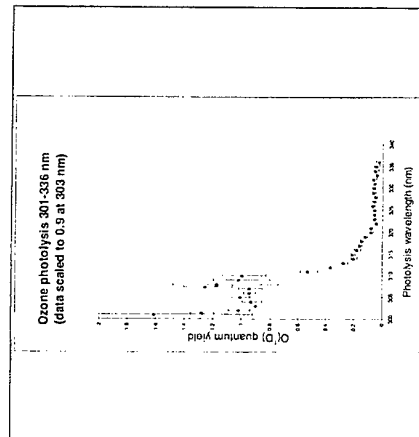
A. J. Hynes, R. C. Richter, C. J. Nien, E. Silvente, M. Zheng and E. S. Saltzman  
*Division of Marine and Atmospheric Chemistry, Rosenstiel School of Marine and Atmospheric Science, University of Miami, 4600 Rickenbacker Causeway, Miami, FL 33149, USA*

The chemistry of the hydroxyl radical, OH, drives chemical transformation in the troposphere and its chemistry has been the subject of particularly intense scrutiny. As a consequence attempts to measure OH concentrations and confirm current theories of fast photochemical cycling have been a major thrust in tropospheric chemistry over the past twenty years. Recent developments in measurement techniques suggest that reliable OH measurements are now possible and a series of instruments have reported both tropospheric and stratospheric OH measurements.

In this work we report on laboratory measurements and a modelling study of some reactions which play an important role in controlling OH concentration levels and [OH]:[HO<sub>2</sub>] ratios.

## O'D Production.

In this work we have focussed on the effects on uncertainties in the quantum yield for the production of O'D,  $\Phi_{O'D}$ , on the concentration of OH predicted by a photochemical model. A model which uses currently recommended (NASA, IUPAC) values of  $\Phi_{O'D}$  significantly (10-20%) underpredicts the peak and average OH concentrations in comparison with a model which uses a more realistic  $\Phi_{O'D}$  at  $\lambda > 320$  nm. These effects become more pronounced at large solar zenith angles. We report a series of preliminary measurements which assess the utility of OH ( $\nu=1$ ) detection as a spectroscopic marker for O'D in the long wavelength photolysis of O<sub>3</sub>. Figure 1 shows the quantum yields and Figure 2 shows a comparison of recent determinations at  $\lambda > 310$  nm. Our results confirm that  $M_{O'D}$  is significant at wavelengths greater than 320 nm and established the threshold for O'D formation at  $\lambda > 335$  nm.



addition to form a weakly bound adduct. The adduct can decompose to reform the reactants or react further with oxygen to form products. We have observed a dramatic enhancement in the observed rate coefficients of both the DMS and DMS-d<sub>6</sub> reactions in the presence of nitric acid. The figure shows the enhancement in the observed rate coefficient for OH + DMS-d<sub>6</sub> in 700 Torr of N<sub>2</sub> at 298 K. Qualitatively, the dependence of the observed rate coefficient on [HNO<sub>3</sub>] is similar to the "oxygen enhancement" in the effective rate coefficient for the reactions of OH with DMS and DMS-d<sub>6</sub>. The rate enhancement observed for OH + DMS-d<sub>6</sub> in 700 Torr of O<sub>2</sub> at 298 K is  $4.5 \times 10^{12}$  cm<sup>3</sup> molecule<sup>-1</sup> s<sup>-1</sup>. Less than 1 Torr of HNO<sub>3</sub> appears to produce an equivalent effect! A simulation of the observed rate enhancement based on the previously reported mechanism, elementary rates and adduct thermochemistry is in qualitative agreement with the observations. Quantitative agreement implies that the frequency of reaction of the OH adduct with HNO<sub>3</sub> exceeds the hard-sphere collision frequency. Such a result may be consistent with the formation of a complex which leads to rearrangement of the OH adduct. These experiments provide a route to the determination of the elementary rates for adduct formation under realistic atmospheric conditions.

To investigate the utility of measurements of vibrational deactivation rates of OH ( $\nu \geq 1$ ) as a route to the limiting high pressure association rate,  $k_{\infty}$ , we have measured rates with DMS, CS<sub>2</sub> and CH<sub>3</sub>SH. We generate OH ( $\nu > 0$ ) chemically via photolysis of ozone followed by O'D + HX. We pump off-diagonal A-X transitions at  $\sim 350$  nm and monitor blue-shifted fluorescence in the diagonal transitions at  $\sim 308$ -320 nm. To test the approach we have measured deactivation rates with H<sub>2</sub>O, NH<sub>3</sub> and CH<sub>4</sub> and find good agreement with previous determinations.

## Comparison of measured deactivation rates for OH ( $\nu = 1, 2, 3$ ):

Collider	k <sub>3</sub>	k <sub>2</sub>	k <sub>1</sub>	Ref
H <sub>2</sub> O	6.94(-11)	2.8(-11) 2.6(-11)	1.6(-11) 1.3(-11)	This work Raiche et al.
NH <sub>3</sub>		1.0(-10) 1.0(-10)	2.5(-11) 2.5(-11)	This work Raiche et al.
CH <sub>4</sub>	4.5(-12) 6.8(-12)	2.0(-12) 2.5(-12) 1.5(-12)	5.1(-13) 5.0(-13) 5.1(-13)	This work Raiche et al. Cheskis et al.
DMS		5.3(-11)	2.6(-11)	This work
CS <sub>2</sub>		1.6(-11)	1.2(-11)	This work
CH <sub>3</sub> SH		2.4(-11)	2.3(-11)	This work

The rates will be compared with thermal measurements and their implications for the determination of  $k_{\infty}$  will be discussed.

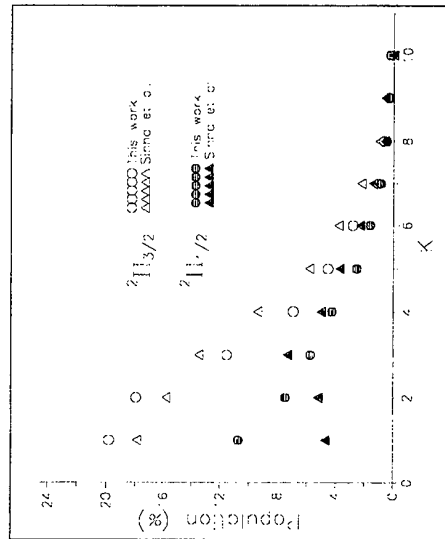
## Mass Resolved REMPI detection of O'D.

We have detected O'D using mass-identified REMPI at 276 nm. The main feature is the (3+1) 3d'  $1\pi^0$ -2p' $1\pi$  transition. The other features are three photon resonances but a number of singlet or "spin-orbit mixed" triplets are candidates for assignment. This is the first reported observation of these transitions for O'D detection.

**Laser Photofragmentation-Laser Induced Fluorescence (LP-LIF) Detection of HO<sub>2</sub>**  
We have developed a scheme for HO<sub>2</sub> detection using photofragmentation followed by LIF detection. HO<sub>2</sub> was generated by laser photolysis of a precursor molecule, via fast chemistry. The radical was photolyzed at 212 nm by a second laser, generating O and OH fragments. The OH was then detected via LIF by a third laser. The second and third laser pulses were generated by a single Nd-Yag pumped dye laser system and the third "detection" pulse overlapped or was slightly delayed with respect to the second "fragmentation" pulse. Under these conditions the OH LIF signal is directly proportional to the HO<sub>2</sub> radical concentration. By varying the delay between the first laser pulse, which initiates production, and the second and third laser pulses, which monitor HO<sub>2</sub> concentration, temporal profiles of the radical were mapped out.

To determine the optimum pumping configuration we have studied the 212 nm photodissociation of HO<sub>2</sub> and determined the energy disposal in the OH and O fragments. We find that OH is formed in v=0 with a little rotational excitation. O atoms are formed predominantly in the O'D state. Figure 3 shows the rotational distributions together with recent work of Sinha et al.

We have demonstrated that LP-LIF has the sensitivity and temporal resolution to be useful for kinetic studies under realistic atmospheric conditions. We have obtained high quality temporal profiles in 300 Torr of N<sub>2</sub> at an initial HO<sub>2</sub> concentration of 5x10<sup>12</sup> cm<sup>-3</sup>. At these concentrations the loss of HO<sub>2</sub> is due to diffusion, disproportionation makes a very small contribution. The s/n at [HO<sub>2</sub>]=2x10<sup>11</sup> cm<sup>-3</sup> is 6, were s/n is defined as (signal-background)/(σ background).



## ATMOSPHERIC FATE OF ALKYL NITRATES: REMOVAL VIA OH REACTIONS AND SOLAR PHOTOLYSIS

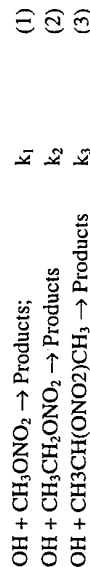
R.K. Talukdar,<sup>a</sup> J. B. Burkholder,<sup>a</sup> S. Herndon,<sup>b</sup> M. Hunter,<sup>b</sup> M. K. Gilles,<sup>a</sup> J. M. Roberts, and A. R. Ravishankara<sup>ab</sup>

*National Oceanic and Atmospheric Administration, Aeronomy Laboratory  
325 Broadway, Boulder CO 80303 USA*

Oxides of nitrogen, NO<sub>x</sub>, are key ingredients in the photochemical production of tropospheric ozone. They may be produced locally or imported from other regions of the troposphere. Alkyl nitrates (RONO<sub>2</sub>) are one class of compounds that may be carriers of nitrogen-oxides from source regions to NO<sub>x</sub>-deficient locations, even over long distances. The efficiency with which they transport NO<sub>x</sub> depends on the atmospheric loss processes for alkyl nitrates. In this paper, laboratory studies of the loss processes are presented and their implication to the atmosphere is discussed. The loss processes considered here are the reactions with OH radicals and UV Photolysis.

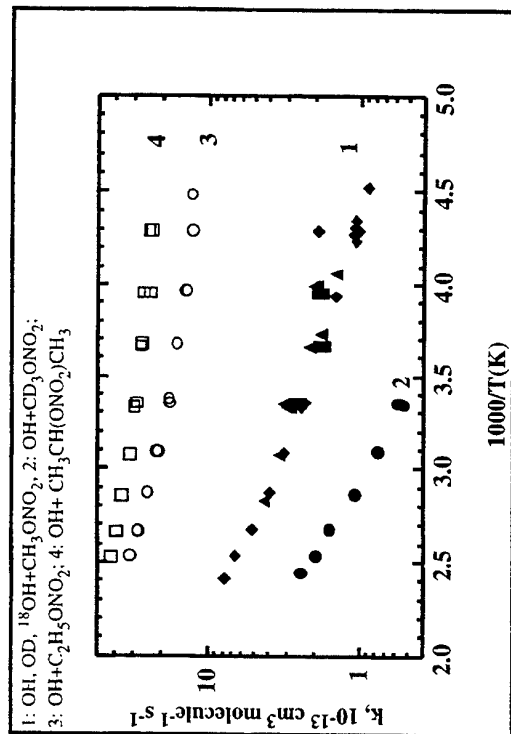
The UV absorption cross sections of methyl, ethyl, and isopropyl nitrates were measured using a diode array spectrometer over the wavelength range 233 to 350 nm and between 240 and 360 K. Photodissociation of methyl nitrate was investigated at 193, 248, and 308 nm using transient absorption and resonance fluorescence detection techniques. Transient absorption was used to measure the yields of NO<sub>3</sub>, CH<sub>3</sub>ONO (formed from the CH<sub>3</sub>O fragment via reaction with NO), HONO, and CH<sub>3</sub>O while atomic resonance fluorescence was used for H and O atoms. Detection of NO<sub>3</sub> involved 662 nm diode laser absorption while the detection of CH<sub>3</sub>ONO, HONO, and CH<sub>3</sub>O utilized a diode array spectrometer. The photodissociation quantum yield for CH<sub>3</sub>ONO<sub>2</sub> was found to be unity with the major products being NO<sub>2</sub> and CH<sub>3</sub>O.

The rate coefficients for the reaction:



were measured using the pulsed photolysis-laser induced fluorescence technique between ~220 and ~400 K. We found large discrepancies between our values and those in the literature. In an attempt to search for systematic errors and explore the mechanisms of these reactions, the rate coefficient for the reactions of <sup>18</sup>OH and OD with CH<sub>3</sub>ONO<sub>2</sub> and those of OH and OD with CD<sub>3</sub>ONO<sub>2</sub> were also measured. Experimental conditions were varied over wide ranges and some measurements were carried out in the presence of O<sub>2</sub>. None of these changes significantly affected the

measured rate coefficients. A few of the measured rate coefficients are shown in the form of an Arrhenius plot in the Figure below. (For the sake of clarity, not all the data is shown).



Based on these studies, we believe that the  $\text{OH} + \text{CH}_3\text{ONO}_2$  reaction proceeds via abstraction of the H atom and that our measured rate coefficients are accurate and applicable to the atmosphere.

The OH rate coefficients, UV absorption cross sections and the photodissociation quantum yields were used to evaluate the atmospheric loss processes for methyl, ethyl, and isopropyl nitrates. It was assumed that the photodissociation quantum yields for ethyl and isopropyl nitrates were unity, as in the case of methyl nitrate. The primary finding was that the photolysis, rather than the reaction with the OH radicals, control the lifetime of alkyl nitrates in the troposphere. These lifetimes vary between 10 and 40 days, with methyl nitrate being the most stable. The kinetics data provides some insight into the mechanism for the OH + alkyl nitrate reactions.

a. Also associated with the Cooperative Institute for Research in Environmental

Research (CIRES), University of Colorado, Boulder CO 80309

b. Also Associated with Department of Chemistry and Biochemistry, University of Colorado, Boulder CO 80303

## THE EFFECT OF OXYGEN PRESSURE IN THE TROPOSPHERIC OXIDATION OF ETHERS

D.P.Starkey, K.A.Holbrook, G.A.Oldershaw and R.W.Walker.

*School of Chemistry University of Hull, UK.*

The oxidation under simulated atmospheric conditions of a large number of compounds has been studied in recent years in connection with atmospheric pollution from various sources [1].

The work described in this paper is concerned with the oxidation of simple aliphatic ethers and also with larger molecules such as methyl- and ethyl tertiary butyl ether which have been used as fuel additives. The oxidation has been carried out by the use of OH radicals generated by the UV photolysis of methyl nitrite and has concentrated largely upon product analysis rather than on relative rate measurements which have received much attention in previous studies.

Oxidation mixtures containing approximately 1000 mTorr of the ether, 400 mTorr of NO and 150 mTorr of methylnitrite were diluted to atmospheric pressure in nitrogen containing variable amounts of oxygen. These mixtures were irradiated using conventional UV sources in either a 0.25L Pyrex or 16.0L Quartz vessel.

Product analyses showed reasonable agreement with other workers as is shown in Table 1 for a mixture containing 20% oxygen. This table also shows the results of Cl-initiated experiments using the photolysis of chlorine in place of methyl nitrite.

**Table 1.** Comparison of experimental results with those of other workers.

	Average yield Ethylformate	Average yield Ethylacetate	Average yield Acetaldehyde
This work Cl initiated	$0.787 \pm 0.035$	$0.0710 \pm 0.007$	$0.114 \pm 0.0127$
This work OH initiated	$0.645 \pm 0.0197$	$0.0702 \pm 0.012$	$0.132 \pm 0.0201$
Eberhard et al. [2]	$0.84 \pm 0.05$	$0.06 \pm 0.01$	$0.10 \pm 0.03$
Eberhard et al. [3]	$0.66 \pm 0.14$	$0.04 \pm 0.03$	$0.08 \pm 0.02$
Wallington [4]	$0.92 \pm 0.06$	$<0.05$	$<0.05$
Prediction (Baldwin) [5]	0.95	0.04	0

The effect of varying the percentage of oxygen on the oxidation of diethylether are shown in Table 2. The results show that neither ethylformate nor ethylacetate yield is much affected by oxygen.

Table 2. Results for diethylether - variation of oxygen pressure

% Oxygen	Ethylformate	Ethylacetate	Acetaldehyde
1	0.673 ± 0.024	0.0752 ± 0.0029	0.101 ± 0.011
20	0.645 ± 0.0205	0.0702 ± 0.0122	0.132 ± 0.020
50	0.638 ± 0.031	0.0844 ± 0.0028	0.161 ± 0.005
Effectively 100	0.660 ± 0.024	0.0998 ± 0.0027	0.147 ± 0.009

It is instructive to consider the ethylacetate/ethylformate ratio as a function of oxygen pressure. The previously accepted mechanisms [3,4] for the oxidation of ethers and other atmospheric additives, under these conditions, would predict a direct dependence of this ratio upon oxygen concentration since ethylformate would be presumed to arise by a decomposition step and ethylacetate by an oxygen dependent step from the most likely radical intermediate. Results will be presented which show that the ratio ethylacetate/ethylformate is largely independent of oxygen pressure.

One possible explanation for this lack of oxygen-dependence could be the involvement of oxygen in the production of both ethylformate and ethylacetate and a possible mechanism is proposed, which is consistent with thermochemical predictions. Similar results have been obtained and are reported for other ethers and also for some hydrocarbons.

## References

- 1) R. Atkinson, *J. Phys. Chem. Ref. Data*, Monograph 2, 1994
- 2) J. Eberhard, M. Semadeni, D. W. Stocker and J. A. Kerr, *Proc. Eurotrac Symposium '92*, Garmisch-Partenkirchen, Germany, P. Borrell et al., Eds., SPB Academic Publishing Co., The Hague, 1992.
- 3) J. Eberhard, C. Muller, D. W. Stocker and J. A. Kerr, *Int. J. Chem. Kin.*, **25**, 639, 1993.
- 4) T. J. Wallington and S. M. Japar, *Environ. Sci. Technol.*, **25**, 410, 1991.
- 5) A. C. Baldwin, J. R. Barker, D. M. Golden and D. G. Hendry, *J. Phys. Chem.*, **81**, 2483, 1977.

## A RELATIVE RATE STUDY OF THE REACTIONS OF ACYLPEROXY RADICALS WITH NO AND NO<sub>2</sub>, PEROXYACETYL NITRATE (PAN) AND PEROXYPROPYONYL NITRATE (PPN) FORMATION UNDER LABORATORY CONDITIONS RELATED TO THE TROPOSPHERE

Stephan Seefeld and J. Alistair Kerr  
EAWAG, Swiss Federal Institute for Environmental  
Science and Technology, ETH Zurich, CH-8600  
Dübendorf, Switzerland

Peroxyacyl nitrates (PANs) are an important component of summer smog. They can cause eye irritation and plant damage. Moreover, PANs are a temporary reservoir for reactive intermediates involved in summer smog formation. It is essential to know the kinetics and mechanisms of their formation and destruction for inclusion in models of atmospheric chemistry.

PANs are formed in the atmosphere as secondary products following the OH-initiated photo-oxidation of aldehydes and the generation of peroxyacyl radicals. The Peroxyacyl radicals may react either with NO<sub>2</sub> to generate PANs or with NO to form radical products and CO<sub>2</sub>:



The ratio of the rate coefficients ( $k_1/k_2$ ) for peroxyacyl nitrate (PAN, R = CH<sub>3</sub>) and peroxypropionyl nitrate (PPN, R = CH<sub>3</sub>CH<sub>2</sub>) have been measured over the temperature range 247–298 K, at a total pressure of ~1 atm. The ratio  $k_1/k_2 = 0.41 \pm 0.03$  (for PAN) and  $0.43 \pm 0.06$  (for PPN) independent of temperature.

The experiments involved flowing a reaction mixture in air, at atmospheric pressure, through an irradiated reactor with a residence time of about 50 s, and analysing the reactants by gas chromatography (GC-ECD-FID) and with an NO<sub>x</sub>-chemiluminescence analyser. The photolysis of biacetyl (for the PAN experiment) and propionyl chloride (for the PPN experiment) were used as the radical sources. The mixing ratios of PAN or PPN were measured as a function of the NO/NO<sub>2</sub> ratio, which was varied during each experiment.

Figure 1 shows a plot of the results from this work for PAN in relation to previous determinations of  $k_1/k_2$  as a function of temperature. Note that in the present study we have been able to extend the relative rate measurements down to a temperature of 247 K and at the same time have considerably improved the precision of the measurements. Above 298 K the decomposition reaction (-1) can not be neglected and these measurements yield a ratio which is underestimated. Also shown in Figure 1 are values of  $k_1/k_2$  calculated from absolute measurements of  $k_1$  and  $k_2$ . Figure 2 shows a similar plot of the present results for PPN.

# OH Radical Initiated Photo-Oxidation of Ethylene Glycol Monoalkyl Ethers

Konrad Stemmler, Wolfgang Mengon, David J. Kinnison and J. Alistair Kerr  
*EAWAG, Swiss Federal Institute for Environmental Science & Technology*

*ETH Zurich, CH-8600 Dübendorf, Switzerland*

Glycol ethers are used extensively as solvents and chemical intermediates and undergo evaporative losses to the atmosphere. The OH radical initiated photo-oxidation of 2-ethoxyethanol and 2-butoxyethanol have been studied in a Teflon bag smog chamber under atmospherically related conditions by irradiating mixtures of methyl nitrite, nitric oxide and the substrate in air at ppm levels. The oxidation products from the gas phase reactions were identified and quantified using chromatographic and mass spectrometric methods. For 2-ethoxyethanol we obtained a detailed picture of the oxidation processes by identifying and quantifying the end-products, which seem to describe all the important oxidation routes under these conditions. A proposed mechanism for the OH radical initiated oxidation of 2-ethoxyethanol is shown in Figure 1A (R=CH<sub>3</sub>). The measured yields of the major products are given in Table 1.

In the 2-butoxyethanol study we observed an analogous product distribution indicating the same pathways as in the 2-ethoxyethanol study, but these only account for ~80 % of the converted glycol ether (Figure 1A with R=CH<sub>2</sub>CH<sub>2</sub>CH<sub>3</sub>). The additionally observed products from 2-butoxyethanol are related to the longer alkyl side chain. A proposed mechanism leading to these additional products is shown in Figure 1B, and the yields are given in Table 1.

Figure 1:

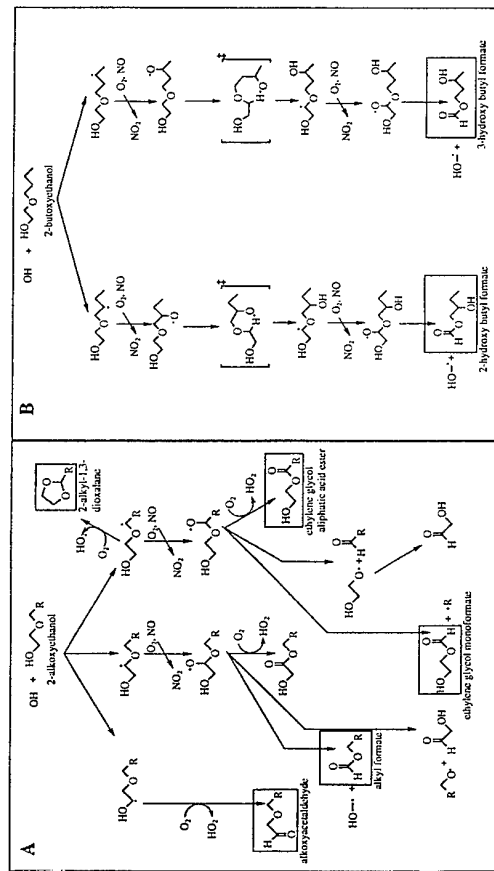
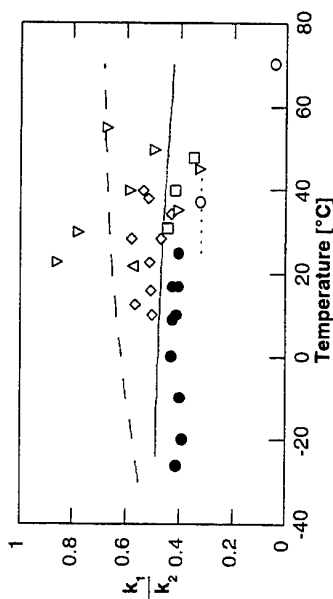


Figure 1A: General mechanism for the OH radical initiated oxidation of 2-ethoxyethanol as well as for the corresponding reactions of 2-butoxyethanol. Observed products are highlighted in boxes.

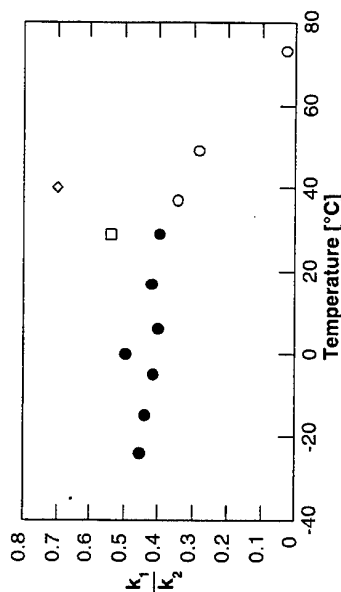
Figure 1B: Proposed mechanism occurring after the H-atom abstraction by the OH-radical from the butyl side chain of 2-butoxyethanol. Only pathways leading to observed products are shown.

Figure 1: Temperature Dependence of the Ratio,  $k_1/k_2$ , for Peroxyacetyl Nitrate (PAN).



Comparison of present data on  $k_1/k_2$  for PAN with literature values: (●) this study, (○) this study, at temperature where reaction (-) is significant; (Δ) Cox et al.[1]; (▽) Cox and Roffey[2]; (□) Kirchner et al.[3]; (◇) Tuazon et al.[4]; (---) Hendry and Kenley[5]; (—) ratio of the absolute rate coefficients of Bridier et al.[6] and Villalta and Howard[7]; (---) ratio of the absolute rate coefficients of Bridier et al.[6] and Maricq and Sente[8].

Figure 2: Temperature Dependence of the Ratio,  $k_1/k_2$ , for Peroxypropionyl Nitrate (PPN).



Comparison of present data on  $k_1/k_2$  for PPN with literature values: (●) this study, (○) this study, at temperature where reaction (-) is significant; (□) Kerr and Stocker[9] (◇) Becker and Kirchner.[10].

## References

- [1] Cox, R. A.; Derwent, R. G.; Holt, P. M.; Kerr, J. A. *Faraday J* 1976, 72, 2061-2075.
- [2] Cox, R. A.; Roffey, M. J. *Environ. Sci. Technol.* 1977, 11, 900-906.
- [3] Kirchner, F.; Zabel, F.; Becker, K. H. *Ber. Bunsenges. Phys. Chem.* 1990, 94, 1379-1382.
- [4] Tuazon, E. C.; Carter, W. P. L.; Atkinson, R. *J. Phys. Chem.* 1991, 95, 2434-2437.
- [5] Hendry, D. G.; Kenley, R. A. *J. Am. Chem. Soc.* 1977, 99, 3198-3199.
- [6] Bridier, L.; Caralp, F.; Loirat, H.; Lesclaux, R.; Veyret, B. *J. Phys. Chem.* 1991, 95, 3594-3600.
- [7] Villalta, P. W.; Howard, C. J. *J. Phys. Chem.*, in press.
- [8] Maricq, M. M.; Sente, I. J. *J. Phys. Chem.*, in press.
- [9] Kerr, J. A.; Stocker, D. W. *J. Photochem.* 1985, 28, 475-489.
- [10] Becker, K. H.; Kirchner, F. *Kinetische Untersuchungen an Peroxynitrat und Peroxyradikalen*, Bergische Universität Gesamthochschule Wuppertal, Fachbereich 9 Physikalische Chemie, 1994.

# KINETIC STUDIES OF THE CONVERSION OF HNO<sub>3</sub> TO NO<sub>x</sub> IN THE TROPOSPHERE

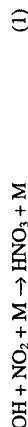
Shaun Carl, John Crowley, Philippe Mirabel\*, Trevor Ingham,  
Geert Moortgat and Paul Crutzen

Max-Planck-Institut für Chemie  
Division of Atmospheric Chemistry  
Mainz, Germany.

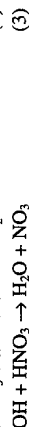
\*Laboratoire de physico-chimie de l'atmosphère  
Strasbourg Cedex, France

Present photochemical models overpredict the tropospheric HNO<sub>3</sub>/NO<sub>x</sub> ratio. The measured HNO<sub>3</sub>/NO<sub>x</sub> ratio is at least a factor of 3 less than that predicted by models.

NO<sub>2</sub> is converted to HNO<sub>3</sub> in about 1 day via:



and is released from HNO<sub>3</sub> by:



The absorption cross section of HNO<sub>3</sub> is well established. The quantum yield for the channel indicated, for wavelengths greater than 222 nm, is close to unity [1]. Process (3) is characterised by a rate constant which decreases with increasing temperature and also shows a negative pressure dependence. This indicates that this reaction proceeds via an energised association complex.

Measurements of tropospheric HNO<sub>3</sub> samples using diffusion denuders show that the species collected is intact HNO<sub>3</sub>·H<sub>2</sub>O [2]. This is also confirmed by thermodynamic calculations of complex formation [3]. The results of our thermodynamic calculations on the gas-phase nitric acid - water system indicate that at temperatures and partial pressures of H<sub>2</sub>O typical of the troposphere, only 30% of HNO<sub>3</sub> is monomeric.

In this study we investigated processes (2) and (3) under conditions when HNO<sub>3</sub> is significantly hydrated to see if the rate of conversion of HNO<sub>3</sub> to NO<sub>2</sub> via the above processes is altered by the presence of water vapour.

## Experimental

All experiments were carried out in a Pyrex absorption/reaction cell with quartz windows and under static conditions. Reaction (3) was monitored by generating OH through dissociation of a small fraction of HNO<sub>3</sub> (typ. 1:2500) using a pulsed excimer laser operating at 248 nm. The excimer laser traversed a path of 104 cm along the centre of the reaction vessel

Table 1

Corrected Yields<sup>a</sup> of the Major Products from the Photo-Oxidation of 2-Butoxyethanol and Comparison with the Corresponding Results from the Photo-Oxidation of 2-Ethoxyethanol

2-butoxyethanol	2-ethoxyethanol
	yield <sup>b,c</sup>
butyl formate	35 ± 11 (28 ± 12) <sup>d</sup>
2-propyl-1,3-dioxalane	2.5 ± 0.5
butoxyacetaldehyde	12 ± 9
ethylene glycol monoformate	39 ± 18.
ethylene glycol monobutyrate	~2.3
propyl nitrate	3.8 ± 1.8
3-hydroxy butyl formate	~19.8
2-hydroxy butyl formate	~4.8
propionaldehyde	~20-30
acetaldehyde	<5
butyraldehyde	<1.1

<sup>a</sup> Corrected for secondary OH radical attack. <sup>b</sup> Expressed as a % of 2-alkoxyethanol reacted.

<sup>c</sup> Error limits are for 95 % confidence intervals and include the errors in analytical responses, the initial bag mixtures, the scatter of results and worst-case estimates of the errors in correcting for secondary OH reactions. <sup>d</sup> Estimated primary yield, excluding the formation as a secondary product from the reaction of the alkoxyacetaldehyde with OH.

## Discussion

An interesting feature of the observed product distribution of 2-butoxyethanol is the high abundance of 3-hydroxy butyl formate. The formation of this product may be explained by reactions following the initial H-atom abstraction at the γ position to the ether linkage in 2-butoxyethanol (see Figure 1B). According to the proposed mechanism, the reactivity with respect to H-atom abstraction by the hydroxyl radical at this site is about 4 times higher than expected by analogy with the corresponding CH<sub>2</sub> group in alkanes. A possible explanation for the enhanced reactivity, may be an initial adduct formation of the hydroxyl radical and the substrate molecule. Our current research is focused on a study of the hydrogen bonded adduct of the hydroxyl radical with the ether oxygen in such a molecule which may be the reactive intermediate responsible for the observed product distribution. An initial *ab initio* calculation (MP2 / 6-31\*) shows that this adduct is stable having a bond energy of ~20 kJ / mol.

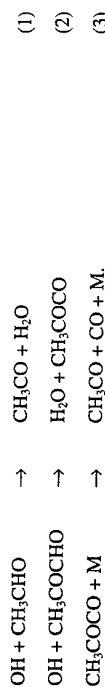
As expected, the most reactive sites towards OH attack in the ether molecules were the CH<sub>2</sub>-groups adjacent to the O atom centre. The distribution of products from the present studies of ethoxyethanol and butoxyethanol shows that the resulting alkoxy radicals of the type RCH(O)·OR do not undergo isomerisations reactions via cyclic transition states and H-atom transfer.

# PRESSURE DEPENDENCE OF THE RATE COEFFICIENT FOR THE REACTION OF CH<sub>3</sub>CO WITH O<sub>2</sub>

John J. Orlando and Geoffrey S. Tyndall,  
Atmospheric Chemistry Division,  
National Center for Atmospheric Research, Boulder CO 80307-3000

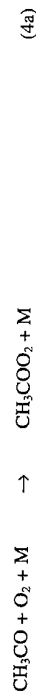
Timothy J. Wallington and Michael D. Hurley,  
Ford Research Laboratory SRL-3083  
Ford Motor Company, P.O. Box 2053, Dearborn MI 48121

The acetyl radical (CH<sub>3</sub>CO) is of importance in the chemistry of the troposphere. It is formed directly in the reaction of OH with CH<sub>3</sub>CHO, or from the decomposition of larger organic species - eg.,



The acetyl radical reacts rapidly with O<sub>2</sub> in the atmosphere and is believed to give the

acetylperoxy radical in large yield:



Direct measurements of  $k_4$  have been obtained previously by McDade *et al.*,<sup>1</sup> who found  $k_4 = 2 \times 10^{-12} \text{ cm}^3 \text{ molec}^{-1} \text{ s}^{-1}$  in the presence of 1-4 Torr He. The high pressure limiting value of  $k_4$  is assumed to be  $5 \times 10^{-12} \text{ cm}^3 \text{ molec}^{-1} \text{ s}^{-1}$ ,<sup>2</sup> by analogy with the rate coefficient for reaction O<sub>2</sub> with ethyl radicals. In addition, previous flow tube studies of the reaction of OH with

CH<sub>3</sub>CHO<sup>3,4</sup> conducted in the presence of O<sub>2</sub> provided evidence for the regeneration of OH, implying OH production from the reaction (4) at low pressure.

well away from the walls. The course of the reaction was followed in real time by continuously monitoring the resulting product, NO<sub>3</sub>, by its non-dissociative absorption, centred at 662 nm, using a cw diode laser. Cell concentrations of HNO<sub>3</sub> were monitored before and after each experimental run by monochromator-selected 212 nm absorption of a D<sub>2</sub> lamp whose beam also traversed the same axis of the absorption/reaction cell as both laser beams. NO<sub>3</sub> concentrations were simply extracted from the Beer-Lambert relationship through absorption at 662 nm.

Various concentrations of H<sub>2</sub>O were admitted to the cell by slowly bubbling N<sub>2</sub> through water at room temperature and passing the gas mixture, at a range of flow pressures, through a condenser held several degrees cooler.

In the absence of any other loss processes for NO<sub>3</sub> and OH, NO<sub>3</sub> will be produced at the same rate as OH is removed via reaction (3) with its concentration asymptotically approaching the initial [OH] produced on photolysis.

In the presence of other removal processes for both NO<sub>3</sub> and OH, the time profile of [NO<sub>3</sub>] will take the following form:

$$[\text{NO}_3]_t = (k_3[\text{OH}]_0 / (k_3 - k_5)) \{ \exp(-k_5 t) - \exp(-k_3 t) \}$$

where  $k_3$  is the pseudo-first-order rate constant for removal of OH and  $k_5$  is the first-order rate constant for removal of NO<sub>3</sub>. Diffusion both of OH and of NO<sub>3</sub> out of the observation region was negligible on the time scales of the measurements. Low conversion of HNO<sub>3</sub> through photolysis together with relatively few averages (6 to 15) ensured that there was no significant build-up of products during measurements in the static cell.

In this way it was possible to measure both the relative photolysis yield of OH at 248 nm (process (2)) and the rate constant for reaction (3) by employing NO<sub>3</sub> as a spectroscopic marker for OH.

A series of measurements were carried out at room temperature in the presence of excess N<sub>2</sub> only and also with N<sub>2</sub>/H<sub>2</sub>O mixtures.

## Results

Our results from studies of reaction (3) in N<sub>2</sub> show the expected behaviour yielding a room-temperature rate constant in agreement with the currently accepted value. As expected, the calculated yield of OH was directly proportional to the HNO<sub>3</sub> concentration. As absolute quantum yields could not be directly measured in these experiments, the results in N<sub>2</sub> (OH quantum yield of unity) provided the comparison for measurements in the presence of H<sub>2</sub>O.

The rate of reaction of OH with HNO<sub>3</sub> (extracted from NO<sub>3</sub> time profiles) slightly decreased with increasing H<sub>2</sub>O pressure (up to 10 Torr), however the overall NO<sub>3</sub> yield, and hence OH yield, showed a marked decrease over the same H<sub>2</sub>O pressure range. These results indicate that there is a significant dependence of overall OH yield on photolysis of HNO<sub>3</sub> in the presence of high concentrations of H<sub>2</sub>O. Using the present, calculated, hydrate fraction as a function of H<sub>2</sub>O pressure we put an upper limit to the quantum yield for production of OH via photolysis of the hydrate of less than 0.1.

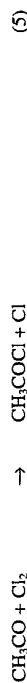
- [1] Turnipseed, A. A., Vaghjiani, G. L., Thompson, J. E. and Ravishankara, A. R., *J. Chem. Phys.*, **1992**, *96*, 5887.
- [2] Benner, C., Lewis, E. A., Eatough, D. J., Eatough, N. L., Huang, A. A., Ellis, E. C., *Am. Chem. Soc.*, **1986**, *92*, 141-ENVR
- [3] Jaeger-Voirol, A., Mirabel, P., and Reiss, H., *J. Chem. Phys.*, **1987**, *87*, 4849.

In this study, rate coefficients and product yields for reaction (4) are determined using

environmental chamber / FT-IR systems at both Ford Motor Company and NCAR.<sup>5,6</sup> Product

yields obtained in photolyses of  $\text{Cl}_2/\text{CH}_3\text{CHO}/\text{O}_2/\text{N}_2$  mixtures over a wide range of pressure

(0.1 to 1100 Torr) are used to obtain values for  $k_4$  relative to  $k_5$ :



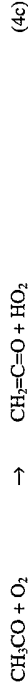
Absolute values for  $k_4$ , obtained using the measured values for  $k_5$  of Maricq and Szenté,<sup>7</sup> are

shown to increase from a constant value of  $7 \times 10^{-13} \text{ cm}^3 \text{ molec}^{-1} \text{ s}^{-1}$  at pressures below 2 Torr,

to a high pressure limiting value of  $3.2 \times 10^{-12} \text{ cm}^3 \text{ molec}^{-1} \text{ s}^{-1}$ . In addition, products yields

obtained in the photolysis of  $\text{Cl}_2/\text{CH}_3\text{CHO}/\text{O}_2/\text{N}_2$  mixtures, with NO or  $\text{NO}_2$  added in some

cases, provide evidence for two low pressure reaction channels, (4b) and (4c):



The rate coefficient and yield data are interpreted in terms of a concerted mechanism in which the acetylperoxy radical (reaction 4a) is increasingly stabilized at high pressure at the expense of the low pressure decomposition channels (reactions 4b and 4c). Branching ratios for the three channels as a function of pressure are provided.

## References

1. C. E. McDade, T. M. Lenhardt, and K. D. Bayes, *J. Photochem.*, **20**, 1, (1982).
2. R. Atkinson, D. L. Baulch, R. A. Cox, R. F. Hampson, J. A. Kerr, and J. Troe, *J. Phys. Chem. Ref. Data*, **21**, 1125 (1992).
3. J. V. Michael, D. G. Keil, and R. B. Klemm, *J. Chem. Phys.*, **83**, 1631 (1985).
4. G. S. Tyndall, T. A. Staffelbach, J. J. Orlando, and J. G. Calvert, *Int. J. Chem. Kinet.*, **27**, 1009 (1995).
5. T. J. Wallington and S. M. Japar, *J. Atmos. Chem.*, **9**, 399 (1989).
6. R. E. Shetter, J. A. Davidson, C. A. Cantrell, and J. G. Calvert, *Rev. Sci. Instrum.*, **58**, 1427 (1987).
7. M. M. Maricq and J. J. Szenté, *J. Phys. Chem.*, in press (1996).

## KINETIC STUDIES ON INTERMEDIATES OF THE ATMOSPHERIC DEGRADATION OF AROMATIC HYDROCARBONS

I. Barnes, K. H. Becker and B. Klotz

Bergische Universität, Physikalische Chemie/FB 9, Gaußstraße 20, D-42097 Wuppertal, Germany

### Introduction

Aromatic hydrocarbons, in particular benzene, toluene and the xylenes, are currently regarded as one of the most important classes of compounds with respect to tropospheric photooxidant formation with a contribution of up to 40 % being predicted in urban areas [1]. The chemical degradation mechanisms used in these predictions, however, are highly speculative.

The main atmospheric fate (90 %) of aromatic hydrocarbons is addition of an OH radical to the aromatic ring. This reaction results in the formation of an aromatic-OH-adduct (1) which will predominately react with molecular oxygen under atmospheric conditions [2]. The products of this reaction, however, are currently not known. Studies by Zetzsch and co-workers showed that  $\text{HO}_2$  is formed from this reaction by a "prompt" mechanism, e.g.  $\text{ARO-OH} + \text{O}_2 \rightarrow \text{HO}_2 + \text{products}$  [3]. The products of such reactions are generally thought to be hydroxylated aromatics like phenol (2) and cresols, see Figure 1, left column. Recent experiments have shown, however, that the formation-yields of such compounds are low under atmospheric conditions [4]. Other previously postulated mechanisms for the reaction of the aromatic-OH-adduct with  $\text{O}_2$  are also depicted in the left column of Figure 1. They include the reaction of a peroxy-radical with NO to give an oxy-radical and  $\text{NO}_2$  ( $\text{ROO} \cdot + \text{NO} \rightarrow \text{RO} \cdot + \text{NO}_2$ ) prior to  $\text{HO}_2$ -formation and are therefore in contradiction to the results mentioned above [3].

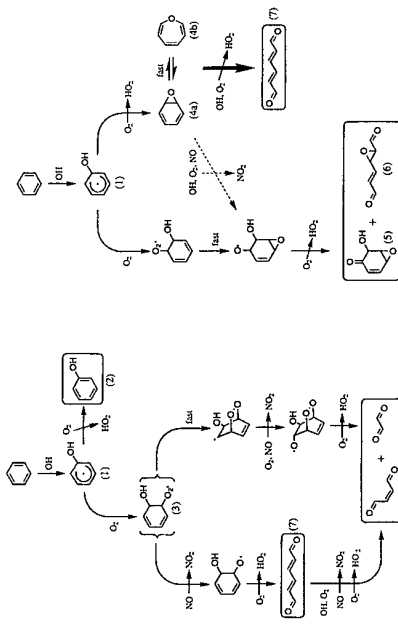


Fig. 1: Previously proposed (left column) and new (right column) mechanisms for the atmospheric degradation of aromatic hydrocarbons, methyl groups being omitted for clarity.

In this study, a new gas-phase mechanism for the reaction of the aromatic-OH-adduct with O<sub>2</sub> is proposed which is consistent with the experimental observation of prompt HO<sub>2</sub> formation. The new mechanism is depicted in Figure 1, in the right column, right pathway. It postulates the formation of benzene-oxide(4a)/oxepin(4b) as an intermediate. The reaction of O<sub>2</sub> with the aromatic-OH-adduct is thought to proceed via H-abstraction from the OH-group of the adduct, leading to the formation of HO<sub>2</sub> and benzene-oxide. Compounds of this type have been given a great deal of attention in the degradation of aromatic hydrocarbons in organisms. Arene-oxides have been positively identified as the primary metabolites of several polycyclic aromatic hydrocarbons [5]. Benzene-oxide/oxepin is considered to be the primary metabolite of benzene [6].

The pathway shown to the left of this mechanism has recently been proposed by Bartolotti and Edney [7], based on theoretical calculations. This mechanism would lead to the formation of HO<sub>2</sub> and 2-hydroxy-7-oxa-bicyclo[4.1.0]hept-4-en-3-one (5) or an epoxy-muconaldehyde (6). Methylated derivatives of these compounds have recently been identified in the photooxidation of toluene [8]. Their formation can, however, also be explained by further reaction of benzene-oxide with OH radicals, as indicated by the dotted arrow in Figure 1, right column.

## Results and Discussion

In order to elucidate the possibility of the involvement of arene oxides and unsaturated 1,6-dicarbonyls in the atmospheric oxidation of aromatics, a study of their atmospheric chemistry has been undertaken. Results of kinetic studies on these compounds with OH- and NO<sub>3</sub>-radicals are presented. The room temperature rate constants were determined using the relative kinetic technique in a large volume (1080 l) photoreactor and are summarised in Table 1. Photolysis of CH<sub>3</sub>ONO/NO mixtures in air was used as the OH radical source, NO<sub>3</sub> radicals were generated by thermal decomposition of N<sub>2</sub>O<sub>5</sub>, which was prepared in a separate bulb by reacting NO<sub>2</sub> with ozone. The results of the kinetic study show that the OH reactions are very fast for all the compounds investigated, a fact which can explain the difficulties in the identification of these compounds in photooxidation experiments on aromatic hydrocarbons. Reaction of the hexadienals with NO<sub>3</sub> is very slow, while that of NO<sub>3</sub> with benzene oxide/oxepin was found to be extremely fast. NO<sub>3</sub> radical reaction might become a very important sink for this compound in smog-chamber experiments performed under conditions of high NO<sub>3</sub> concentrations, where reaction of ozone with NO<sub>2</sub> can give high levels of NO<sub>3</sub> radicals.

Products studies on the OH-initiated oxidation of benzene oxide/oxepin show that its main oxidation products are the hexadienals, which are further oxidised to give unsaturated 1,4-dicarbonyls and 1,2-carbonyls, all of which well known oxidation products of aromatic hydrocarbons. Photolysis of benzene oxide/oxepin leads to the formation of phenol, a fact which might help to explain the large discrepancies observed in the yield of hydroxylated aromatics from the photooxidation of aromatic hydrocarbons by different research groups. If the proposed mechanism is valid, the

yield of hydroxylated aromatic hydrocarbons would be governed by the ratio  $\{(k_{\text{oxepin+OH}}/[\text{OH}]) / (\text{photolysis frequency} \cdot \text{yield}_{\text{m}}(\text{phenol}))\}$ , which might vary considerably under different experimental conditions.

Table 1: Summary of the rate constants determined for the reactions of OH- and NO<sub>3</sub> radicals with unsaturated 1,6-dicarbonyls and benzene oxide/oxepin.

compound	k(OH) [cm <sup>3</sup> molecule <sup>-1</sup> s <sup>-1</sup> ]	k(NO <sub>3</sub> ) [cm <sup>3</sup> molecule <sup>-1</sup> s <sup>-1</sup> ]
E,Z-2,4-Hexadienedial	(10.9 ± 2.2) · 10 <sup>-11</sup>	(5.3 ± 0.4) · 10 <sup>-15</sup>
E,E-2,4-Hexadienedial	(8.8 ± 0.6) · 10 <sup>-11</sup>	(5.3 ± 0.2) · 10 <sup>-15</sup>
E,E-2-Methyl-2,4-hexadienedial	(11.8 ± 0.4) · 10 <sup>-11</sup>	(10.2 ± 0.6) · 10 <sup>-15</sup>
Benzene oxide/Oxepin	(10.0 ± 0.4) · 10 <sup>-11</sup>	(9.2 ± 0.3) · 10 <sup>-12</sup>

In addition to these studies, results from first experiments on the OH-radical initiated oxidation of aromatic hydrocarbons obtained in the European Photoreactor (EUPHORE) in Valencia/Spain are presented. These results indicate that the NO<sub>3</sub> sink observed in various studies on the photooxidation of aromatic hydrocarbons is very likely not an artefact of small reaction vessels.

## References

1. R.G. Derwent, M.E. Jenkin, S.M. Saunders; *Atmos. Environ.* **30** (1996) 181-199.
2. R. Knispel, R. Koch, M. Siese, C. Zetzsch; *Ber. Bunsenges. Phys. Chem.* **94** (1990) 1375-1379.
3. M. Siese, R. Koch, C. Fittschen, C. Zetzsch in: P.M. Borrell, P. Borrell, T. Cvitas, W. Seiler (eds.), Transport and Transformation of Pollutants in the Troposphere. *Proc. EUROTRAC Symp. '94*, SPB Academic Publishing bv. 1994, The Hague, Netherlands, pp. 115-119.
4. K.H. Becker in: P.M. Borrell, P. Borrell, T. Cvitas, W. Seiler (eds.), Transport and Transformation of Pollutants in the Troposphere. *Proc. EUROTRAC Symp. '94*, SPB Academic Publishing bv. 1994, The Hague, Netherlands, p. 67.
5. (a) W. Levin, A. Wood, R. Chang, D. Ryan, P. Thomas, H. Yagi, D. Thakker, K. Vyas, C. Boyd, S.Y. Chu, A. Conney, D. Jerina; *Drug Metab. Rev.* **13** (1982) 555-580. (b) D.M. Jerina, J.W. Daly, B. Witkop, P. Zaltzman-Nierenberg, S. Udenfriend; *J. Am. Chem. Soc.* **90** (1968) 6527-6527.
6. A. Yardley-Jones, D. Anderson, D.V. Parke; *Br. J. Ind. Med.* **48** (1991) 437-444.
7. L.J. Bartolotti, E.O. Edney; *Chem. Phys. Lett.* **245** (1995) 119-122.
8. H. Jeffries; paper presented at the Workshop on Chemical Mechanisms Describing Oxidation Processes in the Troposphere, April 25-28, 1995, Valencia, Spain.

# DISCHARGE FLOW STUDIES OF THE FORMATION OF $\text{Cl}_2\text{O}_3$ FROM THE REACTION BETWEEN $\text{ClO}$ AND $\text{OCIO}$

T. J. Green, M. Islam, J. M. Windsor, K. M. Hickson, C. E. Canosa-Mas and R. P. Wayne

*Physical and Theoretical Chemistry Laboratory, University of Oxford  
South Parks Road, Oxford OX1 3QZ*

The third-order reaction  $\text{ClO} + \text{OCIO} = \text{Cl}_2\text{O}_3$ , has been studied by other workers<sup>1,5</sup> in order to evaluate its importance in polar stratospheric chemistry.

Previous laboratory studies of the reaction have used the flash-photolysis technique to generate  $\text{ClO}$ . The study outlined in this poster utilises the discharge-flow method, coupled with a diode-array spectrometer. Diode-array spectroscopy in the ultra-violet can exploit the absorption of all the oxides of chlorine in the region 200–450 nm, allowing simultaneous detection of several species, in this case  $\text{ClO}$ ,  $\text{OCIO}$  and  $\text{Cl}_2\text{O}_3$ .

$\text{OCIO}$  is produced by passing  $\text{Cl}_2$  gas over sodium chlorite beds:  $\frac{1}{2}\text{Cl}_2 + \text{NaClO}_2 \rightarrow \text{NaCl} + \text{OCIO}$  and dried by passing over  $\text{P}_2\text{O}_5$ .  $\text{Cl}$  atoms are produced by the action of a microwave discharge on  $\text{Cl}_2$ . The reaction of an excess of  $\text{Cl}$  atoms with  $\text{OCIO}$  is used to produce  $\text{ClO}$  in a sliding injector via the reaction  $\text{Cl} + \text{OCIO} \rightarrow \text{ClO} + \text{ClO}$ .

The UV spectrum of  $\text{Cl}_2\text{O}_3$  has been measured between 200 and 330 nm. Table 1 lists the cross sections for  $\text{Cl}_2\text{O}_3$  at 10 nm intervals, between 200 and 330 nm. These are the first measurements which extend down to 200 nm, and show the existence of a secondary peak at  $\lambda = 220$  nm, in addition to the major peak at  $\lambda = 267$  nm.

**Table 1.** Absorption cross sections of  $\text{Cl}_2\text{O}_3$  as a function of wavelength.

Wavelength/nm	Cross section/ $10^{-17} \text{ cm}^2 \text{ molecule}^{-1}$
200	0.61
210	0.80
220	0.92
230	0.87
240	0.89
250	1.12
260	1.49
270	1.58
280	1.22
290	0.70
300	0.35
310	0.15
320	0.05
330	0.01

Using spectroscopic methods to measure the equilibrium concentrations of  $\text{ClO}$ ,  $\text{OCIO}$  and  $\text{Cl}_2\text{O}_3$ , we have determined the equilibrium constant for the reaction  $\text{ClO} + \text{OCIO} + \text{M} = \text{Cl}_2\text{O}_3$  in the range 277K to 233K. Table 2 lists the data obtained. Values of  $\Delta H^\circ$  of 54.3 kJ mol<sup>-1</sup> and  $\Delta S^\circ$  of 120.5 J K<sup>-1</sup> mol<sup>-1</sup> have been determined from a van't Hoff plot of the equilibrium data. These quantities are in good agreement with the data published by Burkholder *et al.*<sup>6</sup>.

**Table 2.** Equilibrium constants for the reaction  $\text{ClO} + \text{OCIO} = \text{Cl}_2\text{O}_3$ .

Temperature/K	Equilibrium constant/ $10^5 \text{ atm}^{-1}$
233	9.89
236	4.12
240	3.53
244	1.63
249	1.23
253	0.76
258	0.62
263	0.30
267	0.21
277	0.07

The rate constant for the formation of  $\text{Cl}_2\text{O}_3$  from the reaction between  $\text{ClO}$  and  $\text{OCIO}$  has been obtained at 243 and 263 K and 2.6 torr. Our data are shown in table 3 along with the data of Burkholder *et al.*<sup>4</sup> calculated from their Troe expression.

**Table 3.** Rate constants for formation of  $\text{Cl}_2\text{O}_3$

Temperature/K	$k/10^{-14} \text{ cm}^3 \text{ molecule}^{-1} \text{ s}^{-1}$	$k/10^{-14} \text{ cm}^3 \text{ molecule}^{-1} \text{ s}^{-1}$
	our data	Burkholder <i>et al.</i> <sup>4</sup>
200	—	3.6
220	—	2.4
240	—	1.6
243	2.1	—
260	—	1.1
263	1.4	—

Preliminary experiments have been performed on the reaction between  $\text{Cl}_2\text{O}_3$  and  $\text{Cl}$  and  $\text{O}$  atoms. The rate constant for the reaction between  $\text{Cl}_2\text{O}_3$  and  $\text{Cl}$  is estimated to be  $2 \times 10^{-11} \text{ cm}^3 \text{ molecule}^{-1} \text{ s}^{-1}$ . The reaction between  $\text{Cl}_2\text{O}_3$  and  $\text{O}$  did not produce a detectable change on the timescale of our experiment and an upper limit for the rate constant of  $1 \times 10^{-15} \text{ cm}^3 \text{ molecule}^{-1} \text{ s}^{-1}$  is suggested.

## REFERENCES

1. G. D. Hayman and R. A. Cox, Chem. Phys. Lett., **155**, 1–7 (1989).
2. A. D. Parr, R. P. Wayne, G. D. Hayman, M.E. Jenkin and R. A. Cox, Geophys. Res. Lett., **17**, 2357–2360 (1990).
3. J. B. Burkholder, J. J. Orlando and C. J. Howard, J. Phys. Chem., **94**, 687–695 (1990).
4. J. B. Burkholder, R. L. Mauldin, R. J. Yokelson, S. Solomon and A. R. Ravishankara, J. Phys. Chem., **97**, 7597–7605 (1993).
5. U. Kirchner, M. Liesner, T. Benter, and R. N. Schindler, STEP-Haloeside/AFEAS Workshop, UCD, Dublin (1993).

STUDIES OF THE REACTION OF  $\text{CF}_3\text{O}_2$  WITH OH

P. Biggs, C. E. Canosa-Mas, A. Vignand and R. P. Wayne

*Physical and Theoretical Chemistry Laboratory, University of Oxford  
South Parks Road, Oxford OX1 3QZ*

The trifluoromethylperoxy radical,  $\text{CF}_3\text{O}_2$ , is a likely product of the atmospheric oxidation of  $\text{CF}_3$ -containing compounds, including hydrofluorocarbons. This work investigates the reaction of  $\text{CF}_3\text{O}_2$  with OH, the latter being an important radical in the troposphere.

Experiments have been conducted to investigate the reaction, in a discharge fast-flow system. The flow tube is equipped with a sliding injector. The  $\text{CF}_3\text{O}_2$  radicals were produced in the main flow by reaction of F atoms with an excess of  $\text{CF}_3\text{H}$ , to produce the  $\text{CF}_3$  radical, and subsequent reaction of  $\text{CF}_3$  with oxygen. The OH radicals were produced in the sliding injector by reaction of H atoms with a slight excess of  $\text{NO}_2$ .  $\text{CF}_3\text{O}_2$  concentrations were measured by titrating with NO and monitoring the  $\text{NO}_2$  produced by laser induced fluorescence (LIF). OH radicals were monitored by resonance fluorescence (RF). Typical radical starting concentrations were  $[\text{OH}]_0 : (0.5 - 2) \times 10^{11}$  molecule  $\text{cm}^{-3}$ , and  $[\text{CF}_3\text{O}_2]_0 : (0.5 - 1) \times 10^{12}$  molecule  $\text{cm}^{-3}$ .

The reactions were carried out at room temperature, with typical flow tube pressures of ca. 2 Torr. Contact times for  $\text{CF}_3\text{O}_2$  and OH were varied between 5 and 30 ms by adjusting the position of the sliding injector. The RF signal was monitored with the fluorine microwave discharge on and off, for each sliding injector position, thus yielding  $[\text{OH}]_t$  (residual concentration after reaction for time  $t$ , with  $\text{CF}_3\text{O}_2$ ) and  $[\text{OH}]_0$  (concentration without  $\text{CF}_3\text{O}_2$  present).

Several sets of experiments were conducted using different concentrations of  $\text{CF}_3\text{O}_2$ . Although  $\text{CF}_3\text{O}_2$  was in excess over OH, its changing concentration over the course of the reaction must be taken into account in order to give a correct rate constant. Modelling showed a fairly linear decrease in the concentration of  $\text{CF}_3\text{O}_2$  with time, and was used to calculate the average concentration,  $[\text{CF}_3\text{O}_2]_{\text{av}}$ .

The slope of a combined plot of  $(\ln\{[\text{OH}]_0/[\text{OH}]_t\}) / [\text{CF}_3\text{O}_2]_{\text{av}}$  against contact time, for all experiments, yielded a second-order rate constant ( $k_1$ ) of  $(4.0 \pm 0.3) \times 10^{11}$   $\text{cm}^3 \text{molecule}^{-1} \text{s}^{-1}$ , where the errors are the 95% confidence limits from the linear regression. Allowing for possible errors in flows and concentrations, we estimate total errors of 15%, so that  $k_1$  is  $(4.0 \pm 0.6) \times 10^{11}$   $\text{cm}^3 \text{molecule}^{-1} \text{s}^{-1}$ .

Although direct observation of the products of the reaction of  $\text{CF}_3\text{O}_2$  with OH was not possible, addition of NO at the end of the flow tube during the reaction showed a recovery of the RF signal to near that for  $[\text{OH}]_0$ . Such an observation is consistent with  $\text{HO}_2$  being one of the products, since  $\text{HO}_2$  reacts with NO to produce OH.

If  $\text{HO}_2$  is indeed one of the products, then  $\text{CF}_3\text{O}$  must also be produced. The reaction of  $\text{CF}_3\text{O}$  with OH has not been taken into account in assessing the value of  $k_1$ . There is no published rate constant ( $k_2$ ) for the reaction between  $\text{CF}_3\text{O}$  and OH, but it has been suggested that the rate constant may be as high as  $1 \times 10^{10}$   $\text{cm}^3 \text{molecule}^{-1} \text{s}^{-1}$  [1]. In the light of this suggestion we have examined the effect on the recovered value of  $k_1$ .

Although modelling may be used to find  $[\text{CF}_3\text{O}]$  produced from reactions of  $\text{CF}_3\text{O}_2$ , there appears to be additional  $\text{CF}_3\text{O}$  produced at the source of  $\text{CF}_3\text{O}_2$ . Direct measurement of  $[\text{CF}_3\text{O}]$  was not possible using our apparatus. However, experiments were conducted introducing  $\text{C}_2\text{H}_6$  into the flow tube.  $\text{C}_2\text{H}_6$  reacts with  $\text{CF}_3\text{O}$ , forming  $\text{CF}_3\text{OH}$  and  $\text{C}_2\text{H}_5$ . Under the conditions of the experiment, the  $\text{C}_2\text{H}_5$  radicals react with the large excess of  $\text{O}_2$ , producing  $\text{C}_2\text{H}_5\text{O}_2$  and eventually  $\text{HO}_2$ . Both products react with NO, introduced at the end of the flow tube, to produce  $\text{NO}_2$ . The  $\text{HO}_2$  also produces OH. Experiments at different concentrations of  $\text{CF}_3\text{O}_2$  showed, upon addition of  $\text{C}_2\text{H}_6$ , RF and LIF signals consistent with  $[\text{CF}_3\text{O}]$  being ca. 2% that of  $[\text{CF}_3\text{O}_2]$ .

The models show that, with such concentrations of  $\text{CF}_3\text{O}$ , if  $k_2$  is  $1 \times 10^{11}$   $\text{cm}^3 \text{molecule}^{-1} \text{s}^{-1}$ , our value of  $k_1$  is unaffected. If  $k_2$  is  $5 \times 10^{11}$   $\text{cm}^3 \text{molecule}^{-1} \text{s}^{-1}$ , our value is reduced by ca. 10% and if  $k_2$  is as large as  $1 \times 10^{10}$   $\text{cm}^3 \text{molecule}^{-1} \text{s}^{-1}$ , it is reduced by ca. 20%. Since there are no published data to substantiate the suggestion that there is a fast reaction between  $\text{CF}_3\text{O}$  and OH, we prefer to quote  $k_1$  as  $(4.0 \pm 0.6) \times 10^{11}$   $\text{cm}^3 \text{molecule}^{-1} \text{s}^{-1}$ .

## Reference:

- [1] A. A. Turnipseed, S. B. Barone, N. R. Jensen, D. R. Hanson, C. J. Howard, A. R. Ravishankara. *J. Phys. Chem.*, **99** (1995), 6000

# THE REACTION OF METHACROLEIN, METHYL VINYL KETONE AND METHYL ACRYLATE WITH NO<sub>3</sub>

C.E. Canosa-Mas, S. Carr, M.D. King, K. Thompson, R.P. Wayne  
*Physical and Theoretical Chemistry Laboratory, University of Oxford*  
*South Parks Road, Oxford OX1 3QZ*

Methacrolein and methyl vinyl ketone are oxidation products of isoprene and are found in appreciable quantities in forested areas [1]. Methyl acrylate is released into the atmosphere from the plastics industry [2].

The kinetics of the reactions of NO<sub>3</sub> with methacrolein, methyl vinyl ketone and methyl acrylate has been studied at room temperature using an absolute and a relative technique. The absolute method used a discharge-flow system at pressures between 2–10 Torr. NO<sub>3</sub> decay being monitored by optical absorption and product NO<sub>2</sub> growth by LIF. The relative-rate technique involved monitoring the decay of substrate and a reference compound in the presence of NO<sub>3</sub> at atmospheric pressure.

Table 1 displays the compounds used as references for the relative-rate experiments and the value of the rate constants for reaction with the NO<sub>3</sub> radical [3]. The values of the experimentally determined rate constants are contained in table 2.

**Table 1** Reference compounds used in relative rate experiments

Compound	NO <sub>3</sub> + methacrolein	NO <sub>3</sub> + methyl vinyl ketone	NO <sub>3</sub> + methacrylate
	propene	acrolein	ethene
$k / \text{cm}^3 \text{ molecule}^{-1} \text{ s}^{-1}$	$(9.5 \pm 2.1) \times 10^{13}$	$(1.16 \pm 0.25) \times 10^{15}$	$(1.85 \pm 0.24) \times 10^{16}$

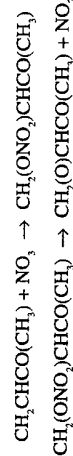
**Table 2.** Rate constants obtained

Technique	$k_{\text{methacrolein} + \text{nitrate radical}} / \text{cm}^3 \text{ molecule}^{-1} \text{ s}^{-1}$	$k_{\text{methyl vinyl ketone} + \text{nitrate radical}} / \text{cm}^3 \text{ molecule}^{-1} \text{ s}^{-1}$	$k_{\text{methyl acrylate} + \text{nitrate radical}} / \text{cm}^3 \text{ molecule}^{-1} \text{ s}^{-1}$
Relative-rate	$(4.0 \pm 1.1) \times 10^{15}$	$(3.9 \pm 1.1) \times 10^{16}$	$(9.6 \pm 2.7) \times 10^{17}$
Discharge-flow	$(9.6 \pm 1.6) \times 10^{15}$	$(7.3 \pm 1.3) \times 10^{16}$	$(3.4 \pm 0.9) \times 10^{16}$

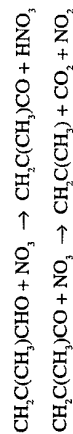
The error limits for the flow-tube determinations of the rate constants are 95% confidence limits, whilst the error limits on the relative-rate values of the rate constants include 95% confidence limits and the error quoted for the reference compound.

The values of the rate constants determined by the flow-tube are approximately twice the values obtained by the relative-rate technique. Possible explanations include the occurrence of fast secondary reactions in the flow-tube involving NO<sub>3</sub> radicals with the primary products of reaction and/or fast reactions with impurities in the organic sample. The rate constants determined by the flow-tube method should therefore only be regarded as upper limits

In the flow-tube experiments, NO<sub>3</sub> was detected for methacrolein and methyl vinyl ketone reacting with the NO<sub>3</sub> radical. No NO<sub>2</sub> has been detected for the reaction between methyl acrylate and the NO<sub>3</sub> radical. However, the higher pressures (8–10 Torr) and low flow velocities needed for this reaction favour N<sub>2</sub>O<sub>5</sub> formation; this process could deplete any product NO<sub>2</sub> to a concentration below the present detection limit of the LIF system. For the reaction of methyl vinyl ketone with the NO<sub>3</sub> radical, the NO<sub>2</sub> (and an epoxide) can be formed by addition of NO<sub>3</sub> to the double bond, followed by collapse of the resulting nitrate



A similar addition pathway is possible between NO<sub>3</sub> and methacrolein, but NO<sub>2</sub> might also be produced by reaction with the acyl radical formed by abstraction of the aldehydic hydrogen.



This behaviour was predicted after NO<sub>3</sub> was detected in the reaction between NO<sub>3</sub> and acetaldehyde in the flow-tube.

Experiments are continuing on the reactions between structurally similar compounds and the NO<sub>3</sub> radical.

## References:

- [1] R.S. Martin, H. Westberg, E. Allwine, L. Aschman, J.C. Farmer, B. Lamb, *J. Atmos. Chem.*, **13** (1991), 1–32
- [2] T.E. Graedel, *Chemical compounds in the atmosphere* (1978) Academic press, New York.
- [3] R.P. Wayne, I. Barnes, P. Biggs, J.P. Burrows, C.E. Canosa-Mas, J. Hjorth, G. Le Bras, G.K. Moortgat, D. Perner, G. Poulet, G. Restelli, H. Sidebottom, *Atmos. Environ.*, **25A** (1991)

# KINETIC STUDY OF $C_2H_5O_2$ : ITS SELF REACTION AND REACTION WITH $HO_2$ BETWEEN 233-363 K

S. Fauvet, E. Henon, M. Touratier, A. Chakir, F. Bohr, J. Brion, D. Daumont and J. Malicet

Laboratoire de Chimie Physique, GSMA, URA D1434, Faculté des Sciences, Université de Reims, Moulin de la Housse, B.P. 1039

51687 REIMS Cedex 2, FRANCE.

email: [abdel.chakir@univ-reims.fr](mailto:abdel.chakir@univ-reims.fr) or [jean.brion@univ-reims.fr](mailto:jean.brion@univ-reims.fr)

Kinetic model elaboration of atmospheric oxidation requires an accurate knowledge of peroxy-radical kinetics. To study the reaction of peroxy-radicals, we have set up the experimental technique of modulated photolysis coupled with single wavelength UV spectroscopy.

The UV absorption spectrum of the  $C_2H_5O_2$  and the kinetic of its self reaction



have been studied over temperature range of [233-363] and at different total pressure [50-200] torr [1]. The room temperature rate constant  $k_{obs}$  had a value of  $(10.3 \pm 0.5) \times 10^{-14} \text{ (cm}^3 \cdot \text{molecule}^{-1} \cdot \text{s}^{-1})$ .

In the range of [233-363] K, the Arrhenius expression derived from the present study is:

$$k_{obs} = 1.56 \times 10^{-13} \exp(-128.0/T) \text{ (cm}^3 \cdot \text{molecule}^{-1} \cdot \text{s}^{-1})$$

Results are discussed with respect to previous kinetic studies of  $C_2H_5O_2$ .

Few studies has been carried out on the reaction between  $C_2H_5O_2$  and  $HO_2$  at low temperature. In addition, a discrepancy between previous works exists. To provide new kinetic data, we are studying this reaction over temperature range [233-363] K at different pressure using modulated photolysis technique.

In addition, a theoretical study [2] has been carried out, involving ab initio and DFT methods, in order to examine the possible structure of intermediate  $RO_4R$  in the self reaction. These results have been compared with experimental data.

- 1) Fauvet, J.P. Ganne, J. Brion, D. Daumont, J. Malicet and A. Chakir. Journal de Chimie Physique., submitted.
- 2) Henon, F. Bohr, A. Chakir, and J. Brion, Chem. Phys. Lett., submitted.

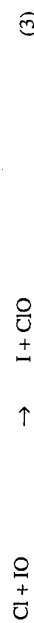
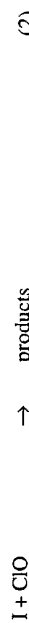
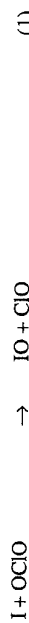
# KINETICS OF THE REACTIONS $I + OClO$ , $I + ClO$ AND $Cl + IO$ . APPLICATION TO THE DETERMINATION OF THE HEAT OF FORMATION OF THE IO RADICAL.

Y. Bedjanian\*, G. Le Bras and G. Poulet.

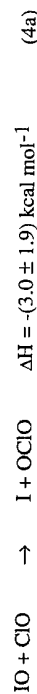
Laboratoire de Combustion et Systèmes Réactifs, CNRS  
45071 Orléans cedex 2, France.

\*Permanent address : Institute of Chemical Physics, National Academy of Sciences,  
375044 Yerevan, Armenia.

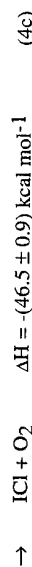
The kinetics of the title reactions have been studied using the discharge-flow mass spectrometric method at  $P \approx 1$  Torr :



The first aim of this investigation was to assess the role of these reactions in the subsequent kinetic study of the reaction of IO with ClO. The latter reaction is of potential importance in stratospheric chemistry since a recent suggestion of a rapid convective transport of short-lived species like  $CH_3I$  to the stratosphere could give importance to ozone depleting cycles initiated by reactions of IO radicals [1]. The reaction between IO and ClO may proceed through several channels :



(4b)



(4d)

Since the products formed in these channels may participate in secondary reactions in the study of reaction (4), independent studies of reactions (1-3) have been carried out. The experimental system has been described earlier [2]. Depending on the reactants, different configurations of the double injector were used. Iodine atoms were

produced from the reaction of molecular iodine with either chlorine or hydrogen atoms. OClO was synthesized in the laboratory and its reaction with Cl was used as the source of ClO radicals. IO radicals were produced from the reaction of oxygen atoms with either molecular iodine or trifluoromethyl iodide. The rate constants obtained are (in  $\text{cm}^3 \text{ molecule}^{-1} \text{ s}^{-1}$ ):

$$\begin{aligned} k_1 &= (9.7 \pm 3.0) \times 10^{-12} \exp[-(1190 \pm 200) / T] & (T = 288-353 \text{ K}) \\ k_2 &\leq 3.7 \times 10^{-15} \text{ (} T = 297 \text{ K)} \text{ and } k_2 \leq 1.7 \times 10^{-14} & (T = 353 \text{ K}) \\ k_3 &= (4.4 \pm 1.0) \times 10^{-11}, \text{ independent of } T & (T = 290-355 \text{ K}) \end{aligned}$$

A direct implication of these kinetic data is the determination of the heat of formation of IO radicals. An upper limit:  $\Delta H_f(\text{IO}) \leq 27.5 \text{ kcal mol}^{-1}$  can be derived from the activation energy measured for reaction (1) and considered as the upper limit of the enthalpy of the reaction. A higher upper limit ( $29.4 \text{ kcal mol}^{-1}$ ) can be obtained from the present value for  $k_1$  and the recent determination of the overall rate constant for reaction (4)[3]. This tends to indicate that the channel forming I + OClO (channel 4a, which is the reverse of reaction 1) would have a branching ratio less than unity. Besides, the upper limit measured for  $k_2$  (which represents an upper limit for the rate constant of the channel forming Cl and IO), combined with the value of  $k_3$  for the reverse reaction, gives  $\Delta H_f(\text{IO}) \geq 25.8 \text{ kcal mol}^{-1}$ .

Consequently, the present determination:  $25.8 \leq \Delta H_f(\text{IO}) \leq 27.5 \text{ kcal mol}^{-1}$ , reduces the current uncertainty on  $\Delta H_f(\text{IO})$ .

The subsequent study of reaction (4) has been performed in the same discharge-flow apparatus. Two sources have been used for both IO (the same ones as above) and ClO (Cl + OClO and Cl + Cl<sub>2</sub>O). The overall rate constant  $k_4$  and the branching ratios for channels (4a), (4b) and (4c) have been measured at 298 K. These results will be also presented and discussed.

**Acknowledgment :** This work has been supported by the EC which is gratefully acknowledged (Project "LEXIS" of the Environment Programme).

## References :

- [1] Solomon, S. ; Garcia, R.P. ; Ravishankara, A.R., *J. Geophys. Res.* **1994**, 99, 20491.
- [2] Lancel, I.T. ; Laverdet, G. ; Le Bras, G. ; Poulet, G., *J. Phys. Chem.*, **1990**, 94, 278.

[3] Gilles, M.K., Turnipseed, A., Burkholder, J.B. and Ravishankara, A.R., presented at the International Conference on Ozone in the Lower Stratosphere, Halkidiki (GR), May 1995.

# RELATIVE RATE MEASUREMENTS FOR ANALOGUES OF MONOTERPENE OXIDATION PRODUCTS USING A PHOTOCHEMICAL REACTOR.

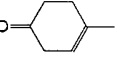
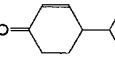
J. B. McQuaid, D. W. Stocker, M. J. Pilling, K. D. Bartle, A. C. Lewis, P. W. Seakins.  
*School of Chemistry, University of Leeds, LEEDS, LS2 9JT, UK*

In the atmosphere volatile organic compounds (VOCs) are degraded by photolysis, reaction with the hydroxyl (OH) radical, and ozonolysis; for many species, the hydroxyl radical reaction is the predominant loss process in the troposphere. To produce realistic models of photochemical oxidation in the troposphere and to assess the impact of anthropogenic activity on air quality the rates of these processes must be determined for anthropogenic and biogenic pollutants as well as their photo-oxidative products. The rate coefficients for the OH radical reaction of a large number of VOCs have been measured (Atkinson, 1994), however, the rate coefficients for the reactions of many of the atmospheric oxidation products of monoterpenes are not known. Isoprene (2-methyl-1,3-butadiene) and monoterpenes are emitted by a wide variety of forest species (e.g. poplar, oak, cotton wood and eucalyptus). Although many of the oxidation products are not readily available, the OH radical rate coefficients may be estimated from structure-activity relationships (Atkinson, 1987). The results reported here are part of a study aimed to expand the database of group rate coefficients to estimate the reactivities of monoterpene oxidation products.

Rate coefficients have been determined by the competitive technique under simulated atmospheric conditions (Atkinson et al; 1981, and Kerr and Stocker, 1986). Synthetic air mixtures containing ppm levels of the test and reference substrates together with the radical source were prepared in 200 dm<sup>3</sup> collapsible Tedlar chamber. Hydroxyl radicals were produced by the photolysis of methyl nitrite in the presence of NO. The reactions were monitored by gas chromatography combined with flame ionisation detection. Known volumes of the gas mixture were withdrawn from the chamber and cryogenically trapped before being flash heated onto a capillary column. The following pairs of substrates were studied: isoprene and trans-2-butene, 3-methyl-2-cyclohexen-1-one and cyclohexene, isophorone and cyclohexene.

Rate coefficients were measured at 298 K. Based on the value  $k(\text{OH} + \text{trans-2-butene}) = 6.4 \times 10^{-11} \text{ cm}^3 \text{ molecule}^{-1} \text{ s}^{-1}$ ,  $k(\text{OH} + \text{isoprene}) = (1.11 \pm 0.06) \times 10^{-10} \text{ cm}^3 \text{ molecule}^{-1} \text{ s}^{-1}$  in good agreement with previous determinations (Atkinson and Aschmann, 1984, Cox et al; 1980, Atkinson, 1994) adding confidence to the results obtained from the present study. Quoted error limits are 95% confidence levels and do not include error associated with the rate coefficient for the reference substrate. Absolute rate coefficients  $k(\text{OH} + 3\text{-methyl-2-cyclohexen-1-one}) = (2.4 \pm 0.4) \times 10^{-11}$

and  $k(\text{OH} + \text{isophorone}) = (3.1 \pm 0.6) \times 10^{-11} \text{ cm}^3 \text{ molecule}^{-1} \text{ s}^{-1}$  based on the value  $k(\text{OH} + \text{cyclohexene}) = 6.77 \times 10^{-11} \text{ cm}^3 \text{ molecule}^{-1} \text{ s}^{-1}$  were obtained. Applying published substituent group rate coefficients to estimate  $k(\text{OH} + \text{isophorone})$   $k(\text{OH} + 3\text{-methyl-2-cyclohexen-1-one})$  leads to an overestimate of the experimental values. The published substituent factor for a  $\beta$ -carbonyl group is based on the reactivity of acyclic compounds in which the OH radical may form a weakly bound complex enhancing reactivity ( $F(\text{C}(\text{=O})-\text{O}) = 0.75$ ). In cyclic compounds this is not geometrically possible and a new substituent factor for  $\beta$ -carbonyl groups in cyclic compounds has been determined;  $F(\text{C}(\text{=O})-\text{O}) = 0.28$  from  $k(\text{HO} + 3\text{-methyl-2-cyclohexen-1-one})$  and 0.26  $k(\text{OH} + \text{isophorone})$ . Cyclic  $\beta$ -carbonyl groups occur in the oxidation products of many monoterpenes, for example  $\beta$ -phellandrene and terpinolene. Estimates of the OH radical reaction rate coefficients and atmospheric lifetimes are given below.

Monoterpene	Oxidation product	$k / 10^{12} \text{ cm}^3 \text{ molecule}^{-1} \text{ s}^{-1}$	Atmospheric lifetimes
$\beta$			Global <sup>a</sup> Rural <sup>b</sup>
Phellandrene		92	6.4 hours 1 hour
Terpinolene		62.5	9.4 hours 1.5 hours

<sup>a</sup> Calculated from the atmospheric budget of  $\text{CH}_3\text{CCl}_3$ , Prinn et al. (1992).

<sup>b</sup> Eisele et al. (1994).

## References

- Atkinson, R. *Int. J. Chem. Kinet.* **19**, 799 (1987).
- Atkinson, R. *J. Phys. Chem. Ref. Data, Monograph No. 2* (1994).
- Atkinson, R., and Aschmann, S. M. *Int. J. Chem. Kinet.* **16**, 1175 (1984).
- Atkinson, R., Carter, W.P.L., Winer, A.M., and Pitts, J.N. Jr. *J. Air Pollut. Contr. Assoc.* **31**, 1090 (1981).
- Cox, R.A., Derwent, R.G. and Williams, M.R. *Environ. Sci. Technol.* **14**, 57 (1980).
- Eisele, F.L., Mount, G. H., Fehsenfeld, F. C., Marovich, E., Parrish, D. D., Roberts, J., Trainer, M. and Tanner, D.J. *J. Geophys. Res.* **99**, 18 605 (1994).
- Kerr, J. A. and Stocker, D. W. *J. Atmos. Chem.* **4**, 253 (1986).
- Prinn, R., Connolly, D., Simmonds, P., Alyea, F., Boldi, R., Crawford, A., Fraser, P., Gutzler, D., Hartley, D., Rosen, R. and Rasmussen, R. *J. Geophys. Res.* **97**, 2445 (1992).

## DEVELOPMENT AND CONSTRUCTION OF A MASTER CHEMICAL MECHANISM (MCM) FOR THE TROPOSPHERE AND APPLICATION TO REGIONAL SCALE PHOTOCHEMICAL OZONE FORMATION IN EUROPE.

S.M. Saunders<sup>1</sup>, M.E. Jenkin<sup>2</sup>, R.G. Derwent<sup>3</sup> and M.J. Pilling<sup>1</sup>

<sup>1</sup>University of Leeds, UK. (Authors to be contacted for MCM computer files)

<sup>2</sup>AEA Technology, Culham, UK. <sup>3</sup>Meteorological Office, Bracknell, UK.

Photochemical models are increasingly used for the assessment of control policies, aimed at reducing exposure to ozone. These models aim to relate peak ozone concentrations found in photochemical pollution episodes to the emissions of the precursors, VOC and NOx from which they are formed. The production of photochemical ozone and other secondary pollutants in the troposphere is governed by the sunlight initiated chemistry, involving NOx and VOC. Development and construction of a detailed chemical mechanism to describe the complete tropospheric oxidation of 120 volatile organic compounds (VOC) is presented. The VOC were selected on the basis of available UK emissions data<sup>1</sup>, and provide approximately 97% mass coverage of the emissions of uniquely identifiable chemical species. The remaining 3% results from minor emissions of approximately a further 100 compounds. The only other major entries in the inventory which could not be treated, were composites, in particular white spirit and kerosene.

The degradation schemes have been constructed using a protocol based on laboratory measurements of the kinetics of the component elementary reactions and are currently being used to provide a detailed mechanism for the production of secondary oxidants, for use in a model of the boundary layer over Europe. The schemes constructed using this protocol are applicable, however, to a wide range of ambient conditions, and may be employed in models of urban, rural or remote tropospheric environments, or for the simulation of secondary pollutant formation for a range of NOx or VOC emission scenarios. These schemes are believed to be particularly appropriate for comparative assessments of the formation of oxidants, such as ozone, from the degradation of organic compounds.

Compilation of the individual VOC degradation schemes has produced a Master Chemical Mechanism (MCM). The organic component of the MCM contains in the region of 7000 reactions and 2500 chemical species. With the exception of 18 aromatic compounds, the chemistry was constructed using the protocol described previously<sup>2</sup>. The aromatic chemistry was based on that used in previous work<sup>3,4</sup>, but was extended to include the reactions of peroxy radicals with HO<sub>2</sub> and NO<sub>3</sub>, and the permutational reactions of the peroxy radicals. Although there are currently many gaps and uncertainties in the details of the atmospheric degradation mechanisms of aromatic compounds<sup>5</sup>, there are several groups active in this field of research<sup>6,7</sup>, and new data are constantly emerging. The difficulties associated with ensuring that there was no species or nomenclature duplication within the compiled mechanism, led to the development of computerised mechanism construction. Details of the format and operation of the computerised system are described herein. Also, due to the large size

of the MCM, it is not possible to provide the listing in hard copy. Full facsimile coding is available, together with associated mechanism and species files via e-mail and the Web. The concepts behind the methodology of the mechanism development and construction are such that as new data become available the MCM can be updated, utilising the computer aided construction format.

The MCM has been implemented in the UK Photochemical Trajectory model<sup>4</sup> to assess regional scale ozone formation across north west Europe and the British Isles. A Photochemical Ozone Creation Potential (POCP) index was generated from the model results showing the relative importance of each VOC in ozone formation, on a mass emitted basis.

- [1] H.J. Rudd - Emissions of volatile organic compounds from stationary sources in the United Kingdom : speciation. Report AEA/CS/16419033/REMA-029 (1995)
- [2] M.E. Jenkin, S.M. Saunders and M.J. Pilling - The tropospheric degradation of volatile organic compounds : a protocol for mechanism development. Atmos. Environ. (in press. 1996)
- [3] R.G. Derwent and M.E. Jenkin - Hydrocarbons and the long range transport of ozone and PAN across Europe. Atmos. Environ. 25A p1661 (1991)
- [4] R.G. Derwent, M.E. Jenkin and S.M. Saunders - Photochemical ozone creation potentials for a large number of reactive hydrocarbons under European conditions. Atmos. environ. 30 p189 (1996)
- [5] R. Atkinson - Kinetics and mechanisms of the gas phase reactions of the hydroxyl radical with organic compounds. J. Phys. Chem. Ref. Data Monograph 2 (1994)
- [6] G. Le Bras (coordinator) - EUROTRAC Annual Report, Part 8 LACTOZ (1993)
- [7] H. Jeffries, Y. Jianzhen and L. Bartolotti - Theoretical and analytical advances in understanding aromatic atmospheric oxidation mechanisms. 210th ACS National Meeting. Paper Number PHYS-15. Chicago, Ill, August 20, (1995)

# ULTRAVIOLET ABSORPTION SPECTRUM, SELF-REACTION AND REACTION WITH NO OF THE BENZOYLPEROXY RADICAL

Virginie Foucher, Françoise Caralp and Robert Lesclaux .

Laboratoire de Photophysique et Photochimie Moléculaire, URA348 CNRS  
Université Bordeaux I, 33405 Talence Cedex, France

The oxidation of toluene  $C_6H_5CH_3$ , one of the most common aromatic compound emitted in the atmosphere, partially results in the formation of benzaldehyde which is rapidly converted into an acylperoxy radical : the benzoylperoxy radical  $C_6H_5C(O)O_2$ .

A flash photolysis /UV absorption technique has been used to study the UV spectrum, the self-reaction, and the reaction with NO of this radical at atmospheric pressure and in the temperature range 298 -400K.

The UV spectrum of  $C_6H_5C(O)O_2$  radical was determined in the wavelength range 245 - 300 nm; a maximum cross section of  $(2 \pm 0.2) \times 10^{-17} \text{ cm}^2 \text{ molecule}^{-1}$  was obtained at 245 nm, value which is considerably higher than those of other peroxy radicals. The determination of the rate constant of the self - reaction of the  $C_6H_5C(O)O_2$  radical ( $k_1$ ) and of its reaction with NO ( $k_2$ ), performed at 298K, gives the following values :

$$k_1 = (1.4 \pm 0.3) \times 10^{-11} \text{ cm}^3 \text{ molecule}^{-1} \text{ s}^{-1}$$

$$k_2 = (1.55 \pm 0.4) \times 10^{-11} \text{ cm}^3 \text{ molecule}^{-1} \text{ s}^{-1}$$

Preliminary results show that the self-reaction displays a negative temperature dependence. This first direct determination of these rate constants confirm the high reactivity associated to reactions of acylperoxy radicals.

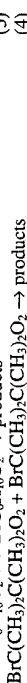
# KINETIC STUDY OF REACTIONS OF PRIMARY, SECONDARY AND TERTIARY $\beta$ -BROMINATED PEROXY RADICALS BETWEEN 275 AND 373K.

Eric Villenave and Robert Lesclaux

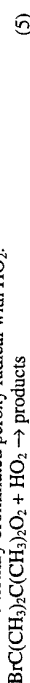
Laboratoire de Photophysique et Photochimie Moléculaire - Université Bordeaux I  
33405 Talence Cedex - France

## Introduction.

The peroxy radical self-reactions are known to present varying rate constants depending principally on the class of the radical or on the position of substitution of H atoms by different functional groups (Lightfoot *et al.*, *Atmos. Environ.* 1992, 26A, 1805). It has been shown recently that substitution of alkylperoxy radicals with OH, or halogen groups may significantly increase self-reaction rate constants (Jenkin *et al.*, *J.Chem.Soc.Faraday Trans.*, 1995, 91, 1911) (Catoire *et al.*, *J.Phys.Chem.*, 1994, 98, 2889). If significant progress has been made in defining structure-reactivity relationships for kinetics of peroxy radicals, only one work to date reports the influence of a functional group on secondary and tertiary peroxy radical reactivities (Jenkin *et al.* 1995). Hence the objectives of the present work were to investigate the effects of a  $\beta$ -substitution with bromine on the self-reaction rate constant of primary, secondary and tertiary peroxy radicals:



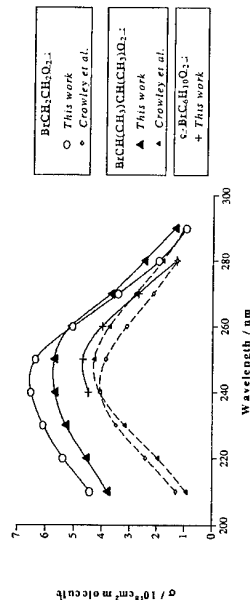
The way the last radical was generated led us to measure, in addition, the kinetics of the reaction of the tertiary brominated peroxy radical with  $\text{HO}_2$ :



Up to now, the size of the radical has been considered as the main factor responsible for the enhancement of the reactivity of peroxy radicals with  $\text{HO}_2$ , with no significant effect of the nature of the substituent on the rate constants having been observed (Lightfoot *et al.* (1992), Catoire *et al.* (1994)).

## Results.

Experiments were performed using flash photolysis and UV absorption spectrometry. Radicals were generated by addition of a bromine atom to an appropriate unsaturated precursor. UV absorption spectra have been recorded for  $\text{BrCH}_2\text{CH}_2\text{O}_2$ ,  $\text{BrCH}(\text{CH}_3)\text{CH}(\text{CH}_3)\text{O}_2$  and  $\text{c-BrC}_6\text{H}_{10}\text{O}_2$  radicals by measuring the initial absorption of the decay traces at different wavelengths. Spectra are shown below, and compared with previous results (Crowley and Moortgat, *J.Chem.Soc.Faraday Trans.*, 1992, 88, 2437):



The chemical mechanism used in the simulations was assumed to be the same as those reported for most peroxy radicals self reactions (Lightfoot *et al.* (1992)) :

# A LABORATORY STUDY OF THE ATMOSPHERIC CHEMISTRY OF $\text{CF}_3\text{CH}_2\text{F}$ (HFC134a) AND $\text{CF}_3\text{CHF}_2$ (HFC125) USING FTIR SPECTROSCOPY

Alam Hasson, Christopher M. Moore and Ian W.M. Smith

*School of Chemistry, The University of Birmingham, Edgbaston, Birmingham B15 2TT*

The proposed and actual replacement of ozone-destroying CFCs (chlorofluorocarbons) by the more benign HFCs (hydrofluorocarbons) has led to intense efforts to understand fully the atmospheric chemistry of this latter class of compounds.<sup>1</sup>

In this poster, we shall describe laboratory experiments on the oxidation of CFC-134a ( $\text{CF}_3\text{CH}_2\text{F}$ ) and CFC-125 ( $\text{CF}_3\text{CHF}_2$ ). In these experiments, F atoms, created by photolysis of  $\text{F}_2$  in the near-ultraviolet, extract an H-atom from the CFC under investigation thereby initiating reaction in a gas mixture at a total pressure of 700 Torr containing a variable amount of  $\text{O}_2$ . The reaction cell (45 dm<sup>3</sup> volume) is internally coated with Teflon to minimise wall reactions and is equipped with White cell mirrors to provide a long optical path length (typically ca. 20 m). This system is coupled to a Nicolet Magnam FTIR spectrometer operated at 0.25 cm<sup>-1</sup> resolution. The temperature of the reaction cell could be varied between 294 and 357 K. In both cases, the substituted alkyl radical which is formed after the abstraction of a hydrogen atom adds  $\text{O}_2$  and two of these peroxy radicals react together to form the substituted alkoxy radicals  $\text{CF}_3\text{CH}_2\text{O}$  or  $\text{CF}_3\text{CHF}_2\text{O}$ . A major interest is the fate of these radicals. In the case of  $\text{CF}_3\text{CH}_2\text{O}$ , abstraction of the remaining H atom by  $\text{O}_2$  is competitive with CC-bond cleavage:



whereas for  $\text{CF}_3\text{CHF}_2\text{O}$  only the second reaction



is possible.

By analysing how the yields of  $\text{CF}_3\text{C}(\text{O})\text{F}$  and  $\text{HFCO}$  depend on  $[\text{O}_2]$  and temperature in experiments on HFC-134a, we have determined

$$k_{1a}/k_{1b} = (3.8 \pm 0.8) \times 10^{-24} \exp(2690 \pm 250) / T \text{ cm}^3 \text{ molecule}^{-1}$$

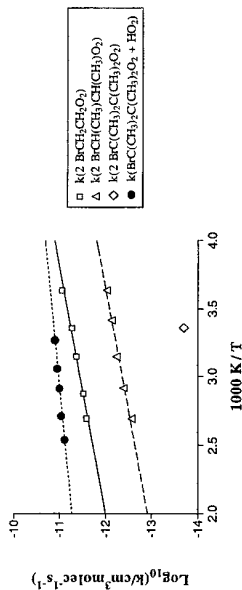
The experiments also show that the reaction between two  $\text{CF}_3\text{CH}_2\text{O}$  reactions yields  $\text{CF}_3\text{C}(\text{O})\text{F}$  as a minor product. In the F-atom initiated oxidation of HFC-125, the yield of  $\text{F}_2\text{CO}$  matches the loss of  $\text{CF}_3\text{CHF}_2$ , suggesting that in this case the reaction between pairs of peroxy radicals,  $\text{CF}_3\text{CHF}_2\text{O}_2$  only produces  $\text{CF}_3\text{CF}_2\text{O}$  and that, under the conditions of the experiments, these yield only  $\text{CF}_3 + \text{F}_2\text{CO}$ . As found by others,  $\text{CF}_3\text{O}_2$  radicals appear to form  $\text{CF}_3\text{O}_3\text{CF}_3$  rather than  $\text{CF}_3\text{O}_2\text{CF}_3$ . Our results will be compared with those from similar studies<sup>1</sup> and their atmospheric implications will be assessed.

T.J. Wallington and O.J. Nielsen in *Progress and Problems in Atmospheric Chemistry*, ed. J.R. Barker (World Scientific, Singapore, 1995) chap. 15.



It becomes more complicated in the case of secondary and tertiary brominated peroxy radicals due, on one hand, to the possible decomposition of the corresponding alkoxy radical and subsequent secondary chemistry, and on the other hand of the dependence of the rate of formation of the peroxy radical on oxygen partial pressure (which could be explained invoking an equilibrium between Br atoms, the alkene and  $\text{O}_2$ ).

Most experiments were performed in one atm of oxygen, reducing unknown secondary chemistry and Arrhenius plots are shown in figure below:



The temperature dependence of the rate constants can be represented by the following expressions:

$$\begin{aligned} -k_1 &= (3.9 \pm 0.81) \times 10^{-14} \exp(1482 \pm 56/T), \text{ giving } (5.6 \pm 1.2) \times 10^{12} \text{ cm}^3 \text{ molecule}^{-1} \text{ s}^{-1} \text{ at } 298 \text{ K, in good agreement with the room temperature value of Crowley and Moortgat } (k_{\text{obs}} = (6.2 \pm 1.2) \times 10^{12}). \\ -k_2 &= (1.16 \pm 0.34) \times 10^{-14} \exp(1219 \pm 82/T), \text{ giving } (6.9 \pm 2.0) \times 10^{13} \text{ cm}^3 \text{ molecule}^{-1} \text{ s}^{-1} \text{ at } 298 \text{ K, also in good agreement with the previous value of Crowley and Moortgat at } 298 \text{ K } (k_{\text{obs}} = (9.6 \pm 1.9) \times 10^{13}). \\ -k_3 &= (2.7 \pm 1.6) \times 10^{-13} \text{ cm}^3 \text{ molecule}^{-1} \text{ s}^{-1} \text{ at room temperature.} \\ -k_4 &= (2.0 \pm 0.9) \times 10^{-14} \text{ cm}^3 \text{ molecule}^{-1} \text{ s}^{-1} \text{ at room temperature.} \\ -k_5 &= (1.38 \pm 0.49) \times 10^{-12} \exp(678 \pm 125/T), \text{ giving } (1.34 \pm 0.48) \times 10^{11} \text{ cm}^3 \text{ molecule}^{-1} \text{ s}^{-1} \text{ at } 298 \text{ K.} \end{aligned}$$

## Conclusion.

All the rate constants of the self-reaction of  $\beta$ -substituted alkylperoxy radicals at 298 K obtained to date are collected in the Table below: (k in  $10^{13} \text{ cm}^3 \text{ molecule}^{-1} \text{ s}^{-1}$ )

X	$\text{XCH}_2\text{CH}_2\text{O}_2$	$\text{XCH}(\text{CH}_3)\text{CH}(\text{CH}_3)\text{O}_2$	$\text{XC}(\text{CH}_3)_2\text{C}(\text{CH}_3)\text{O}_2$
H	0.82	$\sim 0.01^a$	$\sim 0.0003^b$
Cl	33	-	-
Br	56	6.9	0.2
OH	23	6.7	0.04

a:  $k(2 \text{ CH}_3\text{O}_2)$ ; b:  $k(2 \text{ CH}_3)_2\text{CO}_2$ .

This work demonstrates the strong enhancement of the self-reaction rate constants for selected primary, secondary and tertiary alkylperoxy radicals upon Br-atom substitution at the  $\beta$  position (as already observed for OH substitution). However, the decrease of the rate constant from primary to tertiary radicals is still apparent, but in a lesser extent than in the case of unsubstituted radicals.

The reaction of  $\text{HO}_2$  with the tertiary peroxy radical bearing a bromine atom is shown to be fast, having similar Arrhenius parameters to those known for most other peroxy radicals. This shows again that the size of radicals is the major factor contributing to increase the rate constant of this class of reaction and that the influence of the bromine atom is negligible.

# THE USE OF 2D UNSTRUCTURED ADAPTIVE MESHES IN THE MODELLING OF POWER STATION PLUMES

J.D.B.Smith<sup>1</sup>, A.S.Tomlin<sup>2</sup>, G.Hart<sup>2</sup>, M. Berzins<sup>3</sup>, V.Pemington<sup>3</sup>, M.J.Pilling<sup>1</sup>

1: School of Chemistry 2: Dept. of Fuel and Energy 3: School of Computer Studies  
University of Leeds, Woodhouse Lane, Leeds, LS2 9JT, UK

The chemical transformations, leading to the production of secondary pollutants such as ozone, that take place in a power station's plume, change as the plume travels downwind of the source. Close to the chimney, the high levels of NO inhibit the production of ozone, through the formation of NO<sub>2</sub>, but as the plume progresses from the chimney, volatile organic compounds (VOCs) become mixed in from anthropogenic and natural sources, providing alternative routes to the photolytic production of ozone. Modelling these plumes and their interactions with other emissions has become an important part of our attempts to understand the processes occurring in the tropospheric boundary layer.

$$\frac{\partial c}{\partial t} = -\frac{\partial(u c)}{\partial x} - \frac{\partial(w c)}{\partial y} + \frac{\partial}{\partial x} \left( K_x \frac{\partial c}{\partial x} \right) + \frac{\partial}{\partial y} \left( K_y \frac{\partial c}{\partial y} \right) + R(c_1, c_2, c_3, \dots, c_q) + E - (k_1) c \quad (1)$$

A model is described that discretises the two dimensional atmospheric diffusion equation (1) for each chemical species,  $c$ , onto an unstructured triangular mesh using the method of lines. This produces a system of ODEs that are solved as a set of initial value problems. The base mesh can then be refined and de-refined as necessary, according to a pre-determined tolerance applied to the local spatial error. In this fashion, the solution is 'followed' and higher mesh refinement is only provided where the solution dictates that it is.

Using a systematically reduced chemical mechanism, CBMleeds containing 29 species and 57 reactions, the impact of the power station plumes on the regional ozone levels is investigated. The advantages of adaptive grids over fixed grids are shown.

# LABORATORY STUDIES ON THE ATMOSPHERIC PHOTOLYSIS OF NITROUS ACID

Samantha F.M. Ashbourn and R. Anthony Cox

Centre for Atmospheric Science, University Chemical Laboratory, Lensfield Road,  
Cambridge, CB2 1EW, UK

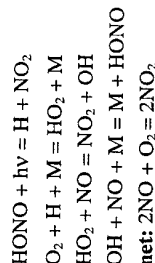
Nitrous acid (HONO) has been established as a common atmospheric pollutant. In sunlight, HONO is photolysed, providing a source of OH radicals which can initiate photo-oxidant formation and thus influence tropospheric oxidising capacity:



Recent work suggests the presence of a second photolysis channel:



This latter channel may help explain apparent anomalously high conversion rates of NO to NO<sub>2</sub> in conditions of poor dispersion in winter, through the reaction sequence:



Laser photolysis experiments<sup>1</sup> in the first absorption band at 355 nm show strong indirect evidence for the production of H atoms in HONO photolysis at wavelengths below the threshold for reaction (2), as originally proposed by Cox. Further evidence comes from comparison of the relative absorption coefficients determined by conventional light absorption methods and by laser photofragment spectroscopy.<sup>2,3</sup>

The steady-state photolysis of HONO is being investigated in a flow system using a UV-visible spectrometer to measure HONO, NO and NO<sub>2</sub>. The apparatus which employs a dual channel diode array absorption set up allows the measurement of small changes in the concentration of HONO, NO and NO<sub>2</sub> in the reaction mixture on photolysis. The aim is to determine wavelength resolved quantum yields for the two channels from measurement of the rate of loss of HONO and formation of NO<sub>2</sub> during

photolysis of HONO, with and without the presence of excess NO, which will suppress the formation of NO by reaction (1).

- 1) Burkholder J.B., Mellouki A., Talukdar R. and Ravishankara A.R. (1992) Rate coefficients for the reaction of OH with HONO between 298 and 373 K, *Int. J. Chem. Kinet.* **24**, 711-725.
- 2) Bongartz A., Kames J., Welter F. and Schurath U. (1991) Near-UV absorption cross sections and trans/cis equilibrium of nitrous acid, *J. Phys. Chem.* **95**, 1076-1082.
- 3) Vasudev R. (1990) Absorption spectrum and solar photodissociation of gaseous nitrous acid in the actinic wavelength region, *Geophys. Res. Lett.* **17**, **12**, 2153-2155.

C37

# KINETICS AND MECHANISM FOR THE OXIDATION OF CHLORINATED ALKANES AND ALKENES.

Marcus Manning, Jack Treacy, and Howard Sidebottom,

*Chemistry Department,  
University College Dublin, Dublin, Ireland.*

The distribution and fate of volatile organohalogen compounds in the atmosphere has recently attracted considerable attention. In particular, it has been shown that chloroacetic acids occur in air, precipitation and plant biomass at levels in excess of those considered to be toxic to vegetation. The source of haloacetic acids is the subject of considerable speculation at the present time. It is frequently assumed that halogenated compounds found in environmental compartments are almost all of anthropogenic origin, however, the concentration of these species observed in the atmosphere indicate that natural sources also make a substantial contribution to the total organohalogen budget.

The aim of this study is to provide mechanisms for the atmospheric degradation of a range of structurally selected organohalogen compounds and to determine the kinetic parameters required to quantify these processes. The results provide structure-reactivity relationships for the reactions which may be used to make reliable predictions concerning the atmospheric oxidation of organohalogen species in general.

# KINETIC STUDIES OF THE REACTION OF HYDROXYL RADICALS WITH OXYGEN-CONTAINING ORGANIC COMPOUNDS

Edward Porter, Jack Treacy and Howard Sidebottom  
*Chemistry Department, University College, Dublin, Ireland.*

Wahid Mellouki, Sophie Téton and Georges LeBras  
*LCSR-CNRS, Orléans, France.*

Marie Thérèse Rayez  
*CNRS, Université Bordeaux, Bordeaux, France.*

Oxygenated compounds have increasing application as water soluble solvents and fuel additives. In addition, they are formed as oxidation products of both aliphatic and aromatic hydrocarbons. The effects of these species on tropospheric ozone and formation of other secondary pollutants following releases into the atmosphere is of some concern. Kinetic data for the reactions of OH radicals with alcohols, ethers, ketones and carboxylic acids have been obtained using both a pulsed laser-laser induced fluorescence technique and a conventional relative rate method. The rate data provide estimates of the atmospheric lifetimes and provide structure-reactivity information on the reactions. The oxygen-containing functional groups in these compounds show long-range activating effects with respect to hydrogen atom abstraction by the OH radical. Thus, the presence of the functional group appears to stabilize the reaction transition states. In an attempt to rationalize the rate data the semi-empirical quantum mechanical method PM3 has been used to investigate the nature of the transition states for the reaction of OH radicals with oxygenated organic molecules.

# KINETICS AND MECHANISMS FOR THE REACTION OF HYDROXYL RADICALS WITH FLUORINATED ETHERS

Niamh O'Sullivan, Jack Treacy, Howard Sidebottom

*Chemistry Department,  
University College Dublin, Dublin, Ireland.*

Fluorinated ethers have been proposed as replacement compounds for chlorofluorocarbons particularly in the area of refrigeration. Fluorinated ethers resemble CFCs in their physical and chemical characteristics, but the presence of at least one hydrogen atom in these compounds means that they are degraded largely in the troposphere following reaction with the hydroxyl radical. Since fluorinated ethers do not contain chlorine, their contribution to stratospheric ozone depletion is expected to be negligible, however, it is important to determine their environmental impact with respect to their Global Warming Potential and degradation products.

In this investigation rate coefficients for the reaction of hydroxyl radicals with a series of fluorinated ethers were determined over the temperature range 250-320K using a conventional photolytic relative rate technique. The results give estimates of the atmospheric lifetimes of these compounds and provide structure-reactivity information on the reactions. Product distribution studies using FTIR spectroscopy and mass spectrometry yield information on the site of OH radical attack on the ethers and also on the reactions of the alkoxy radicals generated in the reactions.

## DECOMPOSITION OF THE ALKOXY RADICAL FROM HFC-134a (CF<sub>3</sub>CFH<sub>2</sub>)

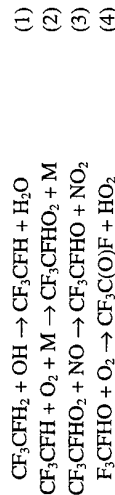
Trine E. Møgelberg, Jens Sehested and Ole J. Nielsen

*Section for Chemical Reactivity  
Environmental Science and Technology Department  
Risø National Laboratory  
DK-4000 Roskilde, Denmark*

Timothy J. Wallington

*Ford Research Laboratory, SRL-E3083  
Ford Motor Company  
Dearborn, P. O. Box 2053  
Michigan 48121-2053, USA*

HFC-134a (CF<sub>3</sub>CFH<sub>2</sub>) is a substitute for CFC-12 in refrigeration and air conditioning units. The current global production of HFC-134a is  $1 \times 10^5$  tonnes yr<sup>-1</sup> and is anticipated to double in the next 25 years [1]. The concentration of HFC-134a in the remote atmosphere is 1.5 ppt and is increasing exponentially at approximately 100% yr<sup>-1</sup> [2]. As with all HFC's HFC-134a has no impact on stratospheric ozone [3]. HFC-134a and has only a modest Global Warming Potential [4]. However, questions have been raised concerning the environmental impact of trifluoroacetic acid [5,6] which is formed from HFC-134a in the atmosphere as a result of the following reaction sequence [7,8,9,10].



Reaction (4) produces CF<sub>3</sub>C(O)F which is hydrolyzed to CF<sub>3</sub>COOH after uptake in cloud and rainwater [11,12]. However, CF<sub>3</sub>COOH production is avoided if CF<sub>3</sub>CFHO radicals decompose instead of reacting with O<sub>2</sub>.



Assessment of the ecological impact of CF<sub>3</sub>COOH requires accurate knowledge of its source, i.e., accurate kinetic data for reactions (4) and (5).

Decomposition of the CF<sub>3</sub>CFHO radical formed in the reaction of CF<sub>3</sub>CFHO<sub>2</sub> radicals with NO was studied at 296 and 393 K using a pulse radiolysis transient VIS-UV absorption absolute rate technique. At room temperature in 1 atmosphere of SF<sub>6</sub> diluent it was found that the majority (79±20)% of CF<sub>3</sub>CFHO radicals formed in the CF<sub>3</sub>CFHO<sub>2</sub>+NO reaction decompose within 3 μs via C-C bond scission. An upper limit

for the lifetime of CF<sub>3</sub>CFHO radicals with respect to C-C bond scission,  $\tau_{\text{CF}_3\text{CFHO}}$ , of <3 μs was obtained at room temperature.

The understanding of the atmospheric chemistry of the CF<sub>3</sub>CFHO radical has been advanced recently by work in our laboratory. Reaction (3) is exothermic by 17 kcal mol<sup>-1</sup> and it was shown that a substantial fraction (64<sup>+12</sup><sub>-23</sub>%) of the CF<sub>3</sub>CFHO radicals produced in reaction (3) possess sufficient internal excitation to undergo prompt decomposition while the remainder are thermalized [i]. To provide further information on k<sub>3</sub> we have conducted an experimental study using the pulse radiolysis technique; results are reported herein. This result is discussed with respect to the current understanding of the atmospheric degradation of HFC-134a. As a part of the present work the rate constant ratio  $k_{\text{CF}_3\text{CFH}+\text{O}_2}/k_{\text{CF}_3\text{CFH}+\text{NO}}$  was determined to be 0.144±0.029 in one atmosphere of SF<sub>6</sub> diluent at 296K.

### References:

1. McCulloch, A., *Environ. Monitor. Assess.*, **1994**, 31, 167.
2. Montzka, S. A.; Myers, R. C.; Butler, J. H.; Elkins, J. W.; Lock, L. T.; Clarke, A. D., *Geophys. Res. Lett.*, **1996**, 23, 169.
3. Wallington, T. J.; Schneider, W. F.; Sehested, J.; Nielsen, O. J., *J. Chem. Soc., Faraday Discussions*, **1996**, 100, 55.
4. Pinnock, S.; Shine, K. P.; Smyth, T. J.; Hurley, M. D.; Wallington, T. J., *J. Geophys. Res.*, **1995**, 100, 23227.
5. Tromp, T. K.; Ko, M. K. W.; Rodrigez, J. M.; Sze, N. D., *Nature*, **1995**, 376, 327.
6. Visscher, P. T., C. W. Culbertson; R. S. Oremland, *Nature*, **1994**, 369, 729.
7. DeMore, W. B.; Sander, S. P.; Golden, D. M.; Hampson, R. F.; Kurylo, M. J.; Howard, C. J.; Ravishankara, A. R.; Kolb, C. E.; Molina, M. J., *JPL Publication 94-26*, **1994**.
8. Wallington, T. J.; Nielsen O. J., *Chem. Phys. Lett.*, **1991**, 187, 33.
9. Bhatnagar, B.; Carr, R. W., *Chem. Phys. Lett.*, **1995**, 238, 9.
10. Peeters, J.; Pultau, V., *Proceedings of CEC/EUROTRAC Workshop on "Chemical Mechanisms Describing Tropospheric Processes"*, Edited by Peeters, September **1992**.
11. Wallington, T. J.; Schneider, W. F.; Worsnop, D. R.; Nielsen, O. J.; Sehested, J.; DeBruyn, W. J.; Shorter, J. A., *Environ. Sci. Tech.*, **1994**, 28, 320A.

# REACTIONS OF DIMETHYLETHER AT 296-666 K

Jesper Platz, Jens Sehested, Knud Sehested  
*Section for Chemical Reactivity*  
*Environmental Science and Technology Department*  
*Risø National Laboratory*  
*DK-4000 Roskilde, Denmark*

Ole J. Nielsen  
*Ford Forschungszentrum Aachen*  
*Dennewartstrasse 25*  
*D-52068 Aachen, Germany*

Dimethylether (DME) has been proposed as an alternative fuel in diesel engine vehicles. The combustion of DME produce less  $\text{NO}_x$  and aerosols compared to the combustion of conventional diesel fuels. To find the reason for this difference, we have studied the kinetics of the reactions between the  $\text{CH}_3\text{OCH}_2$  radical and  $\text{O}_2$ , the self reaction of the  $\text{CH}_3\text{OCH}_2$  radical, and the thermal decomposition of  $\text{CH}_3\text{OCH}_2$  were studied in the temperature range 296-666 K. At temperatures above 473 K the  $\text{O}_2$  was removed by direct reaction with DME. The experimental technique used for these experiments is pulse radiolysis combined time resolved UV absorption spectroscopy. Reactant concentrations used where 1-20 bar of  $\text{SF}_6$ , 10-100 mbar of  $\text{CH}_3\text{OCH}_3$ , and 0.5 mbar of  $\text{O}_2$ .

12. Alternative Fluorocarbon Environmental Acceptability Study, W. M. O. Global Ozone Research and Monitoring Project, Report #20; Scientific assessment of stratospheric ozone, Vol 2, 1989.

- i. Wallington, T.J.; Fracheboud, J.M.; Orlando, J.; Tyndall, G.S.; Sehested, J.; Møgelberg, T.E.; Nielsen, O.J., *J. Phys. Chem.*, submitted 1996.

## ATMOSPHERIC CHEMISTRY OF 1,2-DICHLOROETHANE

Ole J. Nielsen

*Ford Motor Company**Ford Forschungszentrum Aachen**Dennewartstrasse 25**D-52068 Aachen, Germany*

Timothy J. Wallington

*Ford Motor Company**Ford Research Laboratory, SRL-E3083**Dearborn, P.O. Box 2053**Michigan 48121-2053, USA*

Merete Bilde, Trine E. Møgelberg, Jens Sehested

*Section for Chemical Reactivity**Environmental Science and Technology Department**Risø National Laboratory**DK-4000 Roskilde, Denmark*

A pulse radiolysis technique was used to measure the UV absorption spectra of  $\text{CH}_2\text{ClCHCl}$  and  $\text{CH}_2\text{ClCHClO}_2$  radicals over the range 220-300 nm. The self-reaction rate constants were measured. The rate constant for reaction of  $\text{CH}_2\text{ClCHCl}$  radicals with  $\text{O}_2$  in one bar of  $\text{SF}_6$  diluent and the rate constants for the reactions of  $\text{CH}_2\text{ClCHClO}_2$  radicals with  $\text{NO}$  and  $\text{NO}_2$  were determined. A FTIR spectroscopic technique showed that  $\text{CH}_2\text{ClCHClO}$  radicals undergo intramolecular  $\text{HCl}$  elimination and reaction with  $\text{O}_2$ . In 700 Torr of air at 296K the rate constant ratio  $k_{\text{O}_2}/k_{\text{HCl}}$  elimination =  $(2.3 \pm 0.2) \times 10^{-20} \text{ cm}^3 \text{ molecule}^{-1}$ . A lower limit of  $10^5 \text{ s}^{-1}$  was deduced for the rate of decomposition of  $\text{CH}_2\text{ClCHClO}$  radicals at 296 K in 1 bar of  $\text{SF}_6$  diluent. Results are discussed in the context of the atmospheric chemistry of 1,2-dichloroethane.

## ATMOSPHERIC CHEMISTRY OF ACETIC ANHYDRIDE

Lene K. Christensen, Merete Bilde, Trine E. Møgelberg, Jesper Platz, Jens Sehested

*Section for Chemical Reactivity**Environmental Science and Technology Department**Risø National Laboratory*

Timothy J. Wallington

*Ford Motor Company**Ford Research Laboratory, SRL-E3083**Dearborn, P.O. Box 2053**Michigan 48121-2053, USA*

Ole J. Nielsen

*Ford Motor Company**Ford Forschungszentrum Aachen**Dennewartstrasse 25**D-52068 Aachen, Germany*

Gasphase reactions of acetic anhydride were studied by pulse radiolysis/UV absorption technique to determine the kinetics and a smog chamber/FTIR spectroscopic technique was used to determine the reaction products. The study include i) the UV absorption spectrum of the peroxy radical  $\text{CH}_3(\text{CO})\text{O}(\text{CO})\text{CH}_2\text{O}_2$  radical. ii) The rate constant of the self reaction of the  $\text{CH}_3(\text{CO})\text{O}(\text{CO})\text{CH}_2\text{O}_2$  radical. iii) The rate constants for the reactions of  $\text{CH}_3(\text{CO})\text{O}(\text{CO})\text{CH}_2\text{O}_2$  with  $\text{NO}$  and  $\text{NO}_2$ . iv) The fate of the alkoxy radical  $\text{CH}_3(\text{CO})\text{O}(\text{CO})\text{CH}_2\text{O}$ . The reactions are discussed in the context of the atmospheric chemistry of  $\text{CH}_3(\text{CO})\text{O}(\text{CO})\text{CH}_3$ .

## REACTIONS OF CHLORINE ATOMS WITH AROMATIC COMPOUNDS

Barbara O'Leary and Jack Treacy

*Department of Chemistry, Dublin Institute of Technology, Dublin, Ireland*

Howard Sidebottom

*Department of Chemistry, University College Dublin, Dublin, Ireland.*

Reaction with OH radicals is believed to be the dominant loss process for aromatic compounds in the troposphere [1]. However, it has recently been suggested that Cl atoms may play a significant role in the gas phase degradation of volatile organic compounds in marine air masses [2]. Measurements of the ambient concentrations of alkanes [3] and alkyl nitrates [4] in the lower troposphere during the Arctic springtime also provide evidence for the importance of Cl atom reactions in the atmosphere. A growing body of evidence from field experiments, laboratory studies and model calculations suggest that, in addition to HCl, highly reactive chlorine-containing species, such as Cl<sub>2</sub>, HOCl and ClNO, also volatilise from sea salt aerosol in the marine boundary layer. Subsequent photolysis of these compounds may provide relatively high levels of Cl in various regions of the troposphere[5].

The available kinetic data for reactions of Cl atoms with aromatic compounds is very limited. Rate constants at room temperature and 1 atmosphere total pressure have been reported for reaction with benzene, toluene, and xylenes [6,7]. This work involves kinetic studies on the reaction of Cl atoms with a series of aromatic compounds as a function of temperature and pressure. The results provide structure-activity relationships for the reactions.

## References

- [1] R. Atkinson, J. Phys. Chem. Ref. Data, Monograph 2, 1 (1994).
- [2] W.C. Keene, D.J. Jacob, and S.M. Fan, Atmos. Environ., 30A, 1 (1996).
- [3] N.B. Kjeser, J.W. Bottenheim, T. Sideris and H. Niki, Atmos. Environ., 27A, 2979 (1993).
- [4] K. Muthuram, P.B. Shepson, J.W. Bottenheim, B.T. Jobson, H. Niki and K.G. Anlauf, J. Geophys. Res., 99, 25369 (1994).
- [5] P.A. Hooshiyar and H. Niki, Int. J. Chem. Kinet., 27, 1197 (1995).
- [6] T.J. Wallington, L.M. Skewes and W.O. Siegl, J. Photochem. and Photobiol. 45, 167 (1988).
- [7] S.M. Aschmann and R. Atkinson, Int. J. Chem. Kinet., 27, 613 (1995).

# ULTRA-LOW TEMPERATURE REACTIONS OF ELECTRONS, IONS AND RADICALS WITH MOLECULES

B.R. Rowe

*Physique des Atomes, Lasers, Molécules et Surfaces*  
U.R.A. 1203 du C.N.R.S.

*Université de Rennes I, 35042 Rennes Cedex*

More than 100 molecules have been detected in dense interstellar clouds, mostly using millimetre and sub-millimetre spectroscopy. Some of these molecules are complex having as many as 13 atoms and while some are found in our terrestrial environment, others (such as polyacetylenes) are more exotic, and are not found naturally. Theoretical astrochemical models, capable of reproducing the evolution of the observed species, are becoming more and more sophisticated, and nowadays include homogeneous gas phase reactions between electrons, ions and neutrals, as well as reactions involving neutral species on the surface of grains [1]. Despite this sophistication, we are still very far from a full understanding of this topic and a large number of uncertainties exist, particularly with regard to specific reaction rates.

The study of gas phase reactions at the extremely low temperatures (10-100K), typically encountered in the interstellar medium, presents a veritable challenge for the experimenter. In particular, most species (with the exception of hydrogen and helium) have negligible vapor pressures at temperatures close to 10K and condense immediately, forming ices on the walls of cryogenically cooled apparatus. Despite these difficulties, during the 1980's, several groups have developed independent methods to measure rate coefficients for ion-molecule reactions at temperatures well below that of liquid nitrogen. The studies were justified by the key role played by this class of reactions in interstellar chemistry. The ease with which ions can be manipulated, stored and detected by convenient electromagnetic fields allowed specific techniques to be developed, which however, are not adaptable to the study of neutral radicals. We can cite, for example, the drift tube [2], cryogenically cooled ion traps [3], [4], as well as merged beam experiments [5] which allow reaction cross sections at very low energies, to be determined. A method which is much less specific in its application, is to use a supersonic jet as a chemical flow reactor. Thus, at the beginning of the 1980's, the group of Rowe developed such a technique [6], that employs a uniform supersonic flow issuing from a Laval nozzle. This technique is referred to under the name of CRESU (a French acronym for *Cinétique de réaction en Ecoulement Supersonique Uniforme*). Many reactions have been studied by this method for temperatures down to 8K. More recently, Mark Smith and his collaborators [7] have used pulsed free jets to study ion-molecule reactions down to equivalent temperatures of 0.1K (These jets are not in thermodynamic equilibrium).

All these techniques have led to the development of a substantial database of experimental results concerning ion-molecule reactions at ultra-low temperatures that can be compared with current theoretical results, and it is now possible to predict with a higher degree of confidence, the temperature dependence of most ion-molecule

reactions. Of course, there exists many cases which do not obey general rules and research is still very active in this domain.

At the end of the 1980's, almost no results existed concerning the kinetics of reactions between neutral radicals and molecules, below about 80K. On the one hand, interstellar chemistry models favored ionic paths for the formation of molecules. Neutral-neutral reactions were usually believed to exhibit activation barriers and so such reactions were not considered important. On the other hand, most of the techniques, developed for the study of ionic reactions were not adaptable to studies of neutral radicals, anyway. As it has turned out, however, the CRESU method lent itself remarkably well, via the incorporation of the powerful PLP-LIF (Pulsed Laser Photolysis/Laser Induced Fluorescence) technique, to the study of radical-neutral reactions.

This adaptation has been effected in collaboration between the groups of Rowe and Ian Smith of the University of Birmingham, following the construction of a CRESU apparatus at Rennes [8]. In the last five years, 27 reactions, involving the radicals CN, OH, CH and Al have been studied. The LIF technique also allows the internal state (vibration, rotation and spin-orbit) of the reactants and products to be probed and so it can be either verified that they are in Local Thermodynamic Equilibrium (LTE) or their relaxation can be examined. The results that have been obtained have shown in some cases very surprising kinetic behaviors and have opened a new window on interstellar chemistry: It is in fact clear that neutral-neutral chemistry is not negligible in the models of astrochemistry and it has already been shown that its influence on the calculation of molecular abundances, is considerable. A large amount of work remains on the part of theoreticians to reproduce the temperature dependences of these rate coefficients with sufficient confidence.

The formation of interstellar molecules via gas phase ion chemistry implicates the role of electrons through the process of dissociative recombination through which neutrals are formed from large polyatomic ions. The possible presence of Polycyclic Aromatic Hydrocarbons (PAHs) however, in the interstellar medium presents a problem due to their possible capacity to attach electrons at ultra-low temperatures and if this proves to be the case, then this could render current astrochemical models obsolete. There are a number of very sophisticated techniques [9] (Threshold Photoelectron, Rydberg Atom) which allow studies of attachment to be performed at very low electron energies and with an energy resolution, unequalled in other domains ( $\mu\text{eV}$ ). These techniques however, do not allow the molecules, under study, to be cooled to very low temperatures and are therefore difficult to use for very condensable molecules such as PAHs. The CRESU technique has recently been applied to this type of study and, for example, the profound influence of the internal state of the molecules studied ( $\text{CF}_3\text{Br}$  and  $\text{CCl}_2\text{F}_2$ ) upon the attachment rate has been demonstrated.

In conclusion, experimental studies have demonstrated that an extremely rich chemistry, and one, more complex than the simple gas phase ion chemistry of the early models, can develop in the extreme cold of the interstellar medium. Considerable work remains to be done however, as many uncertainties remain concerning the formation paths for interstellar molecules, and particularly for the more complex species.

1) Herbst, E., *Annul Rev. Phys. Chem.*, **46**, 27, 1995.

2) Bohringer, H. and F. Arnold, *Int. J. Mass Spectrom. Ion Proc.*, **49**, 61, 1983.

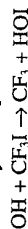
# INVESTIGATIONS OF THE REACTIONS OF OH, H AND O WITH CF<sub>3</sub>I AND THE HEAT OF FORMATION OF HOI: COMPARISONS WITH CH<sub>3</sub>I AND C<sub>2</sub>H<sub>5</sub>I

R. J. Berry,<sup>a</sup> W.-J. Yuan,<sup>b</sup> A. Misra<sup>b</sup> and Paul Marshall<sup>a,b</sup>

<sup>a</sup>Center for Computational Modeling of Nonstructural Materials, Wright Laboratory,  
Wright-Patterson Air Force Base, Ohio 45433

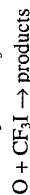
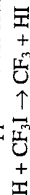
<sup>b</sup>Department of Chemistry, University of North Texas, PO Box 5068, Denton, Texas  
76203-0068

Following the ban on halon production under the Montreal protocols, there is a search for candidates to replace the fire suppression agents CF<sub>3</sub>Br and CF<sub>2</sub>ClBr. For some applications a possible substitute is CF<sub>3</sub>I. In order to improve our understanding of the combustion and atmospheric chemistry of CF<sub>3</sub>I the kinetics of the reaction



have been investigated by the flash photolysis - resonance fluorescence technique to obtain  $k = 9.9 \times 10^{-12} \exp(-12.7 \text{ kJ mol}^{-1}/RT) \text{ cm}^3 \text{ molecule}^{-1} \text{ s}^{-1}$  over the temperature range 280-450 K. Accuracy limits range from 30% at 280 K to 10% at 450 K. The transition state and reaction coordinate for this reaction were characterized at the *ab initio* G2(MP2) level of Gaussian-2 theory, and the results suggest a negligible barrier to the reverse reaction CF<sub>3</sub> + HOI, and thus a small activation energy of  $0 \pm 5 \text{ kJ mol}^{-1}$ . The difference between this quantity and the measured forward activation energy implies  $\Delta H_{298}(\text{HOI}) = -70 \pm 7 \text{ kJ mol}^{-1}$ . As a check on this thermochemistry the enthalpy of formation of the product HOI was analyzed with *ab initio* G2 calculations, by relating  $\Delta_f H(\text{HOI})$  to G2 energies for ICN, ClCN, INO and other small molecules. The result is in good accord with the experimentally-based value.

A similar computational analysis was applied to the reactions



and good accord with literature kinetic data is obtained. The reactions are compared and contrasted with the analogous reactions of CH<sub>3</sub>I with OH, H and O and also OH + C<sub>2</sub>H<sub>5</sub>I, and the implications of the kinetic and thermochemical results for iodine chemistry in flames and the atmosphere are discussed. The tropospheric lifetime of CF<sub>3</sub>I with respect to OH attack is found to be much longer than the photolysis lifetime, and the relative importance of H, O and OH attack and unimolecular decomposition is assessed for CF<sub>3</sub>I in a methane flame.

- 3) Barlow, S.E., J.A. Luine and G.H. Dunn, Int. J. Mass Spectrom. Ion Proc., **74**, 97, 1986.
- 4) Gerlich, D., and S. Homing, Chem. Rev., **92**, 1509, 1992.
- 5) Gerlich, D., XII Int. Symp. on Mol. Beams, V. Aquilanti ed., Perugia, p. 37, 1989.
- 6) Rowe, B.R., G. Dupeyrat, J.B. Marquette, and P. Gaucherel, J. Chem. Phys., **80**, 4915, 1984.
- 7) Hawley, M., T.L. Mazely, L.K. Randeniya, R.S. Smith, X.K. Zeng and M.A. Smith, Int. J. Mass Spectrom. Ion Proc., **80**, 239, 1990.
- 8) Sims I.R., J.L. Queffelec, A. Defrance, C. Rebrion-Rowe, D. Travers, P. Bocherel, B.R. Rowe, and I.W.M. Smith, J. Chem. Phys., **100**, 4229, 1994.
- 9) Dunning F.B., J. Phys. B.: At. Mol. Opt. Phys., **28**, 1645, 1995.

# HEAT OF FORMATION OF CH<sub>2</sub>OH RADICAL: IMPROVED PARTITION FUNCTIONS THAT RECONCILE CONFLICTS AMONG KINETIC EQUILIBRIUM AND PHOTOIONIZATION MASS SPECTROMETRY MEASUREMENTS

Jeffrey W. Hudgens and R. D. Johnson III

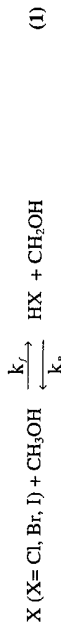
Physical and Chemical Properties Division  
Chemical Science and Technology Laboratory  
National Institute of Standards and Technology

Gaithersburg, MD 20899 USA

Tel. 301-975-2512 and Fax: 301-975-3672

E-mail: Hudgens@enh.nist.gov

The CH<sub>2</sub>OH radical plays important roles in combustion of hydrocarbon fuels, atmospheric pollution chemistry, and interstellar chemistry. Nearly 120 papers have described its properties and reactions. Even so, the heat of formation of CH<sub>2</sub>OH is uncertain. Figure 1 summarizes the experimental determinations of  $\Delta H_{f,298.15}^{\circ}(\text{CH}_2\text{OH})$ . The kinetic equilibrium determinations were obtained from the forward and reverse rates of the reactions:



The ion appearance determinations were obtained from the threshold appearance energy of CH<sub>2</sub>OH<sup>+</sup> from CH<sub>3</sub>OH. After 30 years of study, determinations of  $\Delta H_{f,298.15}^{\circ}(\text{CH}_2\text{OH})$  obtained from these methods seemed irreconcilable.

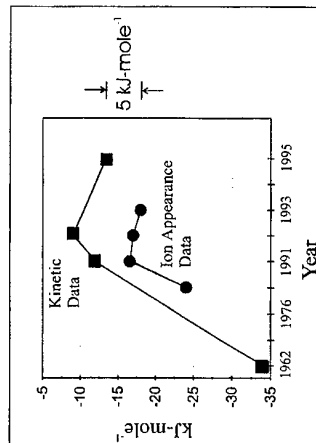


Figure 1. Determinations of  $\Delta H_{f,298.15}^{\circ}(\text{CH}_2\text{OH})$  from kinetic equilibria and ion data.

internal rotation will vary  $S_{298.15}^{\circ}(\text{CH}_2\text{OH})$  by 15 J-(mol-deg)<sup>-1</sup> and  $\Delta H_{f,298.15}^{\circ}(\text{CH}_2\text{OH})$  by 5.6 kJ-mol<sup>-1</sup>.

We have conducted experiments and performed *ab initio* calculations to obtain accurate partition functions for hydroxymethyl radicals and cations. Our results show that previously-accepted spectroscopic data contain substantial conceptual errors and do not include vibrational states residing below 400 cm<sup>-1</sup>. We measured these missing vibrational levels by experimentally observing the extremely weak "hot" bands exhibited in the  $\tilde{B}^2A'(3p) \leftarrow \tilde{X}^2A''$  resonance enhanced multiphoton ionization (REMPI) spectra of CH<sub>2</sub>OH, CH<sub>2</sub>OD, CD<sub>2</sub>OH, and CD<sub>2</sub>OD produced by the reaction of fluorine with methanol. Using optimized MP2/6-311G(2df,2p) calculations, we constructed potential energy surfaces for the radical and cation. Eigenvalues obtained from these potential energy surfaces reproduce the REMPI data and show that the missing levels arise from strongly coupled v<sub>8</sub> torsion (internal rotation) and v<sub>9</sub> CH<sub>2</sub>-wag modes.

Using the new experimental and *ab initio* results, we calculated heat capacities and entropies for the radical and cation using the improved partition functions. The new thermochemical values differ significantly from previous ones. Recalculations of older kinetic equilibrium data using the new entropy,  $S_{298.15}^{\circ}(\text{CH}_2\text{OH}) = 244.170 \pm 0.018$  J-(mol-deg)<sup>-1</sup>, and new heat capacities lower  $\Delta H_{f,298.15}^{\circ}(\text{CH}_2\text{OH})$  by 2-4 kJ/mole. Re-evaluated mass spectrometry data and kinetic equilibrium data lie in agreement and suggest that  $\Delta H_{f,298.15}^{\circ}(\text{CH}_2\text{OH}) = -17.8 \pm 1.3$  kJ-mol<sup>-1</sup>. Our recommended value is also supported by extensive *ab initio* CBS-QCIVAPNO calculations that predict  $\Delta H_{f,298.15}^{\circ}(\text{CH}_2\text{OH}) = -18.4 \pm 1.3$  kJ-mol<sup>-1</sup>.

Previous studies have regarded all vibrational modes as distinct oscillators and rotors. In fact, the v<sub>8</sub> torsion (internal rotation) and v<sub>9</sub> CH<sub>2</sub>-wag modes are strongly coupled and governed by nonharmonic potential energy surfaces. In the radical the CH<sub>2</sub>-wag coordinate has a 156 cm<sup>-1</sup> barrier at the planar configuration and two 1643 cm<sup>-1</sup> barriers to internal rotation. Accurate predictions of the v<sub>8</sub> and v<sub>9</sub> energy levels require simultaneous solutions for motion along both coordinates.

Several previous studies have regarded the hydroxymethyl radical as a totally nonsymmetric species, i.e., as a member of the C<sub>1</sub> point group. In fact, the wavefunctions of hydroxymethyl species belong to the C<sub>s</sub> point group in the rigid molecule picture and to the G<sub>4</sub> permutation-inversion group (which is isomorphic to the C<sub>2v</sub> point group) in the non-rigid molecule picture. Therefore, the proper symmetry number of hydroxymethyl radicals and cations is  $\sigma = 2$ . This symmetry misassignment has also increased errors in some previous entropy calculations.

# VIBRATIONAL RELAXATION OF BENDING MODES OF N<sub>2</sub>O AND OCS BY O ATOMS

Sumith P. Withanage and Leon F. Phillips

*Department of Chemistry, University of Canterbury, Canterbury, NZ*

In previous work [1] we used a new variant of the temperature-jump method to measure the rate of vibrational relaxation of the bending mode of CO<sub>2</sub> by atomic oxygen. The method was to dissociate ozone by flash photolysis in the presence of CO<sub>2</sub> and argon buffer gas, while monitoring the population of a single rotational level belonging to the (010) vibrational state with an infrared diode laser. The photolytic flash served both to produce a known concentration of oxygen atoms and to raise the gas temperature by about 20K. The rate constant was obtained by measuring the relaxation of the population of the vibrational state on a microsecond time-scale with a transient digitizer. We also made preliminary measurements of the relaxation of the bending mode of N<sub>2</sub>O by O atoms, in order to assess the importance of the existence of a bound CO<sub>3</sub> species in the relaxation of CO<sub>2</sub>. However, this comparison was flawed by the ability of O(<sup>1</sup>D), formed in the ozone photolysis, to react chemically with N<sub>2</sub>O.

In the present study we have used NO<sub>2</sub> instead of ozone as the photolytic source of O atoms to avoid the problem with O(<sup>1</sup>D). Quenching of N<sub>2</sub>O(010) by O atoms is slower by a factor of 4 than quenching of CO<sub>2</sub>, which suggests that incipient bond formation with CO<sub>2</sub> may well play a part in the relaxation process. The results are compared with trajectory calculations using the curve-crossing model of Nikitin and Umansky [2]. Final results of the trajectory calculations are not available at the time of writing this preliminary abstract, and the same applies to the results of analogous experiments with OCS, which are intended to determine the effect of having both a heavier collision partner and sulfur d-orbitals available for bonding with O atoms. Trajectory calculations using the curve-crossing model contain two adjustable parameters, namely the crossing radius and a Landau-Zener parameter with the dimensions of velocity. Values for both parameters can be obtained by comparing experimental and theoretical relaxation rates over a range of temperatures. If time permits, the results of preliminary studies in this direction will also be presented.

[1] G.B.I.Scott, D.S.Pollock and L.F.Phillips, Temperature-jump and trajectory studies of the vibrational relaxation of CO<sub>2</sub> by atomic oxygen, *J.Chem.Soc.Faraday Trans.*, 89 (1993) 1183.

[2] E.E.Nikitin and S. Ya. Umanski, Effect of vibronic interactions upon the vibrational relaxation of diatomic molecules. *Faraday Disc.Chem.Soc.*, 53 (1972) 7.

# REACTIONS OF FIRST-ROW TRANSITION METAL ATOMS WITH SIMPLE MOLECULES.

R. Matsui, K. Senba, and Kenji Honma

*Department of Material Science, Himeji Institute of Technology, Kamigori, Hyogo, Japan*

## Introduction

Transition metals play key roles in various chemical processes. Gas phase kinetics of atom and ion is expected to provide basic information to understand more complex processes like catalysis. From a more elementary point of view, one interesting property of transition metal atoms is the high density of low-lying electronic states that results from the near degeneracy of the ns and (n-1)d orbitals. Therefore, the transition metals provide a unique opportunity to study roles of electronic configuration and electronic energy in chemical reactions.

We have measured electronic state-selected reaction rate constants of Ti(<sup>3</sup>F), Ti(<sup>3</sup>F), V(<sup>4</sup>F), and V(<sup>4</sup>D) with some simple molecules by using a discharged-flow tube apparatus.<sup>1</sup>

The results of reactions with oxygen containing molecules, O<sub>2</sub>, NO, and N<sub>2</sub>O, were summarized as the following.

- (1) No difference of rate constants were observed among, spin-orbit sublevels.
- (2) In both metal atoms, the excited states, Ti(<sup>3</sup>F) and V(<sup>4</sup>D), which have 4s<sup>2</sup>3d<sup>n-1</sup> configurations were depleted more efficiently than the ground states, Ti(<sup>3</sup>F) and V(<sup>4</sup>F), which have 4s<sup>2</sup>3d<sup>n-2</sup> configurations.
- (3) The large reactivities of the excited states could be explained by the reaction mechanism where surface crossing between covalent and ionic surfaces takes place.

Here we extended the measurements for the reactions of late transition metals, Co and Ni, with O<sub>2</sub>, NO, and N<sub>2</sub>O. There are some differences in these systems from the reactions of Ti and V. First, no reactive channels are available except for the reaction with N<sub>2</sub>O because of weak bondings of Co-O and Ni-O. Ionization potentials of these atoms are rather high, 7.86eV and 7.635 eV for Co and Ni, respectively, compared with Ti(6.82 eV) and V(6.74 eV). Separation of the spin-orbit sublevels is the other difference, i.e. the larger spin-orbit coupling of Co and Ni split their sublevels wider than those of Ti and V.

## Experimental

Experiment was carried out by using a DC discharge-flow apparatus. The metal atoms were formed by DC discharge (3kV, 10mA) and their concentration were determined by the laser-induced fluorescence. Depletion of the LIF signal was measured as a function of reactant concentration, and they were converted to a rate constant. Typical pressure of He was 0.7Torr and 5% of Ar was added to stabilize the discharge.

## Results and Discussion

Table summarized the rate constants for the depletion of Co and Ni by the interaction upon O<sub>2</sub>. The observed rate constants,  $k_{\text{obs}}$ , are compared with the hard-sphere rate constants,  $k_{\text{HS}}$ 's, and listed in this table. Estimated activation energies,  $E_a$ 's, were calculated by  $E_a = RT \ln(k_{\text{HS}}/k_{\text{obs}})$ .

No depletion was observed for the ground state of Co(<sup>a</sup>F<sub>1</sub>) and the lowest three spin-orbit sublevels of Ni. The other triplet states of Ni showed very slow depletion. Compare with them, the first and second excited states of Co(<sup>b</sup>F<sub>1</sub>, <sup>a</sup>F<sub>1</sub>) and the singlet state of Ni were depleted quite efficiently. The rate constants were observed to be different among the spin-orbit sublevels of Co(<sup>b</sup>F<sub>1</sub>, <sup>a</sup>F<sub>1</sub>). Since no reactive channel is available for all of these states, only possible channel is an electronic energy transfer. One typical rate constant for the electronic energy transfer by the interaction with nonpolar molecule are those for Ti(<sup>a</sup>F<sub>1</sub>) + N<sub>2</sub> and V(<sup>a</sup>D<sub>1</sub>)+N<sub>2</sub><sup>1</sup>. The former is  $(6.5 \pm 2.2) \times 10^{-12} \text{ cm}^3 \text{ s}^{-1}$  and the latter is  $(0.50 \pm 0.03) \times 10^{-12} \text{ cm}^3 \text{ s}^{-1}$ , and the difference was ascribed to the electronic-vibrational energy transfer which is only possible to Ti(<sup>a</sup>F<sub>1</sub>) + N<sub>2</sub>. Compared with these values, the rate constants of the triplet states of Ni are in the same order as that for V + N<sub>2</sub>, and may be explained by the energy transfer with surface crossing. According to the *ab initio* calculation, the singlet Ni-O<sub>2</sub> is predicted to be 75 kJ/mol lower than the Ni(<sup>a</sup>D)+O<sub>2</sub> asymptote<sup>2</sup>, while no deep well is expected for V + N<sub>2</sub>. Our results indicate that this complex is not accessible from any triplet Ni with O<sub>2</sub> without potential barrier.

The rate constants for the excited states of Co are much larger than that of Ti(<sup>a</sup>F<sub>1</sub>) + N<sub>2</sub>, where we concluded that the surface crossing between two repulsive potentials take place. This implies that an attractive potential is important in the case of Co + O<sub>2</sub>. One possibility is the attractive interaction between one of half-filled 3d orbitals of Co and also half-filled  $\pi^*$  orbital of O<sub>2</sub>. In the case of C<sub>2v</sub> symmetry, this interaction makes a stable complex Co-O<sub>2</sub>. More population in the  $\pi^*$  orbital elongate O-O distance and favorable to E-V energy transfer. Enhancement of rate constants by the electronic energy is also consistent with the formation of the intermediate, since more product channels become possible by the larger total energy of the complex.

**Table** Effective bimolecular rate constants for reactions of Co and Ni with O<sub>2</sub> (in 10<sup>-12</sup> cm<sup>3</sup>/s)

Metal Atoms	energy(cm <sup>-1</sup> )	$k_{\text{obs}}$	$k_{\text{HS}}/k_{\text{obs}}$	$E_a$ (kJ/mol)
Co( <sup>a</sup> F <sub>9/2</sub> )	0	NR*	> 3900	20.6
Co( <sup>a</sup> F <sub>7/2</sub> )	816.00	NR		
Co( <sup>a</sup> F <sub>5/2</sub> )	1406.84	NR		
Co( <sup>a</sup> F <sub>3/2</sub> )	1809.33	NR		
Co( <sup>b</sup> F <sub>9/2</sub> )	3482.82	33±3	6	4.5
Co( <sup>b</sup> F <sub>7/2</sub> )	4142.66	57±12	3	3.1
Co( <sup>b</sup> F <sub>5/2</sub> )	4690.18	103±26	2	1.6

Co( <sup>b</sup> F <sub>3/2</sub> )	5075.83	115±24	2	1.3
Co( <sup>a</sup> F <sub>7/2</sub> )	7442.41	75±20	3	2.4
Co( <sup>a</sup> F <sub>5/2</sub> )	8460.81	52±24	4	3.3
$k_{\text{HS}}$		197		
Ni( <sup>a</sup> F <sub>4</sub> )	0	NR	> 3900	20.6
Ni( <sup>a</sup> F <sub>3</sub> )	1332.15	0.1±0.02	2000	18.8
Ni( <sup>a</sup> F <sub>2</sub> )	2216.52	0.6±0.1	330	14.4
Ni( <sup>a</sup> D <sub>3</sub> )	204.79	NR		20.6
Ni( <sup>a</sup> D <sub>2</sub> )	879.81	NR		20.6
Ni( <sup>a</sup> D <sub>1</sub> )	1713.08	0.30±0.06	650	16.1
Ni( <sup>a</sup> D <sub>2</sub> )	3409.93	186±64	1	0.1
$k_{\text{HS}}$		191		

\* NR indicates that the rate constant is smaller than the detection limit,  $5 \times 10^{-14} \text{ cm}^3 \text{ s}^{-1}$ .

## References

- (1) E. Clemmer, K. Honma, and I. Koyano, J. Phys. Chem. **97**, 11480 (1993); K. Honma, M. Nakamura, D. E. Clemmer, and I. Koyano, J. Phys. Chem. **98**, 13286 (1994); K. Honma and D. E. Clemmer, Laser Chem. **15**, 209 (1995); K. Honma, J. Chinese Chem. Soc. **42**, 371 (1995); K. Senba, R. Matsui, and K. Honma, J. Phys. Chem. **99**, 13992 (1995).
- (2) R. A. Blomberg, P. E. M. Siegbahn, and A. Strich, Chem. Phys. **97**, 287 (1985).

# KINETIC AND MECHANISTIC STUDIES OF THE REACTIONS OF ATOMIC CHLORINE WITH A SERIES OF HALOALKANES

C. A. Piety<sup>1a</sup>, J. M. Nicovich<sup>1b</sup>, Y. V. Ayhens<sup>1a,1b,3</sup>, E. G. Estupinan<sup>1c</sup>,  
R. Soller<sup>1c</sup>, M. L. McKee<sup>2</sup>, and P. H. Wine<sup>1a,1b,1c</sup>

1.: Georgia Institute of Technology, Atlanta, GA 30332

a. School of Chemistry and Biochemistry

b. Georgia Tech Research Institute

c. School of Earth and Atmospheric Sciences

2.: Dept. of Chemistry, Auburn University, Auburn, AL 36849

3.: Currently at Dept. of Chemistry and Biochemistry, University of Colorado,  
Boulder, CO 80309

A laser flash photolysis-resonance fluorescence technique has been employed to study the kinetics of reactions of ground state atomic chlorine,  $\text{Cl}(^2\text{P}_1)$ , with a series of haloalkanes as a function of temperature (160–700 K) and pressure (3–600 Torr). The haloalkane reactants investigated include  $\text{CH}_3\text{I}$ ,  $\text{CH}_3\text{Br}$ ,  $\text{CF}_3\text{I}$ ,  $\text{CH}_2\text{ClI}$ ,  $\text{CH}_2\text{ClBr}$ ,  $\text{CH}_3\text{CH}_2\text{I}$ ,  $\text{CD}_3\text{CD}_2\text{I}$ , and  $\text{CF}_3\text{CH}_2\text{I}$ . While some of the reactions studied may play a role in atmospheric chemistry, an important goal of this research was to gain some insight into the physical parameters which control observed reactivity patterns.

At relatively high temperatures, observed kinetic behavior in conjunction with established thermochemistry and available information from the literature (for  $\text{CH}_3\text{Br}$ ,  $\text{CF}_3\text{I}$ ,  $\text{CH}_2\text{ClBr}$ , and  $\text{CH}_2\text{ClI}$  only) suggests that the dominant reaction pathways are hydrogen transfer for  $\text{Cl}(^2\text{P}_1)$  reactions with  $\text{CH}_3\text{I}$ ,  $\text{CH}_3\text{Br}$ ,  $\text{CH}_2\text{ClBr}$ ,  $\text{CH}_3\text{CH}_2\text{I}$ , and  $\text{CF}_3\text{CH}_2\text{I}$ , and iodine transfer for  $\text{Cl}(^2\text{P}_1)$  reactions with  $\text{CF}_3\text{I}$  and  $\text{CH}_2\text{ClI}$ . Arrhenius parameters obtained in the "high temperature" studies are summarized in Table I. Agreement with published kinetic data for  $\text{Cl}(^2\text{P}_1)$  reactions with  $\text{CH}_3\text{Br}$  [1,2],  $\text{CF}_3\text{I}$  [3,4],  $\text{CH}_2\text{ClBr}$  [1] and  $\text{CH}_2\text{ClI}$  [5] is reasonably good. The very fast rate coefficient for the  $\text{Cl}(^2\text{P}_1) + \text{CH}_2\text{ClI}$  reaction appears to be attributable to the fact that the iodine transfer channel is exothermic for this reaction whereas iodine or bromine transfer is endothermic for all other reactions investigated.

At sufficiently low temperatures, observed kinetic behavior suggests that formation of weakly bound adducts becomes the dominant pathway for most reactions studied. Through direct observation of association-dissociation kinetics and associated second- and third-law analyses of the equilibrium data, bond strengths have been evaluated for  $\text{Cl}(^2\text{P}_1)$  adducts with  $\text{CH}_3\text{I}$ ,  $\text{CH}_3\text{Br}$ ,  $\text{CF}_3\text{I}$ ,  $\text{CD}_3\text{CD}_2\text{I}$ , and  $\text{CF}_3\text{CH}_2\text{I}$ ; the results are summarized in Table II. *Ab initio* calculations employing density functional theory at the Becke 3LYP level reproduce experimental bond strengths reasonably well and predict structures where the C–X–Cl bond angles are close to 90 degrees (X = I or Br).

**Table I.** Arrhenius parameters for non-adduct-forming channels in  $\text{Cl}(^2\text{P}_1)$  reactions with the haloalkanes of interest.

haloalkane Range of T (K)	A <sup>a</sup>	E/R (K)	k(298K) <sup>a</sup>	Expt.
$\text{CH}_3\text{I}$	550	1260	8.1	364–694
$\text{CH}_3\text{Br}$	b	b	4.4	197–690
$\text{CF}_3\text{I}$	810	1570	4.2	220–418
$\text{CH}_2\text{ClBr}$	77	897	3.8	222–428
$\text{CH}_2\text{ClI}$	433	-198	800	206–432
$\text{CH}_3\text{CH}_2\text{I}$	634	409	160	350–434
$\text{CD}_3\text{CD}_2\text{I}$	260	383	72	350–434
$\text{CF}_3\text{CH}_2\text{I}$	45	266	18.5	274–434

a. Unit are  $10^{13} \text{ cm}^3 \text{ molecule}^{-1} \text{ s}^{-1}$ .

b. T-dependence was non-Arrhenius:  $k = 3.2 \times 10^{-15} T^{1.26} \exp(-670/T) \text{ cm}^3 \text{ molecule}^{-1} \text{ s}^{-1}$ .

An excellent inverse correlation exists between observed (or calculated) adduct bond strengths and the haloalkane ionization potential. Both the dependence of observed bond strengths on haloalkane ionization potential and the theoretical bond angles are consistent with the formation of 2 center - 3 electron bonds involving interaction between the singly occupied orbital of the chlorine atom and the highest (doubly) occupied molecular orbital of the haloalkane.

**Table II.** Experimental bond strengths ( $D^0$ ) of  $\text{Cl}(^2\text{P}_1)$ -haloalkane adducts.

Haloalkane			
Haloalkane	Ionization Pot. (eV) <sup>a</sup>	$D^0$ (kJ/mol) <sup>b,c</sup>	$D^0_{298}$ (kJ/mol) <sup>b,c</sup>
$\text{CH}_3\text{Br}$	10.54	24.1	24.5
$\text{CF}_3\text{I}$	10.23	30.0	30.1
$\text{CF}_3\text{CH}_2\text{I}$	10.00	46.4	46.6
$\text{CH}_3\text{I}$	9.54	51.5	51.5
$\text{CD}_3\text{CD}_2\text{I}$	9.35	59.0	59.1

a. Ionization potentials taken from reference 6.

b. Adduct entropies and heat capacities calculated using structures obtained from *ab initio* calculations (see text).

c. Reported bond strengths are averages of second- and third-law determinations.

1. E. Tschuikow-Roux, F. Faraji, S. Paddison, J. Niedzielski, and K. Miyokawa, *J. Phys. Chem.* **92**, 1488(1988).
2. T. Gierczak, L. Goldfarb, D. Sueper, and A. R. Ravishankara, *Int. J. Chem. Kinet.* **26**, 719(1994).
3. S. Ahonkhai and E. Whittle, *Int. J. Chem. Kinet.* **16**, 543(1984).
4. E. W. Kaiser, T. J. Wallington, and M. D. Hurley, *Int. J. Chem. Kinet.* **27**, 205(1995).
5. T. J. Wallington, private communication.
6. S. G. Lias, J. E. Bartmess, J. F. Liebman, J. L. Holmes, R. D. Levin, and W. G. Mallard, *J. Phys. Chem. Ref. Data* **17**, Suppl. 1 (1988).

#### Acknowledgments

The experimental component of this research was supported by the National Aeronautics and Space Administration-Upper Atmosphere Research Program. Computer time for the *ab initio* calculations was made available by the Alabama Supercomputer Network.

## REACTIONS OF O(<sup>1</sup>D) WITH CHLORIDES AND FLUORIDES: TOTAL QUENCHING, CHANNEL SPECIFIC RATE CONSTANTS, AND YIELDS OF Cl(<sup>2</sup>P<sub>1/2</sub>)

A.I. Chichinin

*Institute of Chemical Kinetics and Combustion,  
630090, Novosibirsk, Russian Federation*

The kinetics of the reactions of O(<sup>1</sup>D) atoms with M molecules (M=HCl, Cl<sub>2</sub>, COCl<sub>2</sub>, F<sub>2</sub>, XeF<sub>2</sub>, NF<sub>3</sub>, and SF<sub>6</sub>) have been studied by time-resolved laser magnetic resonance (LMR) at 298 K and pressures between 5 and 30 Torr. M/O<sub>2</sub>/He mixtures slowly flowing through a reactor were photolyzed by an excimer laser (KrF, 248 nm). Cl atoms or FO radicals were produced in reactions of O(<sup>1</sup>D) with M molecules. Cl atoms were detected by fine structure <sup>2</sup>P<sub>1/2</sub>-<sup>2</sup>P<sub>3/2</sub> absorption using the 11 P(36) line of <sup>13</sup>CO<sub>2</sub>-laser (882.287 cm<sup>-1</sup>). FO radicals were detected using the 9 P(34) line of CO<sub>2</sub>-laser (1033.488 cm<sup>-1</sup>). The determination of the absolute values for rate constants requires the calibration of LMR signals. In calibration experiments, Cl atoms were produced by COCl<sub>2</sub> photolysis in the absence of ozone; FO radicals were produced by photolysis of XeF<sub>2</sub>/O<sub>2</sub>/N<sub>2</sub> mixture, XeF<sub>2</sub> photodissociation was followed by the F+O<sub>3</sub> → FO+O<sub>2</sub> reaction. In the latter case O(<sup>1</sup>D) atoms were absent because of the rapid quenching of O(<sup>1</sup>D) by N<sub>2</sub>. Results of the study and the literature data are presented in the Table.

Note that reaction of O(<sup>1</sup>D) with F<sub>2</sub> is probably one order of magnitude slower, although it is more exothermic, than the reaction of O(<sup>1</sup>D) with Cl<sub>2</sub>. This preliminary experimental fact is confirmed by rough calculations of the potential energy surface for O(<sup>1</sup>D)+F<sub>2</sub> system.

It was concluded that at low pressures (40±5) % of the deactivation of O(<sup>1</sup>D) by COCl<sub>2</sub> leads to Cl+ClO+CO products, (20±10) % of the deactivation leads to 2Cl+CO<sub>2</sub>, and the rest (40±11) % is Cl<sub>2</sub>+CO<sub>2</sub> channel and physical quenching of O(<sup>1</sup>D).

$R \rightarrow E$  energy transfer due to long-range multipole interaction between OH(OD, HF) and ground state Cl atoms is proposed as a mechanism of Cl(<sup>2</sup>P<sub>1/2</sub>) formation in the O(<sup>1</sup>D)+HCl(DCl), F+HCl reactions. Probabilities of Cl(<sup>2</sup>P<sub>1/2</sub>) formation were estimated with a model, which is close to the Sharma-Brau-Ewing model; reasonably good agreement with experimental results was obtained.

M	$k_M$ , cm <sup>3</sup> /s deactivation	$q_M$ , cm <sup>3</sup> /s reaction only	$q_M/k_M$ , %	$\beta$ , a) %	Ref.
Cl <sub>2</sub>	(2.2 ± 0.2) × 10 <sup>-10</sup>	(1.8 ± 0.6) × 10 <sup>-10</sup>			[1]
	(2.8 ± 0.4) × 10 <sup>-10</sup>	(2.1 ± 0.4) × 10 <sup>-10</sup>	75 ± 10		[2]
	(2.5 ± 0.5) × 10 <sup>-10</sup>	(1.9 ± 0.32) × 10 <sup>-10</sup>	76 ± 12	<5	[3]
HCl	(1.4 ± 0.4) × 10 <sup>-10</sup>				[4]
	(1.5 ± 0.2) × 10 <sup>-10</sup>	(1.0 ± 0.2) × 10 <sup>-10</sup>	67 ± 10		[5]
	(1.5 ± 0.3) × 10 <sup>-10</sup>	(0.94 ± 0.20) × 10 <sup>-10</sup>	63 ± 10	10 ± 4	d)
COCl <sub>2</sub>	(1.8 ± 0.4) × 10 <sup>-10</sup>				[6]
	(7.1 ± 0.9) × 10 <sup>-10</sup>		>80		[7]
	(2.6 ± 0.5) × 10 <sup>-10</sup>	(2.05 ± 0.27) × 10 <sup>-10</sup>	79 ± 18	<10	d)
F <sub>2</sub>		1.4 × 10 <sup>-11</sup>	e)		d)
XeF <sub>2</sub>	(1.6 ± 0.4) × 10 <sup>-10</sup>	(1.4 ± 0.4) × 10 <sup>-10</sup>			d)
NF <sub>3</sub>	(1.2 ± 0.3) × 10 <sup>-11</sup>	(1.0 ± 0.3) × 10 <sup>-11</sup>			d)
SiF <sub>4</sub>	<1.4 × 10 <sup>-11</sup>				d)
SF <sub>6</sub>	(1.8 ± 0.26) × 10 <sup>-14</sup>	1.26 × 10 <sup>-14</sup>	70 ± 10		[8]
		(3.5 ± 1.5) × 10 <sup>-14</sup>			d)

a)  $\beta \equiv [Cl(^3P_{1/2})] / ([Cl(^3P_{1/2})] + [Cl(^3P_{3/2})])$

b)  $q_{HCl}$  is the rate constant of the reaction O(<sup>1</sup>D) + HCl → Cl + OH

c)  $q_{COCl_2} = k_1 + 2k_2$ , where  $k_1$  and  $k_2$  are the rate constants of the reactions O(<sup>1</sup>D) + COCl<sub>2</sub> → Cl + ClO + CO and O(<sup>1</sup>D) + COCl<sub>2</sub> → 2Cl + CO<sub>2</sub>, respectively

d) this work, quoted errors are 2σ

e) only preliminary

- 1) K. Freudenstein, D. Biedenka, Ber. Bunsenges. Phys. Chem., **80**, 42 (1976).
- 2) S. Fletcher, D. Husain, Ber. Bunsenges. Phys. Chem., **80**, 982 (1976).
- 3) P. H. Wine, J. M. Nicovich and A. R. Ravishankara, J. Phys. Chem., **89**, 3914 (1985).
- 4) J. A. Davidson, H. I. Shiff, G. E. Steit, J. R. McAfee, A. L. Schmeltekopf and C. J. Howard, J. Chem. Phys., **67**, 5021 (1977).
- 5) Wine, J. R. Wells and A. R. Ravishankara, J. Chem. Phys., **84**, 1349, (1986)
- 6) R. K. M. Jayanty, R. Simonaitis and J. Heicklen, J. Photochem., **8**, 217 (1976)
- 7) I. S. Fletcher and D. Husain, J. Photochem., **8**, 355 (1978).
- 8) A. R. Ravishankara, S. Solomon, A. A. Turnipseed and R. F. Warren, Science **259**, 194 (1993).

# **DIRECT ABSTRACTION vs. RECOMBINATION-ELIMINATION MECHANISM IN SiH<sub>3</sub> + Cl REACTION.**

A. V. Baklanov, E. N. Chesnokov, A. I. Chichinin

*Institute of Chemical Kinetics and Combustion, Novosibirsk, 630090, Russia.*

This paper reports further studies of the reaction between a silyl radical and chlorine atom initiated in paper [1], in which the rate constant was measured and a possible reaction mechanism discussed. This paper is devoted to the understanding of the detailed mechanism of this reaction.

Two mechanisms can be assumed for the SiH<sub>3</sub>+Cl reaction: direct H atom abstraction



or the formation of the vibrationally excited molecule of silylchloride SiH<sub>3</sub>Cl\* via recombination:



either deactivating further upon collisions with buffer gas molecules:



or eliminating H<sub>2</sub> and HCl via the channels below:



The mechanism of the radical-atom reactions with silyl radical has obtained only minor attention up to now.

In this paper the mechanism of SiH<sub>3</sub>+Cl reaction has been studied by means of two approaches. Firstly, the yield of molecular hydrogen in SiH<sub>4</sub>+Cl and in SiD<sub>4</sub>+Cl systems has been measured by mass-spectrometry to estimate the contribution of the recombination-elimination channel which should mainly result in the formation of H<sub>2</sub> via reaction (4). Secondly, the kinetics of HCl(v) luminescence has been measured experimentally with time-resolved IR-luminescence technique to estimate the contribution of the direct abstraction channel (1).

In both approaches the chlorine atoms have been produced by photolysis of phosgene  $\text{COCl}_2$  with KrF laser radiation (248 nm), which gives two Cl atoms and inert CO molecule. The yield of atomic Cl was varied by changing the laser pulse energy. The yield of molecular hydrogen plotted as a function of the ratio  $[\text{Cl}]_0/[\text{SiH}_4]_0$  is shown in Fig. 1. In excess Cl atom concentration the dependence is saturated and gives the value of the relative yield of molecular hydrogen in this system to be equal to  $\gamma=0.20\pm0.04$ . This yield in the case of  $\text{SiD}_4$  was found to be  $\gamma=0.19\pm0.04$ . This yield can be due to the reaction (4) and the

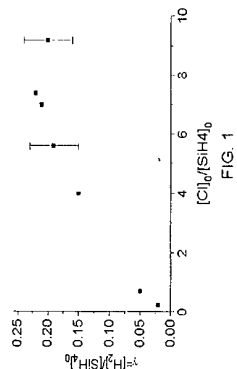


FIG. 1

$\text{SiH}_2+\text{Cl}\rightarrow\text{SiH}_2\text{Cl}^*\rightarrow\text{SiCl}+\text{H}_2$ . Because we cannot exclude the contribution of the last one, we conclude that the measured yield  $\gamma$  is an upper estimate of the contribution of the "recombination-elimination" channel giving rise to the molecular hydrogen (processes (2), (4)) in the reaction  $\text{SiH}_3+\text{Cl}\rightarrow$ . For estimation of the contribution of the recombination-elimination channel (reaction (2)) as a whole it is necessary to estimate the contribution of the channels (3), (5). We have estimated the ratio of the decomposition rate constants of excited  $\text{SiH}_3\text{Cl}^*$  via channels (4) and (5) by means of RRKM calculations to be equal to  $k_4/k_5=1.5$ . These calculations were based on the barrier heights  $E_0$  and transition states vibrational frequencies calculated *ab initio* by Su and Schlegel [5]. The channel of quenching (3) was estimated to be negligible. So we have obtained the upper estimate of the recombination-elimination channel (2) to be near 0.3.

The kinetics of IR-chemiluminescence of vibrationally excited hydrogen chloride  $\text{HCl}(\nu)$  arising in the  $\text{SiH}_4+\text{Cl}$  system has been studied as a function of the ratio  $[\text{Cl}]_0/[\text{SiH}_4]_0$ , varied within the limits 0.25 — 10. The kinetics of  $\text{HCl}(\nu)$  luminescence has been measured experimentally and modeled by numerical solution of a set of differential equations describing a kinetic scheme of the processes occurring in the system under study. This modelling was necessary to subtract the known [5] contribution of  $\text{HCl}(\nu)$  arising in the primary reaction  $\text{SiH}_4+\text{Cl}$ . For the reaction  $\text{SiH}_3+\text{Cl}\rightarrow$  the yields of  $\text{HCl}(1)$  and  $\text{HCl}(2)$  have been determined to be

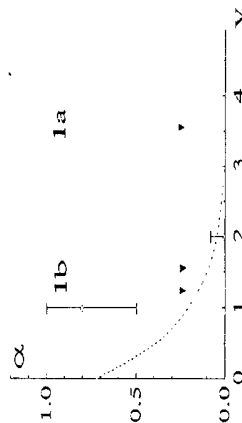


FIG. 2

$\alpha_1=0.8^{+0.2}_{-0.3}$  and  $\alpha_2\leq 0.08$ , respectively (Fig. 2). In Fig. 2 the "prior" distribution of  $\text{HCl}(\nu)$  calculated in the approximation of the unity yield of HCl in reaction  $\text{SiH}_3+\text{Cl}\rightarrow$  is also shown (dashed curve). Taking into account that the whole yield of HCl in this reaction can not be more than 1 we conclude that the distribution is inverted or near that. This indicates on the direct abstraction mechanism to be prevailing in this reaction. The thermochemical limits of the possible  $\text{HCl}(\nu)$  distributions arising in (1a) and (1b) reactions are also shown (dotted arrows). Two limits for the reaction (1b) correspond to two values of singlet-triplet splitting given in literature [4]. The

observed cut at  $\nu=2$  corresponds to the reaction (1b) as a source of observed  $\text{HCl}(\nu)$  distribution. So we conclude that reaction  $\text{SiH}_3+\text{Cl}$  proceeds mainly via direct abstraction mechanism with the final product  $\text{SiH}_2$  to be in triplet ( $^3B_1$ ) state.

The "orbital symmetry correlation" diagram has been considered for the direct  $\alpha$ -abstraction mechanism (abstracted atom is in  $\alpha$ -position to a free electron orbital of radical) in radical-atom and radical-radical reactions. In Fig.3 the scheme of the reaction of "direct abstraction"  $\text{XH}_3+\text{Cl}\rightarrow\text{XH}_2+\text{HCl}$  giving rise to biradical in the triplet T (configuration of unbound electrons  $s^1p^1$ ) and singlet S (configuration  $s^2$ ) states is presented.

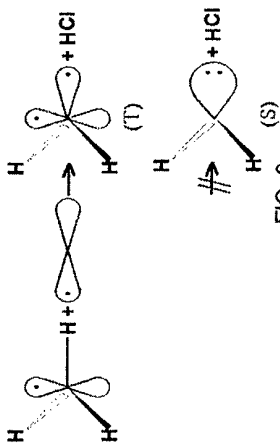


FIG. 3

This figure shows the correlation between initial state of reagents and triplet state of the products from the point of orbital symmetry conservation. Although the picture corresponds to the symmetrical case of planar radical and linear transition state, the orbital symmetry predictions are usually applicable to the unsymmetrical cases too, because they reveal the qualitative features of the orbitals partitioning in the reactions. Qualitatively this picture shows that the initial state of reagents correlates with the state of products with unpaired electrons on the central atom of biradical. This is characteristic for the lowest triplet states of biradicals but not for the lowest singlet ones. So we suppose that direct  $\alpha$ -abstraction mechanism (the abstracted atom is in  $\alpha$ -position to the free electron of radical) can prevail in the radical-atom and radical-radical reactions only if the triplet state of the biradical is accessible from the point of thermochemistry. And if this mechanism is established for some reaction, the biradical should appear in a triplet state. Our results on  $\text{SiH}_3+\text{Cl}\rightarrow$  reaction are in agreement with this prediction.

The Russian Foundation of the Fundamental Researches (project 93-03-05018) and the International Scientific Foundation (project RBK000) provided financial support of this work.

[1]. A.V. Baklanov and A.I. Chichinin, Chem. Phys. 181 (1994) 119.

[2] Thermodynamical properties of the individual substances (in Russian), 3-d ed., (Nauka, 1978).

[3]. P.Ho, M.E.Coltrin, J.S.Binkley and C.F.Melius, J.Phys.Chem. 89 (1985) 4647.

[4]. J. Berkowitz, J.P. Greene, H. Cho and B. Ruscic, J. Chem. Phys. 86 (1987) 1235.

[5]. M.D. Su and H.B. Schlegel, J. Phys. Chem. 97 (1993) 9981.

# KINETICS AND THERMOCHEMISTRY OF BUTYL RADICAL ISOMERS AND SECONDARY PROPYL RADICAL. STUDY OF $R+HBr \leftrightarrow RH+Br$ EQUILIBRIUM

J. A. Seetula

Department of Chemistry, The Catholic University of America, Washington D.C., 20064, USA [Present address: Laboratory of Physical Chemistry, P.O. BOX 55 (A.I. Virtasen aukio 1), FIN-410014 University of Helsinki, Helsinki, Finland]

The kinetics of the reactions of  $n-C_4H_9$ ,  $i-C_4H_9$ ,  $s-C_4H_9$ ,  $t-C_4H_9$  and  $i-C_3H_7$  with  $HBr$  have been investigated in a treatable tubular reactor coupled to a photoionization mass spectrometer. Pulsed, unfocused exciplex laser radiation at 248 nm was used to generate the radical of interest. The reactions were studied under pseudo-first-order conditions. The decay of the radical was monitored as a function of  $HBr$  concentration to determine rate constants of the  $R+HBr$  reaction as a function of temperature range and pressure range. The measured rate constants are independent of the carrier gas density in the pressure range used in this study. All of the reactions studied do have a clear negative activation energy (see Figure). Certain trends in kinetic behaviour of the reactions studied are apparent: 1) The most complex radical has the highest reactivity with  $HBr$ . 2) Activation energy becomes more negative when complexity of the radical increases. 3) These findings are in good agreement with the reactions of bulky alkyl radicals with  $HI$ . 4) Radical reactivity increases parallel with the size of the radical for primary carbon-centered alkyl radicals in the following order:  $CH_3 < C_2H_5 < n-C_3H_7 < n-C_4H_9 \leq i-C_4H_9$ .

The forward reactions were investigated over a wide temperature range from 301 K to 677 K. This kinetic information was combined with rate constants of  $Br+RH$  reactions taken from the literature<sup>a, b</sup> to obtain the heat of formation of the radical at 298 K,  $\Delta H_f^\circ(298)$ , using a Second Law procedure. The results are shown below.

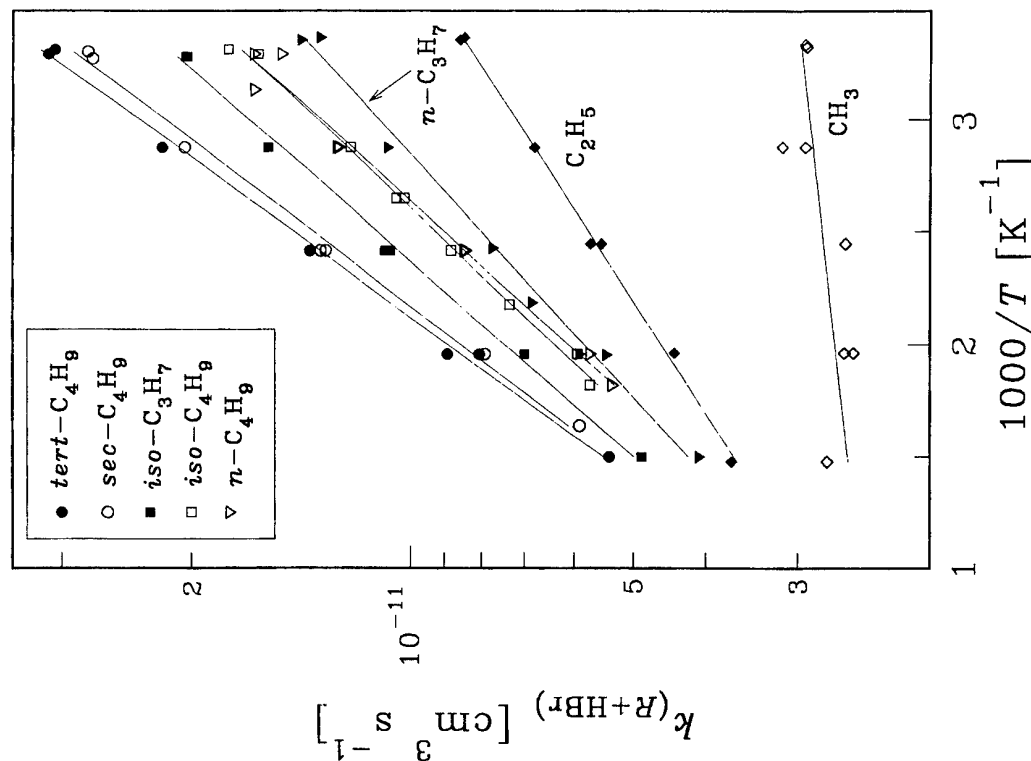
Radical	$\Delta H_f^\circ(298)$ [kJ mol <sup>-1</sup> ]	$S^\circ_{298}$ [J K <sup>-1</sup> mol <sup>-1</sup> ]	C-H Bond Strength at 298 K, [kJ mol <sup>-1</sup> ]
<i>tert</i> -C <sub>4</sub> H <sub>9</sub>	52.7±1.6	317±4	405.2±1.5 a,c
<i>sec</i> -C <sub>4</sub> H <sub>9</sub>	51.0±1.1	314±3	403.5±1.0 b,c
<i>iso</i> -C <sub>4</sub> H <sub>9</sub>	66.7±2.1	330±5	411.2±2.0 a,d
<i>n</i> -C <sub>4</sub> H <sub>9</sub>	72.7±2.2	316±5	425.2±2.1 a,e
<i>iso</i> -C <sub>3</sub> H <sub>7</sub>	80.5±2.2	328±5	425.0±2.1 a,f
	86.6±2.0	281±5	409.1±2.0 a,g

The reverse reaction is taken from (a) Seakins *et al.*, *J. Phys. Chem.* (1992) 96 9847. or (b) Russell *et al.*, *J. Am. Chem. Soc.* (1988) 110 3084.; The meaning of the other

references: (c) (*tert*-C-H bond in *isobutane*), (d) (*sec*-C-H bond in *n*-butane), (e) (*prim*-C-H bond in *iso*-butane), (f) (*prim*-C-H bond in *n*-butane) and (g) (*sec*-C-H bond in propane).

## Acknowledgements.

Support for this research at CUA was provided by the U.S. National Science Foundation (CHE-9102038). I thank the Finnish Combustion Research Program LIEKKI for financial support.



# KINETICS AND BRANCHING RATIOS OF THE REACTIONS

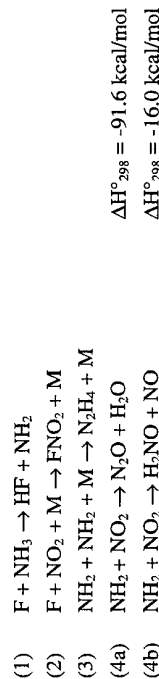
## $\text{NH}_2 + \text{NO}_2 \rightarrow \text{N}_2\text{O} + \text{H}_2\text{O}$ AND $\text{NH}_2 + \text{NO}_2 \rightarrow \text{H}_2\text{NO} + \text{NO}$ STUDIED BY PULSE RADIOLYSIS COMBINED WITH TIME-RESOLVED INFRARED DIODE LASER SPECTROSCOPY.

Hubert Meunier\*, Palle Pagsberg and Alfred Sillesen

*Environmental Science and Technology Department  
Risø National Laboratory, DK 4000 Roskilde Denmark*

*\*Assumption College, Worcester, MA, USA*

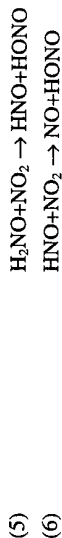
The source reaction  $\text{F} + \text{NH}_3 \rightarrow \text{HF} + \text{NH}_2$  was initiated by pulse radiolysis of  $\text{NH}_3/\text{SF}_6$  mixtures, and the title reactions have been studied by monitoring the decay of  $\text{NH}_2$  and the simultaneous formation of  $\text{N}_2\text{O}$  and  $\text{NO}$  by time resolved infrared diode laser spectroscopy. The primary yield of F-atoms produced by pulse radiolysis of  $\text{SF}_6$  was determined by monitoring the decrease in the infrared absorption of methane consumed in the titration reaction  $\text{F} + \text{CH}_4 \rightarrow \text{HF} + \text{CH}_3$ . Using a strong rotational transition of  $\text{CH}_4$  at  $1348.042 \text{ cm}^{-1}$  the line shape was scanned before and after pulse radiolysis of  $\text{CH}_3\text{SF}_6$  mixtures to determine the initial yield of  $[\text{F}]_0 = \Delta[\text{CH}_4] = (5.7 \pm 0.3) \times 10^{14} \text{ molecules/cm}^3$  obtained with a total pressure of  $\text{SF}_6 = 40 \text{ mbar}$  at  $298 \text{ K}$ . The title reactions were initiated by pulse radiolysis of  $\text{NO}_2/\text{NH}_3/\text{SF}_6$  mixtures, and the following reaction mechanism was found to account for the observed kinetic features and the branching ratios of the product channels.



The kinetics of  $\text{NH}_2$  was studied by monitoring the transient absorption at  $1406.012 \text{ cm}^{-1}$ . In the absence of  $\text{NO}_2$  the we observed simple second order kinetics in accordance with the combination reaction (3) proceeding with a half-life of  $25 \text{ }\mu\text{sec}$ . Under experimental conditions where all F-atoms are consumed in reaction (1) the maximum of the transient absorption signal corresponding to  $[\text{NH}_2]_{\text{max}} = [\text{F}]_0$  was used to derive the absorption cross section at the line center,  $\sigma(\text{NH}_2) = (1.65 \pm 0.17) \times 10^{-18} \text{ cm}^2/\text{molecule}^{-1}$ . From the observed second order decay we have derived an value of  $k_3$

$= (3.6 \pm 0.4) \times 10^{-11} \text{ cm}^3 \text{ molecule}^{-1} \text{ s}^{-1}$ . This value is close to published values of the limiting high pressure rate constant. The high value obtained at a total pressure of  $40 \text{ mbar}$  must be ascribed to the high efficiency of  $\text{M} = \text{SF}_6$  acting as the stabilizing third body. In the presence of  $\text{NO}_2$  we have identified two product channels (4a) and (4b). However, first the decay rate of  $\text{NH}_2$  was studied as a function of the  $\text{NO}_2$  concentration to obtain a value  $k_4 = k_{4a} + k_{4b} = (1.2 \pm 0.1) \times 10^{-11} \text{ cm}^3 \text{ molecule}^{-1} \text{ s}^{-1}$ .

The branching ratios of reactions (4a) and (4b) were determined by monitoring the formation kinetics of  $\text{N}_2\text{O}$  and  $\text{NO}$  using strong rotational transitions at  $1275.493 \text{ cm}^{-1}$  ( $\text{N}_2\text{O}$ ) and  $1849.216 \text{ cm}^{-1}$  ( $\text{NO}$ ). The experiments were carried out using ammonia concentrations in large excess of  $\text{NO}_2$  in order to avoid losses of F-atoms the fast addition reaction (2) which we have investigated recently. (Ref. 1) The yields of  $\text{N}_2\text{O}$  and  $\text{NO}$  were found to increase towards constant values of  $(60 \pm 3)\%$  and  $(40 \pm 4)\%$  under experimental conditions where all  $\text{NH}_2$  radicals were consumed in the reactions (4a) and (4b) without losses in the self reaction (3). Based on the observed formation of  $\text{NO}$  taking place on the same time scale as the  $\text{NH}_2$  decay we have proposed the simple O-atom transfer reaction (4b). However, so far we have no spectroscopic evidence for the formation of the nitroxyl radical,  $\text{H}_2\text{NO}$ . The formation of this radical by the reaction  $\text{F} + \text{NH}_2\text{OH} \rightarrow \text{HF} + \text{H}_2\text{NO}$  has been reported and the nitroxyl radical was identified by far infrared laser magnetic resonance spectroscopy in the range of  $299\text{--}742 \text{ }\mu\text{m}$ . (Ref.2) The nitroxyl radical appears to be remarkably stable. However, in the presence of  $\text{NO}_2$  we have considered reactions (5) and (6).



The  $\nu_3$  band of  $\text{HONO}$  in the range of  $1255 \text{ cm}^{-1}$  is very strong and since we did not observe any product absorption in this region it seems that we can rule out the occurrence of the reactions (5) and (6) at room temperature.

## References

- (1) Pagsberg, A. Sillesen, J.T. Jodkowski and E. Ratajczak Chem.Phys.Lett. **252** (1996) 165
- (2) P.B. Davies, P. Dransfeld, F. Temps and H.Gg. Wagner J.Chem.Phys. **81** (1984) 3763

# LASER-INDUCED FLUORESCENCE AND MASS-SPECTROMETRIC STUDIES OF COPPER ATOM REACTIONS OVER WIDE TEMPERATURE RANGES.\*

David P. Belyung, Jasmina Hranisavljevic, Oleg E. Kashureninov\*, G. Mauricio Santana, and Arthur Fontijn

*High-Temperature Reaction Kinetics Laboratory, The Isermann Department of Chemical Engineering, Rensselaer Polytechnic Institute, Troy, NY 12180-3590*

Paul Marshall

*Department of Chemistry, University of North Texas, Denton, TX 76203-5068*

The reactions of ground state  $\text{Cu}(^2\text{S})$  atoms with  $\text{HCl}$ ,  $\text{Cl}_2$ , and  $\text{N}_2\text{O}$  have been studied in high-temperature fast-flow reactors (HTFFR). The rate coefficient measurements were made using laser-induced fluorescence (LIF) of Cu atoms.

For  $\text{Cu} + \text{HCl}$  the observations yielded  $k(680 - 1500 \text{ K}) = 1.2 \times 10^{-10} \exp(-7719 \text{ K} / T) \text{ cm}^3 \text{ molecule}^{-1} \text{ s}^{-1}$ . Product analysis was achieved by coupling a specially designed HTFFR to a chopped molecular-beam quadrupole mass spectrometer. Those observations, which covered the approximately 1150-1500 K temperature range, showed formation of  $\text{CuCl}$  and the previously unknown species  $\text{HCuCl}$ . Confirmation of the latter assignment was made using DCI. Increasing pressure and decreasing temperature favor the  $\text{HCuCl}$  formation. These findings and this molecular structure are supported by *ab initio* calculations. These also indicate passage through a  $\text{CuClH} \rightarrow \text{HCuCl}$  transition state as the rate controlling step for formation of both products, in agreement with the observed pressure-independence of the overall, Cu-disappearance, rate coefficients.

The measurements for  $\text{Cu} + \text{Cl}_2$  yielded  $k(580 - 1140 \text{ K}) = 2.9 \times 10^{-10} \exp(-84 \text{ K}/T) \text{ cm}^3 \text{ molecule}^{-1} \text{ s}^{-1}$ , which is in accord with an abstraction mechanism. This is further supported by a molecular orbital analysis, which shows that: (i) due to the antibonding character of interacting  $\sigma^*$  orbital on  $\text{Cl}_2$ , the reaction can proceed only via a mechanism that involves bond breaking, and (ii) interaction of the Cu 4s orbital with the  $\sigma^*$  orbital of  $\text{Cl}_2$  in the insertion geometrical arrangement results in net zero orbital overlap. This leaves only  $\text{CuCl} + \text{Cl}$  as the possible products. Similar arguments have been used to explain the reaction between Cd and  $\text{Cl}_2$  and  $\text{O}_2$ .<sup>1</sup>

The  $\text{Cu} + \text{N}_2\text{O} \rightarrow \text{CuO} + \text{N}_2$  reaction had previously been studied from 470 - 1340 K in our laboratory using the pseudo-static MHTP (metals high-temperature photochemistry) technique.<sup>2</sup> The Cu atoms were monitored by hollow cathode lamp

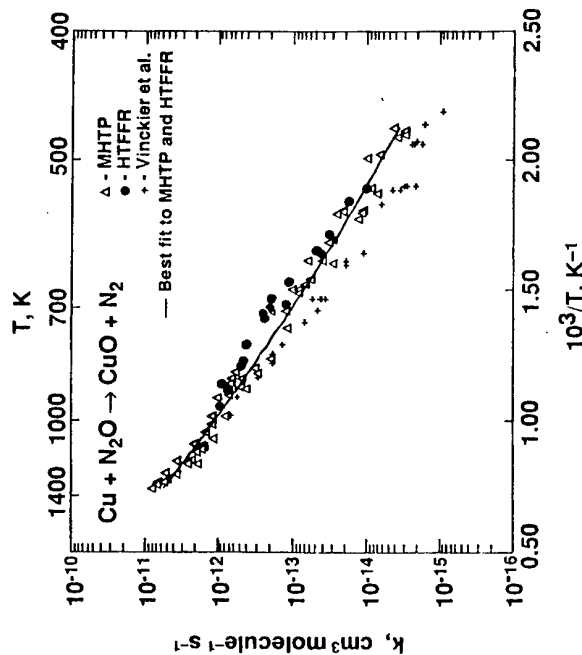
induced fluorescence. A subsequent flow tube study<sup>3</sup> from 460 to 980 K using hollow cathode lamp absorption measurements yielded lower k values, mainly at the lower temperatures, where the scatter is largest. This resulted in a larger activation energy. To investigate this further we have now performed an HTFFR-LIF study of this reaction from 530 to 950 K. As the figure shows this indicated somewhat higher rate coefficients at some temperatures than the MHTP work, but the measurements are well within the joint uncertainties. Combining the HTFFR and MHTP rate coefficients yields  $k(470 - 1340 \text{ K}) = 4.6 \times 10^{-19} (T/\text{K})^{2.61} \exp(-3339 \text{ K}/T) \text{ cm}^3 \text{ molecule}^{-1} \text{ s}^{-1}$ .

## References

- (1) Hranisavljevic and A. Fontijn, J. Phys. Chem. to be submitted.
- (2) Narayan, P. M. Futenko, and A. Fontijn, J. Phys. Chem. **96**, 290 (1992).
- (3) Vinckier, T. Verhaeghe, and I. Vanhees, J. Chem. Soc. Faraday Trans. **90**, 2003 (1994).

\* Work supported by the U.S. National Science Foundation under grant CTS-9301655.

+ On leave from Institute for Structural Macrokinetics, Chernogolovka, Russia.

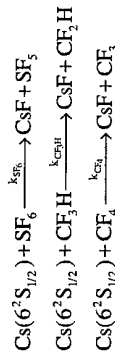


# KINETIC STUDIES OF FLUORINE ATOMS ABSTRACTION BY GROUND STATE ATOMIC CAESIUM, Cs(6<sup>2</sup>S<sub>1/2</sub>), USING TIME-RESOLVED LASER-INDUCED FLUORESCENCE [Cs(7<sup>2</sup>P<sub>3/2</sub> - 6<sup>2</sup>S<sub>1/2</sub>), λ = 455.5 nm] FOLLOWING PULSED IRRADIATION.

E. Martínez, J. Albaladejo, A. Notario, B. Cabañas and E. Jiménez

Universidad de Castilla-La Mancha. Facultad de Ciencias Químicas  
Departamento de Química Física. 13071 Ciudad Real (SPAIN).

Kinetic studies of ground state caesium, Cs(6<sup>2</sup>S<sub>1/2</sub>), following direct time-resolved investigations have been reported in recent years and its collisional behaviour has been reviewed, including its role in combustion science and atmospheric science<sup>(1,2)</sup>. In this context, we have recently described an apparatus<sup>(3)</sup> for the kinetic investigation of this atom, generated by pulsed irradiation and monitored by time-resolved laser-induced fluorescence, in order to characterize absolute rate data for halogen-abstraction at elevated temperatures, in this case, with the fluorine-containing species SF<sub>6</sub>, CF<sub>3</sub>H and CF<sub>4</sub>.



These absolute rate data were compared with those obtained hitherto by time-resolved atomic-resonance absorption spectroscopy in the 'single-shot' mode<sup>(4,5)</sup>.

Cs(6<sup>2</sup>S<sub>1/2</sub>) was generated in a stainless steel reactor by repetitive broad band pulsed photolysis of caesium bromide vapour (which is in equilibrium with its solid at elevated temperatures) in the presence of the reactant gas and excess He buffer gas. The mixture was then flowed through the reactor at a rate ensuring that the system is a slow flow system, kinetically equivalent to a static system. The kinetic decay of Cs(6<sup>2</sup>S<sub>1/2</sub>) was then monitored by laser-induced fluorescence (LIF) using the shorter wavelength component of the strong spin-orbit resolved Rydberg doublet transition at λ=455.5 nm [Cs(7<sup>2</sup>S<sub>3/2</sub>) - Cs(6<sup>2</sup>S<sub>1/2</sub>), λ=459.318 and 455.536 nm, gA=0.65x10<sup>8</sup> and 1.4x10<sup>8</sup> s<sup>-1</sup>, respectively] in preference to the longer wavelength D-line emission [Cs(6<sup>2</sup>P<sub>3/2</sub>) - Cs(6<sup>2</sup>S<sub>1/2</sub>), λ=894.35 and 852.11 nm, gA=0.48 x 10<sup>8</sup> and 1.3 x 10<sup>8</sup> s<sup>-1</sup>, respectively] on account of the sensitivity of the photomultiplier tube employed (Thorn EMI 9813 B). The LIF signals, excited by a pulsed dye-laser pumped by a Nd:YAG laser (CONTINUUM, NDY81 CS-10), were isolated by means of an interference filter centred at λ=455.5 nm and monitored by a gated photomultiplier system.

This signal was then input into the gated integrator (Thorn EMI GB1 A) of a boxcar averager (Stanford Research System, Inc. Model SR250) and finally transferred to a computer via an SR245 computer interface (SRS, Model SR245) for subsequent analysis. The entire experiment was controlled by a pulsed delay generator (SRS Inc. Model DG-535) in combination with a double pulse generator (Pulsetek, Model 233)

used to fire externally the probe laser, and another SR250 boxcar averager unit used to scan the probe laser with respect to the photolysis flash.

The LIF profiles were recorded for different total pressures (p<sub>T</sub>) from dilute mixture of the reactant RF + He of fixed relative composition f, f=[RF]/[He]+[RF] from which the overall first-order rate coefficient, k', for the transient atom was characterised in each case by computerised fitting to the standard form:

$$I_f = \theta_1 + \theta_2 \exp(-k't)$$

The variation of the overall first-order rate coefficient for the caesium atom may be expressed in the form: k'p<sub>T</sub> = β + k<sub>0</sub>/p<sub>T</sub><sup>2</sup>. Hence, a plot of k'p<sub>T</sub> versus p<sub>T</sub><sup>-2</sup> yields k<sub>0</sub>, the absolute second-order rate constant for the reaction in each case, using the appropriate values of f. The present measurements yield the following absolute second-order rate constants, k<sub>0</sub>, for the removal of Cs(6<sup>2</sup>S<sub>1/2</sub>) at the average temperature employed in each case:

Reaction	k <sub>0</sub> /cm <sup>3</sup> mol <sup>-1</sup> s <sup>-1</sup>	T/K	k <sub>0</sub> /cm <sup>3</sup> mol <sup>-1</sup> s <sup>-1</sup>	T/K
Cs + SF <sub>6</sub>	(1.0±0.3) × 10 <sup>-10</sup>	850	(1.3±0.1) × 10 <sup>-10</sup>	830
Cs + CF <sub>3</sub> H	(3.7±1.2) × 10 <sup>-14</sup>	830	(2.4±0.2) × 10 <sup>-12</sup>	833
Cs + CF <sub>4</sub>	(1.9±0.4) × 10 <sup>-15</sup>	840	(7.0±1.2) × 10 <sup>-15</sup>	834

□ This work

□ References 4 and 5

The principal difference between LIF and time-resolved atomic resonance absorption spectroscopy arises in the case of CF<sub>3</sub>H where the result for k<sub>0</sub> from LIF is now closer to that for CF<sub>4</sub>. This new result is concluded to be the chosen value given the nature of the present measurement where the thermochemistry for F-atom abstraction by Cs in both cases for CF<sub>3</sub>H and CF<sub>4</sub> can be calculated as ΔH= +33 and +41 kJmol<sup>-1</sup> (6.7,8,9), respectively. By contrast, fluorine-atom abstraction from SF<sub>6</sub> by Cs is highly exothermic, ΔH= -82 kJmol<sup>-1</sup> (6.7,10), proceeding with close to unit collisional efficiency, and where the role of an electron jump mechanism in determining the magnitude of the cross section (19.7 Å<sup>2</sup>) is favoured both by the ionisation potential (3.8939 eV) (11) of Cs and the electron affinity of SF<sub>6</sub> (0.6 eV) (6).

## REFERENCES

- (1) Husain D, J. Chem. Soc. Faraday Trans. 2, 1989, **85**, 85.
- (2) Plane J.M.C., Int. Rev. Phys. Chem., 1991, **10**, 55.
- (3) Martinez E., Albaladejo J., Notario A. and Husain D., J. Photochem. Photobiol. Chem. A, (1995) in press (paper n° JPC 4253).
- (4) Clay and D. Husain, J. Chem. Res., (S) 1990, 384; (M) 1990, 2944.
- (5) Clay and D. Husain, J. Photochem. Photobiol. Chem. A, 1991, **56**, 1.
- (6) Radzig A.A. and Smirnov B. M., "Reference data on Atoms, Molecules and Ions" (Springer-Verlag, Berlin, 1985).

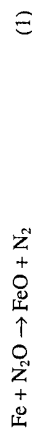
REACTIONS OF ATOMIC Fe AND Fe<sup>+</sup> WITH A SERIES OF OXIDANTS

Rosemary J. Rollason and John M.C. Plane

University of East Anglia  
 School of Environmental Sciences.  
 NORWICH NR4 7TJ

Meteoritic ablation is the major source of layers of metal atoms and ions in the upper atmosphere. These layers, which can be observed by ground-based lidar and rocket-borne mass spectrometry are characterised by many curious features which have yet to be properly explained. These include the relative abundances of the metal layers compared with their meteoritic abundances, differences in the seasonal variations of the layers, and the phenomenon of *sudden* (or sporadic) sodium and iron layers. In order to develop a complete understanding of the processes involved in the formation and behaviour of these layers, laboratory kinetic studies are essential. These studies involve measuring reaction rate coefficients at the low temperatures characteristic of the mesosphere/lower thermosphere region. This kinetic data can then be employed in models of metal layers for comparison with observations.

This poster describes a study of the reactions of Fe with N<sub>2</sub>O and Fe<sup>+</sup> with oxidants including N<sub>2</sub>O and O<sub>3</sub>. The reaction between Fe and N<sub>2</sub>O,



was studied by the pulsed 2-photon dissociation at 193nm of ferrocene vapour to produce Fe atoms in an excess of N<sub>2</sub>O and N<sub>2</sub> bath gas, followed by time-resolved laser induced fluorescence spectroscopy of atomic Fe at 248.3nm. This gave (figure 1):

$$k_1(487 < T < 850\text{K}) = (2.3^{+1.8}_{-1.0}) \times 10^{-10} \exp[(-49.4 \pm 3.0) \text{kJ mol}^{-1} / RT] \text{ cm}^3 \text{ molecule}^{-1} \text{ s}^{-1}$$

(Uncertainties are 2σ.)

The reactions of Fe<sup>+</sup> were studied by the pulsed 4-photon dissociation at 248 nm of ferrocene vapour, producing Fe<sup>+</sup> in an excess of the oxidant and He bath gas. The Fe<sup>+</sup> ions were monitored by time-resolved LIF at 260.0 nm. In the case of the reaction 2,



we obtain,

$$k_2(294 \text{ K} < T < 773 \text{ K}) = (5.3^{+2.3}_{-1.6}) \times 10^{-10} \exp[-(6.2 \pm 1.3) \text{ kJ mol}^{-1} / RT] \text{ cm}^3 \text{ molecule}^{-1} \text{ s}^{-1}$$

In contrast to the neutral Fe reaction, Fe<sup>+</sup> has an open valence s-shell. The reaction is also an ion-molecule process so is assisted by long-range electrostatic forces. Since the reaction is quite exothermic, it is considerably faster than the Fe reaction, as shown in figure 1.

- (7) Huber K.P. and Herzberg G. "Molecular Spectra And Molecular Structure, IV, Constants of Diatomic Molecules" (Van Nostrand, Reinhold, New York 1979).
- (8) Herzberg G. "Molecular spectra and Molecular Structure, III, Electronic Spectra and electronic Structure of Polyatomic Molecules" (Van Nostrand, Reinhold, New York 1966).
- (9) CRC Handbook of Physics and Chemistry, 64th Edition, Eds. Weast R.C., Astle M.J. and Beyer W.H. (CRC Press, Boca Raton, Florida, USA, 1983/84)
- (10) CRC Handbook of Physics and Chemistry, 75th Edition, Eds. Lide D.R., (CRC Press, Boca Raton, Florida, USA, 1994/95).
- (11) CRC Handbook of Physics and Chemistry, 75th Edition, Eds. Lide (CRC Press, Boca Raton, Florida, USA, 1983/84) p 10-206.

The resulting  $\text{FeO}$  and  $\text{FeO}^+$  species are important to study in order to construct models of the upper atmosphere. Reactions (1) and (2) should be an efficient method of producing these oxides for kinetic study, without the complication of having  $\text{O}_3$  in a reactor.

However, in the upper atmosphere, reaction 3 dominates the removal of  $\text{Fe}^+$ :



For this reaction we have obtained the following Arrhenius expression (see figure 1):

$$k_3(236 \text{ K} < T < 386 \text{ K}) = (7.6^{+1.5}_{-1.2}) \times 10^{-10} \exp[-(2.0 \pm 0.4) \text{ kJ mol}^{-1} / RT] \text{ cm}^3 \text{ molecule}^{-1} \text{ s}^{-1}.$$

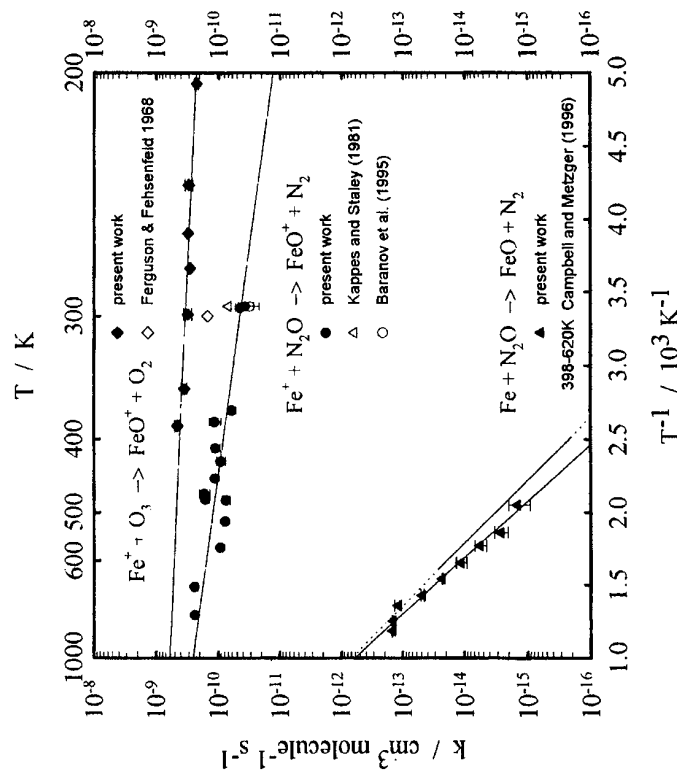


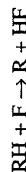
Figure 1 Arrhenius plots ( $\ln(k)$  against  $1/T$ ) for the reactions  $\text{Fe} + \text{N}_2\text{O}$ ,  $\text{Fe}^+ + \text{N}_2\text{O}$  and  $\text{Fe}^+ + \text{O}_3$ .

# KINETICS OF THE REACTIONS OF FLUORINE ATOMS WITH HALOMETHANES OF TYPE $\text{CHCl}_{3-x}\text{F}_x$ ( $x = 0, 1, 2$ , and 3).

F. Louis, P. Devolder, B. Meriaux, J-P Savarysyn  
*Laboratoire de Cinétique et Chimie de la Combustion URA-CNRS 876*  
*Université des Sciences et Technologies de Lille*  
*59655 Villeneuve d'Ascq - France*

M-T Rayez, J-C Rayez  
*Laboratoire de Physicochimie Théorique URA-CNRS 503*  
*Université de Bordeaux I*  
*33405 Talence - France*

The reactions of H-abstraction from halogen-substituted hydrocarbons by fluorine atom attack

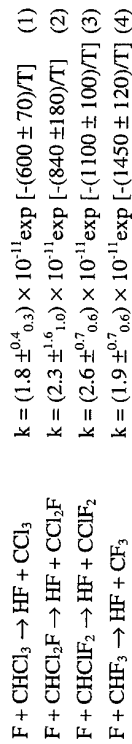


in gas phase play an important role in the incineration of halogenated materials. In laboratory studies, they can be used as sources of haloalkyl radicals in order to investigate the processes of tropospheric photo-oxidation of hydrochlorofluorocarbons (HCFC) and hydrofluorocarbons (HFC) proposed as freon substitutes. If a number of rate coefficient measurements have been performed at room temperature using essentially the relative rate method, limited experimental data are available on the temperature dependence of these reactions.

In this study, we report the measurements of absolute rate coefficients as a function of temperature for the reaction of fluorine atoms with halomethanes of type  $\text{CHCl}_{3-x}\text{F}_x$  ( $x = 0$  to 3) over the temperature range 297-421 K. Furthermore, ab initio calculations are performed in order to gain insight into the reactivity trends along the series. Experimental and theoretical studies on the reactions of halomethanes with fluorine atoms are a complement of our recent studies achieved with chlorine atoms<sup>1,2</sup>.

Experiments were carried out using the conventional discharge flow/mass spectrometric technique (DF/MS). The apparatus has been already described in detail elsewhere<sup>3</sup>. Fluorine atoms were generated by a discharge in a mixture of  $\text{F}_2/\text{He}$  through an alumina tube<sup>4,5</sup> in order to reduce their wall reactions. Initial concentration of fluorine atoms were determined using the fast reaction  $\text{F} + \text{Cl}_2$ <sup>6</sup>. Flow rates of different gases were regulated by calibrated mass flow controllers. The pressure in the flow tube was measured upstream and downstream by a capacitance manometer. All experiments were performed under pseudo-first order conditions with fluorine atoms in excess with respect to halomethanes. The rate coefficients were measured by

monitoring the temporal decay of the intensity of the fragment ions  $\text{CHCl}_2^+$ ,  $\text{F}_x^+$ . Typical experimental conditions were as follows: total pressure 1-3 Torr, average flow velocity  $0.7\text{--}3.5\text{ ms}^{-1}$ ,  $[\text{RH}]_0 = 3 \times 10^{11}\text{--}1.6 \times 10^{13}\text{ cm}^{-3}$  and  $[\text{F}]_0 = 1 \times 10^{13}\text{--}3 \times 10^{14}\text{ cm}^{-3}$ . The following Arrhenius expressions (in  $\text{cm}^3\text{ molecule}^{-1}\text{ s}^{-1}$ ) were obtained:



Uncertainties represent only the statistical errors ( $\pm 2\sigma$ ) of the fits of Arrhenius plots.

The results obtained for the reactions (1) to (3) correspond to the first determinations of Arrhenius expressions using an absolute method. Compared with the only expressions published in the literature and determined using the relative rate method<sup>7</sup>, our expressions lead to different temperature dependences for the reactions (1) to (3), although the values of the rate coefficients obtained at room temperature are in relatively good agreement. Concerning the reaction  $\text{F} + \text{CHF}_3$  (4), our Arrhenius expression is in good agreement with the only expression determined using an absolute method<sup>6</sup> similar to ours (DF/MS).

Ab initio calculations using the program Gaussian 94<sup>8</sup> are also reported for the set of reactions of interest. The geometrical structure, energy and vibrational frequencies were calculated at different levels for reactants, products and transition states. The values of Arrhenius parameters and their evolution along the series of reactions  $\text{F} + \text{CHCl}_{3-x}\text{F}_x$  estimated by these calculations are discussed and compared with the experimental values. Excellent agreement is observed between the experimental<sup>9</sup> values of reaction enthalpies and the ones predicted using the method G2MP2<sup>8</sup>.

## References

- 1) Rayez M.T.; Rayez J.-C.; Sawersyn J.-P. *J. Phys. Chem.* **1994**, *98*, 11342
- 2) Talhaoui A.; Louis F.; Mériaux B.; Devolder P.; and Sawersyn J.-P. *J. Phys. Chem.* **1996**, *100*, 2107
- 3) Sawersyn J.-P.; Lafage C.; Mériaux B.; Tighezza A. *J. Chim. Phys.* **1987**, *84*, 1187
- 4) Rosner D.E.; and Allendorf H.D. *J. Phys. Chem.* **1971**, *75*, 308
- 5) Kolb C.E.; and Kaufman M. *J. Phys. Chem.* **1972**, *76*, 947
- 6) Clyne M.A.A.; McKenney D.J.; and Walker R.F. *Canad. J. Chem.* **1973**, *51*, 3596
- 7) Foon R. and McAskill N.A. *Trans. Faraday Soc.* **1969**, *65*, 3005
- 8) *Gaussian 94* (Revision C.3), M.J. Frisch, G.W. Trucks, H.B. Schlegel, P.M.W. Gill, B.G. Jonhson, M.A. Robb, J.R. Cheeseman, T.A. Keith, G.A. Petersson, J.A. Montgomery, K. Raghavachari, M.A. Al-Laham, V.G. Zakrzewski, J.V. Ortiz, J.B.

Foresman, J. Cioslowski, B.B. Stefanov, A. Nanayakkara, M. Challacombe, C.Y. Peng, P.Y. Ayala, W. Chen, M.W. Wong, J.L. Andres, E.S. Replogle, R. Gomperts, R.L. Martin, D.J. Fox, J.S. Binkley, D.J. Defrees, J. Baker, J.P. Stewart, M. Head-Gordon, C. Gonzalez, and J.A. Pople, Gaussian, Inc., Pittsburgh PA, 1995.

9) DeMore, S.P. Sander, D.M. Golden, R.F. Hampson, J. Kurylo, C.J. Howard, A.R. Ravishankara, C.E. Kolb, M.J. Molina, *Chemical Kinetics and Photochemical Data for Use in Stratospheric Modelling*; Evaluation N° 11, Publication 94-26, Jet Propulsion Laboratory, Pasadena CA, 1994.

# EXPERIMENTAL AND THEORETICAL STUDIES OF THE REACTION OF HYDROXYL RADICALS WITH ACETALDEHYDE OVER AN EXTENDED TEMPERATURE RANGE

Philip H. Taylor, M. Sm. Rahman, M. Arif and B. Dellinger

*Environmental Sciences and Engineering Group, University of Dayton Research  
Institute, 300 College Park, Dayton, Ohio 45469-0132*

Paul Marshall

*Department of Chemistry, University of North Texas, PO Box 5068, Denton, Texas*

76203

Absolute rate coefficients for the reactions of OH with CH<sub>3</sub>CHO, CH<sub>3</sub>CDO, and CD<sub>3</sub>CDO were measured with the laser photolysis/laser-induced fluorescence technique. A large majority of the kinetic data were obtained at 740 torr of helium pressure over the temperature range 295-900 K. Measurements below 600 K exhibited a negative temperature dependence while measurements above 600 K exhibited a positive temperature dependence. CH<sub>3</sub>CHO + OH measurements at 100, 400, and 740 torr helium pressure indicated the lack of a pressure dependence. The reaction mechanism involving OH addition/CH<sub>3</sub> or H-atom elimination and H-atom abstraction was evaluated with a quantum RRK model incorporating *ab initio* calculations on the reactants, transient intermediates and transition-state structures at up to the Gaussian-2 (G2) level of computational theory. A mechanism involving both OH addition/CH<sub>3</sub> elimination and H-atom abstraction from the -CHO group at lower temperatures and H-atom abstraction from the -CH<sub>3</sub> group at elevated temperatures was consistent with the observed bimolecular rate constants. Kinetic isotope effect measurements using CH<sub>3</sub>CDO and CD<sub>3</sub>CDO support the proposed mechanism, and the results are compared with *ab initio* kinetics derived from the G2 potential energy surface. This surface is also compared with G2 results for OH + CH<sub>2</sub>O.

# AB INITIO STUDIES OF THE REACTIONS OF H AND OH WITH CHLOROFLUOROMETHANES

Paul Marshall,<sup>\*ab</sup> M. Schwartz,<sup>a</sup> C. J. Ehlers<sup>b</sup> and R. J. Berry<sup>b</sup>

*<sup>a</sup>Department of Chemistry, University of North Texas, PO Box 5068, Denton, Texas  
76203-0068*

*<sup>b</sup>Center for Computational Modeling of Nonstructural Materials, Wright Laboratory,  
Wright-Patterson Air Force Base, Ohio 45433*

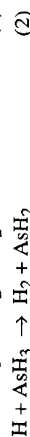
In order to understand the combustion of halogenated species, which are important in waste incineration and fire suppression, kinetic data are required at elevated temperatures. Here we test the capability of *ab initio* methods to furnish such information, and compare the results with experimental data, which in some cases are sparse or do not identify the products. Transition states for the reactions of H and OH with chlorofluoromethanes have been characterized computationally. Geometries and frequencies have been obtained at the HF and MP2 levels with the 6-31 G(d) basis set. Internal rotations were analyzed and several conformations were investigated for some transition states. Evidence for intramolecular hydrogen bonding is discussed. Energy barriers for OH and H attack on fluoromethanes, chloromethanes and chlorofluoromethanes were computed at the Gaussian-2 (G2(ZPE=MP2) or G2(MP2)) levels of theory and the results were used to predict rate constants via transition state theory. These data were compared to kinetic measurements, to test the reliability of the TST results. The *ab initio* results were also used to assess the dominant product channels. For H + fluoromethanes, H-atom abstraction, although less favorable thermochemically than F-abstraction, is the major reaction pathway, while for H + chloromethanes the abstractions of H and Cl have comparable barriers.

# ARRHENIUS PARAMETERS FOR THE REACTIONS OF H ATOMS WITH PH<sub>3</sub> AND AsH<sub>3</sub>

Neville L. Arthur and Ian A. Cooper†

*School of Chemistry, La Trobe University, Melbourne, Victoria, Australia 3083*  
† *Present address: Zeneca Pharmaceuticals, Alderley Park, Macclesfield, Cheshire,  
UK SK10 4TG.*

The reactions of H atoms with PH<sub>3</sub> and AsH<sub>3</sub>



are considered to be active participants in the gas phase chemistry of metal organic chemical vapour deposition (MOCVD) processes used in the manufacture of semiconductor materials. They are also thought to be involved in forming the trace amounts of PH<sub>3</sub> and AsH<sub>3</sub> found in the atmospheres of Jupiter and Saturn. Reliable rate constants for these reactions are therefore needed for computer models designed to throw light on the mechanisms of MOCVD processes and on the evolution of planetary atmospheres.

The flash photolysis system used in this work has been described in detail previously.<sup>1</sup> Briefly, H atoms are produced by mercury-sensitized photolysis of hydrogen by passage of a substrate/hydrogen mixture over a drop of mercury before it enters a quartz cell, where it is illuminated with flashes of light (253.7 nm) from a low-pressure mercury lamp. The concentration of H atoms is followed by monitoring the radiation transmitted through the cell from a Lyman- $\alpha$  lamp, arranged perpendicular to the mercury lamp. The Lyman- $\alpha$  line (121.5 nm) is isolated by a vacuum-ultraviolet monochromator and detected by a solar blind photomultiplier, the signal from which is amplified, digitised and then counted on a multichannel scaler card installed in an IBM compatible PC. The PC also sets the variables which determine the reaction conditions for each experiment: flash time, period between flashes, flow rates, temperature and data collection time. Prior to the experiment, a file is created containing the values of the variables chosen for the series of runs planned. Concentrations were varied by combining the substrate/H<sub>2</sub> mixture with a separate stream of H<sub>2</sub>, and to ensure that a fresh mixture entered the reaction cell prior to each flash, the total flow rate was held constant at 100 standard cm<sup>3</sup> min<sup>-1</sup>. The pressure in the reaction cell was maintained at 500 Torr, and the mercury reservoir was thermostatted at 11°C.

Rate constant measurements were carried out under pseudo first-order conditions ([substrate]  $\gg$  [H]), and with H atom concentrations such that the transmission of Lyman- $\alpha$  radiation followed Beer-Lambert behaviour ([H]  $< 6 \times 10^{-12}$  cm<sup>-3</sup>, corresponding to flash times of less than 6 ms). Under these circumstances the variation of the transmitted Lyman- $\alpha$  intensity with time is given by  $I = I_0 \exp \{-$

$Q[\text{H}]_0 \exp(-k't)\}$ , and  $k'$ , the pseudo first-order rate constant, was obtained by fitting this double exponential function to the experimental decay curve by means of a nonlinear least-squares procedure.

As in previous work<sup>1,2</sup> the value of  $k'$  measured at a given concentration of substrate was found to depend on the flash time, a consequence of the occurrence of secondary reactions. To obtain the true value of  $k'$ , several experiments were carried out at different flash times, and the results extrapolated to zero.  $k'_0$  This value,  $k'_0$  is related to the bimolecular rate constant for H atom attack on the substrate,  $k$ , by  $k'_0 = k[\text{substrate}] + k_w$ , where  $k_w$  is the rate constant for H atom diffusion to the wall of the cell. At each temperature, values of  $k'_0$  were measured at several substrate concentrations, and  $k$  was evaluated from the slope of a plot of  $k'_0$  vs [substrate]. The values obtained were then fitted to the exponential form of the Arrhenius equation, with each point being weighted by the reciprocal of its standard deviation.

The values of the Arrhenius parameters determined in this work are listed and compared with previously published results in the following table.

**Rate constants and Arrhenius parameters for H + PH<sub>3</sub> and H + AsH<sub>3</sub>**

Reaction	T/K	$k/10^{12} \text{ cm}^3 \text{ s}^{-1}$	$A/10^{10} \text{ cm}^3 \text{ s}^{-1}$	$E/\text{kJ mol}^{-1}$	Ref.
H + PH <sub>3</sub>	room	$2.7 \pm 1.0$			3
	209 – 495	$3.8 \pm 0.5^a$	$0.452 \pm 0.039$	$6.15 \pm 0.21$	4
	293 – 472	$3.3 \pm 0.4^a$	$1.09 \pm 0.08$	$8.71 \pm 0.22$	this work
H + AsH <sub>3</sub>	209 – 495	$3.7 \pm 0.3^a$	$0.721 \pm 0.041$	$7.38 \pm 0.16$	best value
	294 – 424	$2.3 \pm 1.7^a$	$2.57 \pm 1.30$	$5.97 \pm 1.33$	this work
	<sup>a</sup> At 300 K.				

This is the first report of the determination of Arrhenius parameters for H atom attack on an As-H bond. A plot of all of the data for H + PH<sub>3</sub> shows that our results are in good agreement with those of Stief and coworkers,<sup>3</sup> and that by comparison the single rate constant of Alexandrov et al.<sup>4</sup> is low. Combination of the data, omitting this point, gives the values for the Arrhenius parameters over the temperature range 209 – 495 K recommended in the table.

## References

- (1) N.L. Arthur and I. A. Cooper, *J. Chem. Soc., Faraday Trans. 2*, 1995, **91**, 3367.
- (2) N.L. Arthur, P. Potzinger, B. Reimann and H.P. Steenbergen, *J. Chem. Soc., Faraday Trans. 2*, 1989, **85**, 1447.
- (3) E. N. Alexandrov, V. S. Arutyunov, I. V. Dubrovina and S.N. Kozlov, *Fizika Goreniya i Vzryva*, 1982, **18**, 73.
- (4) J. H. Lee, J.V. Michael, W.A. Payne, D. A. Whytock and L.J. Stief, *J. Chem. Phys.*, 1976, **65**, 3280.

# TEMPERATURE DEPENDENT RATE CONSTANTS FOR THE REACTIONS OF $\text{CHCl}(\text{X}'\text{A})$ WITH ETHYLENE AND PROPYLENE

C. Rehbein<sup>1</sup> and H.Gg. Wagner

Max-Planck-Institut für Strömungsforschung, Bunsenstrasse 10,  
D-37073 Göttingen, Germany

Rate constants have been determined for the reactions of  $\text{CHCl}(\text{X}'\text{A})$  with ethylene and propylene for a range of temperatures from 217 K to 433 K and 198 K to 511 K.  $\text{CHCl}=\text{CF}_2$  was found to be a suitable precursor for generation of  $\text{CHCl}(\text{X}'\text{A})$  for kinetic measurements under low pressure conditions.  $\text{CHCl}(\text{X}'\text{A})$  was produced by pulsed excimer laser photolysis in a quasistatic thermostatic gas cell and detected via pulsed LIF [1,2]. The removal rates of  $\text{CHCl}(\text{X}'\text{A})$  were determined via the measurement of  $\text{CHCl}(\text{X}'\text{A})$  concentration profiles under pseudo first order reaction conditions.

The value of the rate coefficients at room temperature was  $3.2 \times 10^{+12} \text{ cm}^3 \text{ mol}^{-1} \text{ sec}^{-1}$  and  $8.3 \times 10^{+12} \text{ cm}^3 \text{ mol}^{-1} \text{ sec}^{-1}$  for  $\text{C}_2\text{H}_4$  and  $\text{C}_3\text{H}_6$ , respectively.

The reaction with ethylene was investigated at three different pressures (3.7, 10.3, 18.7 mbar) indicating a positive pressure dependence.

All second order rate constants were fitted to the expression

$$\log k(T) = n \log(T / 295\text{K}) + \log A$$

to reflect the temperature dependence (units of A:  $10^{+12} \text{ cm}^3 \text{ mol}^{-1} \text{ sec}^{-1}$ ) A = 3.2, n = -1.5 for  $\text{C}_2\text{H}_4$  and A = 8.3, n = -1.4 for  $\text{C}_3\text{H}_6$

The reactivity of  $\text{CHCl}(\text{X}'\text{A})$  is discussed and compared with that of methylene and that of mono- and disubstituted halocarbenes.

## References

- 1) A.J. Merer and D.N. Travis. *Can. J. Phys.* **44**, 525 (1966)
- 2) M. Kakimoto, S. Saito and E. Hirota, *J. Mol. spectrosc.* **97**, 194 (1983)

# INFRARED ABSORPTION STUDIES OF THE REACTIONS OF Cl ATOMS WITH HYDROCARBONS\*

Jeffrey S. Pilgrim and Craig A. Taatjes

Combustion Research Facility, Mail Stop 9055, Sandia National Laboratories,  
Livermore, CA 94551-0969

The reaction rate constants for Cl atoms with several small hydrocarbons have been measured using a laser-photolysis / cw infrared absorption method in a newly-designed temperature-controlled multipass cell. Chlorine atoms are generated by excimer photolysis and the reaction progress is monitored by infrared absorption detection of the HCl product. The reactor is outfitted with a multipass cell based on the Herriott design, which allows simultaneous realization of long (12 m) absorption pathlengths and precise temperature control for laser pump-probe experiments.

The hydrogen atom abstraction reactions of chlorine atoms with the smallest alkanes have been measured between 292 and 800 K. The rate coefficient for Cl + methane can be described by a simple Arrhenius fit over this temperature range, yielding Arrhenius parameters which are in reasonable agreement with previous lower-temperature determinations. However, the precision of our measurements is sufficient to establish curvature in the Arrhenius plot, and an improved fit to our data is given by a modified Arrhenius expression,  $k_{\text{CH}_4}(T) = 8.54 \times 10^{-13} (T/298)^{2.07} \exp[-663/T] \text{ cm}^3 \text{ molecule}^{-1} \text{ s}^{-1}$ . An extrapolation of this modified Arrhenius fit also matches the established lower-temperature ( $\sim 200 \text{ K}$ ) measurements for Cl +  $\text{CH}_4$ . In the temperature range 292-600 K the rate with ethane agrees well with earlier investigations, fitting a simple Arrhenius expression. However, as the temperature increases beyond 600 K significant upward curvature in the Arrhenius plot becomes apparent. A modified Arrhenius fit  $k_{\text{C}_2\text{H}_6}(T) = 3.37 \times 10^{-11} (T/298)^{0.69} \exp[149/T] \text{ cm}^3 \text{ molecule}^{-1} \text{ s}^{-1}$  models the experimental data adequately over the entire 292 - 800 K temperature range. The rate coefficient for propane is independent of temperature and equal to  $1.38 (\pm 0.03) \times 10^{-10} \text{ cm}^3 \text{ molecule}^{-1} \text{ s}^{-1}$ . The possible role of spin-orbit excited Cl in the temperature dependence of the primary hydrogen abstraction reaction is discussed.

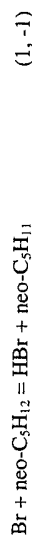
The reactions of Cl atoms with unsaturated hydrocarbons are complicated somewhat by the presence of an addition channel. The kinetics of Cl reacting with ethylene ( $\text{C}_2\text{H}_4$ ) and propylene ( $\text{C}_3\text{H}_6$ ) have been measured as a function of temperature. The two reactions display qualitatively different behaviors reflecting differing competition between abstraction and addition channels. The reaction with ethylene shows a direct abstraction channel, to  $\text{HCl} + \text{C}_2\text{H}_3$ , which competes with addition to a chloroethyl adduct. The abstraction dominates the reaction above  $\sim 450 \text{ K}$ . The direct measurement

# BROMINATION KINETICS OF NEOPENTANE. THE HEAT OF FORMATION OF NEOPENTYL RADICAL

K. Imrik, S. Dóbbé, T. Bérces and F. Márta

Central Research Institute for Chemistry,  
Hungarian Academy of Sciences  
H-1025 Budapest, Pusztaszeri út 59-67, Hungary

The neopentyl radical may be considered as a prototype of larger branched alkyl free radicals. So far, no new thermochemical data have been reported for this radical. In order to provide thermodynamic data for neopentyl radical, we have initiated kinetic investigations of the reactions



The temperature dependence of the rate coefficient for the reaction of Br-atom with neopentane has been investigated using laser flash photolysis technique coupled with Br-atom resonance fluorescence detection. Br-atoms were generated by pulsed excimer laser photolysis of  $\text{CF}_3\text{Br}_2$  at 248 nm. The resonance fluorescence of Br was monitored by a solar blind photomultiplier. The reaction was studied under pseudo-first order conditions, with large excess of neopentane ( $[\text{neo-C}_5\text{H}_{12}] / [\text{Br}] \geq 140$ ). The second-order rate coefficient,  $k_1$ , was obtained from the plot of the pseudo-first-order decay parameter against neopentane concentration.

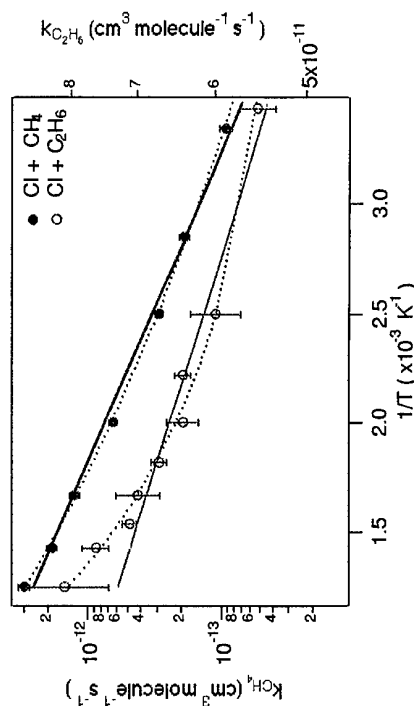
From measurements made in the temperature range of 562-774 K, the rate coefficient expression

$$k_1 = (5.68 \pm 1.27) \times 10^{13} \exp[-(41.89 \pm 1.30) \text{ kJ mol}^{-1} / RT]$$

was derived. No other direct studies of this reaction have been reported, only a single relative rate determination of  $k_1$  appears in the literature. In a gas phase competitive bromination study carried out with GC product analysis over the temperature range of 331-473 K, Fettis et al. [1] derived (with literature data for the Arrhenius parameters of reaction  $\text{Br} + \text{CH}_3\text{Br}$ )  $A_1 = (1.75 \pm 0.25) \times 10^{14} \text{ cm}^3 \text{ mol}^{-1} \text{ s}^{-1}$  and  $E_1 = 59.79 \pm 0.55 \text{ kJ mol}^{-1}$ . Both the A-factor and the activation energy obtained in the present study are

of the pure abstraction channel at 550 - 700 K is well-fit by a simple Arrhenius expression,  $k_{\text{C}_2\text{H}_6} = 1.76 (\pm 0.14) \times 10^{11} \exp[-2290 (\pm 50) / T] \text{ cm}^3 \text{ molecule}^{-1} \text{ s}^{-1}$ . At lower temperatures the chloroethyl adduct establishes an equilibrium with the  $\text{Cl} + \text{C}_2\text{H}_4$ , and the observed time traces have a biexponential component. No evidence is seen for thermal dissociation of the chloroethyl adduct to  $\text{HCl} + \text{vinyl} (\text{C}_2\text{H}_3)$ . However, evidence for a fast reaction of Cl atoms with the chloroethyl adduct is seen; this reaction complicates the analysis of the  $[\text{HCl}]$  time profiles at low temperatures.

The abstraction reaction of Cl with propylene ( $\text{C}_3\text{H}_6$ ), to allyl +  $\text{HCl}$ , is surprisingly slow. At room temperature and 5 Torr total pressure the reaction progresses largely by abstraction, as evidenced by nearly single-exponential  $[\text{HCl}]$  vs. time profiles with no induction period for HCl formation. The apparent rate coefficient for hydrogen abstraction at 293 K and 5 Torr is  $5.6 (\pm 0.3) \times 10^{-12} \text{ cm}^3 \text{ molecule}^{-1} \text{ s}^{-1}$ . The measured  $\text{HCl}$  yield is  $[\text{HCl}]_{\infty} / [\text{Cl}]_{t=0} \sim 0.5$ , indicating that addition contributes 50% to the measured rate coefficient. The Cl + propylene abstraction reaction is thus 20 times slower than the reaction with ethane, which has only twice as many primary hydrogens, despite the large exothermicity (17 kcal/mol) of the abstraction channel. A similar situation is encountered in the reaction of Cl + allene, where no direct abstraction is evident at room temperature despite the exothermic channel to  $\text{HCl} + \text{propargyl}$ . However, the propylene reaction exhibits a negligible temperature dependence over the range 292 - 700 K, indicating no energetic barrier to the abstraction. The possibility of an addition-elimination mechanism for this reaction is considered, which merely underlines the dramatically different reactive behavior towards Cl of the methyl hydrogens in propylene relative to the saturated hydrocarbons.



Arrhenius plot for the reactions of Cl with methane and ethane. The error bars are  $\pm 2\sigma$  precision only. The solid and dashed lines are fits to simple and modified Arrhenius expressions.

lower than the Arrhenius parameters derived from the competitive study. (Examination of the possible causes of the disagreement is under way.)

No experimental kinetic study has been carried out for the reaction between neopentyl radical and HBr, however, the Arrhenius parameters can be estimated: (i) The A-factors reported for the alkyl radical + HBr reactions are between  $5 \times 10^{11}$  and  $1 \times 10^{12} \text{ cm}^3 \text{ mol}^{-1} \text{ s}^{-1}$ , thus we assume  $A_1 = (8 \pm 3) \times 10^{11} \text{ cm}^3 \text{ mol}^{-1} \text{ s}^{-1}$ . (ii) A correlation has been suggested between the logarithm of the rate coefficient for reaction  $R + \text{HBr}$  (where R designates carbon-centred free radicals) and the difference of  $IP(R) - EA(\text{HBr})$  [2]. Using this equation and the assumed  $A_1$ , an activation energy of  $E_1 = -4.9 \pm 2.9 \text{ kJ mol}^{-1}$  is obtained. These estimates are close to the Arrhenius parameters reported for reaction  $\text{C}_2\text{H}_5 + \text{HBr}$  [3].

With the measured kinetic parameters for reaction (1) and the estimated parameters for reaction (-1), both second-law and third-law heats of formation were derived for the neopentyl radical. From the second-law analysis,  $S_{298}(\text{neo-C}_5\text{H}_{11}) = 315 \pm 8 \text{ J mol}^{-1} \text{ K}^{-1}$  and  $\Delta_f H_{298}^\circ = 25.7 \pm 3.3 \text{ kJ mol}^{-1}$ , and from the third-law derivation (with an estimated entropy of  $S_{298}^\circ(\text{neo-C}_5\text{H}_{11}) = 320.0 \text{ J mol}^{-1} \text{ K}^{-1}$ )  $\Delta_f H_{298}^\circ = 28.9 \pm 7.2 \text{ kJ mol}^{-1}$  were obtained. These correspond to the neopentane C-H bond dissociation energy and the neopentyl radical entropy of  $413.5 \pm 8.0 \text{ kJ mol}^{-1}$  and  $317 \pm 8 \text{ J mol}^{-1} \text{ K}^{-1}$ , respectively. The thermochemical properties of the neopentyl radical obtained in the present study are somewhat lower than, but agree within the combined error limits with the recently accepted values [4].

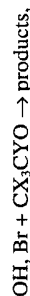
- 1) G.C. Fettes, J.H. Knox and A.F. Trotman-Dickenson, *J. Chem. Soc.*, 4177 (1960).
- 2) T. Bérces and S. Dóbbé, unpublished results.
- 3) J.M. Nicovich, C.A. van Dijk, K.D. Kreutter and P.H. Wine, *J. Phys. Chem.* **95**, 9890 (1991).
- 4) T.J. Mitchell and S.W. Benson, *Int. J. Chem. Kinet.*, **25**, 931 (1993).

# KINETIC STUDIES OF THE REACTIONS OF Br-ATOMS AND OH-RADICALS WITH SELECTED ALDEHYDES AND ACYL-HALIDES

I. Szilágyi, S. Dóbbé, T. Bérces and F. Márta

*Central Research Institute for Chemistry,  
Hungarian Academy of Sciences,  
H-1025 Budapest, Pusztaszeri út 59-67, Hungary*

Aldehydes and acyl-halides are important intermediates formed in the atmospheric degradation processes of halocarbons including the freon replacement compounds, HCFCs and HFCs. In the present work, the kinetics of the reactions of substituted acetaldehydes and acyl-halides with Br and OH have been investigated in the reaction series



where  $\text{X} = \text{H}, \text{Cl}, \text{CH}_3$  and  $\text{Y} = \text{H}, \text{F}, \text{Cl}$ . The reaction  $\text{Br} + \text{CH}_2\text{O}$  has also been studied. These investigations are the extensions of our previous work [1] with the objectives (i) to determine kinetic parameters for use in atmospheric chemistry models; (ii) to investigate structure-activity relationships and (iii) to assess bond dissociation energies for C-H bonds.

Experiments were carried out at room temperature applying the fast flow method coupled with resonance fluorescence detection of Br and OH, respectively. Br-atoms were generated by flowing dilute  $\text{Br}_2/\text{He}$  mixtures through a microwave discharge. OH radicals were obtained via the fast gas-titration reaction  $\text{H} + \text{NO}_2 \rightarrow \text{OH} + \text{NO}$ .

Significant inductive (polar) effect has been observed in the reaction series studied. The rate constant increases with increasing number of methyl groups in the molecule, while decreases with increasing number and increasing electronegativity of the halogen substituent.

Substitution of alkyl H-atoms for  $\text{CH}_3$  in the acetaldehyde molecule gives rise to approximately the same rate enhancement for both the Br and the OH reactions. For example, the rate coefficients of the reactions  $\text{OH} + (\text{CH}_3)_2\text{CHCHO}$  and  $\text{Br} + (\text{CH}_3)_2\text{CHCHO}$  are 2.8 and 3.1 times larger than those of the  $\text{OH} + \text{CH}_3\text{CHO}$  and  $\text{Br} +$

CH<sub>2</sub>CHO reactions, respectively. On the other hand, halogen substitution reduces more the reactivity of the aldehydes in their reactions with Br than with OH.

The inductive effect is also pronounced if halogen substitution is made on the carbonyl group: the OH-radicals react only slowly with acetyl fluoride and acetyl chloride. The rate coefficients for the overall reactions OH + CH<sub>3</sub>CFO → products and OH + CH<sub>3</sub>CClO → products have been found to be  $(4.6 \pm 1.5) \times 10^9 \text{ cm}^3 \text{ mol}^{-1} \text{ s}^{-1}$  and  $(1.0 \pm 0.2) \times 10^{10} \text{ cm}^3 \text{ mol}^{-1} \text{ s}^{-1}$ , respectively. These are about one order of magnitude smaller than the rate coefficient of the reaction between OH and acetone [2], which is a straightforward reference point for the OH + acyl-halide reaction series.

The observed reactivity trends can not be explained by the thermochemistry of the reactions alone. They are due to a great part to the charge transfer character of the transition states, the stability of which increases with increasing number of the electron donating methyl substituents and decreases in the case of the electron withdrawing halogen substituents.

1) S. Dóhé, L.A. Khachatryan, T. Bérces, *Ber. Bunsenges. Phys. Chem.*, **93**, 847 (1989).

2) R. Atkinson, D.L. Baulch, R.A. Cox, R.F. Hampson, Jr., J.A. Kerr, J. Troe, *J. Phys. Chem. Ref. Data*, **21**, 1125 (1992).

# RATE CONSTANT AND PRODUCT BRANCHING FOR THE VINYL RADICAL SELF REACTION AT T = 298 K

R. P. Thorn, Jr., W. A. Payne, and L. J. Stief  
*Laboratory for Extraterrestrial Physics, Code 691  
NASA/Goddard Space Flight Center Greenbelt, MD 20771*

D. C. Tardy  
*Department of Chemistry  
University of Iowa Iowa City, Iowa 52242*

The C<sub>2</sub>H<sub>3</sub> self reaction has the potential to be important in both the relatively low temperatures of planetary atmospheres and the elevated temperatures of combustion processes. The rate constant and product branching for the self reaction of C<sub>2</sub>H<sub>3</sub> has been measured using the discharge-flow kinetic technique coupled to mass spectrometric detection at T = 298 K and 1 Torr nominal pressure (He). C<sub>2</sub>H<sub>3</sub> is produced by the reaction of F with C<sub>3</sub>H<sub>4</sub> which also forms C<sub>2</sub>H<sub>3</sub>F + H. In addition to the C<sub>2</sub>H<sub>3</sub> self reaction, C<sub>2</sub>H<sub>3</sub> also decays by reaction with H and by wall loss processes. The result obtained by parameter fitting the C<sub>2</sub>H<sub>3</sub> decay curves was  $k_1 = (1.41 \pm 0.60) \times 10^{-10} \text{ cm}^3 \text{ molecule}^{-1} \text{ s}^{-1}$  where  $k_1$  is defined by  $d[\text{C}_2\text{H}_3]/dt = 2 k_1 [\text{C}_2\text{H}_3]^2$ . Results from the product studies showed that the recombination product (1,3)-butadiene was not observed at 1 Torr and that the ratio [C<sub>2</sub>H<sub>2</sub>] product formed / [C<sub>2</sub>H<sub>3</sub>]<sub>0</sub> was  $0.65 \pm 0.14$  for the combined C<sub>2</sub>H<sub>3</sub> + C<sub>2</sub>H<sub>3</sub> and C<sub>2</sub>H<sub>3</sub> + H reactions. Both observations are consistent with C<sub>2</sub>H<sub>2</sub> and C<sub>2</sub>H<sub>4</sub> being the exclusive C<sub>2</sub>H<sub>3</sub> + C<sub>2</sub>H<sub>3</sub> products since the maximum yield of C<sub>2</sub>H<sub>2</sub> from the combined C<sub>2</sub>H<sub>3</sub> + C<sub>2</sub>H<sub>3</sub> and C<sub>2</sub>H<sub>3</sub> + H reactions is 0.59.

Our experimental observations at P = 1 Torr and other recent studies at P = 100 and 400 Torr<sup>1,2</sup> show that  $k_1$  is independent of pressure. While our results and an early study<sup>3</sup> at very low pressure (0.065 - 0.20 Torr) show an absence of (1,3)-butadiene (product of C<sub>2</sub>H<sub>3</sub> combination) at P ≤ 1 Torr, the high pressure studies observed a combination / disproportionation ratio of 3.2.

Various mechanisms involving unimolecular isomerizations and/or decompositions have been tested using steady state RRKM calculations. A simple reaction scheme that includes only one unimolecular decomposition step, C<sub>4</sub>H<sub>6</sub><sup>\*</sup> → 2 C<sub>2</sub>H<sub>3</sub>, is inadequate, since the pressures in the present experiments (1 Torr) correspond to the high pressure limit for collisional stabilization of (1,3)-Butadiene. The inclusion of a second unimolecular step that directly produces C<sub>2</sub>H<sub>2</sub>, C<sub>4</sub>H<sub>6</sub><sup>\*</sup> → C<sub>2</sub>H<sub>2</sub> + C<sub>2</sub>H<sub>4</sub>, is also inadequate. Although this mechanism provides the right pressure dependence, it has one major deficiency: there have not been any

# A STUDY OF THE REACTION OF CH RADICALS WITH METHANE ISOTOPOMERS

M.A. Blitz, D.G. Johnson, M. Pesa, M.J. Pilling, S.H. Robertson and P.W. Seakins

*School of Chemistry, University of Leeds, Leeds, LS2 9JT, UK.*

The reaction of CH radicals with methane is uncharacteristic of CH reactions in that there is only one exothermic channel:

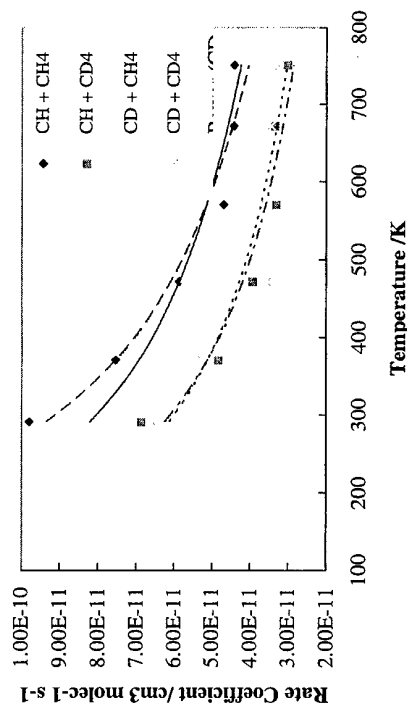


We have investigated the kinetics of this reaction prior to the possibility of using reaction (1) as a calibration reaction for investigating the efficiency of H atom pathways in multichannel CH reactions. The reaction is thought to proceed via the formation of an ethyl intermediate (which can only be stabilized at very high pressures). The mechanism of this reaction is of interest in that although significant atomic rearrangements are required to form the ethyl intermediate the reaction occurs with a slight negative temperature dependence. The potential energy surface close to the entrance channel has been probed using isotopic substitution of both CH and CH<sub>4</sub>.

The reaction has been studied using conventional laser flash photolysis of CH(D)Br<sub>3</sub> with methane in excess over CH, with the time dependent [CH] being monitored by laser induced fluorescence. Pressures and temperatures were varied over the range 50 - 400 Torr and 298 - 778 K.

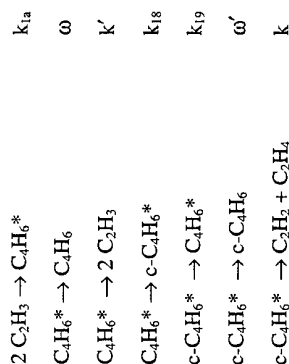
The results are summarized in Figure and Table below.

Temperature Dependence of CH(D) reactions with Methane.



reports of the unimolecular decomposition of (1,3)-butadiene to directly produce C<sub>2</sub>H<sub>2</sub> and C<sub>2</sub>H<sub>4</sub>; only the decomposition producing vinyl radicals has been reported.<sup>4</sup>

The following proposed mechanism provides a more feasible precursor for C<sub>2</sub>H<sub>2</sub> and C<sub>2</sub>H<sub>4</sub>. In this mechanism cyclobutene (c-C<sub>4</sub>H<sub>6</sub>) is formed by the isomerization (k<sub>18</sub>) of chemically activated (1,3)-butadiene. The cyclobutene can: (i) isomerize (k<sub>19</sub>) to (1,3)-butadiene,<sup>5</sup> (ii) be collisionally stabilized (ω), or (iii) decompose (k) to C<sub>2</sub>H<sub>2</sub> and C<sub>2</sub>H<sub>4</sub>. Although the decomposition of cyclobutene has not been observed, the decomposition of cyclobutane to ethylene has been and Arrhenius parameters reported.<sup>6</sup> The following steps make up this mechanism:



The limiting pressure dependencies correlate with what is experimentally observed and the transition pressure from the limiting high and low pressure limits is in the regions where there is no experimental data. At low pressure there is no stabilization so the (1,3)-butadiene and cyclobutene concentrations are zero. At high pressure only (1,3)-butadiene is observed. In the transition region both (1,3)-butadiene and cyclobutene are present. This mechanism indicates that cyclobutene should be observed in the 1-100 Torr range, i.e., when ω ~ k.

## REFERENCES

1. Fahr, A.; Laufer, A.H.; Klien, R.; Braun, W. *J. Phys. Chem.* **1991**, *95*, 3218.
2. Fahr, A.; Laufer, A.H. *J. Phys. Chem.* **1990**, *94*, 726.
3. MacFadden, K.O.; Currie, C.L. *J. Chem. Phys.* **1973**, *58*, 1213.
4. Kiefer, J.H.; Mitchell, K.L.; Wei, H.C. *Int. J. Chem. Kinet.* **1988**, *20*, 787.
5. Carr, R.W.; Walters, W.D. *J. Phys. Chem.* **1965**, *69*, 1073.
6. Benson, S.W.; O'Neal, H.E. "Kinetic Data on Gas Phase Unimolecular Reactions", National Standard Reference Data Series, National Bureau of Standards 21, Washington, D.C. 1970.

# A STUDY OF THE REACTIONS OF THE NITRATE RADICAL WITH 1-PENTENE AND 1-HEXENE OVER THE TEMPERATURE RANGE 298-430K BY LIF DETECTION.

E. Martinez, B. Cabañas, A. Aranda, P. Martin And S. Salgado.

Universidad de Castilla-La Mancha, Dpto Química Física, Facultad de Ciencias.  
Campus Universitario s/n, 13071 Ciudad Real . Spain

Alkenes, in general, are important atmospheric constituents as a result of their involvement in the production of tropospheric ozone and PAN.

The reactions of NO<sub>3</sub> radical with alkenes, dialkenes, cycloalkenes and haloalkenes have been studied using relative and absolute rate techniques<sup>1-3</sup>. All the available kinetic and product data suggest that the initial step in the reaction of nitrate radical with alkenes proceeds predominantly via electrophilic addition of NO<sub>3</sub> to the carbon-carbon double bond<sup>4</sup> to form a radical adduct intermediate which decomposes to epoxide and NO<sub>2</sub>.

The facts of, that the rate constants for reaction of NO<sub>3</sub> with unsaturated hydrocarbons are orders of magnitude large than those for reaction with saturated compounds analogues, which proceed via H-atom abstraction and that rate constants show a typical electrophilic behaviour, support the idea of an addition mechanism. Also Arrhenius parameters derived from these studies are entirely consistent with radical addition processes, with a relatively low activation energies.

This work presents the study of the kinetics of the reactions of the nitrate radical with 1-pentene and 1-hexene. The kinetics of these reactions have been measured using the discharge-flow technique coupled to detection of NO<sub>3</sub> by laser induced fluorescence in the range of temperature 298-430K. Rate constants at different temperatures and Arrhenius parameters for both compounds are shown in table 1.

TABLE 1:

Compound	T/K	K/molec <sup>-1</sup> cm <sup>3</sup> s <sup>-1</sup>	E <sub>a</sub> /kJ mol <sup>-1</sup>	A/molec <sup>-1</sup> cm <sup>3</sup> s <sup>-1</sup>
1-pentene	298	6.1 ± 0.3 x 10 <sup>-14</sup>	14.54 ± 1.34	2.05 ± 0.95 x 10 <sup>-11</sup>
	341	10.9 ± 0.5 x 10 <sup>-14</sup>		
	378	21.1 ± 0.7 x 10 <sup>-14</sup>		
	433	35.1 ± 2.6 x 10 <sup>-14</sup>		
1-hexene	298	9.38 ± 0.7 x 10 <sup>-14</sup>	6.21 ± 0.09	1.24 ± 0.04 x 10 <sup>-12</sup>
	324	12.42 ± 0.4 x 10 <sup>-14</sup>		
	364	15.65 ± 0.6 x 10 <sup>-14</sup>		
	433	22.15 ± 0.9 x 10 <sup>-14</sup>		

Reaction	10 <sup>11</sup> k <sub>298</sub> /cm <sup>3</sup> molecule <sup>-1</sup> s <sup>-1</sup>	Arrhenius Expression/ cm <sup>3</sup> molecule <sup>-1</sup> s <sup>-1</sup>	Reference
CH + CH <sub>4</sub>	9.79 ± 0.37	(2.5 ± 0.3) x 10 <sup>-11</sup> exp [3400 ± 500]/RT]	This work
CH + CH <sub>4</sub>	9.6	(5.0 ± 0.5) x 10 <sup>-11</sup> exp [398 ± 62]/RT]	Ref 1
CD + CH <sub>4</sub>	9.28 ± 0.24	(2.9 ± 0.3) x 10 <sup>-11</sup> exp [2700 ± 450]/RT]	This work
CH + CD <sub>4</sub>	6.86 ± 0.19	(1.8 ± 0.2) x 10 <sup>-11</sup> exp [3200 ± 500]/RT]	This work
CD + CD <sub>4</sub>	6.60 ± 0.26	(2.0 ± 0.2) x 10 <sup>-11</sup> exp [2900 ± 400]/RT]	This work

In general all the reactions are fast and with a slight, but significant, negative temperature dependence. The room temperature value for the reaction of CH with CH<sub>4</sub> is in good agreement with previous work although a somewhat steeper negative temperature dependence was observed in the present work.

As might be expected, isotopic substitution of the CH has little effect on the kinetics, however, deuteration of methane reduces the rate coefficient by approximately 30 % over the entire temperature range.

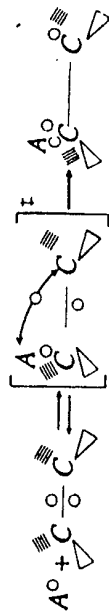
The results of this study will be compared with previous experimental and theoretical work. The isotopic dependence of the reaction appears to be incompatible with a Gorin model for the transition state.

## References

- [1] M.R. Berman and M.C. Lin, *Chem. Phys.* (1983), **82**, 435.

These investigations provide a more complete understanding of the effect of alkenes on tropospheric processes, although it is expected that their individual effect will be small. This study contribute to give a clear picture of the changes in reactivity on the alkene series. The electronic distribution in the  $\pi$ -bond is the primary factor that governs the rate of attack of  $\text{NO}_3$  radical on an unsaturated molecule. For unsymmetric alkenes, the site of attack is effected by steric repulsion, determined by geometrical size and by partial charges on the incoming radical substituents present in the molecule. Thus  $\text{NO}_3$  radical attacks the carbon atom that is least substituted<sup>4</sup>. Addition processes of this type go *via* a three-centre, three-electron type of transition state. In principle, the antibonding character of the  $\pi^*$ -electron in the newly-formed bond which will determine the magnitude of the activation energy of such reaction. The  $\pi^*$ -electron is shared between the three centres as is showed in figure 1.

FIGURE 1



The study of the reactions of  $\text{NO}_3$  with both alkenes (1-pentene and 1-hexene) was also motivated by a desire to compile experimental data to test theoretically and empirically based rate constant predictions developed in this laboratory.<sup>2</sup>

## REFERENCES

- 1) R.P. Wayne, Y. Barnes, P. Biggs, J.P. Burrows, C.E. Canosa-Mas, J. Hjorth, G. Le Bras, G.K. Moortgat, D. Perner, G. Poulet, G. Restelli and H. Sidebottom. *Atmos. Environ.*, 1991 25A.
- 2) E. Martinez, B. Cabañas, A. Aranda and R.P. Wayne. *J.Chem.Soc. Faraday Trans.1996 92(1)*, 53
- 3) E.Martinez, B. Cabañas, A. Aranda, P. Martin and R.P. Wayne. *J. Chem. Soc. Faraday Trans.*, (in press)
- 4) J.M. Tedder and J.C. Walton. *Tetrahedron Lett.*1980, 36, 701
- 5) S.W. Benson. *Thermodynamical Kinetics*, 1976, Second Edition, Wiley, New York.

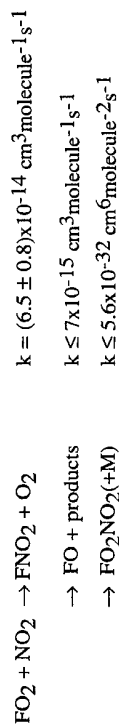
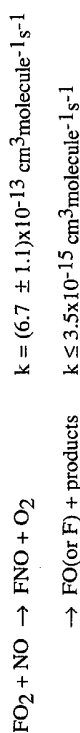
## EXPERIMENTAL STUDY OF $\text{FO}_2$ ELEMENTARY REACTIONS

Yuri R. Bedjanian\*

*Institute of Chemical Physics, National Academy of Sciences  
Yerevan, Armenia*

Kinetics of  $\text{FO}_2$  elementary reactions with  $\text{FO}_2$ ,  $\text{NO}$ ,  $\text{NO}_2$ ,  $\text{NF}_2$ ,  $\text{O}$  and  $\text{N}$  have been studied using EPR/IR LMR - discharge flow technique. Reaction  $\text{F} + \text{O}_2 + \text{M} \rightarrow \text{FO}_2 + \text{M}$  was used to produce  $\text{FO}_2$  radicals and to measure their absolute concentrations.  $\text{FO}_2$  was detected by LMR method using the  $10\text{P}14(\nu = 949.4793\text{cm}^{-1})$  line of a  $\text{CO}_2$ -laser.

At  $T = 298\text{K}$  and in the pressure range  $P = (5 - 30)$  Torr, the following reaction rate constants have been obtained:



**REACTION KINETICS OF O-ATOMS AND H-ATOMS WITH MONO  
METHYL HYDRAZINE AND UNSYMMETRICAL DIMETHYL  
HYDRAZINE ROCKET PROPELLANTS**

Ghanshyam L. Vaghjiani

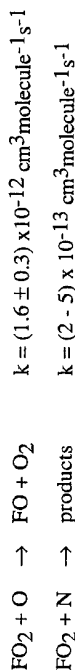
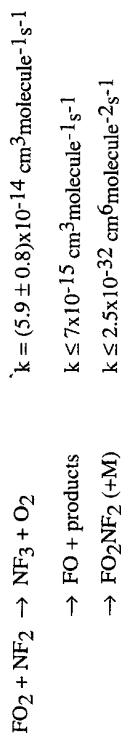
*Hughes STX  
Phillips Lab, PL/RKS  
10 E Saturn Blvd*

*Edwards AFB, CA 93524, USA*

*Tel: (805) 275 5657*

*Fax: (805) 275 6233*

*Email: vaghjiag@lablink.ple.af.mil*



These results show that FO<sub>2</sub> radicals exhibit relatively low reactivity even toward atoms and radicals. Reactions of FO<sub>2</sub> generally proceed through F atom exchange.

#### Acknowledgement

This work was supported by the International Science Foundation (Grant No MVP000). The experiments were partly carried out at the Laboratory of Radical Reactions of the Institute of Chemical Physics, Russian Academy of Sciences.

*\*Present address: CNRS-LCSR, 1c Avenue de la Recherche Scientifique, 45071 Orleans Cedex 2, France*

The reactions of atomic oxygen (O(<sup>3</sup>P)) with diamine fuels like hydrazine (N<sub>2</sub>H<sub>4</sub>), mono methyl hydrazine (CH<sub>3</sub>NNH<sub>2</sub>) and unsymmetrical dimethyl hydrazine ((CH<sub>3</sub>)<sub>2</sub>NNH<sub>2</sub>) are important elementary processes during combustion in bi-propellant (diamine/nitrogen tetroxide (N<sub>2</sub>O<sub>4</sub>)) rocket motors such as those in the Titan launch vehicles. Also, numerous spacecrafts that operate in low earth orbit (LEO), ~ 180 km and above, use N<sub>2</sub>H<sub>4</sub> in attitude-control jets and its methylated analogues are used as fuels for the thruster engines aboard the space shuttle, as well as other spacecrafts in LEO. Although most of the fuel is consumed in the rocket chamber, some escapes in the unburnt state especially at engine shut down. Since the ambient atmosphere at these altitudes consists mainly of atomic oxygen, the ejected fuel fragments are thought to degrade primarily via the O(<sup>3</sup>P) reaction. In order to access the importance of these fuel fragments in such phenomena as the shuttle glow, the contamination of spacecraft surfaces and exhaust plume ultraviolet signatures, an accurate knowledge of the temperature dependences of the reaction rate coefficients together with the product branching ratios for the above and subsequent reactions occurring in these environments is required for detailed kinetic modeling studies.

In this paper we report laboratory measurements of the temperature dependences of the rate coefficients for the gas phase reactions of the alkylated propellants with O-atoms and also with H-atoms. The H-atom reactions are thought to be important in the pyrolysis of these fuels. The reaction mechanisms in these systems will also be discussed.

TIME-RESOLVED STUDY OF THE GAS-PHASE REACTIONS OF  $\text{SiH}_2$   
WITH 1,3-BUTADIENE: KINETICS AND MECHANISM

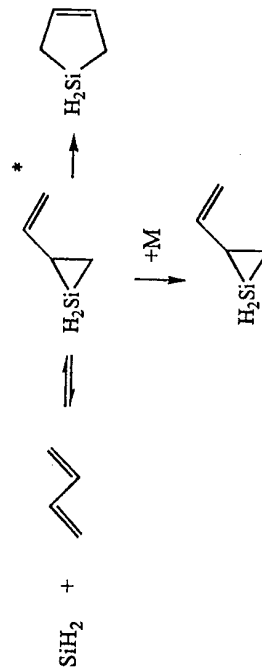
G. Dormer and R. Walsh,

Department of Chemistry, University of Reading, Whiteknights, PO Box 224, Reading  
RG6 2AD, UK.

The title reaction has been investigated by means of laser flash photolysis over the temperature range 300 - 600 K.  $\text{SiH}_2$  was generated by photolysis of both phenylsilane and 4-sila-cyclopentene. The reaction shows good second order kinetic behaviour. The table below shows the rate constants obtained at total pressures of 10 Torr ( $\text{SF}_6$  bath gas). The reaction was also studied as a function of pressure in the range 1-100 Torr and showed a slight pressure dependence of the rate constants. Extrapolation to infinite pressure, at each temperature, gave rate constants which fit the following Arrhenius equation:

$$\log (k^\infty / \text{s}^{-1}) = (-9.57 \pm 0.05) + (3.22 \pm 0.35) \text{ kJ mol}^{-1} / RT \ln 10$$

These figures are consistent with a collision controlled addition reaction and suggestive of a third-body-assisted association process. Independent experiments reveal the formation of 4 silacyclopentene as a product at 150°C (but not at 25°C). The following mechanism is suggested to account for these findings:



Unimolecular (RRKM) modelling is being carried out to verify that the pressure dependence is consistent with those of other silylene addition reactions such as that of  $\text{SiH}_2$  with  $\text{C}_3\text{H}_4$ .<sup>1</sup>

Table of rate constants at 10 Torr

T/K	$k/10^{10} \text{ cm}^3 \text{ molecule}^{-1} \text{ s}^{-1}$
290	$7.4 \pm 0.3$
357	$5.7 \pm 0.3$
418	$4.5 \pm 0.1$
457	$4.1 \pm 0.1$
572	$3.8 \pm 0.2$

1) Al Rubaiey and R. Walsh, *J. Phys. Chem.*, **98**, 5303 (1994).

TIME-RESOLVED STUDY OF THE GAS-PHASE REACTIONS OF  $\text{SiH}_2$   
WITH ACETONE AND OXIRANE: KINETICS, MECHANISM AND  
POTENTIAL ENERGY SURFACE

R. Becerra,

*Instit. Quim. Fis. "Rocasolano", C.S.I.C. C/Serrano 119, 28006 Madrid, Spain;*

P. Cannady,

*Dow Corning Corporation, Midland, Michigan, USA;*

R. Walsh,

*Department of Chemistry, University of Reading, Whiteknights, PO Box 224,  
Reading RG6 2AD, UK.*

Table 1. Rate constants ( $k/10^{-10} \text{ cm}^3 \text{ molecule}^{-1} \text{ s}^{-1}$ ) at 10 Torr ( $\text{SF}_6$ ).

T/K	Oxirane	T/K	Acetone
294	$0.943 \pm 0.023$	295	$4.08 \pm 0.11$
356	$0.652 \pm 0.029$	353	$3.31 \pm 0.04$
397	$0.430 \pm 0.017$	398	$2.64 \pm 0.05$
481	$0.287 \pm 0.010$	473	$1.80 \pm 0.03$
605	$0.183 \pm 0.011$	602	$1.26 \pm 0.05$

Table 2. Arrhenius Parameters (10 Torr,  $\text{SF}_6$ )

Reaction	$\log(A/\text{cm}^3 \text{ molecule}^{-1} \text{ s}^{-1})$	$E_a / \text{kJ mol}^{-1}$
$\text{SiH}_2 + \text{oxirane}$	$-11.41 \pm 0.07$	$-7.99 \pm 0.54$
$\text{SiH}_2 + \text{Me}_2\text{CO}$	$-10.38 \pm 0.08$	$-5.84 \pm 0.60$

The title reactions have been investigated by means of laser flash photolysis over the temperature range 300 - 600 K. Both reactions show good second order kinetic behaviour. Table 1 below shows the rate constants obtained at total pressures of 10 Torr ( $\text{SF}_6$  bath gas). The Arrhenius Parameters for each reaction at this pressure are shown in Table 2. The reactions were also studied as a function of pressure in the range 1 - 100 Torr and both reactions showed slight pressure dependences.

These results indicate (i) that both reactions occur on barrierless potential energy surfaces with the possible intermediacy of transient complexes, and (ii) that both reactions involve formation of products which can, at least partially, revert to reactants. In order to try to characterize intermediates and products, *ab initio* calculations have been carried out at the MP2 level, with energies refined at the MP4 level. These calculations show the following:

- **For  $\text{SiH}_2 + \text{oxirane}$ ,** the initial formation of a donor acceptor complex, *ca* 71 kJ  $\text{mol}^{-1}$  below the reactants. Also on the surface lies 1,2-siloxetane, some 368 kJ  $\text{mol}^{-1}$  lower in energy than the reactants. The final products are  $\text{SiH}_2 + \text{C}_2\text{H}_4$ . Ethene formation has been confirmed experimentally.
- **For  $\text{SiH}_2 + \text{Me}_2\text{CO}$ ,** the system has been modelled by  $\text{SiH}_2 + \text{CH}_2\text{O}$  (for simplicity). An initially formed open chain complex exists at 50 kJ  $\text{mol}^{-1}$  below the reactants, which cyclises with a low barrier to siloxirane, 192 kJ  $\text{mol}^{-1}$  lower in energy than the reactants. The surface beyond this point is still under exploration. However, in the case of  $\text{SiH}_2 + \text{Me}_2\text{CO}$ , propene has been detected experimentally. Calculations rule out its formation via singlet dimethyl carbene.

# ROOM TEMPERATURE OBSERVATION OF GeH<sub>2</sub> AND THE FIRST TIME-RESOLVED STUDY OF SOME OF ITS REACTIONS

R. Becerra,

*Instituto Química Física "Rocasolano", C.S.I.C. C/Serrano 119, 28006 Madrid, Spain;*

S.E. Boganov, M.P. Egorov, O.M. Nefedov,

*Zelinsky Institute of Organic Chemistry, Leninsky Prospekt 47, Moscow 117913, Russia;*

R. Walsh

*Department of Chemistry, University of Reading, Whiteknights, PO Box 224, Reading RG6 2AD, UK.*

Table of rate constants at 295 K

Substrate	$k/\text{cm}^3 \text{ molecule}^{-1} \text{ s}^{-1}$
O <sub>2</sub>	$(6.11 \pm 0.17) \times 10^{-13}$
C <sub>2</sub> H <sub>2</sub>	$(1.29 \pm 0.04) \times 10^{-10}$
i-C <sub>4</sub> H <sub>8</sub>	$(1.24 \pm 0.08) \times 10^{-10}$
1,3-C <sub>4</sub> H <sub>6</sub>	$(3.03 \pm 0.12) \times 10^{-10}$
C <sub>3</sub> H <sub>8</sub>	$< 1.1 \times 10^{-14}$
Me <sub>3</sub> SiH	$(8.18 \pm 0.14) \times 10^{-11}$
DMGCP	$(3.48 \pm 0.16) \times 10^{-10}$

1) Becerra, S.E. Boganov, M.P. Egorov, V.Ya. Lee, O.M. Egorov and R. Walsh, *Chem. Phys. Lett.*, **250**, 111 (1996).

Using a laser flash photolysis/laser probe technique, applied to two different gaseous precursor molecules, we report absorption signals in the wavenumber region 17109–17120 cm<sup>-1</sup>, which we attribute to previously unobserved rotational transitions in the vibronic spectrum of GeH<sub>2</sub>. The spectrum is confirmed by comparison with published fluorescence spectra of the jet cooled species. Time-resolved monitoring of GeH<sub>2</sub> has been carried out using both photolytic sources, yielding second order decay constants for its reactions with O<sub>2</sub>, C<sub>2</sub>H<sub>2</sub>, i-C<sub>4</sub>H<sub>8</sub>, 1,3-C<sub>4</sub>H<sub>6</sub>, C<sub>3</sub>H<sub>8</sub> and Me<sub>3</sub>SiH. The apparent rate constants differ, however, dependent upon the GeH<sub>2</sub> precursor employed. For specific substrates, values obtained using 3,4-dimethylgermacyclopentene (DMGCP) were between 1.5 and 3 times higher than those obtained using phenylgermane. Various indicators (poor yields of transient, excessive concomitant dust formation) lead us to believe that the latter values are wrong. Our results, shown in the table below, are therefore those obtained using the DMGCP precursor. The measurements show that GeH<sub>2</sub> is unreactive towards C-H bonds but inserts readily in Si-H bonds, as well as reacting rapidly (close to the collision rate), with  $\pi$ -bonds. These results represent the first kinetic measurements on GeH<sub>2</sub>. They reveal that GeH<sub>2</sub> is marginally less reactive than SiH<sub>3</sub> in reactions with common substrates. This confirms findings of our earlier study<sup>1</sup> of GeMe<sub>2</sub> which was also found to be slightly less reactive than SiMe<sub>2</sub>. Thus it seems likely that germynes possess the same electrophilic character and substitution effects on reactivity as silylenes. The initial products of the germylene  $\pi$ -addition processes, the germinanes, must be sufficiently stable to permit their formation (although we have not attempted their direct detection). Continuing studies of reaction of GeH<sub>2</sub> with smaller alkenes show pressure dependencies, from which we will be able to extract information about germinane stability.

# RATE CONSTANT FOR THE REACTION BETWEEN HYDROXYL RADICALS AND CHLOROBROMOMETHANE.

V.G. Khamaganov<sup>#</sup>, V.L. Orkin<sup>##</sup>, A.G. Guschin<sup>#</sup>, R.E. Huie<sup>\*</sup> and M.J. Kurylo<sup>\*</sup>

<sup>#</sup>*Institute of Energy, Problems of Chemical Physics, Russian Academy of Sciences, Leninsky Prospekt, 38, Bldg. 2, Moscow 117829, Russia*

<sup>\*</sup>*National Institute of Standards and Technology, Gaithersburg, MD 20899, USA.*

Chlorobromomethane (CBM) is a natural source gas, formed by algal biological processes, which delivers bromine into Earth's atmosphere. In spite of its lower concentration than the main source of atmospheric bromine, CH<sub>3</sub>Br<sup>1</sup>, CBM and other organic bromides can influence the reactive bromine budget in the atmosphere depending on their efficiency of bromine release via both chemical reactions and solar ultraviolet photolysis. Additional interest in chlorobromomethane stems from its effectiveness as a cleaning agent in industrial applications<sup>2</sup> and as a possible fire suppressant. In order to better quantify the atmospheric behavior of this compound, we have determined the rate constant for its reaction with OH and have measured its UV absorption spectrum.

Rate constants were measured by the discharge-flow technique with EPR detection of hydroxyl over the temperature range 298-370K and by the flash photolysis resonance fluorescence technique over the temperature range 277-370K. The resulting parameters obtained, as well as our estimations of both the atmospheric lifetime and ODP for CBM, are presented below.

Molecule	A 10 <sup>12</sup> , cm <sup>3</sup> molec <sup>-1</sup> s <sup>-1</sup>	E/R, K	k(298) 10 <sup>13</sup> , cm <sup>3</sup> molec <sup>-1</sup> s <sup>-1</sup>	Atmospheric Lifetime, yrs	ODP
CH <sub>2</sub> ClBr	3.1	985 ± 67	1.14 ± 0.06	0.43	0.15

## References

1. Scientific Assessment of Ozone Depletion: 1994, World Meteorological Organization, Global Ozone Research and Monitoring Project - Report No. 37 1995, 10.13.
2. Clark, L., Enviro Tech international, personal communication.

# EXPERIMENTAL AND THEORETICAL AB INITIO STUDY OF HYDROGEN ABSTRACTION REACTIONS FROM METHANOL BY H, F, Cl, Br AND OH RADICALS.

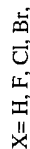
J. Jodkowski, M.T. Rayez and J.C. Rayez

*Laboratoire de Physicochimie Théorique, URA503/CNRS, Université Bordeaux I  
33405, Talence, France*

T. Bércés and S. Dobé

*Central Research Institute for Chemistry, Hungarian Academy of Sciences H-1525  
Budapest, P.O. Box 17, Hungary*

Hydrogen atom abstraction reactions are frequently used in flow systems as the source of free radicals. However, in such reactions, often more than one reactive species are formed in competing reaction channels and may yield species of different reactivities. A good example for this is provided by the hydrogen atom abstraction reactions by H, F, Cl or OH radicals from methanol:



The values of the branching ratios, which are used as inputs in combustion and atmospheric modelling studies, can have a fundamental influence on the outputs of model calculations. In particular, the reaction with Cl is faster than expected for an almost thermoneutral reaction. The causes for this behaviour are not well understood.

## Theory

These reactions are studied using ab initio molecular orbital theory. All geometries of reactants, intermediate complexes and transition states were fully optimized at the (un)restricted Hartree-Fock (U)HF/6-311G(d,p) and Moller-Plesset (U)MP2/6-311G(d,p) levels of theory. Activation energy barriers and heats of reactions have been estimated using both fourth order Moller-Plesset perturbation theory (MP4) and G2 method of Pople and coworkers. Reactions with halogens show a mechanism which involve the formation a long-range loose complexes with halogens which decompose into products. Reactions with H and OH are direct abstractions. Informations on reaction mechanisms and methoxy/hydroxymethyl branching ratios along the series are obtained.

## Experiment

Experiments were carried out by applying both the laser flash photolysis and fast flow techniques. The atoms and radicals consumed or formed in the reactions were detected by resonance fluorescence, laser induced fluorescence and laser magnetic resonance. Arrhenius parameters for the overall reactions and the temperature dependence of the branching ratios have been determined.

# RATE COEFFICIENT MEASUREMENTS OF THE REACTIONS OF C<sub>2</sub>H<sub>2</sub> WITH

## NO AND H<sub>2</sub> AT T = 295 TO 450 K IN THE 2 TO 20 TORR RANGE

H. Van Look, B. Ceursters and J. Peeters

*Department of Chemistry, K.U.Leuven, Celestijnenlaan 200 F, B-3001 Heverlee, Belgium*

The ethynyl radical, C<sub>2</sub>H, is known to play a role in a wide variety of natural and man-made environments. It has been found in abundance in interstellar space<sup>1</sup> and it has been detected in planetary atmospheres<sup>2</sup>. The ethynyl radical is also generally recognized as an important intermediate in hydrocarbon combustion chemistry because of its involvement in the formation of polyacetylenes<sup>3</sup> and possibly of polycyclic aromatic hydrocarbons (PAH) and hence of soot<sup>4</sup>. Its reaction with NO may also be of importance with regard to NO<sub>x</sub>-chemistry<sup>5</sup> in flames in general and its possible role in the so-called "Reburn Technology"<sup>6</sup> in particular.

The quantitative elucidation of the role of C<sub>2</sub>H radicals in combustion processes requires the knowledge of the rate constants at higher temperatures of the elementary formation and destruction reactions.

Absolute rate coefficients of the title reactions were measured at 295 < T < 450 K by means of a pulse laser photolysis / chemiluminescence technique (PLP / CL) that we already applied in other C<sub>2</sub>H kinetic studies, published recently<sup>7</sup>. Ethynyl radicals were generated pulse-wise by 193 nm excimer laser photodissociation of C<sub>2</sub>H<sub>2</sub> (or C<sub>2</sub>HCF<sub>3</sub>) and their real-time pseudo-first-order decay was monitored by the luminescence of CH(A<sup>2</sup>Δ) produced by their reaction with O<sub>2</sub>, present in a high and constant concentration. Experimental conditions of the decay experiments were such that the C<sub>2</sub>H radicals were electronically and vibrationally relaxed.

The temperature dependence of the rate coefficient k(C<sub>2</sub>H + NO), determined for the first time, can be expressed as k(T) = (1.0 ± 0.2) × 10<sup>-10</sup> exp[ -(287 ± 65)/T(K) ] cm<sup>3</sup> molecule<sup>-1</sup> s<sup>-1</sup>; the k(T = 295 K) value of (3.9 ± 0.4) × 10<sup>-11</sup> is independent of the total pressure (2 to 10 Torr He) and agrees with literature data obtained at 20 Torr<sup>8</sup>. The high and pressure-independent rate coefficient indicates that C<sub>2</sub>H + NO is an association-elimination reaction, with HCN + CO or CN + HCO as likely products. In hydrocarbon flames, both HCN and CN should subsequently yield NH or NH<sub>2</sub><sup>9</sup>, each of which can rapidly react with NO to form N<sub>2</sub><sup>5,9,10</sup>. Therefore, it is argued that the

C<sub>2</sub>H + NO reaction is of major importance in NO-reburning chemistry in fuel-rich hydrocarbon flames, where C<sub>2</sub>H is an important intermediate.

Our k(C<sub>2</sub>H + H<sub>2</sub>) result at 295 K, of (6.9 ± 0.7) × 10<sup>-13</sup>, supports the higher of the literature values rather than the slightly lower data (of 4.6 × 10<sup>-13</sup>). In the ab initio Transition State Theory k(T) expression of Harding et al.<sup>11</sup>, we adjusted the barrier height together with the closely correlated ω\*% TS bending frequency in order to fit the average of the literature data at 295 K, k = 5.8 × 10<sup>-13</sup>. The resulting equation, k(T) = 1.31 × 10<sup>-18</sup> T<sup>2.39</sup> exp[ -174/T(K) ] cm<sup>3</sup> molecule<sup>-1</sup> s<sup>-1</sup>, is found to provide a close representation (standard deviation 21 %) of all three available sets of k(T) measurements at higher temperatures<sup>12,13</sup>, including the present data in the 295-440 K range. Combination with the equilibrium constant leads to k(C<sub>2</sub>H<sub>2</sub> + H)(T) = 1.50 × 10<sup>-13</sup> T<sup>1.32</sup> exp[ -15400/T(K) ] cm<sup>3</sup> molecule<sup>-1</sup> s<sup>-1</sup>, implying values at flame temperatures almost 20 times higher than recent recommendations.

### References

- (1) K. D. Tucker, M. L. Kutner and P. Thaddeus, *Astrophys. J.* 1974, **193**, L115.
- (2) D. F. Strobel, *Planet. Space Sci.* 1982, **30**(8), 839.
- (3) U. Bonne, K. H. Homann and H. Gg. Wagner, *Symp. (Int.) on Combust. [Proc.]* 1965, **10**, 503.
- (4) M. Frenklach, D. W. Clary, W. C. Gardiner and S. E. Stein, *Symp. (Int.) on Combust. [Proc.]* 1984, **20**, 887.
- (5) J. A. Miller and C. T. Bowman, *Prog. Energy Combust. Sci.* 1989, **15**, 287 (and references therein).
- (6) C. T. Bowman, *Symp. (Int.) on Combust. [Proc.]* 1992, **24**, 859.
- (7) (a) H. Van Look and J. Peeters, *J. Phys. Chem.* 1995, **99**(44), 16284. (b) J. Peeters, H. Van Look and B. Ceursters, *J. Phys. Chem.*, accepted for publication.
- (8) (a) J. W. Stephens, J. L. Hall, H. Solka, W.-B. Yan, R. F. Curl and G. P. Glass, *J. Phys. Chem.* 1987, **91**(22), 5740. (b) D. R. Lander, K. G. Unfried, G. P. Glass and R. F. Curl, *J. Phys. Chem.* 1990, **94**(20), 7759.
- (9) B. Atakan, A. Jacobs, M. Wahl, R. Weller and J. Wolfrum, *Chem. Phys. Lett.* 1989, **155**(6), 609.
- (10) M. Wolf, D. L. Yang and J. L. Durant, *J. Photochem. Photobiol. A: Chem.* 1994, **80**, 85.
- (11) L. B. Harding, G. C. Schatz and R. A. Chiles, *J. Chem. Phys.* 1982, **76**(10), 5172.
- (12) S. K. Farhat, C. L. Morter and G. P. Glass, *J. Phys. Chem.* 1993, **97**(49), 12789.
- (13) M. Koshi, K. Fukuda, K. Kamiya and H. Matsui, *J. Phys. Chem.* 1992, **96**(24), 9839.

# THE REACTION OF ATOMIC CHLORINE WITH BENZENE

Florence Bertho, Marie-Thérèse Rayez and Robert Lesclaux

*Laboratoire de Photophysique et Photochimie Moléculaire*  
*Université Bordeaux I - URA 348 CNRS -*  
*33405 TALENCE Cedex - FRANCE*

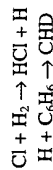
Growing interest has been recently directed towards the chemistry of aromatic compounds, both for combustion and atmospheric applications. However, kinetic studies are scarce for addition reactions to the aromatic ring, even in the case of benzene. For example, the data available for the  $(\text{Cl} + \text{C}_6\text{H}_6)$  reaction exhibit strong disagreement: Atkinson and Aschmann [1] measured  $k(\text{Cl} + \text{C}_6\text{H}_6) = (1.5 \pm 0.9) \times 10^{-11} \text{ cm}^3 \text{ molecule}^{-1} \text{ s}^{-1}$  ( $T=296\text{K}$ , 1 atm of air), whereas both Wallington et al. [2] and Nozière et al. [3] did not observe any reaction in the absence of oxygen, with  $k(\text{Cl} + \text{C}_6\text{H}_6) < 5 \times 10^{-16} \text{ cm}^3 \text{ molecule}^{-1} \text{ s}^{-1}$  ( $T=298\text{K}$ , 1 atm of  $\text{N}_2$ ) [3]. Given those inconsistencies, we have undertaken to investigate again this reaction to clarify the situation.

It is well known that H and OH add to benzenic rings at ambient temperature, the resulting adducts being the cyclohexadienyl (CHD) and hydroxy-cyclohexadienyl (OH-CHD) radicals, respectively. These cyclohexadienyl-type radicals exhibit strong UV absorption around 300 nm with maximum absorption cross sections of about  $1 \times 10^{-17} \text{ cm}^2/\text{molecule}$ . Such a spectrum has also been reported for the (Cl-CHD) radical [4], but this is again inconsistent with the absence of reaction reported in ref. 2 and with a theoretical study of the  $(\text{Cl} + \text{C}_6\text{H}_6)$  reaction [5], which indicates that the (Cl-CHD) radical is unstable.

Experiments were carried out using our flash photolysis / UV absorption technique complemented by ab initio calculations for more detailed information on the thermochemistry of the reaction. The results are as follows:

By flashing  $\text{Cl}_2$  or  $\text{CCl}_4$  in the presence of excess benzene and in the absence of oxygen, at 298K, 373K and 248K, no transient absorption could be observed around 300 nm, where the adduct is expected to absorb strongly. However, transient absorptions were observed in the 220 to 280 nm range, in the presence of oxygen, in agreement with the observations reported by Nozière et al. [3].

In order to check that our experimental conditions were suitable to create cyclohexadienyl-type radicals, we tried to generate the CHD radical by adding  $\text{H}_2$  to the system, according to the reactions:



In such conditions, the characteristic absorption of the CHD radical was clearly observed and could be accounted for by simulation of the reaction system, without taking into account the  $(\text{Cl} + \text{C}_6\text{H}_6)$  reaction. This shows that chlorine atoms preferentially react with  $\text{H}_2$  rather than with benzene ( $[\text{H}_2] = 200 \text{ Torr}$ ;  $[\text{C}_6\text{H}_6] = 20 \text{ Torr}$ ;  $k(\text{Cl} + \text{H}_2) = 1.5 \times 10^{-14} \text{ cm}^3 \text{ molecule}^{-1} \text{ s}^{-1}$ ). Note that this method can be used to generate CHD radicals using our flash photolysis apparatus.

At this stage, it can be seen that the reaction  $(\text{Cl} + \text{C}_6\text{H}_6)$  does not occur in pure  $\text{N}_2$  but does occur in the presence of  $\text{O}_2$ . This indicates that the reaction is equilibrated  $(\text{Cl} + \text{C}_6\text{H}_6 \rightleftharpoons \text{Cl-CHD})$  and that the equilibrium is largely shifted towards the reactants in our conditions.

This can explain the disagreement between the results of Atkinson et al. [1], and those of Wallington and coll. [2,3], obtained in the absence of  $\text{O}_2$ . The ab initio calculations (BAC-MP4 method) have confirmed this hypothesis. The results of calculations are in good agreement with those reported in a separate study [5], and show that the dissociation of the Cl-CHD adduct should be fast around room temperature.

The absorption cross-section of the product formed in excess  $\text{O}_2$  (equilibrium shifted towards the products), has been determined as a function of the wavelength. The shape of the obtained spectrum and absorption cross sections values indicates that the species formed by the reaction of the Cl-CHD adduct with  $\text{O}_2$  is a peroxy radical, but this should be confirmed.

The rate constant of the association reaction  $(\text{Cl} + \text{C}_6\text{H}_6)$  was then investigated by the relative method, using two different chemical systems involving the reactions  $(\text{Cl} + \text{CH}_3\text{OH})$  and  $(\text{Cl} + \text{CHCl}_3)$ , in excess  $\text{O}_2$ . The results obtained are in good agreement:  $k(\text{Cl} + \text{C}_6\text{H}_6) = (8.6 \pm 1.3) \times 10^{-14}$  and  $k(\text{Cl} + \text{C}_6\text{H}_6) = (9.2 \pm 2.1) \times 10^{-14}$  respectively (units of  $\text{cm}^3 \text{ molecule}^{-1} \text{ s}^{-1}$ ), giving the average value:

$$k(\text{Cl} + \text{C}_6\text{H}_6) = (8.9 \pm 1.6) \times 10^{-14} \text{ cm}^3 \text{ molecule}^{-1} \text{ s}^{-1}$$

In addition to the above study, we have used the method described above  $(\text{Cl} + \text{H}_2 + \text{benzene})$  to generate CHD radicals and to measure the rate constants of their self reaction and reaction with  $\text{O}_2$ , which have never been investigated before. Preliminary results give:

$$\begin{aligned} k(\text{CHD} + \text{CHD}) &= 2.5 \times 10^{-11} \text{ cm}^3 \text{ molecule}^{-1} \text{ s}^{-1} \\ k(\text{CHD} + \text{O}_2) &= 1.15 \times 10^{-11} \text{ cm}^3 \text{ molecule}^{-1} \text{ s}^{-1} \end{aligned}$$

## REFERENCES

1. Atkinson, R.; Aschmann, S.M.; Int. J. Chem. Kinet., 1985, **17**, 33.
2. Wallington, T.J.; Skewes, L.M.; Siegl, W.O.; J. Photochem. Photobiol. A., 1988, **45**, 167.
3. Nozière, B.; Lesclaux, R.; Hurley, M.D.; Dearth, M.A.; Wallington T.J.; J. Phys. Chem., 1994, **98**, 2864.
4. Sauer Jr, M.C.; Mani, I., J. Phys. Chem. 1970, **74**, 59.
5. Ritter E.R.; Bozzelli, J.W.; Dean, A.M.; J. Phys. Chem., 1990, **94**, 2493.

## REACTION KINETICS AND ENERGY TRANSFER AT EXTREMELY LOW TEMPERATURES

Stuart G Arkless, Philip L James,  
Ian R Sims and Ian WM Smith

*School of Chemistry, The University of Birmingham, Edgbaston,  
Birmingham B15 2TT, UK*

André Canosa, Sébastien Le Picard,  
Daniel Travers and Bertrand R Rowe

*Université de Rennes I, Département de Physique Atomique et Moléculaire, U.A. au  
C.N.R.S. 1203, Campus de Beaulieu, 35042 Rennes CEDEX, France*

We have developed a new technique which has enabled the determination of rate constants for gas-phase reactions at temperatures as low as 13 K. The PLP-LIF (Pulsed Laser Photolysis-Laser Induced Fluorescence) method of studying free radical kinetics and dynamics has been combined with the CRESU (Cinétique de Réaction en Ecoulement Supersonique Uniforme) technique, which uses supersonic expansion through specially profiled Laval nozzles to provide an environment which is ultra-cold, yet collisional, and therefore fully thermalised. Complementary experiments have also been carried out down to 80 K in novel cooled cells. Results have been published for reactions of CN, OH and CH radicals, and these have aroused considerable interest from theoreticians and astrochemical modellers.

In this contribution, we will review techniques for low temperature kinetics, including the use of both cryogenically-cooled cells and the CRESU. We will report on some of the latest results for reactions of the CH radical down to 13 K, including new work on vibrational relaxation, and the formation of the methyl radical.

A new CRESU apparatus has been constructed at the University of Birmingham, and we will report on the first results on state-to-state collisional energy transfer at ultra-low temperatures using the IR-UV double resonance technique. A tuneable pulsed infra-red laser is used to prepare NO ( $X^2\Pi_{1/2}; v=3$ ) molecules in a single rotational level, and energy transfer into other rovibrational states is probed via ultra-violet laser-induced fluorescence. This technique has been successfully transferred to the ultra-low temperature environment of the CRESU apparatus, and the latest results will be reported.

# THE TEMPERATURE DEPENDENCE OF CH RADICAL REACTIONS UNDER HIGH PRESSURE CONDITIONS

H. Hippler

*Institut für Physikalische Chemie und Elektrochemie,  
Universität Karlsruhe,  
Kaiserstraße 12,  
D-76182 Karlsruhe, Germany*

# STATE-RESOLVED INTRAMOLECULAR AND UNIMOLECULAR BOND FISSION DYNAMICS OF SMALL POLYATOMIC MOLECULES: HOCl AND NO<sub>2</sub>

B. Abel, A. Charvat, H. H. Hamann, N. Lange

*Institut für Physikalische Chemie der Universität Göttingen, Tammannstraße 6,  
37077 Göttingen, Germany*

Small polyatomic molecules like NO<sub>2</sub> and HOCl are excellent model systems for state resolved investigations of intramolecular and unimolecular dissociation dynamics. Characterization of highly excited eigenstates of polyatomic molecules is central to the understanding of their reaction dynamics and intramolecular vibrational energy redistribution (IVR). Although, frequency domain spectroscopy is often thought to only provide "static" information about molecular constants and structure, high resolution (double resonance) spectroscopy at chemically significant energies can also determine the features of complex intra- and unimolecular processes, such as IVR and unimolecular dissociation. The information about mechanisms, timescales, and the extent of IVR is encoded in the 'splittings' and interactions of zeroth-order rovibrational states. While the information on IVR rates can be inferred from the magnitude of those splittings, the information on the extent of IVR is contained in the degree of fractionation of a zeroth-order rovibrational transition. In addition, the zeroth-order assignments of the interacting states, as well as the dependence of the splittings on rotational quantum numbers contain detailed information on IVR mechanisms. Finally, from linewidths measurements the excited state lifetimes of single states can be inferred. In recent experiments we succeeded in measuring the intramolecular and bond fission dynamics of state selected highly excited NO<sub>2</sub> and HOCl molecules using different techniques of optical double resonance spectroscopy (OODRS) and ultra-sensitive intracavity laser absorption spectroscopy (ICLAS).

We have used laser induced fluorescence detected optical V-type double-resonance spectroscopy in a free jet to access and to assign rovibronic (predissociating) states of NO<sub>2</sub> above the dissociation threshold. From the spectra just above the dissociation threshold a large number of transitions to well characterized

# VIBRATIONAL RELAXATION, ISOMERIZATION, AND DISSOCIATION IN OXIRANE

John H. Kiefer, John DiFelice, John Akufo, and Amal Dib

*Department of Chemical Engineering  
University of Illinois at Chicago  
Chicago, Illinois 60607 U.S.A*

The various sequential processes, vibrational relaxation, isomerization to acetaldehyde, and subsequent dissociation of the acetaldehyde, which are initiated by sudden heating of oxirane in a shock wave, have been observed with the laser-schlieren technique. When the relaxed temperature exceeds about 1000 K in mixtures with rare gases, negative isomerization gradients are seen following the fast positive relaxation gradients. The resolution and clear separation of these two processes allows, for the very first time, the extraction of unimolecular incubation times for an isomerization reaction. At very high temperatures, above 1700 K, relaxation and isomerization are followed by decomposition of the acetaldehyde product. This allows an analysis of the acetaldehyde dissociation during and after isomerization, and offers the opportunity to obtain a more decisive answer to the interesting question of whether the isomerization exothermicity is immediately available for this dissociation, as has been proposed (1,2).

## VIBRATIONAL RELAXATION:

Relaxation can be resolved from 400 to 1000 K in the pure gas, and 932 to 2059 K in mixtures of 4% oxirane in krypton; both sets of experiments show the complex double exponential behavior we find routinely in "large" molecules. In these gases the early gradient rises rapidly to a distinct maximum, followed by exponential decay to the base line. That this behavior is seen in both the pure gas and a dilute rare-gas mixture allows the important conclusion that this complex behavior is not a consequence of rare-gas dilution. The profiles can be closely fit with a simple double-exponential, as  $d(p)/dx = A \exp(-t/\tau_1) - B \exp(-t/\tau_2)$ , either allowing both A and B to vary, or setting A=B, thereby fixing the (unobservable) initial ( $t=0$ ) gradient at zero.

Vibrational relaxation times from the above double-exponential fit have been corrected to Bethe-Teller values using the Blythe procedure (3). The resulting  $P^* \tau$  (atm\*microsec) accurately fit the Landau-Teller form with

$$\log(P^* \tau_1) = 20.68 T^{-(1/3)} - 2.0186$$

$$\log(P^* \tau_2) = 10.381 T^{-(1/3)} - 1.8983$$

in the 4% mixture. For the pure gas we find

## DECOMPOSITION OF ACETALDEHYDE:

When oxirane isomerizes to acetaldehyde at moderately high temperatures, the product acetaldehyde will decompose. To understand and include this process, we have made a comprehensive study of the acetaldehyde decomposition in mixtures of acetaldehyde and krypton (4%  $\text{CH}_3\text{CHO}$  - 96% Kr). A complete mechanism has now been developed which accurately predicts density gradients across the temperature range 1532 to 2027 K. The mechanism also accurately predicts product growth curves for major products obtained as part of a TOF reflected shock study (2).

Although acetaldehyde decomposition has already been studied in shock waves (1,2,4), temperatures were typically lower than 1500 K. In order to study the sequential relaxation of oxirane and isomerization to acetaldehyde, most experiments in this current study were

predissociating states with defined energy E and total angular momentum J above the dissociation threshold were analyzed. Specific rate constants  $k(E, J, \dots)$  and lifetime distributions  $P(k(E, J, \dots))$  have been determined from homogeneous linewidths and compared with results from theoretical calculations and time resolved experiments.

In the case of HOCl many overtones and combination bands have been recorded up to the dissociation limit. Strong and weak Fermi-type resonances, as well as Coriolis interactions at  $\approx 65$ -85% of the dissociation energy  $E_0$  have been analysed in terms of intramolecular vibrational energy redistribution. The  $5\nu_1$  band at about 85% of  $E_0$  has been found to be strongly mixed with the  $4\nu_1 + 2\nu_2 + \nu_3$  zero order vibrational state, and both states are coupled to other background states by additional (weaker) interactions. The extent and the magnitude of perturbations in all  $K_a$  bands of the  $5\nu_1/4\nu_1 + 2\nu_2 + \nu_3$  system and additional interactions with other background states may be regarded as the signature of the onset of efficient but restricted intramolecular vibrational energy redistribution in the overtone spectrum of HOCl. The intramolecular dynamics of this small molecule after coherent short pulse excitation of the  $5\nu_1$  zero order state will be discussed in terms of a simple tiers model.

Experimental densities of states  $\rho(E, J)$ , which are important for statistical unimolecular rate theories, have been determined over large energy ranges and at the dissociation threshold  $E_0$ .

# RANDOMISATION AND ISOMERISATION RATE CONSTANTS FOR ISOCYANOGEN

DeLin Shen and Huw O. Pritchard

Department of Chemistry, York University, Downsview, Ontario,  
Canada M3J 1P3

We have argued recently, as the result of a wide-ranging trajectory study of the isomerisation of  $\text{CH}_3\text{NC} \rightarrow \text{CH}_3\text{CN}$ , that it is not possible to obtain reliable kinetic rate behaviour by the use of piecewise synthetic potential energy surfaces<sup>1</sup>. There is, as yet, no suitable global *ab initio* potential energy surface for this reaction, and so we report here an attempt to calculate the important rate parameters for a simpler reaction, the isomerisation of  $\text{CNCN} \rightarrow \text{NCCN}$ .

The potential energy was calculated at 597 geometries in the CNCN well and around the saddle point connecting CNCN with NCCN, in the frozen-core MP2/6-311G\* approximation. These *ab initio* potential energy values were fitted to an analytic function, according to Murrell's many-body formalism, and trajectory calculations were performed on ensembles of between 300 and 1000 sets of initial configurations at energies in the reactive range by using algorithms similar to those already described<sup>1</sup>. At each of seven values of the energy, two parallel sets of calculations were run: one in which the initial conditions were chosen to have random momenta<sup>2</sup> (flying start), and the other in which all atoms were stationary, and in random positions<sup>3</sup> (standing start). In all cases, the flying-start calculations conformed well to the random-gap law: the logarithm of the number unreacted versus the time was a straight line, and the reciprocal of the slope of this line coincided to better than  $\pm 5\%$  with the average lifetime,  $\tau_2$ , of the ensemble with respect to isomerisation.

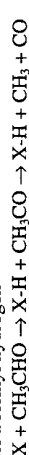
On the other hand, in the standing-start calculations, there were no early isomerisation events, but the frequency of reaction rose to a maximum and then decayed exponentially with the same rate constant as for the flying-start ensemble at the same energy. The simplest explanation of this behaviour is that it takes some time for the motionless atoms to achieve a random set of positions and momenta, after which they decay in the normal random-gap manner. A simple adaptation of the usual integrated rate expression for a pair of consecutive reactions



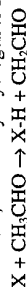
readily yields  $k_1$  if  $k_2 = 1/\tau_2$  is known.

The randomisation rate increases rapidly with increasing energy, roughly in proportion to the density of vibrational states: from reaction threshold ( $\sim 14,000 \text{ cm}^{-1}$  above the zero point) up to  $\sim 35,000 \text{ cm}^{-1}$ , the randomisation lifetime,  $\tau_1 = 1/k_1$ , falls from about 10 ps to about 0.1 ps, whereas the density of vibrational states rises from  $\sim 10^3$  to  $\sim 10^5$  states per wavenumber. The product of  $\tau_1$  in ps with  $\rho(E)$  in states per  $\text{cm}^{-1}$  is roughly  $10^4$  at all energies. This is analogous to the Fermi 'golden rule' normally applied to continuum state mixing.

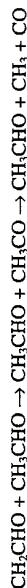
performed at 1500 K or above. At such high temperatures, competing reactions which may be safely ignored at lower temperatures must be recognized. Among such reactions are the abstractions of methyl hydrogens from the parent to form vinyloxy radicals ( $\text{CH}_2\text{CHO}$ ). When hydrogen atoms or methyl radicals ( $\text{CH}_3$ ) react with acetaldehyde molecules, the radicals may abstract either a formyl hydrogen



which propagates the chain, or a methyl hydrogen to form  $\text{CH}_2\text{CHO}$



Once formed,  $\text{CH}_2\text{CHO}$  will either dissociate to form ketene or isomerize to  $\text{CH}_3\text{CO}$ . The acetaldehyde mechanism is very sensitive to the fate of  $\text{CH}_2\text{CHO}$ . Overprediction of ketene formation will result in too much endothermicity, and consistently observed late negative density gradients will not be accurately predicted. Density gradients obtained in this study suggest a vinyloxy radical with sufficiently long lifetime to attack the parent, continuing the chain as



Density gradients were extrapolated to time zero using the derived mechanism, and second order rate constants for the initial dissociation of acetaldehyde



were calculated. These rate constants were then fit with a Gorin RRKM formulation using  $E_0 = 83.0 \text{ kcal/mol}$ ,  $\eta = 0.015$ , and  $\langle \Delta E \rangle_s = 600 \text{ cm}^{-1}$

to give the following second order rate constant valid for 175 torr and 1500 to 2100 K:

$$\log k(\text{cm}^3/\text{mol}\cdot\text{s}) = 74.614 - 15.735 \log T - 111.157 \text{ kcal/mol} / (2.3RT)$$

## ISOMERIZATION AND INCUBATION IN OXIRANE:

When temperatures exceed about 1500 K in 2% mixtures of oxirane and krypton, strong negative density gradients from the exothermic isomerization to acetaldehyde are observed. However, these are preceded by clearly resolved, but sharply defined, positive gradients arising from vibrational relaxation of the oxirane. During this relaxation the isomerization rate must be very slow, in fact it obviously turns on just about where the gradient crosses from positive to negative. This is unimolecular incubation, and the time to zero crossing is a quite unambiguous measure of the incubation time. Experiments on oxirane isomerization were performed over 1535 to 2395 K and pressures covering 145 to 476 torr. Over the range 1535 to 1843 K, incubation times could be reliably determined. At higher temperatures they are too short for accuracy. The results, expressed in the usual ratio to relaxation time, are

$$(P^*\tau)/(P^*\tau_0) = 4645.0/T - 1.0688 \quad (+/- 20\%)$$

These are lower than those obtained in a previous study of incubation in norbornene dissociation (5). Isomerization rates have also been determined, but are complicated by the following decomposition of the acetaldehyde. The complete coupled mechanism is still under development.

## REFERENCES:

- 1) A. Lifshitz and H. Ben-Hamou, *J. Phys. Chem.*, **87**, 1782 (1983).
- 2) R.D. Kern, H.J. Singh, and K. Xie, *Proceedings of the 17th International Symposium on Shock Waves and Shock Tubes*, p.487 (1990).
- 3) P.A. Blythe, *J. Fluid Mech.*, **10**, 33 (1961).
- 4) J. Ernst, K. Spindler, and H.G. Wagner, *Ber. Bunsenges. Phys. Chem.*, **80**, p.645 (1976).
- 5) J.H. Kiefer, S.S. Kumaran, and S. Sundaram, *J. Chem. Phys.*, **99**(5), p. 3531 (1993).

At these energies, all indications are that reaction takes place from a chaotic manifold of states, and so correction for zero-point energy pooling is readily made by statistical considerations. Thus, after allowance for the exclusion of zero-point energy pooling, the isomerisation rate is approximately one-third of the transition state rate calculated with the same potential energy parameters, over the temperature range 400-600K.

#### Acknowledgement

This work was supported by the Natural Sciences and Engineering Research Council of Canada.

#### References

- [1 ] D. Shen and H. O. Pritchard, J. Chem. Soc., Faraday Trans., 1996, 92, 1297.
- [2 ] D. L. Bunker and W. L. Hase, J. Chem. Phys., 1973, 59, 4621.
- [3 ] D. Shen, W.-T. Chan and H. O. Pritchard, J. Chem. Soc., Faraday Trans., 1995, 91, 3747.

## KINETICS, ENERGETICS, AND MECHANISM OF THE UNIMOLECULAR H<sub>2</sub> ELIMINATION FROM ETHANE RADICAL CATIONS

J. Mähnert, F. Güthe, and K.-M. Weitzel

*Institut für Physikalische und Theoretische Chemie, Freie Universität Berlin,  
Takustr. 3, 14195 Berlin, Germany*

At first glance the H<sub>2</sub> elimination from Ethane radical cations is a simple fragmentation reaction which has been extensively studied and thus seems to offer little surprising news. However, so far there was a subtle discrepancy between a relatively small dissociation energy of  $E_0 = 0.572$  eV [1], and the observation of a metastable decay (see e.g. [2]) of the Ethane cation.

We have reinvestigated the H<sub>2</sub> elimination from Ethane radical cations by means of advanced experimental and theoretical methods in order to shed some new light on the kinetics, the energetics, and the mechanism of this reaction. In ZEKEPEPICO experiments [3] on energy selected ions we have measured the breakdown curves of the title reaction [4] at room temperature and at close to 0 K. These data - shown in fig. 1 - indicated that the dissociation energy  $E_0(J)$  is essentially independent of the rotational angular momentum  $J$  of the molecules. This hints at a concerted elimination characterized by a tight transition state.

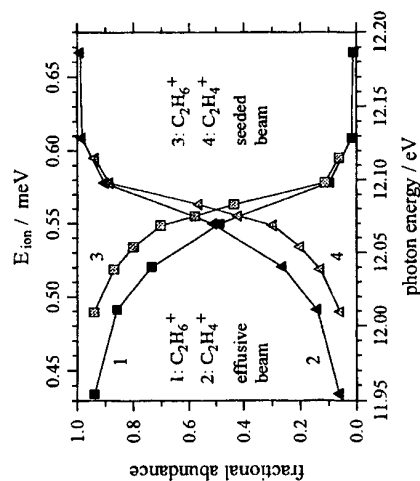


Fig. 1. ZEKE - PEPICO breakdown curves of ethane [4].

In ab initio calculations [5] we have found a complete reaction path leading from the molecular ion to the products. According to these calculations the reaction should proceed by tunneling of H atoms through a barrier for H transfer. Tunneling RRKM calculations on this ab initio potential energy surface predicted a significant kinetic shift in this reaction. The energy dependence of the rate constant  $k(E)$  was so steep that the observation of a metastable reaction should be limited to a very small range of internal energy of the ion. In a recent experiment we have been able to confirm this prediction [6] by measuring the TPEPICOTOF mass spectra at various excitation energies (fig. 2). The rate constant  $k(E)$  of the reaction as determined from the asymmetric TOF profiles increases by two orders of magnitude within 25 meV of ion internal energy. The analysis shows that the reaction proceeds by tunneling of H-Atoms through a barrier with an effective height of  $0.86 \pm 0.05$  eV and an imaginary frequency of  $500 \pm 50$  cm<sup>-1</sup>. By combination of experimental and theoretical investigations we have thus arrived at a fairly advanced picture of the kinetics, the energetics, and the mechanism of this reaction. The final confirmation of the tunneling mechanism can be expected from additional experiments on deuterated Ethane (C<sub>2</sub>D<sub>6</sub>) which are currently in progress.

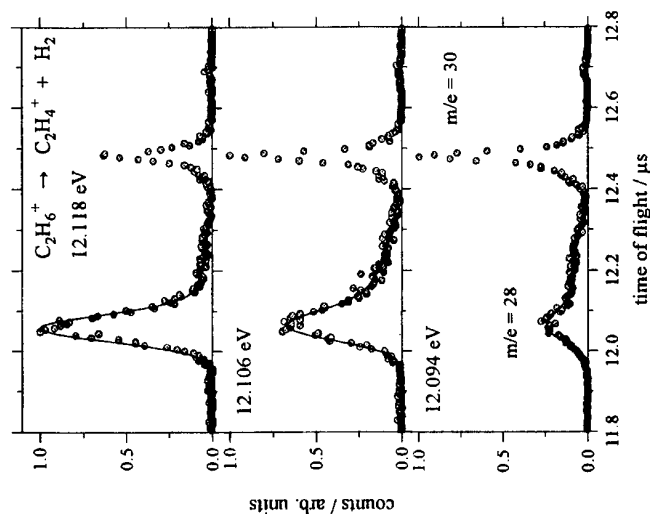


Fig. 2. Experimental and simulated TPEPICO - TOF spectra of ethane.

#### References:

- (1) K.-M. Weitzel, J. Mähner, and H. Baumgärtel, Ber. Bunsenges. Phys. Chem., **97**, 134, (1993)
- (2) J.A. Hipple, R.E. Fox, and E.U. Condon, Phys. Rev., **69**, 347, (1946)
- (3) K.-M. Weitzel, J. Mähner, and M. Penno, Chem. Phys. Lett. **224**, 371, (1994)
- (4) J. Mähner, F. Güthe, and K.-M. Weitzel, Ber. Bunsenges. Phys. Chem., in press
- (5) K.-M. Weitzel, Int. J. Mass Spectrom Ion Proc., **136**, 1, (1994)
- (6) K.-M. Weitzel, and J. Mähner, Z. Phys. Chem., in press

# COLLISIONAL ENERGY TRANSFER: HOW DOES THE ENERGY LEAVE AN EXCITED MOLECULE?

G. Lendvay

*Central Research Institute for Chemistry, Hungarian Academy of Sciences  
H-1525 Budapest, P. O. Box 17, Hungary*

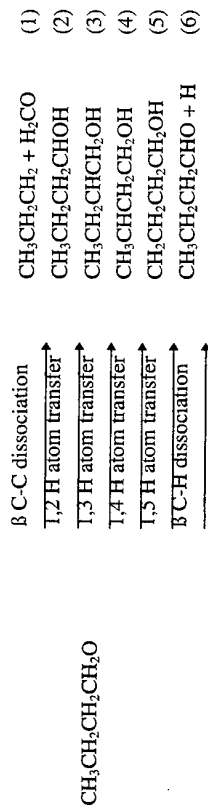
According to the prevailing picture of collisional energy transfer of vibrationally highly excited polyatomic molecules, the active mode through which energy leaves the molecule is a low-frequency bending mode. We performed classical trajectory calculations in which the frequencies of the internal modes of the excited molecule were systematically varied with the purpose of the identification of the active mode. We calculated the average energy transferred per collision as a function of the excitation energy, and the energy transfer probability matrices in some specific cases. The model molecules are CS<sub>2</sub> and CH<sub>4</sub>. We found that decreasing the frequency of a mode generally increases the efficiency of the energy transfer even if the mode is not a bending mode. The transfer of vibrational and rotational energy proves to be coupled, and the degree of coupling depends on the vibrational frequencies. The emerging picture of the mechanism of the energy transfer will be discussed.

# COMPETITIVE UNIMOLECULAR REACTIONS OF THE BUTOXY RADICAL

Béla Viskolcz

*Institute für Physikalische Chemie der Universität Halle-Wittenberg  
FB Chemie Merseburg, Geb. 123; 06099 Halle, Germany*

The butoxy radical (the simplest alkoxy radical that can undergo isomerization via a six-membered transition state) is a prototype of the key intermediates in the photooxidations of most organic compounds in the troposphere. The following unimolecular reactions of the butoxy radical were studied by ab initio methods:



The equilibrium geometries and the transition structures have been optimized at the MP2/6-31G\* level. The stationary points were characterized by calculation of the harmonic vibrational frequencies (MP2/6-31G\* level). The best activation energies at 0 K (19.53, 25.40, 25.10, 17.20, 8.43, 22.94 kcal mol<sup>-1</sup> for reaction 1-6, respectively) were calculated with the MPSAC2/6-311G\*\* method. The barrier heights are in good agreement with experimental values.

The specific rate constants of all individual channels were calculated by the RRKM method based on ab initio molecular orbital calculations (see Fig. below). The results show that in general the 1,5 H-atom transfer is the fastest unimolecular reaction.

Furthermore, the rate of the 1,4 H atom transfer can have the same magnitude as the rate of the β-bond dissociations. The consequences of the calculated barrier heights on the overall kinetics will be discussed.

# KINETIC STUDY OF THE $\text{Sr} + \text{O}_2 + \text{He}$ -REACTION IN THE TEMPERATURE RANGE FROM 303 TO 968 K.

C. Vinckier and J. Helaers

Department of Chemistry, K. U. Leuven  
Celestijnenlaan 200F  
B 3001 Heverlee

A kinetic study of the  $\text{Sr} + \text{O}_2 + \text{He}$ -association reaction (1) was carried out in the temperature range between 303 and 968 K using the fast-flow reactor technique:



Strontium atoms were thermally generated in the gas phase through the vaporisation of strontium metal pellets. The experimental procedure consists of following the strontium atom decay in the presence of molecular oxygen. Atomic absorption spectroscopy at 460.7 nm was used as detection technique.

Since the bimolecular reaction to form  $\text{SrO} + \text{O}$  is endothermic for  $71.6 \text{ kJ mole}^{-1}$  (1) one expects a third-order reaction, which has been clearly established at 303 and 600 K. By varying the total pressure between 6 and 12 Torr, a linear relationship was observed at each temperature between the pseudo second-order rate constant of reaction (1) and the total reactor pressure.

It was also checked that the initial Sr-atom concentration had no systematic effect on the rate constant derived. This could be realised by varying the temperature of the Sr-pellets while keeping the reaction temperature constant.

The temperature dependence of reaction (1) has also been established in the temperature region between 303 and 968 K. The Arrhenius expression is given by equation (2):

$$k_1(T) = 7.2 \pm 0.4 \cdot 10^{-29} \exp \left( \frac{-5.4 \pm 0.3 \text{ kJ/mol}}{RT} \right) \text{ cm}^3 \text{ molecule}^{-2} \text{ s}^{-1} \quad (2)$$

One sees that the  $\text{Sr} + \text{O}_2 + \text{He}$ -association reaction shows an activation energy of  $5.4 \text{ kJ mole}^{-1}$ . This rather unusual kinetic behaviour, considering the third-order character of reaction (1) has also been observed for the analogous Mg- and Ca-atom reactions. Here activation energies of respectively 16.8 and  $10.1 \text{ kJ mole}^{-1}$  have been found (2,3). An explanation might be sought in the closed shell configuration of the alkaline earth

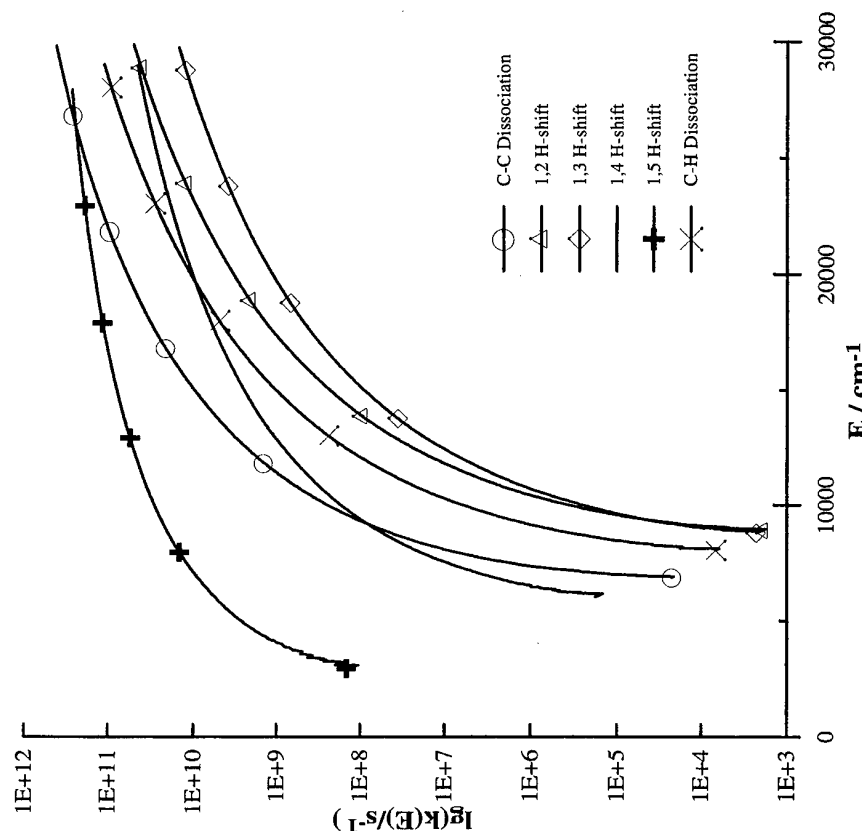


Fig.1 The specific rate constants of unimolecular reactions of butoxy radical.

# DECOMPOSITION OF VIBRATIONALLY EXCITED $C_3H_8$ FORMED BY ASSOCIATION REACTIONS OF H ATOMS WITH $1-C_3H_7$ , $2-C_3H_7$ , AND $C_3H_6$

by K. Scherzer, T. Meinike, J. Triebert, L. Engelmann, and M. Olzmann

*Martin-Luther-Universität Halle-Wittenberg, Standort Merseburg  
Institut für Physikalische Chemie, 06099 Halle, Germany*

We have studied the decomposition of vibrationally excited propane. It is formed by the association of propyl radicals with H atoms. The former are generated, on the one hand, by addition of H atoms to propylene or, on the other hand, via halogen abstraction from halocarbons by H atoms. In this way, the propane molecules formed carry different amounts of internal energy. The investigations were performed at room temperature in a conventional discharge flow tube system with molecular beam sampling and a quadrupole mass-spectrometer. A detailed description is given in [1]. The main products were methane, ethane, propylene, and propane accompanied by smaller amounts of ethylene, butene, and butane. Mass spectra with and without H atoms in the system were employed to obtain product concentrations in the reaction mixture by means of calibration curves. A correction is made to account for overlapping fragmentation patterns of the different hydrocarbons.

For an adequate representation of the reaction systems, up to 28 reactions had to be included in the kinetic modelling procedure. The numerical integration was performed with the LARKIN package [2]. In general, a good agreement between our models and the experimental results was obtained. Figure 1 shows the data points and calculated concentration profiles for the reaction of propylene with H atoms for a typical run.

metals leading to an energy barrier when the metal atom and oxygen are approaching one another on a covalent potential energy surface, leading to the formation of the  $SrO_2$  molecule. In view of the at least partly ionic character of  $SrO_2$  a qualitative relationship can be expected between the height of the barrier and the ionisation energy of the atom: 7.64, 6.11 and 5.69 eV for respectively  $Mg^+$ ,  $Ca^+$  and  $Sr^+$ -atoms. A simplified RRKM calculation based on the Troë-formalism(4) was performed to estimate the bond strength of the  $SrO_2$  molecule. Using the  $^3A_2$ -state of  $SrO_2$  and taking into account a barrier height of  $5.4 \text{ kJ mole}^{-1}$ , bond energies in the range between 285 and  $420 \text{ kJ mole}^{-1}$  were estimated in the temperature range between 303 and 968 K. In how far these calculations are correct remains a matter of debate in view of the uncertainties of the molecular properties of the  $MeO_2$  molecule considered. Based on ab initio calculations a value of  $D_e$  ( $SrO_2$ ) of  $224.6 \text{ kJ mole}^{-1}$  has been derived(5). When a comparison is made between the experimental and theoretical values of  $MeO_2$ -bond energies, one sees that the calculated values are much lower in most cases(2). An explanation for this trend is not available.

The only alkaline earth superoxide bond energy which has been experimentally determined is  $BaO_2$ . In a crossed molecular beam study a value of  $500 \pm 80 \text{ kJ mole}^{-1}$  has been determined(6) so that our estimated range for  $SrO_2$  between 285 and  $420 \text{ kJ mole}^{-1}$  is not that unreasonable.

## References

- (1) H.F. Sullivan, I. Glassman, Combust. Sci. Technol., 4, 241, 1972.
- (2) Plane, "Gas Phase Metal Reactions", A. Fontijn Ed., Elsevier Amsterdam, p29, 1992.
- (3) C. Vinckier, J. Remeysen, J. Phys. Chem., 98, 10535, 1994.
- (4) J. Troë, J. Phys. Chem., 83, 114, 1979.
- (5) C.W. Bauschlicher, H. Partridge, M. Sodupe, S.R. Langhoff, J. Phys. Chem., 96, 9259, 1992.
- (6) H.F. Davis, A.G. Suits, H. Hou, Y.T. Lee, Ber. Bunsenges. Phys. Chem., 94, 1193, 1990.

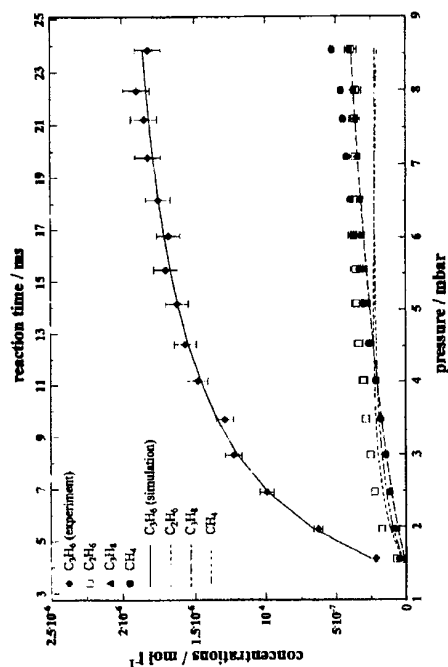


Fig. 1: Concentration-time / pressure profiles for  $\text{H} + \text{C}_3\text{H}_6$ .

Our special interest was the dependence of the ratio  $D / S$  (decomposition / stabilization) of the excited propane on the pressure. For the determination of the  $D / S$  values we used the relation

$$\frac{D}{S} = \frac{[\text{C}_3\text{H}_6]_0 - [\text{C}_3\text{H}_6] - [\text{C}_3\text{H}_8]_s - [\text{C}_4\text{H}_8] - [\text{C}_4\text{H}_{10}]}{[\text{C}_3\text{H}_8]_s}$$

with the initial concentration of propylene  $[\text{C}_3\text{H}_6]_0$ , the actual concentration  $[\text{C}_3\text{H}_6]$  and the stabilized amount of propane  $[\text{C}_3\text{H}_8]_s$ . The latter was separated from the propane produced in the reaction  $\text{CH}_3 + \text{C}_2\text{H}_5$  by using the informations from the modelling procedure.

In Figure 2 calculated and experimental values of  $D / S$  are compared.

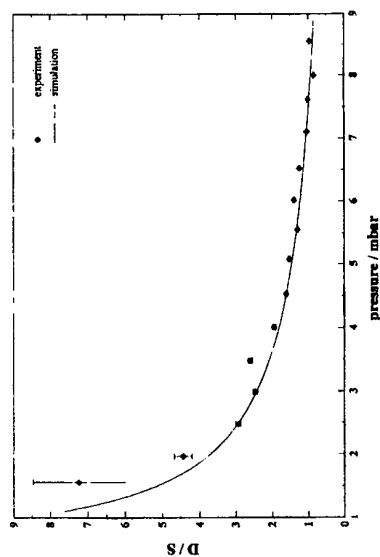


Fig. 2:  $D / S$  in the system  $\text{H} + \text{C}_3\text{H}_6$ .

Between the two addition steps of  $\text{H}$  atoms to propylene and to the propyl radical, respectively, collisional deactivation of the radical occurs. To study these problems, we performed the additional experiments with thermalized propyl radicals, using the propyl bromides as precursors. Compared to  $\text{H} + \text{C}_3\text{H}_6$ , these systems are more complicated, because additional channels for the propane formation are involved.

We will discuss these complications and present a master equation analysis for the propylene system to derive the parameters of the unimolecular decomposition of  $\text{C}_3\text{H}_8$ .

## References

- (1) J. Triebert, T. Meinke, M. Olzmann, and K. Scherzer, *Z. Phys. Chem.*, **191**, 47-57 (1995).
- (2) P. Deuflhard, G. Bader, and U. Nowak, in *Modelling of Chemical Reaction Systems*, Springer Series in Chemical Physics 18, Springer-Verlag, Berlin 1981, p. 38.

# REACTION OF TRIFLUOROMETHYL RADICAL WITH NITRIC DIOXIDE: KINETICS AND MECHANISM

A B Vakhtin

*Institute of Chemical Kinetics and Combustion, Novosibirsk 630090, Russia.*

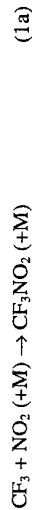
The kinetics of the  $\text{CF}_3 + \text{NO}_2$  reaction was studied at room temperature within the range of total pressure 300-600 Torr. Mixtures containing  $\text{CF}_3\text{NO}$ ,  $\text{NO}$ ,  $\text{NO}_2$ , and helium were irradiated by a pulsed ruby laser ( $\lambda = 694.3 \text{ nm}$ ). The  $\text{CF}_3$  radicals arising in the photodissociation of  $\text{CF}_3\text{NO}$  were involved into competitive pseudo-first-order reactions with  $\text{NO}$  and  $\text{NO}_2$ . The concentration of  $\text{CF}_3\text{NO}$  after the photolyzing pulse was monitored in real time by intracavity absorption of cw He-Ne laser radiation ( $\lambda = 632.8 \text{ nm}$ ) [1]. Measuring the relative amplitudes of the kinetic curves of  $\text{CF}_3\text{NO}$  formation, obtained at different  $[\text{NO}]_0/[\text{NO}_2]_0$  ratios allowed us to obtain the following rate constant for  $\text{CF}_3$  removal by  $\text{NO}_2$ :

$$k_1 = (3.2 \pm 0.7) \times 10^{-11} \text{ cm}^3/\text{s}$$

(the rate constant of the reaction  $\text{CF}_3 + \text{NO} \rightarrow \text{CF}_3\text{NO}$ , measured earlier [1], was used as reference).

This value of  $k_1$  is in reasonable agreement with the values reported by Sugawara et al. [2] ( $2.5 \times 10^{-11} \text{ cm}^3/\text{s}$ ), Francisco and Li [3] ( $2.5 \times 10^{-11} \text{ cm}^3/\text{s}$ ), and Bevilacqua et al. [4] ( $1 \times 10^{-11} \text{ cm}^3/\text{s}$ ) and differs significantly from that obtained by Rossi et al. [5] ( $2.7 \times 10^{-12} \text{ cm}^3/\text{s}$ ).

Analysis of end products has shown that the main carbon-containing products of the  $\text{CF}_3 + \text{NO}_2$  reaction are  $\text{CF}_3\text{NO}_2$  (about 35% of the total product yield) and  $\text{CF}_2\text{O}$  (balance). The product yields differ substantially from those reported in other works [2-5], where no comparable amounts of  $\text{CF}_3\text{NO}_2$  were observed. The results obtained strongly support the mechanism involving association as the primary stage of the reaction:



## Acknowledgement

This work was financially supported by Russian Foundation for Fundamental Research, grant No. 93-03-05018

## References

- (1) A.B. Vakhtin and A.K. Petrov, *Chem. Phys.* **149** (1991) 427.
- (2) K. Sugawara, T. Nakanaga, H. Takeo, and C. Matsumura, *J. Phys. Chem.* **93** (1989) 1894.
- (3) J.S. Francisco and Z. Li, *Chem. Phys. Letters* **162** (1989) 528.
- (4) T.J. Bevilacqua, D.R. Hanson, and C.J. Howard, *J. Phys. Chem.*, **97** (1993) 3750.
- (5) M.J. Rossi, J.R. Barker, and D.M. Golden, *J. Chem. Phys.* **71** (1979) 3722.

# KINETICS AND MECHANISM OF THE REACTION BETWEEN CF<sub>3</sub> AND NO<sub>2</sub>

Emil Ratajczak<sup>a</sup>, Jerzy T. Jodkowski<sup>a</sup>,  
Palle Pagsberg<sup>b</sup> and Alfred Sillesen<sup>b</sup>

<sup>a</sup>*Department of Physical Chemistry, Wrocław University of Medicine,  
Pl. Nankiera 1, 50-140 Wrocław, Poland*

<sup>b</sup>*Environmental Science and Technology Department,  
Risø National Laboratory, DK-4000 Roskilde Denmark*

The reaction of CF<sub>3</sub> radicals with NO<sub>2</sub> was studied in the pressure range 4–88 mbar at 298 K. The reaction was initiated by pulse radiolysis of Ar/CF<sub>3</sub>/NO<sub>2</sub> gas mixture, and both the decay rates of CF<sub>3</sub> radicals as well as the formation rates of CF<sub>2</sub>O and FNO were studied by using time-resolved infrared diode laser spectroscopy. The experimental technique has been described in detail previously [1]. The value of bimolecular rate constant,  $k = (1.5 \pm 0.2) \times 10^{-11} \text{ cm}^3 \text{ molec}^{-1} \text{ s}^{-1}$  obtained from CF<sub>3</sub> decay kinetics monitored, under pseudo-first-order conditions with excess of NO<sub>2</sub>, at 1263.1 cm<sup>-1</sup> and 1266.9 cm<sup>-1</sup>, was found to be pressure independent. The CF<sub>2</sub>O formation kinetics was monitored at 1231.0 cm<sup>-1</sup> and 1263.0 cm<sup>-1</sup> while that of FNO at 1857.2 cm<sup>-1</sup>. The second-order rate constants of the formation both CF<sub>2</sub>O and FNO were found to increase with increasing a total pressure approaching the value of  $1.5 \times 10^{-11} \text{ cm}^3 \text{ molec}^{-1} \text{ s}^{-1}$  at high pressure (see Fig. 1). A comparison of CF<sub>3</sub>+NO<sub>2</sub> rate constant with earlier results at room temperature is shown in Table 1. The experimental findings, in agreement with previous studies [3,4], suggest that the direct formation of CF<sub>2</sub>O and FNO in their vibrational ground states is a main reaction route.

**Table 1.** Comparison of the rate constant for the reaction of CF<sub>3</sub> with NO<sub>2</sub> at room temperature.

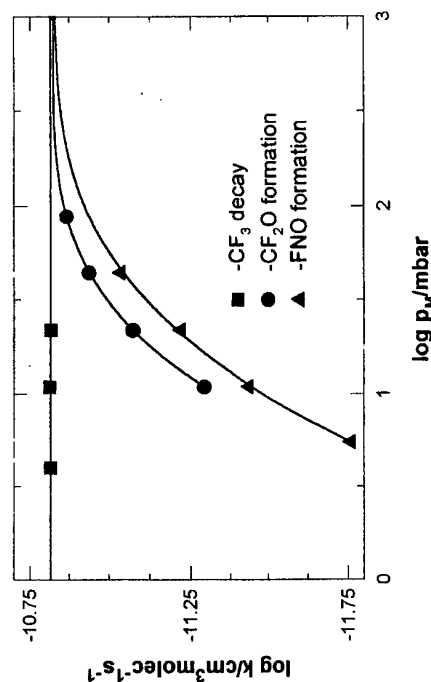
$10^{11} \times k/\text{cm}^3 \text{ molec}^{-1} \text{ s}^{-1}$	Method	References
0.27±0.05	VLPΦ/MS	(2)
2.5±0.3	IRMD/Laser diode absorption	(3)
2.5±0.4	IRMD/Chemiluminescence	(4)
1.5±0.15	PR/Laser diode absorption	this study

Ab initio molecular orbital theory at the MP2/6-31 G(d) and G2 levels has been used in order to examine the energetics of possible reaction paths. All geometries of reactants and products were fully optimized at MP2/G-31G(d) level. The calculated enthalpy -64.5 kcal/mol for the reaction CF<sub>3</sub> + NO<sub>2</sub> → CF<sub>2</sub>O + FNO is in good agreement with that of -64.9 kcal/mol obtained from NASA data [5]. Table 2 shows

calculated enthalpy of formation for some fluorinated reagents. Using the maximum free energy method [6], the values of the high-pressure limiting rate constants of  $1.2 \times 10^{-11}$  and  $2.0 \times 10^{-11} \text{ cm}^3 \text{ molec}^{-1} \text{ s}^{-1}$  were found for other possible reaction paths CF<sub>3</sub> + NO<sub>2</sub> → CF<sub>3</sub>NO<sub>2</sub> and CF<sub>3</sub> + NO<sub>2</sub> → CF<sub>3</sub>ONO.

**Table 2.** Enthalpy of formation

Reagents	Calc. kcal/mol	Exp. [from (5)] kcal/mol
CF <sub>3</sub>	-115.4	-112±1
CF <sub>3</sub> O	-156.6	-157±2
CF <sub>2</sub> O	-150.4	-153±2
CF <sub>3</sub> NO <sub>2</sub>	-167.5	
CF <sub>3</sub> ONO	-182.8	



**Fig. 1.** The CF<sub>3</sub> radical decay kinetics as well as the variation of the constant for the formation of CF<sub>2</sub>O and FNO products.

## References

- (1) P. Pagsberg, E. Ratajczak and A. Sillesen, in: Research in chemical kinetics, Vol. 1, eds. R.G. Compton and G. Hancock (Elsevier, Amsterdam, 1993) p.65.
- (2) M.J. Rossi, J.R. Barker and D.M. Golden, J. Chem. Phys., 71 (1979) 3722.
- (3) K. Sugawara, T. Nakanaga, H. Takeo and C. Matsumura, J. Phys. Chem., 93 (1989) 1894.
- (4) J.S. Francisco and Z. Li, Chem. Phys. Lett., 162 (1989) 528.
- (5) W.B. DeMore, S.P. Sander, D.M. Golden, R.F. Hampson, M.J. Kurylo, C.J. Howard, A.R. Ravishankara, C.E. Kolb and M.J. Molina, Chemical kinetics and photochemical data for use in stratospheric modelling, Evaluation No. 11, JPL Publication 94-26 (1994) 1.
- (6) M. Quack and J. Troe, Ber. Bunsenges. Physik. Chem. 81 (1977) 329.

# THE USE OF MONTE CARLO SIMULATIONS TO EVALUATE KINETIC DATA AND ANALYTIC APPROXIMATIONS

Jan P. Hessler

*Chemistry Division, Argonne National Laboratory  
9700 So. Cass Ave., Argonne, Illinois 60439 U.S.A.*

Experimentalists are always faced with the problem of reducing data to extract physically meaningful information. A particularly vexing problem arises when different models reproduce the data but yield different values for the physical parameters. For over thirty years Monte Carlo simulation techniques have been used to study the statistical behavior of parameters extracted from data. Not only do these simulations provide realistic uncertainties and confidence envelopes of the fit, but they also provide insight into the nature of the model. These insights may be obtained by viewing two-dimensional scatter plots of the fractional changes of the parameters. We will illustrate this approach with examples from  $\text{H} + \text{O}_2 \rightarrow \text{OH} + \text{O}$  and high-pressure rate coefficients. A more complex problem involves models for pressure-dependent rate coefficients in the falloff region. We have modelled methyl-methyl and methyl-hydrogen recombination with five of the most current analytic approximations. All of these reproduce the data to within their uncertainties. However, when Monte Carlo simulation techniques are applied the correlations between the parameters and the nonlinear nature of their behavior become evident. We postulate that the statistical behavior of the parameters of a model may be used to distinguish one model from one another and, thereby, identify those analytic approximations with hold promise for further investigation and utilization.

# EXPERIMENTAL AND THEORETICAL STUDY OF THE $\text{C}_2\text{H}_3 \leftrightarrow \text{H} + \text{C}_2\text{H}_2$ REACTION.

## TUNNELLING AND THE SHAPE OF FALLOFF CURVES.

Vadim D. Knyazev and Irene R. Slagle

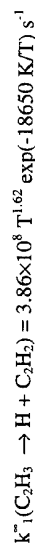
*Department of Chemistry, The Catholic University of America, Washington, DC  
20064, USA*

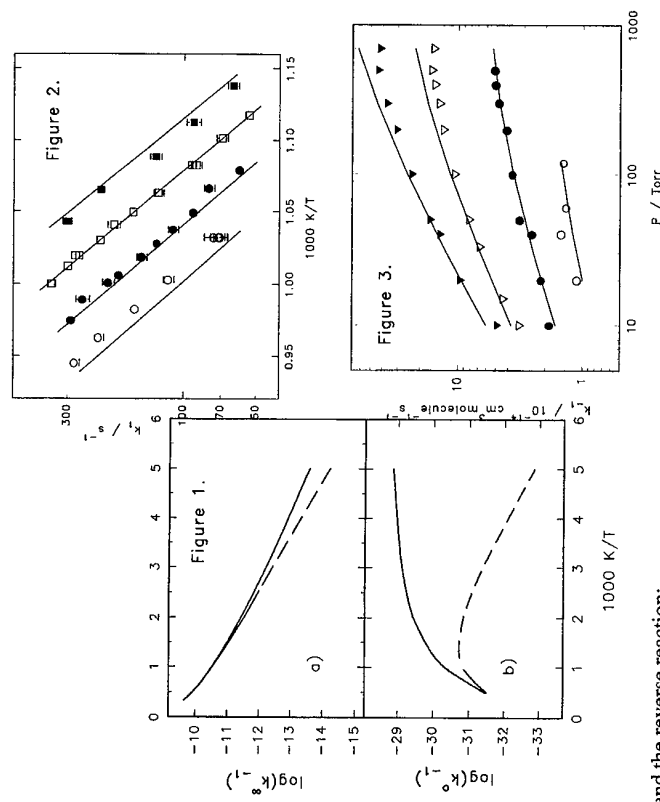
The unimolecular decomposition of the  $\text{C}_2\text{H}_3$  radical was isolated for quantitative study using a heated tubular flow reactor coupled to a photoionization mass spectrometer. Rate constants for the decomposition were determined in time-resolved experiments as a function of temperature (879 - 1058 K) and bath gas density  $((6 - 48) \times 10^{16} \text{ molecule cm}^{-3})$  in He, Ar, and  $\text{N}_2$ . The rate constants are close to the low-pressure limit under the conditions of the experiments.

The potential energy surface and properties of the transition state were studied by ab initio methods. Experimental results of the current and earlier studies of both the direct and reverse reactions were analyzed and used to create a transition state model of the reaction. Fall-off behavior was reproduced using Master Equation modeling with parameters obtained from optimization of the agreement between experimental and calculated rate constants.

The effects of tunneling on the shape of falloff and the values of the low-pressure-limit rate constants were investigated. It was demonstrated that these effects (e.g., Figure 1) exceed those for the high-pressure-limit rate constants by orders of magnitude and cannot be neglected.

The resulting model of the reaction provides the high-pressure limit rate constants for the decomposition reaction:





and the reverse reaction:

$$k_{-1}^{\text{exp}}(\text{H} + \text{C}_2\text{H}_2 \rightarrow \text{C}_2\text{H}_3) = 6.05 \times 10^{-14} T^{1.09} \exp(-1328 K/T) \text{ cm}^3 \text{ molecule}^{-1} \text{ s}^{-1}$$

Among several models of temperature dependence of the collisional energy transfer parameters, the best agreement between the experimental and calculated rate constants (Figures 2 and 3) was achieved with  $\langle \Delta E \rangle_{\text{all}}$  independent of temperature ( $\langle \Delta E \rangle_{\text{all}} = \text{constant}$ ). Values of  $\langle \Delta E \rangle_{\text{all}} = -74 \text{ cm}^{-1}$  (He),  $-115 \text{ cm}^{-1}$  (Ar), and  $-117 \text{ cm}^{-1}$  ( $\text{N}_2$ ) for the average energy loss per collision were obtained using an exponential-down model.

Figure 1. Temperature dependence of (a)  $k_1$  ( $\text{cm}^3 \text{ molecule}^{-1} \text{ s}^{-1}$ ) and (b)  $k_1$  ( $\text{cm}^6 \text{ molecule}^{-2} \text{ s}^{-1}$ ) with (solid lines) and without (dashed lines) accounting for tunneling. The low-pressure effects of tunneling significantly exceed the high-pressure ones. While the high-pressure effects become negligible at temperatures significantly above room temperature, the low-pressure effects remain significant up to 1500 K.

Figure 2. Plot of  $\text{C}_2\text{H}_3$  unimolecular decomposition rate constants ( $k_1$  vs.  $1000/T$ ) for different He densities ( $\text{atom cm}^{-3}$ ). Open circles:  $[\text{He}] = 6 \times 10^{16} \text{ atom cm}^{-3}$ , closed circles:  $[\text{He}] = 12 \times 10^{16} \text{ atom cm}^{-3}$ , open squares:  $[\text{He}] = 24 \times 10^{16} \text{ atom cm}^{-3}$ , closed squares:  $[\text{He}] = 48 \times 10^{16} \text{ atom cm}^{-3}$ . Solid lines represent the results of Master Equation simulation using our best model with  $\langle \Delta E \rangle_{\text{all}} = -74 \text{ cm}^{-1}$ .

Figure 3. Plot of experimental (symbols, Payne, W. A.; Stief, L. J. *J. Chem. Phys.*, **1976**, *64*, 1150) and calculated (lines, current study) rate constants of reaction -1 at different temperatures. Data of Payne and Stief: open circles - 193 K, closed circles - 228 K, open triangles - 298 K, closed triangles - 400 K. Line: master equation fit obtained for the temperatures of experiments using our best model with  $\langle \Delta E \rangle_{\text{all}} = -74 \text{ cm}^{-1}$ .

# PRODUCT BRANCHING-RATIOS IN THE DECOMPOSITION OF THE ETHYL OXY RADICAL

K. Hoyermann<sup>a</sup>, M. Olzmann<sup>b</sup>, J. Seeba<sup>a</sup>, and B. Viskolcz<sup>b</sup>

<sup>a</sup>*Institut für Physikalische Chemie der Universität Göttingen,  
Tammannstr. 6, D-37077 Göttingen, Germany*

<sup>b</sup>*Institut für Physikalische Chemie der Universität Halle-Wittenberg,  
FB Chemie Merseburg, D-06099 Halle, Germany*

The reactions of C<sub>2</sub>H<sub>5</sub> with O, O<sub>3</sub>, NO<sub>3</sub>, and NO<sub>2</sub>, respectively, have been investigated in a discharge flow-reactor at room temperature and pressures between 0.5 and 5 mbar. Reaction products were detected by mass spectrometry with either REMPI or electron-impact ionisation. The observed product pattern is explained in terms of the decomposition of an intermediately formed, chemically activated (indicated by \*), ethyl oxy radical via the reactions



Branching ratios between reactions 1 and 2 were determined, and, additionally, a channel, leading to C<sub>2</sub>H<sub>4</sub> + OH was observed for the oxidants O and O<sub>3</sub>.

The specific rate constants for reactions 1-4 were calculated by RRKM theory based on *ab initio* results (MP2/6-311+G\*\*/MP2/6-31G\*\*) for the potential-energy surface of C<sub>2</sub>H<sub>5</sub>O. By averaging over the molecular distribution functions of C<sub>2</sub>H<sub>5</sub>O\*, according to the different formation reactions, theoretical values for the branching ratios are obtained. As can be seen from Table 1, a reasonable agreement between the measured and the calculated values is achieved, a fact that strongly supports the assumption of an intermediate ethyl oxy radical in the reactions of C<sub>2</sub>H<sub>5</sub> with the above oxidants.

Table 1. Measured and calculated relative branching fractions.

	C <sub>2</sub> H <sub>5</sub> + O		C <sub>2</sub> H <sub>5</sub> + O <sub>3</sub>		C <sub>2</sub> H <sub>5</sub> + NO <sub>3</sub>	
	exp. <sup>a</sup>	calc.	exp.	calc.	exp.	calc.
CH <sub>3</sub> + HCHO	0.32	0.40	0.50	0.50	0.88	0.73
H + CH <sub>3</sub> CHO	0.40	0.44	0.30	0.38	0.25	0.24
OH + C <sub>2</sub> H <sub>4</sub>	0.23	-	0.19	-	-	-
1,3 H shift	-	0.02	-	0.01	-	0.001
1,2 H shift	-	0.14	-	0.11	-	0.03

<sup>a</sup>T. R. Slagle, D. Sarzynski, D. Gutman, J. A. Miller, and C. F. Melius *J. Chem. Soc., Faraday Trans. 2* **84**, 491 (1988).

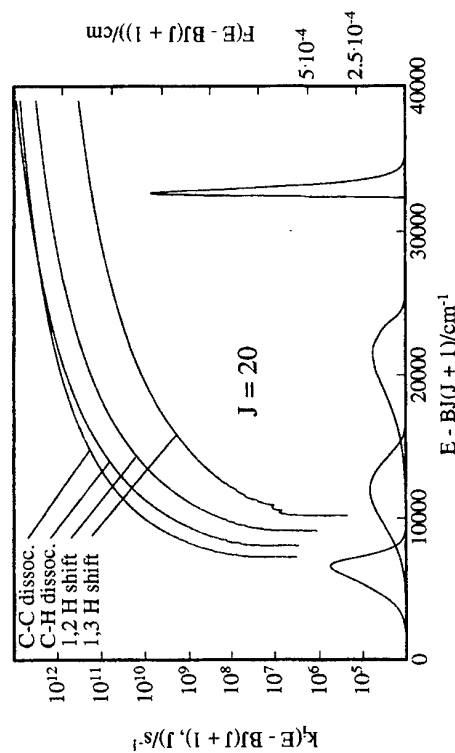


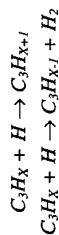
Figure 1. Specific rate constants for reactions 1-4 and nascent molecular distribution functions of C<sub>2</sub>H<sub>5</sub>O\* for the different formation reactions. From low to high energies: C<sub>2</sub>H<sub>5</sub> + NO<sub>2</sub>, NO<sub>3</sub>, O<sub>3</sub>, and O, respectively.

**AB INITIO CALCULATIONS AND QUANTUM STATISTICAL RRRK  
ANALYSES OF THE REACTIONS: (1) PROPYNE+H AND (2) ALLENE+H**

Debasis Sengupta, Jozef Peeters and Minh Tho Nguyen

*Department of Chemistry, University of Leuven  
Celestijnenlaan 200F, B-3001 Leuven, Belgium.*

Formation of polycyclic aromatic hydrocarbons (PAH's) and soot in fossil-fuel combustion are known to be due to the production of benzene in aliphatic flames. Recently, it has been argued that the production of benzene occurs via the self reaction of  $C_3H_3$  radicals. Experimental evidence confirms the high abundance of  $C_3H_3$  radicals in hydrocarbon flames. The evidence of benzene formation via the self reaction of  $C_3H_3$  is also confirmed by ab initio molecular orbital (MO) calculations as there is no activation barrier for such reactions. In general, the  $C_3H_x$  compounds may be closely inter-related by interconversions via the addition or abstraction of H.



The reactions of hydrogen atom with propyne and allene, which can both arise by  $C_3H_3 + H$ , may constitute an important sink for the  $C_3H_x$  species pool via the reaction channel leading to  $C_2H_2$  plus  $CH_3$ . Here we present the results of our theoretical calculations for these two reactions.

We, first, calculate the potential energy surfaces (PES) for both addition of H to the central as well as the terminal C atom in the above reactions by means of higher level ab initio molecular orbital (MO) method. Geometry optimizations were carried out at the MP2/6-31 G (d,p) level and then energy calculations were again performed at the quadratic configuration interaction level with corrections for triple excitations using a larger basis set. Various data, such as activation barriers, vibrational wavenumbers, moments of inertia, obtained from ab initio MO calculations are further utilised to calculate the rate constants of all the reaction channels as a function of temperature and pressure using the bimolecular version of quantum statistical Rice-Ramsperger-Kassel (QRRK) theory coupled with the idea of chemical activation processes. Contributions of various pathways to the total rate constants are critically analysed.

Our calculations show that at lower temperatures the propyne + H reaction mostly proceeds through the addition of H at the terminal C while at higher

temperatures, addition to the central C also becomes important. Propyne to allene conversion in the propyne + H reaction at lower temperatures is primarily due to the addition at the terminal C. At higher temperatures however, it becomes also possible after the addition at the central C atom. On the other hand, acetylene formation at lower temperatures occurs mainly through H addition at the central C atom while at higher temperatures the  $C_2H_2$  production path via the addition at the terminal C becomes competitive. Both effects are due to the importance of H-migrations at high temperatures.

Addition of H to the terminal C in the allene + H reaction is more favourable than that to the central C atom. Allene to propyne conversion in the allene + H reaction primarily proceeds via addition at the terminal C atom while at higher temperatures it is possible through the addition at the central C atom of allene. Formation of acetylene is possible via addition to both the terminal and the central C atom of allene.

Calculated branching ratios for the various products are also compared with the recent experimental results of our group.

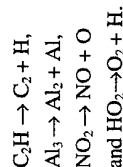
ANALYTICAL THEORY OF ENERGY DISTRIBUTIONS IN THE  
PRODUCTS OF THREE-ATOM UNIMOLECULAR REACTIONS.  
APPLICATION TO SOME PROCESSES GOVERNED BY  
LONG OR SHORT RANGE POTENTIALS

L. Bonnet and J.C. Rayez

Laboratoire de Physicochimie Théorique, URA 503  
Université Bordeaux I and CNRS  
33405 Talence Cedex (France)

Analytical energy distributions among the products of unimolecular three-atom reactions performed in beam experiments are derived within the framework of classical statistical mechanics. For processes governed by long-range forces, it is assumed that the system behaves as if it possessed a unique transition state (TS) in which the nascent products are not subject to any mutual interaction. For reactions involving a barrier, we assume that the energy partitioning between vibrational, rotational and translational motion, from the TS onto the products, does not evolve significantly, especially if the departing atom is sufficiently lighter than those constituting the diatomic molecule (L. Bonnet and J.C. Rayez, *J. Chem. Phys.* **103** (1995) 2929). Moreover, the angular dependence of the potential energy at the TS is supposed to be quadratic. The formulas derived in this work should aid in the characterisation of experimental results and be very useful for the determination of the main factors influencing the statistics of unimolecular reaction dynamics.

This formalism is applied successfully to the following reactions:



Steady-state kinetics in irreversible and equilibrating systems:  
Application to ethane dissociation/methyl recombination.

N.J.B. Green and Z.A. Bhatti

King's College, University of London, Strand, London, WC2R 2LS.

(1) Calculations of unimolecular canonical rate coefficients for a model irreversible dissociation reaction have been performed under the steady-state approximation. The appropriate master equation (ME) matrix is truncated at an energy,  $E'$ , below which all grains are assumed to be Boltzmann populated, e.g., 5 kT below threshold.

Advantages of inversion method over  
diagonalization method

- i) relatively short CPU run time
- ii) Numerically stable (particularly at high pressures where diagonalization method breaks down; see fig 1.)
- iii) Computationally inexpensive

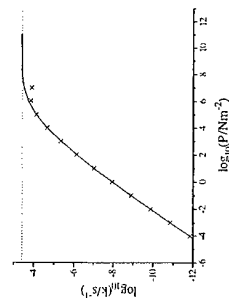


Fig. 1. Comparison of inversion (I) and diagonalization (D) methods. (— I. xxxxx D)

(2) Calculations on the equilibrating system  $\text{C}_2\text{H}_6 \leftrightarrow 2\text{CH}_3$  using a non-linear master equation (the non-linear term arising from the concentration of methyl radicals) show that the fully-reversible scheme can be resolved into steady-state irreversible schemes for dissociation and association.

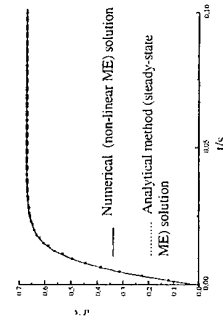


Fig. 2. Comparison of numerical and analytical solutions to dissociation/association (non-linear) master equation.

The non-linear master equation is solved by numerical integration to give the time dependence of the degree of ethane dissociation,  $\zeta$ . The numerical solution can be fitted using an analytic formula involving steady-state (irreversible) rate coefficients for dissociation and association

Ref: N.J.B. Green and Z.A. Bhatti, *Chem. Phys. Letters*, **254**, 358-364, (1996)

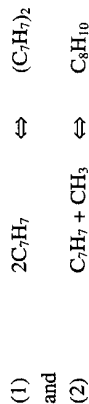
# THE RADICAL-COMBINATION REACTIONS OF BENZYL WITH BENZYL AND BENZYL WITH METHYL

K.R. Henning and K. Luther

*Institut für Physikalische Chemie, Universität Göttingen,  
Tammannstraße 6, D-37077 Göttingen, Germany*

The presence of barriers on the potential surfaces of radical-(re)combination reactions and their importance in combination reaction dynamics are topics of actual interest. Reaction rate measurements over wide temperature ranges can serve as very indicative tools in corresponding research.

As a contribution in this field we will present the results of recent high temperature studies in shock waves on the systems



Reaction (1) was studied in between 980 and 1370 K and reaction (2) - for which experimental rate constants are reported for the first time - between 1270 and 1430 K. The temperature dependent absorption coefficients of bibenzyl and benzyl were redetermined. On this basis a thorough analysis on the resulting temperature dependence of the benzyl-recombination from 300 to 1400 K will be given and be discussed with respect to the opening remark.

# KINETICS OF THE REACTION OF CF<sub>2</sub>Cl RADICALS WITH NO<sub>2</sub>

Gustavo A. Pino, Carlos A. Rinaldi and Juan C. Ferrero

*INFIQC - Departamento de Fisicoquímica, Facultad de Ciencias Químicas,  
Universidad Nacional de Córdoba,  
C.C. 61, Suc. 16, 5016 Córdoba - Argentina*

It is now well established that CFCs (Chlorofluorocarbons) deplete the earth's stratospheric ozone layer through different intermediates produced by the reactions of these radicals with other atmospheric compounds such as O<sub>2</sub> and NO<sub>x</sub>.<sup>i</sup>

It has been informed that the stratospheric photooxidation of the Freon 12 (CF<sub>2</sub>Cl<sub>2</sub>) involves the formation of the CF<sub>2</sub>ClO radical and their unimolecular decomposition by C-Cl bond scission.<sup>ii</sup> The formation of this radical has also been postulated as an intermediate in the reaction of CF<sub>2</sub>Cl radicals with NO<sub>2</sub>.<sup>iii</sup>

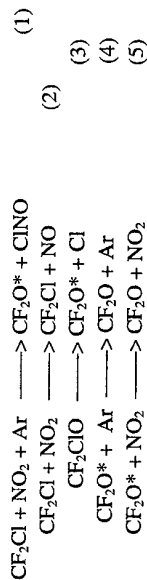
In order to obtain more information on the processes involved, we have studied the reaction of CF<sub>2</sub>Cl radical with NO<sub>2</sub> in presence of Ar.

The CF<sub>2</sub>Cl radicals were produced by IRMPD of CF<sub>2</sub>Cl<sub>2</sub> in a static system. Vibrationally excited CF<sub>2</sub>O was found as a reaction product. Then, the rate of reaction was measured monitoring the IR fluorescence from CF<sub>2</sub>O\* in real time.

In all the experiments the CF<sub>2</sub>Cl<sub>2</sub> pressure was 0.2 Torr and the dissociated fraction per pulse was approximately 0.5% assuring pseudo first order reaction. The NO<sub>2</sub> pressure was varied between 0.2 and 1.0 Torr. The experiments were made with the addition of 1.0 - 10.0 Torr of Ar.

The IR fluorescence was measured with a Sbln detector. The output signal was digitalised and averaged by a computer. The signal showed an initial exponential rise followed by an also exponential decrease, due to collisional relaxation of vibrationally excited CF<sub>2</sub>O. Plots of the rate of increase of the fluorescence intensity as a function of Ar pressure showed a linear behaviour with an interception, indicating the presence of second and third order processes. The value of the second order rate constant is  $k_{2nd} = (1.4 \pm 0.2) \times 10^{12} \text{ cm}^3/\text{molecule.s}$  and the value of the third order rate constant is  $k_{3rd} = (6.5 \pm 0.3) \times 10^{-30} \text{ cm}^6/\text{molecule}^2.\text{s}$ .

The experimental observations can be explained with the following reaction scheme:



From the above reaction scheme, the concentration of CF<sub>2</sub>Cl radicals is given by:

$$[CF_2Cl] = [CF_2Cl]_0 \exp[-(k_1 + k_2) t]$$

# QUANTUM STATE SPECIFIC STUDIES OF THE UNIMOLECULAR DECAY OF DCO ( $\tilde{X}^2A'$ )

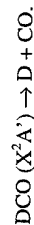
Xiaonong Li\*, C. Stöck\*, F. Temps†

\*Max-Planck-Institut für Strömungsforschung  
Bunsenstr. 10, D-37073 Göttingen

†Institut für Physikalische Chemie, Universität Kiel  
Ohlshausenstr. 40, D-24098 Kiel

The deuterated formyl radical DCO constitutes a nearly unique model system for investigating the unimolecular decay dynamics of highly vibrationally excited molecules.

Using the method of stimulated emission pumping spectroscopy (SEP), DCO can be excited to specific quantum states up to excitation energies of  $18\,200\text{ cm}^{-1}$ , i.e.  $13\,000\text{ cm}^{-1}$  above the asymptotic dissociation limit of  $\text{DCO}(\tilde{X}^2A')$ ,



The SEP spectra show about 150 discrete vibrational levels, which can be identified by their rotational structure. 20 levels correspond to bound vibrational states. The other more than 130 are metastable states, i.e., resonances, which are embedded in the dissociation continuum. The observed highly excited vibrational levels are found to be subject to strong mixings due to a 1:1:2 resonance between the D-CO stretching, C-O stretching, and DCO bending vibrations. Thus, in contrast to HCO, the higher excited vibrational levels of the DCO ( $\tilde{X}^2A'$ ) molecule cannot be described using a simple normal mode picture.

The unimolecular decay rates of the individual  $\text{DCO}(\tilde{X}^2A')$  resonances can be determined from the observed line widths in high resolution SEP spectra. The decay constants of neighbouring states with practically the same amount of energy are found to fluctuate by two orders of magnitude. The observed level energies and lifetimes are compared to predictions by statistical unimolecular rate theory and to results of quantum scattering calculations by Schinke and co-workers.

where  $k_1 = k_1[\text{NO}_2][\text{Ar}] = k_{3rd}$  and  $k_2 = k_2[\text{NO}_2] = k_{2nd}$  and the concentration of vibrationally excited  $\text{CF}_2\text{O}$  is:

$$[\text{CF}_2\text{O}^*] = \{k_1[\text{CF}_2\text{Cl}]_0 / [k_1 + k_5 - k_1' + k_2']\} \times \{ \exp[-(k_1' + k_2')]t \} - \exp[-(k_4' + k_5')t] \}$$

where  $k_4' = k_4[\text{Ar}]$  and  $k_5' = k_5[\text{Ar}]$

Since the IRF signal is proportional to the concentration of  $\text{CF}_2\text{O}^*$ , its temporal evolution is given by the following equation:

$$I(t) = A(\exp^{-k_4't} - \exp^{-k_5't})$$

where  $k_4' = k_1 + k_2$  and  $k_5' = k_4 + k_5$ , are pseudo first-order rate constants for the total rate of disappearance of  $\text{CF}_2\text{Cl}$  radicals and for the collisional relaxation of  $\text{CF}_2\text{O}^*$ .

According to the above reaction scheme, the total rate of disappearance of  $\text{CF}_2\text{Cl}$  radicals is  $1.6 \times 10^{12} \text{ cm}^3/\text{molecule.s}$ , which is lower by a factor of 6 than the value reported by Slagle and Gutman. These authors also reported a second order behaviour for this process, which is also at variance with the present findings. The reason for the variance is not clear at present and further work seems necessary.

The relaxation rate constants, corresponding to steps 4 and 5, were determined to be  $k_4 = (1.2 \pm 0.2) \times 10^{13} \text{ cm}^3/\text{molecule.s}$  and  $k_5 = (1.4 \pm 0.2) \times 10^{12} \text{ cm}^3/\text{molecule.s}$

THE EXTRAORDINARY INTERCONVERSION OF  
1,3-DIMETHYLCYCLOPROPENE AND 1-ETHYLCYCLOPROPENE:  
A KINETIC AND MECHANISTIC STUDY OF A THERMAL  
CYCLOPROPENE-TO-CYCLOPROPENE REARRANGEMENT

H. Hopf, W. Graf Von Der Schulenburg,

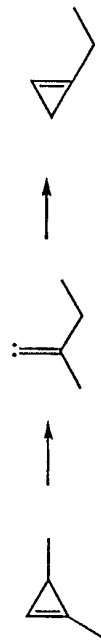
*Institut für Organische Chemie, Technische Universität Braunschweig, Hagenring  
30, 3300 Braunschweig, Germany;*

R. Walsh,

*Department of Chemistry, University of Reading, Whiteknights, PO Box 224,  
Reading RG6 2AD, UK.*

The title compounds have been synthesised and the kinetics of their thermal isomerisations individually investigated in the gas-phase between 200 - 250 °C, in a static system, with GC analysis of the products. Both reactants rearrange by parallel, irreversible unimolecular pathways to form pent-2-yne (the major product in both cases), cis- and trans-penta-1,3-diene. In addition, each reactant cyclopropene generates the other as a transient species in quantities of several percent [in the case of the decomposition of the 1-ethyl isomer, the 1,3-dimethyl isomer is present at levels of more than 10% of the total mixture at its maximum]. This is the first quantitative kinetic study of a cyclopropene-to-cyclopropene interconversion. The Arrhenius Parameters obtained for these processes are shown in the table below.

The mechanism proposed for the interconversion is the following:





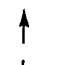
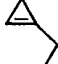

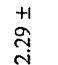





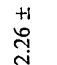
The involvement of the vinylidene species, methyl ethyl vinylidene, is precited by earlier trapping experiments<sup>1</sup>, and rate measurements<sup>2</sup> supporting its involvement in

alkyne formation. In this case the vinylidene species undergoes competitive alkyl group migration to yield pent-2-yne:



The mechanism of this reaction and its further implications will be discussed at the meeting

Table of Arrhenius Parameters

Reaction	log (A/s <sup>-1</sup> )	E <sub>a</sub> /kJ mol <sup>-1</sup>
 → 	overall	13.36 ± 0.08
 → 		164.0 ± 0.8
 → 		166.2 ± 0.6
 → 	overall	13.36 ± 0.09
 → 		160.7 ± 0.9
 → 		156.9 ± 0.5

1) H. Hopf, A. Plagens and R. Walsh, *Liebigs Ann.*, 825 (1996).

2) R. Walsh, C. Wolf, S. Untiedt and A. de Meijere, *JCS Chem. Comm.*, 421 (1992).

THE AZOMETHANE-INITIATED THERMAL REACTION OF  
2-METHYLBUT-2-ENE; ENTHALPY OF FORMATION OF THE RADICAL  
(CH<sub>3</sub>)<sub>2</sub>CH•C(CH<sub>3</sub>)<sub>2</sub>

László Seres

*Institute of Chemistry, Gyula Juhász Teachers' Training College,*

*H-6701 Szeged, POB 396, Hungary*

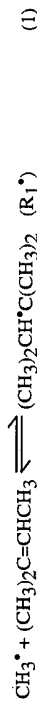
*Zoltán Király and Tamás Körtevényesi*

*Institute of Physical Chemistry, Attila József University,*

*H-6701 Szeged, POB 105, Hungary*

The azomethane (AM)-initiated thermal reaction of 2-methylbut-2-ene (2MB2) was studied in a conventional high-vacuum static system at 540-610 K. The initial concentration of AM was  $7.89 \times 10^{-4}$  mol dm<sup>-3</sup> and that of 2MB2 was  $4.73 \times 10^{-3}$  mol dm<sup>-3</sup> in most experiments. The products were identified by gas-chromatography, mass-spectrometry and Fourier Transform Infrared Spectroscopy. The quantitative analysis was performed with a gas-chromatograph.

The equilibrium constant of the addition reaction



was obtained from the expression

$$K_p = \frac{[\text{R}_1^\bullet]}{[\text{CH}_3^\bullet][2\text{MB2}][\text{R}^\bullet T]} \quad (1)$$

Hydrogen abstraction from the methyl groups of the doubly substituted carbon atom of the parent olefin results in the formation of (E)- and (Z)-isomers of the radical  $^\bullet\text{CH}_2\text{C}(\text{CH}_3)=\text{CHCH}_3$  (12DMA•) and these isomers yield different products on combination with  $\text{CH}_3^\bullet$  and  $\text{R}_1^\bullet$ .

With the assumption that the products of the reactions



(E)- and (Z)- $\text{CH}_3\text{CH}_2\text{C}(\text{CH}_3)=\text{CHCH}_3$  (E3MP2 and Z3MP2)



(E)- and (Z)- $(\text{CH}_3)_2\text{CHC}(\text{CH}_3)_2\text{CH}_2\text{C}(\text{CH}_3)=\text{CHCH}_3$  (E3556TMHp2 and Z3556TMHp2)

are formed only in these elementary steps, the radical concentrations were eliminated from (1) through the rates of formation of the combination products:

$$r(\text{E3MP2}) + r(\text{Z3MP2}) = k_2[\text{CH}_3^\bullet][12\text{DMA}^\bullet]$$

$$r(\text{E3556TMHp2}) + r(\text{Z3556TMHp2}) = k_3[\text{R}_1^\bullet][12\text{DMA}^\bullet]$$

yielding

$$K_p \quad k_3/k_2 = [r(\text{E3556TMHp2}) + r(\text{Z3556TMHp2})]/[r(\text{E3MP2}) + r(\text{Z3MP2})][2\text{MB2}][\text{R}^\bullet T]$$

The rate constant ratio  $k_3/k_2$  was assumed to be temperature-independent. Then, from the exponential form of the van't Hoff equation, the enthalpy of reaction (1) is  $\Delta H_{1,573}^\circ = -103.4 \pm 5.0$  kJ mol<sup>-1</sup>, and  $\Delta_f H_{1,298}^\circ = -105.1 \pm 5.0$  kJ mol<sup>-1</sup>. Finally, the standard enthalpy of formation of  $\text{R}_1^\bullet$  was estimated from the known enthalpies of the other species *via*

$$\Delta_f H_{1,298}^\circ = \Delta_f H_{298}^\circ(\text{R}_1^\bullet) - \Delta_f H_{298}^\circ(2\text{MB2}) - \Delta_f H_{298}^\circ(\text{CH}_3^\bullet)$$

$$\Delta_f H_{298}^\circ(\text{R}_1^\bullet) = \Delta_f H_{1,298}^\circ + \Delta_f H_{298}^\circ(2\text{MB2}) + \Delta_f H_{298}^\circ(\text{CH}_3^\bullet)$$

With  $\Delta_f H_{298}^\circ(2\text{MB2}) = -42.55$  kJ mol<sup>-1</sup> and  $\Delta_f H_{298}^\circ(\text{CH}_3^\bullet) = 146.0$  kJ mol<sup>-1</sup> we obtain  $\Delta_f H_{298}^\circ(\text{R}_1^\bullet) = -1.6 \pm 5.0$  kJ mol<sup>-1</sup>. Finally, the heat of formation of  $\text{R}_1^\bullet$  is best represented by:

$$\Delta_f H_{298}^\circ(\text{R}_1^\bullet) = -1.6 \pm 8.0 \text{ kJ mol}^{-1}$$

where the error limits were increased to allow for possible systematic errors.

If the additivity principle is valid for large alkyl radicals like the present one, through use of Benson's values for the other groups, the group value  $\Delta_f H^\circ[\text{C}(\text{C})_3]$  is 176 kJ mol<sup>-1</sup> and the heat of formation of the radical *tert*-C<sub>4</sub>H<sub>9</sub>• is predicted to be  $\Delta_f H^\circ(\text{tert-C}_4\text{H}_9^\bullet) = 49.5$  kJ mol<sup>-1</sup>, in good agreement with recent determinations.

# CYCLOADDITION REACTIONS OF CF WITH UNSATURATED HYDROCARBONS. CORRELATION OF ACTIVATION ENERGIES AND FREQUENCY FACTORS WITH THE HYDROCARBON IONISATION ENERGIES.

Ilse De Boelpaep, Bart Velters and Jozef Peeters

*Department of Chemistry, University of Leuven, Celestijnenlaan 200F, B-3001 Leuven, Belgium*

Fluorocarbon radicals like CF are important in many aspects of modern society and technology. One of the foremost of these areas of importance concerns the dry-etching techniques for the fabrication of ULSI microcircuits, using fluorocarbon-based plasmas to etch semiconductor and/or oxide layers.

As part of ongoing research on the reactivity and kinetics of CF<sup>1,2</sup>, the absolute rate coefficients of the reactions of CF with several alkenes and alkadienes, in a temperature range of 295K to 455K, have been determined using Pulse Laser Photolysis (PLP) and Laser Induced Fluorescence (LIF) techniques.

CF (X<sup>2</sup>Π, v = 0) radicals were generated by 248 nm laser photolysis of CF<sub>2</sub>Br<sub>2</sub> with a KrF excimer laser. The real-time exponential decay of [CF] at varying concentrations of coreagent, always at very large excess over CF, was followed by LIF, using a Nd:YAG pumped dye laser tuned to the wavelength of the P<sub>11</sub>-bandhead of the A<sup>2</sup>Σ<sup>+</sup> (v'=1) ← X<sup>2</sup>Π (v''=0) transition (223.88 nm)<sup>1</sup>. All experiments were carried out at pressures in the range of 2 Torr to 10 Torr.

The reactions of CF with several alkenes were studied to determine their Arrhenius activation energies E<sub>a</sub> and to verify an expected correlation between the E<sub>a</sub> and the ionisation potential (IP) of the corresponding alkene. James et al. observed negative correlations between the rate constant at 295K and the alkene IP for the analogous reactions of both CCl and CBr<sup>3</sup>. For the reactions of CF with ethene, propene, isobutene and 2,3-dimethyl-2-butene, the experimentally determined temperature dependence of the rate coefficients, in units of cm<sup>3</sup> molecule<sup>-1</sup> s<sup>-1</sup>, can be expressed by the following Arrhenius equations: k(CF+C<sub>2</sub>H<sub>4</sub>) = 7.88×10<sup>-13</sup> exp{(-1.39 kcal mol<sup>-1</sup>)/RT}; k(CF+C<sub>3</sub>H<sub>6</sub>) = 9.07×10<sup>-13</sup> exp{(-0.16 kcal mol<sup>-1</sup>)/RT}; k(CF+i-C<sub>4</sub>H<sub>8</sub>) = 1.08×10<sup>-12</sup> exp{(0.81 kcal mol<sup>-1</sup>)/RT} and k(CF + 2,3-dimethyl-2-butene) = 1.57×10<sup>-12</sup> exp{(1.43 kcal mol<sup>-1</sup>)/RT}.

The experimental activation energies decrease progressively from ethene to 2,3-dimethyl-2-butene. For the latter, the activation energy is negative, indicating that the actual energy barrier is negligibly small; the observed negative temperature dependence is quantitatively compatible with TS theory. The data show that the Arrhenius activation energy increases linearly with the alkene ionisation energy while the frequency factor decreases. The data are consistent with an electrophilic cycloaddition process, where CF inserts in the electron-rich double bond of the alkenes.

The rate constants measured for the reactions of CF with alkadienes can be expressed by the following Arrhenius equations: k(CF+allene) = 3.43×10<sup>-12</sup> exp{(-2.06 kcal mol<sup>-1</sup>)/RT}; k(CF+1,3-butadiene) = 9.14×10<sup>-12</sup> exp{(-1.11 kcal mol<sup>-1</sup>)/RT} and k(CF+isoprene) = 1.24×10<sup>-11</sup> exp{(-0.38 kcal mol<sup>-1</sup>)/RT}. Again, both the frequency factor and experimental activation energy correlate well with the IP of the hydrocarbon concerned. Although this correlation can be attributed to the same cause, it differs quantitatively from that for the alkene reactions. Compared to reactions with an alkene with a similar IP, the alkadiene reactions have (i) a higher energy barrier due to resonance stabilisation of the alkadiene, but on the other hand (ii) a higher frequency factor due to their larger π-electron cloud; both (i) and (ii) are confirmed by our experimental results. For the smaller alkadienes, this leads to rate coefficients that are lower than those of reactions with alkenes with similar IP.

## References

1. Peeters, J., Van Hoeymissen, J., Vanhaelemeersch, S., Vermeylen, D., *J. Phys. Chem.*, **1992**, 96, 1257
2. Van Hoeymissen, J., De Boelpaep, I., Uten, W., Peeters, J., *J. Phys. Chem.*, **1994**, 98, 3725
3. James, F.C., Choi, H.K.J., Ruzsicska, B.P., Strausz, O.P., Bell, T.N., *Frontiers of free radical chemistry*, W.A. Pryor, ed., Academic Press, New York, **1980**, 139

# EXPERIMENTAL AND THEORETICAL STUDY OF PRODUCT YIELDS IN THE REACTIONS OF CF<sub>3</sub>O RADICALS WITH NO<sub>x</sub> (x = 1,2)

R. Zellner, H. Somnitz and G. Bednarek

*Institut für Physikalische und Theoretische Chemie,  
Universität Essen, Universitätsstraße 5, 45117 Essen*

CF<sub>3</sub>O radicals are generated in the atmospheric oxidation of selected fluorinated hydrocarbons. In the stratosphere, NO, NO<sub>2</sub> and CH<sub>4</sub> are the main reaction partners for CF<sub>3</sub>O radicals. Since the alternative reaction with ozone could establish a catalytic cycle of ozone destruction [1], the reactions with NO and NO<sub>2</sub> are of particular interest, in case they do not represent a permanent sink for CF<sub>3</sub>O radicals. Therefore, in addition to the rate coefficient the products of the reactions have to be known as a function of temperature and total pressure.

The rate constants for the reactions of CF<sub>3</sub>O radicals with NO (1) and NO<sub>2</sub> (2) as obtained in our group using a combination of laser photolysis and LIF detection have already been reported [2]. While the reaction with NO has been found to be independent of pressure and temperature, the reaction with NO<sub>2</sub> shows a pressure as well as a slight temperature dependence (T = 222–302 K, p<sub>tot</sub> = 7–107 mbar). The values obtained for these rate constants are:

$$k_1 = (4.5 \pm 1.2) \times 10^{-11} \text{ cm}^3 \text{ s}^{-1}$$

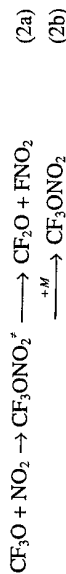
$$k_{2,\text{tot}} = (8 \pm 5) \times 10^{-13} \exp((863 \pm 194) \text{ K}/T) \text{ cm}^3 \text{ s}^{-1}$$

Product studies for the above reactions have been performed using a steady-state photolysis / FTIR spectroscopy technique in the temperature range 247–298 K and at a total pressure of 1000 mbar. As a result from these studies the reaction with NO can be described as



While only CF<sub>2</sub>O could be found in the IR spectra, the formation of FNO as a second product was implied from the F-atom balance. Since the rate coefficient for reaction (1) is independent of temperature, it cannot occur via a direct abstraction of an F atom by NO.

Contrary to the reaction with NO the reaction with NO<sub>2</sub> has two channels, viz.



As a result three different products could be found in the spectra. For reaction (2), the addition channel explains the pressure dependence of the overall rate constant. However the observed temperature dependence is too small for reaction (2a) being an abstraction reaction.

In order to obtain more information about the mechanism of reactions (1) and (2) the potential energy surfaces for both reactions were investigated. Single point energy calculations were performed by density functional theory (DFT) methods on the Becke3LYP level with a triple zeta basis set with polarised and diffuse functions added (6-311+(2df,p)) [3, 4]. The underlying equilibrium geometries were optimised using the MP2 / 6-31G(d) level of theory with full correlation of inner electrons, as were zero-point energies and vibrational frequencies. All *ab initio* calculations were performed using the GAUSSIAN 94 program packages. Microscopic rate constants were derived from the usual RRKM expression

$$k(E) = \frac{\int_0^{E-E_0} \rho^+(E_*) dE_*}{h\rho(E)}$$

In both reactions an activated complex is formed which can be stabilised by collisions to form the adduct or rearrange in a four-centre transition state and subsequently decompose into the molecular fragments. The energy diagram as obtained for reaction (1) is shown in Fig. 1.

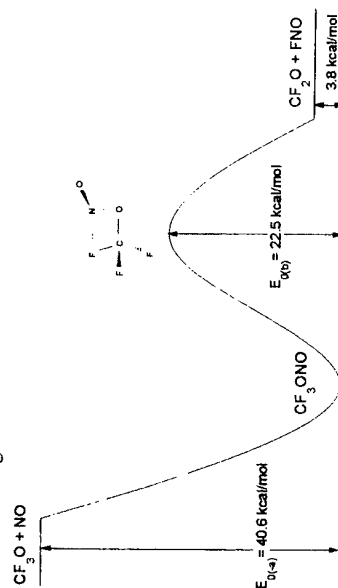


Fig. 1: Energy diagram for the reaction CF<sub>3</sub>O + NO → CF<sub>2</sub>O + FNO

## ASYMMETRIC INTERNAL ROTATION: THEORY AND APPLICATION

Jun Gang, Michael J. Pilling and Stuart H. Robertson

*School of Chemistry, University of Leeds, Leeds, UK LS2 9JT*

A methodology has been developed for treating molecules and radicals with asymmetric internal rotors[1]. The principal difficulty in tackling such species is that the conventional division into internal and external rotation cannot be made because, not only is there Coriolis coupling between internal and external rotations, but also the values of the 'external' moments of inertia are dependent on the internal coordinates used to describe the asymmetric rotor.

Algebraic manipulators were used to construct the full classical kinetic energy expression for the combined external/internal rotation system including all coupling arising from both Coriolis effects and changes in moments of inertia. Butane, pentane and 2-C<sub>4</sub>H<sub>9</sub> radicals, all of which exhibit asymmetric internal rotors, are analysed.

The canonical partition function was then evaluated by performing the appropriate phase space integration. This integration was considerably simplified by applying the theorem due to Aston and Eidinoff[2] which allows direct analytic integration over the conjugate momenta to be performed. The remaining configuration integral depends on the choice of potential describing combined external/internal rotation. Internal potential was assumed to be separable allowing the integration to be expressed as a product of one dimensional integrals. Standard statistical mechanical machinery can be used to determine thermodynamic quantities such as heat capacity, C<sub>p</sub>, and entropy, S. The canonical partition function is the Laplace transform of density of states, N(E). This relation is used to determine N(E) and the sum of states, W(E), for the combined internal-external rotation system by using a combination of techniques based on the convolution theorem and fast Fourier transform. The overall N(E) and W(E) are then derived from this by convoluting with vibrational densities of states determined by direct count together with quantum mechanical corrections.

To assess these techniques an analysis of the experimental data for the reaction



obtained by Knyazev et al[3] has been performed. The data were analysed by using a master equation approach, the microcanonical rate coefficients used in the MBE calculation were obtained by using RRKM theory and the inverse Laplace transform (ILT) technique[4]. Transition state parameters were obtained from ab initio calculations. Internal rotors for both the 2-C<sub>4</sub>H<sub>9</sub> radical and the transition state were treated using the current methodology. The only adjustable parameters that were used are the reaction threshold E<sub>0</sub> and (ΔE)<sub>a</sub> the average energy transferred in a deactivating collision. The best fit values from both techniques are in good agreement.

## References

- 1: J. Gang, M. J. Pilling and S. H. Robertson, *Faraday Trans.*, in press.
- 2: M.L. Eidenoff and J.G. Aston, *J. Chem. Phys.* 3, 379 (1935).
- 3: V. D. Knyazev, I. A. Dubinsky, I. R. Slagle, and D. Gutman, *J. Phys. Chem.*, 98, 11099-11108, 1994.
- 4: S. H. Robertson, M. J. Pilling, D. L. Baulch and N. J. B. Green, *J. Phys. Chem.*, 99, 13452-13460, 1995.

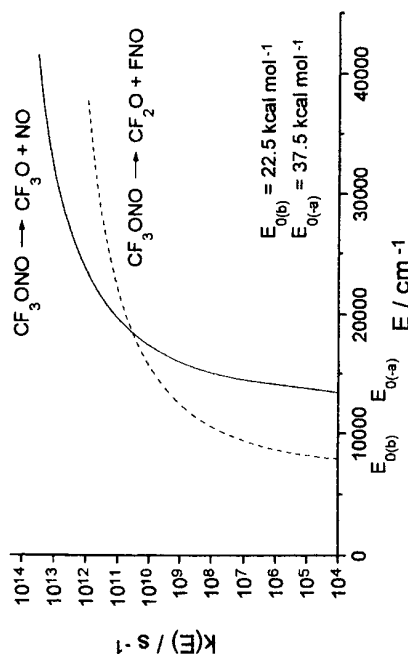


Fig. 2: Microscopic rate constants for the elementary steps (b) and (-a) of reaction (1). The activated complex can also decompose back into the educts. The transition state for this decomposition was assumed to resemble the products (i.e. CF<sub>3</sub>O + NO<sub>x</sub>) and its exact position was determined by variation of the separation of the educt molecules and minimising the sum of states for the transition state. A plot of the microscopic rate constants as a function of total energy ( $k(E)$ ) for reaction (b) and (-a) is shown in Fig. 2. Reaction paths for the abstraction channels could not be found on the potential energy surfaces for these reaction in agreement with the experimental activation energy.

## References

- 1) M.K.W. Ko, N.-D. Sze, J.M. Rodriguez, D.K. Weisenstein, C.W. Heisey, R.P. Wayne, P. Biggs, C.E. Canosa-Mas, H.W. Sidebottom, and J. Treacy, *Geophys. Res. Lett.* 21 (1994) 101
- 2) Presented at the 13th International Symposium on Gas Kinetics, Dublin 1994
- 3) A.D. Becke, *J. Chem. Phys.* Vol 98, No 7, 5648 (1993)
- 4) C. Lee, W. Yang and R.G. Parr, *Phys. Rev. B* 37, 785 (1988)

MASTER EQUATION MODELLING OF  ${}^1\text{CH}_2 + \text{C}_2\text{H}_2 \rightarrow \text{C}_3\text{H}_3 + \text{H}$ 

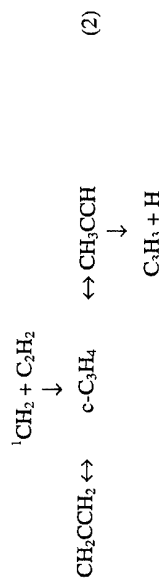
Martin Beasley, Michael J. Pilling and Struan H. Robertson

School of Chemistry, University of Leeds, Leeds, UK LS2 9JT

Polyaromatic hydrocarbons (PAH) are formed during the combustion of hydrocarbon fuels, particularly diesel<sup>1</sup>. PAH, through coagulation and surface reactions, are responsible for the formation of soot particles. It has been proposed that one of the principal reactions leading to PAH is the combination of propargyl radicals;



It is therefore of interest to determine how the propargyl radical is formed. In this study the formation of the Propargyl radical from  ${}^1\text{CH}_2$  and  $\text{C}_2\text{H}_2$  is modelled. The initial product of the association of methylene and acetylene is cyclopropene. The cyclopropene can subsequently isomerize to form either propyne or allene, and it is from propyne that the propargyl radical is formed by loss of H.



The isomerization of the cyclopropene is complicated by the effects of bath gas concentration and so a realistic analysis requires a master equation (ME) approach. An ME model has been constructed based on previous work by Quack<sup>1</sup> and Green et al.<sup>2</sup>. In this model three sets of equations describing the collision activation/deactivation processes are coupled together by reaction terms:

$$\begin{aligned} \frac{d\rho_i^A}{dt} &= \omega \sum_j P_{ij} \rho_j^A - \omega \rho_i^A - k_i^A \rho_i^A + k_{1,i}^B \rho_i^B \\ \frac{d\rho_i^B}{dt} &= \omega \sum_m P_{im} \rho_m^B - \omega \rho_i^B - k_{1,i}^B \rho_i^B - k_{2,i}^B \rho_i^B + k_i^A \rho_i^A + k_r^C \rho_r^C \\ \frac{d\rho_r^C}{dt} &= \omega \sum_s P_{rs} \rho_s^C - \omega \rho_r^C - k_r^C \rho_r^C + k_{2,i}^B \rho_i^B \end{aligned} \quad (3)$$

Microcanonical rate coefficients were calculated using RRKM theory and the exponential down model was used to model the transition kernels. The population of each of the grains is found by diagonalizing the matrix formed by concatenating the three sets of MEs. It is found that the decay of the initial distribution to equilibrium is determined by three eigenvalues one of which is zero.

The isomerization model is further extended by incorporating a time-dependent source term and a reactive loss term from the propyne isomer to the propargyl radical. The overall rate of production of propargyl as well as the overall rate coefficient can thus be obtained.

## References

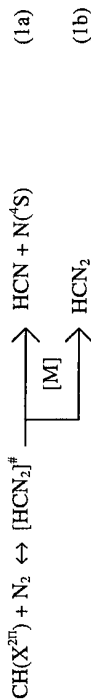
- 1) Y. Yoshihara, A. Kazakov, H. Wang and M. Frenklach, *Twenty-Fifth Symposium (International) on Combustion*, 941 (1994).
- 2) M. Quack *Ber. Bunsenges. Phys. Chem.*, **88**, 94 (1984).
- 3) N.J.B. Green, P.J. Marchant, M.J. Perona, M.J. Pilling and S.H. Robertson, *J. Chem. Phys.*, **96**, 5896 (1992).

# KINETICS OF THE REACTION $\text{CH} + \text{N}_2 \xrightarrow{[M]} \text{PRODUCTS}$ IN THE RANGE 10 - 620 TORR AND 298 - 1059 K

K.H. Becker, H. Geiger and P. Wiesen

*Physikalische Chemie / Fachbereich 9, Bergische Universität - Gesamthochschule  
Wuppertal  
D-42097 Wuppertal, Germany*

In hydrocarbon combustion, the reaction of CH radicals with molecular nitrogen is the initial step of the formation of so called "prompt" NO. Nitrogen oxides are probably the most important pollutants formed by combustion. Accordingly, several experiments have been carried out to study the kinetics of the reaction of CH radicals with molecular nitrogen in detail. For the pressure and temperature dependent reaction a mechanism with two pathways,



an addition channel (1b), which occurs at lower temperatures, and an abstraction reaction (1a), which becomes the dominant pathway at higher temperatures, was proposed.

In the present work, the gas-phase reaction of  $\text{CH}(\text{X}^2\text{I})$  radicals with molecular nitrogen was studied in the temperature range 298 - 1059 K at total pressures between 10 and 620 Torr. CH radicals were generated by excimer laser photolysis of  $\text{CHClBr}_2$  at 248 nm and were detected by laser-induced fluorescence. The investigated reaction shows a strong temperature and pressure dependence. At pressures of 20, 100, and 620 Torr the Arrhenius plots exhibit a strong decrease of the rate constant with increasing temperature. The rate constant is well described by,

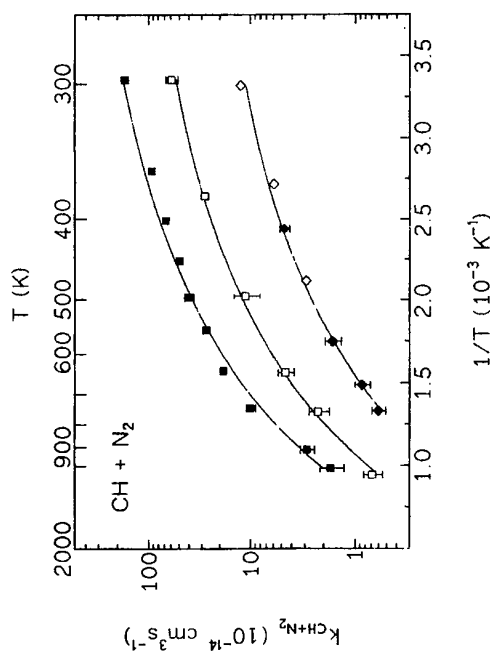
$$k_{(20 \text{ Torr})} = (24 \pm 6) \times T^{-(5.25 \pm 0.05)} \times \exp[-(7.57 \pm 0.83)/RT] \text{ cm}^3 \text{ s}^{-1},$$

$$k_{(100 \text{ Torr})} = (107 \pm 25) \times T^{-(5.25 \pm 0.05)} \times \exp[-(7.38 \pm 0.83)/RT] \text{ cm}^3 \text{ s}^{-1},$$

$$k_{(620 \text{ Torr})} = (1467 \pm 350) \times T^{-(5.48 \pm 0.05)} \times \exp[-(7.82 \pm 1.00)/RT] \text{ cm}^3 \text{ s}^{-1},$$

with  $E_0$  in kJ/mol. The obtained k-values together with literature data of Becker et al. [1] are illustrated in figure 1.

The pressure dependence was studied at temperatures of 298, 410, 561, and 750 K. The rate constants for each temperature were fitted by the Troe formalism [2-4]. The obtained k-values together with literature data are shown in figure 2.



**Figure 1:** Arrhenius plot of the bimolecular rate constant  $k_{\text{CH}+\text{N}_2}$  versus  $1/T$  at individual total pressures (Torr): (○) 620; (◇) 100; (□) 20, this work; (◇) 20, Becker et al. [1]. The solid lines are weighted, non-linear least-squares fits to a three-parameter Arrhenius expression to the corresponding data.

From the calculated values of  $k_0$  and  $k_\infty$ , the Arrhenius expressions,

$$k_0 = (1.1 \pm 0.2) \times 10^{-21} \times T^{(3.5 \pm 0.3)} \times \exp[-(6.4 \pm 0.5)/RT] \text{ cm}^6 \text{ s}^{-1} \quad \text{and}$$

$$k_\infty = (1.9^{+0.3}_{-0.2}) \times 10^{-12} \times \exp[(3.6 \pm 0.4)/RT] \text{ cm}^3 \text{ s}^{-1},$$

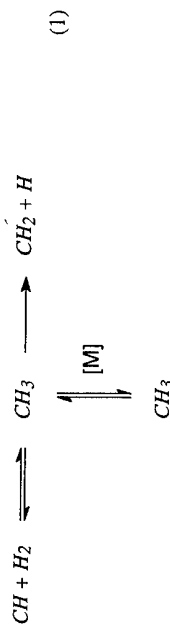
were obtained with  $E_0(k_0)$  and  $E_\infty(k_\infty)$  in units of kJ/mol. Within the range of 298-750 K the temperature dependence of the broadening factor is well described by  $F_c = 0.029 + (173.3 / T)$ .

# MASTER EQUATION ANALYSIS OF THE CH + H<sub>2</sub> REACTION

D.G. Johnson, M.J. Pilling, S.H. Robertson and P.W. Seakins

School of Chemistry, University of Leeds, Leeds, UK, LS2 9JT

Master equation techniques are used to investigate the reaction



which is an important route to the CH<sub>2</sub> radical. The potential energy surface for this reaction is shown schematically in figure 1. Smith and Stewart<sup>1</sup> have investigated this reaction by monitoring the decay of the CH radical by absorption. The results obtained exhibited a negative pressure dependence at higher temperatures (500-700 K). The aim of this study is to analyse this data using both time dependent and independent master equation schemes.

## Time Independent Master Equation

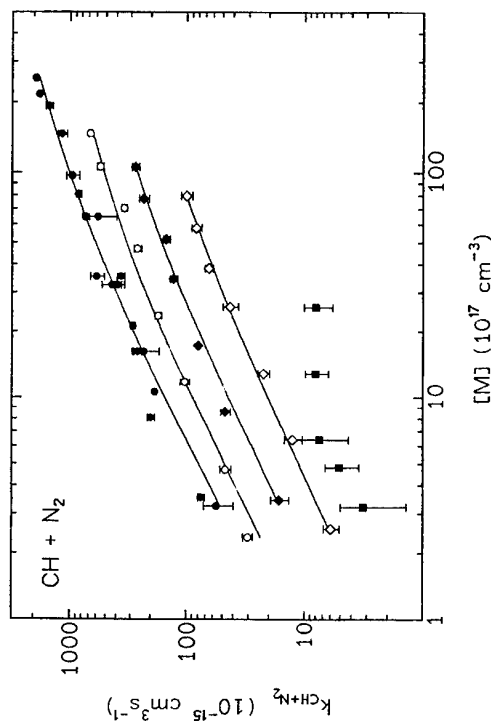
In this approach, the master equation was formulated as<sup>2</sup>

$$\frac{dp}{dt} = \omega(P - I)p - \sum_m K_m p + g \quad (2)$$

where  $\omega(P - I)$  governs collisional activation/deactivation,  $K_m$  is a diagonal matrix that contains the microcanonical rate coefficients for dissociation through channel  $m$ , and  $g$  is the source term given by,

$$g_i = k_b^\infty [\text{CH}][\text{H}_2] \frac{k_i^m N_i \exp(-\beta E_i)}{\sum_i k_i^m N_i \exp(-\beta E_i)} \quad (3)$$

Equation (3) is solved for the steady state by setting the left hand side to zero and using matrix inversion. Results from this approach did not exhibit a negative pressure dependence but did indicate that  $\langle \Delta E \rangle_d$  was strongly temperature dependent.



**Figure 2:** Comparison of the pressure dependencies of the bimolecular rate constant  $k_{\text{CH}+\text{N}_2}$  with Ar as bath gas at different temperatures: (●) 298 K, data of this work and literature data [5-7]; (○) 410 K, this work; (◆) 561 K, this work; (◇) 750 K, this work; (◊) Medhurst et al. [7], 750 K. The solid lines are the results of individual fits of the corresponding data to the expression of Troe [2-4].

## Acknowledgements:

Financial support by the "Deutsche Forschungsgemeinschaft (DFG)" and the "Ministerium für Wissenschaft und Forschung des Landes Nordrhein-Westfalen (MWF)" is gratefully acknowledged.

## References:

- [1] K.H. Becker, B. Engelhardt, H. Geiger, R. Kurtenbach, G. Schrey, P. Wiesen, *Chem. Phys. Lett.*, **195** (1992) 322
- [2] J. Troe, *J. Chem. Phys.*, **66** (1977) 4758
- [3] K. Luther, J. Troe, *J. Symp. (Int.) Combust.*, **17** (1979) 534.
- [4] J. Troe, *Ber. Bunsenges. Phys. Chem.*, **87** (1983) 161
- [5] S.S. Wagal, T. Carrington, S.V. Filseth, C.M. Sadowski, *Chem. Phys.*, **69** (1982) 61
- [6] M.R. Berman, M.C. Lin, *J. Phys. Chem.*, **87** (1983) 3933
- [7] L.J. Medhurst, N.L. Garland, H.H. Nelson, *J. Phys. Chem.*, **97** (1993) 12275

In order to ascertain the origin of the observed negative pressure dependence, a master equation based on an isomerisation approach was utilised<sup>1</sup>. The concentration of  $H_2$  was assumed to be in such an excess that reaction with CH could be modelled as a pseudo-first order process. This allows the effects of vibrational relaxation of the CH radical to be accounted for. The overall scheme can be represented as:

$$\begin{aligned}\frac{dp^m}{dt} &= \omega(P-I)p^m - \sum_{l=0}^2 k_l p^m + k_{b,0}[H_2]p_{v=0} + k_{b,1}[H_2]p_{v=1} \\ \frac{dp_{v=0}}{dt} &= k_{1 \rightarrow 0}p_{v=1} - k_{0 \rightarrow 1}p_{v=0} + K_0 p^m - k_{b,0}[H_2]p_{v=0} \\ \frac{dp_{v=1}}{dt} &= k_{0 \rightarrow 1}p_{v=0} - k_{1 \rightarrow 0}p_{v=1} + K_1 p^m - k_{b,1}[H_2]p_{v=1}\end{aligned}\quad (4)$$

Preliminary results from this study will be presented.

## References

1. I.W.M. Smith and D. Stewart Personal communication
2. S.H. Robertson, M.J. Pilling and D.L. Baulch. *J. Phys. Chem.* **1995**, *99*, 13452
3. N.J.B. Green, P.J. Marchant, M.J. Perona, M.J. Pilling and S.H. Robertson. *J. Chem. Phys.* **1992**, *96*, 5896

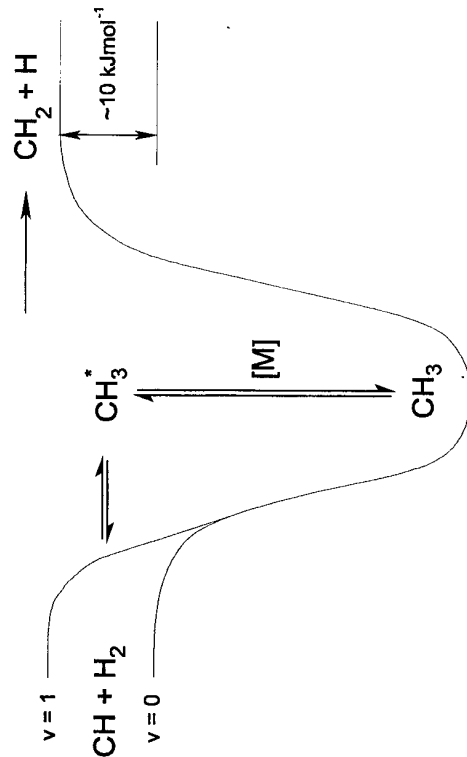


Figure 1.

## QUANTUM CHEMICAL AND QUANTUM STATISTICAL ANALYSIS (QRRK) ON REACTIONS OF $NH_2$ AND $HO_2$ RADICALS

R. Sumathi

*Lehrstuhl für Theoretische Chemie*

*Universität Bonn*

*Wegelerstrasse 12, 53115 Bonn.*

The reaction  $NH_2 + HO_2 \rightarrow$  Products, a reaction of atmospheric interest, has been studied using ab initio molecular orbital calculations with extended basis sets (6-311++G\*\* and 6-311++G(2df,2pd)), and a variety of methods accounting for electron correlation such as MP2 with all electrons, QCISD(T), CAS(8,8) and MRDCl. Also the performance of density functional (DFT) calculations has been investigated. Stationary points on the potential energy surface of  $NH_2 + HO_2$  giving rise to different products,  $HNO + H_2O$ ,  $NH_2O + OH$ ,  $NH_3 + O_2$ ,  $H_2O_2 + NH$ , and  $HNOO + H_2$ , have been optimised and characterised by their Hessian matrix. A new pathway of decomposition via isomerisation to amine oxide, which has hitherto never been identified either, has been considered for HNO formation. Amine oxide and dihydroxamine have been found to be the precursors for HNO formation. An attempt has been made to explain the experimental finding, nonobservation of OH during photolysis of ammonia. A rigorous quantum Rice-Ramsperger-Kassel (QRRK) analysis has been carried out on the chemically activated  $NH_2OOH$  adduct to calculate the apparent rate constants of available reaction channels over a range of temperatures (200-1900K) and pressures (0.001 to 10 atm.) with various bath gases. Our results demand for new experiments with spectroscopic identification of OH radicals.

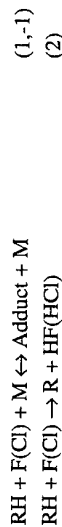
# HALOGEN ATOM ADDUCTS IN THE GAS PHASE

Merete Bilde, Jens Sehested and Trine E. Møgelberg  
*Section for Chemical Reactivity*  
*Environmental Science and Technology Department*  
*Risø National Laboratory*  
*DK-4000 Roskilde, Denmark*

Timothy J. Wallington  
*Ford Motor Company*  
*Ford Research Laboratory, SRL-E3083*  
*Dearborn, P.O. Box 2053*  
*Michigan 48121-2053, USA*

Ole J. Nielsen  
*Ford Forschungszentrum Aachen*  
*Dennewartsstrasse 25*  
*D-52068 Aachen, Germany*

A pulsed radiolysis technique was used to study the kinetics and mechanism of the reactions of F atoms with CH<sub>2</sub>BrCl in the gas phase. The general reaction scheme for halogenated methanes is a two channel mechanism:



where RH is the halogenated methane. Pressure dependency of the adduct formation channel will be discussed. A FTIR spectroscopic technique was used to study the kinetics and mechanism of the reactions of Cl atoms with CH<sub>2</sub>BrCl. UV spectra of alkyl radicals and adducts have been measured using the pulsed radiolysis technique and will be compared with UV spectra of F atom adducts with CH<sub>3</sub>Br and CF<sub>2</sub>BrH, respectively. Halogen atom adducts show characteristic absorptions in the region 270-320 nm.

<sup>1</sup> Scientific Assessment of Ozone Depletion: 1991, World Meteorological Organization global Ozone Research and Monitoring Project - Report No. 25.

<sup>2</sup> F. Wu and R. W. Carr, *J. Phys. Chem.*, 1992, 96, 1743

<sup>3</sup> T. Slagle and D. Gutman, *J. Amer. Chem. Soc.*, 1982, 104, 4741

## DEVELOPMENT AND APPLICATION OF LASER SPECTROSCOPIC TECHNIQUES FOR COMBUSTION DIAGNOSTICS

Marcus Alden

*Division of Combustion Physics, Lund Institute of Technology  
P.O. Box 118, S-221 00 Lund  
Sweden*

During the last decade different laser based diagnostic techniques have become very important tools for the understanding of combustion processes. The main advantages with these techniques are the feature of non-intrusiveness, the high spatial and temporal resolution and the possibilities to measure several species in multiple points. The spectroscopic laser based techniques are mainly used for species concentration measurements (atoms, radical and molecules), temperatures (rotational as well as vibrational temperature) and flow velocities. In the present paper some developments and applications of new as well as more mature techniques will be described. In the field of Coherent anti-Stokes Raman Scattering, CARS, rotational dual broadband CARS has proven to be a clear complement to the more conventional vibrational CARS, especially at elevated pressure ( $> 5$  bar) and lower temperature ( $< 1000$  K). This technique will be described and exemplified by experiments in an IC engine. A variant of vibrational CARS, 2-1 CARS, its advantages and limitations will also be briefly described. In the field of Laser-Induced Fluorescence, LIF, developments of multiphoton detection, multiple species imaging and practical applications in engines and gas turbines will be described. In the area of new techniques, not yet applied in "real" combustion apparatus, Polarization Spectroscopy, PS, and Stimulated Emission, SE, will be described and exemplified by laboratory flame experiments. The paper will be concluded with a discussion of potential laser-induced disturbances in flames caused by the high-power laser beam and how these can be minimized.

## AUTOMATIC GENERATION OF LUMPED MECHANISMS IN THE OXIDATION OF ALKANES

R. Fournet, V. Warth, P.A. Glaude, G.M. Côme, F. Battin-LeClerc and  
G. Scacchi

*Département de Chimie Physique des Réactions  
URA n°328 CNRS, INPL-ENSIC and Université de NANCY I  
I, rue Grandville - BP 451 - 54001 NANCY Cedex - France*

There is an increasing need for the development of well validated and reliable models to represent the combustion phenomena in spark ignited engines, in order to formulate gasolines which present optimal octane number properties and which lead to minimal pollutants formation. These models require the development of chemical mechanisms, to reproduce the combustion reactions, which can be embedded in three dimensional computational fluid dynamic codes in order to be employed to model the reactive flows found in real combustion devices. At the moment, a complete mechanism for modelling the combustion of organic compounds includes several thousands of elementary reactions and thus cannot be incorporated in such codes due to the present limitations of computer hardware. This leads to an urgent need of techniques to reduce the size of complex chemical mechanisms.

Our laboratory has developed a software (EXGAS) which produces automatically generated mechanisms and the associated thermochemical and kinetic data to model the gas-phase oxidation of alkanes or ethers, in a format compatible with CHEMKIN II [1]. A mechanism generated by using EXGAS includes three parts:

- A reaction base (C0-C2 reaction base) including all the unimolecular or bimolecular reactions involving radicals or molecules containing less than three carbon atoms and which lead to radicals or molecular products containing less than three carbon atoms [2].

- A primary mechanism, that is to say a mechanism in which the only molecular reactants are the initial organic molecules and  $O_2$ . This mechanism is generated by writing systematically all the generic propagating reactions,  $O_2$  additions, isomerizations, betascissions, decompositions to cyclic ethers, oxidations, metatheses, for all the radicals created either by initiations or by propagations. The rules which govern the reaction generation are those which are currently used to write the alkanes oxidations mechanisms in the literature [3-5]. In fact, this mechanism can be already simplified during the generation according to the Goldfinger-Letort-Niclaude rules [6] and by lumping the primary molecular products.

- A secondary mechanism including reactions whose reactants are the lumped molecular products formed by the primary mechanism. To avoid an exponential increase of the size of the generated mechanism, the secondary mechanism is not generated in the same comprehensive way as the primary mechanism. The reaction of the lumped molecules produced in the primary mechanism are not elementary steps, but lumped reactions which lead in the smallest number of steps to free radicals and molecules whose reactions are included in the C0-C2 database.

The relevant thermochemical data are calculated by using a software (THERGAS) developed in our department [7] and the kinetic data are either calculated by using a software (KINGAS) [8] or estimated by means of correlations. The kinetic data which are used in the CO-C2 database were found in the literature and are mainly those proposed by Baulch et al. [9] and Tsang et al. [10].

The present work describes a technique of reduction, developed by Ranzi et al. [11], and based on the chemical lumping of species involved in the primary mechanism mentioned above. The first step of the procedure consists to lump the free radicals which have the same molecular formula and the same functional group and to generate automatically the corresponding lumped mechanism. The concentration of a lumped species is equal to the sum of the concentrations of the real isomers, so that there is no mass balance problem with this kind of lumping.

At this stage, the problem is to estimate the rate constants of the lumped reactions which permit to obtain results in a good agreement with the detailed mechanism. A reliable starting point for this optimization is obtained for the lumped reaction as a weighted average of the rate coefficients of the relevant elementary steps in the complete mechanism. More exactly, by assuming that the propagation chains are long, it is possible to apply the quasi-stationary state (AEQS) for each free radicals involved in the detailed mechanism. Thus, the relative concentration of free radicals can be calculated by solving a linear system of equations. For each reaction, we define the rate of the reaction by:

$$r_1 = k_1[Rad]_1,$$

where  $k_1$  represents the rate constant of the  $i^{th}$  reaction and  $[Rad]_1$  the concentration of the free radical involved in this reaction and calculated in the approximation of quasi-stationary state. Now, if we consider two reactions of the detailed mechanism lumped in one reaction, the kinetic constant of the lumped reaction can be written as:

$$k_1 = \frac{k_1 r_1 + k_2 r_2}{r_1 + r_2},$$

where  $k_1$ ,  $k_2$  represent the kinetic constants for the two reactions of the detailed mechanism,  $k_1$  the kinetic constant for the corresponding lumped reaction and  $r_1$ ,  $r_2$  the corresponding rate associated to the detailed reactions. This approach has permitted to strongly reduce the primary mechanism. By example in the case of the oxidation of iso-octane the number of species has decreased from 581 to 92 and from 642 to 100 for the n-heptane. The results obtained give results in a good agreement with those obtained with the complete mechanisms.

In conclusion, this chemical lumping process can be automatically operated, leads to the minimum loss of chemical and kinetic information and provides a good starting point for further mathematical reduction techniques mentioned above. A second step, which has been started recently, consists to perform an automatic optimization of all the kinetic parameters involved in the lumped mechanism in order to obtain results in better agreement with those computed by using the complete mechanism. The technique based on SIMPLEX method with non-linear constraints has been applied "manually" in the case of the oxidation mechanism of n-butane and give good results. However, for increasing mechanism, this procedure no longer works and the development of a new fastest optimisation procedure must be viewed.

## REFERENCES

- (1) Kee R.J., Rupley F.M. and Miller J.A. (1993), "Chemkin II. A fortran chemical kinetics package for the analysis of gas phase chemical kinetics". Sandia Laboratories Report, SAND 89 - 8009B.
- (2) Barbé P., Batin-Leclerc F. and Côme G.M. (1995), *J. Chim. Phys.*, **92**, 1666.
- (3) Fish A. (1968), *Angew. Chem.*, Int. ed., **7**, 45.
- (4) Kirsch L.J. and Quinn C.P. (1984), *J. Chim. Phys.*, **82**, 5.
- (5) Cox R.A. and Cole J.A. (1985), *Comb. Flame*, **60**, 109.
- (6) Laidler K.J. (1987), *Chemical Kinetics*, 3<sup>rd</sup> Ed. Harper & Row.
- (7) Muller C., Michel V., Scacchi G. and Côme G.M. (1995), *J. Chim. Phys.*, **92**, 1154.
- (8) Bloch-Michel V. (1995), *Logiciel d'estimation de paramètres cinétiques de processus élémentaires en phase gazeuse*. Thèse, Nancy.
- (9) Baulch D.L., Cobos C.J., Cox R.A., Franck P., Hayman G.D., Just Th., Kerr J.A., Murrells T.P., Pilling M.J., Troe J., Walker R.W. and Warnatz J. (1994), *Comb. Flame*, **98**, 59.
- (10) Tsang W. and Hampson R.F. (1986), *J. Phys. Chem. Ref. Data*, **15**, n°3, 1087.
- (11) Ranzi E., Faravelli T., Gaffuri P., Pennati G. and Sogaro A. (1995), *Comb. Flame*, **102**, 179.

# OXIDATION OF THE METHYL RADICAL: RATE FOR THE $\text{CH}_3 + \text{O}_2 \rightarrow \text{H}_2\text{CO} + \text{OH}$ CHANNEL

Jan P. Hessler, Hong Du, Paul J. Ogren, and Albert F. Wagner

Chemistry Division, Argonne National Laboratory  
9700 So. Cass Ave., Argonne, Illinois 60439 U.S.A.

The rate coefficient for the titled reactions has been measured by monitoring the time-dependent absorption profile of hydroxyl immediately behind incident shock waves. High  $\text{O}_2$ -to- $\text{CH}_3$  ratios were used to ensure methyl-methyl recombination does not influence the results. We present a rigid-rotor isomerizing model for vibrational relaxation. By using this model we can calculate when  $\text{O}_2$  has attained vibrational equilibrium or extract rate coefficients within the transition region. A more realistic model for secondary chemistry has been developed by including unpublished results of Pilling *et al.* for the high-pressure limit for methanol formation and recent results of Grotheer *et al.* for the  $\text{H}_2 + \text{HCOH}$  channel. When helium is used to efficiently relax the oxygen molecules the equilibrium rate coefficient is given by

$$k(T) = 1.24 \times 10^{-12} \exp \left[ -7172 / T(\text{K}) \right] \text{ cm}^3 \text{ s}^{-1}.$$

This result is in good agreement with RRKM calculations based upon the electronic structure calculations of Walch which give an activation energy of 13.7 kcal/mole (57.3 kJ/mole). Our activation energy agrees with the value reported by Braun-Unkoff *et al.* at the 13th International Symposium on Gas Kinetics. However, at 1200 K our rate is a factor of 3.7 higher.

# KINETIC STUDY OF NCO RADICAL REACTIONS WITH SELECTED MOLECULES AND ATOMS

K.H. Becker, R. Kurtenbach, F. Schmidt, and P. Wiesen

Physikalische Chemie / Fachbereich 9, Bergische Universität - Gesamthochschule  
Wuppertal, D-42097 Wuppertal, Germany

NCO radicals are important intermediates in combustion processes, in particular in the conversion of fuel nitrogen into nitrogen oxides and in the so called "prompt" NO formation process [1]. NCO radicals are formed either by the reaction of HCN with oxygen atoms or the reaction of CN radicals with OH radicals or  $\text{O}_2$ . In addition, the NCO radical is a key intermediate in  $\text{NO}_x$  reduction processes such as the RapRe $\text{NO}_x$  and the thermal De $\text{NO}_x$  process [2,3].

In the present work, the gas-phase reactions of  $\text{NCO}(\text{X}^2\text{I})$  radicals with  $\text{NO}$ ,  $\text{NH}_3$ ,  $\text{C}_2\text{H}_2$  and oxygen atoms were studied over a wide temperature and pressure range. NCO radicals were generated by excimer laser photolysis of  $\text{ClNCO}$  at 248 nm and were detected by laser-induced fluorescence at 438.6 nm.

In Fig. 1 the bimolecular rate constants obtained in the present study are plotted as a function of temperature in comparison with literature data. Using the modified Arrhenius expression  $k(T) = \text{B} \times T^n \exp(-E_0/RT)$ , the rate constant is well described by:

$$k_{\text{NCO}+\text{NO}}(T) = \left(1.45^{+0.55}_{-0.35}\right) \times 10^{-5} \times T^{(-1.98 \pm 0.06)} \times \exp \left[ - \left(3.74^{+0.91}_{-0.83} \right) / RT \right] \text{ cm}^3 \text{ s}^{-1},$$

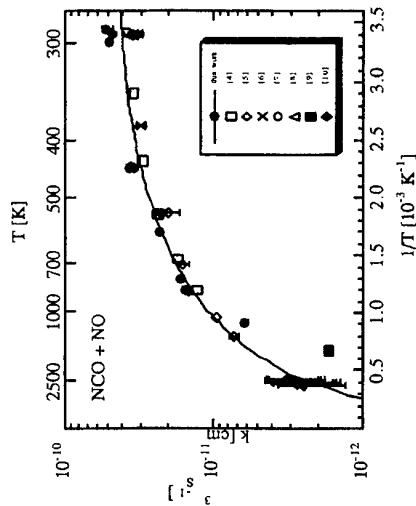
with  $E_0$  in kJ/mol. The results from the present study are in excellent agreement with recent literature data.

The  $\text{NCO} + \text{NH}_3$  reaction was found to be pressure independent. The observed positive temperature dependence could be described by a simple Arrhenius expression with an activation energy of  $(13.9 \pm 0.7)$  kJ/mol, see Fig. 2. Since the Arrhenius plot shows a slight upwards curvature in the temperature range investigated one can use the modified Arrhenius equation to describe the experimental data. This is shown by the solid line in Fig. 2. The rate constant is well described by:

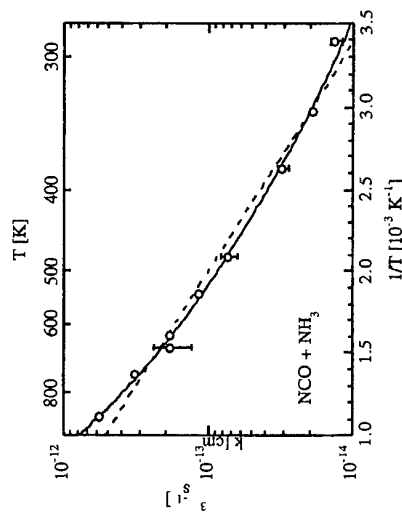
$$k(T) = \left(4.6^{+1.1}_{-1.8}\right) \times 10^{-20} \times T^{(2.48^{+0.06}_{-0.07})} \times \exp \left[ - \left(4.1^{+2.6}_{-0.9} \right) / RT \right] \text{ cm}^3 \text{ s}^{-1},$$

with  $E_0$  in units of kJ/mol. Possible reaction products are  $\text{HNCO}$  and  $\text{NH}_2$  radicals which can be formed by a simple H-atom abstraction from ammonia.

The rate constant of the  $\text{NCO} + \text{C}_2\text{H}_2$  was found to be pressure independent. The positive temperature dependence of the  $k$ -values could be well described in the temperature range 298 - 597 K by a simple Arrhenius expression with an activation energy of  $(7.6 \pm 0.2)$  kJ/mol. Possible reaction products are HCN and HCCO which can be formed via a five-membered cyclic aromatic complex which can undergo a 1,3-H-shift. Further experiments at  $T > 1000$  K as well as a product analysis and calculations of the reaction path would be very helpful to elucidate the reaction mechanism of this reaction.



**Fig. 1:** Temperature dependence of the bimolecular rate constant  $k_{\text{NCO}+\text{NO}}$  for the  $\text{NCO} + \text{NO}$  reaction at 20 Torr total pressure argon. The solid line is a least squares fit of a modified three parameter Arrhenius equation to the corresponding data.



**Fig.2:** Temperature dependence of the bimolecular rate constant  $k_{\text{NCO}+\text{NH}_3}$  at 20 Torr total pressure argon. The dashed line is a weighted, linear least

squares fit of a simple Arrhenius equation, the solid line represents a least squares fit of a modified three parameter Arrhenius fit to the corresponding data.

The reaction of NCO radicals with oxygen atoms was studied in the temperature range 302 - 757 K. The Arrhenius diagram showed a negative temperature dependence with a strong downwards curvature. The rate constant of this reaction is sufficiently described by:

$$k(T) = 1.1 \times 10^{-7} \times T^{-1.3} \text{ cm}^3 \text{ s}^{-1},$$

with  $E_0 = 0$ . The reaction  $\text{NCO} + \text{O}$  possibly leads to the formation of  $\text{NO} + \text{CO}$ .

#### Acknowledgement:

Financial support by the "Deutsche Forschungsgemeinschaft (DFG)" and the "Ministerium für Wissenschaft und Forschung des Landes Nordrhein-Westfalen (MWF)" is gratefully acknowledged.

#### References:

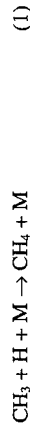
- 1) J.A. Miller and C.T. Bowman, *Prog. Energy Combust. Sci.* 15, 287 (1989).
- 2) D.L. Siebers and J.A. Caton, *Comb. Flame* 79, 31 (1990).
- 3) R.K. Lyon, *Environ. Sci. Technol.* 21, 231 (1987).
- 4) D.Y. Juang, J.-S. Lee, and N.S. Wang, *Int. J. Chem. Kinet.* 27, 1111 (1995).
- 5) B. Atakan and J. Wolfrum, *Chem. Phys. Lett.* 178, 157 (1991).
- 6) R.A. Perry, *J. Chem. Phys.* 82, 5485 (1985).
- 7) G. Hancock and K.G. McKendrick, *Chem. Phys. Lett.* 127, 125 (1986).
- 8) J.L. Cookson, G. Hancock and K.G. McKendrick, *Ber. Bunsenges. Phys. Chem.* 89, 335 (1985).
- 9) R.A. Fifer and H.E. Holmes, *J. Phys. Chem.* 86, 2935 (1982).
- 10) J.D. Mertens, A.J. Dean, R.K. Hanson and C.T. Bowman, *24th Symp. (Int.) Combust., [Proc.]*, (1992) 701.

# TEMPERATURE AND ISOTOPE DEPENDENCE OF THE REACTION OF METHYL RADICALS WITH DEUTERIUM ATOMS

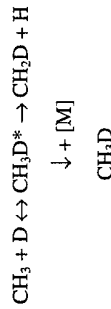
F.L. Nesbitt, W.A. Payne, L.J. Stief, and R.P. Thorn  
*Laboratory for Extraterrestrial Physics, NASA Goddard Space Flight Centre,  
 Greenbelt, MD, 20771, USA.*

M.J. Pilling, S.H. Robertson and P.W. Seakins  
*School of Chemistry, University of Leeds, Leeds, LS2 9JT, UK.*

The reaction of methyl radicals with hydrogen atoms can be an important termination reaction in combustion and simplicity of the reaction has made it an ideal candidate for theoretical study.



In contrast to many other radical recombination reactions, the high pressure limiting rate coefficient,  $k_1^-$ , is predicted to have a positive temperature dependence.<sup>1</sup> Verification of this prediction is difficult as reaction (1) is well into the fall off region under laboratory conditions and significant extrapolations are required. Brouard *et al.* recognised that deuterium atom substitution should, after appropriate correction, yield  $k_1^-$  as reaction degeneracy and zero point energy differences make redissociation of the  $\text{CH}_3\text{D}$  complex to reagents an insignificant process.



However, the values of  $k_1^-$  obtained by Brouard *et al.* from extrapolation of reaction (1) and from the isotopic reaction did not agree casting doubt on either the experimental data, the method of extrapolation or less likely, an unusual isotope dependence of reaction (1).

The reactions of the methyl isotopomers  $\text{CH}_3$ ,  $\text{CH}_2\text{D}$  and  $\text{CHD}_2$  with excess D atoms have been studied by discharge flow/mass spectrometry at 300 K and at pressures of  $\sim 1$  Torr (helium). Methyl radicals and D atoms are generated simultaneously at the tip of a sliding injector by the reaction of F atoms with excess methane and deuterium. Concentrations of methane and deuterium were altered to vary the ratio of reagents. Under these conditions the initially formed methane complex is not stabilised and hydrogen exchange is the predominant reaction.

The generation of methyl radicals is significantly faster than reaction but, along with minor secondary reactions, need to be included in a numerical analysis of the methyl decay curve. Variation of  $[\text{D}]$  gives the bimolecular plot from which the rate coefficients are taken. The following bimolecular rate coefficients were obtained:



The experimental values can be corrected for isotopic substitution and averaged to give a value of  $k_1^- = 2.78 \times 10^{-10} \text{ cm}^3 \text{ molecule}^{-1} \text{ s}^{-1}$  for the high pressure recombination of  $\text{CH}_3 + \text{H}$ . This result is in good agreement with the earlier direct determination via isotopic substitution by Brouard *et al.*

Reanalysis of the  $\text{CH}_3 + \text{H}$  data of Brouard *et al.* using master equation techniques shows that these data are compatible with the present values of  $k_1^-$  and illustrate the problems of making accurate extrapolations of  $k_1^-$  from data in the fall off region.

The reaction of  $\text{CH}_2\text{D}$  with D was also studied at 200 K, with the rate coefficient,  $k_{1\text{c}}^-$ , falling by approximately 35 % from its room temperature value. This result is close to theoretical predictions of Robertson *et al.*

1. Brouard, M.; Macpherson, M.T.; Pilling, M.J. *J. Phys. Chem.* **1989**, *93*, 4047.
2. Robertson, S.H.; Wagner, A.F.; Wardlaw, D.M. *J. Chem. Phys.* **1995**, *103*, 2917.

# KINETICS OF THE $C_2H_3 + H_2 \leftrightarrow H + C_2H_4$ AND $CH_3 + H_2 \leftrightarrow H + CH_4$ REACTIONS

Vadim D. Knyazev, Ákos Bencsura, Stanislav I. Stoliarov, and Irene R. Slagle

Department of Chemistry, The Catholic University of America, Washington, DC  
20064, USA

## The kinetics of the reactions



and

have been studied in the temperature ranges 499-947 K (reaction 1) and 646-1104 K (reaction 2) at He densities  $(6-18) \times 10^{16}$  atom  $cm^{-3}$  by Laser Photolysis / Photoionization Mass Spectrometry. Rate constants were determined in time-resolved experiments as a function of temperature (Figures 1 and 2). Within the above temperature ranges the experimental rate constants can be represented by Arrhenius expressions:

$$k_1 = (3.42 \pm 0.35) \times 10^{-12} \exp(-4179 \pm 67 \text{ K}/T) \text{ cm}^3 \text{ molecule}^{-1} \text{ s}^{-1}$$

$$k_2 = (1.45 \pm 0.18) \times 10^{-11} \exp(-6810 \pm 102 \text{ K}/T) \text{ cm}^3 \text{ molecule}^{-1} \text{ s}^{-1}$$

Experimental values of  $k_2$  are in agreement with the available literature data (Figure 2). Ethylene was detected as a primary product of reaction 1.

The potential energy surface and properties of the transition state for reaction (1,-1) were studied by ab initio methods. Experimental and ab initio results of the current study were analyzed and used to create a transition state model of the reaction. The resulting model provides the temperature dependencies of the rate constants for both direct (1) and reverse (-1) reactions in the temperature range 200-3000 K:

$$k_1 = 1.57 \times 10^{-20} T^{2.56} \exp(-2529 \text{ K}/T) \text{ cm}^3 \text{ molecule}^{-1} \text{ s}^{-1}$$

$$k_{-1} = 8.42 \times 10^{-17} T^{1.93} \exp(-6518 \text{ K}/T) \text{ cm}^3 \text{ molecule}^{-1} \text{ s}^{-1}$$

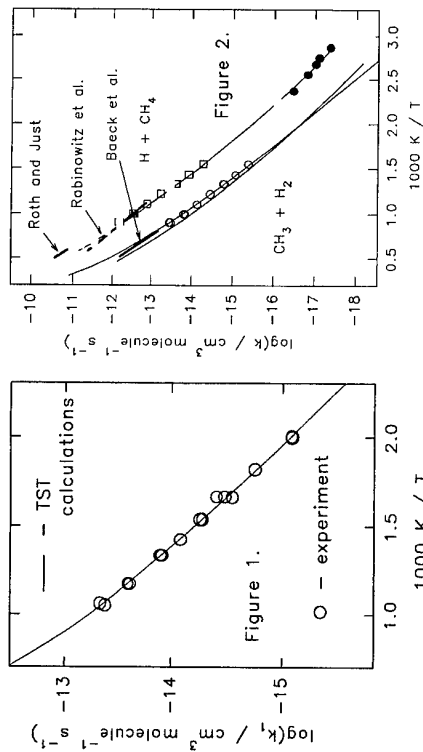


Figure 1.

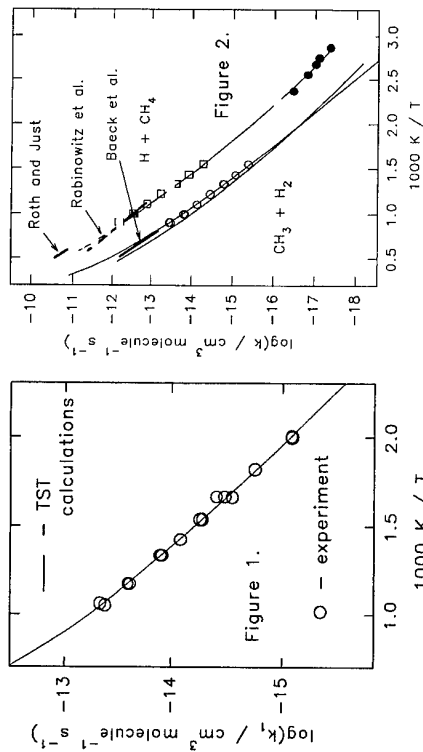


Figure 2.

Figure 1. Experimental and calculated temperature dependencies of the  $C_2H_3 + H_2 \rightarrow H + C_2H_4$  reaction rate constant.

Figure 2. Plot of the rate constants of reactions 2 and -2. Experimental data: open circles -  $k_2$  values of the current study, open squares - the same data converted to  $k_2$  values, closed circles -  $k_2$  values from Marquaire et al. [1], heavy lines -  $k_2$  from Baek et al. [2] and  $k_2$  from Roth and Just [3] and Rabinowitz et al. [4]. Calculated values (thin lines): solid lines -  $k_2$  and  $k_{-2}$  from Marquaire et al. [1], dashed line - recommendation on  $k_2$  from Baulch et al. [5].

## References for Figure 2:

1. Marquaire, P.-M.; Dastidar, A. G.; Manthorne, K. C.; Pacey, P. D. *Can. J. Chem.* **1994**, *72*, 600.
2. Baek, H. J.; Shin, K. S.; Yang, H.; Qiu, Z.; Lissianski, V.; Gardiner, W. C., Jr. *J. Phys. Chem.* **1995**, *99*, 15925.
3. Roth, P.; Just, Th. *Ber. Bunsen-Ges. Phys. Chem.*, **1975**, *79*, 682.
4. Rabinowitz, M. J.; Sutherland, J. W.; Patterson, P. M.; Klemm, R. B. *J. Phys. Chem.* **1991**, *95*, 674.
5. Baulch, D. L.; Cobos, C. J.; Cox, R. A.; Esser, C.; Frank, P.; Just, Th.; Kerr, J. A.; Pilling, M. J.; Troe, J.; Walker, R. W.; Warnatz, J. *J. Phys. Chem. Ref. Data* **1992**, *21*, 411.

# FLOW REACTOR INVESTIGATION OF THE REACTION BETWEEN PHENYL RADICALS AND OXYGEN

R.S. Tranter, H.H. Grotheer, Th. Just.

DLR Stuttgart.

The reaction between phenyl radicals,  $\Phi$ , and  $O_2$  has been identified as a key reaction in soot formation mechanisms. The reaction was investigated in a fast flow reactor over the temperature range 420 K to 850 K and at pressures of 10 mbar and 0.7 mbar. The 10 mbar data is fitted very well by a semi empirical Troe calculation using a reaction enthalpy of 46 kcal mol<sup>-1</sup>. The 0.7 mbar data does not exhibit the expected fall off behaviour and we are investigating this further.

In earlier work Frank et al [1] have studied the title reaction in a shock tube between 1150 and 1500 K. Under their experimental conditions they found that the excited adduct,  $\Phi O_2^*$ , decomposed by two routes, one giving H atoms and the other giving O atoms. These routes are shown with their respective products, quinone and phenoxy, as paths 2a and 2b in Fig.1. Recently, the high temperature channels observed by Frank et al have been confirmed by Michael and Kumaran [2] in their shock tube at Argonne. Although Michael and Kumaran find a different temperature dependency for the two reactions than Frank et al. there is good agreement between the two sets of data over the experimental range.

There have been several studies carried out at lower temperatures than the shock tube work [3]. The agreement between the various data sets is poor although the majority of the data suggest that a rate coefficient of the order  $10^{13}$  cm<sup>3</sup> molecule<sup>-1</sup> s<sup>-1</sup> is reasonable. In 1994 [4] Lin and Yu measured the rate coefficient for the title reaction between 300 K and 500 K and found a rate coefficient of  $1 \times 10^{11}$  cm<sup>3</sup> molecule<sup>-1</sup> s<sup>-1</sup> which was significantly higher than the earlier values. The Lin and Yu method and the earlier measurements monitored  $\Phi$  decay by optical absorption techniques. It was later shown that  $\Phi O_2$  also absorbed at the monitored frequency and this lead to apparently slower losses of  $\Phi$  radicals than were actually occurring. The 1994 data of Lin and Yu were obtained at a frequency where cross absorption did not occur.

At low temperatures, < 500 K, the reaction of  $\Phi + O_2$  is dominated by stabilisation of the excited adduct and is close to the high pressure limit [2,4]. Whereas above 1000 K the stabilisation channel reaches an early steady state and the two decomposition channels 2a and 2b dominate. The reaction scheme is summarised below, Fig. 1. The channel labelled 'w' permits deactivation of  $\Phi O_2^*$  at the wall (see later).

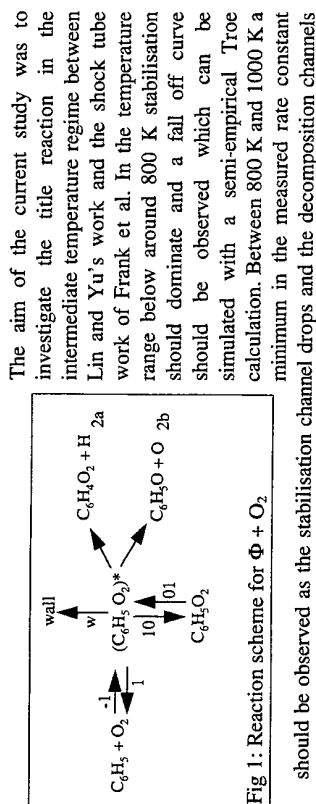


Fig 1: Reaction scheme for  $\Phi + O_2$

The flow reactor has been described in detail elsewhere [5]. Basically it consists of an HF washed, 25.5 mm i.d. quartz tube which is heated by a copper block. The flow tube is coupled to a quadrupole mass spectrometer by a conventional nozzle and skimmer arrangement. Time resolution is achieved by injecting the  $\Phi$  radicals via a movable injector into the main flow which contains  $O_2$ . Phenyl radicals are generated by passing  $\Phi NO$  over a tungsten coil at 900 °C. Approximately 98% of the  $\Phi NO$  is decomposed and initial radical concentrations of  $< 5 \times 10^{11}$  molecules cm<sup>-3</sup> are obtained. The phenyl decays are measured under pseudo first order conditions in an excess of  $O_2$ . Oxygen concentrations between 10 and 1000 times greater than the phenyl radical concentration were used. The bimolecular rate coefficients were extracted by plotting the pseudo first order rate coefficient against  $O_2$  concentration. The phenyl signal was monitored directly using an ionisation energy of 13 eV and a small correction [5] was made for  $\Phi NO$  which survived the pyrolysis source. With this combination of radical source and furnace the maximum achievable temperature in the reactor was 850 K. Reaction products could not be monitored due to the unavoidable formation of side products in the pyrolysis source.

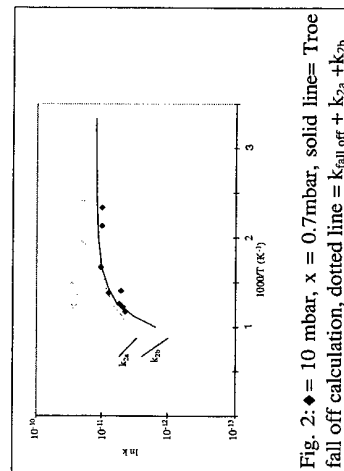


Fig. 2:  $\diamond = 10$  mbar,  $x = 0.7$  mbar, solid line = Troe fall off calculation, dotted line =  $k_{fall\ off} + k_{2a} + k_{2b}$

Within our temperature range it could be expected that the phenyl radical decay curves will exhibit an equilibrium due to the interplay between reactions 1, -1, 10 and 01. However no experimental evidence for this equilibrium has been found.

At 10 mbar the data show the predicted fall off behaviour and a Troe calculation based upon  $\Delta H^\circ = 46$  kcal mol<sup>-1</sup> fits the data very well. Compared to Melius's [6]

value for  $\Delta H^\circ$  this value is high but reasonable. At 0.7 mbar the expected fall off behaviour was not observed. Instead there was a slight increase in the rate coefficient with temperature.

# EXPERIMENTAL AND MODELLING STUDY OF THE OXIDATION OF ISOBUTENE

J.C. Bauge, F. Battin-LeClerc and D. F. Baronet

Département de Chimie-Physique des Réactions  
URA n° 328 CNRS, INPL-ENSIC and Université de Nancy I  
1, rue Grandville - BP 451 - 54001 NANCY Cedex - France

Methyl tert-butyl ether (M.T.B.E.) and Ethyl tert-butyl ether (E.T.B.E.) have high octane numbers (blending research octane number up to 130) and may be added in substantial amounts (up to 10, even 15%) to gasolines to replace lead additives to control engine knock. These oxygenates rapidly produce isobutene as an intermediate. It is then interesting to study the oxidation of this olefin to understand the effect of these ethers on the octane number since isobutene has been identified as their decomposition product responsible for their antiknock effectiveness [1].

The low temperature oxidation was studied in a continuous flow stirred reactor tank (CFSTR) operated at constant temperature (from 833 to 913 K) and pressure (1atm), with fuel equivalence ratios from 3 to 6 and space times ranging from 1 to 10 seconds corresponding to isobutene conversion yields from 1 to 50 %. The main carbon containing products analysed by gas chromatography are carbon monoxide, carbonyl dioxide, methane, ethylene, propene, allene, isoprene, 2-methyl-2-butene, 2-methyl-1-butene, methacrolein and isobutyraldehyde.

The ignition delays of isobutene-oxygen-argon mixtures with fuel equivalence ratios from 1 to 3 were measured behind shock waves. Reflected shock waves permitted to obtain temperatures from 1230 to 1930 K and pressures from 9.5 to 10.5 atm. The onset of ignition was detected by OH radical emission at 306 nm through a quartz window with a photomultiplier fitted with a monochromator at the end of the reaction section.

A mechanism has been proposed to reproduce the profiles obtained for the reactants consumption and the products formation during the slow oxidation and to compute the ignition delays in the shock tube. This one splits into two parts: first, a primary and a secondary mechanism includes reactions involving radicals or molecules containing more than three carbon atoms (135 reversible reactions), this mechanism is then completed by a reaction base for C0-C2 hydrocarbons [2] (440 reactions).

Simulations were performed using the CHEMKIN II software. A correct agreement between the simulated values and the experimental data has been obtained in both reactors, as shown in figure 1 in the case of the shock tube data. The main

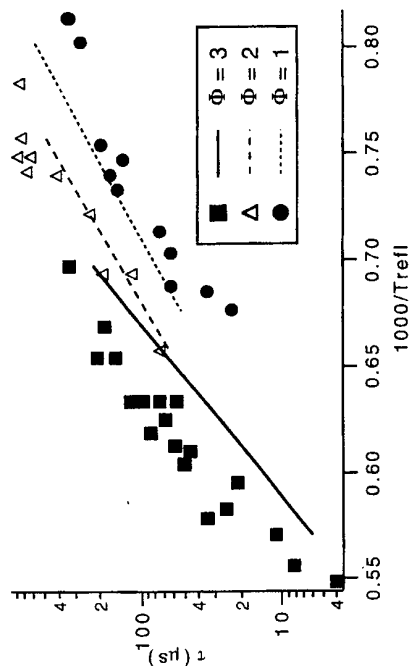
In an attempt to explain this behaviour we have assumed that  $\Phi O_2^*$  can be deactivated at the walls to form some unspecified stable products which do not include  $\Phi O_2$  (path 'w', Fig. 1). Obviously, the wall effect will be more competitive at low pressures than at high pressures. To test this hypothesis a 2D calculation  $\gamma/\gamma_0$  was performed which incorporated reactions 1, -1, 10, 01 and w from Fig.1. The effect of the wall is most sensitive at about 800 K, i.e. under conditions where channels 2a and 2b may be neglected. The wall efficiency is accounted for by a multiplying factor,  $\gamma$ , which represents the fraction of collisions which result in destruction of  $\Phi O_2^*$  at the wall. The results of the calculation are that at 0.7 mbar the simulated phenyl decay coefficient increases by more than a factor of 2 when  $\gamma$  is increased from 0 to 1. When the model was modified to yield stabilised  $\Phi O_2$  as the product of the wall reaction the simulated decay curves changed significantly and an approach to an equilibrium was predicted for both  $\gamma=0$  and  $\gamma=1$ . We have not observed an equilibrium experimentally. However our experimental timescale falls within the approach to equilibrium predicted by the model and does not extend as far as the establishment of the equilibrium. Conversely, at 10 mbar varying  $\gamma$  has virtually no effect on the simulated curves. A more refined calculation which includes energy dependent rate coefficients is currently being performed.

In an attempt to provide 'cleaner' conditions for analysis of the reaction products a new phenyl source utilising  $Na + \Phi Br$  has been tested in a static injector and a mobile version is being constructed. The mobile Na source will also be coupled to a new high temperature reactor which will overlap with the shock tube temperatures. With this new apparatus it should be possible to monitor the reaction products and it may be possible to distinguish between gas phase and wall products thus providing a link between the shock tube work, flow reactor work and the 2D calculations.

## References

1. Frank P., Herzler J., Just Th., Wahl C., 25<sup>th</sup> Int. Symp. Combust., **25**, 833, (1994).
2. Michael J.V., Kumaran S.S., Unpublished work.
3. a) Preidel M., Zellner R.; Ber. Bunsenges. Phys. Chem., **93**, 1417, (1989). b) Baldwin R.R., Scott M., Walker R.W.; 21<sup>st</sup> Int. Symp. Combust. **21**, 991, (1986). c) Fahr A., Mallard W.G., Stein S.E.; 21<sup>st</sup> Int. Symp. Combust. **21**, 825, (1986).
4. Yu T., Lin M.C.; J. Am. Chem. Soc., **116**, 9571, (1994).
5. Schaugg J., Tranter R.S., H.H. Grotheer, 8<sup>th</sup> Int. Symp. Transport Phenomena in Combust. San Francisco, July 1995.
6. Melius C.F. Private communication.
7. Farmanara P., Grotheer H.H., Just Th. Unpublished work.

reaction paths have also been determined for both series of measures by a sensitivity and rate of production analysis.



**Figure 1** Semi-log plot of ignition delays as a function of temperature behind the shock wave for three different equivalence ratios. The three mixtures contain 3.65 % of isobutene. Solid lines are the results of calculations by using the computer model of the reaction system.

## References

- (1) K. Brezinski and F.L. Dryer (1986): "A flow reactor study of the oxidation of isobutylene and an iso-butylene / n-octane mixture", *Combust. Sci. and Tech.*, **45**, 225-232.
- (2) P. Barbé, F. Battin-Leclerc and G.M. Côme (1995): "Experimental and modelling study of methane and ethane oxidation between 773 and 1573 K", *J. Chim. Phys.*, **92**, 1666-1692.

## THE PECULIARITIES OF HYDROCARBON OXIDATION IN A "WALL-LESS" REACTOR UNDER LASER HEATING

Adolph A. Mantashyan

*Institute of Chemical Physics of NAS of Armenia*

The results of the investigations of hydrocarbon-oxygen mixtures conversion processes under the condition of laser heating are represented. The wall of the reactor is being at room temperature. Under such condition the heterogeneous conversion of the initial reagents and the intermediate products is excluded. It becomes possible to carry out the chemical reaction in a "wall-less" reactor and get an information on the processes which take place directly in the gas phase. The results obtained make possible to reveal the main steps of the homogeneous conversion.

The conversion of the simplest hydrocarbons mixtures with oxygen have been studied [1, 2].

The process was carried out under static conditions in a glass cell ( $d=50\text{mm}$ ,  $l=120\text{ mm}$ ), both end of the cell being supported with windows made of NaCl-transparent to IR-radiation of  $\text{CO}_2$  laser.

Propane is the simplest hydrocarbon which shows complete variety of phenomena typical for hydrocarbon oxidation (cool flame, negative temperature coefficient, oscillations etc.) and also represents all types of possible elementary reactions which define the complex of oxidative process.

The process was studied at different  $\text{C}_3\text{H}_8:\text{O}_2$  ratio and different power of laser radiation. Conversion starts up when the radiating power is not less than 11 W. At this the temperature inside a laser beam exceeds 800K. Only propane is consumed during the process, while the oxygen concentration is not changed. Ethylene, propylene, methane and hydrogen were found as main reaction products. Oxygen containing products were detected in a trace concentration and do not exceed 1%. In other words, propane practically undergoes only the cracking reactions. However the conversion does not proceed without oxygen. Apparently this interesting facts are a result of extraordinary non-conventional approach to the realization of hydrocarbon-oxygen mixtures conversion. Chain initiation in a "wall-less" reactor can occur only in a homogeneous way: a)  $\text{RH}+\text{O}_2 = \text{R}+\text{HO}_2$  and provide appropriate rate only at high temperatures. On the other hand  $\text{RO}_2$  radicals formation is impeded because of equilibrium shift in the reversible reaction to the left: b)  $\text{R}+\text{O}_2 \leftrightarrow \text{RO}_2$ . As a result alkyl (R) radicals concentration significantly exceeds that of peroxy ( $\text{RO}_2$ ) radicals, and therefore alkyl radicals reactions take the main role, leading to olefins formation:  $\text{C}_3\text{H}_7 = \text{C}_3\text{H}_6+\text{H}$ ;  $\text{C}_3\text{H}_7 = \text{C}_2\text{H}_4+\text{CH}_3$ , then  $\text{H}+\text{C}_3\text{H}_8 = \text{C}_3\text{H}_7+\text{H}_2$ ;  $\text{CH}_3+\text{C}_3\text{H}_8 = \text{CH}_4+\text{C}_3\text{H}_7$ .

This notion is substantiated by kinetic analysis of the scheme of propane-oxygen mixtures conversion [2]. Analysis was performed using numerical simulation method for different temperatures and isothermal conditions. The reaction scheme involved all possible elementary steps, including reactions with oxygen, branching and positive chain interaction too.

The main conclusion drawn from the obtained results is that the decisive part is played by the reaction of chain initiation and the chain propagation and by the equilibrium reaction (b). During the hydrocarbon oxidation and slow combustion

carried out in a conventional reactor, the chain initiation occurs heterogeneously on the reactor wall.

#### REFERENCES

1. Mantashyan A.A., Khachatryan L.A., Sukiasyan A.A., Kinetika i kataliz, 30, 272 (1989).
2. Mantashyan A.A., Khachatryan L.A., Sukiasyan A.A., Adilkhanyan Dzh.M., Velikyan I.V., Chem. Phys. Reports, 13, 1693 (1995).

F10

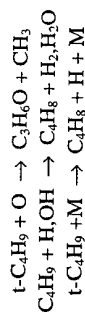
## EXPERIMENTAL EVIDENCE OF UNEXPECTED INTERMEDIATES IN BUTANE FLAMES

B. Walravens, J. Vandooren and P.J. Van Tiggelen

*Laboratoire de Physico-Chimie de la Combustion  
Université Catholique de Louvain  
Louvain-la-Neuve, Belgium*

Experimental flame studies of higher alkanes are rather scarce in the literature. Most of the data available are dealing with either ethane, or propane fuels. According to Fristrom<sup>1</sup> no flame structure of butane flames are reported. A comparison of isobutane/n-butane combustion is achieved by using the molecular-beam mass spectrometry technique for flames burning at low pressure in lean mixtures. Five different flame systems are investigated. Profiles of stable, atomic and radical species are measured as well as temperature. Among the usual species encountered in hydrocarbon flames (H, H<sub>2</sub>, CH<sub>3</sub>, O, OH, H<sub>2</sub>O, C<sub>2</sub>H<sub>2</sub>, CO, CH<sub>2</sub>O, O<sub>2</sub>, Ar, CO<sub>2</sub>, C<sub>2</sub>H<sub>10</sub>) acetone C<sub>3</sub>H<sub>6</sub>O and butenes C<sub>4</sub>H<sub>8</sub> are monitored. Quantitative measurements of their profiles are performed. Acetone and butene occur as intermediates in significant amounts (fig. 1 and 2). The occurrence of both species in the reaction zone raises the question of the decay paths of the initial fuel. The generally accepted "one bond removed rule" for alkyl decomposition introduced in numerical modelling of higher alkane combustion<sup>2</sup> does not take into account those experimental observations.

- In *isobutane* flames the production of both acetone and butene is ascribed to direct reactions of butyl radicals.



- In *n-butane* flames, acetone is not produced and butene is accounted for through radical reactions exclusively.



It appears that radical-radical reactions in higher hydrocarbon flames cannot be neglected. It supplements the usual thermal decomposition reaction ( $\beta$ -scission) in the detailed flame mechanisms. From all these considerations, decay schemes are suggested.

Since in the last stages of the combustion processes i.e. the C<sub>1</sub>- and C<sub>2</sub>-subsystems the kinetics are identical for both fuels (isobutane and n-butane), only the occurrence of dissimilar products in the early stage of the consumption mechanism could have a major effect on the overall aspects of those flames : burning velocity, ion production, induction times, etc... It is specially valid for the induction time because of the lower reactivity<sup>3</sup> of acetone produced in isobutane flame, compared to propionaldehyde produced in n-butane flame. It would be interesting in the future to

extrapolate our conclusions toward flames burning with highly branched hydrocarbons by new appropriate experimental observations.

- (1) R.M. Fristrom. Flame Structure and Processes. Oxford Univ. Press 1995
- (2) J. Warnatz. XXIV Symp. on Combustion, p. 553 (1992)
- (3) J. Vandoreen, A. van der Loos, P. Corillon, H. Leseil and P. J. Van Tiggelen. Joint Meeting of the Portuguese, British, Spanish and Swedish Sections of the Combustion Institute, Funchal, Madeira. 5.2.1. April 1996

**Fresh gases composition**

Flame	% H <sub>2</sub>	% O <sub>2</sub>	% Ar	% iso C <sub>4</sub> H <sub>10</sub>	% n C <sub>4</sub> H <sub>10</sub>	Pressure (kPa)
IP	13.6	78.4	7.0	1.0	-	2.70
IPP	-	89.1	8.0	2.9	-	3.37
NP	13.6	78.4	7.0	-	1.0	2.70
NPP	-	89.1	8.0	2.9	-	3.37
HP	18.6	74.4	7.0	-	-	2.70

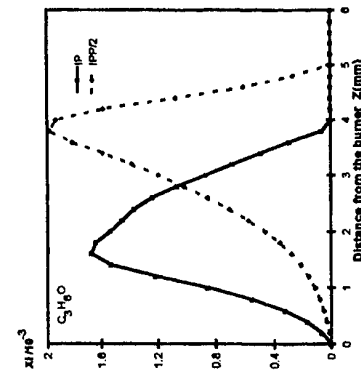


Figure 1

Mole fraction profiles of acetone ( $C_3H_6O$ ), in isobutane flames. Continuous line: IP flame; Dashed line: IPP flame.

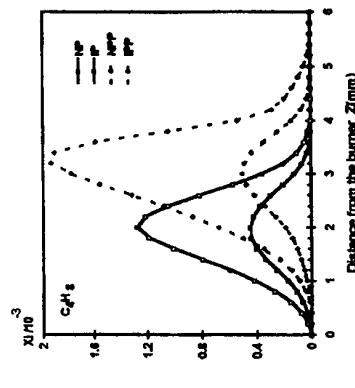


Figure 2

Mole fraction profiles of butene ( $C_4H_8$ ), in the investigated flames. Continuous line: NP and IP flames; Dashed line: NPP and IPP flames. Filled symbols: n-butane; Open symbols: isobutane.

We acknowledge financial support of FRFC (Belgium) through grant #2.9006.88 and a scholarship from I.R.S.I.A. for one of us (BW).

# THE OXIDATION OF N-HEPTANE IN THE PRESENCE OF OXYGENATED OCTANE IMPROVERS: MTBE AND ETBE.

Philippe Dagaut, Ralf Koch, and Michel Cathonnet.

C.N.R.S., Laboratoire de Combustion et Systemes Reactifs  
IC, Avenue de la Recherche Scientifique  
45071 Orleans cedex 2, France

Compression ratio is an important parameter of engine determining its efficiency. Unfortunately, it is limited by the occurrence of engine knock. Engine knock has been reduced in the past by using alkyl lead derivatives. More recently, the increasing use of exhaust catalysts for the reduction of NOX emissions has necessitated the replacement of alkyl lead compounds by chemicals presenting high knock resistance properties. Among these chemicals, tertiary butyl ethers are widely used while their utilization is still under debate. MTBE and ETBE have a research octane number of 118. The effect of methyl-t-butyl ether (MTBE) on the combustion of fuels in engines has been investigated in previous studies by Hoekman (1992) and Osman et al. (1993) and ignition delays have been obtained by Gray and Westbrook (1994) for mixtures of MTBE with propane. The oxidation of neat MTBE has been investigated by means of several techniques including static reactor (Brocard et al., 1983), shock tube (Dunphy and Simmie, 1989 and 1991a; Curran et al., 1992), flow reactor (Norton and Dryer, 1990), research engine (Leppard, 1991), rapid compression machine (Lee et al., 1993), and jet-stirred reactor (Cathonnet et al., 1995). Ethyl-t-butyl ether ignition has been studied in shock tube by Dunphy and Simmie (1991b); its oxidation has been studied by El Kadi and Baronne (1995) in a static reactor, by Leppard (1991) and Kaiser et al. (1991) in a research engine, and by Cathonnet et al., (1995) in a jet-stirred reactor.

From these previous studies, it is not possible to delineate the mechanism involved in engine knock reduction by oxygenated additives, although several mechanisms have been postulated recently (Brocard et al., 1983; Westbrook et al., 1991; Gray and Westbrook, 1994; El Kadi and Baronne, 1995), and the influence of MTBE or ETBE on pollutants emissions is not fully addressed.

In the present study, we have investigated the chemical kinetic effect of MTBE or ETBE on the oxidation of n-heptane from the low temperature oxidation regime (cool flame chemistry) to the high temperature oxidation regime under elevated pressure in order to better understand the octane-enhancing mechanism. Species measurements were used to evaluate the effect of the blending of gasoline by MTBE or ETBE on emissions. The oxidation of n-heptane and mixtures n-heptane-MTBE (50:50) and n-heptane-ETBE (50:50) has been studied experimentally in a high-pressure jet-stirred reactor in a wide range of conditions covering the low and high temperature oxidation regimes (570-1150K,

# STRATEGIES FOR AUGMENTING OH-RADICAL PRODUCTION DURING THE APPROACH TO SPONTANEOUS IGNITION IN HYDROCARBON FUELS

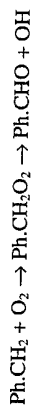
Peter Q. E. Clothier, DeLin Shen, Wai-To Chan and Huw O. Pritchard

Department of Chemistry, York University, Downsview, Ontario,  
Canada M3J 1P3

Key to the efficient operation of diesel engines is the timely spontaneous ignition of the fuel vapour following injection into the combustion chamber. Ignition characteristics of natural fuels vary widely, being particularly poor for those derived from tar sands or from hydro-cracking of heavier heating oil fractions. Moreover, ignition quality can only decline in the future as less attractive sources have to be brought on line. In order to meet National legislated standards for ignition quality (Cetane Number), simple expedients are to add to these low-grade fuels a few-tenths of a percent of free-radical initiators, principally 2-ethylhexyl nitrate or di-*tert*-butyl peroxide.

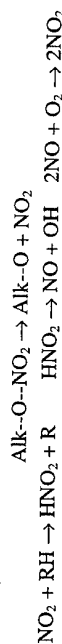
We have shown that not just 'any old radical' will do<sup>1</sup>, and have speculated that what one needs to get the combustion started is the presence of precursors for the formation of OH radicals. Here, we examine two strategies for the low-temperature generation of OH radicals during the pre-ignition phase of the reaction:

*Generation of benzyl-type radicals:* This depends upon the conjecture, supported by *ab initio* calculations at the ROMP2//3-21G level, that OH radicals are readily formed by the sequence of reactions



Benzyl radicals were made by adding to the fuel either dibenzyl mercury ( $\text{Ph}\cdot\text{CH}_2\text{--Hg--CH}_2\cdot\text{Ph}$ ) or  $\omega$ ,  $\omega'$ -azo-toluene ( $\text{Ph}\cdot\text{CH}_2\text{--N=N--CH}_2\cdot\text{Ph}$ ). Both are more effective ignition promoters than 2-ethylhexyl nitrate in our test engine, and dibenzyl mercury was also shown to be a good cetane improver by the ASTM D-613 procedure<sup>2</sup>. Dibenzyl ketone (1,3-diphenyl acetone) is another powerful cetane improver, but here, benzyl radicals per se are not involved, and some 15–20 pathways to the formation of OH radicals are mapped out by *ab initio* molecular orbital methods. Also, pseudo-benzyl radicals  $\text{CH}_2\cdot\text{Ph}\cdot\text{CH}_2\text{CH}_2\cdot\text{Ph}\cdot\text{CH}_2$  formed from [2,2]paracyclophane cause a powerful acceleration in the ignition of diesel fuel<sup>3</sup>.

*Synergy between NO<sub>2</sub> and CH<sub>2</sub>O:* The mechanism by which alkyl nitrates stimulate spontaneous ignition is as follows:



10atm, =1, 0.1% of fuel). The mole fractions of reactants, intermediates and final products have been measured. The influence of the additives on the formation of several pollutants has been addressed. The present results clearly show an influencing effect of MTBE and ETBE on the kinetics of n-heptane oxidation by a reduction of the mixture reactivity in the low temperature regime (570–800K). The results are interpreted in terms of knocking and non-knocking tendencies related to fuel structure and low temperature oxidation mechanism.

## References

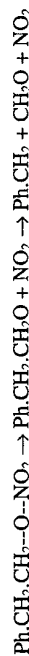
- Brocard, J.C., Baronnet, F. and O'Neal, H.E. (1983). *Combust. Flame*, 52, 25.
- Cathonnet, M., Degaut, P. and Koch, R. (1995). *Deutschen Bunsen-Gesellschaft für Physikalische Chemie, Bremen*, May 25–27.
- Curran, H.J., Dunphy, M.P., Simmie, J.M., Westbrook, C.K. and Pitz, W.J. (1992). 24th Symp. (Int.) on Combustion, The Combustion Institute, Pittsburgh, pp. 769–76.
- Dunphy, M.P. and Simmie, J.M. (1989). *Combust. Sci. Technol.*, 66, 157.
- Dunphy, M.P. and Simmie, J.M. (1991a). *Combust. Flame*, 85, 489.
- Dunphy, M.P. and Simmie, J.M. (1991b). *Int. J. Chem. Kinet.*, 23, 553.
- El Kadi, B. and Baronnet, F. (1995). *J. Chim. Phys.*, 92, 706.
- Gray, J.A. and Westbrook C.K. (1994). *Int. J. Chem. Kinet.*, 26, 757.
- Hoekman, S.K. (1992). *Environ. Sci. Technol.*, 26, 1206.
- Kaiser, E.W., Andino, J.M., Siegl, W.O., Hammerle, R.H. and Butler, J.W. (1991). *J. Air Waste Manage. Assoc.*, 41, 195.
- Lee, D., Hochgreb, S. and Keck, J. (1993). *Proceedings of the Central and Eastern States Sections, The Combustion Institute, New Orleans, March 15–17*, pp. 478–81.
- Leppard, W.R. (1991). *SAE Paper #912313*.
- Norton, T. and Dryer, F.L. (1990). 23rd Symp. (Int.) on Combustion, The Combustion Institute, Pittsburgh, pp. 179–85.
- Osman, M.M., Matar, M.S. and Koreish, S. (1993). *Fuel Sci. Technol. Int.*, 11, 1331.
- Westbrook, C.K., Pitz, W.J. and Leppard, W.R. (1991). *SAE paper 912314*.

However, there is also a strong synergy between NO<sub>2</sub> and formaldehyde because the following two reactions are fast, viz.



This synergy was convincingly demonstrated in engine measurements designed to generate formaldehyde during the pre-ignition phase<sup>3</sup>.

Of course, Alk-O is often R·CH<sub>2</sub>O, and may itself be a ready source of formaldehyde: five different sets of engine measurements along with parallel molecular orbital calculations will be described. One particularly interesting case is the use of phenethyl nitrate as an additive because its thermal decomposition yields NO<sub>2</sub>, formaldehyde and benzyl radicals:



the latter step having a very low activation energy due to the extra resonance energy in the benzyl radical. Unfortunately, this strategy does not work because, although the decomposition has the same activation energy as that of 2-ethylhexyl nitrate, the frequency factor is an order of magnitude smaller because the transition state is much less flexible. Perhaps too, as in atmospheric chemistry, NO may act as a sink for the benzylperoxy radicals?

#### Acknowledgement

This work was supported by Imperial Oil (Products Division), Samia, and by the Natural Sciences and Engineering Research Council of Canada.

#### References

- [1] J. P. Q. E. Clothier, B. D. Aguda, A. Moise and H. O. Pritchard, *Chem. Soc. Reviews*, 22, 101-108 (1993).
- [2] J. P. Q. E. Clothier, D. Shen and H. O. Pritchard, *Combustion Flame*, 101, 383-386 (1995).
- [3] J. P. Q. E. Clothier, H. O. Pritchard and M.-A. Poirier, *Combustion Flame*, 95, 427-429 (1993).

## THE ROLE OF PHENOXY RADICALS AND PHENOLS IN GAS-PHASE 'DIOXIN' FORMATION.

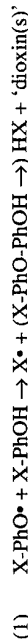
Horst-Henning Grotheer\*, Robert Louw, M. Jacqueline Kanter and Wibo van Scheepingen.

*Center for Chemistry and the Environment, Leiden Institute of Chemistry, Gorlaeus Laboratories, Leiden University; PO Box 9502, 2300 RA Leiden, The Netherlands.  
(E-mail: Louw\_r@chem.leidenuniv.nl)*

*\* On leave from the Institute of Physical Chemistry of Combustion, DLR Stuttgart, Germany.*

Combustion of Cl containing matter is afflicted with the emission of 'dioxins'. Part of the chemistry in incinerators involves catalyzed conversions in the post-combustion train, but the formation and survival of 'predioxins', esp. (chloro)phenols, and generation of polychlorinated dibenzodioxins (PCDDs) and dibenzofurans (DFs) is no doubt inherent in the combustion itself.

In 1983 Shaub and Tsang have addressed the question of the mechanism of gas-phase formation of dioxins from chlorophenol, and came up with the displacement of an (ortho) chlorine in the (poly)chlorinated phenol molecule (Cl-PhOH) by a (chloro)phenoxy radical (Cl-PhO•) - reaction (1a) - as the only important pathway and consequently as the key step. The activation barrier (for the first step of reaction 1a) was modelled at 26 kcal/mol and the overall conclusion was that dioxin formation via this mechanism was insignificant in real incinerators [1].



Recently, Dellinger et. al.[2] have experimentally found rates for gas-phase formation of dioxins from 2,4,6-trichlorophenol to be much larger than predicted by the S&T mechanism. In order to account for this, they adjusted S&T's model Ea down to 19.5 kcal/mol. When they used the analogous tribromophenol, rates to the corresponding dioxins were ca. 500 times larger; this was translated into an Ea for reaction (1b) of only 8.8 kcal/mol [2]. Other pathways to dioxins were not considered, although we have pointed out earlier [3] that in the pyrolysis and slow combustion of phenol and chlorophenols, formation of (chlorinated) DF's and DD's can be satisfactorily described by the combination of two (chlorinated) phenoxy radicals (reaction 2a). Overall rate constants for these condensations are quite large, over 10<sup>8</sup> M<sup>-1</sup>s<sup>-1</sup>, even if (ortho) chlorine is absent; in that case the products are DF's [4,5]. A further example, pentachlorophenol/-phenoxy in an excess of Cl-free phenol, leading to 1,2,3,4-TCDF (not the DD!), is described in ref. [6].

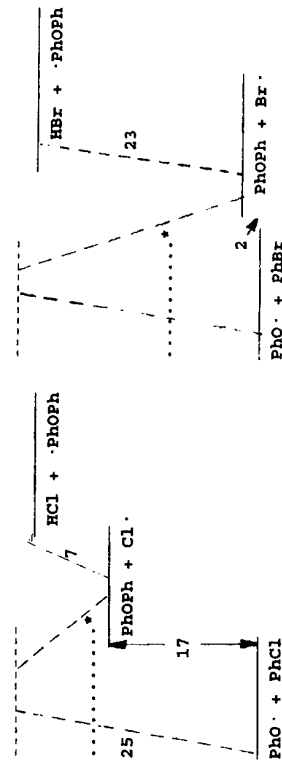
In order to obtain a better insight in this matter - to begin with, in the validity of the Shaub and Tsang model - we have investigated the slow combustion of phenol [PhOH]

together with chlorobenzene [PhCl], i.e. we used PhCl as a model substitute for chlorophenol (reaction 3a). The advantage is that the specific product is diphenylether, PhOPh. Using a quartz backmix-flow reactor at atmospheric pressure, we measured PhOPh for  $728 < T < 984$  K relative to dibenzofuran (DF), the product arising from the condensation of 2 PhO• radicals [4]. Rate and product data were found to yield  $\log A_{3a}$  (M.s units) = 8.7,  $E_{3a}$  = 24.5 kcal/mol. S&T's model is therefore underscored, as is their conclusion that pathway (1a) is unimportant in dioxin formation in incinerators.

With a ratio of  $k_{2a}/k_{3a} \approx 10^5$  at, say 1000 K, reaction (2a) will be faster than (1a) if [Cl•]/[PhO•] is above  $10^{-5}$ , a condition which is likely to be met in practice [7].

For comparison, reactions involving bromobenzene (3b) are also under investigation; remarkably  $k_{3b}$  is almost equal to  $k_{3a}$ , a result which has been validated by a competition between PhCl and pentadeuterated PhBr. This points at **nearly equal** activation energies for both reactions, despite the large difference in bond strengths between C-Cl and C-Br.

Inspection of the enthalpy diagrams for both cases is worth while. It is seen that the low  $E_a$  values suggested by Dellinger et. al. [2] cannot be correct within the framework of the S&T mechanism. Rather, more rapid radical combination occurs in both cases (2a,b).



**FIGURE.**  
Enthalpy diagrams for reactions (3a,b), their reversal, and competitive H-abstraction.

.....\*: transition state levels as proposed by Dellinger et al [2]

Furthermore, knowledge on the reverse process(es), splitting of PhOPh by Cl• or Br• will be highly relevant. The gas-phase chlorination of PhOPh has been described before [8], and at 4 - 500 °C, H-abstraction by Cl• -thence chlorination to ClPhOPh - is a major process \*. In fact, no mention was made about splitting, to give PhCl. We are reinvestigating this chlorination, and have found that both chlorination (H abstraction) and chlorinolysis (reaction -3a) are about equally important [9]. Likewise, the (hitherto unknown) gas-phase reaction between PhOPh and bromine is found to give m- and p-BrPhOPh (plus DF\*), but accompanied by a significant degree of brominolysis -

equivalent with a difference in free energy of ca 1.5 kcal/mol. These halogenation studies corroborate therefore the large activation barriers (of ca 25 kcal/mol) for the displacements (3) of both Cl and Br by phenoxy radicals.

Thermokinetic analysis shows that the displacement of OH in phenol by phenoxy is overall ca 22 kcal/mol endothermic; it should be considerably slower than displacement of Cl in PhCl, but not totally impossible. In fact, when conducting the slow combustion of phenol with benzene as a partner rather than chlorobenzene, the production of diphenylether was diminished by more than a factor of ten.

**In sum**, phenoxy radicals react at best sluggishly with not only chlorobenzene but also in the nearly thermoneutral displacement of Br in bromobenzene.

\* H-abstraction leads to m- and p-ClPhOPh by subsequent chlorination of the respective aryl radicals; in stead of ortho-ClPhOPh, dibenzofuran is formed, by - more rapid - intramolecular addition and loss of H instead of bimolecular reaction of the o-PhOPh• radical with chlorine [8].

## References.

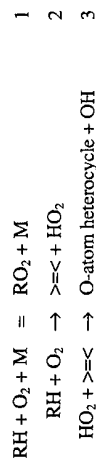
- [1] W.M. Shaub and Wing Tsang, Environ. Sci. Technol. **17**, 721 (1983).
- [2] S.S. Sidhu, L. Maqsud and B. Dellinger, Comb. Flame **100**, 11 (1995).
- [3] J.P.G. Born, R. Louw and P. Mulder, Chemosphere **18**, 401 (1989).
- [4] J.P.G. Born, Thesis, Leiden University (1992).
- [5] I.W.C.E. Arends, R. Louw and P. Mulder, J. Phys. Chem. **97**, 7914 (1993).
- [6] M.J. Kanter and R. Louw, Chemosphere, in press.
- [7] H-Y. Zhang and J.T. McKinnon, Comb. Sci. Technol., submitted.
- [8] J.W. Engelsma and E.C. Kooyman, Recl. Trav. Chim. Pays-Bas **80**, 526 (1961).
- [9] R. Louw and I. Wiater, to be published.

# ESTIMATING THE KINETICS AND THERMODYNAMICS FOR THE OXIDATION OF ALKYL RADICALS.

D.W. Stocker and M.J. Pilling

School of Chemistry, University of Leeds, Leeds, LS2 9JT

The oxidation of alkyl radicals plays a central role in the combustion of alkanes in the temperature range 500–1000 K, the relative importance of the various reaction channels changes with temperature and determines not only the combustion products but also the combustion characteristics. The details of the reaction dynamics are complex and may involve two electronic energy surfaces [1], however, The phenomenological reactions may be represented as:



Measurements of the rate coefficients are sparse and limited to small radicals, rate coefficients for larger radicals can be estimated by applying structure-activity relationships (SAR). In the present paper methods to estimate  $K_p(1)$ , based on group additivity estimates of the thermodynamic properties of alkyl and alkylperoxy radicals, and  $k_1$ ,  $k_2$  and  $k_3$  based on structure-activity relationships are developed. Where appropriate, data have been updated to include the latest recommended kinetic [2] and thermodynamic data [3]

*Group Additivity Estimates of the Thermodynamic Properties of Alkyl and Alkylperoxy Radicals.* The group additivity procedure of Benson has been adopted to estimate the thermodynamic properties of alkyl and alkylperoxy radicals, the group contributions for radical centres and neighbouring groups have been revised to incorporate more recent determinations of the thermodynamic properties of small radicals.  $S^\circ$  and  $C_p$  have been calculated from spectroscopic and ab initio calculations of the vibrational energy levels and barriers to internal rotation,  $\Delta H_f^\circ$  values were taken from recent studies of  $\text{R} + \text{HBr}$  and  $\text{C}_2\text{H}_5 + \text{O}_2$  equilibria. A summary of the group coefficients is given below. Correction factors for non-bonding

Group	$\Delta H_f^\circ$ /kJ K <sup>-1</sup> mol <sup>-1</sup>	$S^\circ$ /J K <sup>-1</sup> mol <sup>-1</sup>	$C_p^\circ(300)$ /J K <sup>-1</sup> mol <sup>-1</sup>
C•-C/H <sub>2</sub>	163.68	135.81	25.44
C•-C <sub>2</sub> /H	175.35	58.16	14.81
C•-C <sub>3</sub>	180.53	-26.65	19.29
C-C•/H <sub>3</sub>	-42.68	126.78	25.90
C-C•/C/H <sub>2</sub>	-22.50	40.24	28.28
C-C•/C <sub>2</sub> /H	-7.72	-50.50	19.00
C-C•/C <sub>3</sub>	0.75	-130.72	17.78
O-C/O•	58.16	156.89	25.93

interactions in radicals have been estimated from ab initio calculations of the energies of the rotational conformers of 1- and 2-butyl radicals [4,5,6]; *gauche* C-C-C• = 3.3 and *gauche* C-C-C•-C = 0.9 kJ mol<sup>-1</sup>. Bond additivity (BA) methods [7] assume non-bonding interactions are the same as in the parent alkanes, the difference in the two approaches is apparent when estimating  $\Delta H_f^\circ$  for branched alkyl radicals, e.g.,  $\Delta H_f^\circ(2\text{-methyl-2-pentane}) = 13.4 \text{ kJ mol}^{-1}$  [8] (updated to include current recommended  $\Delta H_f^\circ(\text{C}_2\text{H}_5)$ ), estimated values are 5.5 (BA) and 12.7 kJ mol<sup>-1</sup> (this work).

*Estimating  $k_{1a}$ .* The reactions of C<sub>3</sub> and larger radicals are assumed to be at or near the high pressure limit,  $k_{1a}(298)$  correlates with the structure of the radical, in particular the nature of the carbon atoms  $\beta$  to the radical centre.

$$k_{1a}(298) = n_p k(\text{C-C}\bullet/\text{H}_3) + n_s k(\text{C-C}\bullet/\text{C}/\text{H}_2) + n_k k(\text{C-C}\bullet/\text{C}_2/\text{H}) + n_q k(\text{C-C}\bullet/\text{C}_3)$$

where, e.g.  $k(\text{C-C}\bullet/\text{H}_3)$  represents a primary group bonded to the radical centre and  $n_p$  is the number of primary  $\beta$  groups.  $k(\text{C-C}\bullet/\text{H}_3) = 7.6$ ,  $k(\text{C-C}\bullet/\text{C}/\text{H}_2) = 7.8$ ,  $k(\text{C-C}\bullet/\text{C}_2/\text{H}) = 2.9$ ,  $k(\text{C-C}\bullet/\text{C}_3) = 2.2 \times 10^{12} \text{ cm}^3 \text{ molecule}^{-1} \text{ s}^{-1}$  suggesting steric hindrance is the main influence behind the SAR as the reaction probably occurs without an energy barrier. Agreement between the estimated rate coefficient for 2-butyl radicals (not used to construct the SAR) with updated experimental data [9] is good  $k_{1a}(\text{est}) = 1.53$  and  $k_{1a}(\text{expt}) = 1.66 \times 10^{11} \text{ cm}^3 \text{ molecule}^{-1} \text{ s}^{-1}$ . Temperature dependent studies the reaction of ethyl, 1-propyl and neopentyl radicals show a slight negative temperature dependence and fit the function  $k = AT^{-2.5}$ .

*Estimating  $k_2$ .* Experimental studies of the reactions of ethyl and 2-propyl radicals show a complex dependence on temperature and pressure, consistent with direct competition between reactions (1) and (2). The rate coefficients correlate well with the number of abstractable hydrogen atoms

$$k_2(750 \text{ K}) = n_p k_{\text{primary}} + n_s k_{\text{secondary}} + n_q k_{\text{tertiary}}$$

$k_{\text{primary}} = 2.7$ ,  $k_{\text{secondary}} = 8.9$ ,  $k_{\text{tertiary}} = 5.2 \times 10^{14} \text{ cm}^3 \text{ molecule}^{-1} \text{ s}^{-1}$ , the order of reactivity probably reflects experimental uncertainty and steric factors. The estimated rate coefficient for tert-butyl radicals, not included in determining the SAR coefficients, is within a factor 1.5 of an updated indirect experimental determination [10]:  $k_2(\text{est}) = 2.4$  and  $k_2(\text{expt}) = 3.2 \times 10^{13}$

# THE USE OF NON-THERMAL ATMOSPHERIC PRESSURE ELECTRICAL DISCHARGES FOR THE REMOVAL OF NO<sub>x</sub> FROM GASEOUS EMISSIONS

C. Fitzsimmons, J.T. Shawcross and J.C. Whitehead

Chemistry Department, Manchester University,  
Manchester, M13 9PL.

As a result of increasingly stringent environmental legislation and public concern, the reduction of NO<sub>x</sub> and SO<sub>x</sub> (DeNO<sub>x</sub> and DeSO<sub>x</sub>) and particulate matter has become the subject of intense research. The application of non-thermal, atmospheric pressure plasmas is being extensively investigated due to their potential to simultaneously remove NO<sub>x</sub>, SO<sub>x</sub> and soot without the need for a catalyst. The aim is to be able to use non-thermal plasmas for the after-treatment of combustion exhaust gases from chimney stacks and diesel engines more efficiently than current technology. The main priority for exhaust after-treatment technology is that processing of waste gas should preferably produce benign species such as N<sub>2</sub>, CO<sub>2</sub>, and H<sub>2</sub>O as by-products.

An investigation into the DeNO<sub>x</sub> potential of a non-thermal atmospheric pressure electrical discharge plasma is reported with emphasis made upon the reaction mechanism responsible for DeNO<sub>x</sub> in both a reductive and oxidative atmosphere in an attempt to simulate conditions found in a diesel exhaust. Results are reported for plasma treatment of NO<sub>2</sub> and NO / NO<sub>2</sub> mixtures in both N<sub>2</sub> and air at atmospheric pressure, monitoring the reaction product using a long path gas cell, FTIR spectrometer. The dominant reaction pathways are discussed and indicate that oxidative and reductive chemistry can be initiated by the plasma depending upon the ratio of N and O atoms and the moisture content. In N<sub>2</sub> buffer gas, DeNO<sub>x</sub> reactions are found to be dominated by N radicals forming N<sub>2</sub>O and N<sub>2</sub> with little NO<sub>2</sub> production. In air, the reaction of NO / NO<sub>2</sub> is believed to be dependant upon the formation of O atoms and ozone and produces NO<sub>2</sub> almost exclusively. It is found that

cm<sup>3</sup> molecule<sup>-1</sup> s<sup>-1</sup> the level of agreement reflects uncertainty in the SAR coefficients and experimental data. Temperature dependent data for ethyl and isopropyl radical reactions show non-Arrhenius behaviour;  $k_2 \approx A \exp(1280/T)$ .

**Estimating  $k_3$ .** The rate limiting step is probably addition of HO<sub>2</sub> to the double bond, activation energies for reactions involving the addition of electrophilic radicals to double bonds increases with the ionisation potential of the alkene. For reaction (3)  $E_a/R = 19.17$   $I_p(\text{alkene}) - 9273$ .  $I_p(\text{alkene})$  is related to the degree of substitution around the double bond which in turn influences the pre-exponential factor through steric effects:  $\ln(A/\text{cm}^3 \text{ molecule}^{-1} \text{ s}^{-1}) = 0.0182$   $I_p(\text{alkene}) - 44.88$ . Estimated rate coefficients are within a factor 3 of experimental data, e.g. for isobutene  $k_3(\text{est}) = 0.68$  and  $k_3(\text{expt}) = 1.8 \times 10^{-16} \text{ cm}^3 \text{ molecule}^{-1} \text{ s}^{-1}$  [11].

## References

- 1 Pilling, M.J., S.H. Robertson and P.W. Seakins, *J. Chem. Soc. Faraday Trans. 91*, 4179 (1995).
- 2 Baulch, D.L., C.J. Cobos, R.A. Cox, P. Frank, G. Hayman, T. Just, J.A. Kerr, T. Murrells, M.J. Pilling, J. Troe, R.W. Walker, J. Warnatz, *J. Phys. Chem. Ref. Data* **23**, 847 (1994).
- 3 Kerr, J.A., in *CRC Handbook of Chemistry and Physics*, 74th edition, D.R. Lide editor, CRC Press, Boca Raton, pp 9-135 (1993).
- 4 Chen, Y., A. Rauk and E. Tschuikow-Roux, *J. Phys. Chem.* **94**, 6250 (1990).
- 5 Knyazev, V.D. and I.R. Slagle, *J. Phys. Chem.* **100**, 5318 (1996).
- 6 Gang, J. Private communication.
- 7 Lay, T.H., J.W. Bozzelli, A.M. Dean and E.R. Ritter, *J. Phys. Chem.* **99**, 14514 (1995).
- 8 Seres, L. M. Görgényi and J. Farkas, *Int. J. Chem. Kinet.* **15**, 1133 (1983).
- 9 Lenhardt, T.M., C.E. McDade and K.D. Bayes, *J. Chem. Phys.* **72**, 304 (1980).
- 10 Evans, G.A. and R.W. Walker, *J. Chem. Soc. Faraday Trans. 1* **75**, 1458 (1979).
- 11 Walker unpublished work

# COMBINED SHOCK TUBE TIME RESOLVED ATOMIC AND MOLECULAR ABSORPTION STUDIES

L. Batt, M.M. Law, V. Mahe\*, S.K. Ross and P.C. Wraight

*University of Aberdeen, Scotland, U.K.*

We have built a shock tube for use in high temperature studies of reactions important in combustion and pyrolysis. To date temperature ranges of 1000-3000K are accessible. However the apparatus is robust enough to access much higher temperatures using stronger shocks.

The advent of our newly developed time resolved spectrometer, based upon a CCD array, has meant that the apparatus allows the simultaneous monitoring of transient species by both atomic absorption resonance spectroscopy (ARAS) and molecular absorption spectroscopy from 200-900nm. These two detecting systems are at essentially coincident positions but disposed at right angles to one another.

We have recently obtained absorption spectra for CN using  $C_2N_2$  as a source. Temperatures of 2000-3000K are required for the production of suitable concentrations. An absorption spectrum of CN from a typical shock experiment is shown on page 2. This corresponds to the violet system  $B^2\Sigma - X^2\Sigma$ . There are several objectives associated with the study of CN. The vibration-rotation excitation can be used to measure the shock temperature. Preliminary calculations predict a potential accuracy of  $\pm 30$  degrees at 3000K. A second objective is to study the reactions of CN with O and  $O_2$ . These reactions are important in relation to the modelling of the "Fuel Nitrogen Mechanism". A preliminary study has been carried out with  $C_2N_2$  as a source of CN. Raw data for the decomposition process using the CCD camera together with a temporal absorbance profile is shown on page 2. Preliminary data for the dissociation of  $N_2O$  and the production of O using atomic resonance absorption spectroscopy is

the presence of NO with  $NO_2$  in air serves to limit oxidation of NO to  $NO_2$  with no higher oxidation state  $NO_x$  formed. It is believed that this is due to the formation of an NO /  $NO_2$  oxidation-reduction cycle where further oxidation of  $NO_2$  is less likely due to competing reactions. For  $NO_2$  in air, the chemistry is dominated by O /  $O_3$  reactions to higher oxidation state  $NO_x$  species such as  $N_2O_5$  and  $HNO_3$ . As the  $O_2$  concentration of the air used (~23%) is higher than a typical diesel engine exhaust (~8-15%) the plasma chemistry studied here is believed to be more oxidative than it would be for a diesel. The higher moisture content of a diesel exhaust would also mean that  $HNO_3$  formation would be enhanced. The  $DeNO_x$  potential of non-thermal plasma gas processing is found to be dependant upon the plasma input energy with maximum  $DeNO_x$  and plasma activity corresponding to an average input power of 3 - 5W.

Detailed kinetic mechanisms and the results of modelling studies of the plasma chemistry will be presented.

This work was supported by EPSRC via the Total Technology Studentship scheme with support from AEA Technology plc.

also shown on page 2. In particular one can observe the arrival of both the incident and reflected shock in addition to the absorption at 130.6nm due to the formation of O atoms.

\*Université d'Orléans, France

F17

## COMPLEX OSCILLATIONS IN SIMPLE COMBUSTION REACTIONS

Stephen K Scott & Barry R Johnson

*School of Chemistry, The University, Leeds, LS2 9JT*

Combustion reactions are excellent examples of dynamical systems. They contain many steps whose reaction rates depend on the concentration of more than one species and so are 'nonlinear' processes, and which exhibit thermal feedback through the combination of the overall reaction exothermicity and the Arrhenius dependence of their rate constant. Chemical feedback is also common through processes such as chain branching cycles (autocatalysis) or chain termination. It is therefore not surprising that these reactions show behaviour typical of nonlinear dynamical systems in general.

It is well known that the simplest of combustion reactions, that between hydrogen and oxygen in a closed vessel, has three explosion limits at increasing pressures which separate quiescent and explosive reaction. Less familiar is the observation of regular, periodic reaction at pressures between the first and second limits when the reaction is studied in an open system<sup>1</sup>. For an equimolar reaction mixture simple repetitive ignitions are observed over a range of temperatures and pressures; all the fuel is consumed in each ignition with an accompanying temperature spike reaching above 2500K. Such phenomena can be explained in terms of a simple isothermal reaction mechanism combined with the outflow of the inhibitory product water, and replenishment of the feed reactants<sup>2</sup>. For stoichiometric mixtures more complex, but still periodic, behaviour occurs where smaller secondary ignitions appear between the large ignitions, attributable to the coupling of the mechanism above with thermal effects. These complex, or mixed mode, ignitions are categorised as  $L^s$ , where  $L$  is the number of large ignitions and  $s$  the number of small ignitions per repeating unit, and are all of the form  $1^s x$  where  $1 < x < 10$ .  $x$  is constant at fixed parameter values but increases with temperature.

Regular temporal oscillations in temperature have also been reported for the oxidation of ethane, butane and ethers, the decomposition of di-tertiarybutylperoxide, and the reaction between  $H_2$  and  $Cl_2$ . More complex behaviour has been reported in the oxidation of acetaldehyde, when external forcing of the gas flows can produce aperiodic cool flames, and in carbon monoxide oxidation where chaotic ignition series arise naturally<sup>3</sup>. Waves of reaction, in the form of spirals, have also been reported recently in butane oxidation in a flow tube reactor.

In the present work we return to hydrogen oxidation but now investigate fuel rich compositions. Mixtures of  $6.5 - 8.5 H_2 : 3 O_2$  were studied in a continuous flow

stirred tank reactor at pressures of 10 - 25 mmHg and residence times of 1.5 - 4 s, with reaction monitored via a fine wire thermocouple. At the highest pressures within the oscillatory region both the simple and complex  $L^S$  oscillatory ignitions previously described are observed, where the secondary ignitions occur well before the thermocouple response to the first ignition has died away. However, under certain conditions new repeating units have now been discovered. Initially  $1^0$  waveforms can give way to  $1^1$  through a mixing of the two via an intermediate  $1^{0.1}$  (or  $2^1$ ) repeating unit. On increasing the temperature further the  $1^1$  waveform can then produce a  $1^2$  waveform via  $1^1 1^2$ , and on up to  $1^1 1^6$  (Figure 1) before giving way to  $1^*$  ( $\lambda \geq 6$ ) oscillations before the transition to small, high frequency period 1 ignitions ( $0^1$ ). Sequences of  $1^0 1^1$  are equally common.

At lower pressures ( $\leq 14$  mmHg) different behaviour is observed. The regular large  $1^0$  waveform is replaced by a new mixed mode oscillation. Again this is composed of large and small ignitions, but unlike before the secondary ignitions are almost separate from the first large ones: up to 3 secondary events can develop. The transition to  $0^1$  is also different. This new mixed mode gives way to a waveform of alternately smaller ignitions (Figure 2). This is reminiscent of the period doubling and halving seen in CO oxidation<sup>3</sup> but a new feature for hydrogen.

The transitions between different waveforms occur at different places as the ambient temperature is reduced, a phenomenon known as hysteresis. A state where no repeating unit can be determined (Figure 3) can be reached from the  $0^1$ . This aperiodicity and all the new behaviour observed in these fuel rich systems is currently under examination by numerical investigation of small and large scale kinetic mechanisms in order to determine the origin and underlying attractor structure of this behaviour. Such complicated waveforms are common in other nonlinear chemical systems such as the Belousov-Zhabotinsky<sup>4</sup> reaction.

- 1 B R Johnson, J F Griffiths & S K Scott *J. Chem. Soc. Faraday Trans.* **87** 523 (1991)
- 2 B R Johnson, S K Scott & A S Tomlin *J. Chem. Soc. Faraday Trans.* **87** 2539 (1991)
- 3 B R Johnson, J F Griffiths & S K Scott *Chaos* **1** 387 (1991)
- 4 J L Hudson, M Hart & D Marinko *J. Chem. Phys.* **71** 1601 (1979)

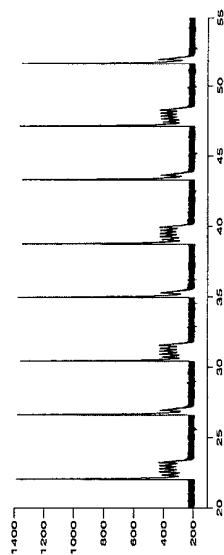


Figure 1 Stabilised  $1^1 1^5$  mixed mode waveform.

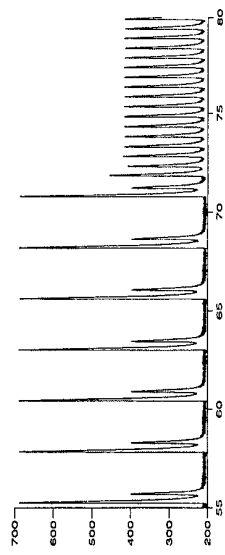


Figure 2 Period halving transition between mixed mode  $1^1$  and simple  $0^1$  waveforms.

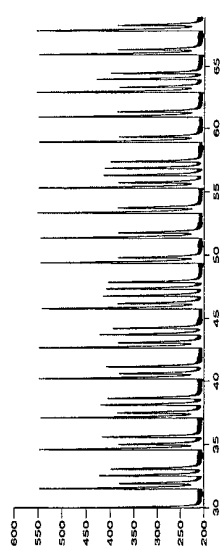


Figure 3 Aperiodic waveform established on decreasing the ambient temperature.

# EXTENSION OF A COMPREHENSIVE METHANE OXIDATION MECHANISM TO INVESTIGATE NITROGEN SPECIES PROFILES IN FLAMES.

K.I. Hughes and A. Tomlin  
*Department of Fuel and Energy, University of Leeds*  
*Leeds, LS2 9JT, UK*

A. Clague, and M.J. Pilling  
*School of Chemistry, University of Leeds*  
*Leeds, LS2 9JT, UK*

T. Turányi  
*Department of Physical Chemistry*  
*Eötvös University*  
*H1518 Budapest-112, P.O. Box 32*

and  
*Central Research Institute for Chemistry*  
*H-1525 Budapest, P.O. Box 17*  
*Hungary*

A comprehensive chemical mechanism to describe the oxidation of methane has been developed, consisting of 351 irreversible reactions with 37 species. To facilitate its widespread use, it is available in a CHEMKIN data file. Comprehensive documentation is also included for each reaction, giving its literature reference along with the applicable temperature range and an estimation of the maximum uncertainty. Where possible, rate coefficient expressions are based on recent evaluated rate data. When necessary, additional documentation is provided in the data file detailing possible alternative rate expressions and/or product channels. The mechanism has been validated against a wide range of experimental measurements including laminar flame velocities, laminar flame species profiles, and ignition delay times.

The mechanism has been extended to include the chemistry of nitrogen and sulfur species, and has been tested against the data on nitrogen species profiles in flames available on the GRI-mech 2.11 [www.gri.me](http://www.gri.me) page [1]. This poster gives the results relevant to the nitrogen species, and in selected cases shows the results obtained from using KINALC as a post processor to the sensitivity analysis data produced by PREMIX.

- [1]. C.T. Bowman, R.K. Hanson, D.F. Davidson, W.C. Gardiner, Jr., V. Lissianski, G.P. Smith, D.M. Golden, M. Frenklach and M. Goldenberg.  
[http://www.me.berkeley.edu/gri\\_mech/](http://www.me.berkeley.edu/gri_mech/)

## HYDROCARBON OXIDATION CHEMISTRY FOR APPLICATION IN ENGINES: HANDLING THE COMPLEXITY

C. Morley

*Shell Research and Technology Centre, Thornton,  
PO Box 1, Chester CH1 3SH, U.K.*

The performance of internal combustion engines is affected in several ways by the chemical kinetics of the fuel oxidation. The emphasis here is on aspects which depend on fuel composition. With the exception of some unusual fuels such as hydrogen or ethyne, the flame propagation during the main (high temperature) combustion is influenced mainly by the energetics of the fuel rather than the detailed structure, and is not discussed here. On the other hand, fuel chemical structure has a very large influence on two phenomena: the reactions between 700 and 1000K which lead through autoignition to knock in the unburned fuel/air mixture; and the speciation of exhaust hydrocarbon emissions which arise from the partial oxidation at between 1000 and 1500K during the exhaust process of fuel which has survived the main combustion. Modelling gasoline autoignition chemical kinetics has a number of problems. Comprehensive models have been developed for hydrocarbons up to  $C_8$  and beyond and successfully reproduce fuel structure effects. However, even for a fuel consisting of a single chemical species a comprehensive model contains several thousand species. This is sustainable with current computing capabilities for a homogeneous system but is impractical if the chemistry is combined with fluid mechanics. There are systematic methods of reducing such schemes, based essentially on applying steady state approximations to species selected by an analysis of the time scale associated with their chemistry.

These different time scales have been illustrated experimentally in an autoignition system by perturbing it and observing the subsequent relaxation. A cool flame was stabilised in a flowing hydrocarbon air mixture and its products photolysed to produce OH radicals, which were observed by laser fluorescence. The OH disappearance was complex and could be fitted to a the sum of three exponential decays, the time constants of which are interpreted as reflecting the chemistry of OH, organic peroxy radicals and organic hydroperoxides, respectively. Rates of chain termination and branching can be individually determined. While a number of factors prevent this experiment giving precise elementary data, the results from a number of alkanes are consistent with, and help to confirm, current mechanisms.

As an alternative to the comprehensive approach, simplified models aim to capture the essential chemical behaviour by using a relatively small number of generalised species. There are several examples in the literature using various degrees of empirical fitting of

parameters. For the investigation of the effect of composition of practical fuels, it is essential that these models handle mixtures - a gasoline can have 100 to 200 significant constituents. A method has been developed in which allows the complicated structurally-dependent alkane chemistry to be reduced to a few parameters - essentially the rates of chain propagation, branching and termination. These are then combined with explicit elementary reactions for the smaller species to provide a description of ignition delays etc., although detailed species information is of course not generated. Alkane oxidation is now reasonably well understood in outline (although there is very little experimental work going on to extend the quantitative information for gas phase rate constants involving moderate sized organic species at temperatures of interest). Mechanisms for aromatics, which comprise a large fraction of commercial fuels, are less developed. In spite of the uncertainties, it is clear that a crucial role is played by benzyl and related radicals. Their inertness means that their concentrations can build up, allowing radical-radical reactions to play a significant role in the autoignition. Modelling shows that the reaction of benzylic radicals with  $HO_2$  is responsible for a synergistic effect and a minimum in the octane number in mixtures of alkanes and aromatics. The influence of chemical kinetics on hydrocarbon exhaust emissions is considerable but is difficult to model. Most of the fuel which escapes the main combustion is trapped in the piston top crevice and its oxidation during exhaust process is under very inhomogeneous conditions. Some progress has been made towards the development of a sufficiently simplified description of the physical conditions and estimates of the relative yield of exhaust products can be made. Alkane chemistry is at least qualitatively clear but there are still large uncertainties with respect to the chemistry of alkenes and aromatics.

The generation of complex reaction mechanisms has been traditionally done by hand but there is an increasing interest in the use of computer techniques. These apply a set of rules for the occurrence of reactions and the structural dependence of the rate constants. Potential advantages are consistency, reviewability, the capability for sensitivity analysis for generic reaction types, and ease of extension and updating. Real disadvantages are the difficulty of excluding large numbers of insignificant reactions. Recent developments in the automatic combustion mechanism generation are briefly reviewed and a new interactive implementation described. Its application to neopentane oxidation - a system that has provided much of the mechanistic understanding of peroxy radical chemistry - has allowed the validity of some of the assumptions in previous interpretations to be tested. In summary, there has been progress in applying kinetics to assessing the practical performance of engine fuels, but there remains a dearth of fundamental rate data under appropriate conditions.

# CHEMICAL KINETIC MODELLING OF HYDROCARBON OXIDATION

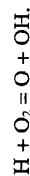
C. Mohamed and J.F. Griffiths

*School of Chemistry, The University, Leeds LS2 9JT, UK*

H.J. Curran, W.J. Pitz and C.K. Westbrook

*Lawrence Livermore National Laboratory, Livermore, CA 94550*

The oxidation of hydrocarbons and related compounds is a complex process involving many intermediate compounds, which ultimately leads to the final products of combustion, CO<sub>2</sub> and H<sub>2</sub>O. The process of oxidation is known to develop through a radical chain mechanism. An important manifestation of this mechanism is chain branching which renders the process capable of self-acceleration and which occurs at both low and high temperatures. Chain branching processes are controlled by two different mechanisms in these two distinct temperature regimes, which depend on the nature of the intermediate species formed in the combustion process. At low temperatures (< 900 K), branching proceeds through a series of molecular oxygen additions to radical species with  $[R] + [O_2] \leftrightarrow [RO_2] > 1$ . Subsequent internal hydrogen abstractions ultimately lead to the formation of two hydroxyl radicals in addition to another oxygenated radical species. At high temperatures,  $[R] + [O_2] \leftrightarrow [RO_2] < 1$ , and thus O<sub>2</sub> addition to alkyl radical is less important than  $\beta$ -scission with chain branching proceeding through the reaction



At intermediate temperatures ( $900 \leq T \leq 1200$  K) both low and high temperature oxidation schemes are important. This region is normally characterized by a two-stage ignition phenomenon in which an early weak ignition is followed by a later and much stronger second stage ignition.

A comparison of results obtained experimentally in a rapid compression machine and computationally using a detailed chemical kinetic model are discussed. These results are significant in that they include both low and intermediate temperature chemical kinetics. Results are reported for a number of hydrocarbons for isomers of C<sub>5</sub> to C<sub>8</sub>.

# OXIDATION AND AUTO-IGNITION OF HYDROCARBONS AT HIGH PRESSURE IN THE LOW AND INTERMEDIATE RANGE OF TEMPERATURE

## COMPARISON BETWEEN 1-PENTENE AND n-PENTANE

R. Minetti, M. Ribaucour, A. Roubaud, L.R. Sochet

*Laboratoire de Cinétique et Chimie de la Combustion URA CNRS 876  
Université des Sciences et Technologies de Lille  
F-59655 Villeneuve d'Ascq Cedex - France*

The influence of a double bond in the auto-ignition chemistry of aliphatic hydrocarbons has been examined by comparing the behaviour of 1-pentene and n-pentane under rapid compression in the same parametric conditions. Auto-ignition delay times, light emission, pressure jump and pre-ignition intermediate products have been measured in the rapid compression machine of Lille for stoichiometric hydrocarbon-air mixtures in the low and intermediate temperature range (700 to 900 K) and at relatively high pressures (6.8 to 9.2 bar). Both fuels present a similar phenomenology of auto-ignition: a lower temperature limit of ignition at ca. 700 K, a marked negative temperature coefficient range of the reaction rate, a two-stage ignition in the lower temperature range and a one-stage ignition at higher temperatures. However, a comparison of the delay times of the cool flame ignition and the normal flame ignition versus the temperature of the core gas at a similar compressed charge density shows marked quantitative differences between the two fuels (Fig. 1). The total ignition delay times are longer for 1-pentene in the whole range of investigated temperatures and the cool flame event disappears at a lower core gas temperature. The negative temperature coefficient region is also narrower. These results were confirmed by the observation that the intensity of the light emission and the pressure jump associated with the cool flame are weaker. All the observed features point out to a lower reactivity of 1-pentene as compared to n-pentane in the considered experimental conditions.

Chemical analysis were performed on samples drawn from the reaction mixture after the cool flame emission in exactly the same conditions of temperature and pressure for both hydrocarbons to detect possible differences in the main reaction pathways. The initial hydrocarbon consumption and the intermediate species nature and concentrations were determined. The main light products formed from 1-pentene are ethanal, propenal, butanal, butene, ethene, and propene. The main C<sub>5</sub> products are 1,3-pentadiene (2.3 % of 1-pentene consumed) and propyloxirane (1.3 % of 1-pentene consumed). The minor C<sub>5</sub> products are 2,4-dimethyloxetane, 2-ethyl-3-methyloxirane, 2-methyltetrahydrofuran, 2-ethyloxetane, pentanal, and pentalen. The initial 1-pentene

# CHEMICAL UPGRADING OF RAPESEED OIL METHYL ESTERS BY THERMOCONVERSION

D. Archambault and F. Billaud

Département de Chimie Physique des Réactions.  
ENSIC-INPL, URA No. 328 CNRS.

1, rue Grandville, BP 451, 54001 Nancy, France

Our laboratory is interested in non alimentary rapeseed oil upgrading by other means than the production of biodiesel fuel obtained by transesterification of rapeseed oil. The aim of this study is to produce  $C_{10}$  -  $C_{14}$   $\alpha$ -olefins and  $C_{6:1}$  -  $C_{12:1}$  unsaturated esters. These products have a high added value in the fields of biodegradable lubricants and oils (poly  $\alpha$ -olefins, industrial lubricants, ...). surfactants ( $\alpha$ -olefin sulfonates, linear alkyl benzene sulfonates, alkyl polyglucosides, ...) and plastic monomers (Rilsan, ...).

Thermoconversion of methyl oleate (major rapeseed oil methyl esters) diluted with nitrogen was investigated in a tubular flow reactor between 500 and 700°C at atmospheric pressure. The residence time ranged from 0.2 to 1.2 seconds. A specific device for the condensation of cracking effluents was used for the fractionated recovery of liquid and gaseous effluents. The latter were analyzed online by an infrared analyzer and by gas chromatography. The cracking products in the liquid effluent were identified by gas-chromatography / mass-spectrometry coupling.

The effects of temperature and residence time on the cracking reaction were studied. The main products were linear 1-olefins, n-paraffins and unsaturated methyl esters. We also observed  $CO$ ,  $CO_2$  and  $H_2$  in the gas fraction. The best yields of  $C_{10}$  -  $C_{14}$   $\alpha$ -olefins and  $C_{6:1}$  -  $C_{12:1}$  unsaturated esters were obtained at about 600°C and for a flow time of about 1.2 seconds with a molar ratio of 10 mole of nitrogen / 1 mole of methyl oleate.

consumption is 28 %. The main light products formed from n-pentane are: ethanal, propene, ethene, 2-pentene, 1-butene, propanal, propanone. The main C5 products are 1- and 2-pentenones (15 % of n-pentane consumed) and 2-methyltetrahydrofuran (4 % of n-pentane consumed). The minor C5 products are 2,4-dimethylpentane, 2-ethyl-3-methylpentane, propylpentane, 2-ethylpentane, pentanal, pentenone and pentenal. The consumption of n-pentane is 30 %.

The measurements of relatively high amounts of butanal and propylpentane in 1-pentene oxidation is in sharp contrast to the observation of Prabhu et al [1] who claim that these products were not observed to be dominant in a lean 1-pentene/air mixture oxidized in a pressurized flow reactor in the same range of temperature and pressure as ours. The presence of these two products in our system has been proved by comparing chromatographic retention times and mass spectra of a commercial sample for butanal and a sample of propylpentane synthesized by the classical reaction of methylchloropentanoic acid with 1-pentene for propylpentane.

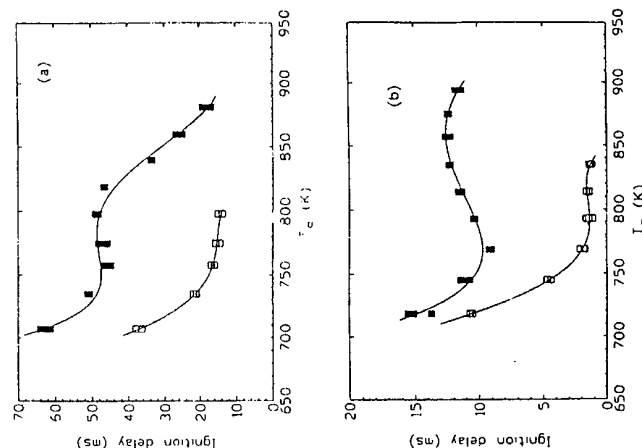


Fig. 1: Auto-ignition delays versus core gas temperature. Pressure range 7-9 bar.

(a) 1-pentane (b) 1-pentene, • cool flame delay times, ■ normal flame delay times

S.K. Prabhu, R.K. Bhat, D.L. Miller, and N.P. Cernansky, 1-Pentene oxidation and its interaction with nitric oxide in the low and negative temperature coefficient regions, Combustion and Flame, 104, 377-390, (1996).

## THE MECHANISM OF ETHYLENE PYROLYSIS AT SMALL CONVERSIONS

J. M. Roscoe,

Department of Chemistry,  
Acadia University, Wolfville, Nova Scotia, Canada B0P 1X0

and

I. S. Jayaweera, A. L. MacKenzie and P. D. Pacey,

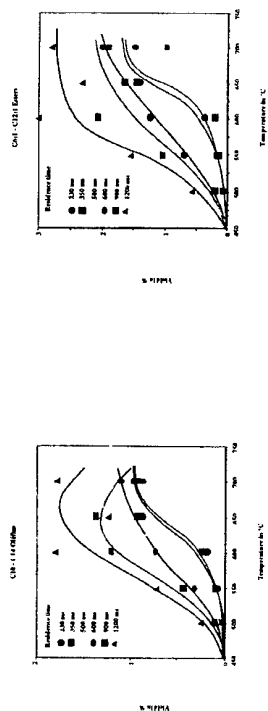
Department of Chemistry,  
Dalhousie University, Halifax, Nova Scotia, Canada B3H 4J3

Kinetic modeling is used in conjunction with measurements of product yields to develop a mechanism for the pyrolysis of ethylene at 896 K and ethylene pressures ranging from approximately 3 to 78 kPa. The major products, roughly in order of importance, were 1,3-C<sub>4</sub>H<sub>6</sub>, C<sub>2</sub>H<sub>6</sub>, 1-C<sub>4</sub>H<sub>8</sub>, H<sub>2</sub>, C<sub>3</sub>H<sub>6</sub>, and CH<sub>4</sub>. Trace amounts of C<sub>3</sub>H<sub>8</sub>, C<sub>4</sub>H<sub>10</sub>, and *cis*- and *trans*-2-C<sub>4</sub>H<sub>8</sub> were also observed. Ethylene conversions were always less than 4%. An induction period was observed for all products except H<sub>2</sub>, and was followed by a steady rate, which was of second order for all products except 1,3-C<sub>4</sub>H<sub>6</sub>. The induction periods could be fitted to the equation<sup>1</sup>

$$[A] \quad [X]/t = \frac{R_X^{\text{ss}} \tau}{t \ln 2} \ln \left\{ \cosh \left( \frac{t \ln 2}{\tau} \right) \right\}$$

in which  $R_X^{\text{ss}}$  is the steady-state rate just before the onset of autoacceleration,  $t$  is the residence time in the reactor and  $\tau$  is the induction period. The values of  $R_X^{\text{ss}}$  and  $\tau$  were adjusted using nonlinear least squares analysis to optimize the fit to the data. Rates of autoacceleration beyond the induction period were calculated as  $[X]/t^2$ . The pressure dependences of the parameters above were described as conventional log-log order plots.

The experimental data could be described by a kinetic model consisting of 31 elementary reactions. The model was tested by using it to calculate product yields as a function of reaction time for each of the experimental reaction conditions. These results were then analysed in the same way as the experimental results, producing kinetic parameters which could be compared directly with those evaluated from the experimental data. The following tables indicate the quality of agreement with the experimental results.



Yield of C10-C14 α-olefins

Yield of C6-1 - C12-1 esters

The Arrhenius parameters for the overall thermal decomposition of methyl oleate were calculated. In a tubular reactor of stainless steel the rate equation

$$\log(k/s^{-1}) = 4.60 - 10294/2.3T$$

was determined in the temperature range of 500 to 700°C.

A mechanistic simulation model was developed. The primary mechanism consisted of 408 free radical and 1 non-elementary reactions. We simulated this mechanism by using the CHEMKIN code package [1]. This is a Fortran program for predicting homogeneous gas phase chemical kinetics for different reactor systems. To simulate the experimental tubular flow reactor, a series of micromixed perfectly stirred reactors was used.

The model explains the consumption of the reactant and the formation of the main products.

This research is supported by CNRS (Ecotech) - ADEME - Communauté Urbaine du Grand Nancy and AGRICE.

(1) R.J. Kee, F.M. Rupley, J.A. Miller Chemkin-II: A Fortran chemical kinetics package for the analysis of gas phase chemical kinetics, Sandia Report, Supersedes SAND 89-8009B, September 1989

Table 1  
Orders of Quantities Determined From Experiments

Quantity	Experimental	Model
$\tau$	-0.99±0.31	-1.10±0.05
$R_{CH_4}^*$	2.22±0.17	1.98±0.02
$R_{C_2H_6}^*$	2.00±0.16	1.99±0.04
$R_{C_3H_8}^*$	1.62	1.74±0.02
$R_{C_4H_{10}}^*$	2.05	1.97±0.02
$[H_2]/t^2$	1.56±0.10	0.98±0.01
$[CH_4]/t^2$	1.98±0.18	1.99±0.01
$[C_2H_6]/t^2$	1.74±0.09	1.96±0.01
$[C_3H_8]/t^2$	1.97	2.14±0.01

Table 2  
Fitted Parameters in Equation [A] from Experiment and from Predictions of the Final Model.

Pressure (kPa)	S/V (cm <sup>-1</sup> )	$\tau$ (s)		$R_X^{ss} \times 10^{10}$ (mol L <sup>-1</sup> s <sup>-1</sup> )	
		Experimental	Model	Experimental	Model
X = CH <sub>4</sub>					
3.1	3	-----	0.70	1.3±0.1	1.55
4.6	3	-----	0.50	3.4±0.5	3.50
4.7	10	0.27±0.04	0.48	3.7±0.1	3.60
7.0	9	0.28±0.02	0.29	11.0±0.3	7.70
7.8	9	0.23±0.04	0.24	12.2±0.5	9.10
9.8	9	0.11±0.02	0.20	23 ± 1	15.0
17.3	14	-----	0.11	74 ± 6	47.5
X = C <sub>3</sub> H <sub>6</sub>					
3.1	3	-----	0.70	6.3±0.2	7.20
4.6	3	-----	0.50	16 ± 2	16.3
5.6	10	0.24±0.03	0.33	20.8±0.7	21.8
7.0	9	0.16±0.01	0.27	48 ± 1	34.5
17.3	14	0.12±0.02	0.11	192 ± 6	221
X = 1,3-C <sub>4</sub> H <sub>6</sub>					
4.7	10	0.40±0.05	0.43	76 ± 3	80.0
7.8	9	0.34±0.03	0.24	171 ± 5	190
X = 1-C <sub>4</sub> H <sub>8</sub>					
4.7	10	0.65±0.05	0.42	28 ± 1	22.0
7.8	9	0.34±0.03	0.24	78 ± 2	60.0

Table 3  
Rates of Auto-acceleration. [X] × 10<sup>19</sup>/t<sup>2</sup> mol L<sup>-1</sup> s<sup>-1</sup>

Pressure (kPa)	S/V (cm <sup>-1</sup> )	H <sub>2</sub>		CH <sub>4</sub>		C <sub>3</sub> H <sub>8</sub>		C <sub>3</sub> H <sub>6</sub>	
		Expt.	Model	Expt.	Model	Expt.	Model	Expt.	Model
4.6	3	-----	11.4	1.5±0.3	0.38	10±2	3.7	4.1±0.4	1.6
9.8	9	-----	49.0	7±1	3.0	50±4	33.3	-----	13.5
10.3	3	-----	24.0	6.9±0.8	1.87	45±4	17.4	20 ± 1	8.02
20.0	9	40±8	47.0	-----	7.46	80±20	70.2	-----	33.3
26.1	3	70±20	51.0	-----	10.6	140±60	92.6	-----	52.2
26.7	9	66±3	126	-----	22.2	172±1	230	-----	99.5
41.6	9	160±20	168	-----	48.3	420±80	471	-----	219
53.2	9	160±40	241	-----	86.5	700±200	837	-----	395
66.4	9	290±20	321	-----	144	1100±200	1370	-----	663
77.6	9	350±20	310	-----	170	1700±200	1540	-----	811

## REFERENCES

1. P.D. Pacey and J.H. Wimalasena, *J. Phys. Chem.*, **88**, 5658-5660 (1984).
2. J.M. Roscoe, I.S. Jayaweera, A.L. Mackenzie and P.D. Pacey, *Int. J. Chem. Kinet.*, **28**, 181-193 (1996).

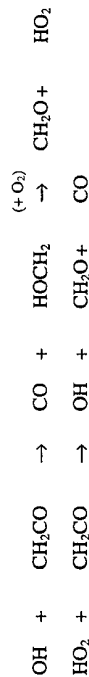
## THE GAS-PHASE AUTOXIDATION OF KETENE

Peter J. Roden, Moray S. Stark, and David J. Waddington,

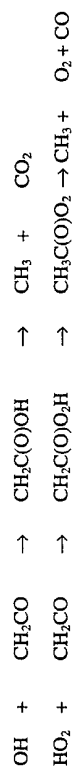
*Department of Chemistry, University of York, Heslington, York, YO1 5DD, UK.*

Ketene and the ketyl radical have been reported as important intermediates in the oxidation of hydrocarbons and related compounds (1), and specifically in the oxidation of methane (2), acetylene (3), and acetone (4). However, there have only been two detailed studies of the autoxidation of ketene itself in the gas phase, by Barnard and Kirschner (5) and by Michaud and Ouellet (6,7). Their findings, obtained over a temperature range of 603-748K, are broadly similar, the major products being carbon monoxide, carbon dioxide and formaldehyde. These products were also observed in a later study on the reaction of ketene with hydroxyl radicals (8).

These experimental results cannot easily be rationalised using the mechanisms proposed by earlier workers (5-7). Indeed some of the reactions they proposed now appear unnecessarily complex. We have therefore constructed a reaction mechanism to model their results (eg. figure 1). Addition of hydroxyl and hydroperoxyl radicals to the  $\beta$ -carbon atom of ketene account for the majority of the observed products.



However the rate and the autocatalytic character of the reaction appear to be governed by addition of radicals to the  $\alpha$ -carbon atom. In the simulations, radical chain branching is by the decomposition of methylhydroperoxide (observed as a product at 603 K), with the methyl radicals formed predominantly by addition of hydroxyl (9) and hydroperoxyl (10) radicals to the  $\alpha$ -carbon, followed by an internal hydrogen transfer reaction.



It is difficult to simulate the rapid, autocatalytic overall rate of reaction for ketene autoxidation without having an unusually fast rate for the addition of hydroperoxyl to ketene. This is consistent with recent work (11) on the epoxidation of acrolein by peracetyl radicals, which

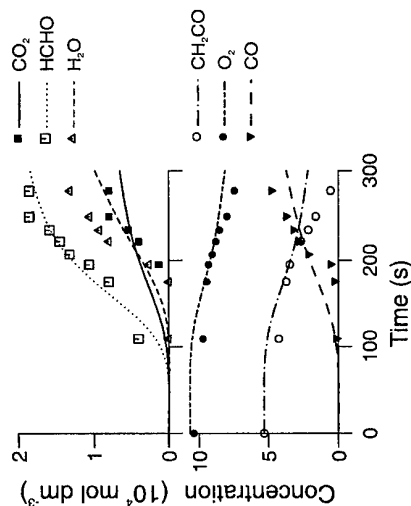


Figure 1. Autoxidation of ketene. Conditions, 603 K, 80 mbar,  $[\text{CH}_2\text{CO}]/[\text{O}_2]_{\text{initial}} = 1/2$ .

The points are experimental results of Michaud and Ouellet (7) and the lines are simulations.

## References

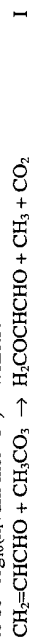
1. Salooja, K. C., *Combust. Flame*, **10**: 11-21 (1966).
2. Dagaut, P., Boettner, J., Cathonnet, M., *Combust. Sci. and Technol.*, **77**: 127-148 (1991).
3. Miller, J. A., Mitchell, R. E., Smooke, M. D., Kee, R. J. *19th Symp. (Int.) on Comb., The Combustion Institute*, Pittsburgh, 1982, p 181-196.
4. Barnard, J. A., Honeyman, T. W., *Proc. Roy. Soc. London A*, **279**: 236-247 (1964).
5. Barnard, J. A., Kirschner, E., *Combust. Flame*, **11**: 496-500 (1967).
6. Michaud, P., Ouellet, C., *Combust. Flame*, **12**: 395-398 (1968).
7. Michaud, P., Ouellet, C., *Canad. J. Chem.*, **49**: 297-302 (1971).
8. Faubel, C., Wagner, H. G., Hack, W., *Ber. Bunsenges. Phys. Chem.*, **81**: 689-692 (1977).
9. Brown, A. C., Canosa-Mas, C. E., Parr, A. D., and Wayne, R. P., *Chem. Phys. Lett.*, **161**: 491-496 (1989).
10. Tidwell, T. T., *Ketenes*, J. Wiley & Sons, New York, 1995, p636-639.
11. Roden, P. J., Stark, M. S. and Waddington, D. J., *The Epoxidation of Acrolein by Acetylperoxy Radicals*, 14th Int. Symp. on Gas Kinetics, Leeds University, 1996.

# THE EPOXIDATION OF ACROLEIN BY ACETYLPEROXY RADICALS

Peter J Roden, Moray S Stark and David J Waddington.

*Department of Chemistry, University of York, York, YO1 5DD, United Kingdom.*

An understanding of the mechanism of the gas phase autoxidation of alkenes depends in turn on an understanding of the behaviour of the resulting unsaturated aldehydes in the process (1). However, little work has been done on the autoxidation of these species. It is known though, that the low temperature autoxidation of acrolein (produced during the oxidation of propene) is anomalously slow in comparison with the oxidation of acetaldehyde or propanal (2). Chain branching for aldehyde oxidation is considered to be via decomposition of the acylperoxide. However, this route may not be so readily available for acrolein. There is an alternative route for acylperoxy radicals, which can epoxidise acrolein instead of abstracting a hydrogen atom. In preliminary experiments, the epoxide of acrolein (oxiran-2-yl carboxaldehyde) was identified in the autoxidation of acrolein and in these studies the rate constant for the related reaction of epoxidation of acrolein by acetylperoxy radicals (reaction 1) has been examined at 383 K and found to be  $\log_{10}(k_1/\text{dm}^3\text{mol}^{-1}\text{s}^{-1}) = 4.1 \pm 0.5$ .



Acetylperoxy radicals were produced by the slow autoxidation of acetaldehyde in a static reactor in the presence of small quantities of 1-butene and acrolein. The rate of formation of oxiran-2-yl carboxaldehyde relative to that of 1,2-epoxybutane was determined by GC FID, with product identification by GC MS (figure 1). A previously measured rate constant for the epoxidation of 1-butene by acetylperoxy radicals (3) allowed the rate constant for the epoxidation of acrolein to be determined.

This rate constant is more than two orders of magnitude faster than would be expected from the correlation that exists between the rate constant for epoxidation by peroxy radicals and the ionisation energy of the double bond (4) (figure 2).

The rate of hydrogen abstraction by acetylperoxy radicals from acrolein has also been examined for this work and found to be at least ten times slower than the corresponding abstraction from acetaldehyde. Work is currently being carried out to find whether the anomalously fast rate of epoxidation of acrolein by acylperoxy radicals allows the reaction to play a significant role during acrolein autoxidation.

## References

1. Stark, M.S. and Waddington, D.J., *Int J Chem Kinet*, **27**, 123-151 (1995).
2. Newitt, D.M., Baxt, L.M. and Kelkar, V.V., *J Chem Soc*, 1703-1710 (1939).
3. Selby, K. and Waddington, D.J., *J Chem Soc Perkin Trans II*, 1715-1718 (1975).
4. Ruiz Diaz, R., Selby, K. and Waddington, D.J., *J Chem Soc Perkin Trans II*, 360-363 (1977).

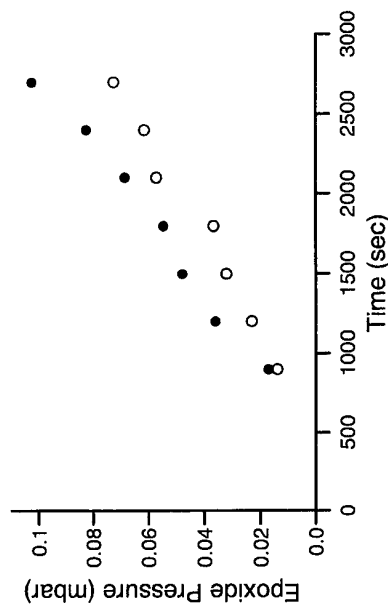


Figure 1. The growth of oxiran-2-yl carboxaldehyde (●) and 1,2-epoxybutane (○) during the co-oxidation of acetaldehyde, acrolein and 1-butene. Conditions: 383K, 400 mbar total pressure, 133 mbar  $\text{CH}_3\text{CHO}$ , 133 mbar  $\text{O}_2$ , 13.3 mbar  $1\text{-C}_4\text{H}_8$ , 13.3 mbar  $\text{C}_2\text{H}_3\text{CHO}$ , 107 mbar He.

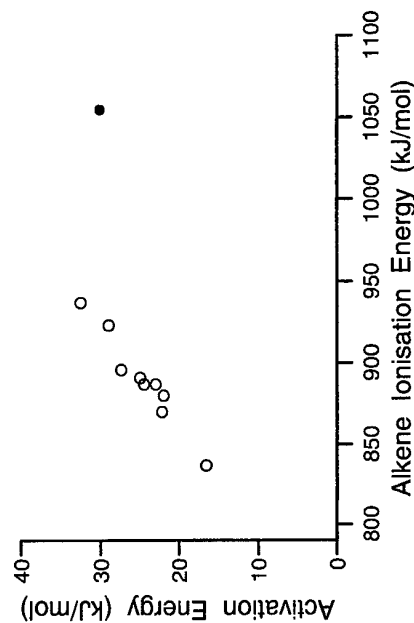


Figure 2. Activation energy for the reaction of acetylperoxy radicals with alkenes related to the alkene ionisation potential of the alkenes. The plot shows the correlation that exists for mono-alkenes (○) and the anomalous behaviour of acrolein (●).

# ACTIVE INTERMEDIATES IN THE CHAIN OXIDATION OF DICHLOROSILANE

N.M.Rubtsov, V.I.Chernysh, G.I.Tsvetkov

*Russia, Institute of Structural Macrokineitics Ras, Moscow Region,  
142432, P/O Chernogolovka*

The wide application of  $\text{SiO}_2$  thin films in integrated circuits processing evokes an increasing interest to silanes oxidation. The branching chain nature of these reactions has been established, but the kinetic mechanisms have not been yet assigned. This work is aimed at the detection and identification of the active intermediates in the branching chain reaction of the oxidation of dichlorosilane (DCS) with molecular oxygen.

The experiments were carried out under static and flow conditions over the pressure range 0.5-5 Torr and the temperature range 293-393 K. The quartz reactor of cylindrical shape (12 cm high, 12 cm in diameter) had inlets for electrical power supply and gas evacuation as well as optical windows. The ignition was provided by rapidly heated nichrome wire coil. The gas mixtures contained 25% DCS with oxygen. It has been shown that the reaction occurs in oscillatory regime under flow conditions at fixed pressure at 293 K after several forced ignitions at 2 Torr; in this case the intensity and period of ignitions are constant in time. It should be noted that these oscillations take place outside of self-ignition area (the lower temperature of self-ignition is 340 K under our conditions). These regimes are presumed to be associated with nonlinear reactions involving the long-lived intermediate containing -Si-O-Si- fragments. The oscillations become attenuated at the temperature above 330 K turning into slow stationary combustion in the absence of any marked warming-up ( $< 4^\circ$ ).

The emission spectra were recorded at 293 K. The light emitted in oscillatory regime was brought in focus on the enter slit of the 600 grooves/cm grating monochromator VM-25 (Germany). The scanning speed of the spectrum was fitted in such a way that 1-2 ignitions occurred during 1 nm scanned. The light emission has been observed over the following intervals of wavelengths:  $\text{SiO}^* (A^1 \Pi \rightarrow X^1 \Sigma)$  [1] in the range 220-280 nm;  $\text{SiCl}_2^* (A^1 B_1 \rightarrow X^1 A_1)$  in the range 300-380 nm [2]; the continuous emission caused by the blackbody radiation from the solid  $\text{SiO}_2$  particles over 400 nm in accordance with the studies of the rarified flame of the oxidation of silane [3]. It should be noted that silylene radicals in combustion of silanes are experimentally detected for the first time.

The intensive absorption due to short-lived intermediate in the range of 210-260 nm (maximum 220 nm) has been observed under static conditions. The simultaneous recording of the above mentioned intermediates as well as conductivity (revealed recently [4]) during the single ignition has been performed. It has been shown that the peaks of the signals are staggered in time. The first peak in time is  $\text{SiCl}_2^*$  (coincident with  $\text{SiO}^*$ ), the second is the absorption peak, the third is the visible emission coincident with conductivity peak. Indeed, the detectable conductivity is observed when the first peaks ( $\text{SiCl}_2^*$  and  $\text{SiO}^*$ ) take place. It has been also shown that 10% additives (to fuel) of  $\text{SF}_6$  have a decreasing effect only on the absorption, visible emission and conductivity signals. It means that the absorbing intermediate contains Si-O bonds, since  $\text{SF}_6$  has influence mainly on  $\text{SiO}_2$  formation [5].

1. R.Shanker, C.Linton, R.D.Verma. Mol.Spectr. 1976, v.60, N1, p.197.
2. D.Sameith, J.P.Monch, H.J.Tiller et al. Chem.Phys.Lett., 1986, v.128, p.483.
3. C.Coda, O.Fujivara. Comb. and Flame, 1988, v.73, p.187.
4. V.V.Azatyay, A.S.Lukashev, S.S.Nagorny et al. Kinetika i Kataliz, 1993, v.34, N3, p.404.
5. V.P.Karpov, N.M.Rubtsov, O.T.Ryzhkov et al. Proc. of the Zel'dovich memorial, Moscow, 1994, v.2, p.33.

## LINEAR CHAIN BRANCHING IN THE OXIDATION OF DICHLOROSILANE

N.M.Rubtsov, V.V.Azatyay, S.M.Temchin, V.I.Chernysh, O.T.Ryzhkov  
*Russia, Institute Of Structural Macrokinetics Ras,  
Moscow Region, 142432, P/O Chernogolovka*

The branching chain reactions of the oxidation of silane and its derivatives are widely used in the integrated circuits processing. However, the kinetic mechanisms of these reactions have not been revealed at present. Thus, the assignment of the nature of particles taking part in linear branching and the measurement of the effective rate constant of this process are quite valuable.

This work describes the kinetic approach based on the study of the dependence  $[A]$  of the lower pressure limit of self-ignition on the initial concentrations of fuel and oxidizer, temperature and reactor diameter [1].

The experiments were carried out under static conditions over the temperature range 373 - 513 K and over the pressure range 0.5 - 10 Torr. The diameters of heated quartz reactors were in the range of 2 - 6.5 cm. The gas mixtures of dichlorosilane (DCS) with oxygen were prepared prior to experiment and contained DCS in the range of 5 - 50 %.

The first part of the experiments was carried out over the interim area of chain break in reactors previously treated with 30 - 50 self-ignitions at required temperature until the lower pressure limit of the self-ignition  $P$  became constant. It has been found that the values of the lower pressure limit are independent on the oxygen content in the mixture and decrease with increase in DCS content. It means that molecular oxygen does not take part in linear branching process, i.e. the condition of self-ignition at the lower limit takes the form:

$$n K_1 (DCS) = K_2$$

In this case  $1/K_2 = 1/K_2'' + 1/K_2'$  ( $1 < n \leq 2$ ) is the stoichiometry coefficient,  $K_1$  - the effective rate constant of linear branching,  $K_2'$  - the rate constant of the chain break over the interim area,  $K_2'' = 23.2 D / d^2 P$  - the rate constant of the diffusive chain break,  $D = D'(T/273)^{1.6}$ ,  $D'$  - the mass diffusivity of the active centre participating in linear branching at NTP (estimated as 0.2 cm<sup>2</sup>/s),  $d$  - the reactor diameter,  $P$  - the pressure of the lower limit

of the self-ignition,  $T$  - temperature). The data handling (at  $n = 2$ ) gave the following values [2]:

$$K_1 = (4 \pm 1) 10^{-11} \exp(-(27.6 \pm 4.0) \text{ kJ/mole} / RT) \text{ cm}^3 / \text{s}; K_2'' = 100 \pm 300 \text{ s}^{-1}.$$

It has been also found, that the values of the lower limit of the self-ignition are markedly higher in freshly washed (with 10% HF) reactors, i.e. the chain break in thus treated reactors is close to the diffusive type. This part of experiments was carried out in such a way that the reactor was washed with 10% HF after each self-ignition. The experimental data for different diameters were calculated by equation [1]:

$$P^2 d^2 = 23.2 D T / (2 K_1 \gamma 10^{19}) \quad (\gamma \text{ is the mole fraction of DCS}).$$

It is evident that the  $K_1$  value obtained from the latter equation conforms with the one derived independently above on the basis of the experimental data for the chain break over the interim area.

1. N.N.Semenov. A selection of problems of chemical kinetics and reactivity. Moscow, Ac.Sci.USSR. 685 p.

2. O.T.Ryzhkov, V.V.Azatyay, N.M.Rubtsov, S.M.Temchin. Kinetika i kataliz 1995, v.36, N1, p.99-102.

# THE CHEMIONIZATION IN THE LOW TEMPERATURE (293K) BRANCHING CHAIN REACTION OF THE CHLORINATION OF DICHLOROSILANE

V.V.Azatyán, N.M.Rubtsov, S.M.Temchin, V.I.Chernysh, G.I.Tsvetkov  
*Russia, Institute Of Structural Macrokinetics Ras, 142432, Moscow  
Region, P/O Chernogolovka*

In our previous works charged particles formed by chemionization have been revealed in the branching chain low temperature reactions of the oxidation of silane and dichlorosilane (DCS) at low pressures [1]. We have aimed to extend the scale of this class of chain processes, i.e. to demonstrate chemionization both for DCS oxidation and DCS chlorination, moreover the chemical nature of the latter reaction has not been yet clarified. The present work describes the investigation of DCS-chlorine reaction.

The experiments were carried out under static conditions at 293 K and pressures up to 6 torr. The quartz reactor of cylindrical shape (4 cm in diameter) had inlets for electrical power supply and gas evacuation as well as optical windows for simultaneous recording of chemiluminescence and conductivity. The latter was measured by means of electrical probes. The chlorine was initially allowed to bleed into the reactor up to the required pressure  $P = 0.2-3$  Torr.

It has been found that the self ignition occurs immediately after mixing at  $P > 1$  Torr (DCS: chlorine = 1:1) without any distinct induction period. The latter arises at  $P < 1$  Torr and amounts up to 6 s at the lower self-ignition limit (0.55 Torr). The existence of the self-ignition limit and its dependence on the surface state show the branching chain character of the chlorination of DCS. The changes in conductivity during the self-ignition events were recorded under conditions specified. The time of the total change in conductivity was equal to the one of chemiluminescence and amounted to 3 s. One can see, according to  $\tau = x^2 / 2 D$ , that the heat

released would be practically dissipated on the surface during the self-ignition ( $\tau$  is the characteristic heating time,  $x$  the characteristic dimension and  $D$  - mass diffusivity close to thermal diffusivity). Therefore the heat released is not sufficient for any marked warming-up.

The concentration of charged particles was estimated from the dependence of the current density  $J$  on electrical field tension  $E$  in the instrumental cell consisting of two copper plates as electrical probes placed in reactor:  $J = (en_+ \mu_+ + en_- \mu_-) E$  ( $e$  is electron charge,  $n_+$ ,  $n_-$ ,  $\mu_+$ ,  $\mu_-$  - concentrations and mobilities of positive and negative charged particles). The ionization degree is small at low temperatures, so  $n_+ = n_- = n$ . The very fast trimolecular reaction  $e + Cl_2 + Cl_2 \rightarrow Cl_2 + Cl_2^-$  occurs, so the characteristic time of electron conductivity is rather small ( $10^{-3}$  s) in comparison with the time of combustion, and the electron conductivity contribution into the whole conductivity is markedly low. Thus,  $\mu_+ = \mu_- = \mu$  is a mobility of ions. The upper limit of the mobility of chlorine ions in molecular chlorine was estimated as  $190 \text{ cm}^2 / \text{V s}$  at 4 Torr. Under our conditions ( $J = U/SR$ ,  $U=50 \text{ mV}$ ,  $S=20 \text{ cm}^2$ ) one can estimate the low limit of the concentration of charged particles  $n = J/2e\mu E > 5 \cdot 10^6$  charge units/ $\text{cm}^3$ .

It has been shown that the emission spectrum of the ignition recorded with the optical spectra analyser OSA-500 (Germany) supplied with 600 grooves/cm grating monochromator corresponds to  $\text{SiHCl}$  ( $1 B_1 - 1 A_1$ ) [2]. The fact that initial pressure and the pressure of the end products are equal implies the stoichiometry of reaction:  $\text{SiH}_2 \text{Cl}_2 + 2 \text{Cl}_2 \rightarrow \text{SiCl}_4 + 2 \text{HCl} + 136 \text{ kcal/mole}$ . The energy released in the reaction of addition of chlorine atom to  $\text{SiHCl}$  ( $1 B_1$ ) amounts to about 170 kcal/mole, that may be enough for the formation of the pair:  $\text{SiHCl}_2 + e$ .

1. V.V.Azatyán, A.S.Lukashev, S.S.Nagorny et al. Kinetika i Kataliz, 1993, v.34, N3, p.404.

2. P.Ho, W.G.Breiland. Appl.Phys.Lett, 1983, v.43, p. 125.

# EXPERIMENTAL RESULTS TESTIFYING TO CHAIN BRANCHING IN THE PROCESS OF 1,1-DIFLUOROETHANE CHLORINATION

I.R.Begishev

*Higher Engineering Fire Service Technical School, 4, Galushkina St. Moscow  
129301, Russia*

V.A.Poluektov

*Karpov Institute of Physical Chemistry, Moscow, Russia*

The problem of chain branching in hydrocarbons chlorination reactions is not fully understood yet. Nevertheless experimental data received while studying photoignition of  $\text{Cl}_2 + \text{CF}_3\text{HCH}_3$  mixtures validly prove their existence.

$\text{CF}_3\text{HCH}_3$  chlorination in a gaseous phase initiated by light goes with a high rate at atmospheric pressure and normal ambient temperature. The substitution of a hydrogen atom by a chlorine atom in the difluoroethane molecule occurs most rapidly in position 1. The chain length of the chlorination reaction reaches the meaning of  $10^5$ . Chain breaking mainly occurs during interaction of chlorine atoms with halohydrocarbon radicals. The substitution rate of the first hydrogen atom by chlorine at  $T=293\text{K}$  is almost two orders as high as that of the second hydrogen atom. The reaction rate of photochlorination in a wide range of reagents concentration change is described by the equation

$$\frac{d[\text{RCI}]}{dt} = K(W_i[\text{RH}][\text{Cl}_2])^{0.5}$$

where  $W_i$  is the formation rate of the reaction initial centres. At the mercury lamp light intensity of  $I=2 \times 10^{21}$  quantum/ $\text{m}^2 \cdot \text{s}$   $\text{CF}_3\text{HCH}_3 + \text{Cl}_2$  mixtures are intensely heated and can ignite. Photoignition of such mixtures in long (in the direction of a light flux) reaction vessels has an unusual character.

Steel cylindrical vessels 0.05 m in diameter and from 0.2 till 1.0 m in length were used. One end of them were closed with a quartz glass. The temperature of the reacting mixture was measured by tungsten-rhenium thermocouples ( $d=20 \times 10^{-6}$  m) spaced along the vessel axis.

Under the light flux action the mixture ( $\text{CF}_3\text{HCH}_3 + \text{Cl}_2$ ) is initially heated in the vicinity of the quartz window through which the light is let into the vessel and then after a short period of time the mixture is intensely heated in the depth of the vessel where the flame does occur. We've called such a phenomenon a two-centered ignition.

In other similar gaseous systems ( $\text{CF}_3\text{H}_2 + \text{Cl}_2$ ,  $\text{CCl}_3\text{H}_2 + \text{Cl}_2$ ) we've not observed such a phenomenon, the flame occurred in the vicinity of the quartz window and then spread over the reaction vessel.

An unusual space - time ignition profile is explained by 1,1-difluoroethane chlorination reaction kinetic peculiarities. First it is connected with lack of energy evolving at the first stage for flame propagation and secondly with a considerable difference in the substitution reaction activation energies of the first and second hydrogen atoms by chlorine in the molecule  $\text{CF}_3\text{HCH}_3$  ( $E_1=7.5$  kJ/mole,  $E_2=29.3$  kJ/mole). At light initiation the chemical reaction rate is the highest in the vicinity of the quartz window. At this point as a result of the first chlorination stage the reaction mixture is most intensely heated. In a long reaction vessel locally heating region expands freely. This leads to the temperature decrease of the heated mixture within this region and correspondingly to the reducing of the reaction rate and heat evolving rate during further stages. Ignition is impossible here.

The following experiments will help to comprehend the flame appearance in the depth of the reaction vessel. At light pulse ignition of  $\text{CF}_3\text{HCH}_3 + \text{Cl}_2$  mixture the temperature decrease in the nearest to light source centre right after the temperature initiation ceased inside the vessel and a high temperature centre appeared in a dark period after a considerable time interval ( $>0.5$  s). In our opinion the cool mixture ignition during a dark period may occur only as a result of chain branching in the process of  $\text{CF}_3\text{HCH}_3$  chlorination.

Power chain branching through an excited molecule  $\text{HCl}$  is known to be impossible because of its low energy. In  $\text{CF}_3\text{HCH}_3 + \text{Cl}_2$  system power chain branching could occur at the dissociation of halocarbon molecule having an ability of storing a sufficient quantity of energy as a result of a successive substitution of several H-atoms by chlorine. Chain branching and ignition seat formation occur in the depth of the vessel because  $\text{CF}_3\text{ClCH}_3$  quantity which was formed there during the light action is minimal. The experiments prove  $\text{CF}_3\text{ClCH}_3$  to be an effective retarder for the process of photoignition at a low temperature.

# THE ROLE OF HETEROGENEOUS REACTIONS IN GASEOUS PHASE OXIDATION OF FLUOROOLEFINS AT CLOSE TO ATMOSPHERIC PRESSURES

I.R. Begishev

*Higher Engineering Fire Service Technical School, 4, Gdushkina St. Moscow  
129301, Russia*

It is generally accepted that the influence of the reactor vessel walls can be seen in chain reactions in gaseous phases only at low pressures ( $10^2$ - $10^4$  Pa) and it is basically accounted for originating and breaking of reaction chains on the walls. At higher pressures chain originating and active particles decaying mainly occur in the vessel volume, that's why the role of heterogeneous reactions under these conditions was considered to be extremely low. As for the role of the surface in chain development reactions it can also be clearly seen at low pressures as the rate of heterogeneous chain development is quite comparable with the rate of chain development in a gaseous phase. (According to V.Azatyany [1]).

A great effect of reaction vessel walls condition has been discovered during the investigation of fluoroolefin-oxygen mixtures self-ignition at pressures (0,4 - 4,0)  $10^5$  Pa in cylindrical vessel with 0,05 m in diameter and 0,2 m in long. The temperature of fluoroolefin self-ignition in oxygen has been noticeably decreasing after several mixture ignitions in the reactor (reactor vessel ageing). In some cases concentration ignition area spreading also took place. At atmospheric pressure self-ignition temperature of oxygen mixtures has decreased from 535K to 515K for hexafluoropropylene; from 461K to 412K for tetrafluoroethylene and from 440K to 314K for trifluorochloroethylene.

Efficient activation energies of chemical reaction in the region of low and high pressures considerably differed. For example, in case of hexafluoropropylene efficient activation energy obtained according to the dependence of  $\ln P/T$  on  $1/T$  at pressures lower than atmospheric was 18,1 kJ/mole and at pressures higher than atmospheric was nearly 140 kJ/mole. Despite the changes in the oxidation mechanism the effect of vessel walls on the self-ignition process remained strong at high pressures too.

The analysis of experimental results leads to the conclusion that the effect of reaction vessel walls is due to the participation of surface adsorbing of active particles in the chain development reactions. At the mixture burning the formed active particles-intermediate products of the reaction - are adsorbed on the reaction vessel walls. Vacuuming the vessel between the experiments doesn't remove them completely.

Reacting with the molecules from a gaseous phase they contribute to the ignition of a fresh mixture.

The participation of adsorbed active particles in chain development reactions is confirmed by the experiments with photochemical initiation. The effect of the 1 kW mercury lamp UV-light on the reaction mixtures  $C_3F_6+O_2$  and  $C_2F_3Cl+O_2$  led to a decrease in self-ignition temperature. As for  $C_2F_4+O_2$  mixture its change under the light effect was complex. At pressures higher than atmospheric an insignificant self-ignition temperature increase took place whereas at lower pressures the temperature sharply decreased. In this mixture the light effect caused change in the limit nature which testified to the light initiated chain ignition. But the difference in its values in a fresh and aged vessel is kept. In some cases this difference is greater than the change caused by the light effect. Under chlorine sensitizing photoignition in mixtures  $C_3F_6+O_2$  initial reaction centres formation mainly take place in the reaction vessel volume. In this case surface condition of vessel walls also remains as it was. Thus the experimental results obtained testify to the significant role of heterogeneous reactions in gaseous phase oxidation of fluoroolefins at pressures close to atmospheric.

(1) Azatyany V.V. Uspekhi khimii **54**, N 1, 33-61 (1985).

# GAS - PHASE KINETICS AND MECHANISMS OF THE CF<sub>3</sub> RADICAL REACTIONS WITH UNSATURATED COMPOUNDS

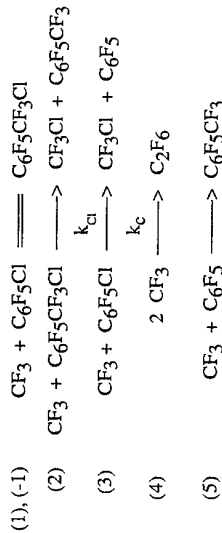
J. D. Nieto, C.A.Rinaldi, O. S. Herrera, S. I. Lane and E. V. Oexler

INFIQC - Departamento de Fisicoquímica. Facultad de Ciencias Químicas.  
Universidad Nacional de Córdoba  
C.C. 61, suc. 16, 5016 Córdoba - Argentina

There have been many gas phase studies of the reactions of the CF<sub>3</sub> radicals with a variety of organics compounds, as a result of which the kinetic parameters of these reactions are now well established<sup>1</sup>. There is, however, little information about the reactions of CF<sub>3</sub> radicals with halobenzenes and in particular Arrhenius parameters for the addition and abstraction reactions. We have studied the reaction of CF<sub>3</sub> radicals with chloropentafluorobenzene in the temperature range 318 - 653 K in order to gain insight into the reaction mechanism and derive the corresponding kinetic parameters.

The photolysis of perfluoroacetic anhydride (PFAA) with light from a high pressure mercury lamp, was used as the CF<sub>3</sub> radical source in the temperature range 318 - 473 K. Products were identified by GC, IR and MS. Runs were carried out at low conversion of C<sub>6</sub>F<sub>5</sub>Cl, less than 2 %. Under these conditions the main products identified were CF<sub>3</sub>Cl, C<sub>2</sub>F<sub>6</sub>, C<sub>6</sub>F<sub>5</sub>CF<sub>3</sub>, CO<sub>2</sub> and CO. Taking into account that the amount of CO<sub>2</sub> formed from the photolysis of PFAA measures the quantity of CF<sub>3</sub> radicals produced, the rate of addition of CF<sub>3</sub> to the aromatic ring can be estimated from a radical material balance.

If the following general reaction scheme is applicable :



and considering that reaction (3) is negligible at low temperatures the following expression is obtained for the addition reaction (1) :

$$k_{\text{add}}/k_c^{1/2} = R_{\text{add}}/R_{\text{C}_2\text{F}_6}^{1/2} [\text{C}_6\text{F}_5\text{Cl}]$$

and the addition rate parameters can be summarized in the following equation, between 318 and 373 K :

$$\log \{ (k_{\text{add}}/k_c^{1/2}) \text{ mol}^{-1/2} \text{ cm}^3/2 \text{ s}^{-1/2} \} = (4.46 \pm 0.10) - (22.48 \pm 0.70) / \theta$$

with  $\theta = 2.303 \text{ RT kJ mol}^{-1}$ .

It was found that the addition reaction becomes reversible above 400 K and the rate constant can be correlated with the ionization energy of C<sub>6</sub>F<sub>5</sub>Cl and other halosubstituted aromatic compounds, as has been shown for the rate coefficient of the addition reactions of other electrophilic species such as OH to benzene and its substituted derivatives<sup>2,3</sup> and NO<sub>3</sub> to alkenes<sup>4</sup>.

In the temperature range 573 - 653 K, the CF<sub>3</sub> radicals produced by photolysis of CF<sub>3</sub>I react with C<sub>6</sub>F<sub>5</sub>Cl only by abstraction of the chlorine atom (reaction 3), with the following Arrhenius parameters relative to CF<sub>3</sub> recombination:

$$\log \{ (k_{\text{Cl}}/k_c^{1/2}) \text{ mol}^{-1/2} \text{ cm}^3/2 \text{ s}^{-1/2} \} = (6.24 \pm 0.10) - (52.65 \pm 0.86) / \theta$$

with  $\theta = 2.303 \text{ RT kJ mol}^{-1}$ .

The Arrhenius parameters for the chlorine abstraction reaction were estimated using the Bond Strength-Bond Length (BSBL) semiempirical method. Good agreement was obtained with the experimental values as for the hydrogen abstraction reaction from pentafluorobenzene<sup>5</sup>, previously studied in our laboratory.

We are also investigating the reaction of CF<sub>3</sub> with thiophene and preliminary results indicate that the addition channel is dominant at low temperature.

## References

- 1- NIST Chemical Kinetics Database. Version 5.0 (1992).
- 2- K. Lorenz and R. Zellner, *Ber. Bunsenges. Phys. Chem.*, **87**, 629 (1983).
- 3- M. Rinke and R. Zetzsch, *Ber. Bunsenges. Phys. Chem.*, **88**, 55 (1984).
- 4- G. Marston, P.S. Monks, C.E. Canosa-Mas and R.P. Wayne, *J. Chem. Soc. Faraday Trans.*, **89**, 3899 (1993).
- 5- S.I. Lane, E.V. Oexler and E.H. Staricco, *Int. J. Chem. Kinet.*, **23**, 361 (1991).

## MECHANISM OF "CHLORO-PYROLYSIS" OF METHYL CHLORIDE

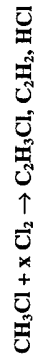
Paul-Marie Marquaire, Marwan Al Kazzaz and René Fournet

Département de Chimie Physique des Réactions

CNRS URA 328, ENSIC - INPL Université

address: DCPR-ENSIC - BP 451 - 1 rue Grandville - 54001 NANCY Cedex - FRANCE

The "chloro-pyrolysis" of methyl chloride is a  $\text{CH}_3\text{Cl} / \text{Cl}_2$  gas phase reaction at high temperature, under no flame condition ... In specific conditions [1], the reaction produces mostly vinyl chloride, acetylene and HCl other products are  $\text{C}_2\text{H}_4$ ,  $\text{CH}_4$ ,  $\text{C}_2\text{H}_2$  and  $\text{CH}_2\text{Cl}_2$ .

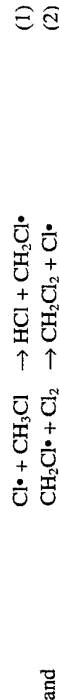


The "chloro-pyrolysis" produces  $\text{C}_2$  hydrocarbons even though it is well known that the thermal reaction between  $\text{CH}_3\text{Cl}$  and  $\text{Cl}_2$  is a chlorination reaction which produces chloromethanes.

In the first experimental study, at  $950^\circ\text{C}$ , 40ms and 5% of chlorine, we have obtained a vinyl chloride selectivity of 30% and 30% for the  $\text{C}_2$  hydrocarbons, for a conversion of about 15%. The "chloro-pyrolysis" is the second step of the MTV process (Methane To Vinyl Chloride), a new way for upgrading Natural Gas [2].

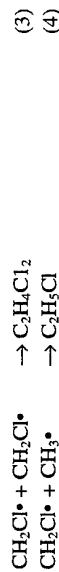
A detailed radical mechanism is proposed, it is in agreement with others studies [3-5], and it explains our experimental results of "chloro-pyrolysis".

The primary mechanism allows to understand the reaction, in particular the very strong influence of temperature. At low temperature the reaction is a long chain reaction of chlorination [3]:

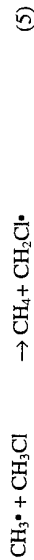


With a negative "activation energy", the primary chain length decreases when the temperature increases. At high temperature, it is a short chain reaction with radical coupling reactions. The radicals concentrations are:

$\text{CH}_2\text{Cl}\cdot > \text{CH}_3\cdot \gg \text{Cl}\cdot$ , according to these reactions:

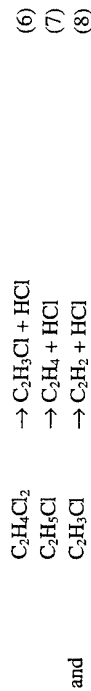


The methane formation comes from:

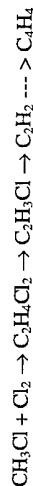


It is particularly important to note that  $\text{CH}_2\text{Cl}\cdot$  radical concentration controls the  $\text{C}_2$  selectivity by the competition between two elementary reactions: (2) and (3).

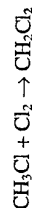
The secondary reactions explain the formation of others products. The decomposition of  $\text{C}_2\text{H}_4\text{Cl}_2$  and  $\text{C}_2\text{H}_5\text{Cl}$  lead to vinyl chloride and ethylene



Our experimental results on  $\text{CH}_3\text{Cl}/\text{Cl}_2$  reaction can be interpreted by a competition between two major pathways:  
- the "chloro-pyrolysis" (short chain reaction):



- the "classical" chlorination (long chain reaction):



The "chloro-pyrolysis" is similar to the pyrolysis, but the presence of chlorine induces a pyrolysis at lower temperature and/or lower reaction time. In these conditions, the addition of chlorine has a beneficial effect on the pyrolysis of  $\text{CH}_3\text{Cl}$ : - the reaction can produce  $\text{C}_2\text{H}_3\text{Cl}$  - the soot formation decreases, but the chlorine gives two by-products:  $\text{CH}_2\text{Cl}_2$  and HCl.

As our "Chloro-pyrolysis of Methyl Chloride", other gas phase processes use chlorine for methane activation: - the Benson process [6]: methane/chlorine flame - the Gorin process [7]: pyrolysis of  $\text{CH}_3\text{Cl}$  - the "CCOP" Senkan process [8]: oxy-pyrolysis of  $\text{CH}_3\text{Cl}$ . These "chlorine catalysed" processes produce  $\text{C}_2$  hydrocarbons, but under specific conditions, our reaction produces vinyl chloride.

This work has been funded by **Gaz de France** (GDF).

## REFERENCES

- 1) P.M. Marquaire, Y. Muller and M.-Al Kazzaz, Fr Patent No.2 711 649 (1995).
- 2) P.M. Marquaire, M.-Al Kazzaz, Y. Muller and J. SaintJust, *4th International Natural Gas Conversion Symposium* - Kruger National Park (South Africa), 19-23 November 1995; Studies in Surface Science and Catalysis (in press).
- 3) B.E. Kurtz, Ind. Eng. Chem. Process Des. Develop., 11 (1972) 332.
- 4) M. Weissman and S.W. Benson, Int. J. Chem. Kin., 16 (1984) 307.
- 5) S.B. Karra and Senkan S.M., I&EC. Res., 27 (1988) 1163.
- 6) S.W. Benson, US Patent No. 4 199 533 (1980).
- 7) E. Gorin, US Patent No. 2 320 274 (1943).
- 8) S.M. Senkan, US Patent No. 4 714 796 (1987).

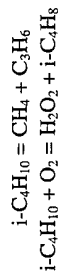
THE HETERO-HOMOGENEOUS AUTOXIDATION  
OF ISOBUTANE AT 800 K. A SIMPLE TECHNIQUE  
FOR DETERMINING RATE CONSTANT PARAMETERS.

R. Zils, D. Perrin and R. Martin

*Université Henri Poincaré, Nancy 1 and INPL, Laboratoire de Chimie Radicalaire,  
U.A. 328 CNRS, BP 239, 54506 VANDŒUVRE-LES-NANCY Cedex (FRANCE).*

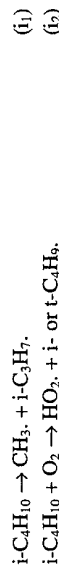
Most of data concerning  $\text{HO}_2$ , + alkane reactions have been obtained using the decomposition of tetramethylbutane in the presence of  $\text{O}_2$  in aged boric acid-coated Pyrex vessels as a source of  $\text{HO}_2$ .<sup>(1)</sup> In these vessels, the surface is inert to oxygenated radicals and surface effects are negligible. In other cases, kinetic data have been obtained in KCl-coated vessels in which oxygenated radicals are efficiently destroyed at the surface.<sup>(2)</sup>

It is shown in the present paper that a  $\text{PbO}$ -coated Pyrex reactor of surface-to-volume ratio  $23 \text{ cm}^{-1}$  is very efficient in destroying peroxy radicals and allows to obtain reliable kinetic data concerning the autoxidation of alkanes. First results of a kinetic study of the thermal reaction of 50-100 Torr of isobutane in the presence of 1-50 Torr oxygen are described. In this  $\text{PbO}$ -coated reactor, the only observed stoichiometries are:



The rate of oxygen consumption is practically equal to that of isobutene production. Rates of methane and of propene production are also practically equal. No molecular hydrogen and no carbon oxides are observed. The rates of product formation are second order in isobutane. Those of  $\text{CH}_4$  (or  $\text{C}_3\text{H}_6$ ) and of isobutene are 0.5 and 0.8, respectively, in oxygen. All the concentration-time profiles are linear.

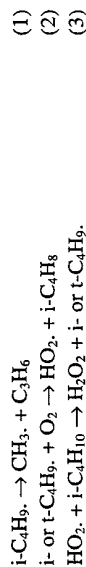
These observations are consistent with a free-radical scheme in which chains are initiated by the homogeneous steps:



and terminated at the  $\text{PbO}$ -coated surface:



The homogeneous propagation steps:



account for the observed products.

Arrhenius parameters of these steps are evaluated. An analysis of the scheme gives  $k_2/k_1$ ,  $k_3 k_1/k_w$  and  $k_2/k_1$ .

These results are confirmed by a more detailed scheme analysed by computer.

- 1) R.W. WALKER, Twenty-Second Symposium on Combustion - The Comb. Inst. 1988, p 883-892.
- 2) R.R. BALDWIN et al., J. Chem. Soc. Faraday Trans., 1991, **87**, 2147-50.

## HIGH TEMPERATURE PYROLYSIS OF CYCLOPENTADIENE

K. Roy, P. Frank

*DLR Institute for Physical Chemistry of Combustion, Stuttgart, Germany.***Introduction**

Cyclic  $C_5$ -hydrocarbons are considered to play an important role as intermediates in the degradation of aromatic hydrocarbons. As a first step in investigating high temperature  $C_5$ -reactions, the decomposition of cyclopentadiene has been investigated. Only few experimental studies are available. Gey et al. [1] have published an ab-initio calculation supported by experiments in a regular oven, for the decomposition of cyclopentadiene. Butler and Bruinsma et al. [2] executed flow reactor experiments. Colket [3] and very recently, Bureat and Dvinyaninov [4] investigated the decomposition of cyclopentadiene in a single-pulse shock tube with relatively high initial concentrations.

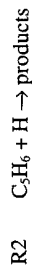
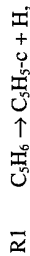
**Experimental**

The high purity stainless steel shock tube consists of a test section of 6 m and a driver section of 4 m length. The test section is evacuated by a turbomolecular pump to about  $10^{-7}$  mbar before each experiment. The measurements were performed behind the reflected shock front close to the end flange. ARAS was used to monitor the time dependent concentration profiles of H-atoms. The H-atom concentrations were measured at  $\lambda_o$  (121.6 nm) by using an oxygen spectral filter. The atomic concentration profiles reported here are based on calibration experiments.

Cyclopentadiene was obtained by distillation from di-cyclopentadiene with a purity of better than 99% (controlled by mass spectrometry). The initial concentrations of cyclopentadiene for the experiments ranged from 0.5 to 8 ppm. The pressures for all experiments were about 2 bar, observation time was 1 ms. The sensitive ARAS technique allowed the high temperature reactions to be studied in highly diluted mixtures. These low initial concentrations strongly reduce, within the time scale of the experiment ( $t \leq 800 \mu s$ ), the number of important subsequent reactions which had to be considered for the evaluation of the measured concentration profiles.

**Results and Modelling**

In the investigated temperature range, all the experimental H-absorption profiles clearly reveal that H-atoms are formed without any detectable induction delay. The evaluation of the measured H-profiles showed, that for low initial concentrations the cyclopentadiene decay in the temperature range of 1260 K to 1530 K can be simulated essentially by using only reactions R1 and R2.



This is caused by the high dilution of the reactant which reduces the influence of secondary reactions considerably. The experiments show that besides the H-producing step the H-consumption by reaction R2 leads to a decreasing H-atom growth rate in the latter stage of the reaction progress. Therefore, for a first evaluation of  $k_1$ , only these two reactions were used.

The rate constant for the major H-consuming reaction step  $C_3H_6 + H \rightarrow \text{products}$  was determined in a separate series of experiments. For a direct determination of the rate constant, the consumption of H-atoms was monitored. Therefore, mixtures of cyclopentadiene (about 10 ppm) and ethyl iodide (about 1 ppm) were prepared. Ethyl iodide served as H-atom source [5]. At temperatures  $T \geq 1150$  K the production of H-atoms is fast and leads to initial concentrations of H equal to the initial concentration of  $C_3H_5I$ . Thus by monitoring the I-atom concentrations, the initial concentration of H-atoms can be easily determined. These investigations were carried out for temperatures below 1280 K, where the influence of reaction R1 is negligible.

**Discussion**

The evaluated rate constants for the unimolecular decomposition reaction of cyclopentadiene are shown in the Arrhenius plot of fig 1. From this diagram the rate constant for R1:

$$k_1 = 1.1 \times 10^{15} \exp(-38760/T) \text{ s}^{-1} \text{ was deduced.}$$

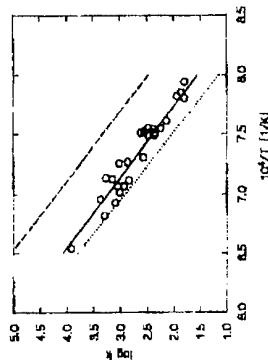


Fig. 1. Arrhenius diagram for reaction R1.  
Full line: this work; -----: Ref.[4]; .....: Ref.[3]

From the experiments with mixtures of cyclopentadiene and ethyl iodide a global rate coefficient for the H-consuming reaction channel of  $k_2 = 7.2 \times 10^{13} \exp(-1781/T) \text{ cm}^3 \text{ mol}^{-1} \text{ s}^{-1}$  was deduced. As there is at present no possibility to identify products, a discussion about the branching into plausible product channels can be made by taking into consideration the results of Emdee et al.[6] and of Dean [7]. This leads to the result that there is a major H-consuming pathway

## HIGH TEMPERATURE PYROLYSIS OF PHENOL

C. Horn, P. Frank

DLR, Institute of Physical Chemistry of Combustion, Stuttgart, Germany.

## Experimental

Phenol is believed to play an important role during the oxidation of aromatics. However, the mechanism of the thermal decay of this species is still poorly understood. Therefore, we performed shock tube experiments on highly diluted mixtures of phenol in Ar. The initial phenol concentrations were between 10 and 50 ppm, the temperature ranged from 1450 to 1650 K behind the reflected shock; the typical post shock pressure was between 2 and 2.5 bar.

The time dependent absorption at  $\lambda_1 = 121.6$  nm and  $\lambda_2 = 151.0$  nm was monitored simultaneously, close to the end flange. At these wavelengths, resonance absorption of H atoms and CO molecules, allows to deduce time dependent concentration profiles of the two species, sufficiently free from interferences. The relationship between absorption and concentration was given by calibration curves.

In a separate series of experiments, the absorption at  $\lambda_3 = 130.2$  nm was also measured, allowing us to determine O atom concentrations.

For investigating the reaction of phenol with H atoms, a series of experiments was performed with ethyl iodide and phenol diluted in Ar at temperatures below 1300 K, i.e. below the temperature when phenol starts to decay. In this temperature range ethyl iodide is suitable as source for H atoms [1].

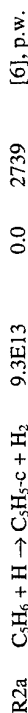
Phenol exhibits a strong tendency for adsorption at metallic surfaces. Therefore we worked with a tube heated to 70°C. To control the precise phenol concentration, before each shock run samples were drawn at the end flange and quantitatively analyzed by absorption spectroscopy.

## Results

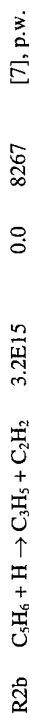
A typical concentration profile for H and CO at 1536 K with an initial concentration of 20.5 ppm phenol is shown in fig.1.

While the CO - concentration is increasing steadily, the H - concentration shows a maximum at about 300  $\mu$ s after the start of the reaction. Furthermore, what is the most important point, even at the very beginning of the reaction the CO concentration exceeds the H concentration by far.

This behaviour is observed over the whole temperature range. At  $T > 1570$  K, however, the CO concentrations in our experiments reach a plateau which is equal to the initial phenol concentration. The measurement of the O atoms showed, that below 1650 K there is no production of O atoms. Previously performed measurements on OH production [2] during the phenol decay showed, that the OH production is also negligible under our conditions ( $[\text{OH}]_{\text{max}} < 1\% [\text{C}_6\text{H}_5\text{OH}]_0$ ).



and a second H-consuming reaction step



The evaluation procedure of ref. [6] is based on measurements in a flow reactor at temperatures about 1100 K to 1200 K. The rate constant  $k_{2b}$  has been calculated from that of the reverse reaction which results from QRRK calculations performed by Dean [7]. From these data a branching ratio of about 0.67 at 1280 K is calculated. Using this value and the total rate constant of the present work, the Arrhenius expressions for R2a and R2b have been calculated.

## References

- [1] Gey, E., Ondrushka, B., Zimmermann, G., J. Prakt. Chem. **1987**, 329 (3), 511
- [2] Butler, R.G., Msc. Thesis Princeton University **1992**, (b) Bruisma, O.S.L., Tromp, P.J.J., de Sauvage Nolling, H.J.J., Moulijn, J.A., FUEL **1988**, 67, 334
- [3] Colket, M.B., **1990**, Eastern States Section of Combustion Institute annual meeting Orlando, Paper #1
- [4] Burcat, A., Dvinyaninov, M., **1996**, Comb. Flame, to be published.
- [5] Wintergerst, K., Frank, P., Proc. 19th Internat. Symposium on Shock Waves, Springer **1993**, pp. 77-82.
- [6] Endee, J.L., Brezinsky, K., Glassman, I., J. Phys. Chem. **1992**, 96: 2151
- [7] Dean, A.M., J. Phys. Chem. **1990**, 94: 1432

## Discussion

In a first attempt to model our results, we used the reaction mechanism proposed by Lovell et al. [3], who performed flow reactor experiments on the pyrolysis of phenol. They assumed an H - abstraction from phenol forming phenoxy + H as the first step which is followed by the dissociation of phenoxy to CO + cyclopentadienyl ( $C_5H_5$ ) and by further subsequent reactions.

This assumption is not in agreement with our measurements. Using the mechanism of ref. [3], the production of H should be higher than that of CO. As we always find more CO than H, the model would require a very fast H consumption after the initial step:

He et al. have performed shock tube experiments on phenol + H [4]. They propose a reaction channel yielding phenoxy plus  $H_2$  with  $k_1 = 1.15 \times 10^{-14} \exp(-6240/T) \text{ cm}^3/(\text{mol s})$  and a second channel yielding benzene + OH with  $k_2 = 2.21 \times 10^{-13} \exp(-3990/T) \text{ cm}^3/(\text{mol s})$ . Our experiments on phenol + H could be modelled very well with those values.

To simulate at least the first 200  $\mu\text{s}$  of the H - profiles of the phenol pyrolysis experiments, either the value of  $k_1$  or the value of  $k_2$  has to be raised by two orders of magnitude which is in contradiction to He's and our measurements. Furthermore, such an increase in  $k_1$  would lead to a much higher CO - concentration at the lower end of our temperature range.

The second channel yielding benzene + OH would produce too large OH concentrations. At the upper temperature range the final concentration of CO equals the initial phenol concentration. This is also in contradiction to a fast OH - producing channel.

This argument can also be used to rule out a fast third channel yielding phenyl +  $H_2O$ .

The necessary H consumption by reaction with the highly reactive cyclopentadienyl radical also cannot simulate the profile: even with a reaction rate of  $5 \times 10^{-14} \text{ cm}^3/(\text{mol s})$  (which would be close to the collision number), the simulated H concentrations in the beginning of the reaction would exceed the measured ones by a factor of three to five.

Therefore we have to conclude, that the first step in the pyrolysis of phenol is a rearrangement of the phenol to a tautomer followed by the abstraction of CO:



The CO - profiles can be modelled very well by an overall rate coefficient  $k_3 = 1.0 \times 10^{-12} \exp(-30600/T)$  for reaction R3:  $C_6H_5OH = C_3H_6 + CO$  summing up these two steps. The Arrhenius diagram is shown in fig. 2.

The CO abstraction as the first step in the pyrolysis of phenol has already been proposed by Cypriès and Bettens [5], who replaced the hydroxyl - H of phenol by tritium and then pyrolyzed this species. The tritium was afterwards exclusively found in the  $C_3H_6$  - species (or rather  $C_3H_5T$  - species) which was detected by mass spectroscopy. This species might probably be cyclopentadiene as this had been found by means of GC in the flow reactor measurements of Lovell et al. [3]. The pyrolysis of this species then dominates the H production. Extensive investigations on the pyrolysis of cyclopentadiene are currently being made so that we hope to be able to interpret our H signals soon.

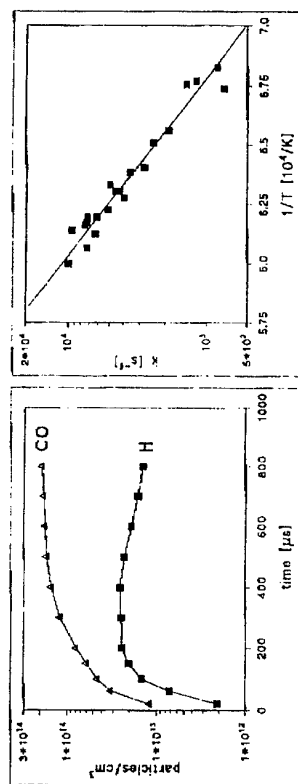


Figure 1

Figure 2

**Fig.1:** Concentration profiles of H (squares) and CO (triangles).  
T = 1536 K, p = 2.38 bar,  $[Phenol]_0 = 20.5 \text{ ppm}$

**Fig.2:** Arrhenius diagram for the reaction R3:  $C_6H_5OH = C_3H_6 + CO$

## References:

- [1] K. Wintergerst, P. Frank : *Proc. 19th Int. Symposium on Shock Waves, Springer 1993, pp. 77-82*
- [2] C. Naumann : *DLR Stuttgart, unpublished results.*
- [3] A.B. Lovell, K. Brezinsky, I. Glassman : *Int. J. Chem. Kin. Vol. 21, 547 - 560 (1989)*
- [4] Y.Z. He, W.G. Mallard, W. Tsang : *J. Phys. Chem. 92, 2196 - 2201 (1988)*
- [5] R. Cypriès, B. Bettens : *Tetrahedron, Vol. 30, 1253 - 1260, (1974)*

## SILANE THERMAL DECOMPOSITION

A.A. Onischuk, V.P. Strunin, M.A. Ushakova, V.N. Panfilov

*Institute of Chemical Kinetics and Combustion, Russian Academy of Sciences,  
Siberian Branch, Novosibirsk, 630090, Russia.*

The process of silane thermal decomposition results in a solid product of variable composition. For the same experimental conditions the mass-spectrometric analysis of the gas-phase products and the investigation of solid product (amorphous hydrogenated silicon, formed as aerosol particles) were carried out. The silane decomposition was carried out in a flow reactor for the mixtures  $\text{Ar} + \text{SiH}_4$  with the reactor temperature  $800 \leq T \leq 1000$  K. The total mixture pressure was 39 kPa. The initial silane molar fraction ( $c_s$ ) was in the range  $1.5 \times 10^{-4} \leq c_s \leq 5 \times 10^{-2}$ . The solid product was analyzed by the methods of hydrogen evolution, IR and ESR spectroscopy. The contents of polyhydride groups ( $\text{SiH}_2$ ), monohydride groups ( $\text{SiH}$ ) and paramagnetic centers were determined [1,2].

The following experimental results were obtained. At the initial stage of reaction the acceleration of silane decomposition and disilane and hydrogen formation occurs. The effective activation energy ( $E_{\text{eff}}$ ) of silane decomposition decreases with decreasing silane molar fraction:

$$E_{\text{eff}} \approx [275 + 23.8 \times \log_{10}(c_s)] \text{ kJ/mol.}$$

We found also, that a decrease in  $c_s$  causes the decrease in the relative rate of silane consumption  $W_s = (d[\text{SiH}_4]/dt) / [\text{SiH}_4]_0$  and disilane relative concentration  $[\text{Si}_2\text{H}_6]/[\text{SiH}_4]_0$  (where  $[\text{SiH}_4]_0$  is the initial silane concentration and  $[\text{SiH}_4]$ ,  $[\text{Si}_2\text{H}_6]$  are silane and disilane concentrations during the reaction). The essential solid product formation begins at silane conversion  $> 4\%$ . At low conversions the hydrogen in solid product is mainly contained as polyhydride groups, formed from gas-phase silylenes ( $\text{Si}_2\text{H}_5$ ). At high silane conversions the monohydride groups, forming from hydrogen depleted gas-phase intermediates are prevailing in the solid product. The fraction of hydrogen, contained in solid product as constituent of polyhydride groups decrease with  $c_s$  decreasing.

To give a qualitative explanation of the above experimental data the kinetic modeling was carried out.

Arrhenius Parameters of Reaction Steps, used in modeling

rxn. no	reaction	A	E
1	$\text{SiH}_4 \rightarrow \text{SiH}_2 + \text{H}_2$	$1.0 \times 10^{12}$	217
-1	$\text{SiH}_2 + \text{H}_2 \rightarrow \text{SiH}_4$	$1.9 \times 10^{12}$	0
2	$\text{SiH}_4 + \text{SiH}_2 \rightarrow \text{Si}_2\text{H}_6$	$1.3 \times 10^{14}$	0
-2	$\text{Si}_2\text{H}_6 \rightarrow \text{SiH}_2 + \text{SiH}_4$	$2.4 \times 10^{15}$	215
3	$\text{Si}_2\text{H}_6 + \text{SiH}_2 \rightarrow \text{Si}_3\text{H}_8$	$2 \times 10^{14}$	0
-3	$\text{Si}_3\text{H}_8 \rightarrow \text{SiH}_2 + \text{Si}_2\text{H}_6$	$4.9 \times 10^{15}$	222
4	$\text{Si}_2\text{H}_6 \rightarrow \text{H}_3\text{SiSiH} + \text{H}_2$	$7.9 \times 10^{15}$	236
-4	$\text{H}_3\text{SiSiH} + \text{H}_2 \rightarrow \text{Si}_2\text{H}_6$	$1.9 \times 10^{12}$	0
5	$\text{SiH}_4 + \text{H}_3\text{SiSiH} \rightarrow \text{Si}_3\text{H}_8$	$1.3 \times 10^{14}$	0
-5	$\text{Si}_3\text{H}_8 \rightarrow \text{SiH}_4 + \text{H}_3\text{SiSiH}$	$9.3 \times 10^{14}$	209
6	$\text{H}_3\text{SiSiH} \rightarrow \text{Si}_2\text{H}_4$	$6.2 \times 10^9$	6.5
-6	$\text{Si}_2\text{H}_4 \rightarrow \text{H}_3\text{SiSiH}$	$1.3 \times 10^{10}$	52.7
7	$\text{Si}_2\text{H}_4 \rightarrow \text{Si}_2\text{H}_2 + \text{H}_2$	$7 \times 10^{12}$	140

(Units:  $\text{cm}^3$ , mol, s, kJ)

We assume, that, precursors of solid product are silylenes ( $\text{SiH}_2$ ,  $\text{SiH}_3\text{SiH}$ ) and hydrogen depleted intermediates. Hydrogen depleted intermediates can result from dissociation of disilene  $\text{H}_2\text{Si=SiH}_2$  (reaction 7) and its higher homologs. The concentrations of these homologs are likely to be low and may be neglected. An example of solid product formation reaction due to hydrogen depleted intermediates may be:



In our modeling the stage (7) limited the solid sink process.

The modeling testifies that initially, silane decomposition follows reactions (1) and (2) which leads to the accumulation of intermediates  $\text{Si}_2\text{H}_6$ ,  $\text{Si}_3\text{H}_8$ ,  $\text{SiH}_2$ ,  $\text{H}_3\text{SiSiH}$ ,  $\text{Si}_2\text{H}_4$ . As the concentrations of the above mentioned intermediates increase, the rate of silane consumption via reaction (5) becomes substantial. This silane consumption acceleration leads to the acceleration of hydrogen, disilane, trisilane and other intermediate formation. These computation results agree with the experimentally observed initial acceleration of silane consumption and disilane and hydrogen formation.

It was shown experimentally, that solid product forming on the walls results in additional silane decomposition. The conclusion was drawn, that the solid product reactivity is related to the dangling bonds located on the surface of interconnected microvoids and channels.

## References:

- 1) Onischuk, A.A., Strunin, V.P., Ushakova, M.A. and Panfilov, V.N., *phys. stat. sol.(b)* **186**, 43-55 (1994).
- 2) Onischuk, A.A., Strunin, V.P., Ushakova, M.A., Samoilova, R.I. and Panfilov, V.N., *phys. stat. sol.(b)* **193**, 25-38 (1996).

# MECHANISM REDUCTION FOR TROPOSPHERIC CHEMISTRY

M.J. Pilling and G. Zeng

*School of Chemistry, University of Leeds, Leeds LS2 9JT U.K.*

A detailed butane oxidation mechanism has been constructed with 510 elementary reactions of 185 species; it represents the degradation chemistry over a wide range conditions in the troposphere. A set of ordinary differential equations (ODEs) has been compiled to describe the kinetics of the mechanism. The reduction of this mechanism has been carried out for a range of tropospheric conditions which are characterized by extremely low, intermediate and high [NO] respectively.

The mathematical tools used for mechanism reduction are based on sensitivity analysis, which provides a quantitative measure of the dependence of species concentrations and rates on the concentrations of other species or on the rate parameters. Principal component analysis (PCA) is also employed and, in combination with the sensitivities, allows the classification of reactions into groups of differing time-scale and the understanding of the coupling within these groups. The initial removal of the redundant species from the mechanism significantly simplifies the structure, and makes the application of the PCA more efficient because there are fewer parameters. The application of the PCA to the rate sensitivity matrix enables the identification of the redundant reactions in the group by studying eigenpairs of the symmetric matrix. The separation of the eigenvalues illustrates the significances of the reaction groups, and the corresponding eigenvectors describe the combinations of the reactions within a group. Fast reversible reactions can be identified in pairs from the eigenvector elements. Identification of the redundant reactions can also be effected by studying the reaction rates and their relative contributions to the net production rates of various species.

The reduction depends strongly on the initial conditions and the model objectives. The criterion for the reduction was to reproduce the concentration of ozone, as well as PAN and OH within the specific accuracies from the solutions of the reduced model. The specific accuracies are related to the requirements of practical atmospheric modelling or measurement.

Further simplification of the mechanism was achieved by application of the quasi-steady-state approximation (QSSA) to the reduced schemes obtained from the sensitivity analysis, by reducing the number of ODEs. The criterion for the selection of QSSA species is the calculation of the QSSA errors produced by applying the QSSA along the reaction trajectory.

This mechanism was reduced to 64 reactions of 32 species (including 8 QSSA species) in the remote marine scenario, 76 reactions of 44 species (including 11 QSSA species) in the remote rural scenario and 53 reactions of 38 species (including 22 QSSA species) in the polluted scenario. The reduced schemes represent the optimum procedures for the regional conditions described above and the different degradation paths that butane follows as a function of the different initial conditions and ratios.

## References

- Turanyi T., *J. Math. Chem.*, **5**, 203, (1990)
- Turanyi T., *New J. Chem.*, **14**, 795, (1990)
- Tomlin A. S., Pilling M. J., Turanyi T., Merkin J. H., Brindley J., *Combust. Flame*, **91**, 107-130, (1992)
- Jenkin M. E., Sanders S. M., Pilling M. J., in press, (1996)
- Madronich S. and Calvert J. G., *J. Geophys. Res.*, **95**, 5697-5715, (1990)
- Greenberg J. P. and Zimmerman P. R., *J. Geophys. Res.*, **89**, 4767-4778, (1984)
- Fahey D. W. et al., *J. Geophys. Res.*, **91**, 9781-9793, (1986)
- Bowman F. M. and Seinfeld J. H., *J. Geophys. Res.*, **99**, 5309-5324, (1994)
- Turanyi T., Tomlin A. S., Pilling M. J., *J. Phys. Chem.*, **97**, 163-172, (1993)

# KINALC: A PROGRAM FOR THE KINETIC ANALYSIS OF GAS-PHASE REACTION SYSTEMS

Tamas Turanyi

*Department of Physical Chemistry*  
*Eotvos University*  
*H-1518 Budapest-112, P.O.Box 32, Hungary*  
*and*  
*Central Research Institute for Chemistry*  
*H-1525 Budapest P.O.Box 17, Hungary*

KINALC is a postprocessor to any CHEMKIN [1] based simulation program. It has been interfaced to the programs of the CHEMKIN package (SENKIN, PREMIX, PSR, SHOCK, and EQLIB) and also to the RUN1DL [2] package. KINALC carries out three types of analysis: processing sensitivity analysis results, extracting information from reaction rates and stoichiometry, and providing kinetic information about the species. KINALC can extract the important pieces of information from the sensitivity results dumped by the simulation programs. It can also calculate the sensitivity of objective functions, formed from the concentrations of several species. The program can suggest a list of rate limiting steps. The most advanced handling of sensitivity information is the principal component analysis [3] of the sensitivity matrix. This eigenvector-eigenvalue analysis shows which parameters have to be changed simultaneously for a maximum change of the concentration of several species. This information can be used for uncertainty analysis, parameter estimation, experimental design, and mechanism reduction.

KINALC can carry out rate-of-production analysis with detailed output and gives a summary of important reactions. The matrix of normed reaction rate contributions can also be considered as the sensitivity of reaction rates, and the principal component analysis of this matrix is an alternative way for mechanism reduction. The program can calculate the fluxes of elements from species to species and the contribution of each reaction to these fluxes.

Reduction of the number of species can be based on the study of strength of kinetic connections among the species, calculated by the program. Also, it can estimate the instantaneous error of QSSA species [4] and thus enables the proper selection of QSSA species.

KINALC has been designed to be very user friendly. It accepts simple keywords and may provide a detailed explanation of the results. The program does all the mechanical work and leaves only the task of thinking for its user.

KINALC has a modular structure and can be easily extended by other methods for the analysis of reaction mechanisms and can be interfaced easily to other simulation programs.

The program is available from the World Wide Web at address  
<http://chem.leeds.ac.uk/Combustion/Combustion.html>

[1] Kee RJ, Rupley FM, Miller JA  
CHEMKIN-II: A FORTRAN Chemical Kinetics Package for

the Analysis of Gas-phase Chemical Kinetics  
Report SAND89-8009, Livermore, 1989

[2] Rogg B

RUN1DL: A computer program for the simulation of one-dimensional chemically reacting flows

Report CUED/A-THERMO/TR39, Cambridge, 1991

[3] Vajda S, Valko P., Turanyi T

Int.J.Chem.Kinet.,17,55-81(1985)

[4] Turanyi T, Tomlin AS, Pilling MJ

J.Phys.Chem.,97,163-172(1993)

# MOLECULAR BEAM REACTION DYNAMICS OF ATOMS AND RADICALS

P. Casavecchia

*Dipartimento di Chimica, Università di Perugia, 06100 Perugia, Italy*

The goal of chemical reaction dynamics is to learn about the forces that control chemical reactivity, that is, for each chemical reaction, to learn about the nature of the potential energy surface (PES) that governs the nuclear motions.<sup>1,2</sup> The physical observables that are most sensitive to the nature of the PES are reaction cross sections, especially if differential in angle. When converged quantum mechanical scattering calculations on an assumed PES can be performed, comparison of calculated and experimental cross sections provides an unambiguous test of the PES. This test has only been possible, so far, for the benchmark three-atom reactions  $D+H_2$ ,  $H+D_2$  and  $F+H_2$ , and has occurred only within the past several years following exciting advancements in molecular beam and laser spectroscopic techniques, as well as quantum reactive scattering methods and electronic structure calculations.<sup>3</sup> The same experimental advances have recently allowed to extend the dynamical investigation to a large variety of atoms and small radical reactions.<sup>4</sup> At the same time, the increasing access to powerful computers given to quantum chemists and dynamicists has led to great strides in calculating PES by *ab initio* methods for many other atom and radical reactions and in treating the reaction dynamics by improved approximate methods, which can be tested against exact calculations on prototype systems.<sup>4</sup>

In this lecture, after a brief overview of the recent progress in the field of chemical reaction dynamics, we will discuss results on reactions of atoms (O, N, Cl) and radicals (OH) with simple molecules, which have been recently obtained in our laboratory by using the crossed molecular beam scattering method with rotating mass spectrometric detection.<sup>2,5,6</sup> Emphasis will be on three-atom ( $A + BC$ ) and four-atom ( $AB + CD$ ) reactions for which the interplay between experiment and theory is the

strongest and the most detailed. In particular, we will extend the same kind of very fundamental comparison, which has been carried out for  $H+H_2$  and  $F+H_2$ , to a third chemical reaction,  $Cl+H_2$  and will show that, after 150 years, we are well on the way to a complete quantitative understanding of the simplest chlorine reaction.<sup>7</sup>

The lecture will also emphasize the detailed comparison between scattering observables and results of quantum (approximate) as well as quasiclassical dynamical calculations on *ab initio* potential energy surfaces for some simple radical reactions of the  $AB + CD$  type. Included in the set of examples will be the benchmark four-atom reactions  $OH + H_2 \rightarrow H_2O + H$  and  $OH + CO \rightarrow CO_2 + H$  in an effort to assess the current status of theory *versus* experiment as we go beyond  $A + BC$  systems.<sup>8</sup>

Extension of dynamical studies, under single collision conditions, to reactions of atomic nitrogen<sup>9</sup> and other radicals will also be discussed.

## References

- 1) D.R. Herschbach, Y.T. Lee, and J.C. Polanyi "Nobel Lectures 1986", in: *Nobel Lectures in Chemistry 1981-1990*, eds. T. Frängsmyr and B.G. Malmström (World Scientific, Singapore, 1992).
- 2) P. Casavecchia, *Science Spectra* (1996), in press.
- 3) W.H. Miller, *Ann. Rev. Phys. Chem.* **41**, 245 (1990); D.M. Neumark, Y.T. Lee *et al.*, *J. Chem. Phys.* **82**, 3045 (1985); D.E. Manolopoulos, D.M. Neumark *et al.*, *Science* **262**, 1852 (1993); L. Schnieder *et al.*, *Science* **269**, 207 (1995); J.F. Castillo *et al.*, *J. Chem. Phys.* **104**, 6531 (1996).
- 4) See: *Advanced Series in Physical Chemistry- Vol. 6, The Chemical Dynamics and Kinetics of Small Radicals*, eds. K. Liu and A. Wagner (World Scientific, Singapore, 1995).
- 5) M. Alagia, N. Balucani, P. Casavecchia, D. Stranges, and G.G. Volpi, *J. Chem. Soc. Faraday Trans. (Faraday Research Article)* **91**, 575-596 (1995).
- 6) P. Casavecchia, N. Balucani, and G.G. Volpi, in *Ref. 4*, ch. 9; in *Research in Chemical Kinetics*, Vol.1, ed. by R.G. Compton and G. Hancock (Elsevier, Amsterdam, 1993), pp.1-63.
- 7) M. Alagia, N. Balucani, L. Cartechini, P. Casavecchia, E.H. van Kleef, G.G. Volpi, F.J. Aoiz, L. Banares, D.W. Schwenke, T.C. Allison, S.L. Mielke, and D.G. Truhlar, submitted.
- 8) M. Alagia, N. Balucani, P. Casavecchia, D. Stranges, G.G. Volpi, D.C. Clary, A. Kliesch, and H.-J. Werner, *Chem. Phys.* (1996), in press.
- 9) M. Alagia, N. Balucani, L. Cartechini, P. Casavecchia, E.H. van Kleef, and G.G. Volpi, to be published.

# PREDISSOCIATION DYNAMICS OF THE $A^1A''$ STATE OF HNO STUDIED BY CAVITY RING-DOWN SPECTROSCOPY

Andrew J. Orr-Ewing, Jonathan Pearson, Martyn D. Wheeler,

Michael N.R. Ashfold and Richard N. Dixon

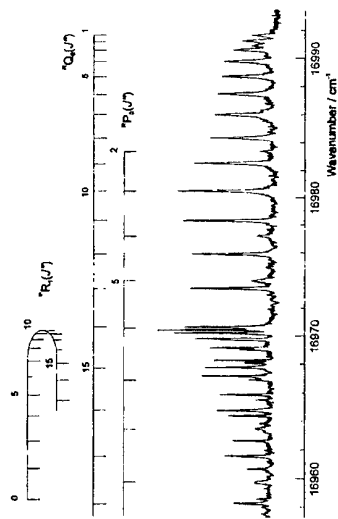
*School of Chemistry, University of Bristol, Bristol BS8 ITS, UK*

The predissociation dynamics of the  $A^1A''$  state of HNO have been investigated by measurement of the lifetime-broadened widths of rotational lines of the  $A^1A''$ - $X^1A'$  transition by cavity ring-down spectroscopy (CRDS). CRDS is a highly sensitive form of absorption spectroscopy<sup>1</sup> because of the very long pathlengths established through absorbing samples: typically, we can achieve pathlengths of 100 km in a 1.5-m long absorption cell. It is a technique better suited than LIF to studies of molecular predissociation if the excited state dissociation lifetime is short compared to its fluorescence lifetime. This study illustrates such a case where the  $A^1A''$ - $X^1A'$  LIF spectrum of HNO breaks off above the dissociation limit for formation of  $H(^2S) + NO(X^2Ti)$ .<sup>2</sup> The CRD spectrum, however, extends well beyond the dissociation limit (we have identified transitions to rotational states lying up to 2400  $cm^{-1}$  above the dissociation limit of 16450  $cm^{-1}$ ).<sup>3</sup> The predissociation dynamics of  $HNO(A^1A'')$  can thus be explored by measuring the lifetimes of individual rotational levels of this electronic state from the broadening of rotationally resolved spectral lines.

The lifetime-dependent Lorentzian components of the lineshapes of numerous rovibrational features of the  $A^1A''$ - $X^1A'$  CRD absorption spectrum were deconvoluted from the Doppler and laser line profiles to obtain lifetimes and predissociation rates for individual  $|v_1v_2v_3\rangle JK\rangle$  states. Here, the labels  $v_1$ ,  $v_2$ , and  $v_3$  denote the number of quanta of the N-H stretch, N=O stretch, and H-N-O bending vibrations respectively. HNO is a near-prolate symmetric top and  $K$  ( $=K_a$ ) can be regarded as a good quantum number. We have measured line broadening (of up to 0.3  $cm^{-1}$ ) in transitions to all vibronic states above the predissociation threshold (the 100 and 020 states, for which the higher  $K$  levels are above the dissociation limit, and the 101, 030, 110, and 111 states).

In three substates (100  $K=5$ , 101  $K=1$  and 110  $K=4$ ) strongly J-dependent linewidths are seen. The 100  $K=5$  and 101  $K=1$  substates show a maximum linewidth midway through the observed spectral transitions while the linewidths for 110  $K=4$  increase with J. Some transitions to rotational levels of the 100  $K=5$  state have markedly asymmetric lineshapes.

Linewidths also generally increase with  $K$ . Linewidths for transitions to states involving excitation of the bending mode (the 101 and 111 states) are considerably larger than those for which  $v_3=0$ .



CRD spectrum of the  $A^1A''$ - $X^1A'$  101-000 band, 1-0 subband. Our observations clarify the predissociation mechanism suggested by previous absorption<sup>4,5</sup> and LIF<sup>6,7</sup> studies. The  $A^1A''$  state is coupled via a-axis Coriolis coupling to discrete, quasi-bound, highly vibrationally excited levels of the ground state which, in turn, are coupled to the electronic ground state continuum corresponding to dissociation to  $H(^2S) + NO(X^2Ti)$ . Calculations using accurate potential energy surfaces for the  $X^1A'$  and  $A^1A''$  states demonstrate that the quasi-bound vibrational levels involve predominantly  $N=0$  stretching, which is only weakly coupled to the dissociative N-H coordinate. These states are thus sufficiently long lived to support rotational levels narrow enough in energy to give rise to the J-dependent predissociation rates described above.

- (1) O'Keefe and D.A.G. Deacon, *Rev. Sci. Instrum.*, **59**, 2544 (1988).
  - (2) Dixon, M. Noble, C.A. Taylor, and M. Delhoume, *Faraday Discuss. Chem. Soc.*, **71**, 125 (1981).
  - (3) Pearson, PhD thesis, University of Bristol (1996).
  - (4) Bancroft, J.M. Hollas, and D.A. Ramsay, *Can. J. Phys.*, **40**, 322 (1962).
  - (5) Freedman, *Chem. Phys. Lett.*, **44**, 605 (1976).
  - (6) Dixon, K.B. Jones, C.A. Taylor, and S. Carter, *Mol. Phys.*, **42**, 455 (1981).
- Dixon and C.A. Rosser, *J. Mol. Spec.*, **110**, 262 (1985).

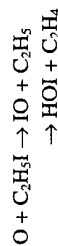
# ROLE OF INTERSYSTEM CROSSING IN THE DYNAMICS OF O(<sup>3</sup>P) ATOMS REACTING WITH ALKYL AND ALLYL IODIDE MOLECULES

by J.J. Wang, D.J. Smith and R. Grice

*Chemistry Department, University of Manchester, Manchester, M13 9PL, UK.*

Reactive scattering has been measured for O(<sup>3</sup>P) atoms with C<sub>2</sub>H<sub>3</sub>I, (CH<sub>3</sub>)<sub>2</sub>CHI, (CH<sub>3</sub>)<sub>3</sub>CI and C<sub>3</sub>H<sub>5</sub>I molecules at initial translational energies E ~ 50 and 15 kJ mol<sup>-1</sup>.

The O + C<sub>2</sub>H<sub>3</sub>I reaction [1] follows two reaction pathways



with isotropic scattering at low initial translational energy and scattering which favours the backward hemisphere at higher initial translational energy more strongly for the IO than the HOI reaction product. The O + (CH<sub>3</sub>)<sub>2</sub>CHI, (CH<sub>3</sub>)<sub>3</sub>CI reactions [2] show similar behaviour at high initial translational energy. However the O + C<sub>3</sub>H<sub>5</sub>I reaction yields only IO reaction product, which favours scattering in the backward direction at both initial translational energies.

These results show unequivocally that, while the O + C<sub>2</sub>H<sub>3</sub>I reaction necessarily commences on the triplet <sup>3</sup>A" potential energy surface, intersystem crossing occurs in the entrance valley to the singlet <sup>1</sup>A' potential energy surface in the OIC<sub>2</sub>H<sub>5</sub> configuration. The singlet OIC<sub>2</sub>H<sub>5</sub> intermediate involves a dative OI covalent bond but rearrangement via a 5 membered ring transition state involving divalent O atom bonding abstracts an H atom from the terminal CH<sub>3</sub> group forming HOI product. The O + C<sub>2</sub>H<sub>5</sub>I reaction occurs entirely via the singlet OIC<sub>2</sub>H<sub>5</sub> intermediate at low initial translational energy but the excess IO backward scattering observed at higher initial translational energy indicates a contribution from direct reaction via the triplet OIC<sub>2</sub>H<sub>5</sub> transition state.

The O + (CH<sub>3</sub>)<sub>2</sub>CHI, (CH<sub>3</sub>)<sub>3</sub>CI reactions show a higher yield of HOI product compared with IO product, in line with the increased number of terminal CH<sub>3</sub> groups capable of forming a 5 membered ring transition state. However the same proportion of the total reaction cross section ~ 4/5 arises from intersystem crossing to the singlet potential energy surface while ~ 1/5 arises from direct reaction over the triplet potential energy surface, for all the alkyl iodide reactions at an initial translational energy E ~ 50 kJ mol<sup>-1</sup>.

The O + C<sub>3</sub>H<sub>5</sub>I reaction involves direct reaction via the triplet transition state at both initial translational energies. A higher proportion of the total reaction cross section arises from direct reaction over the triplet potential energy surface rather than from intersystem crossing to the singlet potential energy surface in comparison to the alkyl iodide reactions. This is attributed to facile reaction over the triplet surface which is unimpeded by a potential energy barrier for the strongly exoergic allyl iodide reaction. The stability of the singlet OIC<sub>3</sub>H<sub>5</sub> intermediate is depleted by the increased reaction exoergicity, which may also contribute to increased IO scattering in the backward direction. In all cases reaction appears to be confined to small impact parameter collisions with b<sub>m</sub> ≤ 2.5 Å, due to the weak long-range interaction of the ground state O(<sup>3</sup>P) atoms with the alkyl and allyl iodide molecules.

(1) Wang, D.J. Smith and R. Grice, *J. Phys. Chem.*, **100**, 6620 (1996).

(2) Wang, D.J. Smith and R. Grice, *J. Phys. Chem.*, in press.

# PULSED, CROSSED, SUPERSONIC MOLECULAR BEAM STUDIES OF REFRACTORY ATOM REACTIONS :

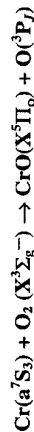


Christian Naulin, Ian M. Hedgecock and Michel Costes

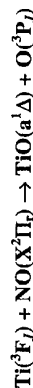
URA 348 CNRS, *Photophysique et Photochimie Moléculaire*,

Université Bordeaux I, 33405 Talence Cedex, France

In recent years, the combination of pulsed nozzle sources and pulsed laser techniques has prompted novel crossed molecular beam studies of bimolecular gas phase reactions. The pulsed nozzle beam - pulsed UV laser combination has proved to be a powerful tool for the generation of intense supersonic beams of transient species, truly useful in reactive scattering experiments. Atom beams of metallic and refractory elements have been generated in this laboratory by laser ablation of the corresponding solid in the early stage of the carrier gas pulse expansion. This technique is extremely versatile and can be employed for any element, provided it can be handled as a solid rod at room temperature; it has been, so far, applied to oxidation reactions of ground state Al, Mg, C and Si, and will be exemplified with the two title reactions.



This reaction has been studied at relative translational energies varying between 0.3 and 0.6 eV. [1] The  $\text{Cr}(a^7S_3)$  reactant and the  $\text{CrO}(X^3\Pi_0)$  product have been probed by laser-induced fluorescence. The reaction exhibits a translational energy threshold at  $\epsilon_r \sim 0.40$  eV. The analysis of the CrO internal energy partitioning just above the threshold leads to a reaction endoergicity:  $\Delta\epsilon_0 = 0.38 \pm 0.09$  eV, and to a CrO bond-dissociation energy:  $D_0(\text{CrO}) = 4.74 \pm 0.09$  eV.



This reaction has been studied at relative translational energies varying between 0.1 and 0.5 eV. Both  $\text{Ti}(^3F_2)$  and  $\text{NO}(X^2\Pi_1)$  reactants and the  $\text{TiO}(a^1\Delta)$  product have been probed by laser-induced fluorescence. The reaction exhibits an apparent translational energy threshold around  $\epsilon_r \sim 0.2$  eV for production of  $\text{TiO}(a^1\Delta, v=1)$ , as observed on the  $(c^1\Phi \leftarrow a^1\Delta)$  (1-1) R bandhead region: at this energy, the excitation limit in  $v=0$  is about  $J < 50$ , which allows for observing (0-0) P branch, up to the excitation limit, with only little overlap with (1-1) band (the P(50) line of the (0-0) band lies in the vicinity of the (1-1) band origin). The analysis of the  $\text{TiO}(a^1\Delta, v=0)$  rotational energy distribution under these conditions leads to a reaction exoergicity (for ground-state reactants and products)  $\Delta\epsilon_0 = -0.37 \pm 0.08$  eV and to a TiO bond-dissociation energy:  $D_0(\text{TiO}) = 6.87 \pm 0.08$  eV.

- [1] I.M. Hedgecock, C. Naulin and M. Costes, *Chem. Phys.* 207 (1996) 379.

# ROTATIONAL AND SPIN-ORBIT EFFECTS IN THE DYNAMICS OF $\text{O}(^3P_j) + \text{HYDROCARBON REACTIONS}$

Gillian M. Sweeney, Allister Watson and Kenneth G. McKendrick

Department of Chemistry, The University of Edinburgh, Edinburgh EH9 3JJ, U.K.

We have used laser photolysis of  $\text{NO}_2$  in conjunction with laser-induced fluorescence detection of the nascent OH product to investigate the dynamics of the reactions of  $\text{O}(^3P_j)$  with a series of saturated hydrocarbons. [1,2]

We confirm previous observations[3] of very low fractions of OH rotational energy release for the higher homologues such as isobutane and cyclopropane. By photolysing  $\text{NO}_2$  at shorter wavelengths to produce translationally hotter  $\text{O}(^3P_j)$  atoms, we have been able to extend the measurements to the previously unstudied parent members of the series, ethane and methane. The rotational energy release remains low, being only marginally greater than that for the higher members. This suggests that  $\text{CH}_4$  and  $\text{C}_2\text{H}_6$  follow smoothly on the previously observed trends, consistent with a proposed strong collinear constraint. No preference for either OH  $\Lambda$ -doublet component was observed, also consistent with a collinearly constrained reaction.

An interesting further feature of the results for all the systems examined is non-statistical population of the OH spin-orbit states, even accounting for the spatial degeneracies of individual levels in the two spin-orbit manifolds. We have clarified the correlations of fine-structure surfaces from  $j=2$ , 1 and 0 of  $\text{O}(^3P_j)$  to  $\Omega' = 3/2$  and  $1/2$  of OH in these systems at different levels of electronic adiabaticity. It is found that the observed OH spin-orbit distributions are not well reproduced in a fully adiabatic,  $\Omega$ -conserving limit, as illustrated in Fig.1. The inclusion of exit channel mixing alone is not sufficient to obtain satisfactory agreement. However, the further addition of strong non-adiabatic coupling between entrance channel surfaces of the same  $\Omega$  and parity results in a much improved prediction, as also shown in Fig. 1.

We have also shown that the non-adiabatic mixing required in the successful model is compatible with previous independent studies of elastic[4] and inelastic scattering[5,6] of  $\text{O}(^3P_j)$  with similar partners. The entrance channel surfaces, and the couplings between them, have been characterised in magnetically-selected molecular beam scattering experiments[4]. Although non-adiabatic couplings do not contribute substantially to the observed total scattering, we believe they are important for the subset of relatively high energy, low impact parameter collisions which lead to reaction. Similarly, the observed[5] and predicted[6] propensities for inelastic,  $j$ -changing collisions of  $\text{O}(^3P_j)$  are compatible with the strong coupling of specific surfaces required in our model.

An interesting corollary of this work is the predicted  $j$ -dependence of the reactivity of  $O(^3P_j)$ . The successful model suggests only a moderate decline in reactivity in the order  $j=2$  to 1 to 0, in marked contrast to a much more dramatic decline which would be observed if the system behaved fully adiabatically.

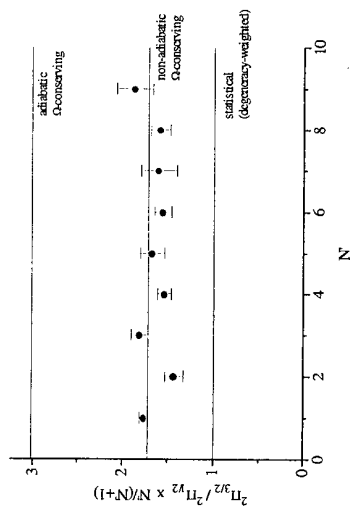


Figure 1 Degeneracy-corrected observed and predicted OH spin-orbit ratios for the reaction of  $O(^3P_j)$  with cyclohexane. The successful prediction incorporates strong non-adiabatic mixing of particular fine-structure surfaces.

- [1] (a) A. Watson, *PhD Thesis, The University of Edinburgh*, 1994.  
(b) G. M. Sweeney, *PhD Thesis, The University of Edinburgh*, (in preparation, 1996).
- [2] G. M. Sweeney, A. Watson and K. G. McKendrick, (manuscript in preparation).
- [3] P. Andresen and A. C. Luntz, *J.Chem.Phys.* **72**, 5842 (1980).
- [4] V. Aquilanti, R. Candori, L. Mariani, F. Pirani and G. Liuti, *J.Phys.Chem.* **93**, 130 (1989).
- [5] Z. Ma and K. Liu, *Chem.Phys.Lett.* **213**, 269 (1993).
- [6] R. Jaquet, V. Staemmler, M. D. Smith and D. R. Flower, *J.Phys.B* **25**, 285 (1992).

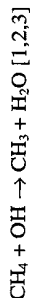
# QUANTUM SCATTERING CALCULATIONS ON THE $NH_3 + OH \rightarrow NH_2 + H_2O$ REACTION.

Gunnar Nyman

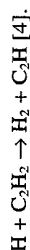
Department of Physical Chemistry  
Göteborg University  
S-412 96 Göteborg, Sweden

In 1976 the first accurate cross sections for a chemical reaction,  $H + H_2 \rightarrow H_2 + H$ , obtained by a quantum mechanical treatment were reported by Schatz and Kuppermann. In 1993 the quantum dynamics for the four-atom reaction  $OH + H_2 \rightarrow H + H_2O$  were solved in full-dimensionality for total angular momentum zero on a single Born-Oppenheimer potential energy surface by Manthe, Seideman and Miller. These calculations provide reaction probabilities, though not yet state-to-state reaction probabilities, and are enormously important as they make it possible to test approximate calculations.

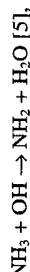
Simultaneously there is a need to find accurate quantum dynamical methods to treat larger reactions. The approach used here, is to treat only a few degrees of freedom explicitly quantum dynamically while all other degrees of freedom are treated with an adiabatic approach. This technique has recently been applied to the seven-atom reaction



and the five-atom reaction



Here the six-atom reaction



which is of practical importance in the combustion of nitrogen from fossil fuels and in the atmosphere, is treated with this technique.

In essence the so called Rotating Bond Approximation (RBA), developed by Clary to treat four-atom reactions, is used. In the scattering calculations,  $NH_2$  is treated as a pseudo-atom Q and the reaction is written



The quantum numbers  $v$ ,  $j$ ,  $m$  and  $n$  represent the QH vibration, the OH rotation, the  $H_2O$  bend and a local OH stretch of  $H_2O$  respectively. These degrees of freedom, and the relative translation, are explicitly treated in the scattering calculations by using the RBA. All other degrees of freedom are treated by an adiabatic approach.

A reduced dimensionality potential energy surface (RDP) is developed. The term reduced dimensionality potential is used as the surface is an explicit function of a reduced number of coordinates. The RDP combines an accurate potential function for  $H_2O$  with a LEPS function to describe the N-H and OH reactive bonds. The potential has accurate reactant and product ro-vibrational energy levels and a vibrationally adiabatic groundstate barrier height of 2.8 kcal/mol in accord with ab initio calculations [6].

# COLLISIONAL ENERGY TRANSFER AT EXTREMELY LOW TEMPERATURES: RATE COEFFICIENTS FOR STATE-TO-STATE ROVIBRONIC RELAXATION OF

NO( $X^2\Pi$ ,  $\Omega = 1/2, \nu = 3, J$ ) BY He DOWN TO 27 K

Philip L James, Ian R Sims and Ian WM Smith

*School of Chemistry, The University of Birmingham, Edgbaston, Birmingham B15 2TT, UK*

A CRESU (Cinétique de Réaction en Ecoulement Supersonique Uniforme) apparatus has recently been commissioned in our laboratories in Birmingham. The intention is to study a range of molecular processes at ultra-low temperatures (down to 10 K). In this paper, we shall report the first results obtained with the new apparatus: namely, rate coefficients for state-to-state rovibronic relaxation of NO in its ground electronic state in collisions with He - and possibly Ar. These measurements yield the first state-to-state rate coefficients for rotational energy transfer at temperatures as low as 27 K.

The new apparatus, like its French cousin in Rennes, relies on expansion through a Laval nozzle to generate a relatively dense, supersaturated and supersonic flow of gas in which frequent collisions ensure that a translational and rotational temperature is established.<sup>1,2</sup> In our experiments, tuneable infrared laser pulses are used to excite a sub-set of NO molecules to a specific rotational state in the  $X^2\Pi_{1/2}$ ,  $\nu = 3$  level. This ca. 1.80  $\mu\text{m}$  radiation is provided by difference frequency mixing the output from a dye laser with residual fundamental from the injection-seeded Nd:YAG pump laser.

In these *IR-UV double resonance* experiments, the frequency-doubled output of a Nd:YAG-pumped dye laser is used to detect NO molecules in ( $X^2\Pi$ ,  $\Omega = 1/2, \nu = 3, J$ ) via excitation in the  $A^2\Sigma^+ - X^2\Pi$  (0,3) band and subsequent off-resonance fluorescence in the (0,0) band. Experiments of two kinds are performed. To obtain the *total* rate of relaxation from the initially populated  $\Omega = 1/2, \nu = 3, j$  level the frequency of the UV probe laser is tuned to an absorption from the initially populated level in the  $A^2\Sigma^+ - X^2\Pi$  (0,3) band and the time delay between the excitation and probe lasers is scanned. To determine *state-to-state* rates, the time delay between the two lasers is fixed at a

Cumulative reaction probabilities obtained in the RBA scattering calculations are presented. Some of the features in these are related to quantized transition states [7] gating the flux.

It is shown that the  $\text{OH}(j=0) + \text{NH}_3(v=0) \rightarrow \text{H}_2\text{O} + \text{NH}_2$  reaction mainly produces  $\text{H}_2\text{O}$  in its vibrational ground state. For reaction out of  $\text{OH}(j=0) + \text{NH}_3(v=1)$ ,  $\text{H}_2\text{O}$  is mainly formed with one quantum of energy in the local vibrational stretch. The local stretch is essentially a superposition of the symmetric and asymmetric normal mode stretches wherefore these calculations predict that experimentally, excitation of these two modes should be observed.

The so called J-shifting approximation, which facilitates rate constant calculations, is tested against centrifugal sudden calculations. The agreement is good for energies in the tunneling regime. At higher energies the agreement is not quite as good. We have previously found the J-shifting approximation to work well for the  $\text{CH}_4 + \text{OH} \rightarrow \text{CH}_3 + \text{H}_2\text{O}$  reaction in the tunneling regime.

Thermal rate constants were calculated and found to be in reasonable agreement with experimental results. In particular, the experimentally observed temperature dependence of the rate constant is reproduced quite well.

Tunneling was found to dominate the rate constant at room temperature. The importance of tunneling has interesting implications for quasiclassical trajectory calculations. Many of the ongoing efforts to account for the problem of zero-point energy leakage in trajectory calculations can be expected to offset the current partial cancellation between this error and the lack of tunneling.

## References.

1. G. Nyman and D. C. Clary, JCP 101, 5756 (1994).
2. G. Nyman, D. C. Clary and R. D. Levine, Chem. Phys. 191, 223 (1995).
3. G. Nyman, CPL 240, 571 (1995).
4. D. Wang and J. M. Bowman, JCP 101, 8646 (1994).
5. G. Nyman, JCP 104, (1996).
6. J. C. Corchado, J. Espinosa-Garcia, W.-P. Hu, I. Rossi and D. G. Truhlar, JPC 99, 687 (1995).
7. D. C. Chatfield, R. S. Friedman, G. C. Lynch, D. G. Truhlar and D. W. Schwenke, JCP 98, 342 (1993)

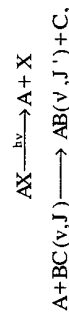
# DETERMINATION OF THE STATE-RESOLVED DIFFERENTIAL CROSS SECTION FOR THE REACTION OF H + D<sub>2</sub> AT 2.2 eV

Russell J. Low, Hao Xu, Neil E. Shafer-Ray<sup>1</sup> and Richard N. Zare

*Department of Chemistry, Stanford University*

*Stanford CA 94305, USA.*

For the photoinitiated bimolecular reaction of the form



the most intuitive method of determining the state-to-state differential cross section would be to use crossed molecular beams of the reagents, and observe the products as a function of scattering angle. This technique has been successfully applied to a few systems, but in the case of the H + H<sub>2</sub> reaction and its isotopic variants, usually only the product vibrational state is resolved.

An alternative technique with improved sensitivity, which allows the study of such a reaction in a single gas stream, is the *photoloc* technique (*photo*initiated bimolecular reactions where analysis is based on the *law of cosines*). Under favourable conditions, with AX considered to be stationary with respect to BC, it can be shown that a measurement of the laboratory frame speed distribution of the AB product in a given rovibronic state can lead to a determination of the full differential cross section. Following this strategy, we have measured the state-selective differential cross section for the bimolecular reaction



at a collision energy of 2.2 eV. A schematic of the experiment is shown in figure 1. (a) A gas mixture of HI and D<sub>2</sub> is coexpanded into a vacuum chamber and then the reaction is initiated by laser photolysis of the HI precursor at ~213 nm. (b) A delay of 20 ns allows time for the products to form. (c) Sub-Doppler bandwidth laser radiation excites the HD product to long-lived Rydberg states to achieve state as well as velocity selection. (d) The Rydberg HD molecules drift for 600 ns. (e) The HD Rydberg molecules are then ionized with a pulsed electric field, which is followed by time-of-flight (TOF) detection (f). The TOF spectra is analysed and yields information on the speed distribution of the HD (v'=4, J=3) reaction product in the laboratory frame.

small value (ca. 30 ns) and the frequency of the UV probe laser is scanned. From the relative intensities of the lines in the A<sup>2</sup>Σ<sup>+</sup> - X<sup>2</sup>Π (0,3) band, it is possible to find the rate coefficients for transfer between specific initial and final states in the process of collisionally-induced transfer.<sup>3</sup>

It is anticipated that results will be reported for transfer from initial rotational levels j = 0.5 and j = 6.5. The rate coefficients will be compared with those previously measured at temperatures between 295 K and 80 K.<sup>3</sup>

<sup>1</sup> I.R. Sims, J.-L. Queffelec, A. Defrance, C. Rebrion-Rowe, D. Travers, P. Bocherel, B.R. Rowe, and I.W.M. Smith *J Chem. Phys.*, **100**, 4229 (1994).

<sup>2</sup> I.R. Sims and I.W.M. Smith, *Ann. Rev. Phys. Chem.*, **46**, 109 (1995).

<sup>3</sup> M. Islam, I.W.M. Smith and J.W. Wiebrecht, *J. Chem. Phys.*, **103**, 9676 (1995).

# PHOTODISSOCIATION OF JET-COOLED $\text{CH}_3\text{ONO}$ AND $\text{CH}_3\text{SNO}$ AT 355 nm: ALIGNMENT OF THE NO PHOTOFRAGMENT

G. Kennedy, C. Ning and J. Pfab

Department of Chemistry, Heriot-Watt University, Edinburgh, EH14 4AS

The photodissociation of alkyl nitrites and alkyl thionitrites in the near-UV continues to attract considerable interest among theoreticians and experimentalists with recent research concentrating on the quantum state distributions and vector properties of the NO photofragment and experiments with jet-cooled, nearly mono-energetic molecules. The work to be reported at the Symposium summarises our most recent measurements of the rotational alignment of the  $\text{NO}(\nu''=0,1)$  photofragment from the photodissociation of jet-cooled  $\text{CH}_3\text{ONO}$  and  $\text{CH}_3\text{SNO}$  at 355 nm. We have used polarised photolysis and polarised laser-induced fluorescence (LIF) on the  $\gamma$ -bands of the nascent NO to measure the alignment, that is the spatial correlation of the J-vector of highly rotationally excited fragments with the transition moment vector associated with the parent electronic transitions involved.

Fig.1 shows the schematic of our experimental set-up. The polarisation of the probe laser was retained in the horizontal plane whilst the polarisation of the photolysis laser was controlled to be either horizontal or vertical by turning the polariser and the Fresnel rhomb. Alignments of each rotational state of the NO fragment were measured by scanning the corresponding rotational lines with two different polarisations of the photolysis beam

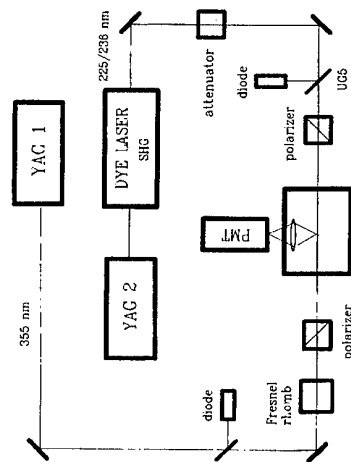


Fig. 1 Schematic of the pump-probe experiments

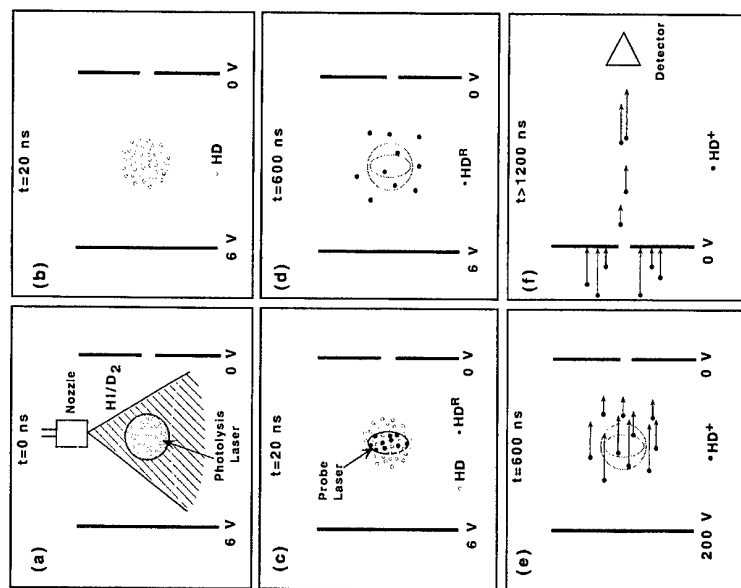


Figure 1. Schematic Diagram of the Experimental Procedure.

From the TOF spectrum, we obtain the state-specific differential cross section of the reaction. In order to improve the resolution of this measurement, it has been necessary to carefully calibrate the instrument response function. This calculation has been achieved by observing the photolysis of  $\text{HDS} \rightarrow \text{HD}(\nu'=4, J=3) + \text{S}$  at  $\sim 130$  nm under identical conditions.

These measurements of the differential cross section, which offer greater sensitivity than conventional crossed beam techniques, provide more stringent tests of theoretical models. In particular, at the high collision energies used in these studies, the importance of the quantum resonance and geometric phase effects can be tested.

R.J.L. wishes to thank the Royal Commission for the Exhibition of 1851 for a postdoctoral research fellowship. This work is supported by the US National Science Foundation.

<sup>1</sup> Permanent Address: Department of Chemistry, University of Oklahoma, Norman, Oklahoma, 73019.

In the experiment each scan of a rotational line involved 500 laser shots for each pump-probe geometry. Integrated line intensities were used to calculate the alignment employing Dixon's formulae, and all the following alignment data were obtained from the average of two independent scans.

Fig.2 shows the measured alignment of the  $\text{NO}(\nu''=1)$  photofragment from the photodissociation of methylthionitrite at 355 nm. The alignment was positive and increased slightly with  $J$  approaching 0.5 in good agreement with previous room temperature measurements. The positive alignment is in agreement with the  $(n, \pi^*)$  character of the  $S_1 \leftarrow S_0$  transition of the parent molecule at 355 nm with the transition moment perpendicular to the molecular plane. For high  $J$  ( $J > 30.5$ ) the alignment has a value close to +0.5, that is substantially lower than the high  $J$  limit of 0.8, indicating that the geometry changes on electronic excitation or that the lifetime is relatively long. Lifetimes of the order of 200 fs have been deduced before but are not in agreement with the substantial width of the structured, but predissociated parent absorption features.

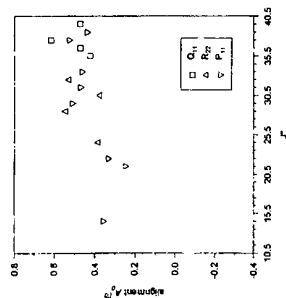


Fig. 2 The alignment of  $\text{NO}(\nu''=1)$  from photolysis of  $\text{CH}_3\text{ONO}$  at 355 nm.

In contrast to the vibrationally structured absorption of the alkyl nitrites the near-UV absorption spectrum of alkyl thionitrites arises from a typical unstructured dissociation continuum peaking close to 355 nm for the methyl derivative.

Fig.3 shows alignment measurements for  $\text{NO}(\nu''=1)$  from the photolysis of methylthionitrite at 355 nm. Here the measured alignment is negative indicating a  $(\pi, \pi^*)$  transition with an in-plane transition moment. The alignment at high  $J$  approaches a value of -0.25 which is again significantly lower than the high  $J$  limit of -0.4. The shape of the absorption continuum indicates that the electronic transition projects the molecule to a rather repulsive potential with dissociation times considerably less than 100 fs. The low value of the negative alignment may therefore also be due to out-of-plane distortion of the molecule in the  $S_2$  excited state.

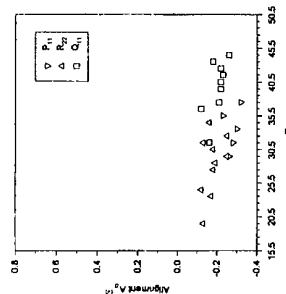


Fig.3 The alignment of  $\text{NO}(\nu''=1)$  from photolysis of  $\text{CH}_3\text{SNO}$  at 355 nm.

In conclusion alignments for NO at high  $J$  up to 44 have been measured for both methyl nitrite and methyl thionitrite. In both cases there was little difference between the two spin-orbit manifolds of NO. The measured alignments were significantly smaller

than the high  $J$  limits of +0.8 for positive and -0.4 for negative alignments, indicating that out-of-plane motions in the upper state play a significant role in both cases. The origin of these alignment effects and the very contrasting mechanism of methyl and methyl thionitrite photodissociation will be discussed in detail on the basis of parent absorption spectra, NO product state distributions and alignment measurements for  $\text{NO}(\nu = 0 \text{ and } 1)$ .

# ROTATIONAL EFFECTS IN STATE-TO-STATE COLLISION-INDUCED ENERGY TRANSFER IN THE SiF $C^2\Delta - B^2\Sigma^+$ SYSTEM

Colin J. Randall, Neil A. Jackson and Kenneth G. McKendrick

*Department of Chemistry, The University of Edinburgh, Edinburgh EH9 3JJ, U.K.*

Laser excitation of ground state SiF radicals generated in a discharge-flow system has been used to prepare selected rotational population distributions in the SiF  $C^2\Delta$  excited state. Collision processes of these excited radicals were investigated by time- and wavelength resolving the fluorescent emission. [1-3]

It was established that at the typical pressures of these experiments the initially prepared rotational distributions remained largely unaltered by collisions during the  $C^2\Delta$  state fluorescence lifetime, as illustrated in Fig.1. Excitation at the  $Q_1$  head (more correctly the combination of the  $Q_1$  and  $Q_{P21}$  heads) populated  $j$  values centred around 12.5. In contrast, the  $P_1$  head forms at a much higher  $j$  of around 34.5. The dependence of the collisional behaviour on initial rotational state,  $j$ , could therefore be reliably investigated. The  $j$ -dependence of the total collisional removal by simple collision partners such as  $H_2$  and  $N_2$  has been measured, with an initial analysis indicating at most a weak variation with  $j$ .

It has previously been found [2] that collisions with certain partners transfer a fraction of the  $C^2\Delta$  molecules to the lower-lying  $B^2\Sigma^+$  state. Surprisingly, the predominant  $B^2\Sigma^+$  product channels involve very substantial vibronic energy gaps ( $\sim 5000\text{ cm}^{-1}$ ). More highly dispersed B-X fluorescence spectra, such as those in Fig.2, have now revealed that an unusually large fraction of the available energy is released as SiF rotation.[3] Increased initial rotational angular momentum is found to lead to a corresponding increase in rotation of the product. There is greater SiF  $B^2\Sigma^+$  product rotation for  $N_2$  than for  $H_2$ .

These observations can be rationalised within a limiting model in which the three contributions to the final angular momentum from initial rotation, from linear to angular momentum conversion, and from sudden impulsive recoil, respectively, add vectorially. The strong repulsion necessary to explain the results is consistent with the valence-Rydberg character of the collision-induced transition, which causes a dramatic increase in the SiF effective electronic volume. The suddenness of the transition is also compatible with Franck-Condon control of the

vibrational distributions found in previous measurements.[2] We also believe that distinct contrasts with the collisional behaviour of the nominally isoelectronic SiCl states[4,5] can be explained by relatively subtle differences in the arrangements of the potential energy curves. The presence of a  $2\Delta - 2\Sigma^+$  curve-crossing in the isolated SiCl molecule enhances the role of long-range interactions with the quencher, in contrast to SiF where a relatively close encounter is required to induce a surface crossing.

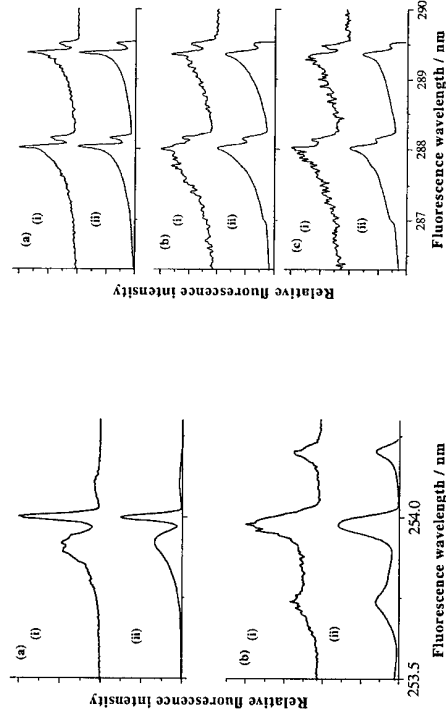


Figure 1 Dispersed fluorescence spectra of the SiF  $C^2\Delta-X^2\Pi_{3/2}$  (0,0) sub-band following excitation on the  $C^2\Delta-X^2\Pi_{1/2}$  sub-band.

(a)  $Q_1$  excitation; (b)  $P_1$  excitation.

In each case, (i) experimental spectrum (total pressure 2.5 Torr); (ii) best-fit simulation.

Figure 2 Collisionally produced SiF B-X (0,0) emission spectra.

(a)  $Q_1$  excitation, 1 Torr  $H_2 + 1.5$  Torr Ar;

(b)  $P_1$  excitation, 1 Torr  $H_2 + 1.5$  Torr Ar;

(c)  $Q_1$  excitation, 1 Torr  $N_2 + 1.5$  Torr Ar.

In each case: (i) experiment; (ii) simulation.

[1] C. W. Watson and K. G. McKendrick, *Chem. Phys.* **187**, 79 (1994).

[2] C. W. Watson and K. G. McKendrick, *Chem. Phys.* **187**, 87 (1994).

[3] N.A. Jackson, C. W. Watson and K. G. McKendrick, *Chem. Phys. Lett.* **243**, 564 (1995).

[4] J. B. Jeffries, *J. Chem. Phys.* **95**, 1628 (1991).

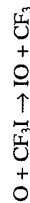
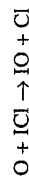
[5] S. Singleton and K. G. McKendrick, *J. Phys. Chem.* **97**, 1389 (1993).

# ROLE OF INTERSYSTEM CROSSING IN THE DYNAMICS OF THE O(<sup>3</sup>P) + ICl, CF<sub>3</sub>I REACTIONS

D.D. Wells, S. Mohr, K.M. Goonan, M. Hammer and R. Grice

*Chemistry Department, University of Manchester, Manchester, M13 9PL*

A supersonic beam of ground state O(<sup>3</sup>P) atoms seeded in He buffer gas with a peak velocity ~ 3.7 km s<sup>-1</sup> has been produced from a high temperature RF discharge source. Differential cross sections have been measured [1] for the reactions



up to initial translational energies  $E \sim 100 \text{ kJ mol}^{-1}$ . Both reactions exhibit mildly peaked angular distributions favouring the forward direction and product translational energy distributions which peak at low energy with a tail extending up to higher energy. This attributed to efficient intersystem crossing from the lowest triplet potential energy surface to form a persistent OIR complex on the underlying singlet potential energy surface in each case. The efficiency of intersystem crossing is related to the contribution of charge transfer interaction of the form  $\text{OI}^+ + \text{R}^-$  to the electronic wavefunction of the <sup>3</sup>A" potential energy surface.

L.J. Powell, D.D. Wells, J.J. Wang, D.J. Smith and R. Grice, *Molec. Phys.*, **87**, 865 (1996).

# REACTIONS OF O(<sup>1</sup>D) WITH HCl AND CF<sub>3</sub>Br

A Laganà, A. Riganelli, G. Ochoa de Aspuru

*Dipartimento di Chimica,*

*Università di Perugia, Perugia, Italy*

Maria L. Hernandez

*Departamento de Física de la Atmósfera*

*Universidad de Salamanca, Salamanca, Spain*

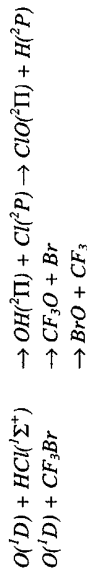
G. Lendvay

*Department of Homogeneous Reaction Kinetics,*

*Hungarian Academy of Sciences, Budapest, Hungary*

## Introduction

Reactive processes we recently investigated are:



Calculations for these reactions were carried using classical trajectories and reduced dimensionality techniques. For the O(<sup>1</sup>D) + HCl reaction both a model (LAGROBO[1]) potential and a polynomial of Bond order coordinates fitted to *ab initio* potential energy values[2] were used. Theoretical estimates of the experimental observables obtained from extensive trajectory calculations have been compared with measured data. In particular, the calculations reproduced the backward-forward shape of the measured product angular distribution including the backward bias. The calculations reproduced also the measured branching ratio at the two energies of the experiment. We also calculated the rate coefficient for both the OH and the ClO channel at different temperatures.

Similar calculations were performed for the O(<sup>1</sup>D) + CF<sub>3</sub>Br reaction.[3] To reduce the dimensionality of the problem the CF<sub>3</sub> radical was treated as a single particle of mass 69 a.m.u.. This is motivated by the fact that at the investigated energies CF<sub>3</sub> never fragments. The calculated exoergicities for the formation of the CF<sub>3</sub>O and BrO products are 37.63 kcal/mol and 30.08 kcal/mol, respectively, which are somewhat smaller (especially the former one) than the values credited by the accepted thermochemistry. The physical quenching and intersystem crossing were not included in the theoretical treatment since an electronically adiabatic approach has been adopted. A suitable potential energy surface was built using the LAGROBO model. On this potential energy surface we performed quasiclassical trajectory calculations in

order to obtain theoretical estimates of the product distributions, cross sections and rate coefficients for each reaction channel. For the processes leading to  $BrO + CF_3$  and to  $CF_3O + Br$  a rate coefficient of  $1.55 \times 10^{-10} \text{ cm}^3 \text{ molecule}^{-1} \text{ s}^{-1}$  and  $0.11 \times 10^{-10} \text{ cm}^3 \text{ molecule}^{-1} \text{ s}^{-1}$ , respectively, was obtained. This finding is in agreement with what can be inferred from kinetic studies, which, as already mentioned in the introduction, indicate that  $BrO$  formation is the dominant reactive pathway. To compare with the measured rate coefficient these two values were summed together. In this way a value of  $1.65 \times 10^{-10} \text{ cm}^3 \text{ molecule}^{-1} \text{ s}^{-1}$  was obtained which compares reasonably well with the measured data[4] of  $0.41 \times 10^{-10} \text{ cm}^3 \text{ molecule}^{-1} \text{ s}^{-1}$ . The calculations were extended to higher temperatures to estimate the temperature dependence of the rate coefficients.

## References

- (1) E. Garcia and A. Laganà, **103**, 5410 (1995); A. Laganà, G. Ochoa de Aspuru, E. Garcia, *J. Phys. Chem.* **99**, 17139 (1995)
- (2) M.L. Hernandez, C. Redondo, A. Laganà, G. Ochoa de Aspuru, M. Rosi, and S. Scamellotti, *J. Chem. Phys.* xx, xx (1996)
- (3) P. Casavecchia, A. Laganà, G. Ochoa de Aspuru, G. Lendvay, M. Alagia, N. Balucani, E.H. Van Kleef and G.G. Volpi, *Chem. Phys. Letters* (in the press)
- (4) P.H. Wine, J.R. Wells, and A.R. Ravishankara, *J. Chem. Phys.* **84**, 1349 (1986).

## CAN CLASSICAL MECHANICS BE USED TO STUDY COLLISION-INDUCED VIBRATIONAL ENERGY TRANSFER AT LOW TEMPERATURES?

M.J.T. Jordan and D.C. Clary

*Department of Chemistry, University of Cambridge, Cambridge CB2 1EW and  
Department of Chemistry, University College London, London WC1H 0AG.*

Quasi-classical trajectories and quantum vibrational close-coupled infinite order sudden approximation (VCC-IOS) calculations have been used to study collision-induced vibrational energy transfer in  $S_1$  *p*-difluorobenzene at 40 K. Vibration to translation transfer was examined from four initial levels:  $30^2$ ,  $8^2$ ,  $27^1$  and  $6^1$  with colliders ranging from He to Kr. The classical simulations reproduced all the features seen experimentally<sup>1</sup> for initial excitation of the  $30^2$  and  $8^2$  vibrational modes. Some results are shown in Fig 1. The VCC-IOS quantum scattering calculations agreed well with experiment for the He collider and allowed ambiguities in the experimental assignment of destination levels following initial excitation of  $27^1$  and  $6^1$  to be resolved. The good agreement observed between quantum and classical results indicates that, although lacking the detail of the quantum calculations, classical mechanics is adequate for studying these systems even at extremely low energies.

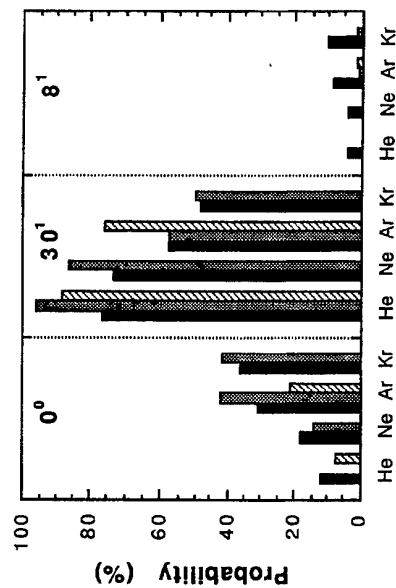


Figure 1. Product destination levels following excitation of  $30^2$ . Solid bars represent experimental results from Ref. 1, dotted bars have been calculated from classical trajectories and hashed bars are VCC-IOS quantum results.

(1) Mudjijono and W.D. Lawrance, *J. Chem. Phys.*, **104**, 7444 (1996)

## MEASUREMENT OF ENERGY TRANSFER RATE COEFFICIENTS FOR THE HYDROXYL RADICAL AT LOW TEMPERATURES BY LIF

Angela E. Bailey, Dwayne E. Heard and Michael J. Pilling.

*School of Chemistry, University of Leeds, Leeds, LS2 9JT.*

The hydroxyl radical, OH, is an important atmospheric species, being responsible for the removal of almost all trace pollutants. Tropospheric OH concentrations are low, around  $10^6 \text{ molec.cm}^{-3}$ , with a lifetime shorter than 1 second, therefore a sensitive and selective measuring technique is required to obtain accurate values of OH concentration.

Laser-induced-fluorescence (LIF) is among the techniques being developed for this purpose. LIF involves laser excitation of a particular absorption line in the OH spectrum and quantitative detection of the resultant fluorescence. In order that the method be calibrated accurately information about rates of electronic quenching and rovibrational energy transfer must be known. Although such energy transfer processes are well characterized at room temperature<sup>1</sup>, a data set of rates of quenching at low temperatures is required for calibration of the FAGE technique<sup>2</sup> for atmospheric OH measurement. Quenching from the  $v' = 0$  level of the  $A^2\Sigma^+$  excited state of OH by various atmospheric colliders has been studied using LIF in a cooled cell.

The figure shows quenching cross sections for the colliders  $\text{CO}_2$ ,  $\text{O}_2$  and  $\text{N}_2$  determined for a range of temperatures down to 236 K. Cross sections were found to increase with decreasing temperature though the change is small for  $\text{O}_2$  and  $\text{N}_2$  over the temperature range studied. For  $\text{CO}_2$  the cross section ( $A^3$ ) showed a marked increase from  $62.9 \pm 1.9$  at 292 K to  $81.0 \pm 2.4$  at 236 K.

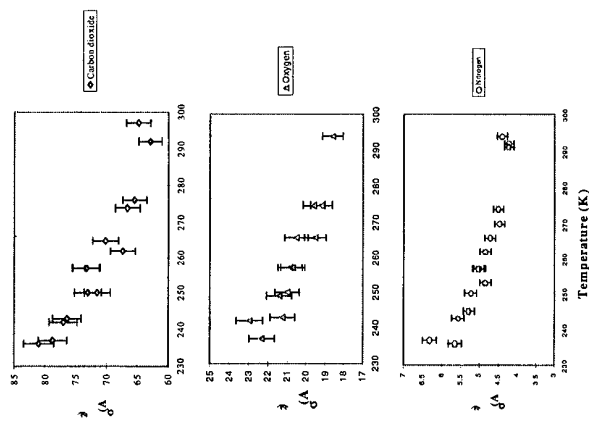
The data set has now been extended to include measurements for temperatures down to 200 K and experimentation is being carried out on rates of quenching and vibrational energy transfer from the  $v' = 1$  level of the first electronically excited state. The increase in rates of quenching with decreasing temperature is consistent with the

formation of a collision complex and is due to the role of long range attractive forces in complex formation<sup>3</sup>.

### References

1. I.J. Wysong, J. B. Jeffries and D. R. Crosley, *J. Chem. Phys.*, **92**(9), 5218 (1990).
2. M. R. Heal, D. E. Heard, M. J. Pilling and B. J. Whitaker, *J. Atm.. Sci.*, **52** (19), 3428 (1995)
3. P. W. Fairchild, G. P. Smith and D. R. Crosley, *J. Chem. Phys.*, **74**, 1795 (1983).

Variation on quenching cross section with  
temperature for various colliders



# A VISUALISATION OF AN ATMOSPHERIC FREE-JET EXPANSION

David J. Creasey, Dwayne E. Heard, Michael J. Pilling and Benjamin J. Whitaker  
*School of Chemistry, University of Leeds, Leeds, LS2 9JT*

Martin Berzins and Roger Fairlie  
*School of Computer Studies, University of Leeds, Leeds, LS2 9JT*

The hydroxyl radical, OH, performs a pivotal role in both tropospheric and stratospheric chemistry and has a result there has been extensive research undertaken in order to develop a field based system capable of measuring its low concentration, which is typically around  $10^6$  molecules  $\text{cm}^{-3}$ .

In order to develop and construct an atmospheric field experiment to monitor the hydroxyl radical at the low tropospheric concentrations a detailed study of a free-jet expansion was performed to assist the choice of optimum nozzle size and cell geometry. By the use of the laser induced fluorescence technique a thorough characterisation has been achieved, with LIF being used to probe the rotational temperature and gas density within a molecular beam of ambient air expanded through a variety of different nozzles. Shock structures are observed with steep gradients in both temperature and density, the density information inferred from OH signals measured with absence of fluorescence quenching. Excited state lifetime measurements within the jet enable the cross-section for electronic quenching of  $\text{OH } A^2\Sigma^+ v'=0$  by air to be estimated as low as 25 K.

In addition to experimental work a two-dimensional computational fluid dynamics simulation of the free-jet expansion was performed. The simulation is able to reproduce the experimental results and provides a detailed visualisation of all shock structures.

The OH signal detected is dependent on several parameters:

$$\text{Signal} = k [\text{OH}] f_i B_i f_{\text{gate}} \phi_i$$

where  $k$  contains all terms associated with fluorescence collection (collection solid angle, transmission of optics, filters, quantum yield of detector...),  $f_i$  is the population of OH in state  $i$ ,  $B_i$  is the Einstein coefficient for absorption from state  $i$ ,  $\phi_i$  is the fluorescence quantum yield of the excited state following laser excitation from  $i$ , and  $f_{\text{gate}}$  is the fraction of the fluorescence that is collected by the temporal gate of the detector. Only  $k$  is independent of position of probing inside the free-jet expansion of our FAGE experiment, therefore, carrying out a detailed characterisation of the expansion allows us to optimise our experiment and ultimately develop a field experiment capable of detecting OH in the atmosphere.

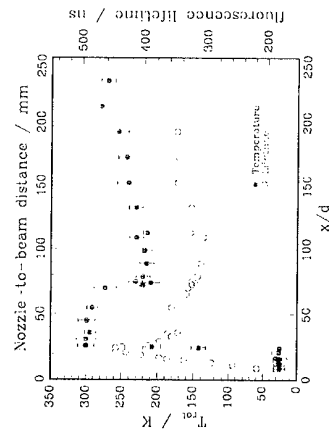


Figure 1. Rotational temperature measurements and fluorescence lifetimes at varying points in the free-jet expansion for the 1mm nozzle.

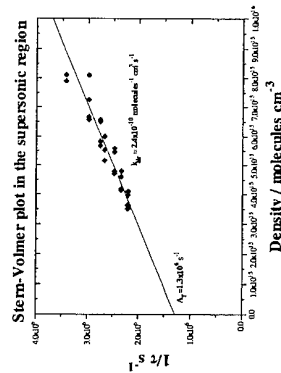


Figure 2. The Stern-Volmer plot at 25 K shows the rate constant by air to be  $2.4 \times 10^{10}$  molecules $^{-1}$  cm $^3$  s $^{-1}$ .

# REMOVAL RATES OF THE QUENCHING OF GROUND AND LOW VIBRONICALLY EXCITED NCO BY SIMPLE MOLECULES

(N<sub>2</sub>, O<sub>2</sub>, NO, CO<sub>2</sub>, N<sub>2</sub>O AND SO<sub>2</sub>)

José A. Fernández, Pilar Puyuelo, María N. Sánchez Rayo, Fernando Castaño  
and D. Husain<sup>#</sup>

*Departamento de Química Física. Universidad del País Vasco. Apartado 644. 48080 Bilbao, Spain.*

*<sup>#</sup>Department of Chemistry. University of Cambridge. Cambridge CB2 1 England. U.K.*

NCO is a linear open shell molecule with a doubly degenerate bending  $v_2(\Pi)$ . The vibrational angular momentum couples to the electronic one,  $\Lambda$ , yielding the vibronic angular momentum,  $K$ , whose quantum numbers are determined as  $K = |\pm 1 \pm \Lambda|$ . The magnitude of the interaction and subsequent splitting is measured by the so-called Renner expansion parameter,  $\epsilon$ , and the effect results in a classic breakdown of the Born-Oppenheimer adiabatic approximation known as the Renner-Teller effect. The spin-orbit coupling also contributes to split further the quantum levels; so the degenerate  $^2\Pi$  ground electronic states splits into  $\Omega = 1/2$  and  $3/2$  fine structure components and the other states couple in a similar way, resulting a wealth of states.

The influence of the symmetry of the molecular vibronic states on the efficiency of removal rates by molecules of well characterised symmetry is a fundamental subject in chemical dynamics. The vibrational relaxation of the open-shell species has been little studied, although a considerable interest has arisen on rotational relaxation, particularly in the explanation of the lambda doublet propensity rules in  $^2\Pi$  electronic states. This work reports a study of five of the lower NCO vibronic states, prepared by IRMPD of PhNCO and probed by laser induced fluorescence and their quenching by ground states simple molecules of different symmetries, N<sub>2</sub>, O<sub>2</sub>, NO, CO<sub>2</sub>, N<sub>2</sub>O and SO<sub>2</sub>, in order to study the influence of the symmetry terms on the reaction rates. The interpretation of the experimental results is done by a simple kinetic model of coupled differential equations. A discussion of the model approximations and the conclusions is also presented.

# DIRECT MEASUREMENTS OF REMOVAL RATES OF ELECTRONICALLY EXCITED NCO( $\tilde{A}^2\Sigma^+(0,0,0)$ ) BY SIMPLE MOLECULES.

J. A. Fernández, I. Merelas, María N. Sánchez Rayo, F. Castaño and D. Husain<sup>#</sup>.

*Departamento de Química Física. Universidad del País Vasco. Apartado 644. 48080 Bilbao, Spain.*

*<sup>#</sup>Department of Chemistry. University of Cambridge. Lensfield Road, Cambridge CB2 1EW. England. U.K.*

Direct measurements of the rate constants at room temperature for collisional removal of NCO( $\tilde{A}^2\Sigma^+(0,0,0)$ ) by O<sub>2</sub>( $^3\Sigma_g^-$ ), N<sub>2</sub>( $^1\Sigma_g^+$ ), NO( $^2\Pi$ ), CO<sub>2</sub>( $^1\Sigma_g^+$ ), N<sub>2</sub>O( $^1\Sigma_g^+$ ), SO<sub>2</sub>( $^1A$ ) and precursor phenyl isocyanate PhNCO are reported. NCO( $X^2\Pi(0,0,0)$ ) was prepared by infrared multiple photon dissociation (IRMPD) of PhNCO followed by tunable dye laser pumping at the transition NCO( $\tilde{A}^2\Sigma^+(0,0,0)$ )  $\leftarrow$  X<sup>2</sup> $\Pi_{3/2}(0,0,0)$ . Removal is very efficient and the rates for the gases mentioned were measured to be  $2.05 \pm 0.2$ ,  $15.2 \pm 0.2$ ,  $32.0 \pm 3.0$ ,  $8.52 \pm 0.4$ ,  $6.46 \pm 0.2$ ,  $27.1 \pm 1.0$  and  $51.8 \pm 5.0$  (at a laser fluence of  $43 \text{ J/cm}^2$ ) in  $10^{11} \text{ cm}^3 \text{ molecule}^{-1} \text{ s}^{-1}$  units. An upper limit of the rate constant for physical quenching of NCO( $\tilde{A}$ ) by Ar is also reported as  $<1 \cdot 10^{13} \text{ cm}^3 \text{ molecule}^{-1} \text{ s}^{-1}$ . The rate data are analysed by their correlation with the well depth of the partners, discussing its consequences and obtaining a NCO( $\tilde{A}^2\Sigma(0,0,0)$ ) pair well depth of  $69 \pm 20 \text{ K}^{1/2}$ .

# INFLUENCE OF ROTATIONAL AND VIBRATIONAL EXCITATION ON THE INTERSYSTEM CROSSING ( $c^1\Pi, v=0, J \rightarrow A^3\Pi, v, N$ ) OF NH AND ND IN COLLISIONS WITH MOLECULAR OXYGEN

J. Hohmann and F. Stühli

*Physikalische Chemie I, Ruhr-Universität Bochum, D-44780 Bochum, Germany*

The intersystem crossing (ISC) reactions  $\text{NH}(c^1\Pi, v=0, J) \rightarrow \text{NH}(A^3\Pi, v, N)$  and  $\text{ND}(c^1\Pi, v=0 \text{ and } 1, J) \rightarrow \text{ND}(A^3\Pi, v, N)$  induced by collisions with  $\text{O}_2(X^3\Sigma_g^-)$  were investigated as a function of rotational and vibrational excitation of the  $\text{NH}/\text{ND}(c)$  state. Competing processes such as rotational relaxation and collisional quenching, were studied too in this work.

Single rotational levels of  $\text{NH}/\text{ND}(c)$  were generated by first photolyzing  $\text{HN}_3/\text{DN}_3$  at 248 nm with an KrF excimer laser, which yields metastable  $\text{NH}/\text{ND}(a)$ . Subsequent pumping on the  $(c, v'=0, J' \leftarrow a, v''=1, J'')$  and the  $(c, v'=1, J' \leftarrow a, v''=2, J'')$  transitions by dye laser light at around 360 nm produced the desired excited levels.

The population distributions of fluorescence obtained after population of single rotational levels  $J$  in  $\text{NH}(c, v=0)$  and  $\text{ND}/\text{ND}(A)$  resulting from inelastic collisions with  $\text{O}_2$  were probed by monitoring the  $c \rightarrow a$  and  $A \rightarrow X$

$X$  emissions at about 326 and 336 nm, respectively, hence avoiding stray light for these (0,0) bands. A typical series of fluorescence spectra is displayed in Fig. 1 for  $\text{NH}(c, v=0, J=1-6)$ . It indicates the various efficiencies for the generation of  $\text{NH}(A, v=0, 1, 2)$ .

The following trends were observed:

- For ISC starting from low rotational states,  $J$ , of  $\text{NH}(c)$ , mainly  $v=0$  and  $v=1$  in  $\text{NH}(A)$  are formed. With increasing  $J$ , the population of  $\text{NH}(A, v=2)$  increases at the expense of  $v=1$ .
- For excitation of  $\text{ND}(c, v=0)$ , the formation of  $\text{ND}(A)$  solely in the vibrational ground state was detected.
- For  $\text{ND}(c, v=1)$ , vibrational excitation in  $\text{ND}(A)$  up to  $v=3$  was monitored.

Fig. 2 displays a number of rate constants,  $k^Q$ , for the total quenching and,  $k^{\text{ISC}}$ , for the singlet-triplet intersystem crossing in collisions with  $\text{O}_2$ . In the case of  $\text{ND}(c)$ , a few constants for  $v=1$  are included. These and other data will be described in more detail and discussed.

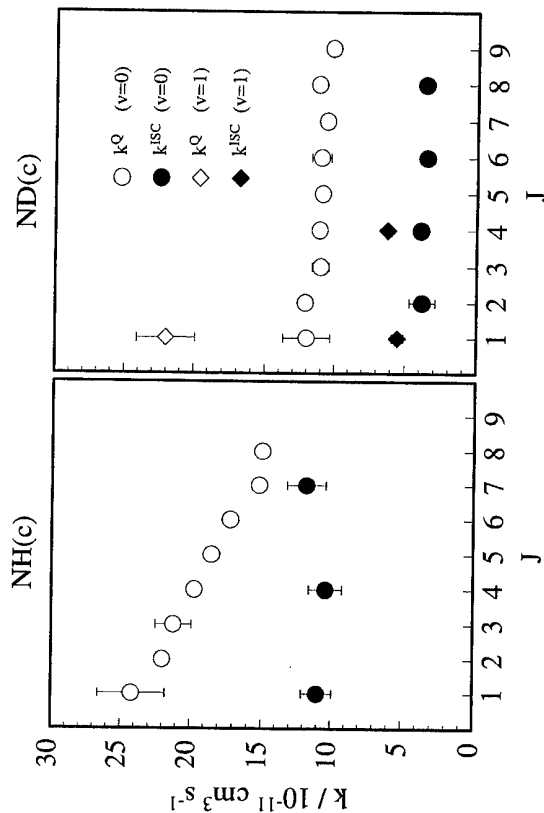


Fig. 2. Rate constants for the electronic quenching,  $k^Q$ , and the intersystem crossing to  $\text{NH}/\text{ND}(A^3\Pi, v)$ ,  $k^{\text{ISC}}$ , of singly excited rotational levels  $J$  of  $\text{NH}/\text{ND}(c^1\Pi, v)$  in collisions with  $\text{O}_2$ .

Financial support by the Deutsche Forschungsgemeinschaft (Stu 59/33-1) is gratefully acknowledged.

# THE QUENCHING OF METASTABLE $\text{NH}(\text{b}^1\Sigma^+)$ BY AMMONIA: A COMPLEX-FORMING BIMOLECULAR REACTION

St. Höser<sup>a</sup>, M. Olzmann<sup>b</sup>, U. Blumenstein<sup>a</sup>, and F. Stuhl<sup>a</sup>

<sup>a</sup> *Physikalische Chemie I, Ruhr-Universität, Bochum, D-44780 Bochum, Germany*

<sup>b</sup> *Institut für Physikalische Chemie der Universität Halle-Wittenberg,*

*D-06099 Halle, Germany*

The quenching of metastable  $\text{NH}(\text{b}^1\Sigma^+)$  and  $\text{ND}(\text{b}^1\Sigma^+)$  by  $\text{NH}_3$  and  $\text{ND}_3$ , respectively, has been studied in the presence of the diluent gases He, Ar,  $\text{N}_2$ , and  $\text{SF}_6$ . Rate constants were determined by measuring directly the removal rates of the metastables at bath gas densities

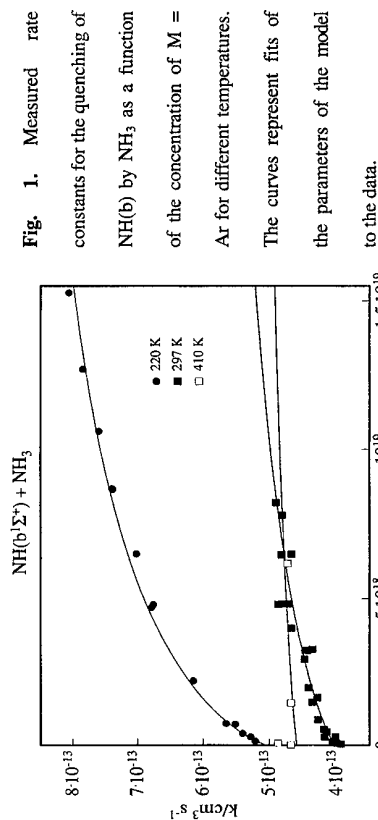


Fig. 1. Measured rate constants for the quenching of  $\text{NH}(\text{b})$  by  $\text{NH}_3$  as a function of the concentration of  $M = \text{Ar}$  for different temperatures. The curves represent fits of the parameters of the model to the data.

between  $\sim 10^{16}$  and  $\sim 10^{19} \text{ cm}^{-3}$  and in the temperature range from 220 to 410 K. Examples of the constants are shown in Fig. 1. Values between  $3 \cdot 10^{-13}$  and  $8 \cdot 10^{-13} \text{ cm}^3 \text{s}^{-1}$  were obtained for

$\text{NH}(\text{b}) + \text{NH}_3$ , whereas the rate constants for the deuterated species are lower by about one order of magnitude. In general, besides this isotope effect, a complicated dependence on the pressure, the nature of the bath gas, and the temperature is observed. This behavior is explained by assuming reactive quenching via complex formation for at least part of the reaction. It is suggested that this quenching proceeds on the first excited singlet surface of  $\text{N}_2\text{H}_4$ . Based on some gross features of the underlying potential-energy surface, a master equation was set up and solved with a stepladder model for the transition probabilities and specific rate constants from RRKM theory. A consistent set of parameters was found, which describes the complicated behavior observed over the whole range of experimental conditions, including the isotope effect. In Fig. 1, the good agreement between the measured and the calculated rate constants is demonstrated and, in Fig. 2, a schematic diagram of the derived potential-energy profile is given. The significance of these parameters will be discussed in view of the unknown potential-energy surface of  $\text{N}_2\text{H}_4$  in its first excited singlet state.

# CHEMICAL RELAXATION OF UPPER VIBRATIONAL OH( $v=7-9$ ) STATES IN REACTION WITH O<sub>2</sub>. IMPLICATION TO THE THEORY OF NIGHT SKY HYDROXYL EMISSION.

Yu.M. Gershenzon, V.M. Grigorieva, A.S. Kukui, D.V. Shalashilin and  
S.Ya. Umanskiy,  
A.F. Dodonov\* and V.V. Zelenov\*.

*Institute of Chemical Physics, RAS,  
4 Kosygin St., 117977 Moscow, Russian Federation*

*\*Institute for Energy Problems of Chemical Physics, RAS,  
38 Leninskii prosp., 117977 Moscow, Russian Federation*

The reaction of the upper vibrational states OH( $v=7-9$ ) with O<sub>2</sub> has been studied by mass-spectrometric probing of O<sub>3</sub> diffusion cloud in a fast flow of He containing H atoms with or without O<sub>2</sub> additive [1]. OH( $v=7-9$ ) states were generated in the reaction (1) of O<sub>3</sub> flowed out through a capillary in a flux of He+H+(O<sub>2</sub>)



An increase in the HO<sub>2</sub> concentration in the mixing zone due to the reaction was established and measured.



The experiments have been carried out at T=298 K, P=4.45 Torr, [H] = 3.8 x 10<sup>13</sup> cm<sup>-3</sup>, Δ[O<sub>2</sub>] = 1.7 x 10<sup>15</sup> cm<sup>-3</sup>.

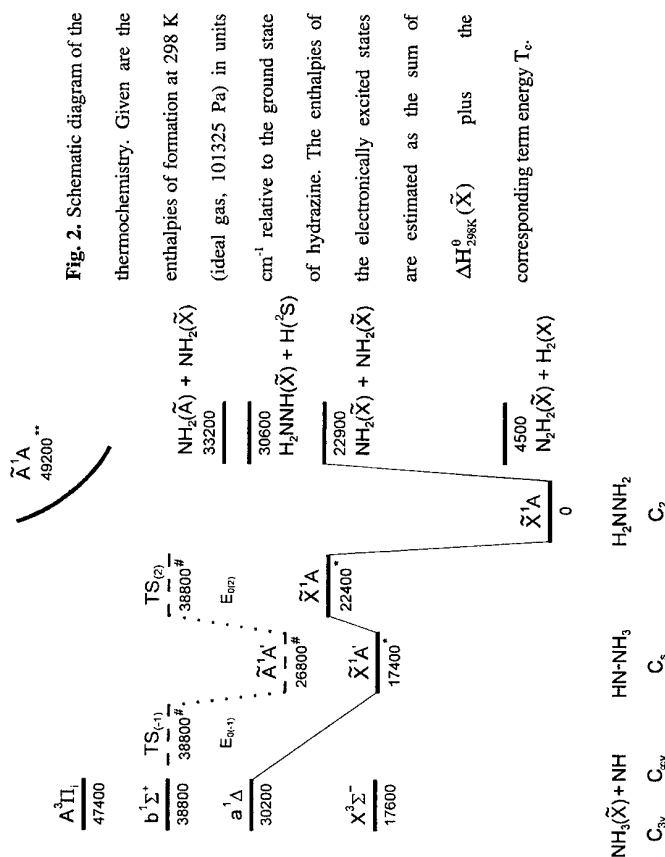
Relations of rate constants of reaction (2) and relaxation (3)



have been estimated using the measured value of Δ[HO<sub>2</sub>]. The reaction (2) rate has been found to be about 40-80 times slower than the total rate of upper states quenching in collisions with O<sub>2</sub>, process (3). This is an important result for the theory of nightglow OH( $v$ ) Meinel emission.

Two extreme kinetic models of OH( $v$ ) emission have been supposed [2,3]. The first one suggests single quantum relaxation in OH( $v$ ) collisions with air molecules (N<sub>2</sub>, O<sub>2</sub>, O) for all vibrational states  $v=1-9$ . The second extreme case, called in [2] as a sudden death model, assumes the total vibrational OH energy loss in collisions with air molecules.

Recent laboratory studies [4] and trajectory simulations [5] showed that collisions with O<sub>2</sub> are more effective than those with N<sub>2</sub> and O-atoms for OH( $v=7-9$ ) in the mesosphere. In this connection, the result obtained does not provide a physical basis



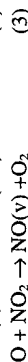
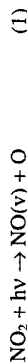
# TIME RESOLVED FTIR STUDIES OF VIBRATIONAL ENERGY TRANSFER FROM NO(<sup>2</sup>Π<sub>1/2,3/2</sub>, v) BY NO<sub>2</sub> AND O<sub>2</sub>

C. G. Hickman, E. L. Moore and G. Hancock

*Physical and Theoretical Chemistry Laboratory, Oxford University,  
South Parks Road, Oxford, OX1 3QZ, U. K.*

Vibrational relaxation of NO(v) with a range of collision partners, such as NO<sub>2</sub>, NO and O<sub>2</sub> [1, 2, 3], has been extensively studied as it is a test bed for theories of vibrational energy transfer, such as SSH theory.

Data were generated by photolysing NO<sub>2</sub> at 308 nm in the presence of appropriate gases, and monitoring the resulting IR emission with a stop-scan TR-FTIR instrument. Spectra in the NO region were modelled to give time resolved populations of NO(v) (v=1-3), with the population of NO(v=0) found from a surprisal plot of the nascent vibrational distribution. Quenching rates for each vibrational level were found by fitting the experimental data to the following kinetic model:



with rate constants and vibrational distributions for process (3) taken from the work of Smith et al. [4].

The resulting state specific rate constants are ( $\pm 2\sigma$  error limits):

NO(v)	kNO <sub>2</sub> /10 <sup>-12</sup> cm <sup>3</sup> molecule <sup>-1</sup> s <sup>-1</sup>	kO <sub>2</sub> /10 <sup>-14</sup> cm <sup>3</sup> molecule <sup>-1</sup> s <sup>-1</sup>
1	1.9 ± 0.2	4.6 ± 0.6
2	2.9 ± 0.3	5.9 ± 1.4
3	4.8 ± 0.7	14 ± 1

These values are generally in good agreement with previous values [1, 2, 3, 5]. For NO<sub>2</sub> the rate constant for v=1 is consistent with prior observations [3], whilst the values for v=2,3 are previously unreported. The reduced probabilities P<sub>v</sub>/v are found to be independent of |ΔE| in contradiction with theory. Conversely for O<sub>2</sub>, the rate constants are consistent with previous studies and theory.

## References

1. I. J. Wysong *J. Chem. Phys.* **101**, 2800, (1994).
2. I. J. Wysong *Chem. Phys. Lett.* **227**, 69, (1994).
3. R. P. Fernando and I. W. M. Smith *J. Chem. Soc. Faraday Trans.* **77**, 459, (1981).
4. I. W. M. Smith, R. P. Tuckett and C. J. Whitham *Chem. Phys. Lett.* **200**, 615, (1992).
5. B. D. Green, G. E. Caledonia, R. E. Murphy and F. X. Robert *J. Chem. Phys.* **76**, 2441, (1982).

for realization of the sudden death model in the chemical relaxation process (2). A collisional loss of the total vibrational energy in process (3) also can not be accepted as quenching due to reasons pointed out in [1, 4, 5]. Thus, the sudden death model is not realized for the upper levels.

As was shown by Grigorjeva et al [6], the single quantum relaxation of OH(v=7-9) on O<sub>2</sub> is also not the process to describe the relative population of OH(v). We do not consider that both the sudden death and stepwise models are appropriate to explain the nightglow populations of OH(v=4-9) states [6].

A new model of nightglow OH(v) emission [6] includes single quantum relaxation for lower OH(v=1-6) levels and mainly three quantum relaxation for upper OH(v=7-9) states in collisions with O<sub>2</sub>.

In our model, the middle states OH(v=4-6) are "fed" by 2-3 quantum transitions in the processes:



The sink of OH(v=4-6) is realized in both the stepwise deactivation on O<sub>2</sub> and in OH(v=4-6) + O → O<sub>2</sub> + H reaction. This model describes well the observed relative [OH(v)]/[OH(v=9)] populations in the airglow [6]. A more detailed analysis of space and energy OH(v) distribution will be published elsewhere.

This work was supported by the Russian Foundation for Basic Research (grant #9303-5495) and the International Science Foundation (grants NEQ 000 and NEQ 300).

## References:

- (1) Kukui, V. V. Zelenov, A. F. Dodonov, V. M. Grigorjeva, and Yu. M. Gershenson, *Khimicheskaya Fizika*, **15**(5), 67, 1996 (in Russian).
- (2) McDade I.C., and E. J. Llewellyn, *J. Geophys. Res.*, **92**, 7643, 1987.
- (3) McDade I.C., *Planet Space Sci.*, **39**, 1049, 1991.
- (4) Chalamala B.R., and R. A. Copeland, *J. Chem. Phys.*, **99**, 5807, 1993; Knutsen K., and R. A. Copeland, *EOS Trans. A.G.U.*, (34) Fall meeting Suppl., 472, 1993.
- (5) Shalashilin, S. Ya. Umanskii, and Yu. M. Gershenson, *J. Chem. Phys.*, **168**, 315, 1992; D. V. Salashilin, A. V. Mitchenko, S. Ya. Umanskii, and Yu. M. Gershenson, *J. Phys. Chem.*, **99**, 11627, 1995.
- (6) Grigorjeva, Yu. M. Gershenson, D. V. Shalashilin, and S. Ya. Umanskii, *Chem. Phys. Repts.*, **13**, 1577, 1995, Translated from Russian, *Khimicheskaya Fizika*, **13**, 3, 1994, (in Russian).

# QUANTUM YIELDS AND PHOTOFRAGMENT SPECTROSCOPY OF ATMOSPHERICALLY IMPORTANT SPECIES

Stephen M. Ball, Gus Hancock, Shouna E. Martin and John C. Pinot de Moira

*Oxford Centre for Applied Kinetics,  
Physical and Theoretical Chemistry Laboratory, Oxford University,  
South Parks Road, Oxford OX1 3QZ, U.K.*

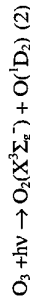
We will report on the relative quantum yields ( $\Phi$ ) of the  $O(^1D_2)$  fragments from photolysis of ozone at wavelengths between 300 and 325nm. Two identical tuneable dye lasers were employed, the first to photolyse ozone and the second to form  $O(^1D_2)$  ions from the fragments in a 2+1 Resonance Enhanced Multi-photon Ionization (REMPI) process. The quantum yield measurements were conducted on a bulk sample of ozone at room temperature and placed on an absolute scale by comparison with previous studies.

We found the  $O(^1D_2)$  quantum yield broadly agrees with our previous measurements of the  $O_2(a^1\Delta_g)$  quantum yield at wavelengths between 300 and 325nm [1]. The  $O(^1D_2)$  yields have a constant value close to unity at wavelengths below the threshold for process (1) at 310nm.



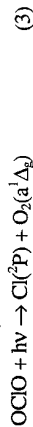
Beyond 310nm, the yield drops rapidly, reaching  $\Phi=0.2$  near 320nm, the fragments presumably being from photolysis of internally excited ozone molecules. A yield of 20% is contrary to the zero yield recommended by NASA for atmospheric modelling of  $O(^1D_2)$  production [2], and, owing to the larger solar flux penetrating into the troposphere at these wavelengths, the higher measured  $O(^1D_2)$  yields are expected to change calculated  $O(^1D_2)$  production rates at ground level by up to a factor of two [3].

At wavelengths above 320nm the quantum yield is small, but non zero. It is expected that these fragments derive from either the photolysis of the small fraction of doubly vibrationally excited ozone molecules or from the spin forbidden process (2).

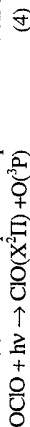


We will also report on translational energy measurements of the fragments formed from the laser photodissociation of OCIO between 321 and 331nm. The translational energy measurements were made by photolyzing OCIO in a molecular beam and then using the same laser pulse to perform multi-photon ionization of the photofragments. The ions were produced in the source region of a modified Wiley-McLaren TOF mass spectrometer and were detected as a function of time following the REMPI pulse. The fields in the spectrometer were chosen to allow the velocities of the neutral fragments to be determined from their flight time profiles. A detailed description of the time-of-flight mass spectrometer is given elsewhere [4]. There is evidence from previous studies [5] that a minor channel for

the dissociation of OCIO is (3) and wavelengths were chosen at which REMPI of  $O_2(a^1\Delta_g)$  ( $v=0$ , low  $J$ ) was known to occur, i.e.  $\lambda \approx 330$ nm.



However, the TOF spectra show no signal from  $O_2^+$  at  $m/e=32$ , implying there is no detectable formation of  $O_2(a^1\Delta_g)$  ( $v=0$ , low  $J$ ) from channel (3) at these photolysis wavelengths. Rather, large signals were observed from  $ClO^+$ , presumably from dissociation of OCIO to ClO via channel (4) and subsequent multiphoton ionization of ClO.



Furthermore, aligning the polarization of the photolysis laser parallel to the detection axis produced forward and backward peaks in the ClO fragment velocities along the detection axis. While, aligning the photolysis polarization perpendicular to the detection axis produced a single peak centred around zero velocity, indicative of an anisotropic dissociation via a parallel transition (anisotropy parameter,  $\beta$ , positive).

Also present in the TOF spectra are signals from  $Cl^+$  at  $m/e=35$  and 37, possibly formed following absorption by  $ClO^+$ . These signals show an isotropic kinetic energy distribution. A very weak signal is observed at  $m/e=16$  from  $O^+$ , which shows a strong alignment between velocity and photolysis vectors.  $O^+$  is thought to derive from prompt one laser photolysis of  $ClO^+$  via a separate pathway to the one above.

1. S.M. Ball and G. Hancock; *Geophys. Res. Lett.* **22** (1995) 1213
2. W.B. DeMore, S.P. Sander, D.M. Golden, R.F. Hampson, M.J. Kurylo, C.J. Howard, A.R. Ravishankara, C.E. Kolb, M.J. Molina, Chemical kinetics and photochemical data for use in stratospheric modeling. *Evaluation number 11*, JPL publication 94-26, (1994).
3. M. Müller, A. Kraus and A. Hofzumahaus; *Geophys. Res. Lett.* **22** (1995) 679
4. S.M. Ball, G. Hancock, J.C. Pinot de Moira, C.M. Sadowski, F. Winterbottom; *Chem. Phys. Lett.* **245** (1995) 1
5. H.F. Davis and Y.T. Lee; *J. Phys. Chem.* **96** (1992) 5681

# SCALAR AND VECTOR PROPERTIES OF THE REACTION $\text{O}^3\text{P} + \text{H}_2\text{S}^1\text{A}_1 \rightarrow \text{OH}(\text{X}^2\text{A}) + \text{SH}(\text{X}^2\text{A})$

M.L. Costen, G Hancock and G.A.D Ritchie

*Physical and Theoretical Chemistry Laboratory, South Parks Road,  
 Oxford, OX1 3QZ, United Kingdom.*

The scalar properties of the OH product of the titled reaction have been measured using the LIF pump and probe technique, the  $\text{O}^3\text{P}$  atoms being produced by 355nm photolysis of  $\text{NO}_2$ . The rotational, spin-orbit and 7-doublet distributions for OH ( $v''=1$ ) are found to be non-statistical and rotationally hot with population upto the exothermic limit.

Experiments are in progress to determine the vector properties of the reaction by utilising polarised Doppler limited spectroscopy. Analysis of the shape of a Doppler profile can yield the vector correlations occurring between the relative velocity vector of the reagents,  $\mathbf{k}$ , the relative velocity vector of the products,  $\mathbf{k}'$ , and the rotational angular momentum of the product molecule,  $\mathbf{J}$  [1]. More recently it has been shown that in favourable cases the differential scattering cross-section and energy disposal in the cofragment can also be deduced [2,3]. Preliminary analysis to determine the differential scattering cross-section and translational speed distribution for the  $v''=1$ ,  $N=6$  level suggests largely sideways scattering of the OH, with a narrow translational energy distribution reflecting low rotational excitation in the cofragment SH.

The dynamics are interpreted as describing a planar transition state with out of plane rotation of the  $\text{H}_2\text{S}$  transferring to OH product rotation. Detailed models such as that suggested lead to predictions about the dynamics of other OH levels, and the SH fragment formed with them. The SH product can also be probed using the same techniques allowing testing of both the analysis of the doppler profiles and the models presented.

## References:

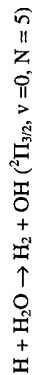
- [1] R.N.Dixon, *J.Chem.Phys.*, 1986, **85**, 1866.
- [2] H.L.Kim, M.A.Wickramaarachchi, X.Zheng, G.E.Hall, *J.Chem.Phys.*, 1994, **101**, 2033.
- [3] M.Brouard, M.Lambert, C.L.Russell, J.Short, J.P.Simons, *Faraday Discuss.*, 1995, **102/15**.

# STATE SPECIFIC DIFFERENTIAL CROSS-SECTIONS FOR THE $\text{H} + \text{H}_2\text{O}$ REACTION VIA POLARISED DOPPLER-RESOLVED LASER SPECTROSCOPY.

M. Brouard, G.A.J. Markillie and K.E.W. McGrath

*Physical and Theoretical Chemistry Laboratory, South Parks Road, Oxford, OX1  
 3QZ, United Kingdom*

Doppler-resolved, polarised laser induced fluorescence has been employed in a study of the stereodynamics of the velocity aligned, hot atom reaction



at a mean centre-of-mass collision energy of 1.49 eV. The velocity aligned H atoms were produced by polarised photodissociation of  $\text{H}_2\text{S}$  at a wavelength of 225nm [1].

Doppler-resolved profiles of both A-doublet levels were recorded in collinear and orthogonal geometries. Composite profiles were then obtained from the data [2,3], and fitted with an array of generated basis functions. The weighting of the basis functions was then used to deduce the centre-of-mass differential cross-section for each A-doublet component [4].

The results of the analysis indicated that both A-doublets had very similar differential cross-sections, with the OH product being isotropically scattered in the centre-of-mass frame. It was concluded that the results were consistent with the concept of a cone of acceptance, which is small for collision energies just above the barrier to reaction and opens as the collision energy increases, thus allowing higher impact collisions to lead to reaction. This explains the broad spread in angular scattering in this experiment, and the exclusively forward distribution measured at the lower collision energy employed by Casavecchia [5].

## References

- [1] G.P. Morley, I.R. Lambert, D.H. Mordaunt, S. Wilson, M.N.R. Ashfold, R.N. Dixon and C.M. Western; *J. Chem. Soc. Faraday Trans.*, **89**, (1993), 3865
- [2] F.J. Aoiz, M. Brouard, P.A. Enriquez and R. Sayos; *J. Chem. Soc. Faraday Trans.*, **89**, (1993), 1427
- [3] R.N. Dixon; *J. Chem. Phys.*, **85**, (1986), 1886
- [4] M. Brouard, H.M. Lambert, S.P. Rayner and J.P. Simons; *Mol. Phys.*, in press
- [5] M. Alagia, N. Balucani, P. Casavecchia, D. Stanges and G.G. Volpi; *J. Chem. Soc. Faraday Trans.*, **91**, (1995), 575

# CN VIBRONIC DISTRIBUTIONS PRODUCED BY THE EXOERGIC INDIRECT REACTIONS $N + CH \rightarrow CN + H$ , $N + C_2 \rightarrow CN + C$ AND $C + NO \rightarrow CN + O$ .

N. Daugey, A. Bergéat, A. Schuck, P. Caubet, G. Dorthé, P. Halvick\*, M. T. Rayez\* and J. C. Rayez\*.

*Laboratoire de Photophysique et Photochimie Moléculaire and  
Laboratoire de Physico-Chimie Théorique\*, Université Bordeaux I, 33405 Talence, France.*

Little attention has been paid to the dynamics of "indirect" reactions involving long-lived complexes since they have been believed to exhibit a more or less statistical behaviour. In a theoretical investigation of exoergic indirect collinear three-atom reactions, on a single potential-energy surface, Halvick and Rayez<sup>1</sup> found non-statistical vibrational distributions of the diatomic product, which can be linked to the anisotropy of the well: the higher the anisotropy, the greater the departure from the statistical distribution. Systematic experimental studies are thus needed to check the dynamic trends theoretically predicted. The above-mentioned exoergic three-atom indirect reactions, yielding the same radical CN, appeared interesting to study because all of them involve deep potential-energy wells between the reactants and the products.

The  $N + CH$  and  $N + C_2$  reactions were recently performed in a low pressure (1 Torr He) fast-flow reactor with thermalized reactants. Clean production of CH and  $C_2$  was achieved by the reaction of K vapor with  $CHBr_3$  and  $C_2Cl_4$  in a microfurnace tapering into a nozzle. The reaction temperature decayed from 460 K at the nozzle exit (where mixing with atomic nitrogen occurred) to 310 K, 100 mm downstream, so that the mean thermal energy of the reactants decayed from 0.10 eV to 0.07 eV. The mean total energy available to the products varied from 4.40 to 4.37 eV for the  $N + CH$  reaction and from 1.66 to 1.63 eV for  $N + C_2$ . In the simulation matching vibrational distributions recorded at different distances, we assumed the nascent CN vibrational distribution to be constant all along the reactor.

The energy available to the products from the  $N + CH$  reaction can populate  $CN(X^2\Sigma^+)$  up to  $v_A = 19$ ,  $CN(A^1\Pi)$  up to  $v_A = 16$  and  $(B^2\Sigma^+)$  up to  $v_B = 4$ . However, the reactants in their ground electronic states, namely  $N(^4S_u)$  and  $CH(X^2\Pi)$ , do not correlate with  $CN(B^2\Sigma^+) + H(^2S_g)$ . A strong chemiluminescence has been observed from all vibrational levels of  $CN(A^1\Pi)$  up to  $v_A = 16$  while a chemiluminescence from  $B^2\Sigma^+$  exclusively in  $v_B = 0$  was observed. The latter chemiluminescence was shown to result from the collisional transfer between  $CN(A^1\Pi)$ ,  $v_A = 10$  and  $CN(B^2\Sigma^+)$ ,  $v_B = 0$ .  $CN(A^1\Pi)$  arises both from direct production from the reaction and collisional transfer from  $CN(X^2\Sigma^+)$  vibrational levels. The latter levels could be probed up to  $v_A = 9$  by laser-induced fluorescence. The simulation of the evolution with the distance of the stationary vibrational populations of  $CN(A^1\Pi)$  and  $CN(X^2\Sigma^+)$ , taking into

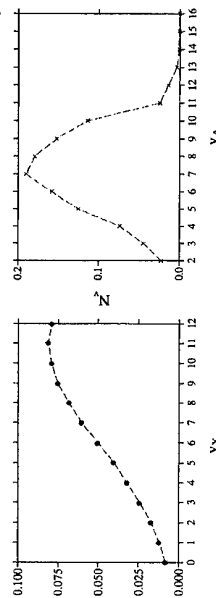


Fig. 1.  $CN(X^2\Sigma^+)$  and  $(A^1\Pi)$  nascent vibrational distributions from the reaction  $N + CH \rightarrow CN + H$ .

account the collisional and radiative transfers between vibronic states, led to a strong nascent population inversion on both states with a maximum, respectively, at  $v_A = 11$  and  $v_A = 7$  (Fig. 1).

The  $A^1\Pi$  state of  $C_2$  lying only 0.09 eV above  $X^1\Sigma_g^+$ , both states were involved in the reaction  $N + C_2$ . The CN vibrational distribution, though non-inverted, departs significantly from that expected on a statistical basis whatever can be the  $C_2$  state (Fig. 2).

The  $C + NO$  reaction was performed some years ago in a crossed-beam apparatus at two collision energies yielding total available product energies of 1.33 and 1.50 eV. Non-statistical CN vibrational distributions were found<sup>2</sup> (Fig. 3).

For the  $C + NO$  reaction, the theoretical vibrational distribution calculated from the ground-state potential energy surface, for which the well anisotropy is small, is in fair agreement with that obtained experimentally. For other reactions, the vibrational distributions have not as yet been calculated. For  $N + CH$ , many surfaces are involved with anisotropic wells so that the vibrational inversion is consistent with the expected trend. For  $N + C_2$  surfaces with anisotropic and isotropic wells are involved so that no definite conclusion can be drawn.

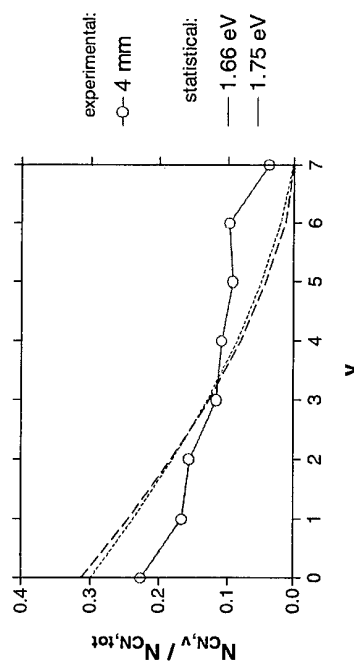


Fig. 2.  $CN(X^2\Sigma^+)$  nascent vibrational distribution from the reaction  $N + C_2 \rightarrow CN + C$ .

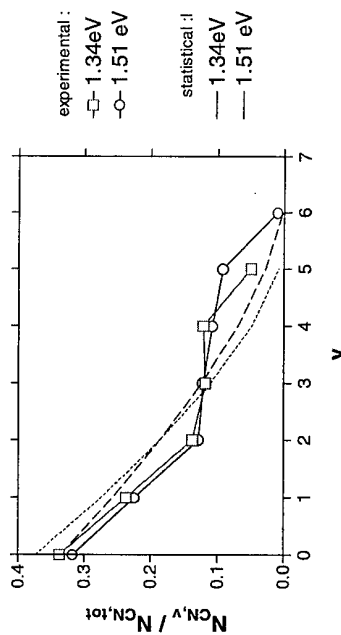


Fig. 3.  $CN(X^2\Sigma^+)$  nascent vibrational distribution from the reaction  $C + NO \rightarrow CN + O$ .

## References:

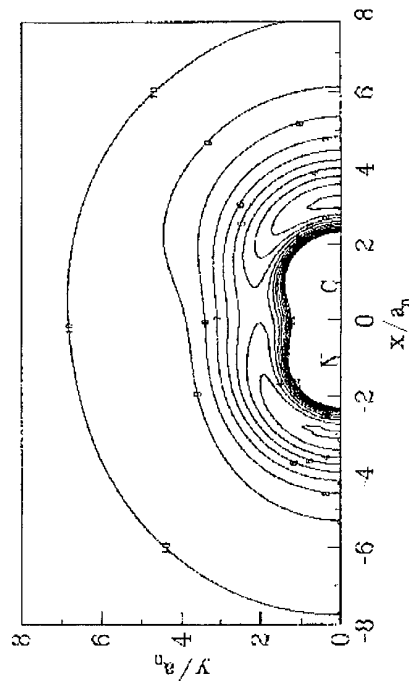
1. P. Halvick, J.C. Rayez, M. T. Rayez and B. Duguay, *Chem. Phys.* **114**, 375 (1987).
2. C. Naulin, M. Costes and G. Dorthé, *Chem. Phys.* **153**, 519 (1991).

# ACCURATE SINGLE-VALUED DOUBLE MANY-BODY EXPANSION POTENTIAL ENERGY SURFACE FOR HCN( $X^1\Sigma^+$ )

S.P.J. Rodrigues and A.J.C. Varandas

*Departamento de Química, Universidade de Coimbra  
P-3049 Coimbra Codex, Portugal*

Knowledge of the title potential energy surface is crucial for studying the spectroscopy of the HCN and HNC isomers, and to calculate the rate constant of the isomerization reaction  $\text{HCN} \leftrightarrow \text{HNC}$ . Although various potentials have been proposed, none is fully satisfactory. Moreover, no attempt has been made to describe properly the high regions of the potential energy surface below dissociation. At these regions, long range forces are expected to predominate, and hence should have an important role on the spectroscopy and dynamics at such regimes. In this work, we have used existing



**Figure 1:** Optimized contour plot of H moving around NC (internuclear distance variation between 2.0 and 2.4  $a_0$ ) for the calculated potential energy surface. Contours start at  $-0.490 E_h$ , with successive intervals of  $0.022 E_h$ .

$\text{HCN} \leftrightarrow \text{HNC}$  *ab initio* CCSD(T) calculations [1], and new FV-CAS calculations for CHN geometries, in conjunction with atom-diatom long range coefficients obtained from a recently developed model [2], to determine an accurate single-valued double many body expansion [3, 4] (DMBE) potential energy surface for HCN ground state.

Figure 1 shows an optimized contour plot of the obtained potential energy surface. The minima of the HCN and HNC structures are the main features of this Figure together with the saddle point which connects them,  $\text{HCN}^\ddagger$ . We note that the hydrogen isocyanide and the isomerization saddle point lie  $5140 \text{ cm}^{-1}$  and  $16832 \text{ cm}^{-1}$  above the HCN global minimum, respectively.

The new reported potential energy surface is globally valid and compares well with the most accurate reported so far. Thus, it is recommended for future adiabatic studies on the  $\text{HCN} \leftrightarrow \text{HNC}$  system. In particular, it can be employed for studies of the unimolecular dissociation through the reactions  $\text{HCN} \rightarrow \text{H} + \text{CN}$  and  $\text{HNC} \rightarrow \text{C} + \text{NH}$ , and the  $\text{HCN} \leftrightarrow \text{HNC}$  isomerization reaction.

**Acknowledgments:** This work has the support of the Junta Nacional de Investigação Científica e Tecnológica, Portugal, under programmes PRAXIS XXI and FEDER (Contract 2/2.1/QUI/408/94).

## References

- 1) Bowman, B. Gadzy, J. Bentley, T.J. Lee, and C.E. Dateo, *J. Chem. Phys.* **99**, 308 (1993).
- 2) Varandas and S.P.J. Rodrigues, *Chem. Phys. Lett.* **245**, 66 (1995).
- 3) Varandas, *Adv. Chem. Phys.* **74**, 255 (1988).
- 4) Varandas, *Chem. Phys. Lett.* **194**, 333 (1992).

# DYNAMICS STUDY OF THE H + ArO<sub>2</sub> REACTION OVER A WIDE RANGE OF TRANSLATIONAL ENERGIES

J.M.C. Marques, W. Wang, A.A.C.C. Pais and A.J.C. Varandas

*Departamento de Química, Universidade de Coimbra  
P-3049 Coimbra Codex, Portugal*

We report a detailed trajectory study of the H + ArO<sub>2</sub> reaction over the range of translational energies  $0.25 \leq E_{tr}/\text{kcal mol}^{-1} \leq 131.4$ . The ArHO<sub>2</sub> potential energy surface has been written as a pairwise summation of realistic EHFACE2<sup>1</sup> potentials for the interactions involving Ar, and the reliable DMBE IV<sup>2</sup> potential energy surface for the chemically stable triatomic species. Using a novel scheme<sup>3</sup> to identify all fourteen channels arising from a general atom+triatom reactive collision, the HO<sub>2</sub>, O<sub>2</sub>, ArH, ArOH, OH, and ArO products have been identified in batches of 1500 or 3000 trajectories for each value of the translational energy. Cross sections for the hydroperoxyl radical formation have then been calculated for the translational energies  $0.25 \leq E_{tr}/\text{kcal mol}^{-1} \leq 8.0$ , and used to obtain the termolecular rate coefficient for the three-body recombination process  $\text{H} + \text{O}_2 + \text{Ar} \rightarrow \text{HO}_2 + \text{Ar}$  employing a chaparron mechanism<sup>3</sup>. Also reported are reactive cross sections for formation of O<sub>2</sub>. Moreover, we have studied<sup>4</sup> the dynamical behaviour of energized HO<sub>2</sub> molecules which arise from the H + ArO<sub>2</sub> collisions at low translational energies. In turn, the decay curves for the unimolecular dissociation reaction



are shown in Figure 1. Clearly, the curve of panel (a) shows two decay regimes associated with different elementary step processes, while that of panel (b) shows that the dominant behaviour corresponds to prompt dissociation. The formation of OH has also been studied, and compared with the corresponding process in the absence of argon<sup>5</sup>; some results are gathered in Figure 2, where the solvation effects due to the argon atom are clearly patent.

**Acknowledgements:** The support of Junta Nacional de Investigação Científica e Tecnológica (Portugal) and EC is gratefully acknowledged.

## References

- 1) Varandas and J. Dias da Silva, *J. Chem. Soc., Faraday Trans. 2* **82**, 593 (1986).
- 2) Pastrana, L.A.M. Quintales, J. Brandão, and A.J.C. Varandas, *J. Phys. Chem.* **94**, 8073 (1990).

- 3) Varandas, A.A.C.C. Pais, J.M.C. Marques, and W. Wang, *Chem. Phys. Lett.* **249**, 264 (1996).
- 4) Marques, W. Wang, A.A.C.C. Pais and A.J.C. Varandas, submitted for publication.
- 5) Varandas, *J. Chem. Phys.* **99**, 1076 (1993).

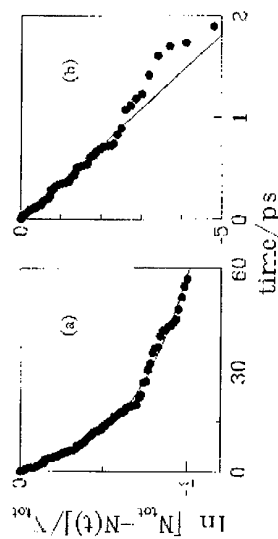


Figure 1: Logarithm of the decay rate of the HO<sub>2</sub>\* complexes as a function of time. Panel (a) refers to the H + ArO<sub>2</sub> initial translational energy of 2.0 kcal mol<sup>-1</sup>, while panel (b) corresponds to 19.1 kcal mol<sup>-1</sup>. The lines represent least-squares fits.

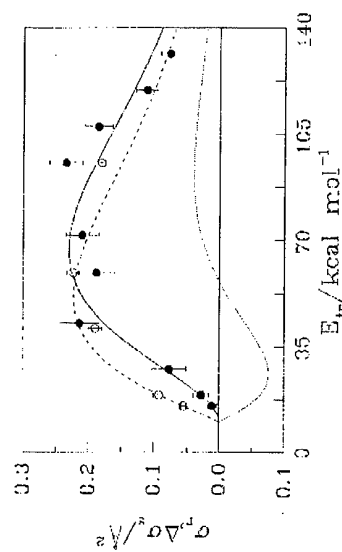


Figure 2: Cross sections for OH formation as a function of the translational energy: ● and —, this work; ○ and —, QCT results (Ref. 5); —, Δσ<sub>OH</sub> (difference between the solid and dashed lines). The lines for σ<sub>OH</sub> represent least-squares fits, while the points indicate the calculated cross sections. The error bars are also shown.

# MOLECULAR BEAM AND QUASICLASSICAL TRAJECTORY STUDIES OF THE REACTION DYNAMICS OF $O(^1D) + H_2$ AND $O(^1D) + D_2$

M. Alagia, N. Balucani, L. Cartechini, P. Casavecchia, E.H. van Kleef, and G.G. Volpi  
*Dipartimento di Chimica, Università di Perugia, 06100 Perugia, Italy*

P.J. Kuntz

*Hahn-Meitner-Institute für Kernforschung Berlin, D 1000 Berlin 39, Germany*

J.J. Sloan

*Department of Chemistry, University of Waterloo, Waterloo, Canada N2L 3G1*

The reaction  $O(^1D)+H_2 \rightarrow OH+H$  has been the subject of considerable experimental and theoretical work over the last 20 years because of its fundamental and practical importance (atmospheric chemistry and combustion).<sup>1</sup> However, despite extensive investigation, its reaction dynamics is still not well understood. In particular, it is not clear what is the relative role of insertion and abstraction mechanisms, and the product vibrational distribution remains somewhat uncertain. In order to shed more light into the dynamics of this reaction, we have undertaken a detailed study of  $O(^1D)+H_2$  and  $O(^1D)+D_2$  at different collision energies ( $E_c$ ) by using the crossed molecular beam (CMB) scattering method with rotating mass spectrometric detection.<sup>2</sup> This work is an extension of previous CMB work<sup>3</sup> and a complement to recent work<sup>4</sup> on the systems  $O(^1D)+D_2$  and  $O(^1D)+HD$  carried out in crossed pulsed beam experiments using Doppler-shift measurements in a REMPI H-atom detection scheme. We exploit the generation of intense supersonic beams of atomic oxygen containing also significant concentrations of  $O(^1D)$  by high pressure radio frequency discharge<sup>5</sup> and the fact that the reaction  $O(^3P)+H_2$  has an activation barrier of about 8.5 kcal/mol, well above the experimental reactant translational energies. Simultaneously, quasiclassical trajectory (QCT) calculations on a semiempirical potential energy surface (PES)<sup>6</sup> have been undertaken at the same energies of the experiment to probe the reliability of the PES and assist the analysis of the molecular beam data.

Product angular and velocity distributions have been measured at  $E_c=1.9$ , 3.0 and 4.0 kcal/mol for  $O(^1D)+H_2$  and  $E_c=5.3$  kcal/mol for  $O(^1D)+D_2$ . A fit in terms of a single couple of product angular and translational energy distributions in the center-of-mass (c.m.) frame indicates (i) a modest fraction of energy released as translational motion of the products, which points to a high internal (ro-vibrational) excitation, and (ii) a preferential backward scattering of the product with respect to the oxygen direction. A more detailed analysis in terms of separate angular and translational energy distributions for the various product vibrational levels involved, indicates an inverted vibrational distribution, considerably hotter than that predicted by the QCT computations. The results are compared with the vibrational distributions obtained at a

somewhat lower average collision energy ( $\approx 1$  kcal/mol) by laser-induced-fluorescence,<sup>6</sup> chemical laser<sup>7</sup>, and infrared-chemiluminescence<sup>8</sup> experiments.

The main result of the QCT calculations on the PES of Ref. 4 is that, in all cases, the c.m. angular distribution is found to be symmetric or slightly forward scattered and the product translational energy distribution considerably hotter (i.e., the  $OH(v')$  distribution colder) than the experiment, which points to some inadequacies of the semiempirical PES. The fact that the c.m. angular distribution is not symmetric indicates that  $O(^1D)$  direct-insertion into the  $H_2(D_2)$  bond does not dominate the overall reaction mechanism; but the abstraction pathway could start to contribute at these translational energies, which would not be surprising considering that the barrier to collinear abstraction is calculated to be less than 0.2 kcal/mol.<sup>9</sup> A suggestive interpretation of the preferred backward scattering, even in the case of a very rapid formation, following direct insertion, of a highly excited  $H_2O$  molecule intermediate, which is very short lived and dissociates within a few bending vibrations before the energy can randomize, is afforded by a detailed analysis of the reactive trajectories. It is found that a large majority of them explore the deep potential well of the  $H_2O$  intermediate once or twice: while those making a traversal of the well once (i.e., experiencing one bending vibration) are strongly forward scattered, those making two traversals of the well (i.e., experiencing two bending vibrations) are strongly backward scattered. The QCT results indicate that the former type of trajectories are somewhat more numerous than the second type, while the reverse would be in accord with the experiment, again pointing to some deficiencies of the PES. More theoretical work is clearly needed, as also suggested by a recent three-dimensional quantum dynamics study.<sup>1</sup>

## References

- 1) T. Peng, D.H. Zhang, J.Z.H. Zhang, and R. Schinke, *Chem. Phys. Lett.* **248**, 37 (1996), and references therein.
- 2) M. Alagia, N. Balucani, P. Casavecchia, D. Stranges, and G.G. Volpi, *J. Chem. Soc. Faraday Trans. (Faraday Research Article)* **91**, 575-596 (1995); P. Casavecchia, N. Balucani, and G.G. Volpi in: *Advanced Series in Physical Chemistry - Vol. 6, The Chemical Dynamics and Kinetics of Small Radicals*, eds. K. Liu and A. Wagner (World Scientific, Singapore, 1995), ch. 9.
- 3) R.J. Buss, P. Casavecchia, T. Hirooka, S.J. Sibener, and Y.T. Lee, *Chem. Phys. Lett.* **82**, 386 (1981).
- 4) D.-C. Che and K. Liu, *J. Chem. Phys.* **103**, 5164 (1995).
- 5) P.J. Kuntz, B.I. Niefer, and J.J. Sloan, *J. Chem. Phys.* **88**, 3629 (1988).
- 6) K. Mikulecky and K.-H. Gericke, *J. Chem. Phys.* **96**, 7490 (1992), and refs. therein.
- 7) Y. Yuang, Y. Gu, C. Liu, X. Yang, and Y. Tao, *Chem. Phys. Lett.* **127**, 432 (1986).
- 8) P.M. Aker and J.J. Sloan, *J. Chem. Phys.* **85**, 142 (1986).
- 9) S.P. Walch and L.B. Harding, *J. Chem. Phys.* **88**, 7653 (1988).

# MOLECULAR BEAM STUDIES ON THE DYNAMICS OF BIMOLECULAR REACTIONS OF ATOMIC NITROGEN: $N(^2D) + D_2$ AND $N(^2D) + C_2H_2$

M. Alagia, N. Balucani, L. Cartechini, P. Casavecchia, E.H. van Kleef, and G.G. Volpi  
*Dipartimento di Chimica, Università di Perugia, 06100 Perugia, Italy*

Despite extensive literature on gas-phase reactions of "active nitrogen", there appear to be no experimental studies on the dynamics of N-atom reactions under single collision conditions.

Here, we report on the first dynamical investigation of bimolecular N-atom reactions, in which product angular and velocity distributions are measured by using a high resolution crossed beam apparatus with rotatable mass spectrometric detector.<sup>2</sup> Continuous supersonic beams of N atoms are generated by radio-frequency discharge in high pressure (300–400 mbar)  $N_2$ /rare gas mixtures through a water cooled quartz nozzle (250  $\mu$ m diameter). By using 2.5%  $N_2/He$ , Ne mixtures, dissociation fractions larger than 60% and velocity spreads of about 20% are attained. The beams are characterized by Stern-Gerlach magnetic analysis<sup>3</sup>: 75% of the N atoms are found in the ground  $^4S$  electronic state and 25% in the first excited  $^2D$  and  $^2P$  states (lying 2.39 eV and 3.56 eV, respectively, above the ground state) with relative population of 3:1.

The first reaction we have looked at is that with acetylene leading to HCCN + H. The reactions of N atoms with hydrocarbons are significant in a wide variety of systems, including the chemistry of the atmospheres of Titan and Neptune, nitrogen chemistry in hydrocarbon combustion, the chemistry of interstellar and circumstellar clouds and laboratory studies of the reactions of hydrocarbons with "active nitrogen". The HCCN (cyanomethylene or cyanocarbene) radical represents the first step in the formation of nitriles in many environments, from combustion to interplanetary chemistry, and has attracted much experimental and theoretical attention over the years.<sup>4</sup> According to very recent theoretical calculations,<sup>5</sup> the reaction of  $N(^4S)$  with acetylene is nearly thermoneutral:



The room temperature rate constant for the  $N(^4S)$  reaction is reported<sup>6</sup> to be very small ( $k_{298} \sim 10^{-16}$  cc molec<sup>-1</sup>s<sup>-1</sup>), which points to a high activation energy. The reaction of acetylene with  $N(^2D)$  is instead strongly exoergic:

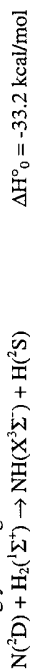


and is expected to proceed with much larger cross section. Recently, formation of the HCCN radical from this reaction has been suggested<sup>7</sup> to be the first step in the formation of cyanogen, dicyanogen, HCN, etc., in the atmosphere of Titan. Since  $N(^4S)$  is well known to be characterized by a low reactivity, many reactive processes in various environments leading to N-containing compounds may well be due to reactions of  $N(^2D)$ . The possible reaction of  $N(^2P)$  is expected to be slow on the basis of simple

adiabatic electronic energy correlation diagrams, with physical quenching being the most probable process.

From angular and velocity distribution measurements of the HCCN product we conclude that cyanomethylene formation arises from the reaction of  $C_2H_2$  with  $N(^2D)$ . At the collision energies of 3.1 kcal/mol and 9.5 kcal/mol the reaction is found to proceed through a long-lived complex and an osculating complex, respectively. The product energy partitioning is determined, and the lifetime of the intermediate cyanomethyl ( $H_2CCN$ ) radical is estimated.

The reaction of ground state atomic nitrogen with molecular hydrogen is considerably endoergic ( $\Delta H^\circ_0 = 21.7$  kcal/mol), while that of electronically excited  $N(^2D)$  is strongly exoergic:



We have measured angular and velocity distributions of the NO product from the isotopic variant  $N(^2D) + D_2$  at  $E_c = 5.1$  kcal/mol and determined angular and translational energy distributions in the center-of-mass frame. The reaction is found to proceed by direct insertion via the ground state  $^2B_1$  potential surface of the  $NH_2$  radical. The results are compared with those of the similar reaction  $O(^1D) + D_2$  studied at the comparable  $E_c$  of 5.3 kcal/mol and which is known to proceed by a direct path via the  $^1A_1$  surface of  $H_2O$ ; considerable differences are found. The  $N(^2D) + H_2$  reaction is sufficiently simple to be amenable to theoretical treatment; indeed, very recently, potential energy surfaces for the ground and excited states of  $NH_2$  have been calculated by van Hemert *et al.*<sup>8</sup>, which should allow in the near future reaction dynamics calculations.

## References

- 1) A.N. Wright and C.A. Winkler, *Active Nitrogen*, Academic Press, N.Y. (1968).
- 2) M. Alagia, N. Balucani, P. Casavecchia, D. Stranges, and G.G. Volpi, *J. Chem. Soc. Faraday Trans. (Faraday Research Article)* **91**, 575 (1995).
- 3) B. Brunetti, G. Liuti, F. Pirani, E. Luzzatti, *Chem. Phys. Lett.* **84**, 201 (1981).
- 4) M.C. McCarthy, C.A. Gottlieb, A.L. Cooksy, and P. Thaddeus, *J. Chem. Phys.* **103**, 7779 (1995), and references therein; N. Goldberg, A. Fiedler, and H. Schwarz, *J. Phys. Chem.* **99**, 15327 (1995), and references therein.
- 5) J.S. Francisco, *Chem. Phys. Lett.* **231**, 372 (1994), and references therein.
- 6) D.A. Safrany and W. Jaster, *J. Phys. Chem.* **72**, 3305 (1968); J.V. Michael, *Chem. Phys. Lett.* **76** (129) 1980.
- 7) Y.L. Yung, *Icarus* **72**, 468 (1987).
- 8) M.C. van Hemert, R. Vetter, G.J. Kroes, and E.F. van Dishoeck, in: *IAU Symposium 178 "Molecules in Astrophysics, Probes and Processes"*, Leiden 1-5 July 1996, Book of Abstracts, p. 190.

# DYNAMICS OF THE HYDROGEN EXCHANGE REACTIONS $H + D_2$ AND $H + D_2O$

R.A. Brownsword, M. Hillenkamp, T. Laurent, R.K. Vatsa,  
H.-R. Volpp & J. Wolfrum

*Physikalisch-Chemisches Institut der Universität Heidelberg,  
Im Neuenheimer Feld 253, 69120 Heidelberg, Germany*

The collision dynamics of the atom exchange reactions of  $H + D_2$  and  $H + D_2O$  have been studied at well-defined translational energies by H and D atom vacuum ultraviolet laser-induced fluorescence. H atoms were generated by excimer laser photolysis at 248 or 193 nm of  $H_2S$  or  $HCl$ , at corresponding centre-of-mass translational energies of 0.87, 1.55 and 1.97 eV for  $H + D_2$  and 2.20 eV for  $H + D_2O$ . VUV probe laser radiation was generated by sum-frequency mixing in a Kr/Ar mixture, and could be tuned over the range 121.5 - 121.6 nm to record Doppler LIF spectra of both H and D atoms under single-collision conditions.

Calibration of the D atom LIF signal against the photolytically produced H atom signal allowed the absolute reactive cross-sections  $\sigma$  for the two title reactions to be determined. Doppler profiles were recorded for different geometries of photolysis laser electric vector  $E$  and probe laser propagation direction  $k$ , from which the average energy released into translation,  $\langle E_T \rangle$ , could be calculated via the second moment of the D atom laboratory velocity distribution. The following values for  $\sigma$  and  $\langle E_T \rangle$  were obtained:

	$E_{cm} / \text{eV}$	$\sigma / \text{\AA}^2$	$\langle E_T \rangle$
$H + D_2 \rightarrow HD + D$	0.87	$0.97 \pm 0.11$	$0.86 \pm 0.12$
	1.55	$1.23 \pm 0.32$	$0.47 \pm 0.06$
	1.97	$1.31 \pm 0.26$	$0.55 \pm 0.04$
$H + D_2O \rightarrow HOD + D$	2.20	$0.36 \pm 0.15$	$0.58 \pm 0.09$

The absolute reaction cross-section data for  $H + D_2$  are in good agreement with the most recent previous measurements on this system. The translational energy release data are consistent with previous results obtained in the 1.0 - 1.3 eV range and show a pronounced decrease with increasing collision energy. This behaviour is predicted theoretically and may be due to the operation of a less "direct" atom exchange mechanism operating at higher energies. Direct comparison of the  $H + D_2O$  results with theory is not yet possible, but values of  $\sigma = 0.65 \text{ \AA}^2$  and  $\langle E_T \rangle = 0.6$  have been obtained from QCT studies of the  $H + H_2O$  system. Theoretical studies of the  $H + D_2O$  reaction are desirable in order to make detailed comparison with experiment in this prototypical four-atom reactive system.

# CHEMILUMINESCENCE AND PRODUCT ROTATIONAL POLARISATION IN $Mn + O_2 \rightarrow MnO^*(A^6\Pi, A^6\Sigma^+) + O$

Matthew A Spence and Martin R Levy  
*Department of Chemical and Life Sciences, University of Northumbria  
Ellison Place, Newcastle upon Tyne NE1 8ST, UK.*

The  $MnO(A^6\Sigma^+ \rightarrow X^6\Sigma^+)$  band system is well known, and was observed some time ago in this laboratory as chemiluminescence, at  $\lambda > 570$  nm, from  $Mn + O_2$ ,  $NO_2$ ,  $CO_2$ ,  $SO_2$  and  $N_2O$  [1,2]. Reinvestigations now indicate that, in all cases, the emission extends well into the infra-red, ie beyond the known range of the  $A^6\Sigma^+ \rightarrow X^6\Sigma^+$  system. Translational excitation functions measured in the red (570-690 nm) and infra-red (780-900 nm) regions show different functionalities, with lower thresholds in the IR. In addition, the latter emission is found to be preferentially polarised *perpendicular* to the initial relative velocity vector  $k$ , while the former is *parallel* polarised. This suggests the presence of a lower-lying, previously unknown, emitting  $MnO^*(A^6\Pi)$  state.

In this report we concentrate on the results for  $Mn + O_2$ . As before, the reaction has been studied by means of a laser-ablated beam of Mn atoms, of wide velocity range and containing several metastable states ( $a^6D$ ,  $z^6P$ ,  $a^4D$ , ...) in addition to the ground state ( $a^6S$ ). A time-of-flight technique has been employed to determine the excitation functions  $\sigma(E_T)$ , where  $E_T$  = the nominal collision energy in the beam-gas configuration. To measure the polarisation of the chemiluminescence, and its energy dependence, the Earth's magnetic field has been excluded by means of 3 mutually orthogonal pairs of Helmholtz coils.

The excitation functions, in the range  $E_T = 0-1500 \text{ kJ mol}^{-1}$ , have been analysed by means of the multiple line-of-centres approach [3],

$$Y(E_T) = E_T \sigma(E_T) = \sum \sigma_k (E_T - E_k),$$

where  $k = 0, 1, 2, 3, \dots$ ,  $\sigma_k$  can be positive or negative, and each term only contributes from its threshold  $E_k$ . In contrast to the earlier measurements [2],  $Y(E_T)$  is now found for both channels to be composed of several linear processes, albeit with threshold curvature due to the collision energy spread at each nominal  $E_T$ . The parameters  $\sigma_k$  and  $E_k$  are obtained by non-linear least-squares regression.

For the IR emission, the  $\sigma_k$  values imply two separate processes with initial thresholds  $\sim 46$  and  $\sim 187 \text{ kJ mol}^{-1}$ . From the energetics, these are identified as due to reaction of the  $a^4D$  and  $a^6D$  states of Mn respectively. In both of these channels,  $-\sigma_1 \gg \sigma_0$ , indicating the presence of a *forward transition state shift* with increasing collision energy. The  $E_T$  value at which this shift occurs,  $E_s$ , is estimated tentatively from the derived parameters to be  $\sim 379$  and  $\sim 279 \text{ kJ mol}^{-1}$  respectively.

The red yield function consists of rather more linear sections, and its  $\sigma_k$  values can only be satisfactorily separated into 4 separate processes. The initial thresholds,  $\sim 49$ ,  $109$ ,  $203$  and  $264 \text{ kJ mol}^{-1}$ , appear to derive from reaction of  $a^4D$ ,  $z^6P$ ,  $a^6D$  and  $a^6D$  atoms respectively.

The three highest threshold processes, at least, again show significant forward shifts in the reaction transition state with increasing collision energy.

The polarisation of the  $\text{MnO}^*(\text{A}^6\Sigma^+ \rightarrow \text{X}^6\Sigma^+)$  emission is readily analysed to yield  $\langle P_2(\hat{j}' \cdot \hat{k}) \rangle$ , the mean value of the second moment of the Legendre expansion of the correlation between  $\mathbf{k}$  and the  $\text{MnO}^*$  rotational angular momentum  $\mathbf{j}'$ . For the  $\text{A}^6\Pi \rightarrow \text{X}^6\Sigma^+$  system, the derived values of  $\langle P_2(\hat{j}' \cdot \hat{k}) \rangle$  are not unique, depending on the Hund's coupling case which applies. Nonetheless, the trend with collision energy remains the same.

Both band systems display a sharp increase in  $\langle P_2(\hat{j}' \cdot \hat{k}) \rangle$  corresponding to onset of  $\text{Mn}^*(\text{a}^6\text{D}_J)$  reaction. Below this threshold, the small signal level of the  $\text{z}^8\text{P}_J$  and/or  $\text{a}^4\text{D}_J$  processes gives rise to considerable noise on the data; but it is clear that  $\langle P_2(\hat{j}' \cdot \hat{k}) \rangle$  is essentially zero. However, as collision energy increases above the  $\text{a}^6\text{D}_J$  threshold, the sharp rise in  $\langle P_2(\hat{j}' \cdot \hat{k}) \rangle$  is followed by a rapid fall, and then a slow increase to higher energies still.

These results suggest that, at collision energies in the threshold region, the  $\text{Mn}^*(\text{a}^6\text{D}_J)$  reaction occurs in a plane which contains  $\mathbf{k}$ , so that  $\mathbf{j}'$  tends to be oriented at right angles thereto. The sharp rise originates predominantly from the increasing proportion of this channel relative to the total observed signal. The subsequent fall however indicates the opening up, to wider impact parameters as collision energy increases, of reaction configurations which do not contain  $\mathbf{k}$ .

For each emission band system, the energy at which the slow, high energy rise in  $\langle P_2(\hat{j}' \cdot \hat{k}) \rangle$  begins is close to the derived value(s) of  $E_0$  for the  $\text{a}^6\text{D}_J$  reaction. We believe this to be the first corroborative evidence that a transition state shift is indeed occurring, and is accompanied by a change in dynamics. The slow rise is entirely consistent with competition between a shifted process, with high  $\langle P_2(\hat{j}' \cdot \hat{k}) \rangle$  at low impact parameters, and the unshifted process, with low  $\langle P_2(\hat{j}' \cdot \hat{k}) \rangle$ , at high impact parameters.

As in other Mn atom reactions [4,5], the forward shift suggests an initial transition state located in the exit valley, and may reflect the influence of ionic-covalent curve crossings. With increasing collision energy, there may be insufficient time for the  $\text{O}_2$  to stretch to the equilibrium  $\text{O}_2^-$  distance, so that the vertical electron affinity, rather than the adiabatic value, becomes more important. The more repulsive interaction is then likely to lead to a stronger correlation of  $\mathbf{j}'$  perpendicular to  $\mathbf{k}$ .

## References

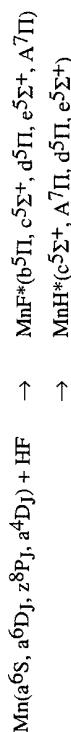
1. M R Levy, *J. Phys. Chem.* **93**, 5195 (1989).
2. M R Levy, *J. Phys. Chem.* **95**, 8491 (1991).
3. M R Levy, *Research Chem. Kinetics* **1**, 163 (1993).
4. D A Newnham and M R Levy, *J. Phys. Chem.* **100**, 2799 (1996).
5. D L Herbertson and M R Levy, *J. Phys. Chem.* **100**, 2809 (1996).

## MnF AND MnH CHEMILUMINESCENCE IN THE REACTION $\text{Mn} + \text{HF}$

Timothy J Hughes and Martin R Levy

*Department of Chemical and Life Sciences, University of Northumbria  
Ellison Place, Newcastle upon Tyne NE1 8ST, UK.*

A pulsed, laser-ablated beam of Mn atoms in different long-lived states has been employed to investigate the production of chemiluminescence in the competing reactions



Translational excitation functions  $\sigma(E_T^0)$  ( $E_T^0$  = nominal collision energy in the beam-gas configuration) have been measured in a number of spectral regions:

$\lambda/\text{nm}$	MnF system expected	MnH system expected
> 780 (IR)	$\text{b}^5\Pi \rightarrow \text{a}^5\Sigma^+$	$\text{c}^5\Sigma^+ \rightarrow \text{a}^5\Sigma^+$
590-690 (red)	$\text{c}^5\Sigma^+ \rightarrow \text{a}^5\Sigma^+$	weak $\text{A}^7\Pi \rightarrow \text{X}^7\Sigma^+$
570-620 (orange)	weak $\text{c}^5\Sigma^+ \rightarrow \text{a}^5\Sigma^+$	$\text{A}^7\Pi \rightarrow \text{X}^7\Sigma^+$
490-510 (green)	$\text{d}^5\Pi \rightarrow \text{a}^5\Sigma^+/\text{X}^7\Sigma^+$	weak $\text{d}^5\Pi \rightarrow \text{a}^5\Sigma^+$
417-470 (blue)	$\text{e}^5\Sigma^+ \rightarrow \text{a}^5\Sigma^+$	$\text{e}^5\Sigma^+ \rightarrow \text{a}^5\Sigma^+$
330-380 (UV)	$\text{A}^7\Pi \rightarrow \text{X}^7\Sigma^+$	--

Although the MnF and MnH systems overlap, the different endothermicities of the completely ground state reactions, respectively  $\sim 144$  and  $\sim 436$  kJ mol $^{-1}$ , allow the emitting species to be identified.

The IR, red, orange and green results have been successfully analysed by means of the multiple line of centres model [1],

$$Y(E_T) = E_T \cdot \sigma(E_T) \sim \sum \alpha_k (E_T - E_k),$$

where  $k = 0, 1, 2, 3, \dots$ ,  $\alpha_k$  can be positive or negative, and each term only contributes from its threshold  $E_k$ .

In the IR region, the data indicate 3 separate  $\text{MnF}^*(\text{b}^5\Pi)$  production processes, without any significant contribution from  $\text{MnH}^*(\text{c}^5\Sigma^+)$ . The Mn reagent states responsible are the metastable levels  $\text{a}^4\text{D}_J$  and  $\text{a}^6\text{D}_J$ , the latter giving rise to the two dominant, higher energy processes. With increasing collision energy, both of these  $\text{a}^6\text{D}_J$  processes appear to be accompanied by forward transition state shifts,  $\sim 15\%$  and 26% respectively, before the onset of depletion.

Similar  $\text{MnF}^*(\text{c}^5\Sigma^+)$  behaviour appears to be occurring in the red region. However, here the transition state shifts are not so easily extracted. Measurements in the orange

## RELAXATION KINETICS IN EXCITED CH/CD

M.A. Blitz, M. Pesa, M.J. Pilling and P.W. Seakins.  
*School of Chemistry, University of Leeds, Leeds. LS2 9JT.*

## Introduction

CH( $^2\Pi$ ) kinetic studies have generally used photolytic sources of CH, eg. CHBr<sub>3</sub>. The generated CH is formed initially electronically, vibrationally and rotationally excited. The rotational and doublet electronic excited states will rapidly relax to the ground-state. However, the vibrational states have appreciable lifetimes. While ideally CH kinetics should be performed when all the degrees of freedom are thermalized, this study involves the monitoring of the CH ground-electronic vibrational states in order to ascertain if vibrational relaxation may affect CH chemical kinetics.

## Experimental

Typically 0.7 mTorr of bromoform/deuterated bromoform was photolysed using ca. 100 mJ/pulse of 248 nm light. The excited CH/CD was monitored ( $v=0,1,2$ ) using laser induced fluorescence; scanning the delay between the pump and probe to map out time profiles of the states. The buffer gas, Ar and He, was varied between 5-120 Torr and the temperature varied between 295-468 K.

## Results

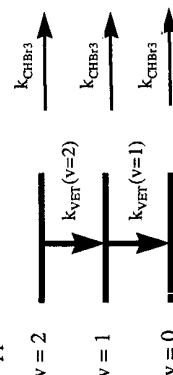
The CH/CD( $v=0$ ) data was characterised by an early time gain followed by loss. This behaviour also described the CH/CD( $v=1,2$ ) data but the gain was more ill defined in these cases. Initially the traces were fitted to the general loss and gain equation:

$$[\text{CH}(v=0,1,2)]_t = A e^{-Bt} - C e^{-Dt}$$

For CH/CD( $v=0$ ) the loss parameter, B, represented the rate constant for the reaction of CH/CD( $v=0$ ) with bromoform; this was independent of total pressure.

For the  $v=1,2$  states the B parameter was pressure dependent. This pressure dependence represents the quenching of the vibrational state; rate constant for vibrational energy transfer,  $k_{\text{VET}}$ .

As a first approximation the scheme:



was considered to explain the data. All the traces were simultaneously fitted to this scheme. This scheme failed to balance the observed CH/CD concentrations in the

region indicate that, for at least one of the  $a^6D_J$  processes, product vibrational excitation increases with rising collision energy. In addition there seems to be some emission from  $\text{MnH}^*(A^7\Pi)$ , the threshold indicating that  $\text{Mn}^*(a^6D_J)$  is again the precursor.

In the green region, the emission appears to derive from  $\text{MnF}^*(d^5\Pi)$ , formed via single  $a^4D_J$  and  $a^6D_J$  processes, plus a high energy contribution from  $\text{MnH}^*(d^5\Pi)$ . The blue and UV data display quite a different functionality: the predominant process in each case follows an initial dependence

$$Y(E_T) = \sigma_0(E_T - E_0)^2,$$

over wide energy range, before going over to the multilinear form. Such behaviour is explained by microcanonical transition state theory [2] as originating from the participation of two, rather than one, vibrational mode at the critical transition state - ie there appears to be a somewhat attractive, long-lived interaction. The thresholds indicate that the emitting species are  $\text{MnF}^*(e^5\Sigma^+, A^7\Pi)$ , and that for each the reagent state is  $\text{Mn}^*(a^4D_J)$ . In the  $A^7\Pi$  case, this is a particularly surprising result, as a quartet-sextet spin change must be occurring.

The observation of forward transition state shifts for formation of the lower  $\text{MnF}^*$  states suggests that ionic-covalent curve crossings may play a role in this reaction [3-5]. For production of the two highest states, however, an alternative explanation may apply. Since both the  $a^6D_J$  and  $a^4D_J$  states of Mn have the same  $\dots 3d^6 4s^1$  configuration, the greater degree of attraction shown by the more excited  $a^4D_J$  state may result from 3d-4s hybridisation involving electrons of opposite spin [5-7]. This would allow one empty sd hybrid to point towards the HF, with the filled hybrid pointing in the opposite direction. Such a mechanism is impossible in  $\text{Mn}(a^6D_J) + \text{HF}$ , as all the unpaired 3d electrons have the same spin as the single 4s electron; a more repulsive interaction would therefore be anticipated.

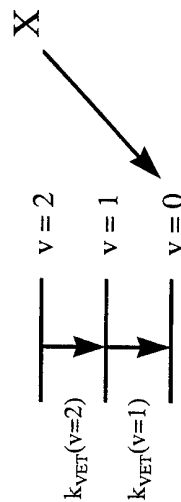
## References

1. M R Levy, *Research Chem. Kinetics* **1**, 163 (1993).
2. A González Ureña, *Mol. Phys.* **52**, 1145 (1984).
3. D A Newnham and M R Levy, *J. Phys. Chem.* **100**, 2799 (1996).
4. D L Herbertson and M R Levy, *J. Phys. Chem.* **100**, 2809 (1996).
5. D L Herbertson and M R Levy, *J. Phys. Chem.* **100**, in press (1996).
6. M R A Blomberg, U B Brandemark, P E M Siegbahn, K B Mathisen and G Karlström, *J. Phys. Chem.* **89**, 2171 (1985).
7. C W Bauschlicher Jr, P S Bagus, C J Nelin and B O Roos, *J. Chem. Phys.* **85**, 354 (1986)

system; gain terms predicted larger concentrations of CH/CD than were observed. Also gain terms predicted different rate constants to the upper level loss terms.

The above mechanism requires an additional gain of CH/CD to the system; certainly for the  $v=0$  level.

#### Extended Mechanism



This scheme now balances the observed loss and gain; the CH/CD concentrations balance and rate constants are consistent. Analysing the above scheme using simultaneous fitting to all traces generated  $k_{\text{VET}}$  consistent with the results of the general loss and gain equation. Typically the  $[\text{CH}(v=1)]$  was 10–20% of  $[\text{CH}(v=0)]$ . The concentration of X was consistently larger than  $[\text{CH}(v=1)]$  but not as well defined. The X species is best coupled to the CH/CD( $v=0$ ) via a pressure independent mechanism; based on  $X^2$  and more consistent  $k_{\text{VET}}$ . X cannot be impurities in the buffer gas. A tentative speculation is that X is the CH/CD (a  $\Sigma^+$ ) state. X is coupled to CH/CD( $v=0$ ) with a rate constant ca.  $2 \times 10^{-4} \text{ s}^{-1}$ ; this is consistent with a spin forbidden transition.

## RESULTS

	T/K	$k_{\text{VET}(v=1)}/10^{-14} \text{ cm}^3 \text{ s}^{-1}$	$k_{\text{VET}(v=2)}/10^{-14} \text{ cm}^3 \text{ s}^{-1}$	$X/10^{-4} \text{ s}^{-1}$
CH-Ar	295	3.3	4.4	2.3
	383	4.2	6.0	1.7
CH-He	468	5.8	8.3	5.7
	295	0.7	1.2	1.0
CD-He	383	1.7	2.7	1.4
	468	2.2	4.6	6.5
CD-Ar	295	0.2	-	2.2
	383	0.7	-	2.6
CD-Ar	468	1.2	-	2.2
	295	0.4	-	3.6
	383	0.6	-	1.5

## Conclusions

The CH/CD( $v=0$ ) has gain terms that are consistent with vibrational energy transfer and also a species that is coupled pressure independently to it. Both these gain terms can occur on the time scale of CH/CD chemical kinetics. Therefore CH/CD kinetics, especially pressure dependent determinations, should model the gain as well as the loss in order to determine the best rate parameters for CH reactions.

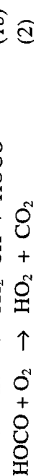
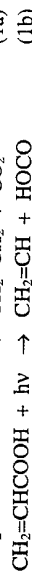
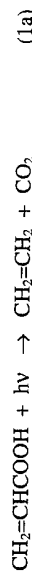
# STATE-SPECIFIC PRODUCT YIELDS USING INFRARED DIODE LASER SPECTROSCOPY: $\text{CO}_2$ PRODUCED IN THE PHOTOLYSIS OF ACRYLIC ACID AND THE REACTION: $\text{O}_2 + \text{HOCO} \rightarrow \text{CO}_2 + \text{HO}_2$

Michael Osborne and Ian W.M. Smith

School of Chemistry, The University of Birmingham, Edgbaston, Birmingham B15 2TT

Using diode lasers tunable in the range 1800–2400  $\text{cm}^{-1}$ , time-resolved experiments which employ kinetic infrared absorption spectroscopy are being performed to monitor the chemical products and the product states of chemical and photochemical reactions. The reactions are initiated by flash photolysis and in each experiment a record of transmitted intensity is obtained with the diode tuned to the frequency of an absorption in the infrared spectrum of a reagent or product of the reaction.

Here we shall describe experiments in which acrylic acid ( $\text{CH}_2=\text{CHCOOH}$ ) is photolysed by a broad band flashlamp in the absence and presence of  $\text{O}_2$ . The recorded traces of absorption *versus* time show that there are two sources of  $\text{CO}_2$ , one which is 'prompt' on the time resolution of our experiments and which is present whether or not  $\text{O}_2$  is present. Clearly it arises directly from photolysis of the acrylic acid. In addition,  $\text{CO}_2$  is formed in a slower secondary process. These observations are consistent with a mechanism which involves competitive photochemical channels which produce (a)  $\text{CH}_2=\text{CH}_2 + \text{CO}_2$  and (b)  $\text{CH}_2=\text{CH} + \text{HOCO}$ , followed by the reaction of HOCO with  $\text{O}_2$  when  $\text{O}_2$  is present.



By comparing the strength of absorption signals at short delays in the absence of  $\text{O}_2$  and in the presence ca. 1 Torr of  $\text{O}_2$ , it is possible to measure the branching ratio for the two channels (1a) and (1b) for photolysis of  $\text{CH}_2=\text{CHCOOH}$ . Preliminary results suggest that this ratio is close to unity. In addition, we shall report measurements of:

- (a) the rate constant for reaction (2), derived from observing the time-dependence of the 'non-prompt'  $\text{CO}_2$  absorption signals, and
- (b) the vibrational state distributions of  $\text{CO}_2$  produced in the photochemical channel (1) and in the reaction of HOCO with  $\text{O}_2$ .

Preliminary results indicate that the rate constant for (2b) is close to the value of  $1.9 \times 10^{12} \text{ cm}^3 \text{ molecule}^{-1} \text{ s}^{-1}$  reported by Petty, Harrison and Moore<sup>1</sup> and, surprisingly, that the  $\text{CO}_2$  formed in both processes is quite 'cold' vibrationally, as in the  $\text{OH} + \text{CO}$  reaction.<sup>2</sup>

<sup>1</sup> J.T. Petty, J.A. Harrison and C.B. Moore, *J. Phys. Chem.* **97**, 11194 (1993).

<sup>2</sup> M.J. Frost, P. Sharkey and I.W.M. Smith, *Farad. Discuss. Chem. Soc.* **91**, 305 (1991)

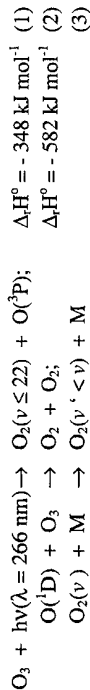
# THE CHEMICAL AND PHOTOCHEMICAL FORMATION AND RELAXATION OF VIBRATIONALLY EXCITED OXYGEN FOLLOWING THE PHOTOLYSIS OF OZONE AT 266 nm

Ian W.M. Smith, Andrew C. Symonds, Richard P. Tuckett and Gary N. Ward

*School of Chemistry, The University of Birmingham, Edgbaston, Birmingham B15 2TT, U.K.*

There is intense interest in the formation and relaxation of  $O_2$  following the proposal that vibrationally excited  $O_2$  might participate in the production of  $O_3$  in the upper atmosphere. Although the major channel in the photodissociation of  $O_3$  between 200 and 300 nm produces  $O_2(^1\Delta_g) + O(^1D)$ , ca. 10% of the products are  $O_2(^3\Sigma_g^-) + O(^3P)$ , with the  $O_2$  being produced in vibrational levels ( $v \leq 22$ ).

In this poster, a description will be given of experiments on the formation and relaxation of vibrationally excited  $O_2$  in and following the photolysis of  $O_3$  at 266 nm:



In our experiments,  $O_3$  is photolysed at 266 nm.  $O_2$  in specific vibrational levels is then observed via laser-induced fluorescence in the  $(0,v)$  bands of the  $B^3\Sigma_u^- - X^3\Sigma_g^-$  system.

Experiments have been performed with different concentrations of  $N_2$  present. With  $[N_2]$  small or zero, highly excited  $O_2$  is formed principally in reaction (2) and we shall report the distribution between  $v = 18$  and 23. With a large excess of  $N_2$  present ( $[N_2]:[O_3] = 3000$ ), the  $O(^1D)$  atoms are quenched rather than undergo reaction (2). In this case, vibrationally excited  $O_2$  is only formed in the photochemical step (1) up to  $v = 22$ .

We shall report the relative  $O_2$  vibrational populations in levels close to this energetic limit and the relaxation rates for  $O_2(v = 21)$  and  $O_2(v = 22)$  with  $M = O_2, N_2, NO_2, CO_2, N_2O, CH_4$  and He. Our results will be compared with those from the related investigations of Slinger,<sup>1</sup> Wodtke<sup>2</sup> and Houston<sup>3</sup> and their co-workers, as well as with the relaxation rates that we have measured previously for  $O_2(v = 8-11)$ .<sup>4</sup>

<sup>1</sup> H. Park and T.G. Slinger, *J. Chem. Phys.*, **100**, 287 (1994).

<sup>2</sup> (a) C.A. Rogaski, J.A. Mack and A.M. Wodtke, *Farad. Discuss. Chem. Soc.* **100**, 229 (1995); (b) J.A. Mack, K. Mikulecky and A.M. Wodtke, in press (1996).

<sup>3</sup> R.L. Miller, A.G. Suits, P.L. Houston, R. Toumi, J.A. Mack and A.M. Wodtke, *Science*, **265**, 1831 (1994).

<sup>4</sup> M. Klatt, I.W.M. Smith, R.P. Tuckett and G.N. Ward, *Chem. Phys. Lett.*, **224**, 253 (1994).

# RATES OF RADICAL-RADICAL REACTIONS MEASURED BY ULTRAVIOLET CAVITY RING-DOWN ABSORPTION SPECTROSCOPY

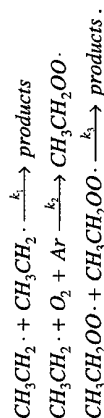
Dean B. Atkinson and Jeffrey W. Hudgens

*Physical and Chemical Properties Division  
Chemical Science and Technology Laboratory  
National Institute of Standards and Technology  
Gaithersburg, MD 20899 USA*

Tel. 301-975-2512 and Fax: 301-975-3672

E-mail: [Hudgens@enh.nist.gov](mailto:Hudgens@enh.nist.gov)

In this study we report the use of cavity ring-down spectroscopy for measurements of self-reaction rates of ethyl and ethylperoxy radicals and the reaction rate of ethyl radicals and oxygen:



The purpose of these experiments is to validate the use of cavity ring-down spectroscopy (CRDS) as a tool for measuring free radical kinetics. The few previous studies that have used CRDS detection have not examined reactions with known rate constants. In the present chemical system the rate constants  $k_1$  and  $k_2$  are well-known at 300K. CRDS can measure absolute free radical concentrations with great sensitivity. This is important because free radical kinetic studies are very susceptible to interference from side-reactions, which can be minimized by keeping the radical concentrations low. These experiments are also the first to use CRDS to measure rate coefficients in the ultraviolet spectrum. Because most organic radicals have strong ultraviolet absorptions, this paper may encourage more widespread use of this technique.

In our experimental apparatus a resonant cavity is constructed from two high reflectivity ( $R=99.8+\%$ ) mirrors. Frequency doubled light from a tunable pulsed dye laser ( $\Delta t \sim 20$  nsec) is injected into the cavity through the center of one mirror. Behind the second mirror we place a high-speed photomultiplier to monitor the transmitted light. Within the empty cavity the injected light decays exponentially with a rate determined predominantly by the mirror reflectivity. Absorbance is determined by measuring the decrease in cavity ring-down time induced by absorbing radicals. We can easily observe 1% reductions of ring-down times with moderate signal averaging. The empty cavity ring-down times (1/e time) for our mirrors at 220 nm and 270 nm are approximately 400 and 800 nsec, respectively. These ring-down times translate into base sensitivities for absorbance of 80 and 40 ppm, respectively.

Our rate constant measurements are based upon absorbance measurements of ethyl and ethylperoxy radical concentrations at 220 nm and 270 nm, respectively. The ring-

down cavity encompasses a slow-flow laser flash-photolysis reactor. In the reactor a XeCl excimer laser beam (308 nm, 20 nsec) crosses the ring-down cavity axis at right angles and photolyzes Cl<sub>2</sub> to produce Cl atoms. The Cl atoms react with excess ethane to produce ethyl radicals. This configuration produces a well-defined reaction zone and a well-defined absorption pathlength for the CRDS measurements, enabling determinations of absolute radical concentrations.

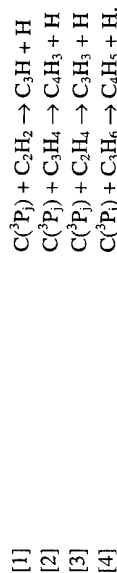
The ethyl radical self-reaction rate coefficient was measured at 300 K and 665 Pa (5 torr),  $k_1 = 2 \times 10^{11} \text{ cm}^3 \text{ sec}^{-1}$ . As expected, this rate constant agrees well with previous measurements of  $k_1$  obtained at higher pressures. A second set of experiments, also at 300 K, enabled determinations of the association rate coefficient,  $k_2$ , and the self-reaction rate constant of ethylperoxy radicals,  $k_3$ .

# CROSSED BEAM REACTION OF CARBON ATOMS WITH UNSATURATED HYDROCARBONS: CARBON-HYDROGEN EXCHANGE AS A MEANS TO BUILD UP CARBON-BEARING SPECIES

R.I. Kaiser, Y. T. Lee, and A. G. Suits

*Chemical Sciences Division  
Lawrence Berkeley National Laboratory  
Berkeley, CA 94720, USA*

Crossed beam reaction of ground state carbon atoms with a variety of unsaturated hydrocarbon molecules have been studied under well-defined conditions, yielding full double-differential cross sections. The following carbon atom reactions were studied at collision energies between 8 and 120 kJmol<sup>-1</sup>:



The carbon-hydrogen exchange channels dominate the reactively scattered products. The crossed beam method allows insight into the dynamics of the reaction and reveals additional information on the reaction intermediate and product isomers when the observed dynamics are compared to what is expected based on energetics and ab initio calculations.

Reaction [1] proceeds through a short-lived C<sub>3</sub>H<sub>2</sub> trans propenediylidene complex (1) on the triplet surface. (1) undergoes rearrangement to vinylideneacetylene and cyclopropenylidene or propargylene, followed by a nearly simple bond rupture via a symmetric transition state to 1-C<sub>3</sub>H with an exit barrier of about 5-8 kJmol<sup>-1</sup>. A second exit channel passes an asymmetric transition state and is quenched with increasing collision energy. The identification of the C<sub>3</sub>H isomer in this channel is under investigation. Substitution of a H atom by a methyl group [2] leads to a long-lived C<sub>4</sub>H<sub>4</sub> complex stabilized by the additional vibration modes of the CH<sub>3</sub> group. Its decomposition leads to butenynyl (1) or butatrienyl radicals.

Reaction (3) involves two distinct microchannels, both initiated by attack of the carbon atom on the ethylene π-orbital via a loose, reactant-like transition state located at the centrifugal barrier. One involves the excitation of C-axis rotations of the cyclopropenyl complex, followed by ring opening to triplet allene, followed by H atom emission to yield the ground state propargyl radical. The second channel involves A-axis rotations of the complex, and a strong correlation of initial and final angular momentum in this case yields a forward scattered angular distribution for the propargyl radical product. These studies reveal the importance of the carbon-hydrogen exchange reactions for the buildup of carbon bearing species in combustion processes and in chemistry in interstellar clouds and the outflows of carbon stars.